AD

AD-E401 178

SPECIAL PUBLICATION ARLCD-SP-84001

STRUCTURES TO RESIST THE EFFECTS OF ACCIDENTAL EXPLOSIONS VOLUME III - PRINCIPLES OF DYNAMIC ANALYSIS

MICHAEL DEDE
FREDERICK SOCK
SHAFOR LIPVIN-SCHRAMM
ORVAL DOBBS

AMMANN & WHITNEY
TWO WORLD TRADE CENTER
NEW YORK, NY 10048

JUNE 1984

U.S. ARMY ARMAMENT RESEARCH AND DEVELOPMENT CENTER

LARGE CALIBER WEAPON SYSTEMS LABORATORY

DOVER, NEW JERSEY

DTIC
ELECT
SELECTED
DEC 0 3 1984
E

84   11   27   046

The views, opinions, and/or findings contained in this report are those of the author(s) and should not be construed as an official Department of the Army position, policy, or decision, unless so designated by other documentation.

Destroy this report when no longer needed. Do not return to the originator.

REPORT DOCUMENTATION PAGE	READ INSTRUCTIONS BEFORE COMPLETING FORM

1. REPORT NUMBER	2. GOVT ACCESSION NO.	3. RECIPIENT'S CATALOG NUMBER
Special Publication ARLCD-SP-84001	AD-A148895	

4. TITLE (and Subtitle)	5. TYPE OF REPORT & PERIOD COVERED
STRUCTURES TO RESIST THE EFFECTS OF ACCIDENTAL EXPLOSIONS - VOLUME III - PRINCIPLES OF DYNAMIC ANALYSIS	Final
	6. PERFORMING ORG. REPORT NUMBER

7. AUTHOR(s)	8. CONTRACT OR GRANT NUMBER(s)
Michael Dede, Frederick Sock, Sharon Lipvin-Schramm, and Norval Dobbs	DAAK10-82-C-0112

9. PERFORMING ORGANIZATION NAME AND ADDRESS	10. PROGRAM ELEMENT, PROJECT, TASK AREA & WORK UNIT NUMBERS
Ammann & Whitney Two World Trade Center New York, NY 10048	

11. CONTROLLING OFFICE NAME AND ADDRESS	12. REPORT DATE
ARDC, TSD STINFO Div [DRSMC-TSS(D)] Dover, NJ 07801	June 1984
	13. NUMBER OF PAGES
	415

14. MONITORING AGENCY NAME & ADDRESS(if different from Controlling Office)	15. SECURITY CLASS. (of this report)
ARDC, LCWSL Energetic Systems Process Div [DRSMC-LCM-SP(D)] Dover, NJ 07801	Unclassified
	15a. DECLASSIFICATION/DOWNGRADING SCHEDULE

16. DISTRIBUTION STATEMENT (of this Report)

Approved for public release; distribution unlimited.

17. DISTRIBUTION STATEMENT (of the abstract entered in Block 20, if different from Report)

18. SUPPLEMENTARY NOTES

This report covers Volume III of six volumes which will eventually be published as a tri-service design manual and was written under contract DAAK10-82-C-0112. The project was sponsored by the Department of Defense Explosives Safety Board. The ARDC project leader for the effort was Joseph P. Caltagirone.

19. KEY WORDS (Continue on reverse side if necessary and identify by block number)

Structural design	Protective structures	Ultimate resistance
Dynamic response	Explosive manufacturing facilities	Design for pressure
Dynamic analysis	Explosives safety	Design for impulse
Blast resistant design	Protective technology	Dynamic design
Blast walls	Resistance-deflection functions	Impulse design

20. ABSTRACT (Continue on reverse side if necessary and identify by block number)

This report, in six volumes, details design procedures for structures which are subjected to the effects of accidental explosions. The procedures cover the determination of the blast environment (blast and fragments) and then structural design. This volume, "Principles of Dynamic Analysis," in particular, contains the procedures for analyzing structural elements subject to blast overpressures. It discusses the basic principles of dynamics as well as procedures for calculating the various components used to perform the analyses. Also presented

(CONTINUED ON REVERSE)

DD _{1 JAN 73} 1473   EDITION OF 1 NOV 65 IS OBSOLETE

20. ABSTRACT (cont)

are resistance-deflection functions for various elements including both one-
and two-way panels as well as beam elements. These functions include the
elastic, elasto-plastic, and plastic ranges of response. In addition, a
discussion of dynamic equivalent systems (single- and multi-degree-of-freedom
systems) is presented. A step-by-step numerical integration of an element's
motion under dynamic loads using the acceleration-impulse-extrapolation method
or the average acceleration method and design charts for simplified loads is
illustrated. It also includes methods for analyzing elements subjected to
impulse type loadings, that is, loadings whose durations are short in com-
parison to the time to reach maximum response of the elements. Example
problems and solutions using these procedures are also included.

ACKNOWLEDGEMENT

i

TABLE OF CONTENTS

LIST OF FIGURES

LIST OF FIGURES (Continued)

LIST OF FIGURES (Continued)

LIST OF FIGURES (Continued)

LIST OF FIGURES (Continued)

LIST OF FIGURES (Continued)

LIST OF FIGURES (Continued)

LIST OF FIGURES (Continued)

LIST OF TABLES

VOLUME III
PRINCIPLES OF DYNAMIC ANALYSIS

INTRODUCTION

3-1 Purpose

The purpose of this six volume manual is to present methods of design for protective construction used in facilities for development, testing, production, maintenance, modification, inspection, disposal and storage of explosive materials.

3-2 Objectives

The primary objectives are to establish design procedures and construction techniques whereby propagation of explosion (from one building or part of a building to another) or mass detonation can be prevented and protection for personnel and valuable equipment will be provided.

The secondary objectives are:

    (1) Establish the blast load parameters required for design of protective structures;

    (2) Provide methods for calculating the dynamic response of structural elements including reinforced concrete, structural steel, etc.;

    (3) Establish construction details and procedures necessary to afford the required strength to resist the applied blast loads;

    (4) Establish guide lines for siting explosive facilities to obtain maximum cost effectiveness in both the planning and structural arrangements; providing closures, and preventing damage to interior portions of structures due to structual motion, shock, and fragment perforation.

3-3 Background

For the first 60 years of the 20th century criteria and methods based upon the results of catastrophic events have been used for the design of explosive facilities. The criteria and methods did not include a detailed or reliable quantitative basis for assessing the degree of protection afforded by the protective facility. In the late 1960's quantitative procedures were set forth in the first edition of the present manual, "Structures to Resist the Effects of Accidental Explosions." This manual was based on extensive research and development programs which permitted a more reliable approach to design requirements. Since the original publication of this manual, more extensive publication, more extensive testing and development programs have taken place. This additional research was directed primarily towards materials other than reinforced concrete which was the principal construction material referenced in the initial version of the manual.

Modern methods for the manufacture and storage of explosive materials, which include many exotic chemicals, fuels, propellants, etc., required less space for a given quantity of explosive material than was previously needed. Such concentrations of explosives increase the possibility of the propagation of accidental explosions (one accidental explosion causing the detonation of other explosive materials). It is evident that a requirement for more accurate design techniques has become essential. This manual describes rational design methods to provide the required stuctural protection.

These design methods account for the close-in effects of a detonation including associated high pressures and nonuniformity of the blast loading on protective structures or barriers as well as intermediate and far-range effects which are encountered in the design of stuctures which are positioned away from the explosion. The dynamic response of structures, constructed of various materials, or combination of materials, can be calculated, and details have been developed to provide the properties necessary to supply the required strength and ductility specified by the design. Development of these procedures has been directed primarily towards analyses of protective structures subjected to the effects of high explosive detonation. However, this approach is general and is applicable to the design of other explosive environments as well as other explosive materials as numerated above.

The design techniques set forth in this manual are based upon the results of numerous full- and small-scale structural response and explosive effects tests of various materials conducted in conjunction with the development of this manual and/or related projects.

3-4 Scope of Manual

This manual is limited only by variety and range of the assumed design situation. An effort has been made to cover the more probable situations. However, sufficient general information on protective design techniques has been included in order that application of the basic theory can be made to situations other than those which were fully considered.

This manual is generally applicable to the design of protective structures subjected to the effects associated with high explosive detonations. For these design situations, this manual will generally apply for explosive quantities less than 25,000 pounds for close-in effects. However, this manual is also applicable to other situations such as far or intermediate range effects. For these latter cases the design procedures as presented are applicable for explosive quantities up to 500,000 pounds.

Because the tests conducted so far in connection with this manual have been directed primarily towards the response of structural steel and reinforced concrete elements to blast overpressures, this manual concentrates on design procedures and techniques for these materials. However, this does not imply that concrete and steel are the only useful materials for protecitve construction. Tests to establish the response of wood, brick blocks, plastics, etc. as well as the blast attenuating and mass effects of soil are contemplated. The results of these test may require, at a later date, the supplementation of these design methods for these and other materials.

Other manuals are available which enable one to design protective structures against the effects of high explosive or nuclear detonations. The procedures in these manuals will quite often complement this manual and should be consulted for specific applications.

Computer programs, which are consistent with the procedures and techniques contained in the manual, have been approved by the appropriate representative of the U.S. Army, the U.S. Navy, the U.S. Air Force and the Department of Defense Explosive Safety board (DDESB). These programs are available through the following repositories:

1.   Department of the Army

Commander and Director
U.S. Army Engineer
Waterways Experiment Station
Post Office Box 631
Vicksburg, Mississippi   39180

Attn: WESKA

2.   Department of the Navy

Officer-In-Charge
Civil Engineering Laboratory
Naval Battalion Construction Center
Port Hueneme, California 93043

Attn: Code L51

3.   Department of the Air Force

Aeorspace Structures
Information and Analysis Center
Wright Paterson Air Force Base
Ohio 45433

Attn: AFFDL/FBR

Limited number of copies of the above program are available for each repository upon request.   The individual programs are identical at each repository.   If any modifications and/or additions to these programs are required, they will be submitted by the organization for review by DDESB and the above services. Upon concurrence of the revisions, the necessary changes will be made and notification of these changes will be made by the individual repositories.

3-5 Format of Manual

This manual is subdivided into six specific volumes dealing with various aspects of design. The titles of these volumes are as follows:

Volume I - Introduction
Volume II - Blast, Fragment and Shock Loads
Volume III - Principles of Dynamic Analysis
Volume IV - Reinforced Concrete Design
Volume V - Structural Steel Design
Volume VI - Special Considerations in Explosive Facility Design

Appendix A pertinent to a particular volume and containing illustrative examples of explosive effects and structural response problems appears at the end of each volume.

Commonly accepted symbols have been used as much as possible. However, protective design involves many different scientific and engineering fields, and, therefore, no attempt has been made to standardize completely all the symbols used. Each symbol has been defined where it is first introduced, and a list of the symbols, with their definitions and units, is contained in Appendix B of each volume.

VOLUME CONTENTS

3-6 General

This Volume contains the procedures for analyzing structural elements subject to blast overpressures. These procedures are contained in the next eleven sections; Section 3-7 deals with a simplified discussion of the basic principles of dynamics as well as the procedures for calculating the various components used to perform the dynamic analyses. Presented in Sections 3-8 through 3-15 are resistance-deflection functions for various elements including both one- and two-way panels as well as beam elements. These functions include the elastic, elasto-plastic, and plastic ranges of response. In addition, a discussion of dynamic equivalent systems is presented in Sections 3-16 and 3-17. These include single- and multi-degree-of-freedom systems. Presented in this Section also are methods for calculating load and mass factors required to perform the dynamic analyses.

Sections 3-18 through 3-20 include both a step-by-step numerical integration of an element's motion under dynamic loads utilizing the Acceleration-Impulse-Extrapolation Method or the Average Acceleration Method and design charts for idealized loads. Presented also in these Sections are methods for analyzing elements subjected to impulse type loadings; that is, loadings whose durations are short in comparison to the time to reach maximum response of the elements.

- 4 -

BASIC PRINCIPLES

3-7 General

The principles used in the analysis of structures under static load will be reviewed briefly, since the same principles are used in the analysis and design of structures subjected to dynamic loads. Two different methods are used either separately or concurrently in static analysis: one is based on the principle of equilibrium, and the other on work done and internal energy stored.

Under the application of external loads, a given structure is deformed and internal forces developed in its members. In order to satisfy static equilibrium, the vector sum of all the external and internal forces acting on any free body portion of the stucture must be equal to zero. For the equilibrium of the structure as a whole, the vector sum of the external forces and the reactions of the foundation must be equal to zero.

The method based on work done and energy considerations is sometimes used when it is necessary to determine the deformation of a structure. In this method, use is made of the fact that the deformation of the structure causes the point of application of the external load to be displaced. The force then does work on the structure. Meanwhile, because of the structural deformations, potential energy is stored in the structure in the form of strain energy. By the principle of energy conservation, the work done by the external force and the energy stored in the members must be equal. In static analysis, simplified methods such as the method of virtual work and the method of the unit load are derived from the general principle of energy conservation.

In the analysis of statically indeterminate structures, in addition to satisfying the equations of equilibrium, it is necessary to include a calculation of the deformation of the strucuture in order to arrive at a complete solution of the internal forces in the structure. The methods based on energy considerations such as the method of least work and the method based on Castigliano's theorems are generally used.

For the analysis of structures under dynamic loading, the same two methods are basically used; but the load changes rapidly with time and the acceleration velocity and, hence, the inertia force and kinetic energy are of magnitudes requiring consideration. Thus, in addition to the internal and external forces, the equation of equilibrium includes the inertia force and the equation of dynamic equilibrium takes the form of Newton's equation of motion:

$$F - R = Ma \qquad \qquad \text{3-1}$$

where F = total external force as a function of time
          R = total internal force as a function of time
          M = total mass
          a = acceleration of the mass

As for the principle of conservation of energy, the work done must be equal to the sum of the kinetic energy and the strain energy:

$$WD = KE + SE \qquad \qquad \text{3-2}$$

- 5 -

where   WD = work done
         KE = kinetic energy
         SE = strain energy

and the strain energy includes both reversible elastic strain energy and the irreversible plastic strain energy. Thus, the difference between structures under static and dynamic loads is the presence of inertial force (Ma) in the equation of dynamic equilibrium, and of kinetic energy in the equation of energy conservation. Both terms are related to the mass of the structure; hence, the mass of the structure becomes an important consideration in dynamic analysis.

In the dynamic analysis of structures, both the energy balance equation and the force balance equation are applied with explicit description of the external forcing function F, and the internal resisting forcing function R. The difference between these forcing functions is the inertia force as described above. The following is a discussion of the details of how these forces are utilized in the design of structures which respond in the ductile mode.

In the design of a structure to resist the blast from an HE explosion, the total external force acting on the structure can be obtained by the principles discussed Volume II. The design method also consists of the determination of the total internal force, i.e. the resistance of the structure required to limit calculated deflections of the individual members and the structure as a whole under the external force (blast loading), to within prescribed maximum values. The determination of the resistance of the individual members of the structure is presented in Sections 3-8 through 3-17. Subsequent sections of this manual present the principles and methods of dynamic analysis and equations, charts, and procedures for design.

RESISTANCE - DEFLECTION FUNCTIONS

3-8   Introduction

Under the action of external loads, a structural element is deformed and internal forces set up. The sum of these internal forces tending to restore the element to its unloaded static position is defined as the resistance. The resistance of a structural element is a reactive force associated with the deflection of the element produced by the applied load. It is convenient to consider the resistance as an equivalent load in the same manner as the applied load, but opposite in direction. The variation of the resistance vs. displacement is expressed by a resistance-deflection function and may be represented graphically. An idealized resistance-deflection function for an element spanning in two directions and covering in the complete flexural range to incipient failure is shown in figure 3-1.

As load is applied to a structural element, the element deflects and, at any instant, exerts a resistance to further deformation, which is a function of its units stiffness K, until the ultimate unit resistance r_u (total resistance is $r_u A$ where A is the element area) of the element is reached at deflection X_p. The intial portion of the resistance-deflection diagram is composed of

- 6 -
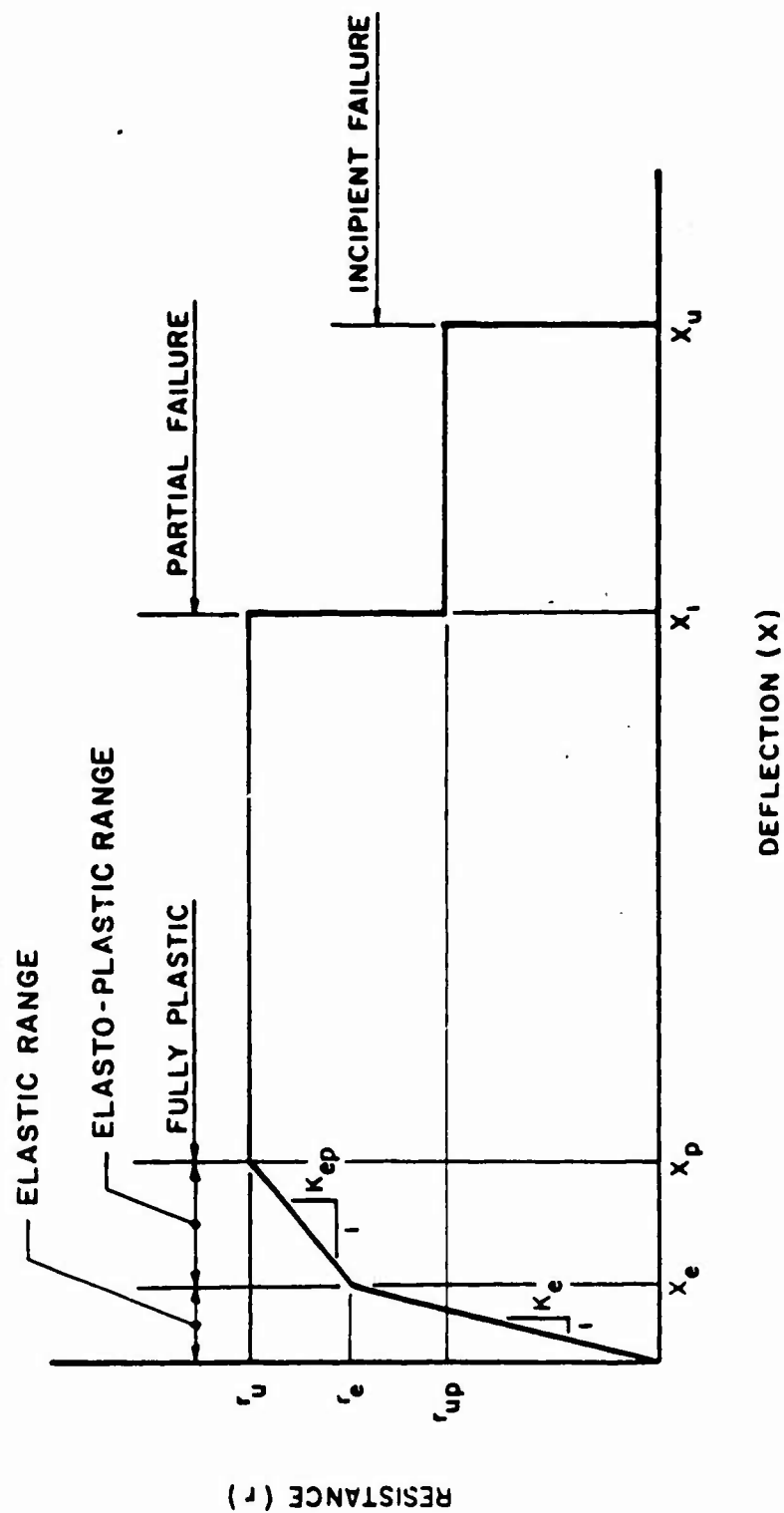
Figure 3-1   Typical resistance-deflection function for two-way element

the elastic and elasto-plastic ranges, each with its corresponding stiffness, the transition from one range to another occurring as plastic hinges are formed at points of maximum stress (yield lines). The number of elasto-plastic ranges required before the ultimate resistance of a particular element is reached depends upon the type and number of supports, and the placement of reinforcing steel (in the case of reinforced concrete elements). For example a beam with simple supports subjected to uniformly distributed loads needs only one plastic hinge to develop the ultimate resistance (or full plastic strength) of the element; whereas for the same beam fixed at both ends, more than one plastic hinge is required.

In subsequent paragraphs, various procedures, equations and illustrations are presented to enable the designer to determine the resistances of both one- and two-way elements. The procedures outlined apply mainly to reinforced concrete elements and so do the equations appearing in the text, unless the equations are given as part of an illustrative example. However, they can also be used for structural steel elements as well as other structural elements such as aluminum, plastics, etc. Equations have been derived for specific cases most often encountered in practice. These are applicable for structural steel and reinforced concrete elements of uniform thickness in both the horizontal and vertical directions. Before the equations and figures can be used for reinforced concrete element, however, the reinforcing steel across any yield line must have a uniform distribution in both the vertical and horizontal directions; however, the reinforcement across the positive yield lines can be different from that across the negative yield lines and the reinforcing pattern in the vertical direction different from that in the horizontal direction.

Regardless of whether it is reinforced concrete or structural steel element, any opening in the element must be compact in shape and small in area, compared to the total area of the element.

3-9   Ultimate Resistance

3-9.1   *General*

The ultimate resistance of an element depends upon:

     (1)   The distribution of the applied loads.
     (2)   The geometry of the element (length and width).
     (3)   The number and type of supports.
     (4)   The distribution of the moment capacity or reinforcement in the case of reinforced concrete elements.

The distribution of the loads depends upon the design range of the element; i.e., high, intermediate or low pressure. For intermediate and low pressure ranges, it can be assumed that the pressure is uniform across the surface of the element although it varies with time. At high pressure ranges, however, the blast loads are variable across the surface of the element. However, for structural steel elements and concrete elements utilizing laced reinforcement, or for concrete elements with standard shear reinforcement which sustain relatively small deflections, a good estimate of the resulting deflections can be made using the resistance functions conforming to those of uniformly loaded elements.

- 8 -

The other factors that affect the ultimate resistance of an element are predetermined by the requirements of the protective structure (where the element is used) and the magnitude of the blast output.

3-9.2 *One-Way Elements*

The ultimate resistance of a one-way reinforced concrete element with an elastic distribution of its reinforcing steel is based on the moment capacity at first yield since all critical sections yield simultaneously. For one-way reinforced concrete elements (such as beams or slabs) with non-elastic distribution of reinforcing steel and for structural steel elements, the ultimate resistance is a function of the moment capacity at the first yield plus the added moment capacity due to subsequent yielding at other critical sections.

Values of the ultimate resistance for one-way elements are shown in table 3-1 where the following symbols are used:

M_N = ultimate negative unit moment capacity at the support.
M_p = ultimate positive unit moment capacity at midspan.
L = length
r_u = ultimate unit resistance
R_u = total ultimate resistance

Table 3-1 applies to both beams and slabs. However, special attention must be paid to the units used for the respective element. The moment capacity of a slab is expressed for a unit strip of the slab (inch-pounds per inch) whereas the total moment capacity (inch-pounds) is considered for a beam. Consequently, the resistance of a slab is expressed in load per unit area (psi) where the resistance of a beam is expressed in load per length along the beam (pounds per inch).

3-9.3 *Two-Way Elements*

The amount of data available on the limit analysis of retangular steel plates is very limited. However, an elementary approach imagines a mechanism formed of straight yield lines, as is customary in reinforced concrete. This approach for reinforced concrete elements will be considered appropriate for structural steel elements.
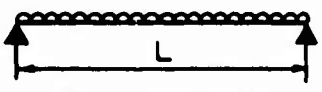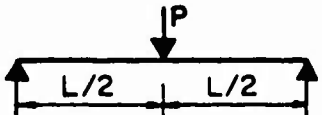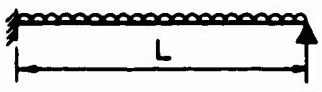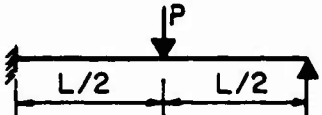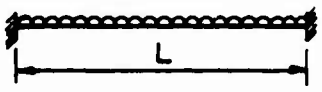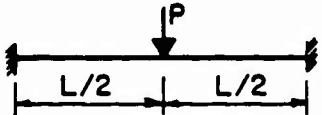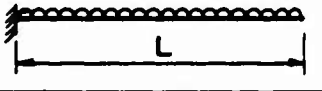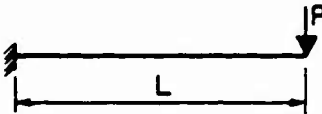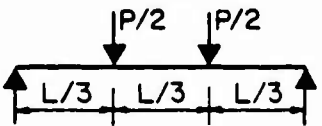
In the design of two-way reinforced concrete elements, it is not necessary to define accurately the stress distribution during the initial and intermediate stages of loading since the ultimate load capacity can be readily determined by the use of yield line procedures. The yield line method assumes that after inital cracking of the concrete at points of maximum moment, yielding spreads until the full moment capacity is developed along the length of the cracks on which failure will take place. Several illustrative examples of the simplified yield or crack lines for two-way elements are illustrated in figure 3-2.

In using the yield line solution, the inital step is to assume a yield line pattern (as shown in figure 3-2) applying the following rules:

(1) To act as plastic hinges of a collapse mechanism made up of

- 9 -

Table 3-1   Ultimate Unit Resistances for One-Way Elements

Edge Conditions and Loading Diagrams	Ultimate Resistance
	$r_u = \dfrac{8\,M_p}{L^2}$
	$R_u = \dfrac{4\,M_p}{L}$
	$r_u = \dfrac{4\,(M_N + 2\,M_p)}{L^2}$
	$R_u = \dfrac{2\,(M_N + 2\,M_p)}{L}$
	$r_u = \dfrac{8\,(M_N + M_p)}{L^2}$
	$R_u = \dfrac{4\,(M_N + M_p)}{L}$
	$r_u = \dfrac{2\,M_N}{L^2}$
	$R_u = \dfrac{M_N}{L}$
	$R_u = \dfrac{6\,M_p}{L}$
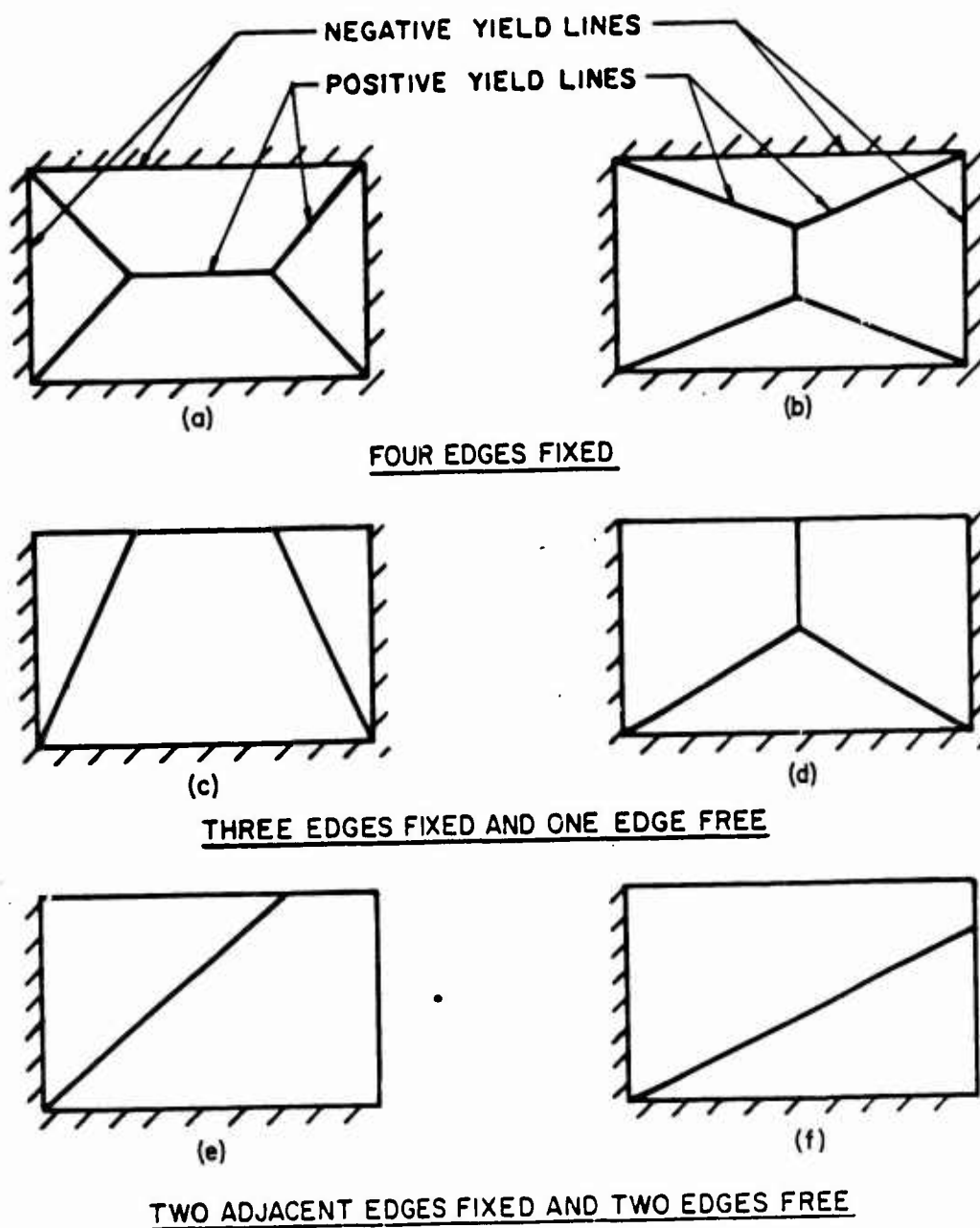
Figure 3-2   Idealized yield line locations for several two-way elements

plane segments, yield lines must be straight lines forming axes of rotation for the movements of the segments.

(2) The supports of the slabs will act as axes of rotation. A yield line may form along a fixed support and an axis of rotation will pass over a column.

(3) For compatibility of deformations, a yield line must pass through the intersection of the axes of rotation of the adjacent slab segments.

Tests indicate that the actual location and extent of these lines on reinforced concrete elements differ only slightly at failure from the theoretical ones. Use of the idealized yield lines results in little error in the determination of the ultimate resistance and the error is on the side of safety.

The corner sections of two-way elements are stiff in comparison to the remainder of the member; therefore, straining of the reinforcement which is associated with the reduced rotations at these sections will be less. To account for the corner effects, the design of any one particular section of a two-way element should consider a variation of the moment capacity along the yield lines rather than a uniform distribution.

This variation is approximated by taking the full moment capacity along the yield lines, except in the corners where two-thirds of the moment capacity over the lengths described in figure 3-3 are used. The variation applies to both the negative moments along the supports and the positive moments at the interior.

The ultimate unit resistance can be determined from the yield line pattern using either the principle of virtual work or the equations of equilibrium. Each approach has its advantages; in general, the virtual work method is easier in principle but difficult to manipulate algebraically since it involves differentiating a usually complex mathematical expression for a minimum value of resistance. The equilibrium method, which is used in this manual, also has its disadvantages. Since equilibrium requires that the shear forces acting on each side of a yield line have to be equal and opposite, correction forces (also known as nodal forces) have to be introduced around openings in two-way members and at free edges, and these correction forces may not be available from simple analysis. However, in three of the six cases shown in figure 3-2, (cases c, e, f), nodal forces exist; but their effects are negligible.

In order to calculate the ultimate unit resistance r_u of a two-way element, the equation of equilibrium of each sector formed by the yield lines is expressed in terms of the moments produced by the internal and external forces. The sum of the resisting moments acting along the yield lines (both positive and negative) of each sector is equated to the moment produced by the applied load about the axis of rotation (support of the sector), assuming that the shear forces are zero along the positive yield lines.

$$\Sigma M_N + \Sigma M_p = Rc = r_u Ac \qquad\qquad 3\text{-}3$$

- 12 -
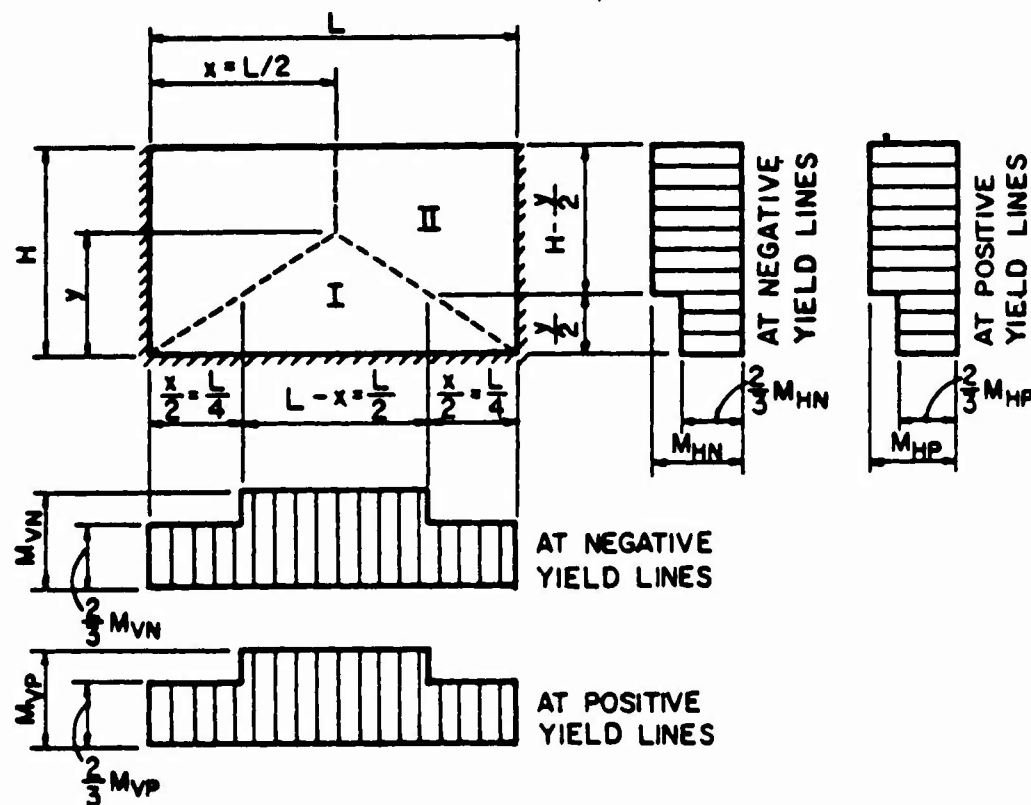
a) YIELD LINES AND DISTRIBUTION OF MOMENTS
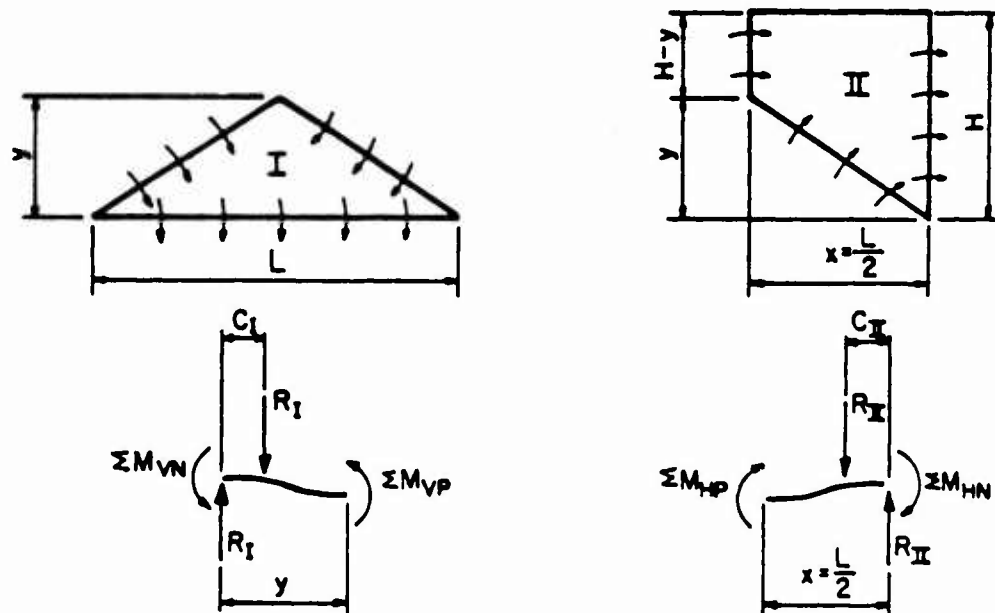
b) FREE-BODY DIAGRAMS FOR INDIVIDUAL SECTORS

Figure 3-3   Determination of ultimate unit resistance

-13-

where M_N = sum of the ultimate unit resisting moments
acting along the support (negative yield lines)

M_p = sum of the ultimate unit resisting moments
acting along the interior failure lines (positive
yield lines)

R = total ultimate resistance of the sector

c = distance from the centroid of the load to
the line of rotation of the sector

r_u = ultimate unit resistance of the sector

A = area of the sector

Once the equations of equilibrium are known for all sectors, the ultimate resistance is obtained either by solving the equations simultaneously or by a trial and error procedure noting that the unit resistance of all sectors must be equal.

To illustrate the above procedure (equation 3-3), consider the two-way concrete element shown in figure 3-3 which is fixed on three edges and free on the fourth, and where the nomenclature is as follows:

L = length of element

H = height of element

x = yield line location in horizontal direction

y = yield line location in vertical direction

M_{VN} = ultimate unit negative moment capacity in
the vertical direction

M_{VP} = ultimate unit positive moment capacity
in the vertical direction

M_{HN} = ultimate unit negative moment capacity
in the horizontal direction

M_{HP} = ultimate unit positive moment capacity
in the horizontal direction

The nomenclature as stated in the paragraph above is strictly applicable to two-way elements which are used as walls. However, when roof slabs or other horizontal elements are under consideration, the preceding nomenclature will also be applicable if the element is treated as being rotated into a vertical position.

The first step in the solution is to assume the location of the yield lines as defined by the coordinates x and y. It should be noted that in some cases, because of geometry, the value of x and y will be known and therefore need not be evaluated. In this example, the negative reinforcement in the horizontal direction at opposite supports is assumed to be equal; therefore, the vertical yield line is located at the center of the span and the value of x is numerically equal to L/2 (a, fig. 3-3). However, in other cases, neither the location of x nor y will be known, and the solution will require the determination of both coordinates.

Once the yield lines have been assumed, the distribution of the resisting moments along the yield lines is determined. In the case at hand, the reduced moments, as a result of the increased stiffness at the corners, act over lengths equal to x/2 and y/2 in the horizontal and vertical directions, respectively (a, fig. 3-3). The equations of equilibrium are then written for

- 14 -

each sector with the use of the free body diagrams (b, fig. 3-3). For the triangular sector I:

$$M_{VN} = (2/3)M_{VN}(L/4 + L/4) + M_{VN}(L/2)$$

$$= (5/6)M_{VN}L \qquad\qquad 3\text{-}4$$

$$M_{VP} = (2/3)M_{VP}(L/4 + L/4) + M_{VP}(L/2)$$

$$= (5/6)M_{VP}L \qquad\qquad 3\text{-}5$$

$$C_I = y/3 \qquad\qquad 3\text{-}6$$

$$R_I = (M_{VN} + M_{VP})/C_I$$

$$= [5L(M_{VN} + M_{VP})]/2y \qquad\qquad 3\text{-}7$$

$$A_I = Ly/2 \qquad\qquad 3\text{-}8$$

$$r_u(\text{Sector I}) = R_I/A_I$$

$$= [5(M_{VN} + M_{VP})]/y^2 \qquad\qquad 3\text{-}9$$

For the trapezoidal sector II, a similar procedure gives

$$M_{HN} = (2/3)M_{HN}(y/2) + M_{HN}(H - y/2)$$

$$= M_{HN}(H - y/6) \qquad\qquad 3\text{-}10$$

$$M_{HP} = (2/3)M_{HP}(y/2) + M_{HP}(H - y/2)$$

$$= M_{HP}(H - y/6) \qquad\qquad 3\text{-}11$$

$$C_{II} = (1/3)(L/2)[2(H-y) + H]/(H + H - y)$$

$$= [L(3H - 2y)]/6(2H - y) \qquad\qquad 3\text{-}12$$

$$R_{II} = (M_{HN} + M_{HP})/C_{II}$$

$$= [(6H - y)(2H - y)(M_{HN} + M_{HP})]/L(3H - 2y) \qquad\qquad 3\text{-}13$$

$$A_{II} = (1/2)(L/2)(H + H - y)$$

$$= [L(2H - y)]/4 \qquad\qquad 3\text{-}14$$

$$r_u(\text{Sector II}) = R_{II}/A_{II}$$

$$= [4(M_{HN} + M_{HP})(6H -y)]/L^2(3H - 2y) \qquad\qquad 3\text{-}15$$

Equations 3-9 and 3-15 are the equations of equilibrium for the triangular (I) and the trapezoidal (II) sectors, respectively. As mentioned previously, these equations can be solved simultaneously or by a trial and error procedure. In the latter method, values of y are substituted into both equations until r_u (sector I) is equal to r_u (sector II).

- 15 -

If a numerical solution based on the above procedure (equation 3-3) yields negative values for either x, y or r_u, then the assumed yield line location is wrong. In this example, the only other possible yield line pattern ($x \leq L/2$) would be as shown in figure 3-2c.

The solution of equation 3-3 is universally applicable for any two-way element. If the negative reinforcement in the horizontal direction had been unequal at the opposing supports, the value of $x = L/2$ would have changed, and all three sectors wold have had to be considered to determine x, y and hence, r_u.

Simultaneous solution of equations 3-9 and 3-15 reveals that the locations of the yield lines are a function of the ratio of the spans L/H and the ratio of the sum of the unit vertical to horizontal moment capacities as follows:

$$r_u(\text{Sector I}) = r_u(\text{Sector II}) \qquad 3\text{-}16$$

$$5(M_{VN} + M_{VP})/y^2 = [4(M_{HN} + M_{HP})(6H - y)]/L^2(3H - 2y) \qquad 3\text{-}17a$$

$$L^2(M_{VN} + M_{VP})/H^2(M_{HN} + M_{HP}) =$$

$$[4y^2(6 - y/H)]/[5H^2(3 - 2y/H)] \qquad 3\text{-}17b$$

$$(L/H)[(M_{VN} + M_{VP})/(M_{HN} + M_{HP})]^{1/2} =$$

$$(y/H)[(4(6 - y/H)/5(3 - 2y/H)]^{1/2} \qquad 3\text{-}17c$$

Equation 3-17c, which relates the location of the yield lines to the moment capacity of the element, is used to plot figure 3-6. Knowing the location of the yield lines, the resistance of the two-way element can be obtained from either equation 3-9 or 3-15 which are also presented in table 3-2.

Using the procedure outlined above, the values of the ultimate unit resistances for several two-way elements with various support conditions are given in tables 3-2 and 3-3, the nomenclature confirming to that previously listed. Table 3-2 covers the special cases where opposite supports provide the same degree of restraint thus resulting in symmetrical yield line patterns. Table 3-3 deals with the general cases when the yield line patterns are not symmetrical (that is, when opposite supports provide different restraints). Yield line location ratios x/L and y/H for the same elements are depicted in figures 3-4 through 3-20.

Figures 3-4 and 3-5 show the location of the yield lines for two-way elements with two adjacent edges supported and the other two free. In each of these figures eight curves are shown which represent different ratios of the positive to the negative moment capacities in both the vertical and horizontal directions. Figures 3-6 through 3-16 illustrate the yield line location for two-way elements with three edges supported and one edge free. Figures 3-6 and 3-11 covers the case when the yield line pattern is symmetrical (opposite supports provide the same degree of restraint). Figures 3-17 through 3-20 show the yield line location for two-way elements with four sides supported.

- 16 -

Table 3-2   Ultimate Unit Resistances for Two-Way Elements (Symmetrical Yield Lines)
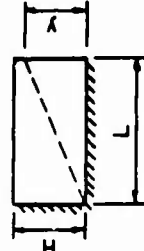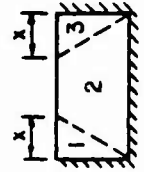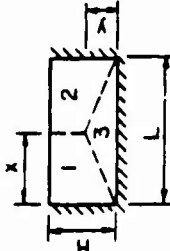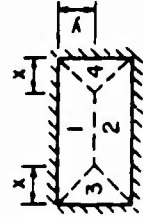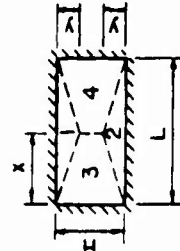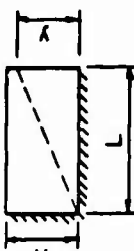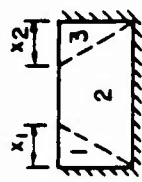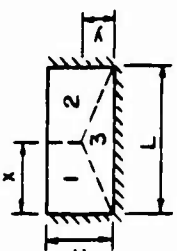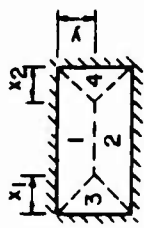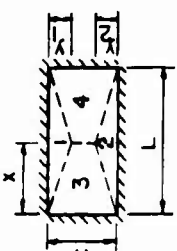
Edge Conditions	Yield Line Locations	Limits	Ultimate Unit Resistance
Two adjacent edges supported and two edges free		$x \leq L$	$\dfrac{5(M_{HN}+M_{HP})}{x^2}$ OR $\dfrac{6LM_{VN}+(5M_{VP}-M_{VN})x}{H^2(3L-2x)}$
		$y \leq H$	$\dfrac{5(M_{VN}+M_{VP})}{y^2}$ OR $\dfrac{6HM_{HN}+(5M_{HP}-M_{HN})y}{L^2(3H-2y)}$
Three edges supported and one edge free		$x \leq \dfrac{L}{2}$	$\dfrac{5(M_{HN}+M_{HP})}{x^2}$ OR $\dfrac{2M_{VN}(3L-x)+10xM_{VP}}{H^2(3L-4x)}$
		$y \leq H$	$\dfrac{5(M_{VN}+M_{VP})}{y^2}$ OR $\dfrac{4(M_{HN}+M_{HP})(6H-y)}{L^2(3H-2y)}$
Four edges supported		$x \leq \dfrac{L}{2}$	$\dfrac{5(M_{HN}+M_{HP})}{x^2}$ OR $\dfrac{8(M_{VN}+M_{VP})(3L-x)}{H^2(3L-4x)}$
		$y \leq \dfrac{H}{2}$	$\dfrac{5(M_{VN}+M_{VP})}{y^2}$ OR $\dfrac{8(M_{HN}+M_{HP})(3H-y)}{L^2(3H-4y)}$

Table 3-3   Ultimate Unit Resistances for Two-Way Elements (Unsymmetrical Yield Lines)

Edge Conditions	Yield Line Locations	Limits	Ultimate Unit Resistance
Two adjacent edges supported and two edges free		$x \leq L$ $y \leq H$	Same as in Table 3-2
Three edges supported and one edge free		$x \leq \dfrac{L}{2}$ $y \leq H$	$\dfrac{5(M_{HN1}+M_{HP1})}{X_1^2}$ OR $\dfrac{5(M_{HN3}+M_{HP})}{X_2^2}$ OR $\dfrac{(5M_{VP}-M_{VN2})(X_1+X_2)+6M_{VN2}L}{H^2(3L-2X_1-2X_2)}$ $\dfrac{(M_{HN1}+M_{HP})(6H-Y)}{X^2(3H-2Y)}$ OR $\dfrac{(M_{HN2}+M_{HP})(6H-Y)}{(L-X)^2(3H-2Y)}$ OR $\dfrac{5(M_{VN3}+M_{VP})}{Y^2}$
Four edges supported		$x \leq \dfrac{L}{2}$ $y \leq \dfrac{H}{2}$	$\dfrac{(M_{VN1}+M_{VP})(6L-X_1-X_2)}{Y^2(3L-2X_1-2X_2)}$ OR $\dfrac{(M_{VN2}+M_{VP})(6L-X_1-X_2)}{(H-Y)^2(3L-2X_1-2X_2)}$ $\dfrac{5(M_{HN1}+M_{HP})}{X_1^2}$ OR $\dfrac{5(M_{HN2}+M_{HP})}{X_2^2}$ $\dfrac{5(M_{VN1}+M_{VP})}{Y_1^2}$ OR $\dfrac{5(M_{VN2}+M_{VP})}{Y_2^2}$ $\dfrac{(M_{HN1}+M_{HP})(6H-Y_1-Y_2)}{X^2(3H-2Y_1-2Y_2)}$ OR $\dfrac{(M_{HN2}+M_{HP})(6H-Y_1-Y_2)}{(L-X)^2(3H-2Y_1-2Y_2)}$
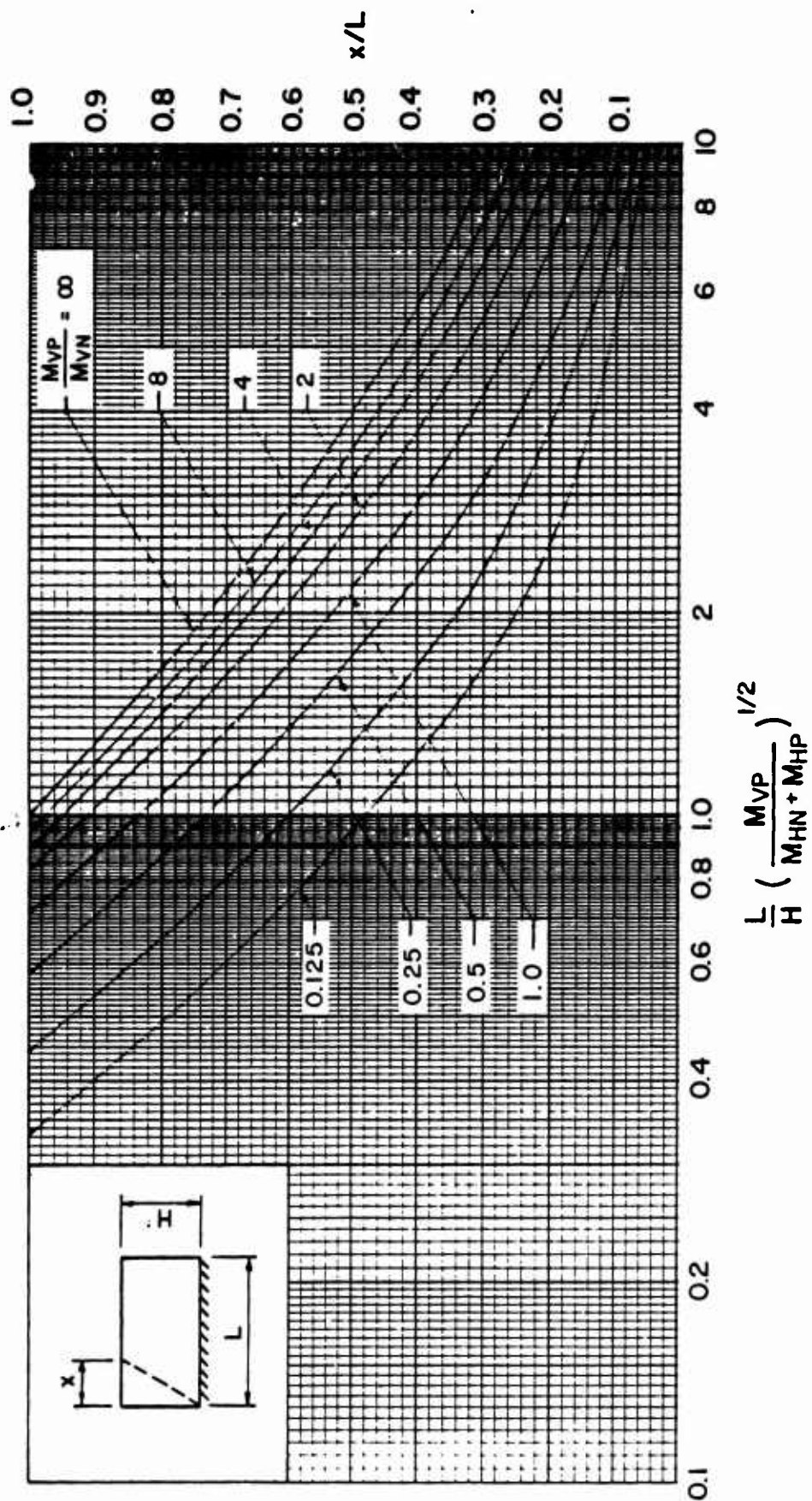
Figure 3-4   Location of yield lines for two-way element with two adjacent edges supported and two edges free (values of x)

-19-
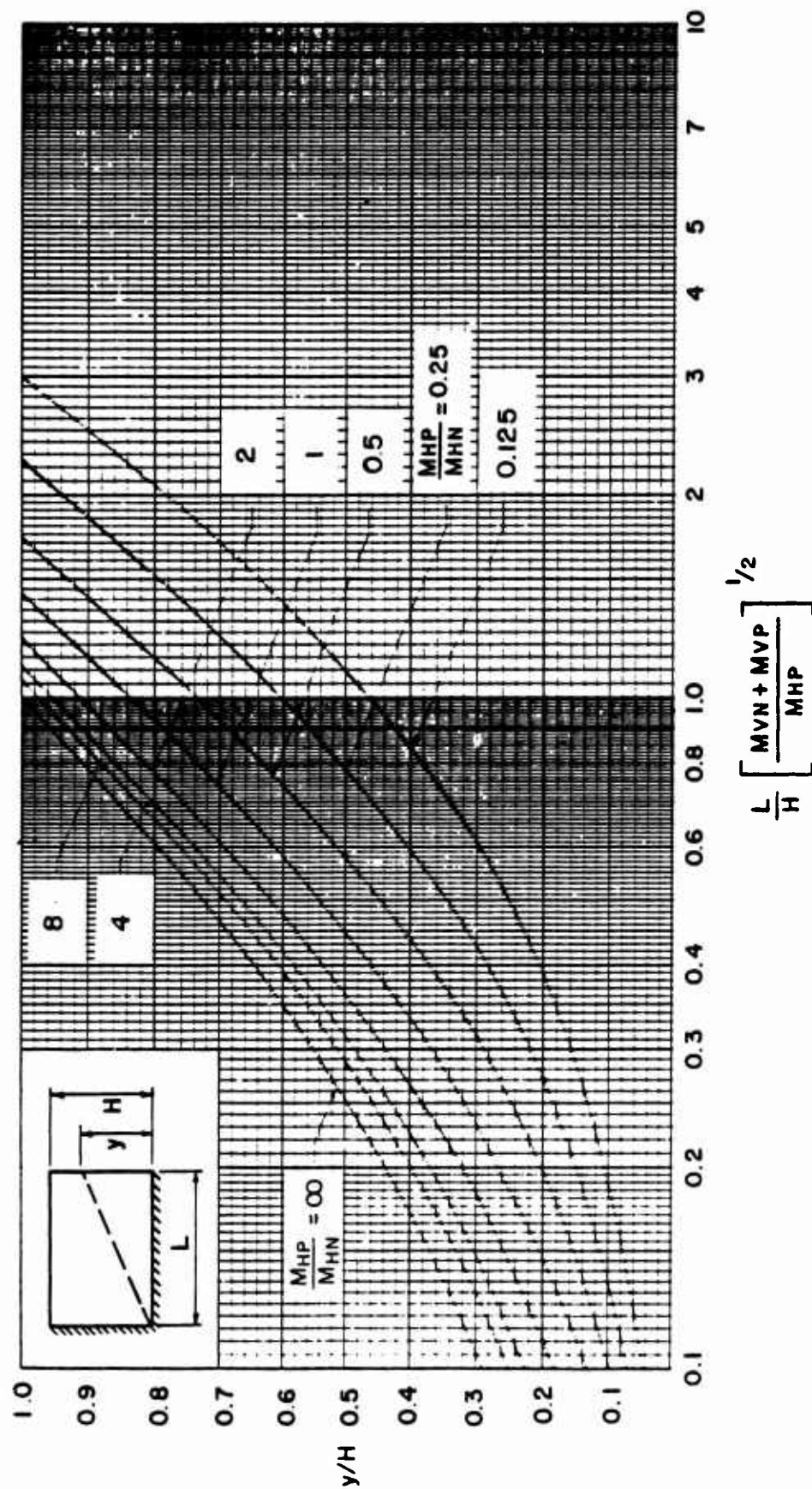
Figure 3-5   Location of yield lines for two-way element with two adjacent
              edges supported and two edges free (values of y)
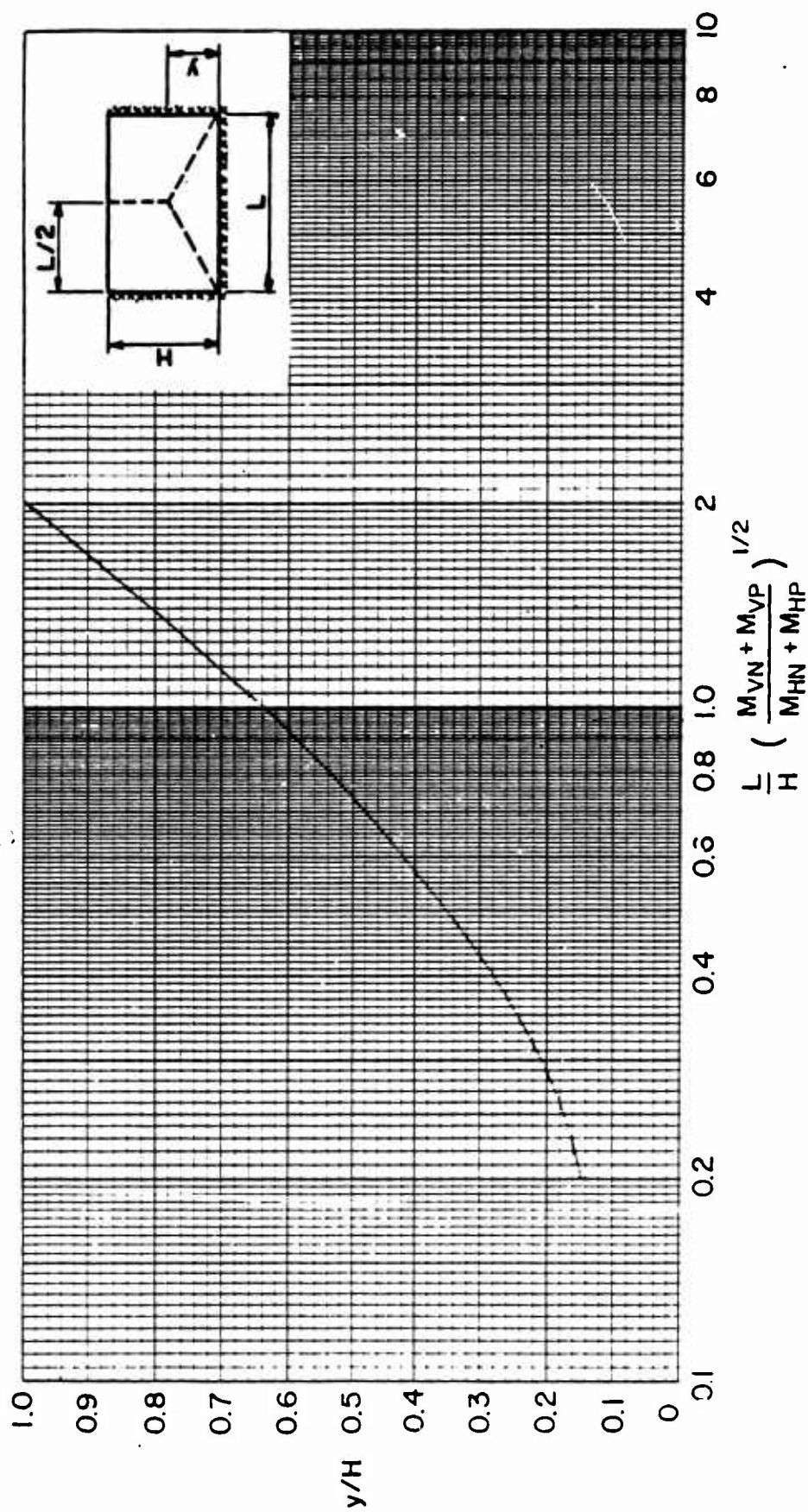
Figure 3-6   Location of symmetrical yield lines for two-way element with three
edges supported and one edge free (values of y)
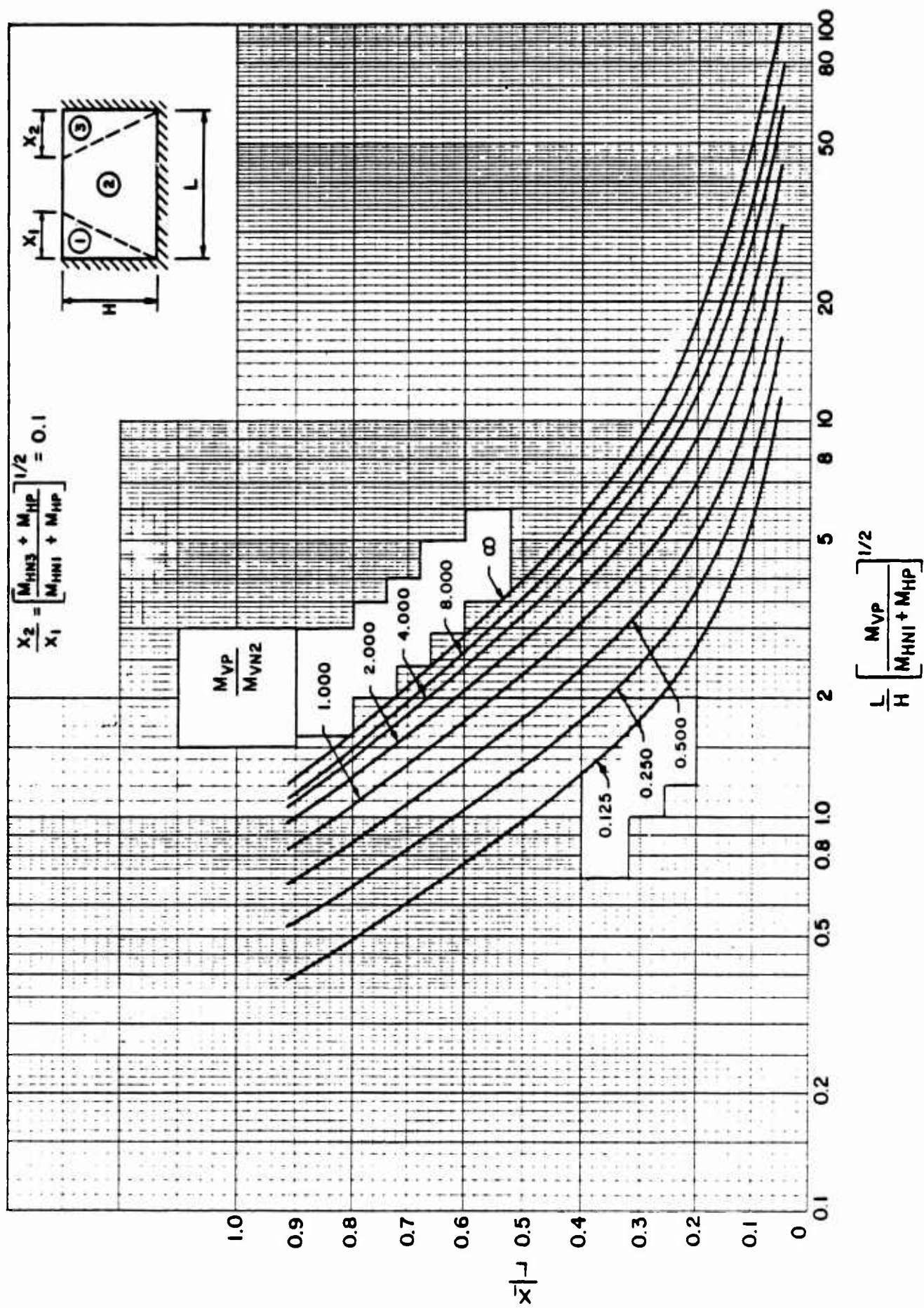
Figure 3-7   Location of unsymmetrical yield lines for two-way element
with three edges supported and one edge free ($X_2/X_1 = 0.1$)
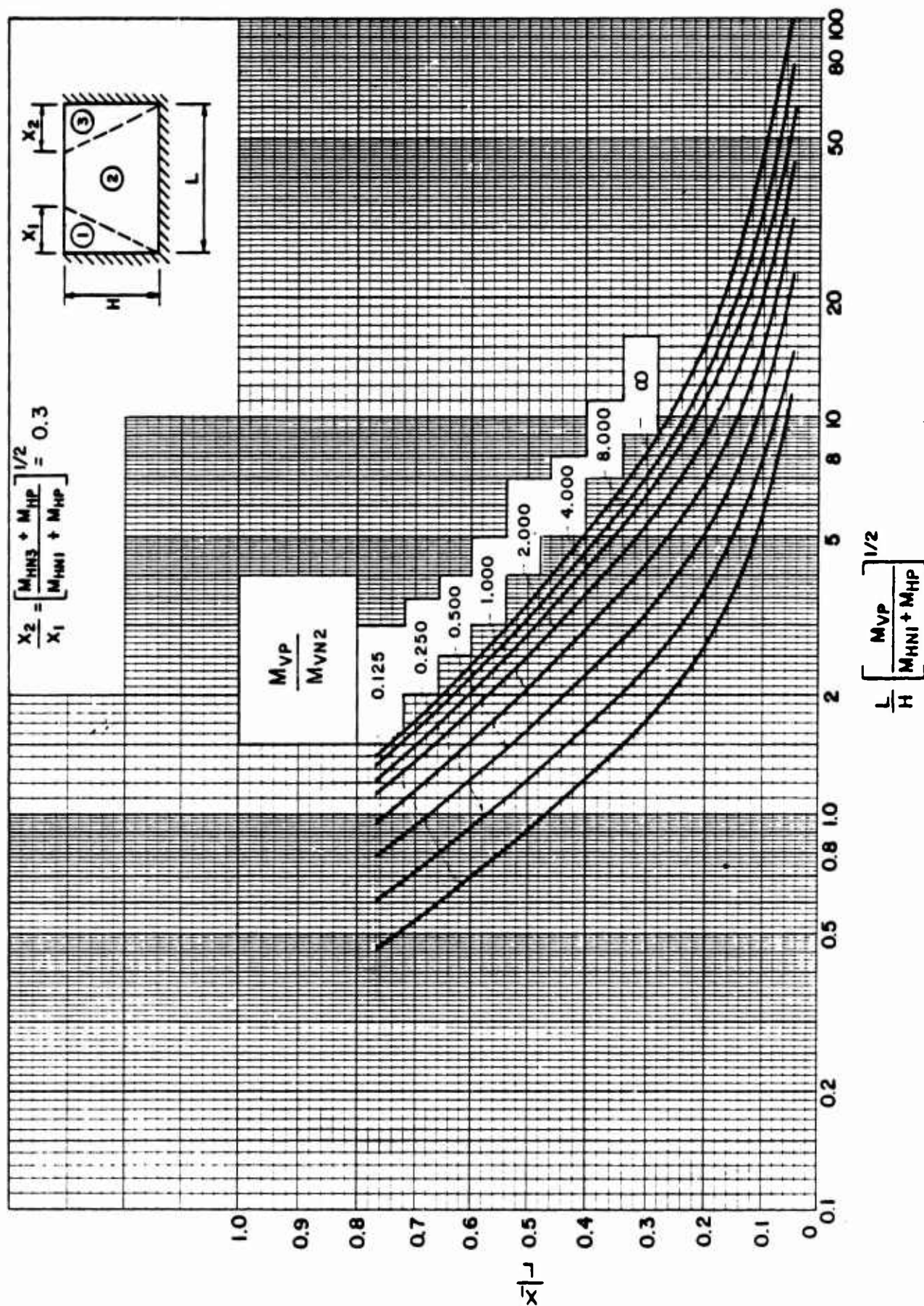
Figure 3-8 Location of unsymmetrical yield lines for two-way element with three edges supported and one edge free ($X_2/X_1 = 0.3$)
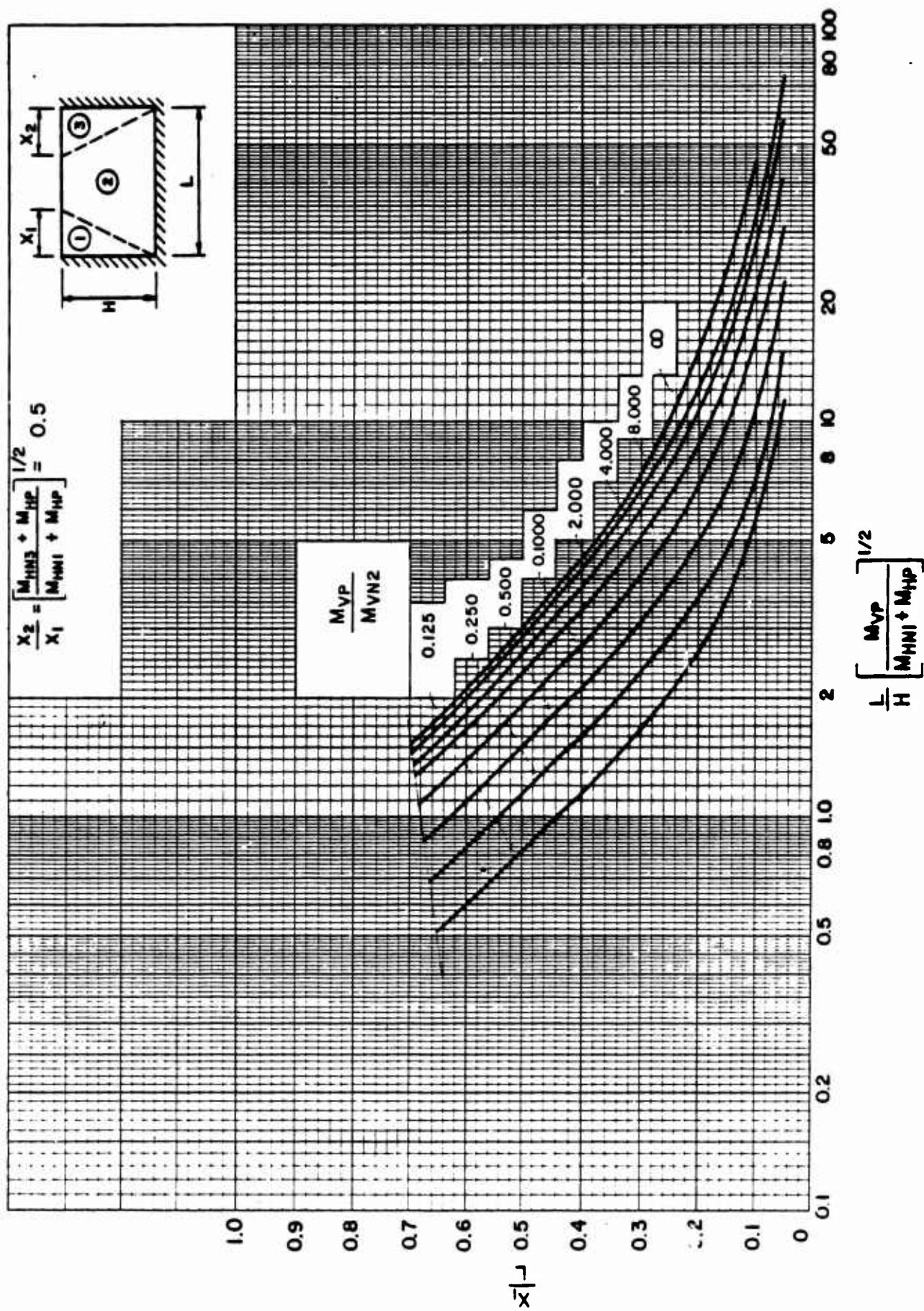
Figure 3-9   Location of unsymmetrical yield lines for two-way element with three edges supported and one edge free ($X_2/X_1 = 0.5$)

$$\frac{X_2}{X_1} = \left[\frac{M_{HN3} + M_{HP}}{M_{HN1} + M_{HP}}\right]^{1/2} = 0.5$$

$$\frac{L}{H}\left[\frac{M_{VP}}{M_{HN1} + M_{HP}}\right]^{1/2}$$

$$\frac{X_1}{L}$$

$$\frac{M_{VP}}{M_{VN2}}$$

0.125
0.250
0.500
0.1000
2.000
4.000
8.000
∞
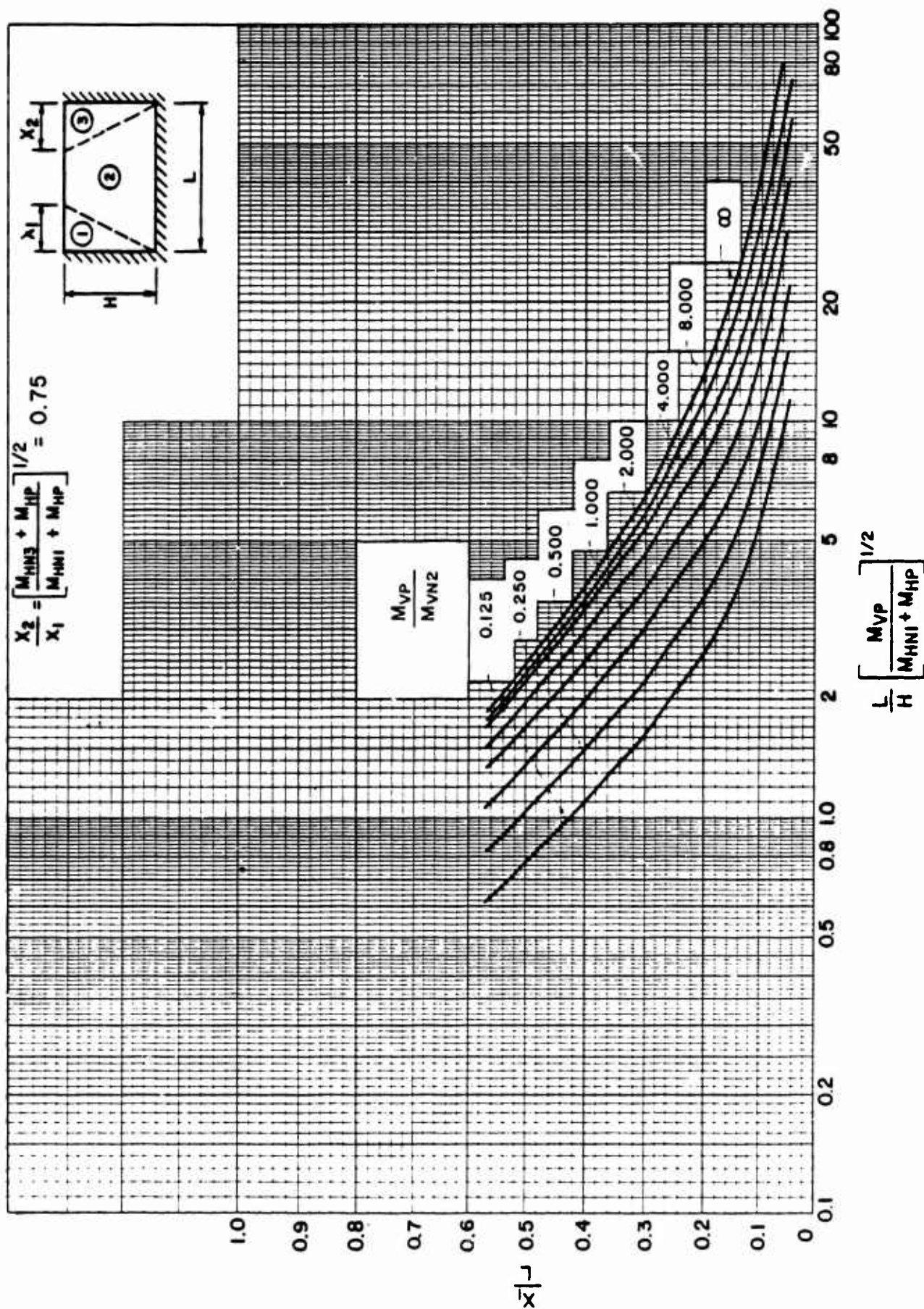
Figure 3-10   Location of unsymmetrical yield lines for two-way element with three edges supported and one edge free ($X_2/X_1 = 0.75$)
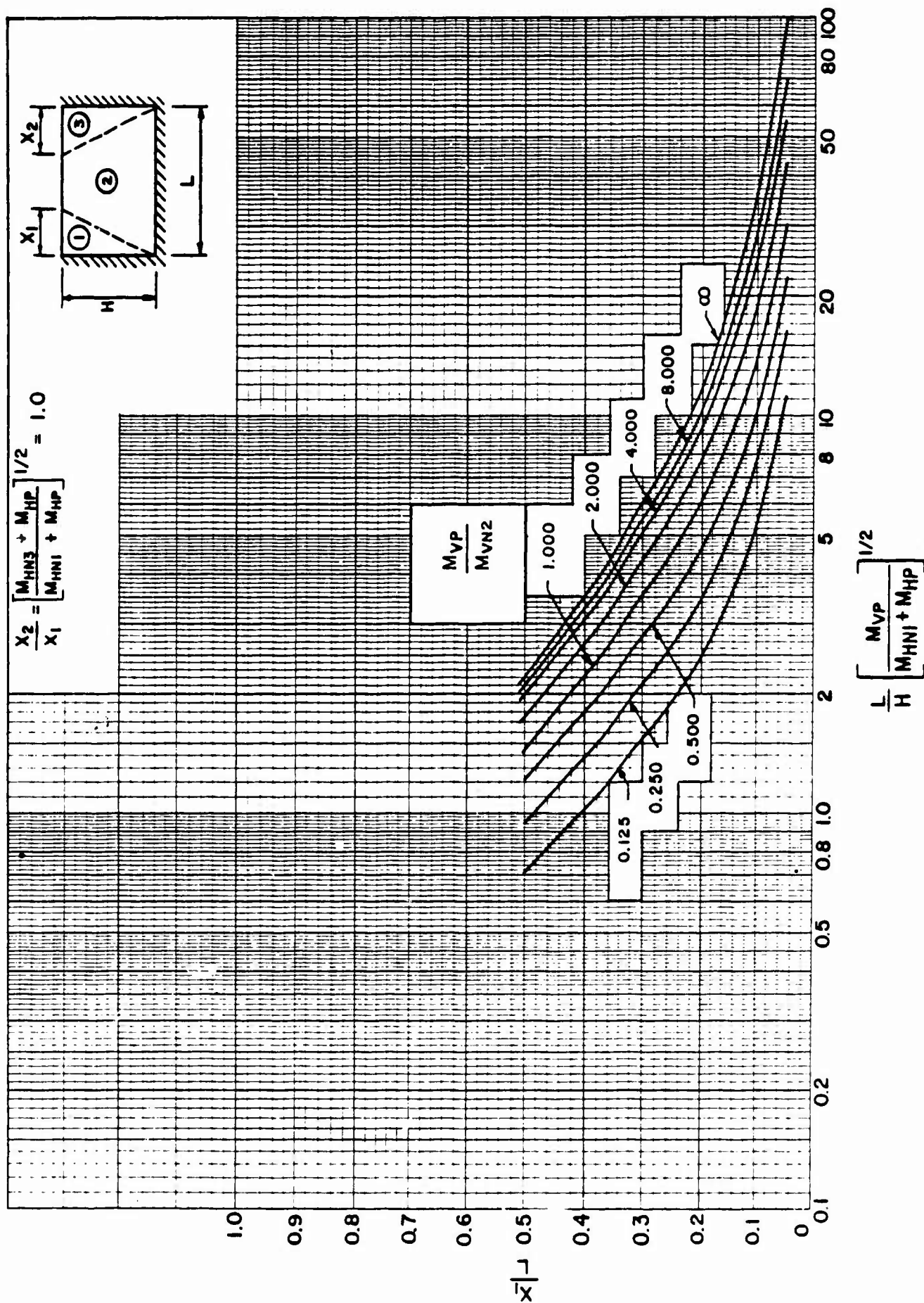
Figure 3-11   Location of unsymmetrical yield lines for two-way element with three edges supported and one edge free ($X_2/X_1 = 1.0$)
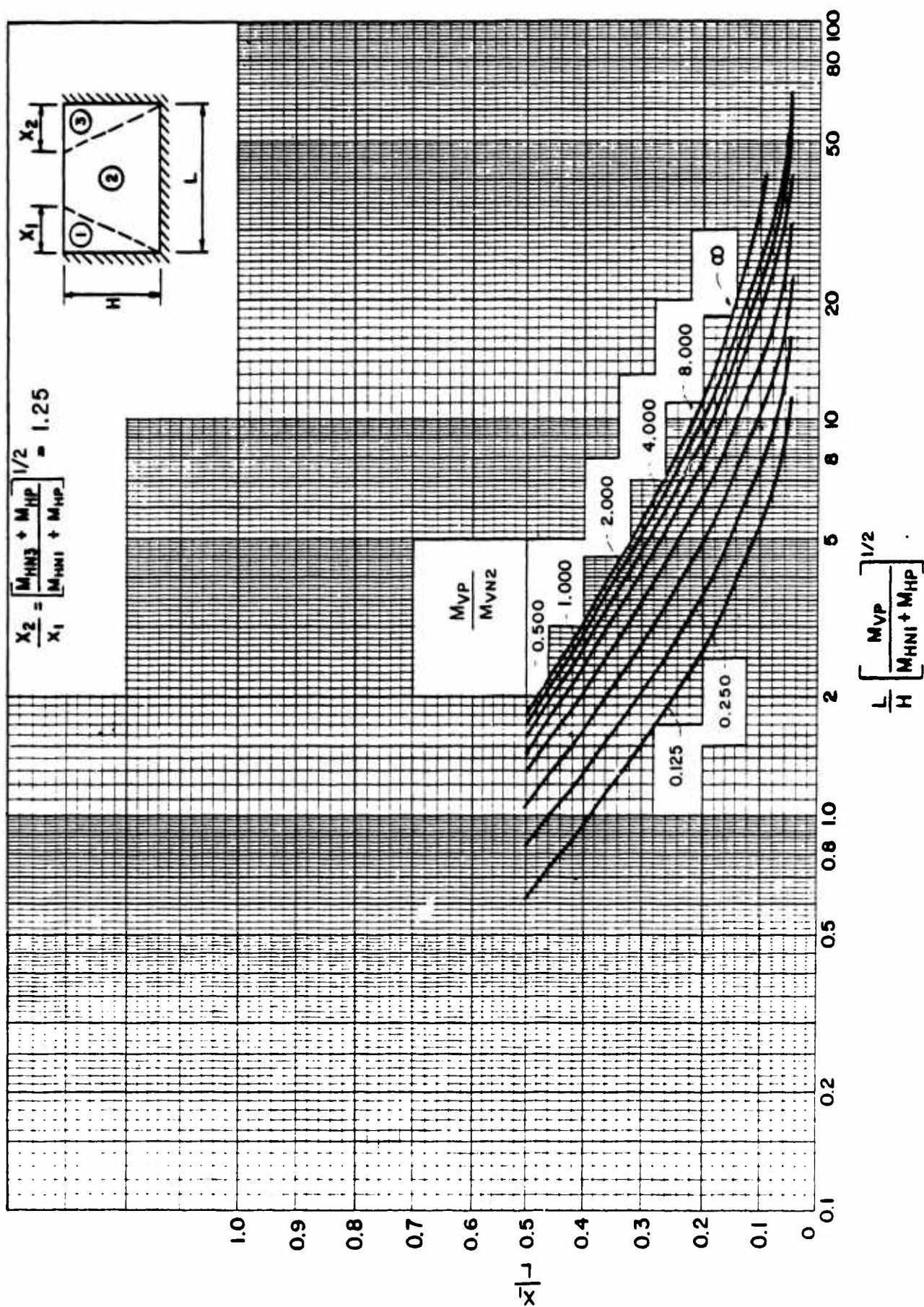
Figure 3-12   Location of unsymmetrical yield lines for two-way element with three edges supported and one edge free ($X_2/X_1=1.25$)
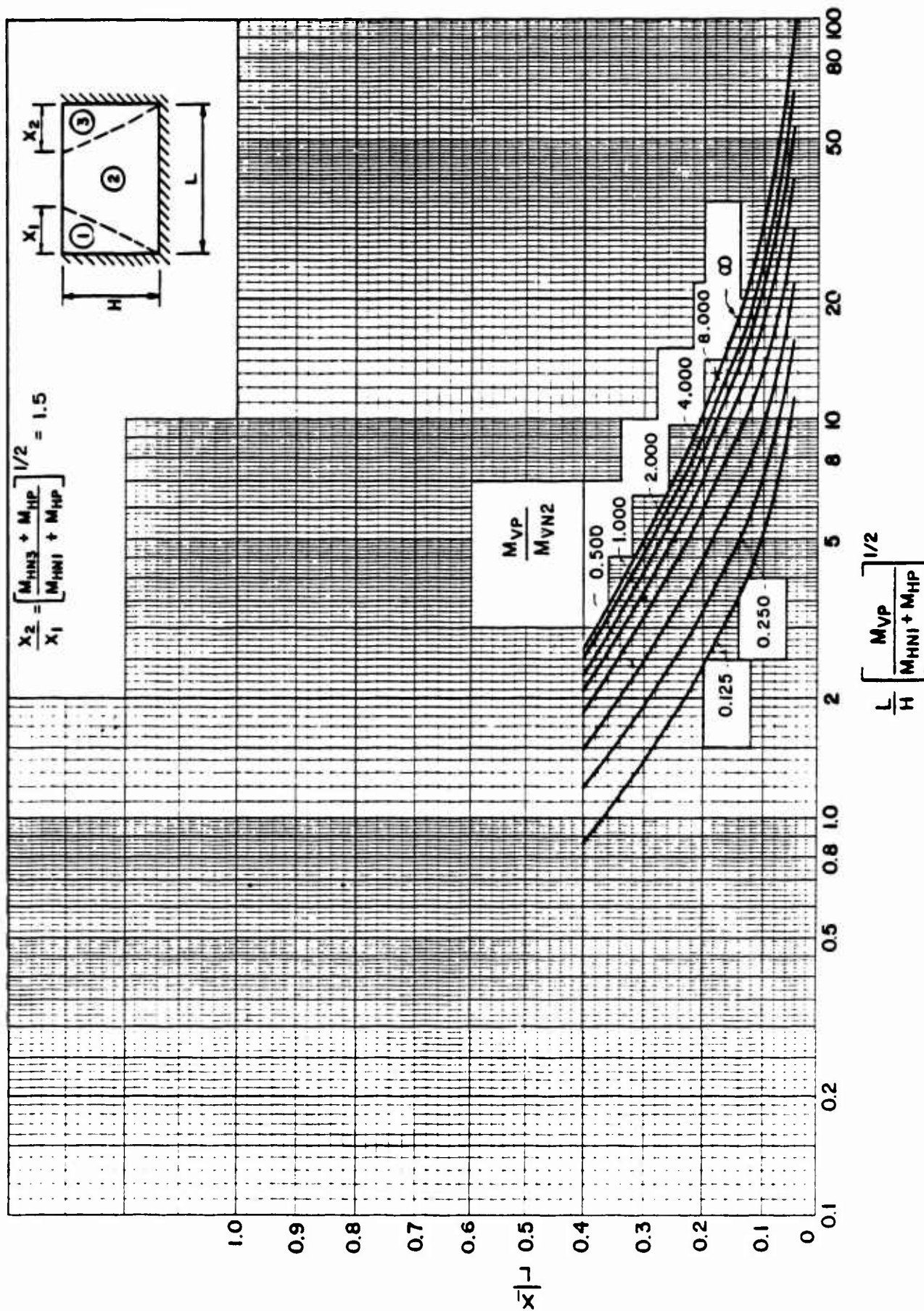
Figure 3-13   Location of unsymmetrical yield lines for two-way element with three edges supported and one edge free ($X_2/\ell_1 = 1.5$)
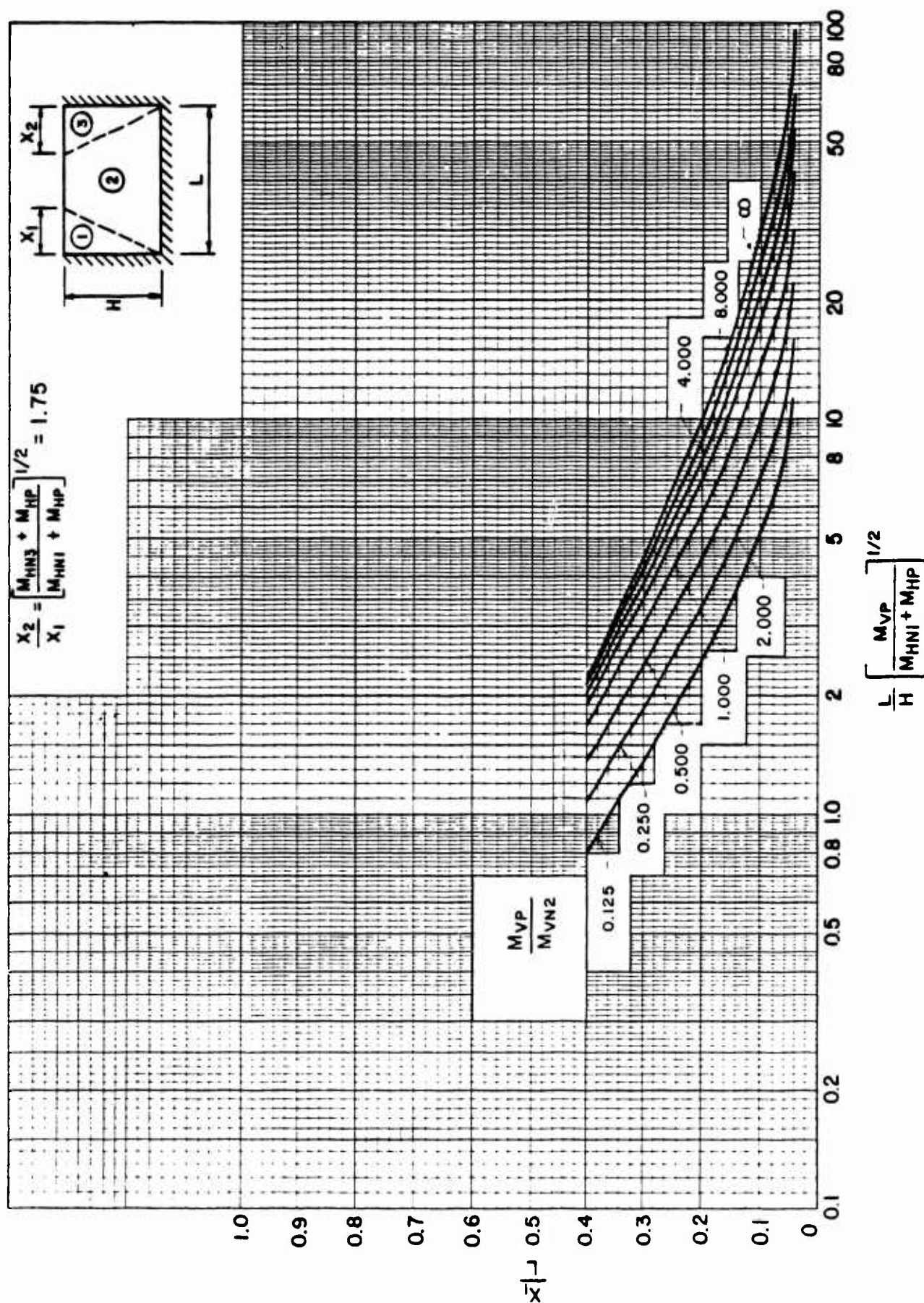
Figure 3-14   Location of unsymmetrical yield lines for two-way element with three edges supported and one edge free (X_2/X_1 = 1.75)
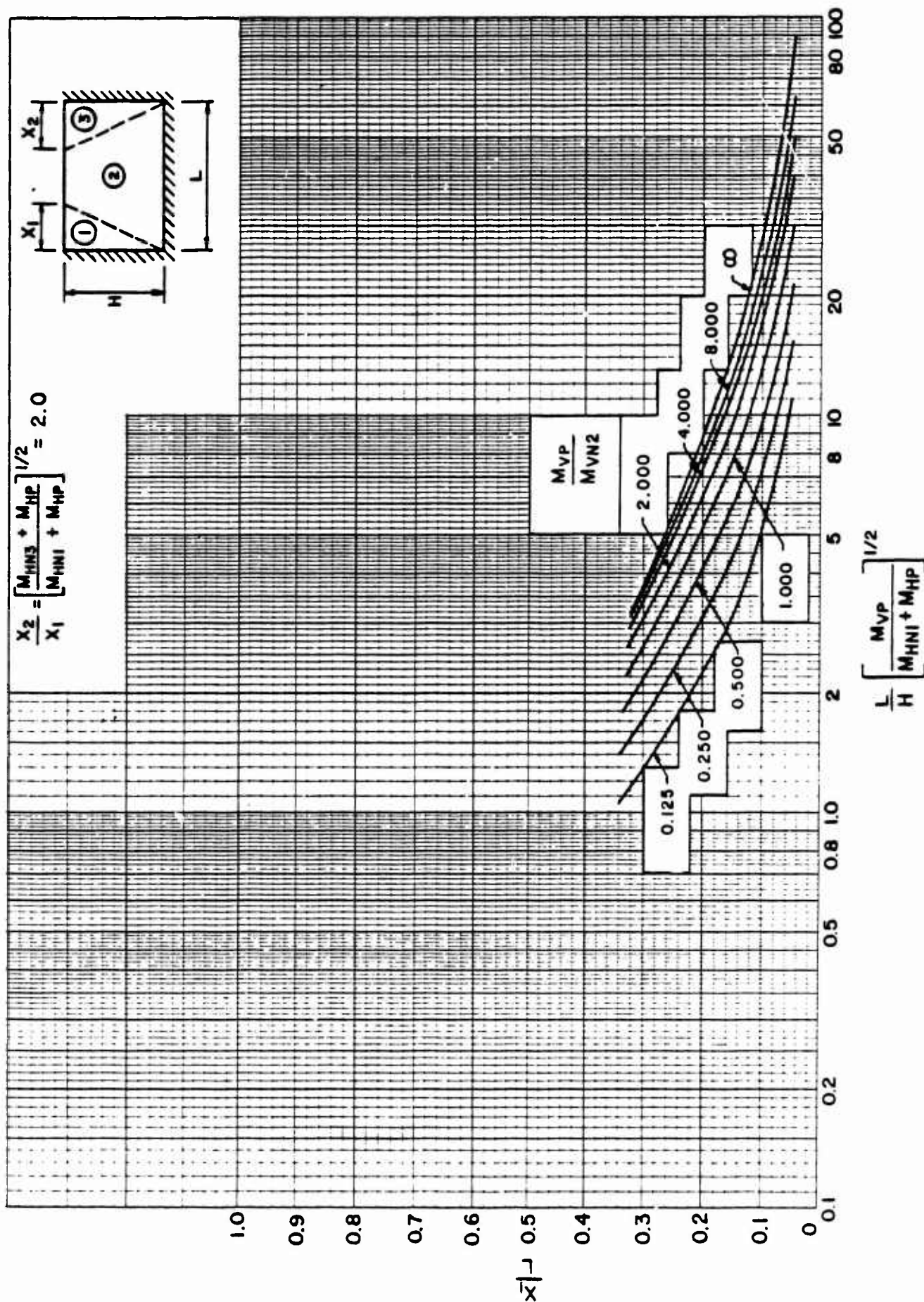
Figure 3-15   Location of unsymmetrical yield lines for two-way element with three edges supported and one edge free ($X_2/X_1 = 2.0$)
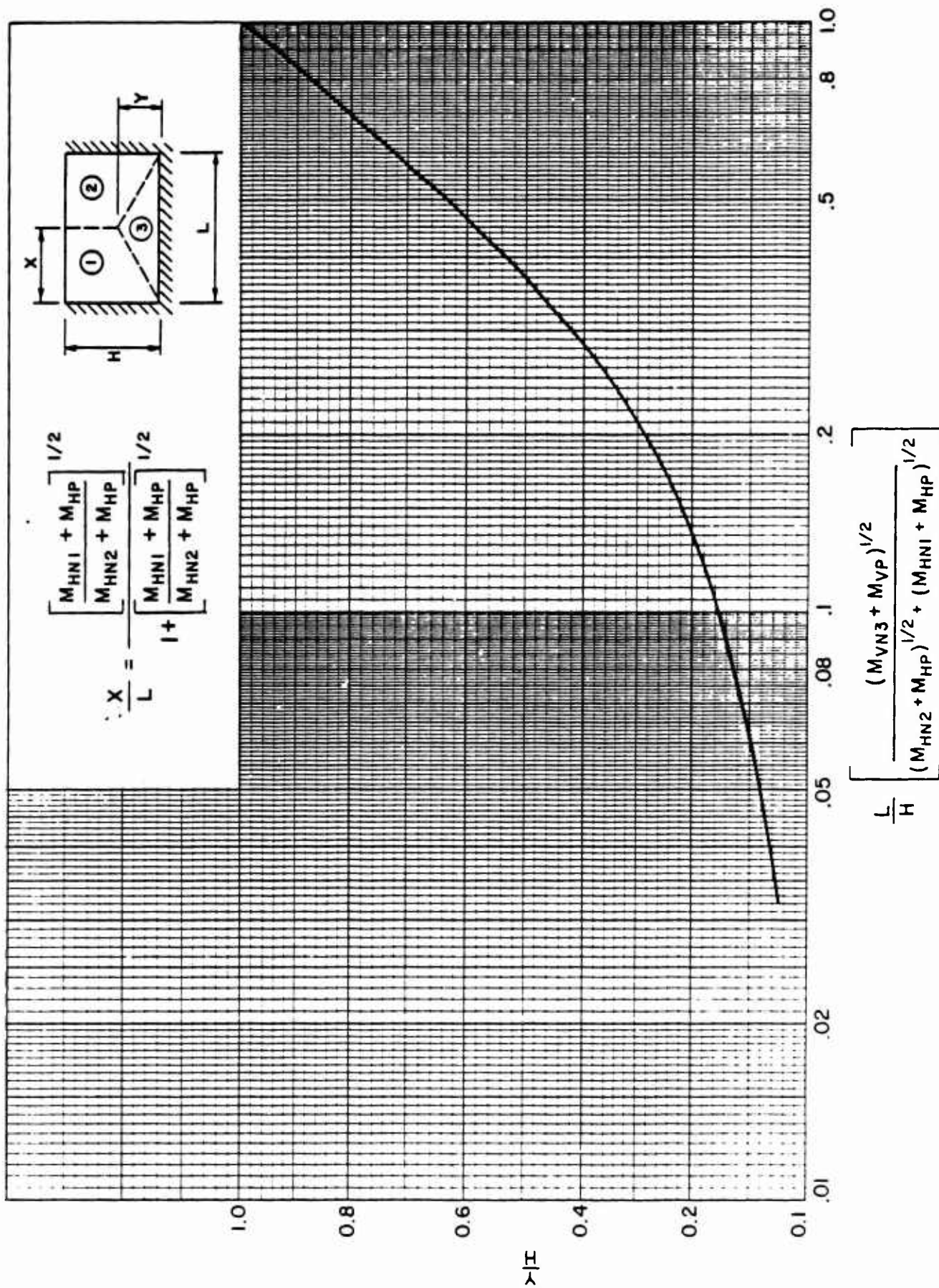
Figure 3-16   Location of unsymmetrical yield lines for two-way element with three edges
supported and one edge free (values of y)

$$\frac{X}{L} = \frac{\left[\dfrac{M_{HN1} + M_{HP}}{M_{HN2} + M_{HP}}\right]^{1/2}}{1 + \left[\dfrac{M_{HN1} + M_{HP}}{M_{HN2} + M_{HP}}\right]^{1/2}}$$

$$\frac{L}{H}\left[\frac{(M_{VN3} + M_{VP})^{1/2}}{(M_{HN2} + M_{HP})^{1/2} + (M_{HN1} + M_{HP})^{1/2}}\right]$$

$\frac{Y}{H}$

-31-
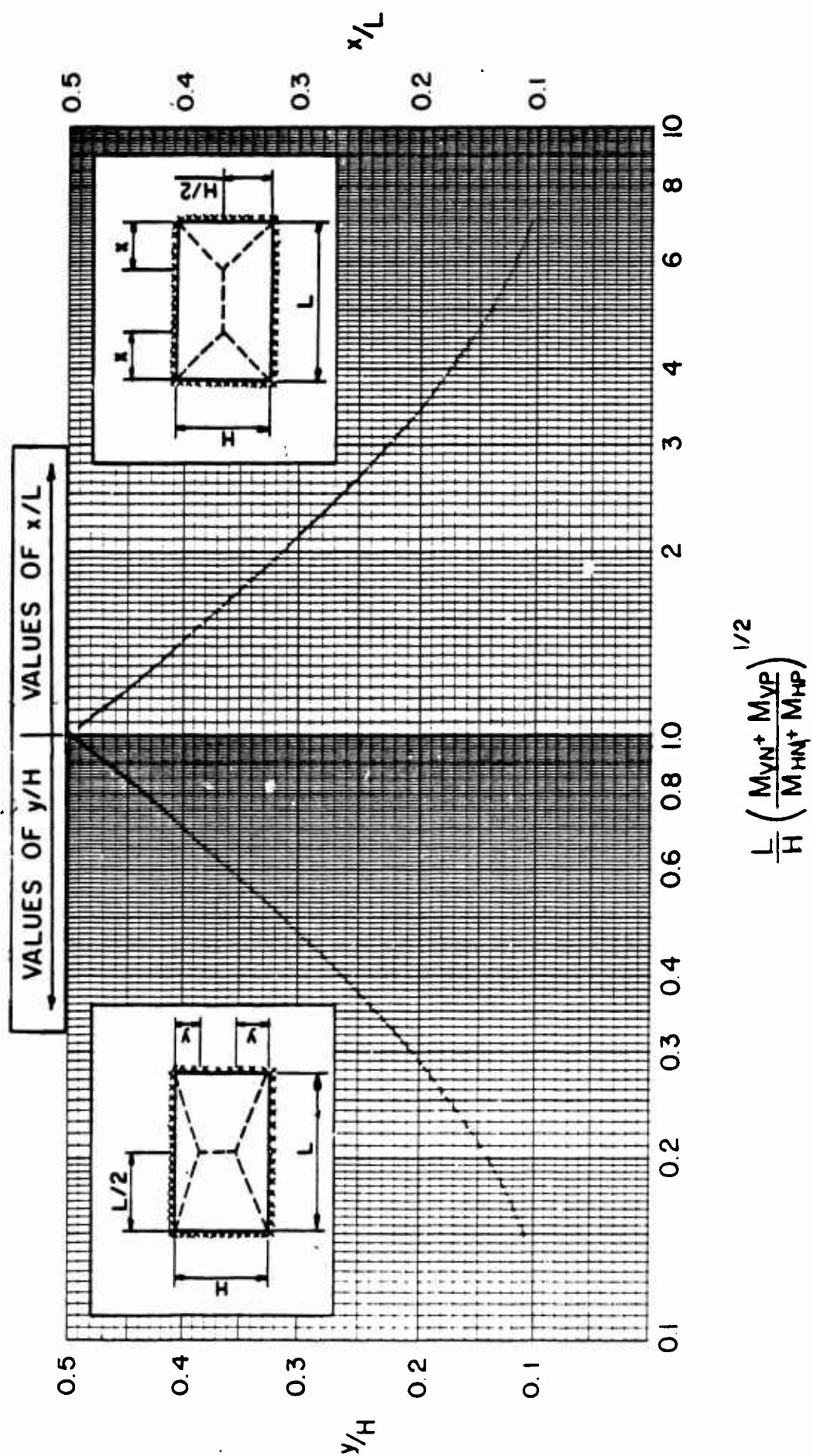
Figure 3-17   Location of symmetrical yield lines for two-way element with four edges supported
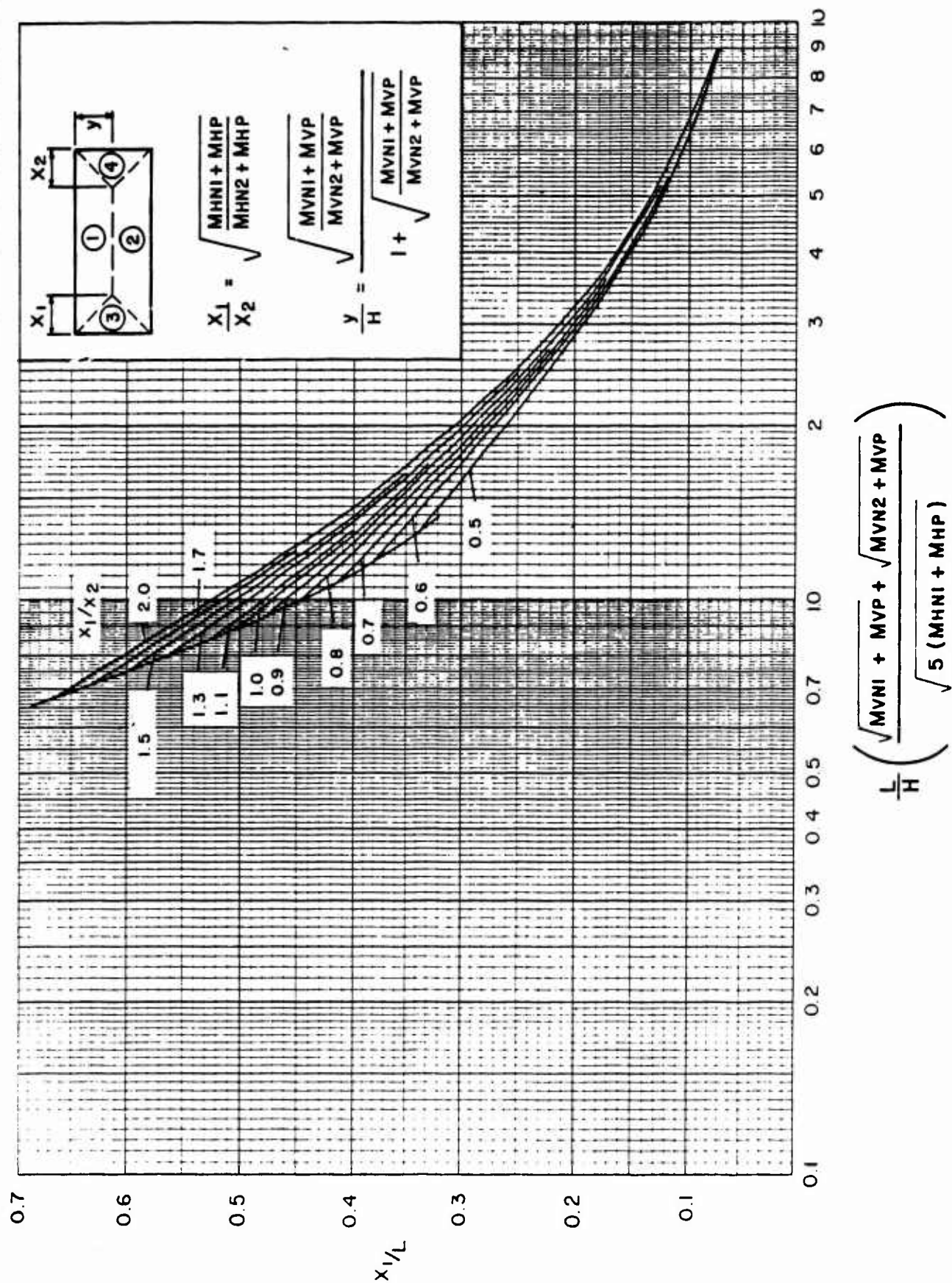
Figure 3-18   Location of unsymmetrical yield lines for two-way element with four edges supported (values of X_1)

-33-
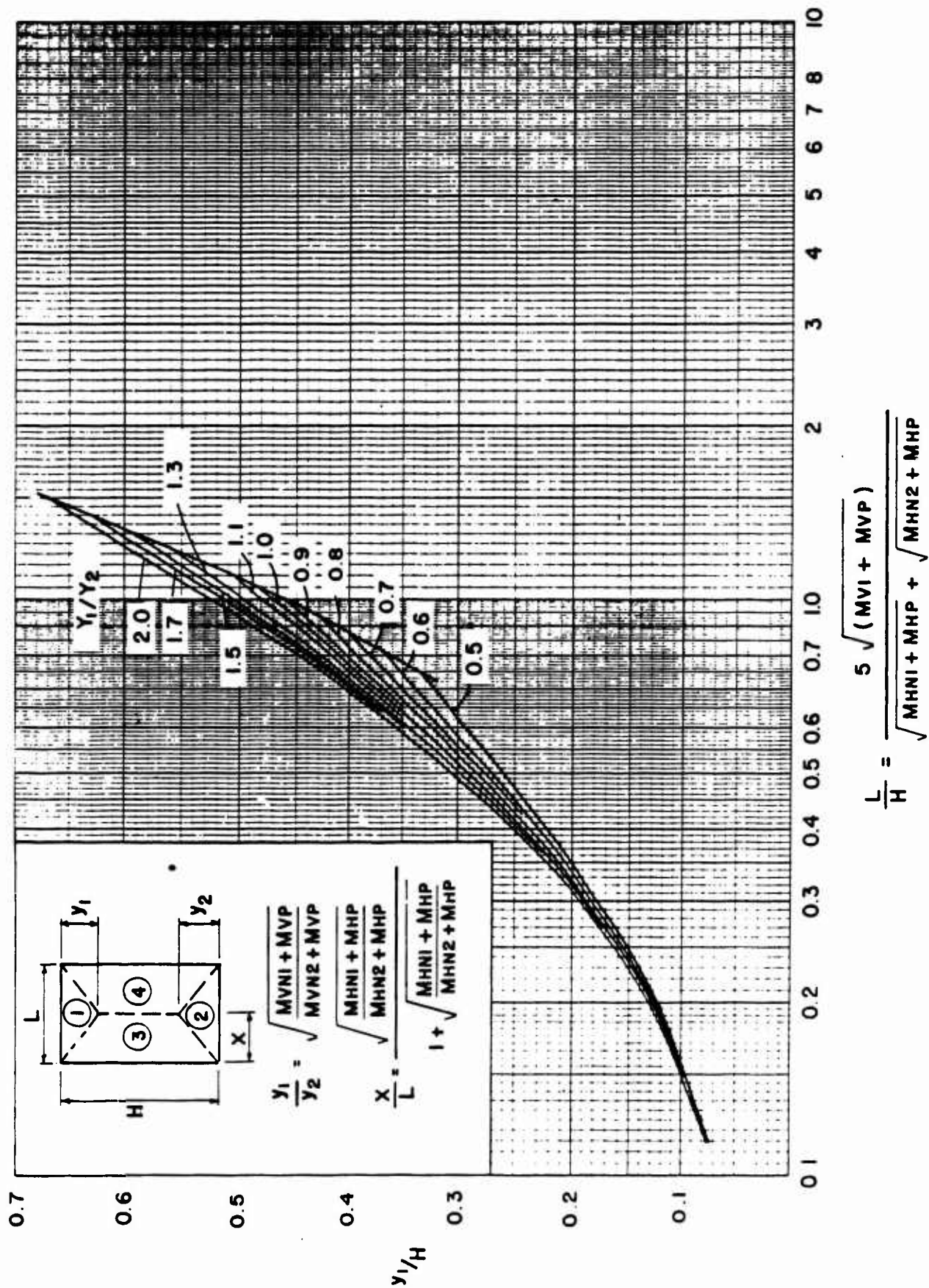
Figure 3-19   Location of unsymmetrical yield lines for two-way element with four edges supported (values of Y_1)
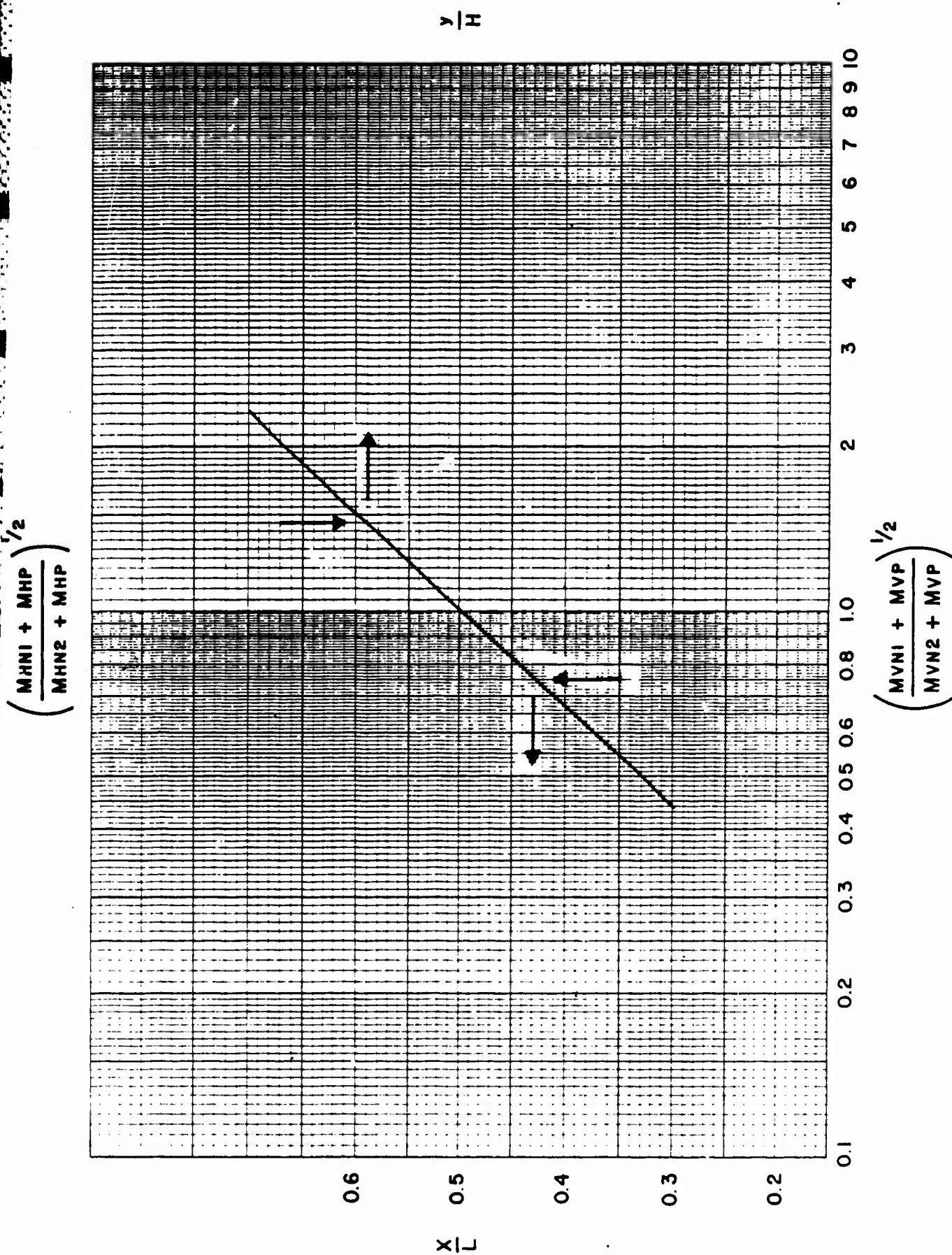
Figure 3-20   Location of unsymmetrical yield lines for two-way element with four edges
            supported (values of x/L and y/H)

Figure 3-17 covers the special case when opposite supports provide the same degree of restraint thus resulting in a symmetrical yield pattern. An example illustrating the use of some of these figures is provided in Appendix A.

3-9.4 *Openings in Two-Way Elements*

The use of openings in two-way elements, whether for access as a door opening or for visual communication as in the case of observation ports, is permissible with certain reservations. It is difficult to state exact rules concerning openings, but their effect on the design is generally a function of location, size and shape.

Small compact openings with approximate areas of less than 5 percent of the panel area and located away from regions of high stress can usually be ignored in the design. However, as in the case of conventional design, reinforcement at least equal to the amount interrupted should be placed adjacent to the opening. For example, in figure 3-21, the openings shown in (a) and (b) can be disregarded. If the opening in (b) were made more rectangular as in (c), then the design must be modified to account for the change in the yield lines and, hence, the change in the resistance. This change in resistance is a function of both the shape and the location of the opening.

Door openings invariably require special analysis because of their size. As depicted in (d), (e) and (f), figure 3-21, the presence of door openings causes gross relocations of the yield lines which generally propagate from the corners of the openings. Since the door also sustains the blast loading, concentrated line loads are present around the periphery of such openings. These concentrated loads must be included in the analysis since they change the resistance. As previously outlined for solid elements and for this case also, the yield line locations are assumed and each sector is individually analyzed. The presence of line loads modifies equation 3-3 to

$$\Sigma M_N + \Sigma M_p = r_u Ac + M_c \qquad\qquad 3\text{-}18$$

where M_c is the moment of the concentrated loads about the line of rotation of the sector being considered. Solution of elements with openings is most easily accomplished through a trial and error procedure by setting up the simultaneous equations for each sector and assuming various values of x and y until the several values of r_u agree to within a few percent.

3-10 Post-Ultimate Resistance

In general, the two-way elements described in this manual exhibit a post-ultimate resistance after initial failure occurs as indicated in figure 3-1. Prior to this partial failure, the element is spanning in two directions with a resistance equal to the ultimate resistance r_u. At a particular deflection, denoted as X_1, failure occurs along one side or two opposite sides, and the element then spans in one direction with the reduced post-ultimate unit resistance r_{up} until complete failure occurs at deflection X_u. One-way elements do not exhibit this behavior.

The location of the yield lines determines the presence or absence of this range. If the yield lines emanating from the corners of the elements bisect the 90-degree corner angle, then all supports fail simultaneously and there is

- 36 -
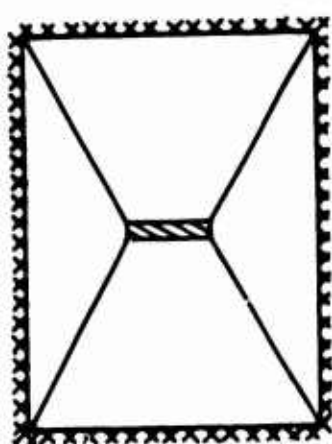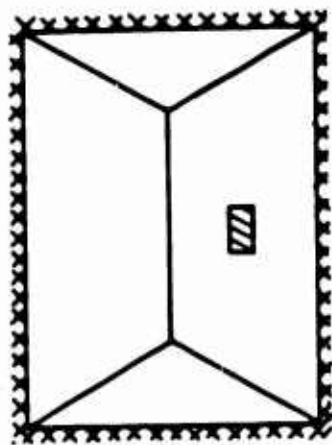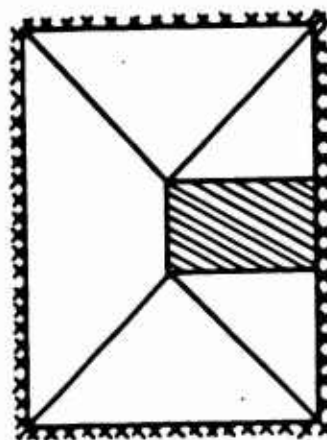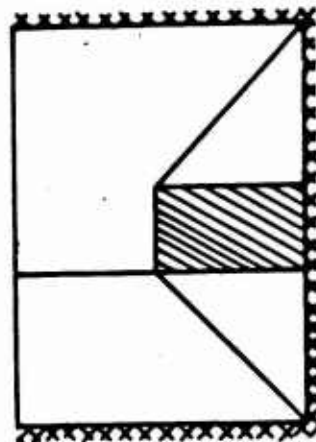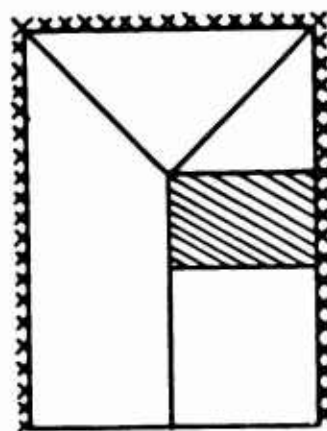
Figure 3-21   Effects of openings on yield lines locations

no post-ultimate range. As previously shown, the location of the yield lines for a particular element is a function of L/H and the ratio of the unit vertical to horizontal moment capacities. Post-ultimate resistances for two-way elements are shown in table 3-4.

3-11   Partial Failure and Ultimate Deflection

Partial failure deflection X_1, for two-way elements and ultimate deflections X_u for both one-way and two-way elements are a function of the angle of rotation of the element at its supports and the geometry of the sectors formed by the position yield lines.

Once the ultimate resistance r_u is reached (full moment capacity developed along the yield lines), the structural element becomes a mechanism which rotates with no further increase in either the moment or curvature between the hinges. For one-way elements, the rotation continues and the deflection increases until either the maximum deflection X_m is reached or failure occurs at θ max. The equations for the maximum deflection X_m in the range $0 < X_m < X_u$ for several one-way elements as a function of the rotation angle θ and the ultimate deflection X_u are given in table 3-5, when the values for X_u are based on the development of a maximum support rotation, θ max., prior to failure.

Actually, the maximum support rotation will vary with the material type and geometry of the element. The criteria for partial and incipient failure for concrete and structural steel elements can be found in Volumes IV and V respectively.

For two-way elements, the rotations of all the sectors must be considered in order to define the deflections of partial and incipient failure. Prior to partial failure $(0 < X_m < X_1)$, the maximum deflection is a function of the larger angle of rotation formed along either the vertical or horizontal supports. At deflection X_1, this larger angle equals θ max, and failure occurs along this support. Beyond this point, the element spans in one direction until the angle of rotation at the adjacent supports (in the direction opposite to that at which failure has already occured) reaches θ at which time total collapse occurs $(X_m = X_u)$.

To illustrate the above, consider a two-way element (fig. 3-22) which is fully restrained on four edges and whose positive yield lines are defined by $H/2 < x < L/2$ and $y = H/2$. Denoting θ_H as the angle of rotation in the horizontal direction (along vertical supports) and θ_V as the vertical angle of rotation (along horizontal supports), the maximum deflection X_m at the center of the element prior to reaching the deflection X_1 is

$$X_m = (H \tan \theta_V)/2 \qquad\qquad 3-19$$

and at the partial failure deflection X_1 where θ_V max

$$X_1 = (H \tan \theta_{max})/2 \qquad\qquad 3-20$$

Table 3-4   Post-Ultimate Unit Resistances for Two-Way Elements
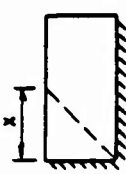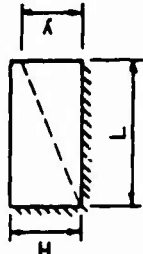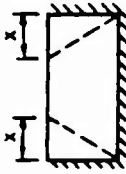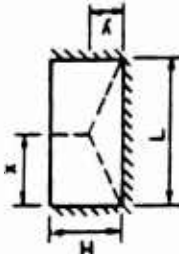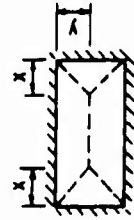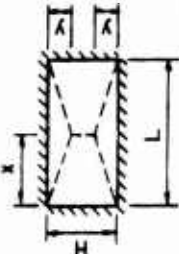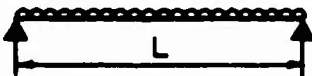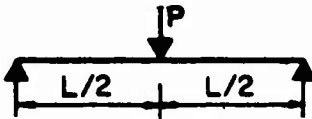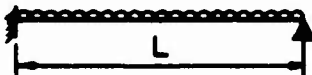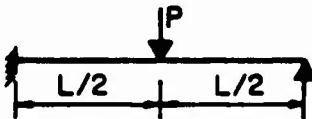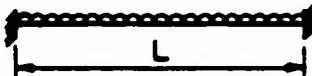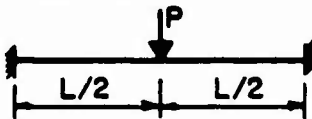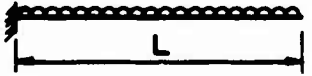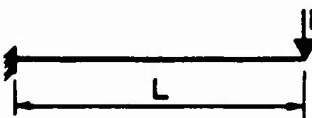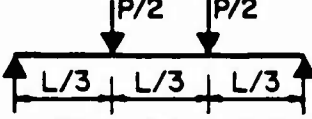
Edge Conditions	Yield Line Locations	Limits	Post – Ultimate Unit Resistance
Two adjacent edges supported and two edges free		$x < H$	$2\,M_{VN}/H^2$
		$x > H$	$2\,M_{HN}/L^2$
		$y < H$	$2\,M_{HN}/L^2$
		$y > L$	$2\,M_{VN}/H^2$
Three edges supported and one edge free		$x < H$	$2\,M_{VN}/H^2$
		$x > H$	$8\,(M_{HN}+M_{HP})/L^2$
		$y < L/2$	$8\,(M_{HN}+M_{HP})/L^2$
		$y > L/2$	$2\,M_{VN}/H^2$
Four edges supported		$x < H/2$	$8\,(M_{VN}+M_{VP})/H^2$
		$x > H/2$	$8\,(M_{HN}+M_{HP})/L^2$
		$y < L/2$	$8\,(M_{VN}+M_{VP})/H^2$
		$y > L/2$	$8\,(M_{HN}+M_{HP})/H^2$

Table 3-5   General and Ultimate Deflections for One-Way Elements

Edge Conditions and Loading Diagrams	Maximum Deflection, X_m	Ultimate Deflection, X_u
	$\dfrac{L}{2} \tan \theta$	$\dfrac{L}{2} \tan \theta \max$
	$(L/2) \tan \theta$	$(L/2) \tan \theta \max$
	$\dfrac{L}{2} \tan \theta$	$\dfrac{L}{2} \tan \theta \max$
	$(L/2) \tan \theta$	$(L/2) \tan \theta \max$
	$\dfrac{L}{2} \tan \theta$	$\dfrac{L}{2} \tan \theta \max$
	$(L/2) \tan \theta$	$(L/2) \tan \theta \max$
	$L \tan \theta$	$L \tan \theta \max$
	$L \tan \theta$	$L \tan \theta \max$
	$(L/3) \tan \theta$	$(L/3) \tan \theta \max$

-40-

ELEVATION

$$H/2 \leq x \leq L/2$$

$$y = H/2$$
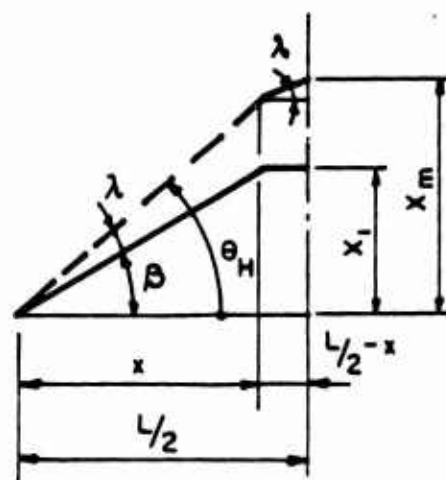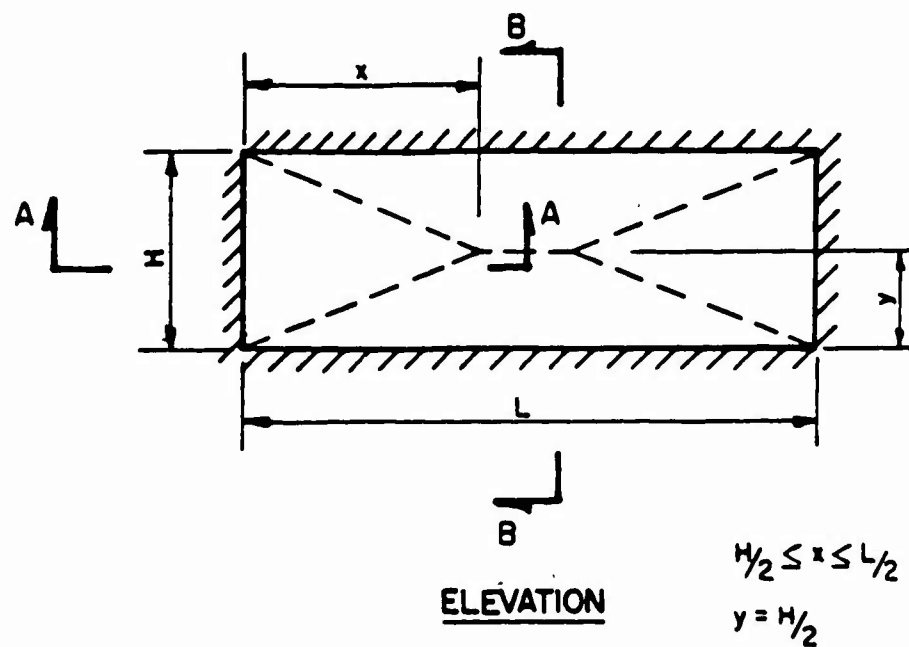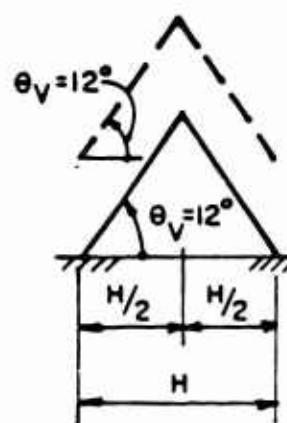
SECTION A-A   SECTION B-B

— PARTIAL FAILURE
--- INCIPIENT FAILURE

Figure 3-22   Deflection of two-way element

-41-

Referring to figure 3-22, the deflected shape at deflection X_1 is indicated by the solid line and θ_H has value β which is defined as

$$\beta = \tan^{-1}(X_1/x) = \tan^{-1}(H \tan \theta_{max}/2x) \qquad 3\text{-}21$$

As the element continues to deflect the angle of rotation θ_H increases, its magnitude becoming equal to

$$\theta_H = \lambda + \beta \qquad 3\text{-}22$$

where λ is the angular rotation in excess of β. For a two-way element which undergoes partial failure but does reach incipient failure, the maximum deflection in the range $X_1 \leq X_m \leq X_u$ becomes

$$X_m = x \tan \theta_H + [(L/2) - x] \tan (\theta_H - \beta) \qquad 3\text{-}23$$

When θ_H equal θ_{max}, the ultimate deflection X_u at incipient failure is

$$X_u = x \tan \theta_{max} + [(L/2 - x)] \tan [\theta_{max} - \tan^{-1}(H \tan \theta_{max}/2x)]$$

$$3\text{-}24$$

Equations 3-19 through 3-24 are specifically for two-way elements described in figure 3-2 and will vary for other two-way elements with different material properties and geometry.

The maximum deflection X_m for several two-way elements in the ranges $0 \leq X_m \leq X_1$, and $X_1 \leq X_m \leq X_u$ as a function of the rotation angles θ_H and θ_v are given in table 3-6 along with the values of partial failure (X_1) and ultimate (X_u) deflections. The support which fails at partial deflection X_1 is also indicated.

3-12 Elasto-Plastic Resistance

As stated in Section 3-8, the initial portion of the resistance function (fig. 3-1) generally is composed of an elastic and one or more elasto-plastic ranges. The elastic unit resistance r_e is defined as the resistance at which first yield occurs; similarly, the elasto-plastic unit resistance r_{ep} is the resistance at which second yields subsequently occur. Where all hinges form in a member at one time, r_e will be equal to the ultimate unit resistance r_u; where two or more hinges are formed at separate times, the maximum value of r_{ep} will be equal to r_u (depending upon the hinges formed, one or more values of r_{ep} may exist).
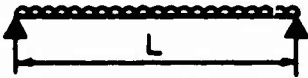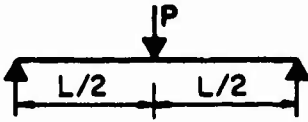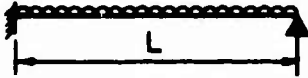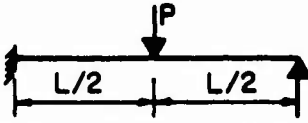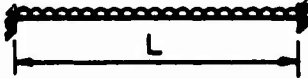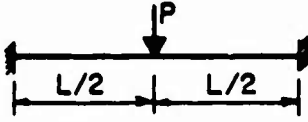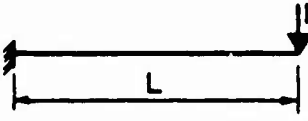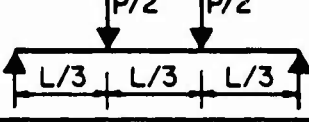
These resistances for one-way elements are listed in table 3-7. In those cases where the elasto-plastic resistance is equal to the ultimate resistance, the value can be determined from table 3-1.

The determination of the elasto-plastic resistances of two-way elements is more complicated than that for one-way elements, since the resistance varies with the span ratio and, in the case of reinforced concrete elements, with the placement of the reinforcement. Data for calculating the resistances of two-way elements during the elasto-plastic ranges (graphically summarized in Figure 3-23) are presented in figures 3-24 through 3-38.

Table 3-6   General, Partial Failure, and Ultimate Deflections for Two-Way Elements

Edge Conditions	Yield Line Location	Limits	Maximum Deflection, X_m ($0 < X_m < X_i$)	Maximum Deflection, X_m ($X_i < X_m < X_u$)	Partial Failure Deflection X_i	Ultimate Deflection, X_u	Support Failing at Deflection X_i
Two adjacent edges supported and two edges free	(diagram)	$x \leq H$	$x\tan\theta_H$	$H\tan\theta_V$	$x\tan\theta_{max}$	$h\tan\theta_{max}$	H
		$x \geq H$	$H\tan\theta_V$	$x\tan\theta_H + (L-x)\tan\left[\theta_H - \tan^{-1}\left(\frac{\tan\theta_V}{x/H}\right)\right]$	$H\tan\theta_{max}$	$x\tan\theta_{max} + (L-x)\tan\left[\theta_{max} - \tan^{-1}\left(\frac{\tan\theta_{max}}{x/H}\right)\right]$	L
	(diagram)	$y \leq L$	$y\tan\theta_V$	$L\tan\theta_H$	$y\tan\theta_{max}$	$L\tan\theta_{max}$	L
		$y \geq L$	$L\tan\theta_H$	$y\tan\theta_V + (H-y)\tan\left[\theta_V - \tan^{-1}\left(\frac{\tan\theta_H}{y/L}\right)\right]$	$L\tan\theta_{max}$	$y\tan\theta_{max} + (H-y)\tan\left[\theta_{max} - \tan^{-1}\left(\frac{\tan\theta_{max}}{y/L}\right)\right]$	H
Three edges supported and one edge free	(diagram)	$x \leq H$	$x\tan\theta_V$	$H\tan\theta_V$	$x\tan\theta_{max}$	$H\tan\theta_{max}$	H
		$x \geq H$	$H\tan\theta_V$	$x\tan\theta_H + \left(\frac{L}{2}-x\right)\tan\left[\theta_H - \tan^{-1}\left(\frac{\tan\theta_V}{x/H}\right)\right]$	$H\tan\theta_{max}$	$x\tan\theta_{max} + \left(\frac{L}{2}-x\right)\tan\left[\theta_{max} - \tan^{-1}\left(\frac{\tan\theta_{max}}{H}\right)\right]$	L
	(diagram)	$y \leq \frac{L}{2}$	$y\tan\theta_V$	$\frac{L\tan\theta_H}{2}$	$y\tan\theta_{max}$	$\frac{L\tan\theta_{max}}{2}$	L
		$y \geq \frac{L}{2}$	$\frac{L\tan\theta_H}{2}$	$y\tan\theta_V + (H-y)\tan\left[\theta_V - \tan^{-1}\left(\frac{\tan\theta_H}{2y/L}\right)\right]$	$\frac{L\tan\theta_{max}}{2}$	$y\tan\theta_{max} + (H-y)\tan\left[\theta_{max} - \tan^{-1}\left(\frac{\tan\theta_{max}}{2y/L}\right)\right]$	H
Four edges supported	(diagram)	$x \leq \frac{H}{2}$	$x\tan\theta_H$	$\frac{H\tan\theta_V}{2}$	$x\tan\theta_{max}$	$\frac{H\tan\theta_{max}}{2}$	H
		$x \geq \frac{H}{2}$	$\frac{H\tan\theta_V}{2}$	$x\tan\theta_H + \left(\frac{L}{2}-x\right)\tan\left[\theta_H - \tan^{-1}\left(\frac{\tan\theta_V}{2x/H}\right)\right]$	$\frac{H\tan\theta_{max}}{2}$	$x\tan\theta_{max} + \left(\frac{L}{2}-x\right)\tan\left[\theta_{max} - \tan^{-1}\left(\frac{\tan\theta_{max}}{2x/H}\right)\right]$	L
	(diagram)	$y \leq \frac{L}{2}$	$y\tan\theta_V$	$\frac{L\tan\theta_H}{2}$	$y\tan\theta_{max}$	$\frac{L\tan\theta_{max}}{2}$	L
		$y \geq \frac{L}{2}$	$\frac{L\tan\theta_H}{2}$	$y\tan\theta_V + \left(\frac{H}{2}-y\right)\tan\left[\theta_V - \tan^{-1}\left(\frac{\tan\theta_H}{2y/L}\right)\right]$	$\frac{L\tan\theta_{max}}{2}$	$y\tan\theta_{max} + \left(\frac{H}{2}-y\right)\tan\left[\theta_{max} - \tan^{-1}\left(\frac{\tan\theta_{max}}{2y/L}\right)\right]$	H

Table 3-7 Elastic and Elasto-Plastic Unit Resistances for One-Way Elements.

Edge Conditions and Loading Diagrams	Elastic Resistance, r_e	Elasto - Plastic Resistance, r_{ep}
	r_u	—
	R_u	—
	$\dfrac{8M_N}{L^2}$	r_u
	$\dfrac{16M_N}{3L}$	R_u
	$\dfrac{12M_N}{L^2}$	r_u
	$\dfrac{8M_N}{L}$	R_u
	r_u	—
	R_u	—
	R_u	—
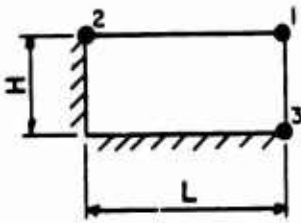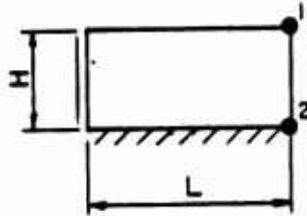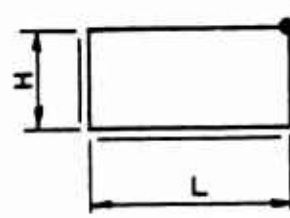
FIG. 3-24   FIG. 3-25   FIG. 3-26
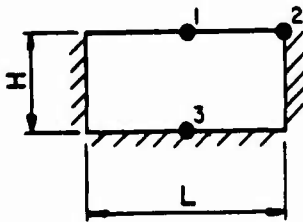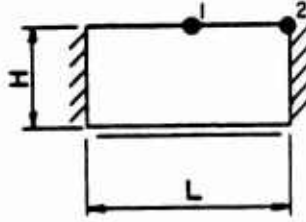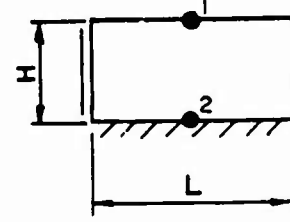
FIG. 3-27   FIG. 3-28   FIG. 3-29
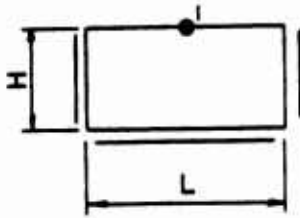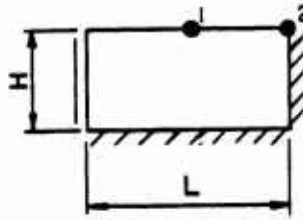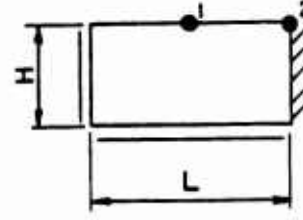
FIG. 3-30   FIG. 3-31   FIG. 3-32
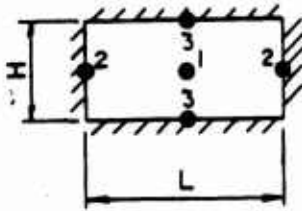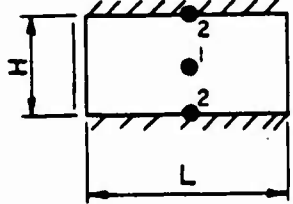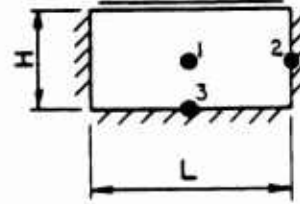
FIG. 3-33   FIG. 3-34   FIG. 3-35
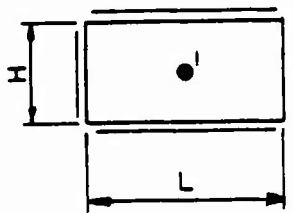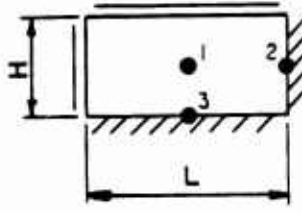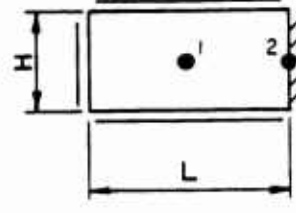
FIG. 3-36   FIG. 3-37   FIG. 3-38

LEGEND: EDGE CONDITIONS

FREE   SIMPLE   FIXED
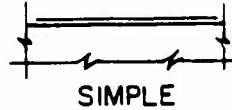
Figure 3-23   Graphical summary of two-way elements

-45-
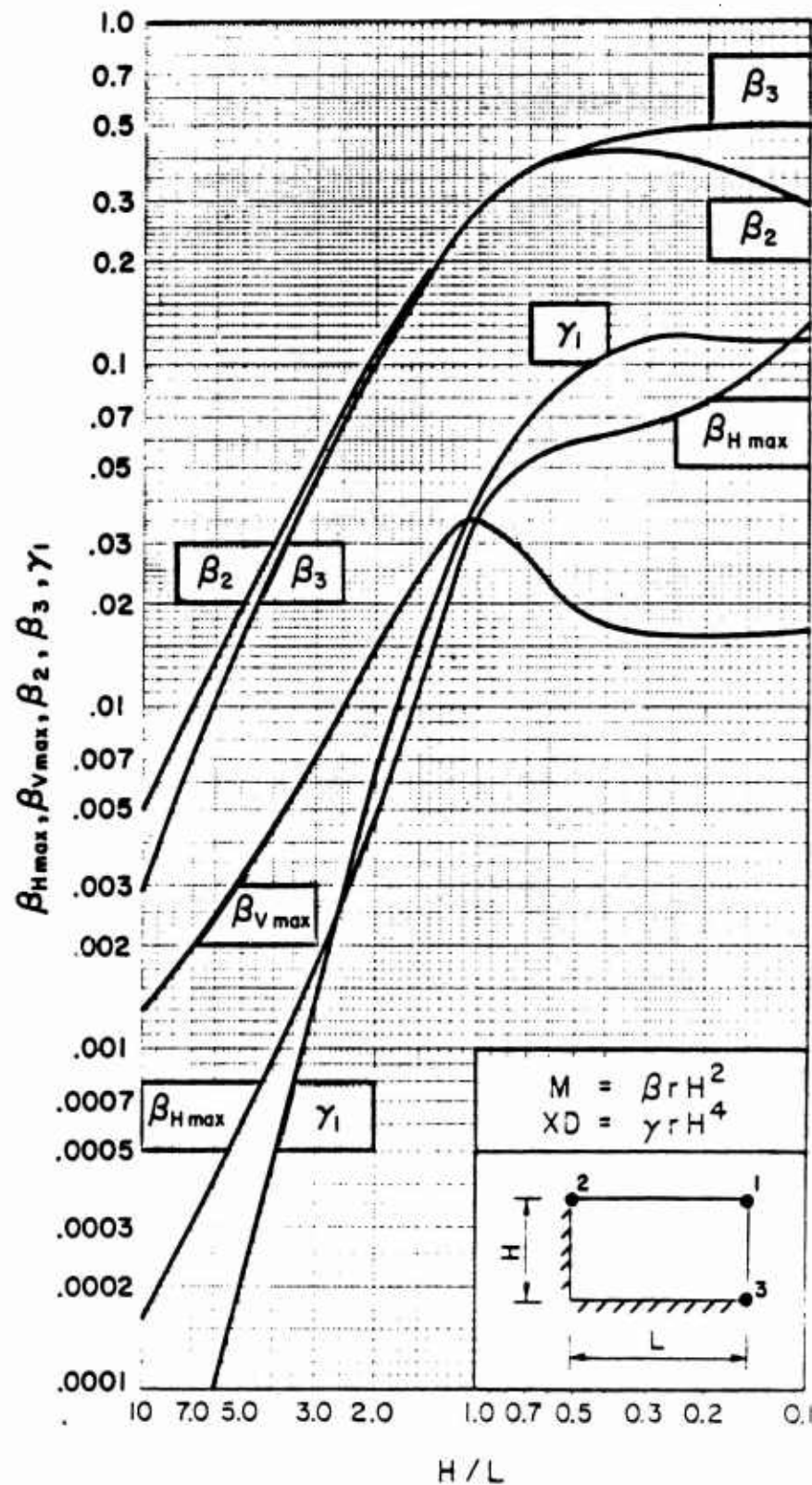
Figure 3-24 Moment and deflection coefficients for uniformly-loaded, two-way element with two adjacent edges fixed and two edges free
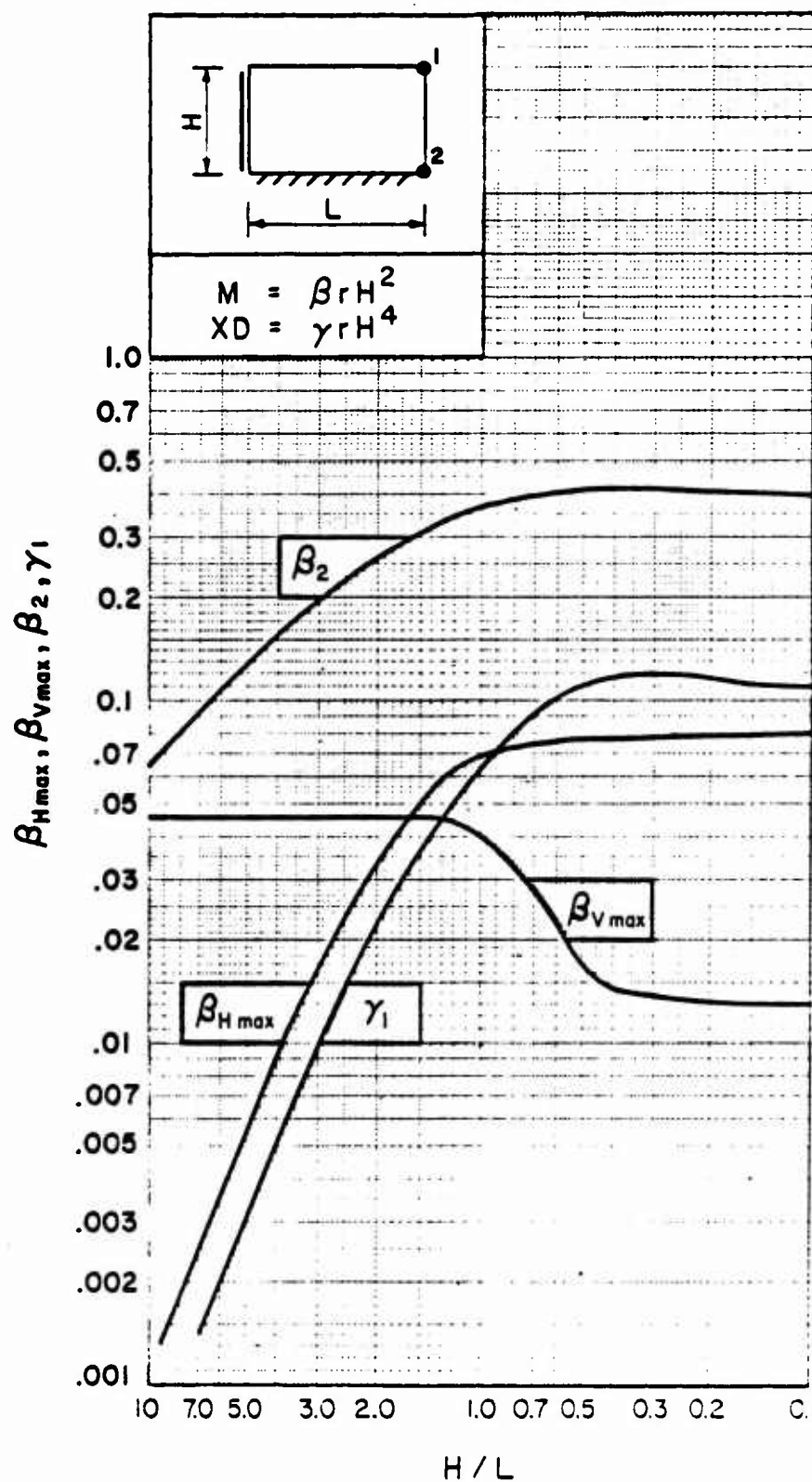
Figure 3-25   Moment and deflection coefficients for uniformly-loaded, two-way element with one edge fixed, an adjacent edge simply-supported and two edges free
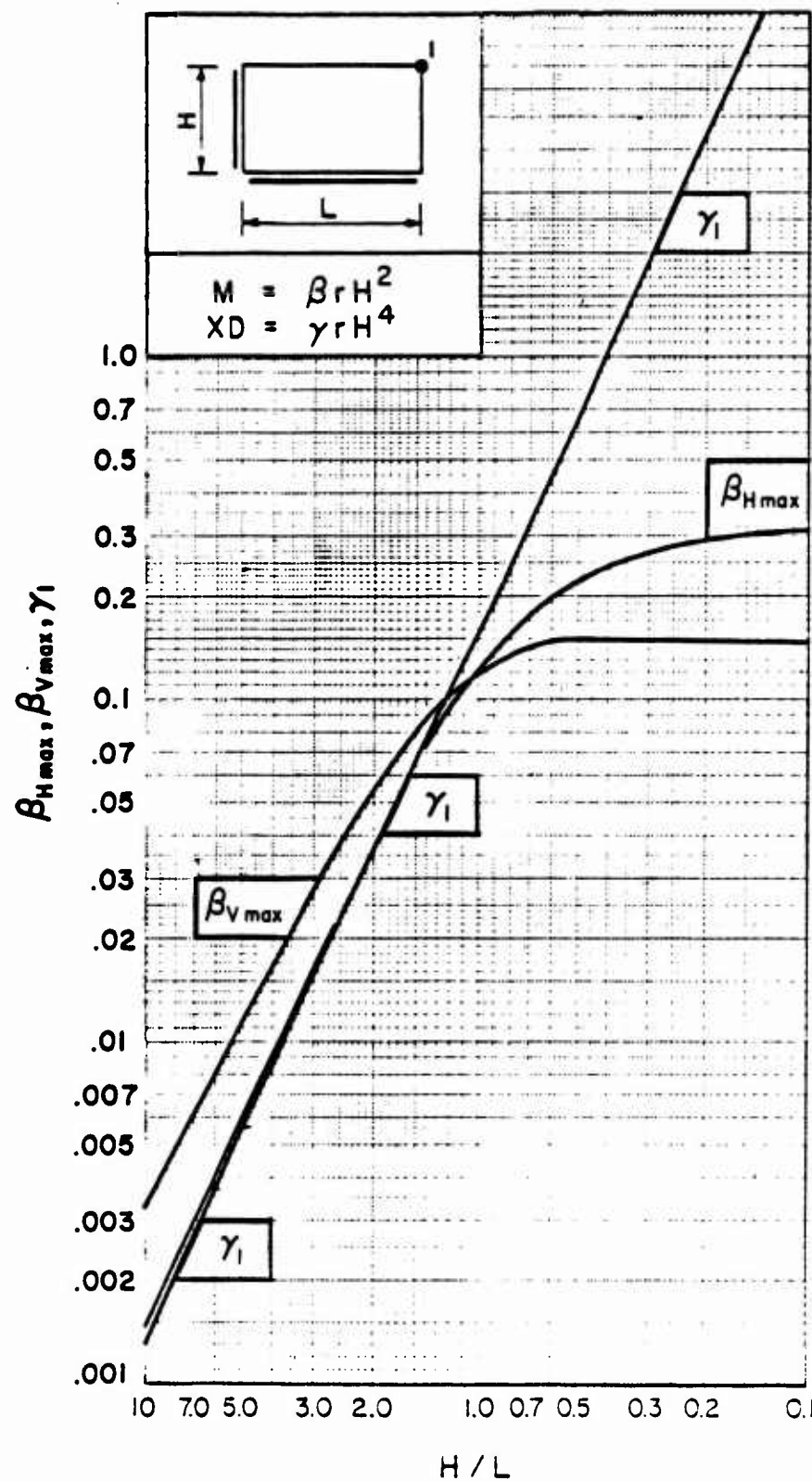
Figure 3-26   Moment and deflection coefficients for uniformly-loaded, two-way element with two adjacent edges simply-supported and two edges free
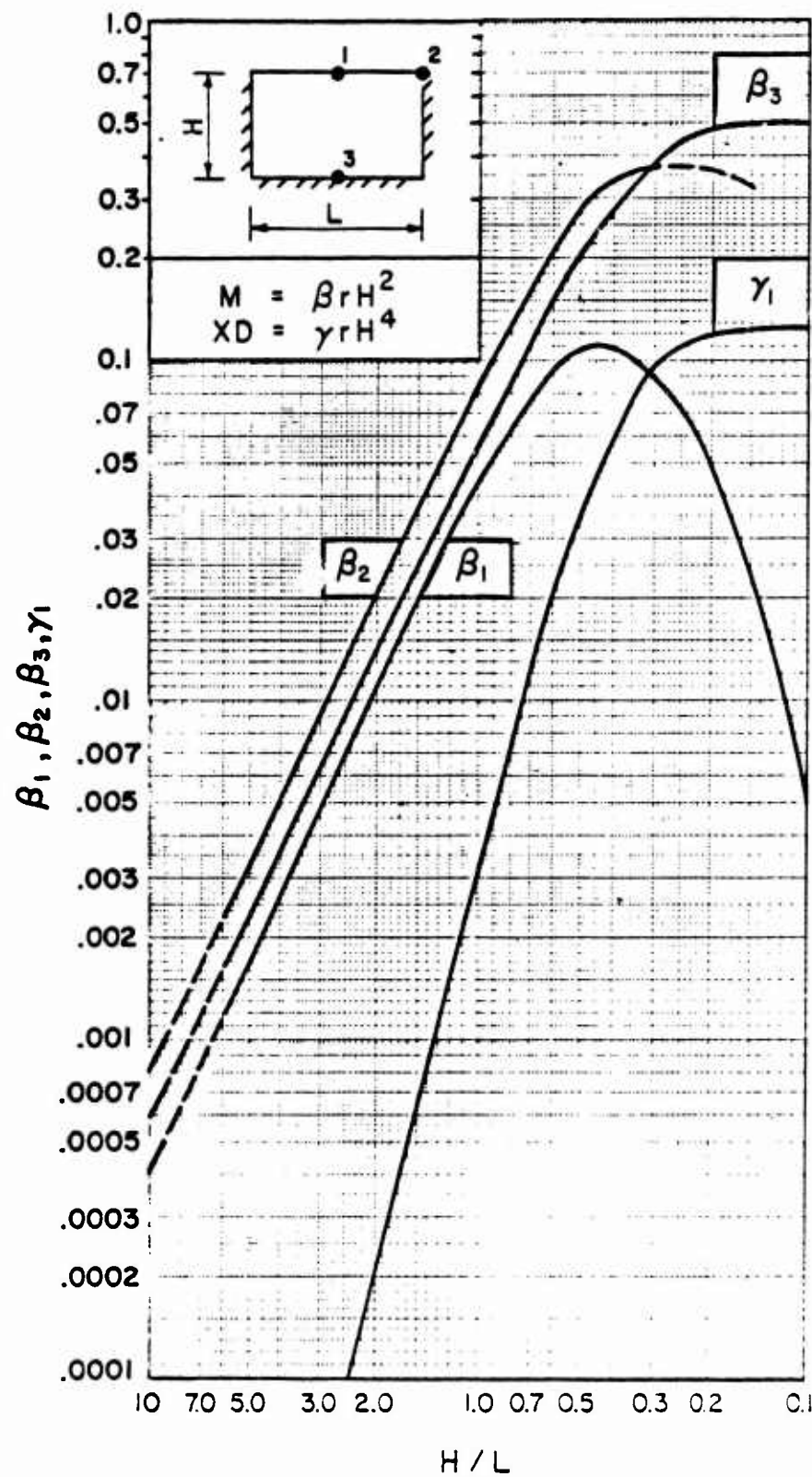
Figure 3-27   Moment and deflection coefficients for uniformly-loaded, two-way element with three edges fixed and one edge free
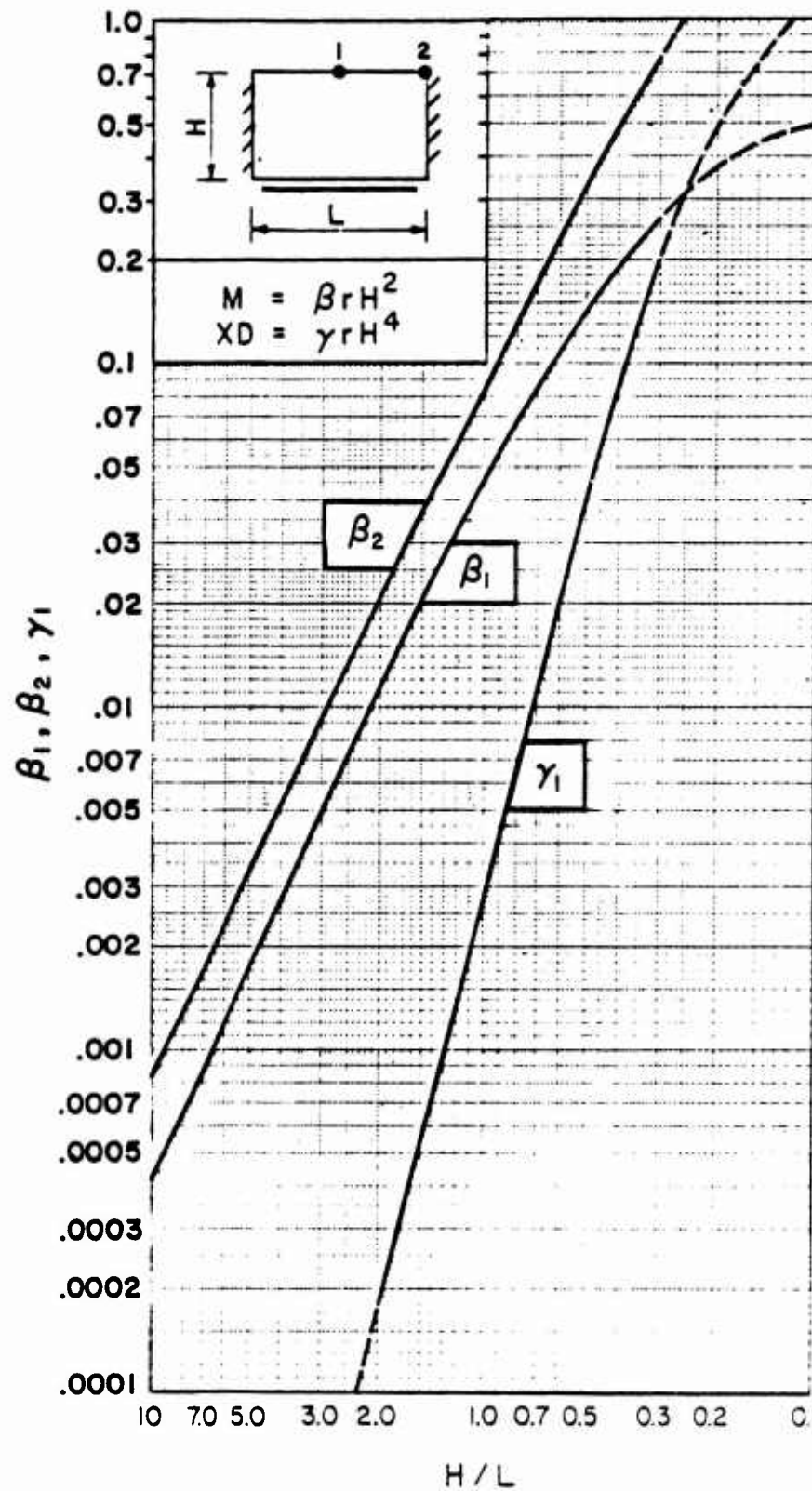
Figure 3-28   Moment and deflection coefficients for uniformly-loaded, two-way element with two opposite edges fixed, one edge simply-supported and one edge free
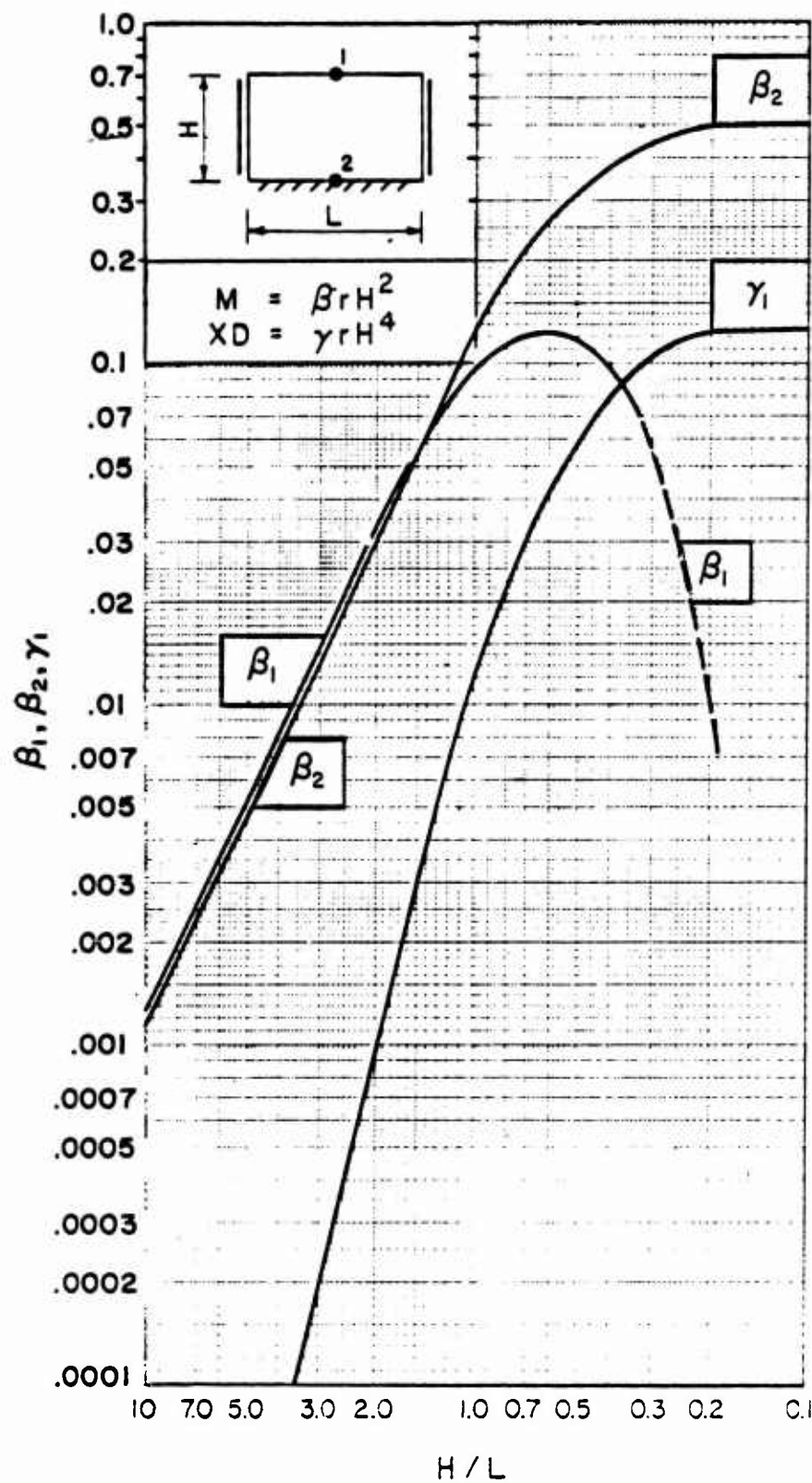
Figure 3-29   Moment and deflection coefficients for uniformly-loaded,
two-way element with two opposite edges simply-supported,
one edge fixed, and one edge free
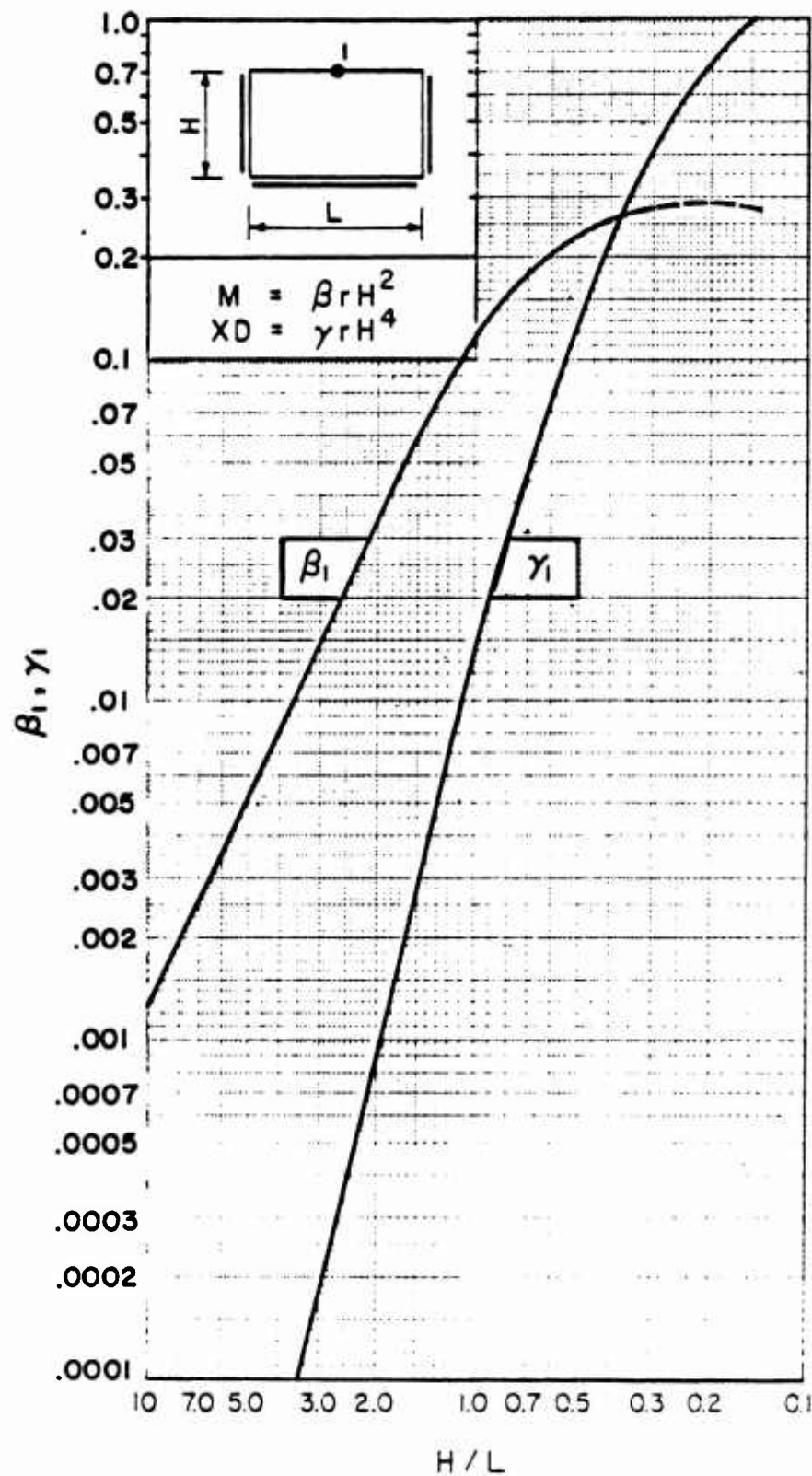
Figure 3-30   Moment and deflection coefficients for uniformly-loaded, two-way element with three edges simply-supported and one edge free
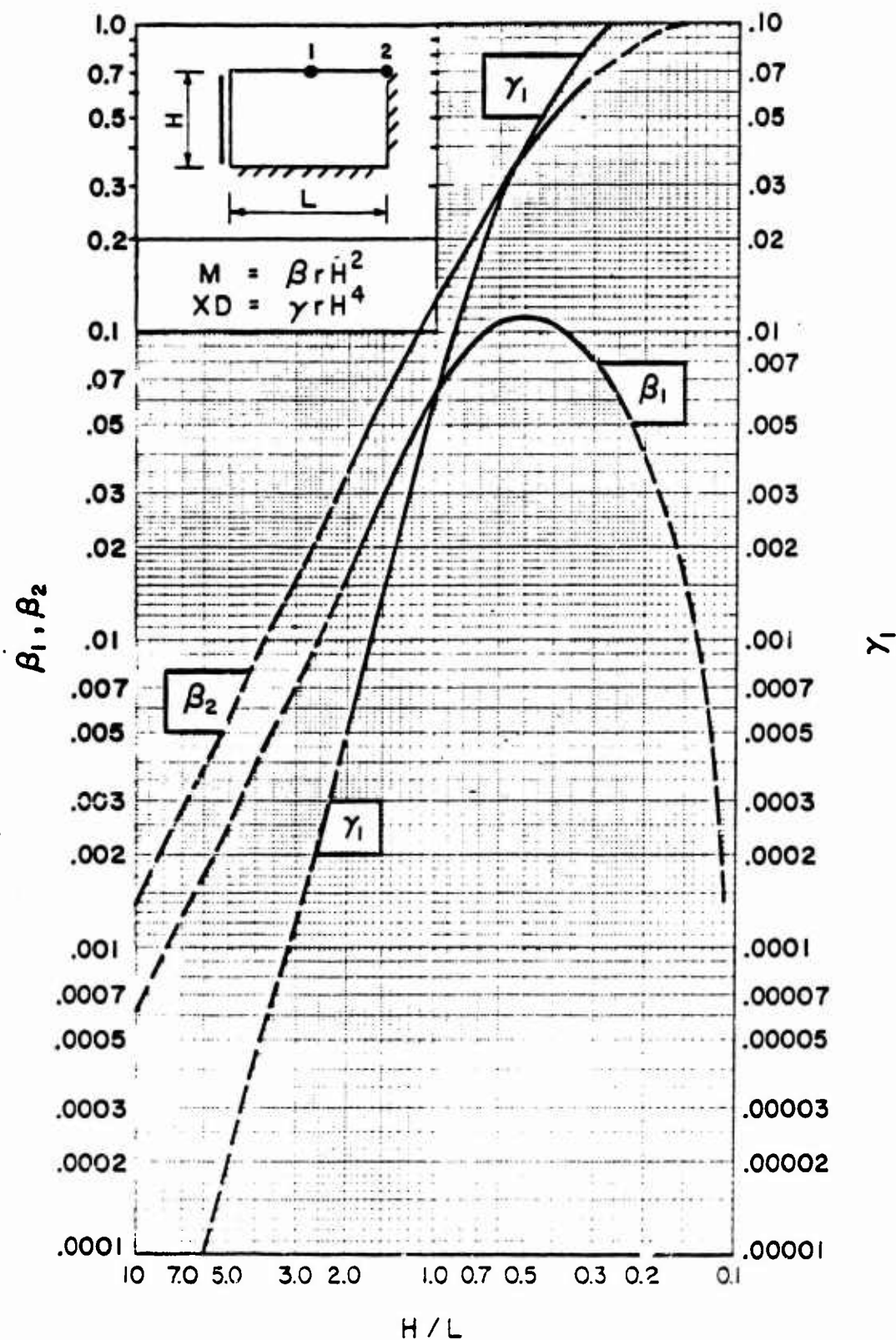
Figure 3-31   Moment and deflection coefficients for uniformly-loaded, two-way element with two adjacent edges fixed, one edge simply-supported, and one edge free
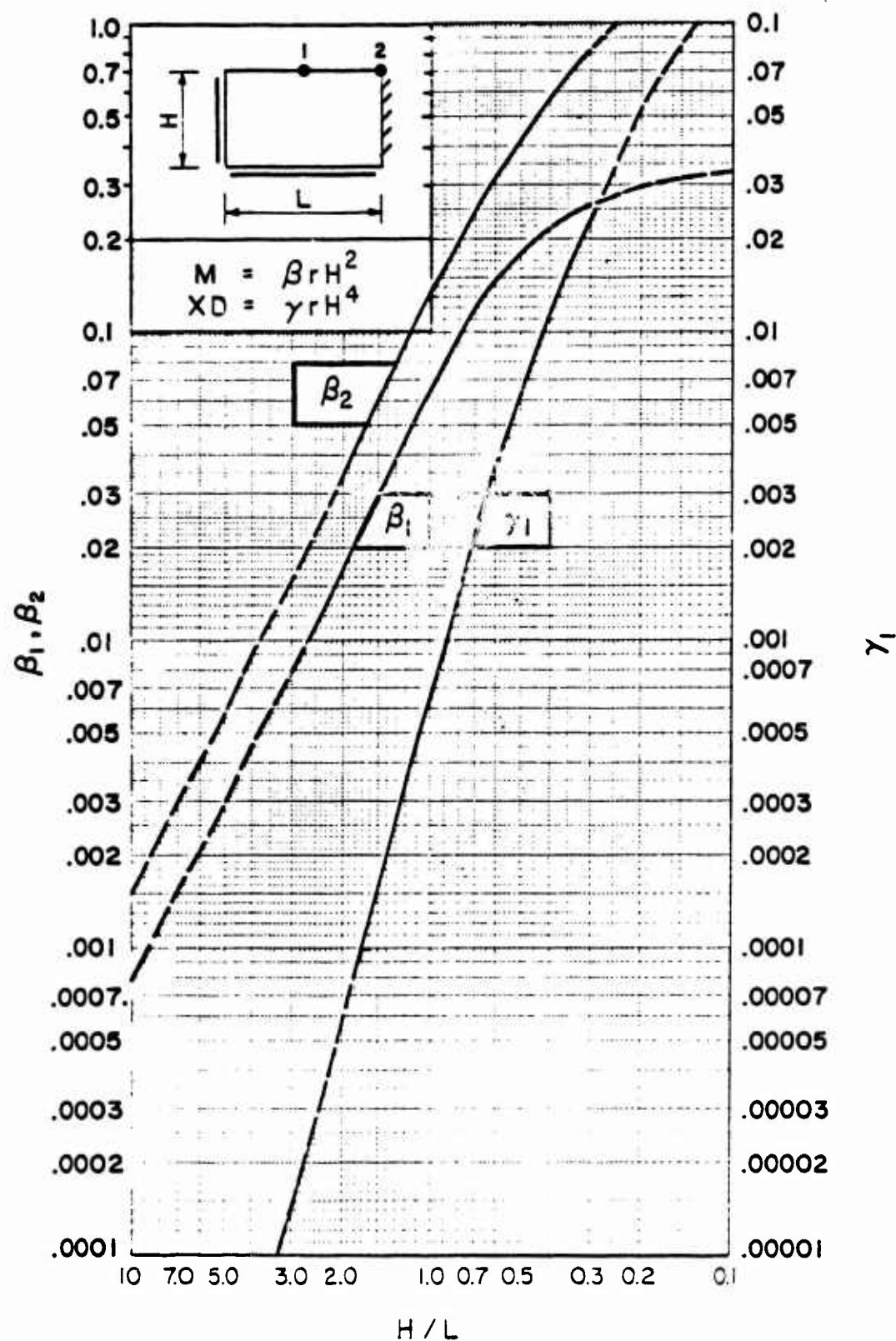
Figure 3-32   Moment and deflection coefficients for uniformly-loaded, two-way element with two adjacent edges simply-supported, one edge fixed, and one edge free
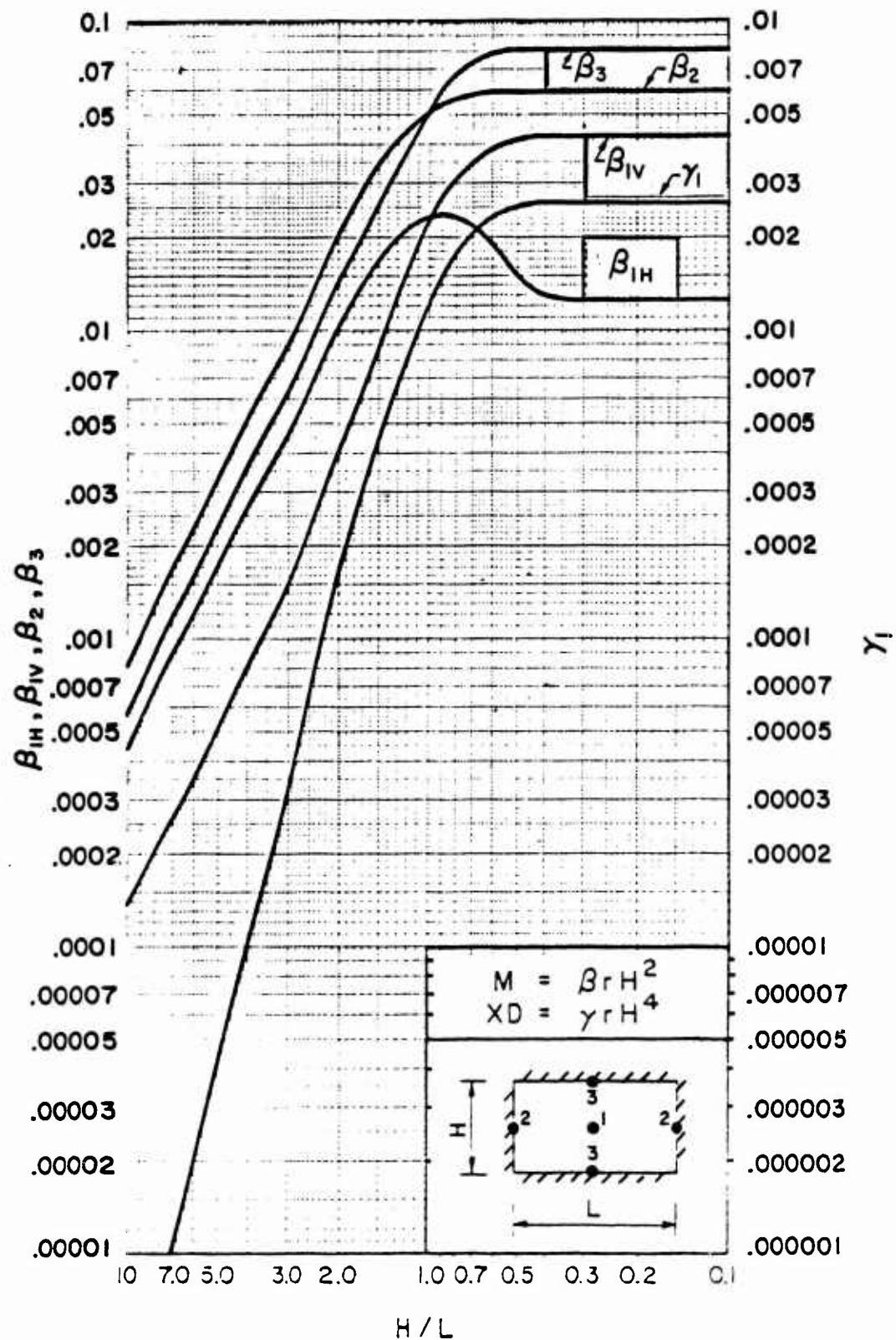
Figure 3-33   Moment and deflection coefficients for uniformly-loaded, two-way element with all edges fixed
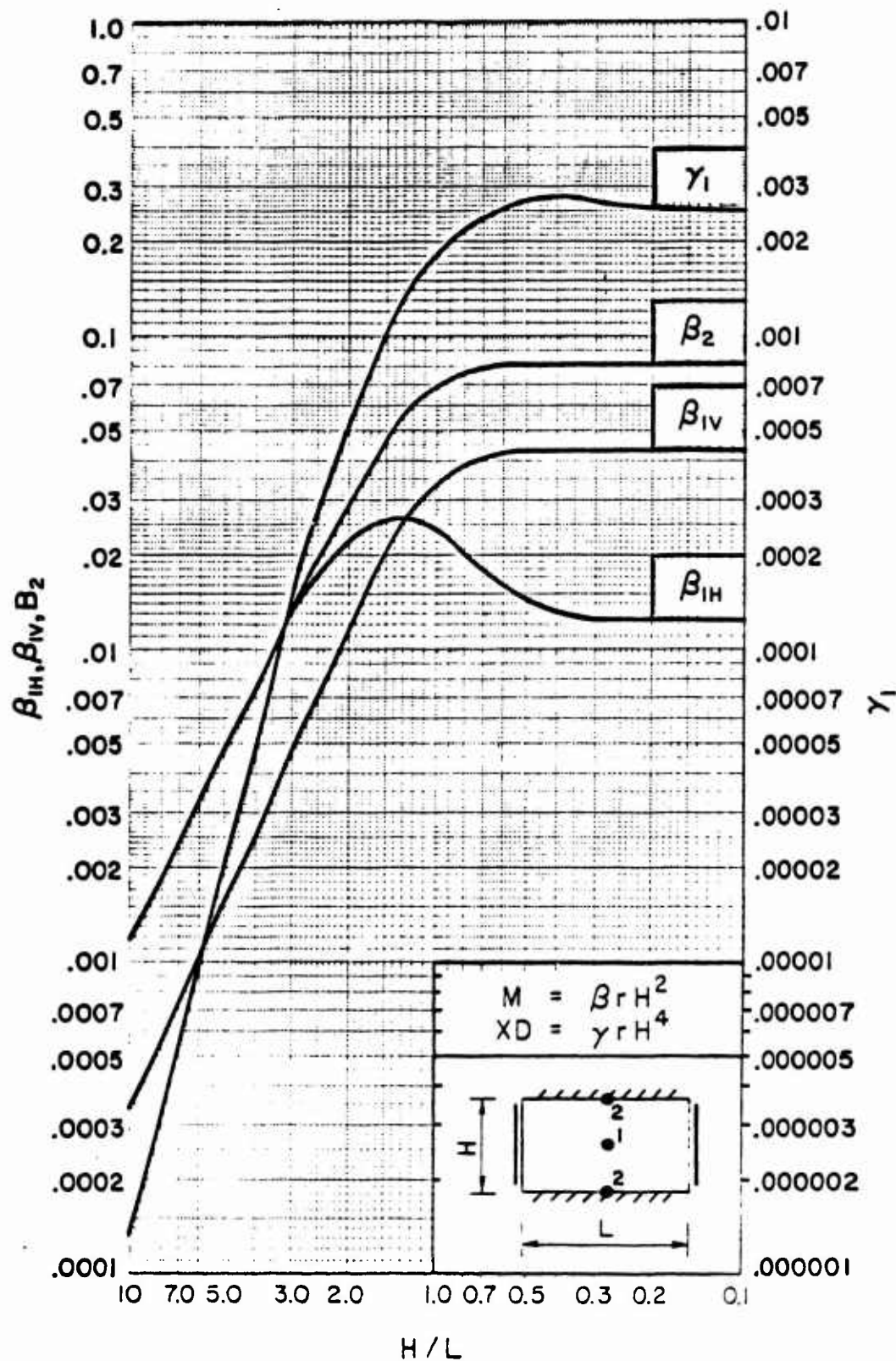
Figure 3-34   Moment and deflection coefficients for uniformly-loaded, two-way element with two opposite edges fixed and two edges simply-supported
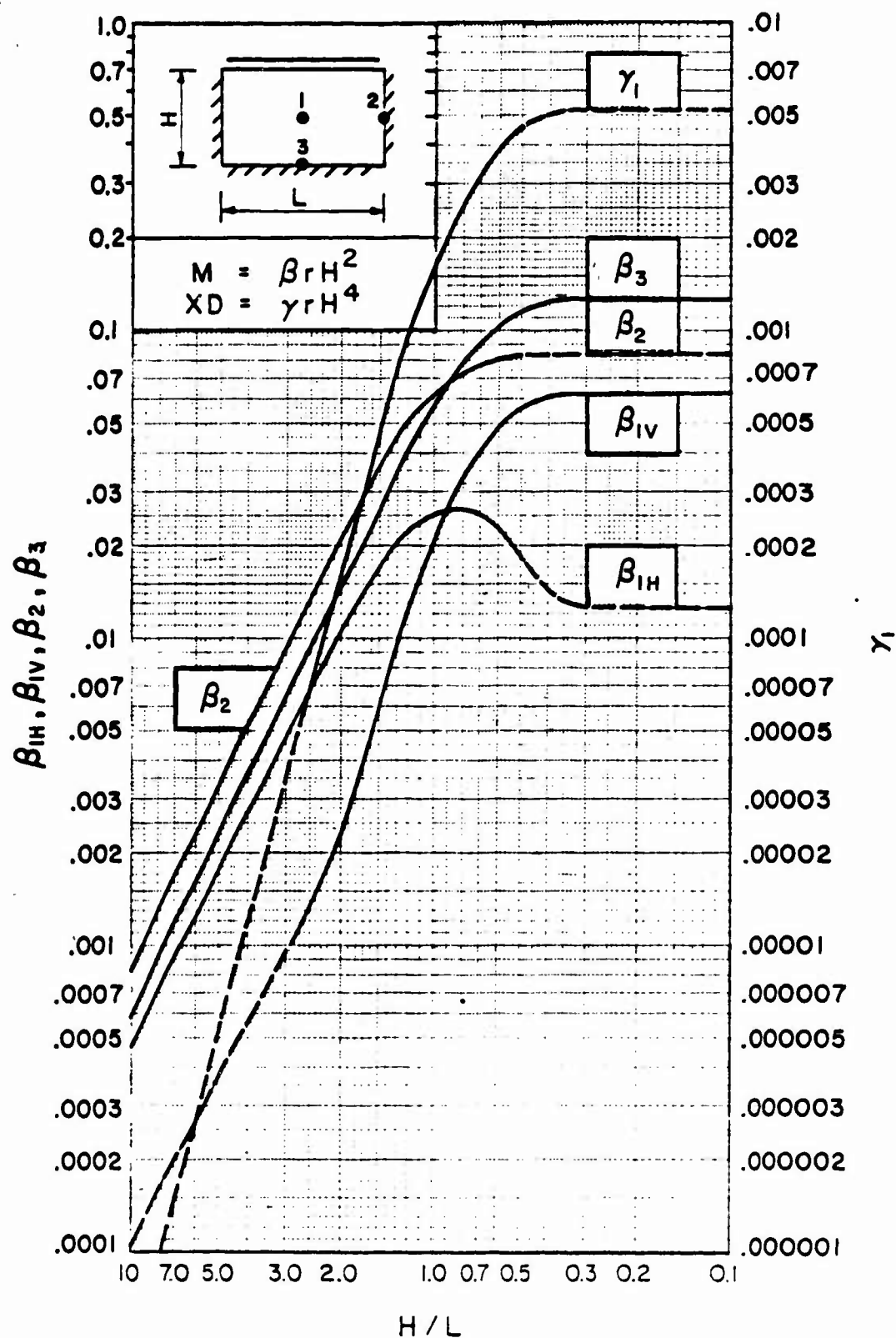
Figure 3-35   Moment and deflection coefficients for uniformly-loaded, two-way element with three edges fixed and one edge simply-supported
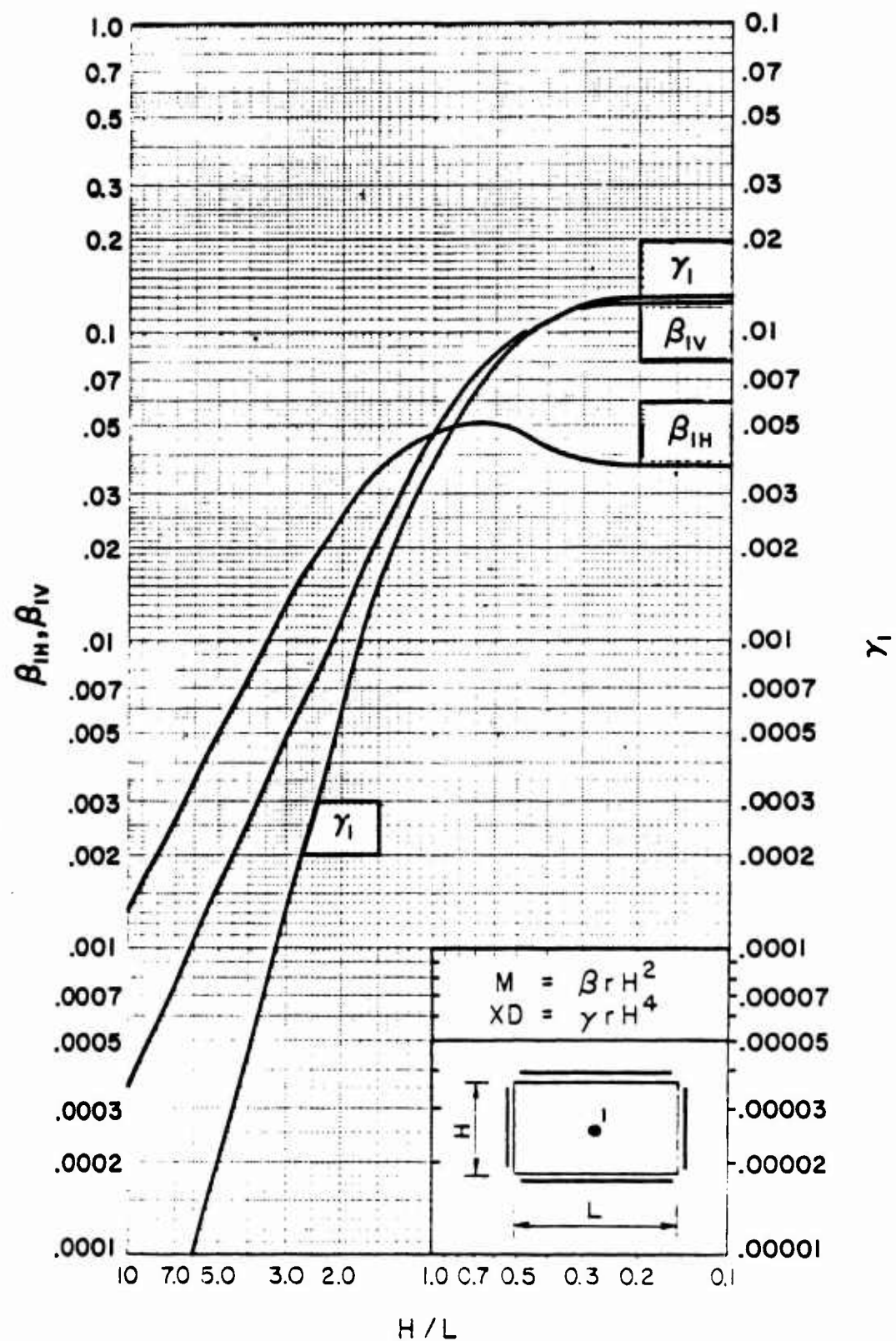
Figure 3-36   Moment and deflection coefficients for uniformly-loaded, two-way
element with all edges simply-supported
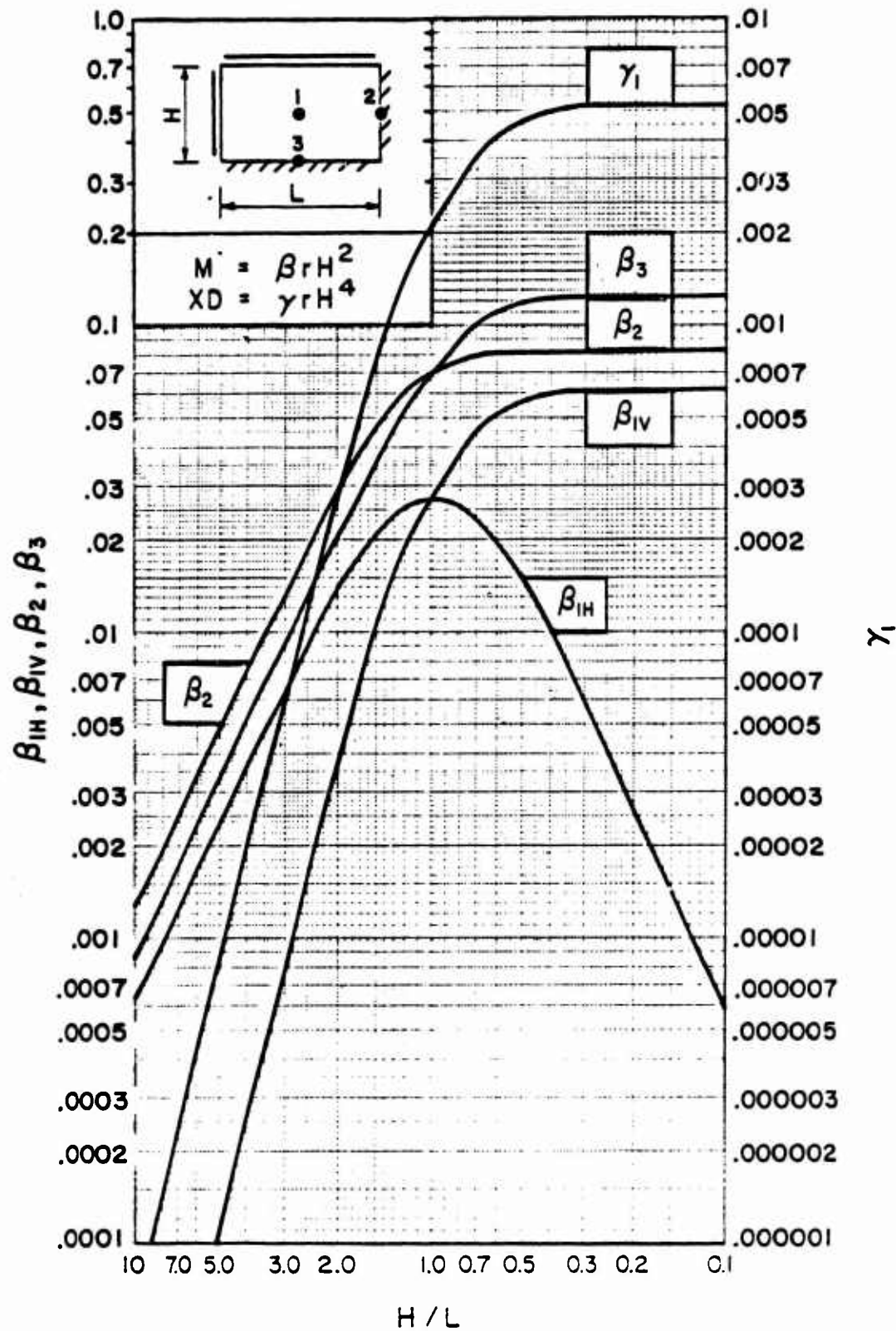
Figure 3-37   Moment and deflection coefficients for uniformly-loaded, two-way
element with two adjacent edges fixed, and two edges simply-
supported

-59-
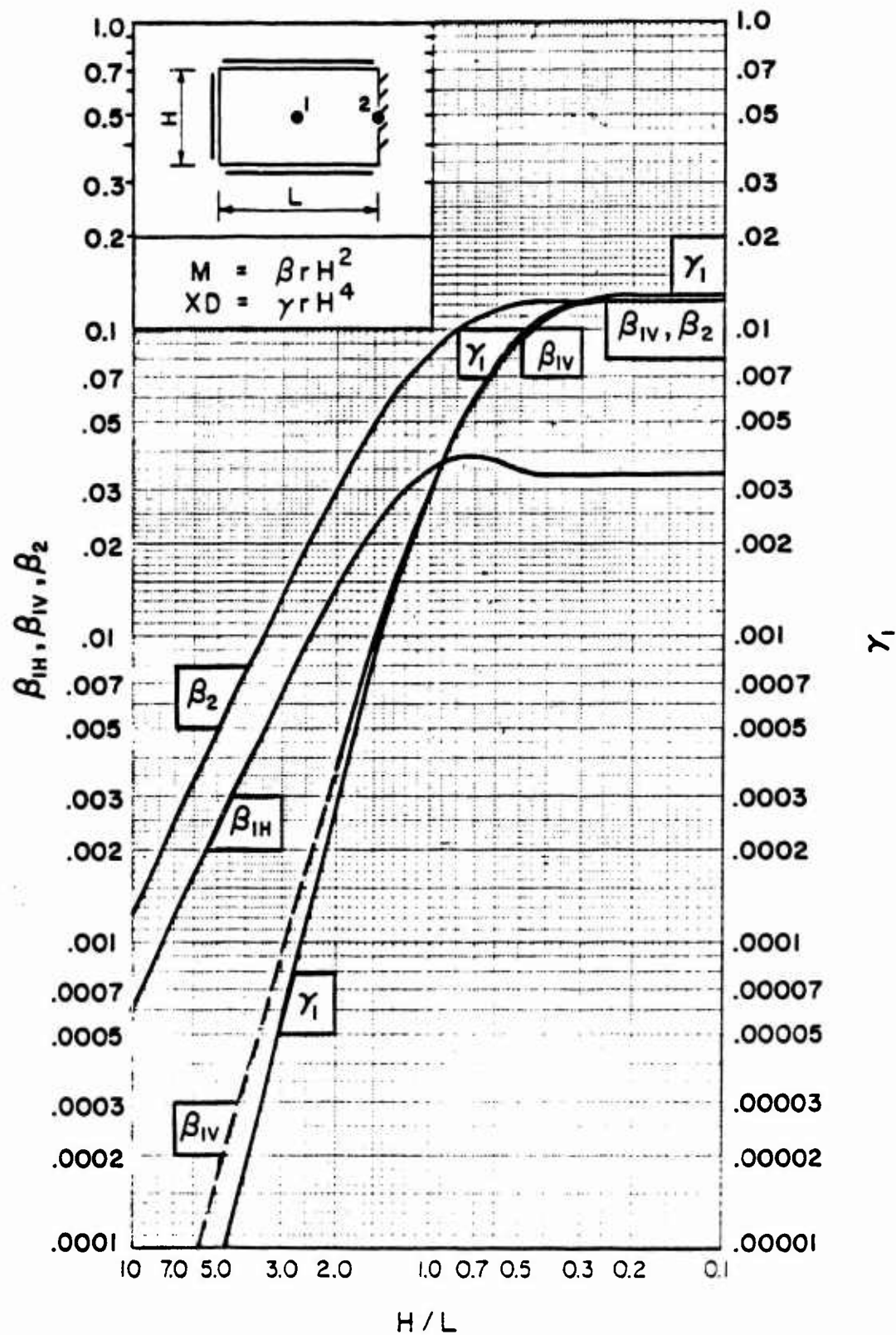
Figure 3-38   Moment and deflection coefficients for uniformly-loaded, two-way element with three edges simply-supported and one edge fixed

Figures 3-24 through 3-26 are for a two-way element supported on two adjacent sides and free at the others. Figures 3-27 through 3-32 are for a two-way element supported on three sides and free on the fourth, while figures 3-33 through 3-38 are for elements fixed on four sides. The resistances in each range can readily be determined using the coefficients β, the subscript referring to the points listed in the accompanying illustration.

For example, in figure 3-27, for an element fixed on three sides and free on the fourth, if the ultimate unit resisting moments M_u are known for points 1, 2 and 3, a resistance r for each point can be calculated from

$$r = M_u/\beta H^2 \qquad\qquad 3\text{-}25$$

where the values of β are found in figure 3-27. The smallest value of resistance r, (say at point 2) corresponds to the first yield and is equal to r_e. Next, the moments at the remaining two points are computed for this value of r_e, and the differences between these and the ultimate values are determined. These differences represent the remaining moment capacities available for additional load. At r_e, the elements supports become free, fixed, and simply-supported on opposite sides. Using the moment differences and entering figure 3-26 two values of the change in resistance can be calculated as above, the smaller being Δr and therefore:

$$r_{ep} = r_e + \Delta r \qquad\qquad 3\text{-}26$$

In similar fashion, the resistance at the end of each range can be determined until the ultimate unit resistance r_u is reached.

3-13   Elasto-Plastic Stiffnesses and Deflections

The slopes of the elastic and elasto-plastic ranges of the resistance function are defined by the stiffness K of the element:

$$K = r/X \qquad\qquad 3\text{-}27$$

where r is the unit resistance and X is the deflection corresponding to the value of r. The elastic range stiffness is denoted as K_e, the elasto-plastic range as K_{ep}, while in the plastic range the stiffness is zero.

Typical resistance-deflection functions used for design are shown in Figure 3-39. One- and two-step systems are generally used for one-way elements while two- and three-step systems are used for two-way elements. Two way elements fixed on all four sides will exhibit a four step system. As can be seen from the figure, the elastic range stiffness

$$K_e = r_e/X_e \qquad\qquad 3\text{-}28$$

the elasto-plastic stiffness for a two-step system

$$K_{ep} = (r_u - r_e)/(X_p - X_e) \qquad\qquad 3\text{-}29$$

and for a three-step system, the elasto-plastic stiffnesses

$$K_{ep} = (r_{ep} - r_e)/(X_{ep} - X_e) \qquad\qquad 3\text{-}30$$

- 61 -
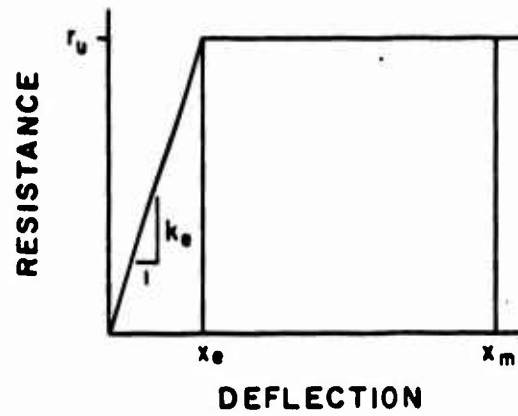
(a) ONE STEP ELASTO-PLASTIC SYSTEM
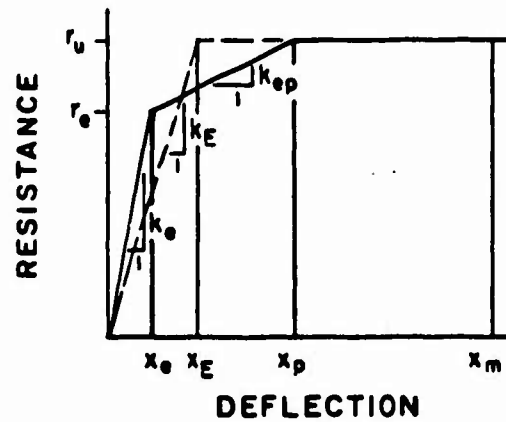
(b) TWO STEP ELASTO-PLASTIC SYSTEM
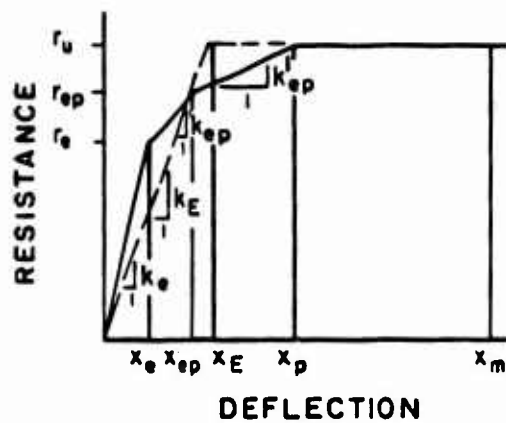
(c) THREE STEP ELASTO-PLASTIC SYSTEM

Figure 3-39   Resistance-deflection functions for limited deflections

-62-

and

$$K'_{ep} = (r_u - r_{ep})/(X_p - X_{ep}) \qquad \text{3-31}$$

The elastic and elasto-plastic stiffnesses of one-way elements are given in table 3-8 as a function of the modulus of elasticity E, moment of inertia I, and span length. Knowing the resistances and stiffnesses, the corresponding elastic and elasto-plastic deflections can be computed from the above equations.

The determination of the elasto-plastic stiffnesses and deflections of two-way elements is more complicated than for one-way elements since another variable, namely, the aspect ratio L/H, must be considered. For two-way elements, the deflections at the end of each range of behavior is obtained from the γ coefficients presented in figures 3-24 through 3-38. The deflection for each range of behavior is obtained from

$$XD = \gamma r H^4 \qquad \text{3-32}$$

where D, the flexural rigidity of the element is defined as

$$D = EI/(1-v^2) \qquad \text{3-33}$$

E is the modulus of elasticity, I is the moment of inertia, and v is Poisson's ratio. It must be realized that except for the elastic range, the values of X (the displacement) and r in Equation 3-32 represent change in deflection and resistance from one range of behavior to another. Therefore, for two-way members the change in deflection and resistance (as previously explained) is obtained from figures 3-24 through 3-38 and the stiffnesses are computed from equations 3-28 through 3-33.

3-14 Resistance-Deflection Functions for Design

3-14.1 *General*
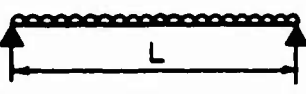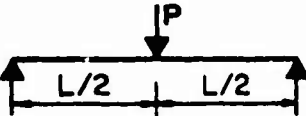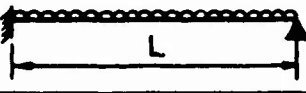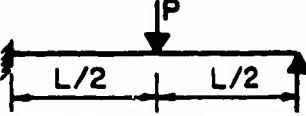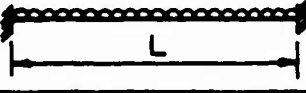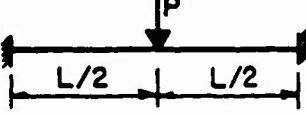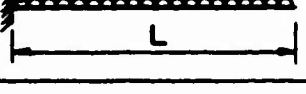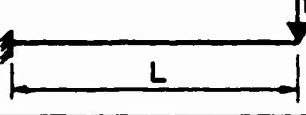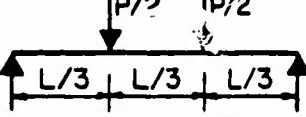
The resistance-deflection function used for design depends upon the maximum permitted deflection according to the design criteria of the element being considered. This maximum deflection X_m can be categorized as either limited or large. In the limited deflection range, the maximum deflection of the system is limited to the elastic, elasto-plastic and plastic ranges. When the maximum deflection falls in the large deflection range, the response of the system is principly within the plastic range and the elastic and elasto-plastic ranges need not be considered. The error resulting from the omission of the elastic and elasto-plastic portions in this analysis is negligible.

The support rotation that corresponds to limited deflection varies for the different materials used in protection design. The response criteria for each material is obtained from the volume that describes the design procedures for that material.

3-14.2 *Limited Deflections*

When designing for limited deflections, the maximum deflection X_m of the element is kept within the elastic, elasto-plastic, and limited plastic ranges, and the resistance-deflection function for design takes the form shown

Table 3-8 Elastic, Elasto-Plastic and Equivalent Elastic Stiffnesses for One-Way Elements

Edge Conditions and Loading Diagrams	Elastic Stiffness, K_e	Elasto-Plastic Stiffness, K_{ep}	Equiv. Elastic Stiffness, K_E
Simply supported, uniform load, span L	$\dfrac{384EI}{5L^4}$	—	$\dfrac{384EI}{5L^4}$
Simply supported, concentrated load P at midspan ($L/2$, $L/2$)	$\dfrac{48EI}{L^3}$	—	$\dfrac{48EI}{L^3}$
Fixed-simple, uniform load, span L	$\dfrac{185EI}{L^4}$	$\dfrac{384EI}{5L^4}$	$\dfrac{160EI^*}{L^4}$
Fixed-simple, concentrated load P at midspan ($L/2$, $L/2$)	$\dfrac{107EI}{L^3}$	$\dfrac{48EI}{L^3}$	$\dfrac{106EI^*}{L^3}$
Fixed-fixed, uniform load, span L	$\dfrac{384EI}{L^4}$	$\dfrac{384EI}{5L^4}$	$\dfrac{307EI^*}{L^4}$
Fixed-fixed, concentrated load P at midspan ($L/2$, $L/2$)	$\dfrac{192EI}{L^3}$	$\dfrac{48EI^{**}}{L^3}$	$\dfrac{192EI^*}{L^3}$
Cantilever, uniform load, span L	$\dfrac{8EI}{L^4}$	—	$\dfrac{8EI}{L^4}$
Cantilever, concentrated load P at free end, span L	$\dfrac{3EI}{L^3}$	—	$\dfrac{3EI}{L^3}$
Simply supported, loads $P/2$ at third points ($L/3$, $L/3$, $L/3$)	$\dfrac{56.4EI}{L^3}$	—	$\dfrac{56.4EI}{L^3}$

* Valid only if $M_N = M_p$

** Valid only if $M_N < M_p$

-64-

in figure 3-39 a, b, and c for a one-step system, a two-step system, and a three-step system, respectively. The design charts presented in Section 3-19.3 were established for a one-step system; for two- and three-step systems, these charts can be used if the resistance-deflection functions are replaced with equivalent elastic resistance-deflection functions defined by K_E and X_E as indicated by the dotted lines in figure 3-39. The equivalent elastic stiffness K_E and the eqivalent maximum elastic deflection X_E are calculated such that the area under the dotted curve is equal to the area under the solid curve, thereby producing the same potential energy in each system. The equivalent maximum elastic deflection X_E for the two-step and three-step systems shown is expressed by equations 3-34 and 3-35, respectively.

$$X_E = X_e + X_p(1 - r_e/r_u) \qquad\qquad 3\text{-}34$$

$$X_E = x_e(r_{ep}/r_u) + X_{ep}(1 - r_e/r_u) + X_p(1 - r_{ep}/r_u)$$

$$3\text{-}35$$

The equivalent elastic stiffness K_E in each case is equal to

$$K_E = r_u/X_E \qquad\qquad 3\text{-}36$$

One-way elements exhibit one- and two-step resistance deflection curves depending on the type of supports. Consequently, the equivalent elastic stiffness K_E is given for one-way elements in table 3-8. The equivalent elastic deflection can then be calculated from equation 3-36. Two-way elements generally exhibit two- and three-step resistance-deflection curves which are a function of not only the type of supports but also of the aspect ratio L/H of the element. The equivalent elastic deflection X_E of the element under consideration must be calculated from equations 3-34 and 3-35 for two- and three-step systems, respectively. The value of K_E for the system can then be obtained from equation 3-36.

3-14.3 Large Deflections

When designing for a large deflection, it can be assumed without significant error that the resistance rises instantaneously from zero to its ultimate value r_u at the onset of the blast loading thus neglecting the elastic and elasto-plastic ranges. The design resistance function for one-way elements is approximated by a constant plastic range resistance as shown in figure 3-40a, while for two-way elements, the resistance function becomes that shown in figure 3-40b, where the maximum deflection X_m can be either smaller or larger than the partial failure deflection X_1.

3-15 Support Shears or Reactions

Support shears or reactions are a function the applied load and the maximum resistance attained by an element, its geometry and yield line location. However, for short duration blast loads, the support shears can be reasonably estimated by neglecting the applied load. Therefore, the ultimate support shear can be assumed to be developed when the resistance reaches the ultimate value, r_u.
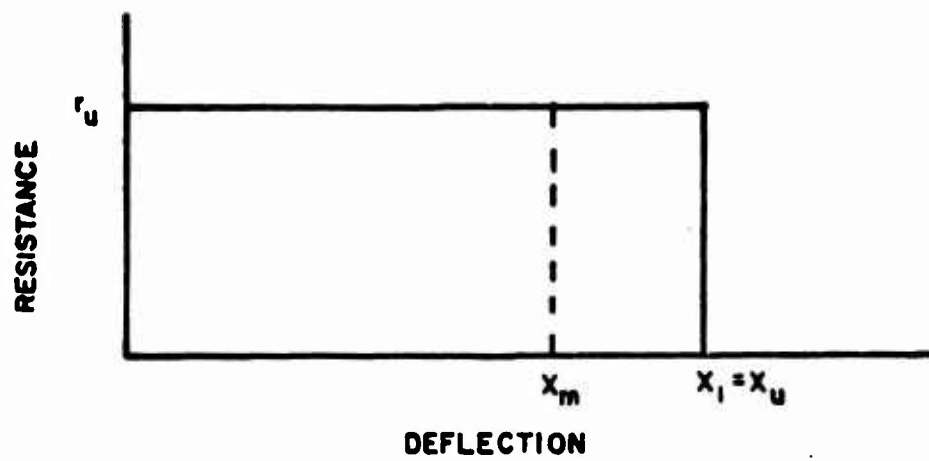
a) ONE-WAY ELEMENT
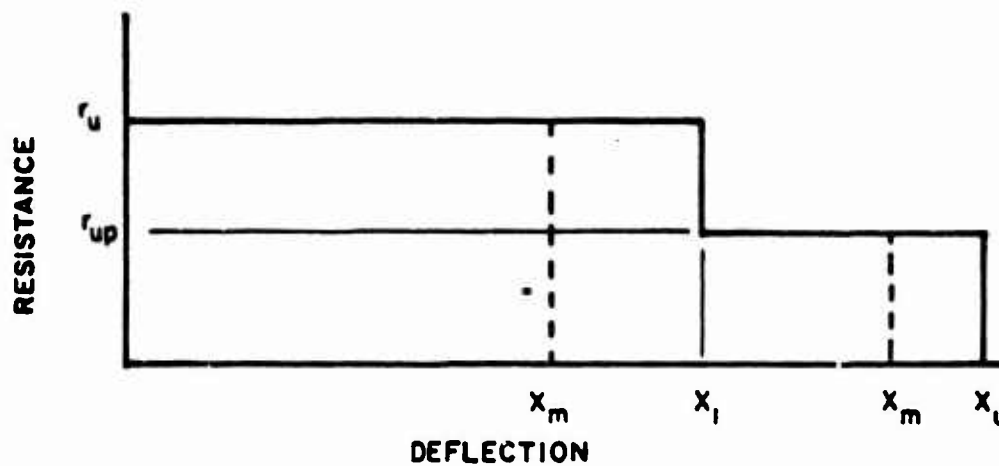
b) TWO-WAY ELEMENT

Figure 3-40   Resistance-deflection functions for large deflections

Equations for the ultimate support shears V_s for one-way elements are given in table 3-9. For those cases where an element does not reach its ultimate resistance, the support shears are obtained based upon elastic theory for the actual resistance r attained by the element.

For two-way elements, the ultimate shears acting at each section are calculated by use of the "yield line procedure" previously outlined for the determination of the ultimate resistance r_u. The shear along the support is assumed to vary in the same manner as the moment varies (2/3 V at the corners and V elsewhere) to account for the higher stiffness of the corners (fig. 3-41). Since the shear is assumed to be zero along the interior (usually positive) yield lines, the total shear at any section of a sector is equal to the resistance r_u times the area between the section being considered and the positive yield lines. Referring to figure 3-41, the support shear V_{sV} for the triangular sector I is

$$(2/3)V_{sV}(L/4 + L/4) + V_{sV}(L/2) =$$

$$r_u(Ly/2) \qquad\qquad 3\text{-}37$$

$$V_{sV} = 3r_u y/5 \qquad\qquad 3\text{-}38$$

and for the trapezoidal sector II

$$(2/3)V_{sH}(y/2) + V_{sH}(H - y/2)$$

$$r_u(L/2)[(H - y + H)/2] \qquad\qquad 3\text{-}39$$

$$V_{sH} = [3r_u L(2-y/H)]/2(6 - y/H) \qquad\qquad 3\text{-}40$$

Values of the ultimate support shears V_{sH} and V_{sV} for several two-way elements derived as above are presented in tables 3-10 and 3-11. Table 3-10 gives the ultimate support shears for the case where opposite supports provide the same degree of restraint resulting in symmetrical yield line patterns. Table 3-11 is for completely general situations where opposing supports provide different degrees of restraint and result in the formation of unsymmetrical yield lines. In these cases, the ultimate support shears are not equal at opposing supports.
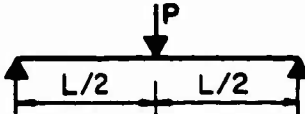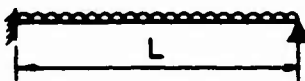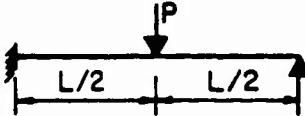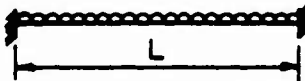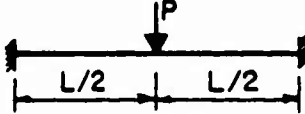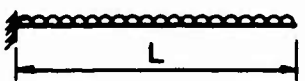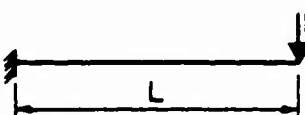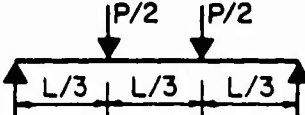
For the situations where the ultimate resistance of an element is not attained, the support shears are less than the ultimate value. The proportion of the total load along each support as well as the distribution of the shears along the support is assumed to be the same as previously cited for the ultimate support shear. Therefore, the support shears corresponding to the resistance r of the element is obtained from the equations presented in tables 3-10 and 3-11 by replacing r_u with the actual resistance attained (r_e, r_{ep}, etc.).

DYNAMICALLY EQUIVALENT SYSTEMS

3-16 Introduction

In dynamic analysis, there are only three quantities to be considered: (1) the work done, (2) the strain energy, and (3) the kinetic energy. To evaluate

Table 3-9 Support Shears for One-Way Elements

Edge Conditions and Loading Diagrams	Support Reactions, V_s
	$\dfrac{r_u L}{2}$
	$\dfrac{R_u}{2}$
	L. Reaction $\dfrac{5 r_u L}{8}$ R. Reaction $\dfrac{3 r_u L}{8}$
	L. Reaction $\dfrac{11 R_u}{16}$ R. Reaction $\dfrac{5 R_u}{16}$
	$\dfrac{r_u L}{2}$
	$\dfrac{R_u}{2}$
	$r_u L$
	R_u
	$\dfrac{R_u}{2}$
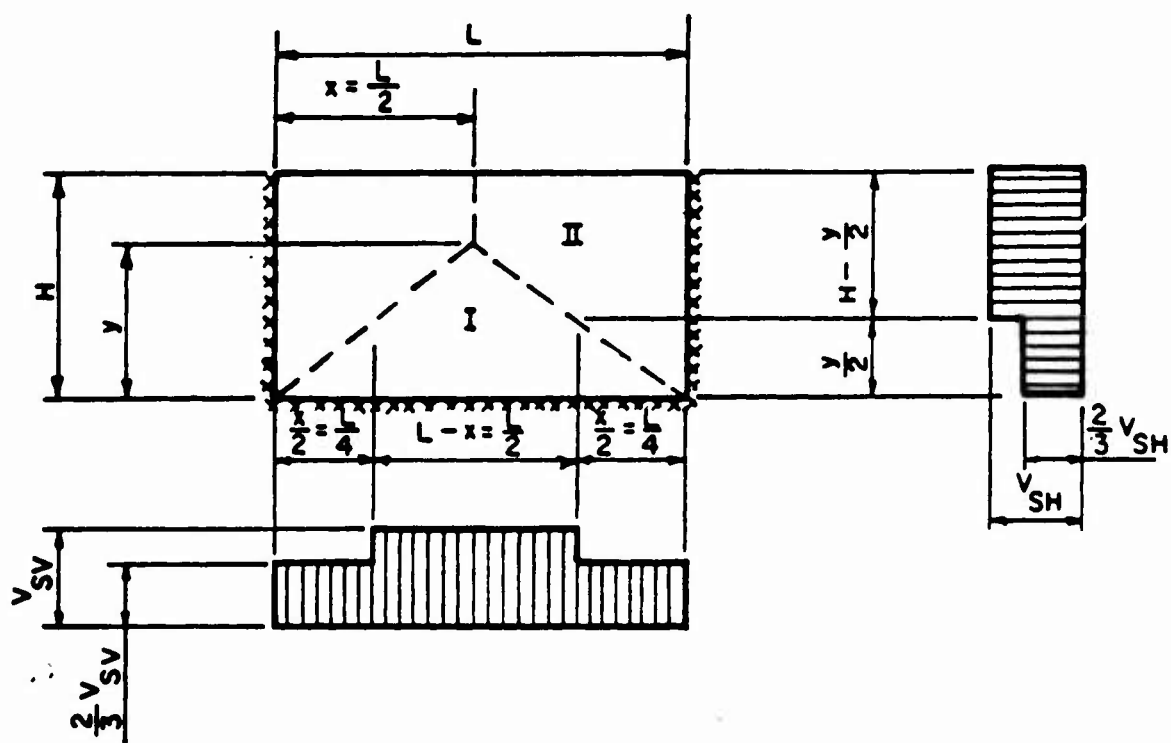
Figure 3-41   Determination of ultimate support shear

-69-

Table 3-10 Ultimate Support Shears for Two-Way Elements (Symmetrical Yield Lines)
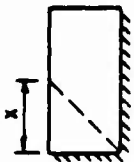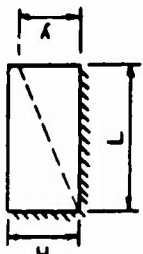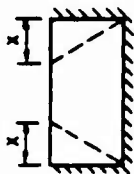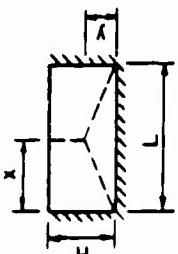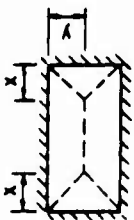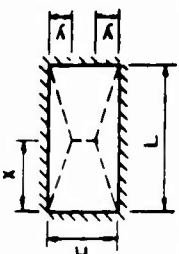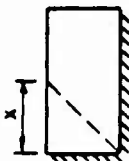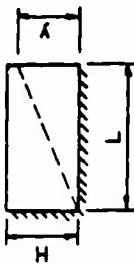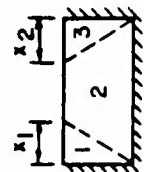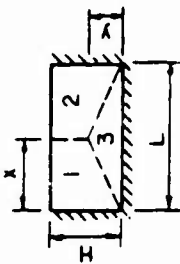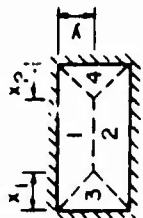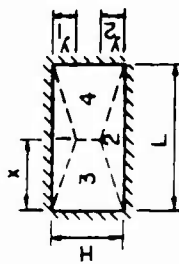
Edge Conditions	Yield Line Locations	Limits	Horizontal shear, V_{sH}	Vertical shear, V_{sV}
Two adjacent edges supported and two edges free		$x \leq L$	$\dfrac{3r_u x}{5}$	$\dfrac{3r_u H\left(2-\frac{x}{L}\right)}{\left(6-\frac{x}{L}\right)}$
		$y \leq H$	$\dfrac{3r_u L\left(2-\frac{y}{H}\right)}{\left(6-\frac{y}{H}\right)}$	$\dfrac{3r_u y}{5}$
Three edges supported and one edge free		$x \leq \frac{L}{2}$	$\dfrac{3r_u x}{5}$	$\dfrac{3r_u H\left(1-\frac{x}{L}\right)}{\left(3-\frac{x}{L}\right)}$
		$y \leq H$	$\dfrac{3r_u L\left(2-\frac{y}{H}\right)}{2\left(6-\frac{y}{H}\right)}$	$\dfrac{3r_u y}{5}$
Four edges supported		$x \leq \frac{L}{2}$	$\dfrac{3r_u x}{5}$	$\dfrac{3r_u H\left(1-\frac{x}{L}\right)}{2\left(3-\frac{x}{L}\right)}$
		$y \leq \frac{H}{2}$	$\dfrac{3r_u L\left(1-\frac{y}{H}\right)}{2\left(3-\frac{y}{H}\right)}$	$\dfrac{3r_u y}{5}$

Table 3-11   Ultimate Support Shears for Two-Way Elements (Unsymmetrical Yield Lines)

Edge Conditions	Yield Line Locations	Limits	Horizontal shear, V_{sH}	Vertical shear, V_{sV}
Two adjacent edges supported and two edges free		$x \leq L$ $y, \leq H$	Same as in Table 3-10	Same as in Table 3-10
Three edges supported and one edge free		$x_1 \leq \dfrac{L}{2}$ $x_2 \leq \dfrac{L}{2}$ $y \leq H$	$\dfrac{3x_1 r_u}{5}$ $\dfrac{3x_2 r_u}{5}$ $\dfrac{3r_u x(2H-y)}{6H-y}$ $\dfrac{3r_u x(L-x)(2H-y)}{6H-y}$	$\dfrac{3r_u H(2L-x_1-x_2)}{6L-x_1-x_2}$ $\dfrac{3r_u y}{5}$
Four edges supported		$x_1 \leq \dfrac{L}{2}$ $x_2 \leq \dfrac{L}{2}$ $y_1 \leq \dfrac{H}{2}$ $y_2 \leq \dfrac{H}{2}$	$\dfrac{3r_u x_1}{5}$ $\dfrac{3r_u x_2}{5}$ $\dfrac{3r_u x(2H-y_1-y_2)}{6H-y_1-y_2}$ $\dfrac{3r_u(L-x)(2H-y_1-y_2)}{6H-y_1-y_2}$	$\dfrac{3r_u y(2L-x_1-x_2)}{6L-x_1-x_2}$ $\dfrac{3r_u(H-y)(2L-x_1-x_2)}{6L-x_1-x_2}$ $\dfrac{3r_u y_1}{5}$ $\dfrac{3r_u y_2}{5}$

the work done, the displacement at any point on the structure under externally distributed or concentrated loads must be known. The strain energy is equal to the summation of the strain energies in all the structural elements which may be in bending, tension, compression, shear or torsion. The kinetic energy involves the energy of translation and rotation of all the masses of the structure. The actual evaluation of these quantities for a given structure under dynamic load would be complicated. However, for practical problems, this can be avoided by using appropriate assumptions.

In most cases, a structure can be replaced by an idealized (or dynamically equivalent) system which behaves timewise in nearly the same manner as the actual structure. The distributed masses of the given structure are lumped together into a number of concentrated masses. The strain energy is assumed to be stored in several weightless springs which do not have to behave elastically; similarly, the distributed load is replaced by a number of concentrated loads acting on the concentrated masses. Therefore, the equivalent system consists merely of a number of concentrated masses joined together by weightless springs and subjected to concentrated loads which vary with time. This concentrated mass-spring-load system is defined as an equivalent dynamic system.

Although all structures possess many degrees of freedom, one mode usually predominates in the response to short duration loads; thus, for all practical purposes, this one mode may be considered to define the behavior of the structure and the problem can be simplified by considering a single-degree-of-freedom system whose properties are those of the fundamental mode of the structures. A single-degree-of-freedom system is defined as one in which only one type of motion is possible or, in other words, only one coordinate is required to define its motion. Such a system is shown in figure 3-42 which consists of a concentrated mass on a frictionless surface attached to a weightless spring and subjected to a concentrated load. A single displacement variable x is sufficient to describe its motion. The material presented herein will be limited to single-degree-of-freedom systems only.

Many structures, however, exist which can not be adequately described by the first vibration, particularly when consideration of dynamic strain is necessary. For these situations, a two (or more)-degree-of-freedom analysis may be required. Procedures are presented in section 3-19.2 for performing these analyses.

Two fundamental methods are available for treating simple systems subjected to dynamic forces. The first of these methods is concerned with solving the differential equations of the system by either classical, numerical or graphical means. The second method of analysis and chart solutions depend on solutions which have been determined by the use of the first method and are approximate solutions to the problems in hand. There is a third method which may also be very useful in vibrational problems; this involves the energy equation.

In the following paragraphs the design factors used to determine the equivalent dynamic system that is used to analyze structural elements are defined and the methods used to obtain these factors are discussed.
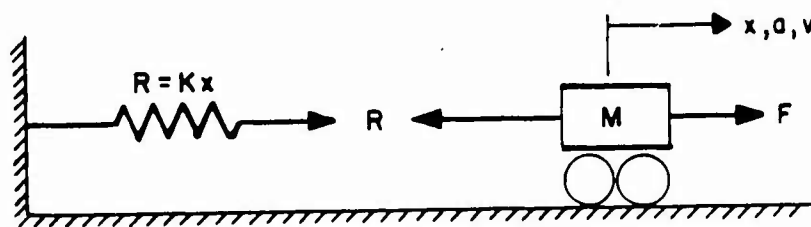
Figure 3-42   Typical single-degree-of-freedom system

3-17   Dynamic Design Factors

3-17.1   *Introduction*

The values of the mass and external force used in the equation of motion
(equation 3-1) are the actual values only if all the elements of the mass of
the structure experience the same force and, consequently, move as a unit, in
which case, the entire mass may be assumed to be concentrated at its center of
gravity. In other cases, the assumption of uniform motion of the entire mass
cannot be made without introducing serious error. This is true for members
with uniformly distributed mass which bend or rotate under load. In such
cases, the motion of the particles of mass varies along the length of the
member. Beams, slabs, etc., with such distributed mass actually have an
infinite number of degrees of freedom; however, such structural elements can
be represented by an equivalent single-degree-of-freedom system.

In order to define an equivalent one-degree system, it is necessary to
evaluate the parameters of that system; namely, the equivalent mass M_E, the
equivalent spring constant K_E and the equivalent load F_E. The equivalent
system is selected usually so that the deflection of the concentrated mass is
the same as that for a significant point of the structure. The single-degree-
of-freedom approximation of the dynamic behavior of the structural element may
be achieved by assuming a deflected shape for the element which is usually
taken as the shape resulting from the static application of the dynamic
loads. The assumption of a deflected shape establishes an equation relating
the relative deflection of all points of the element.

The accuracy of the computed deformation of the single-degree-of-freedom
system is dependent on the assumed deflected shape and the loading region.
For example, in the impulsive loading realm, if the assumed deformed shape for
a simply supported beam is taken to be a parabola, then the exact solution
will be obtained for the deflection of the beam. In the quasi-static loading
realm, however, the static deformed shape gives the exact answer. For blast
resistance design, however, the differences in either a static deformed shape
or a first mode approximation is negligible and thus either way is
permissible. Usually, though, the static deformed shape is easier to use as
it covers both symmetric and asymmetric deformation.

To permit rapid design of structural elements subjected to dynamic loads, it
is convenient to introduce design or transformation factors. These factors
are used to convert the real system to the equivalent system. To obtain them,
it is necessary to equate the relations expressing the kinetic energy, strain
and work done on the actual structural element deflecting according to the
assumed deflected shape, with the corresponding relations for the equivalent
mass and spring system.

3-17.2   *Load, Mass and Resistance Factors*

3-17.2.1 *Load Factor.* The load factor is the design or transformation factor
by which the total load applied on the structural element is multiplied to
obtain the equivalent concentrated load for the equivalent single-degree-of-
freedom system. If the actual total load on the structure is F and the
equivalent load is F_E, the load factor K_L is defined by the equation

- 74 -

$$K_L = F_E/F \qquad \text{3-41}$$

The load factor is derived by setting the external work done by the equivalent load F_E on the equivalent system equal to the external work done by the actual load F on the actual element deflecting to the assumed deflected shape.

For a structure with distributed loads;

$$WD = F_E \delta_{max} = \int_L p(x)\delta(x)dx \qquad \text{3-42a}$$

where

δ_{max} = maximum deflection of actual structure
$p(x)$ = distributed load per unit length
$\delta(x)$ = deflection at any point of actual structure
L = length of structure

rearranging terms

$$F_E = \int_L p(x)\varphi(x)dx \qquad \text{3-42b}$$

$$\text{3-43}$$

where $\qquad \varphi(x) = \delta(x)/\delta_{max}$

and is called the shape function.

NOTE. The shape function, $\varphi(x)$ is different for the elastic range and the plastic range and therefore the load factor, K_L, will be different.

For example; the shape factor for a simply supported beam with a uniformly distributed load, in the elastic rangers is defined as

$$\varphi(x) = (16/5L^4)(L^3x - 2Lx^3 + x^4) \qquad \text{3-44a}$$

while for the plastic range

$$\varphi(x) = 2x/L \qquad x < L/2 \qquad \text{3-44b}$$

For a structure with concentrated loads

$$WD = F_e \delta_{max} = \sum_{r=1}^{i} F_r \delta_r \qquad \text{3-45a}$$

where

F_r = r^{th} concentrated load
δ_r = deflection at load r
i = number of concentrated loads

rearranging terms

$$F_E = \sum_{r=1}^{i} F_r \varphi_r \qquad \text{3-45b}$$

where the shape factor is defined as

$$\text{3-46}$$

$$\varphi_r = \sum_{r=1}^{i} \delta_r/\delta_{max}$$

Again there is a K_L for the elastic range and a K_L for the plastic range. However, for a single concentrated load located at the point of maximum

deflection (i.e. the center of a simply supported or fixed-fixed beam, or the end of a cantilever beam) φ_r is equal to one for both the elastic and plastic ranges and therefore K_L is equal to one for both ranges.

Values for K_L for one-way elements are presented in table 3-12. Equation 3-41 through 3-46 were used to calculate these values. An example calculating K_L is shown in Appendix A.

3-17.2.2 *Mass Factor.* The mass factor is the design or transformation factor by which the total distributed mass of an element is multiplied to obtain the equivalent lumped mass of the equivalent single-degree-of-freedom system. If the total mass of the actual element is M and the mass of the equivalent system is M_E, the mass factor K_M is defined by the equation

$$K_M = M_E/M \qquad\qquad 3\text{-}47$$

K_M can be obtained by setting the kinetic energy of the equivalent system equal to the kinetic energy of the actual structure as determined from its deflected shape.

For a structure with continuous mass

$$KE = 1/2 M_E (\omega \delta_{max})^2 = 1/2 \int_0^L m(x)[\omega \delta(x)]^2 dx \qquad 3\text{-}48a$$

where ω = natural circular frequency
           $m(x)$ = distributed mass per unit length

rearranging terms

$$M_E = \int_0^L m(x)\varphi^2(x)dx \qquad\qquad 3\text{-}48b$$

where the shape function $\varphi(x)$ is based on the deflected shape of the element due to the applied loading and not to the distribution of the mass. Since the deflected shape of the element is different for the elastic and plastic ranges, $\varphi(x)$, and therefore K_M, will also be different.

Using equations 3-47 and 3-48, values for K_M were calculated for one-way elements with constant mass. These values are shown in table 3-12.

For a concentrated mass system,

$$KE = 1/2 M_E (\omega \delta_{max})^2 = 1/2 \sum_{r=1}^{i} M_r (\omega \delta_r)^2 \qquad 3\text{-}49a$$
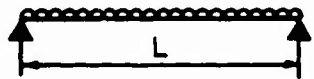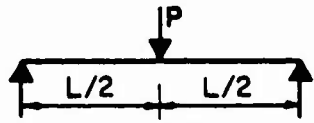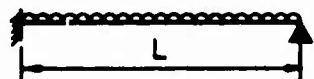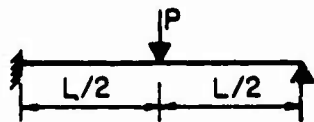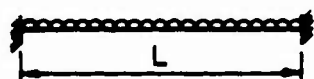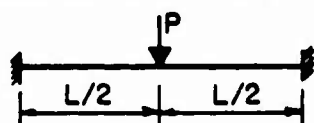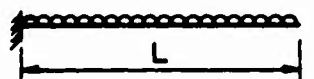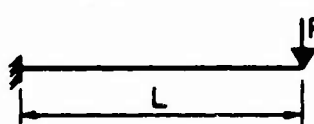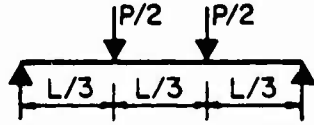
where

M_r = r^{th} mass
δ_r = deflection of mass r
i = number of lumped masses

rearranging terms

$$M_E = \sum_{r=1}^{i} M_r \varphi_r^2 \qquad\qquad 3\text{-}49b$$

- 76 -

Table 3-12 Transformation Factors for One-Way Elements

Edge Conditions and Loading Diagrams	Range of Behavior	Load Factor K_L	Mass Factor K_M	Load-Mass Factor K_{LM}
Simply supported, uniform load (L)	Elastic	0.64	0.50	0.78
	Plastic	0.50	0.33	0.66
Simply supported, concentrated load P at midspan (L/2, L/2)	Elastic	1.0	0.49	0.49
	Plastic	1.0	0.33	0.33
Fixed-simple, uniform load (L)	Elastic	0.58	0.45	0.78
	Elasto-Plastic	0.64	0.50	0.78
	Plastic	0.50	0.33	0.66
Fixed-simple, concentrated load P at midspan (L/2, L/2)	Elastic	1.0	0.43	0.43
	Elasto-Plastic	1.0	0.49	0.49
	Plastic	1.0	0.33	0.33
Fixed-fixed, uniform load (L)	Elastic	0.53	0.41	0.77
	Elasto-Plastic	0.64	0.50	0.78
	Plastic	0.50	0.33	0.66
Fixed-fixed, concentrated load P at midspan (L/2, L/2)	Elastic	1.0	0.37	0.37
	Plastic	1.0	0.33	0.33
Cantilever, uniform load (L)	Elastic	0.40	0.26	0.65
	Plastic	0.50	0.33	0.66
Cantilever, concentrated load P at free end (L)	Elastic	1.0	0.24	0.24
	Plastic	1.0	0.33	0.33
Simply supported, two concentrated loads P/2 at third points (L/3, L/3, L/3)	Elastic	0.87	0.52	0.60
	Plastic	1.0	0.56	0.56

An example of calculations for finding K_M can be found in Appendix A.

3-17.2.3 *Resistance Factor* . Resistance factor is the design factor by which the resistance of the actual structural element must be multiplied to obtain the resistance of the equivalent single-degree-of-freedom system. To obtain the resistance factor, it is necessary to equate the strain energy of the structural element, as computed from the assumed deflection shape, and the strain energy of the equivalent single-degree-cf-freedom system. If the computed total resistance of the structural element is R and the equivalent total resistance of the equivalent system is R_E, then the resistance factor is defined by the equation

$$K_R = R_E/R \qquad\qquad 3\text{-}50$$

Since the resistance of an element is the internal force tending to restore the element to its unloaded static position, it can be shown that the resistance factor K_R must always equal the load factor K_L.

3-17.3 *Load-Mass Factor*

The load-mass factor is a factor formed by combining the two basic transformation factors, K_L and K_M. It is merely the ratio of the mass factor to the load factor, and it is convenient since the equation of motion may be written in terms of that factor alone. The equation of motion of the actual system is given as

$$F - R = Ma \qquad\qquad 3\text{-}51$$

and for the equivalent system

$$K_L F - K_L R = K_M Ma \qquad\qquad 3\text{-}52a$$

which can be re-written as

$$F - R = (K_M/K_L)Ma \qquad\qquad 3\text{-}52b$$

or $\qquad F - R = K_{LM}Ma = M_e a \qquad\qquad 3\text{-}52c$

where $\qquad K_{LM}$ = load-mass factor

$$= K_M/K_L \qquad\qquad 3\text{-}53$$

and $\qquad M_e$ = effective total mass of the equivalent system

when expressed in terms of the unit area of the element, equation 3-52c can be written as

$$f - r = K_{LM}ma = m_e a \qquad\qquad 3\text{-}54$$

Values of load, mass and load-mass factors are presented in table 3-12. Equation 3-53 was used to calculate the load mass factor.

Instead of computing the several factors above, the load-mass factors in the elastic and elasto-plastic ranges can be determined by relating the primary mode of vibration of the member to that of an equivalent single-degree-of-freedom system. In the plastic range, it can be assumed that neither the

moment nor the curvature changes between the plastic hinges under increasing deflection. This behavior results in a linkage action, consideration of which can be used to evaluate the effective plastic mass as follows:

In figure 3-43, a portion of a two-way element bounded by the support and the yield line is shown. The equation of angular motion for this section is

$$\Sigma M = I_m \ddot{\theta} \qquad\qquad 3-55$$

where ΣM = summation of moments

I_m = mass moment of inertia about the axis of rotation

$\ddot{\theta}$ = angular acceleration

Substituting in equation

$$Fc - (\Sigma M_N + \Sigma M_p) = (I_m/L_1)a \qquad\qquad 3-56a$$

where a is the acceleration. Dividing through by c

$$F - (\Sigma M_N + \Sigma M_p)/c = (I_m/cL_1)a \qquad\qquad 3-56b$$

Since the second term is the resistance R

$$F - R = (I_m/cL_1)a = M_e a \qquad\qquad 3-56c$$

and the load-mass factor K_{LM} for the sector shown is

$$K_{LM} = I_m/cL_1 M \qquad\qquad 3-57$$

where c is the distance from the resultant applied load to the axis of rotation, L_1 is the total length of the sector normal to the axis of rotation and M is the total mass of the sector.

When the element is composed of several sectors, each sector must be considered separately and the contributions then summed to determine the load-mass factor for the entire element.

$$K_{LM} = \Sigma(I_m/cL_1)/M \qquad\qquad 3-58$$

For elements of constant depth and, therefore, of constant unit mass, the above equation can be written in terms of the area moment of inertia I and the areas A of the individual sectors.

$$K_{LM} = \Sigma(I/cL_1)/A \qquad\qquad 3-59$$

Table 3-13 gives the load-mass factors for the elastic and elasto-plastic response ranges for various two-way elements. The values given in the table apply for two-way elements of uniform thickness and supported as indicated. Also if there are openings in the element, they must be compact in shape and small in area compared to the total area of the element.

·
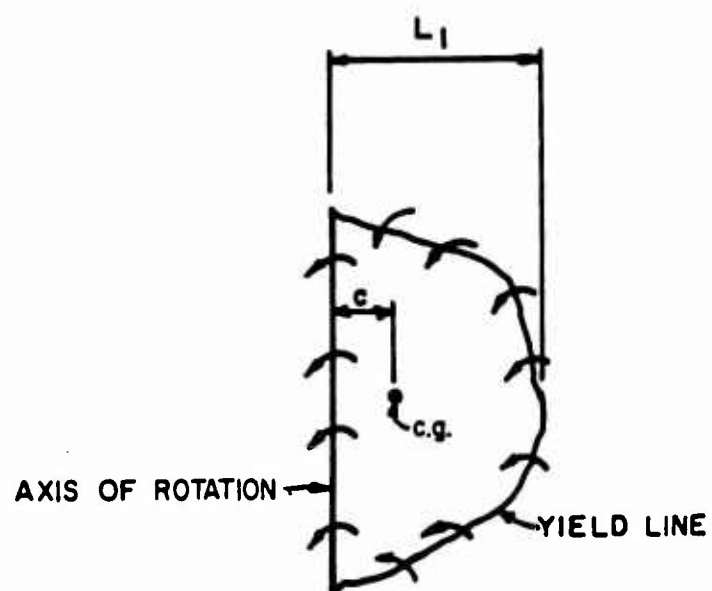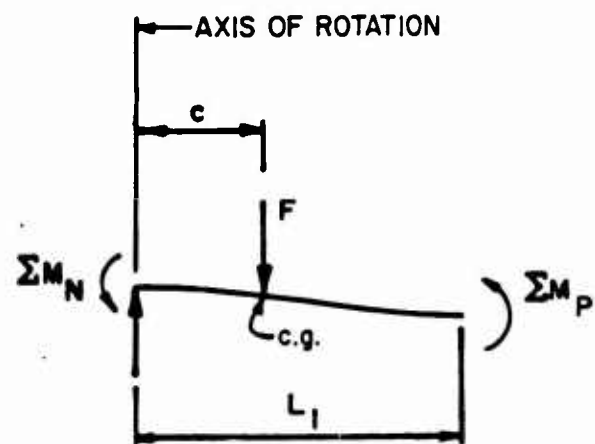
Figure 3-43   Determination of load-mass factor in the plastic range

Table 3-13   Load-Mass Factors in the Elastic and Elasto-Plastic Ranges for Two-Way Elements
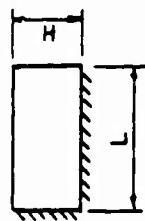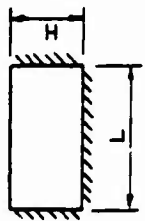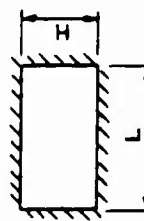
Support Conditions		Value of L/H	Elastic and Elasto - Plastic Ranges (Support Conditions)				
			All Supports Fixed	One Support Simple Other Supports Fixed	Two Supports Simple Other Supports Fixed	Three Supports Simple Other Supports Fixed	All Supports Simple
Two adjacent edges supported and two edges free		ALL	0.65	0.66	—	—	0.66
Three edges supported and one edge free		L/H<0.5	0.77	0.77	0.79	—	0.79
		$.5{\leq}L/H{\leq}2$	$0.65-0.16(\frac{L}{2H}-1)$	$0.66-0.144(\frac{L}{2H}-1)$	$0.65-0.186(\frac{L}{2H}-1)$	—	$0.66-0.175(\frac{L}{H}-1)$
		L/H ≥ 2	0.65	0.66	0.65	—	0.66
Four edges supported		L/H=1	0.61	0.61	0.62	0.63	0.63
		$1{\leq}L/H{\leq}2$	$0.61+0.16(\frac{L}{H}-1)$	$0.61+0.16(\frac{L}{H}-1)$	$0.62+0.16(\frac{L}{H}-1)$	$0.63+0.16(\frac{L}{H}-1)$	$0.63+0.16(\frac{L}{H}-1)$
		L/H ≥ 2	0.77	0.77	0.78	0.79	0.79

Figure 3-44 gives the load-mass factors for the plastic response of various two-way elements. The load-mass factors are a junction of support condition and yield line location. These two-way elements must conform to the following limitations:

    (1) Element must be of constant thickness.

    (2) Opposite support must provide the same restraint so that a symmetrical yield line pattern occurs.

    (3) Any openings must be compact in shape and small in area compared to the total area of the element.

3-17.4 *Natural Period of Vibration*

To determine the maximum response of a system either by numerical methods or design charts (both methods are described in Section 3-19), the effective natural period of vibration is required. This effective natural period of vibration, when related to the duration of a blast loading of given intensity and a given structural resistance, determines the maximum transient deflection X_m of the structural element.

The effective natural period of vibration is

$$T_n = 2\pi(m_e/K_E)^{1/2} = 2\pi(K_{LM}m/K_E)^{1/2} \qquad\qquad 3\text{-}60$$

where m_e = the effective unit mass

     K_E = the equivalent unit stiffness of system

The values used for the effective mass and stiffness for a particular element depends on the allowable maximum deflection. When designing for completely elastic behavior, the elastic stiffness is used. In all other cases the equivalent elasto-plastic stiffness, K_E, is used. The elastic value of the effective mass is used for the elastic range, while in the elasto-plastic range the effective mass is the average of the elastic and elasto-plastic values. For small plastic deflections, the value of the effective mass is equal to the average of the plastic value and the equivalent elastic value. The plastic effective mass is used for large plastic deflections.

DYNAMIC ANALYSIS

3-18 Introduction

Structural elements must develop an internal resistance sufficient to maintain all motion within the limits of deflection prescribed for the particular design. The load capacity of the member depends on the peak strength developed by the specific member (see Volumes IV and V) and on the ability of the member to sustain its resistance for a specific though relatively short period of time. This section describes the methods used for the analysis of structural elements subjected to dynamic loads, and these elements are divided into three groups, namely: (1) elements which respond to the pressure only (low pressure range), (2) elements which respond to pressure-time relationship
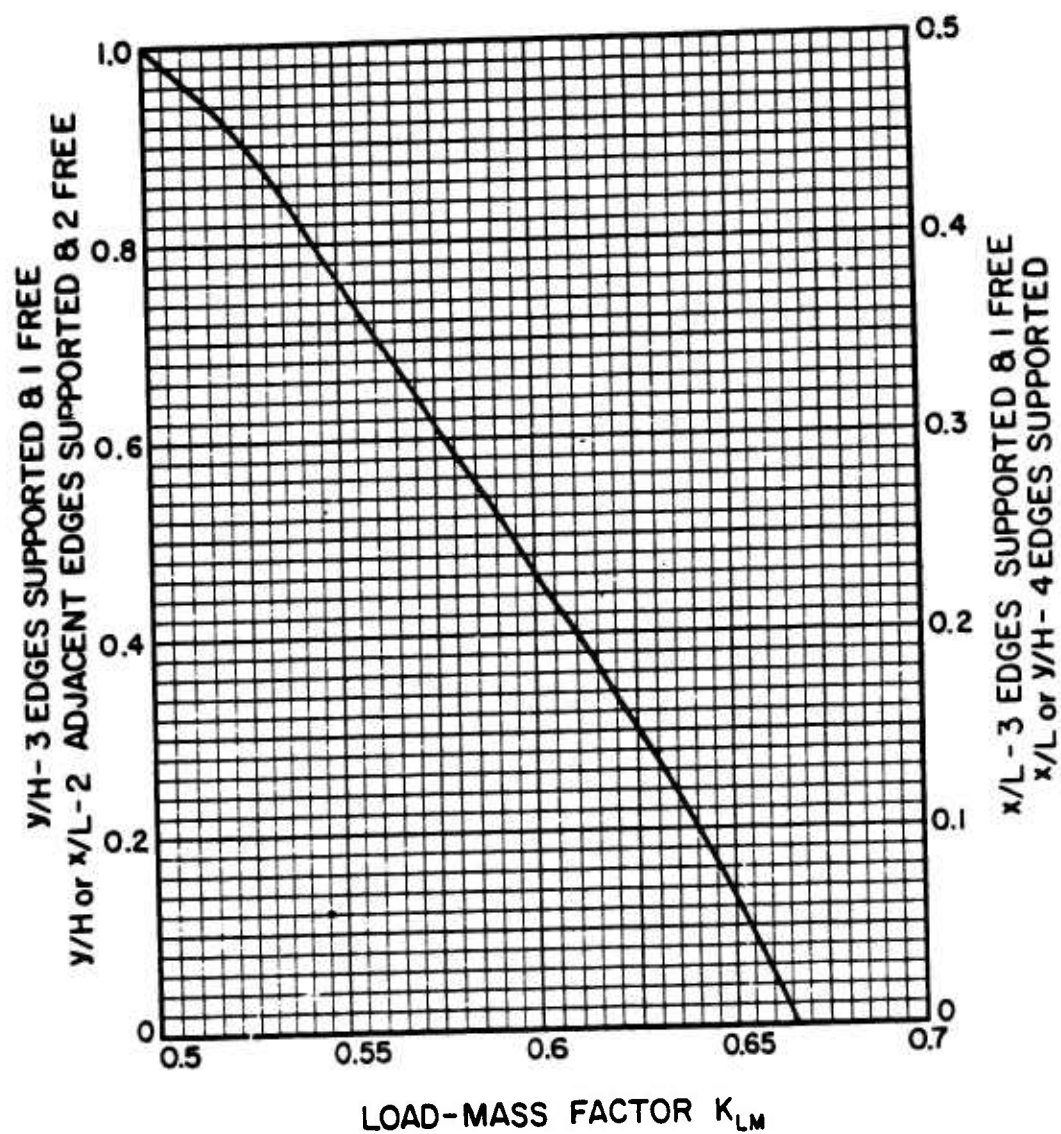
Figure 3-44   Load mass factors in plastic range for two-way elements

-83-

(intermediate-pressure design range) and (3) elements which respond to the impulse which corresponds to the high pressure design range.

The method of analysis is different for the groups of elements. Those elements that respond to pressure only (this is still a pressure-time relation) and those that respond to pressure-time relationship may be analyzed using either numerical methods or design charts, while elements that respond to the impulse are analyzed using either design charts for large deflection or an impulse method for designs with limited deflections.

The method of analysis employing numerical techniques provides a solution that is obtained by a step-by-step integration, and is generally applicable for any type of load and resistance function. This method of analysis is presented in this section. Also presented is the result of a systematic analysis of single-degree dynamic systems for several idealized loadings plotted in non-dimensional design charts.

3-19   Elements Which Respond to Pressure Only and Pressure-Time Relationship.
3-19.1   *General*

To analyze these elements, the true magnitudes for the pressure-time relationship of the applied blast loads must be known. The determination of the dynamic response of these systems is accomplished using numerical techniques or design charts which relate the dynamic properties of the element (natural period of vibration, resistance, and deflection) to those of the blast overpressures.

3-19.2   *Analysis by Numerical Methods*

The numerical method of analysis involves a step-by-step integration procedure, starting at zero time, when displacement and the velocity of the system are presumably known. The time scale is divided into several discrete intervals, and one progresses by successively extrapolating the displacement from one time station to the next. As the time interval in the sequence of time is reduced, i.e., as the number of discrete intervals is increased, the accuracy of the numerical method is improved.

3-19.2.1 *Single-Degree-Of-Freedom Systems* . As stated previously, a single degree of freedom system is one in which only one coordinate is essential to define its motion. The equation of motion for the single-degree-of-freedom system shown in figure 3-42 can be expressed as:

$$F - kx - cv = Ma$$ 3-61

when c = damping constant

There are several methods that can be used to numerically integrate equation 3-61, but the two procedures applied to this problem will be the average acceleration, and the acceleration-impulse extrapolation methods.

3-19.2.1.1 *Average Acceleration Method* . In the average acceleration method, the velocity and displacement at any time t are expressed as

$$v_t = v_{t-1} + 1/2 (a_t + a_{t-1}) \Delta t$$ 3-62

$$x = x_{t-1} + 1/2 \ (v_t + v_{t-1}) \ \Delta t \qquad\qquad 3\text{-}63$$

Substituting equation 3-62 into equation 3-63,

$$x = x_{t-1} + v_{t-1} \ \Delta t + 1/4 \ (a_t + a_{t-1}) \ \Delta t^2 \qquad\qquad 3\text{-}64$$

Substituting equations 3-62 and 3-63 into equation 3-61, we have

$$F - k \ [x_{t-1} + 1/2 \ (v_t + v_{t-1}) \ \Delta t] - c \ [v_{t-1} + 1/2 \ (a_t + a_{t-1}) \ \Delta t] = Ma \qquad 3\text{-}65$$

Equation 3-65 can be simplified to

$$a = \frac{1}{m + (1/2)c \ \Delta t + (1/4)k \ \Delta t^2} \quad [F - k \ (x_{t-1} + v_{t-1} \ \Delta t + 1/4 a_{t-1} \ \Delta t^2)$$

$$- c \ (v_{t-1} + 1/2 \ a_{t-1} \ \Delta t)] \qquad\qquad 3\text{-}66$$

The integrating procedure can be summarized as follows:

Step 1. At t = 0: Compute: a_0 using equation 3-61 and specified values for x_0(t = o), v_0(t = o), and F(t = o). .

Step 2. Increment time: t = t + Δt

Step 3. At t = t + Δt: Compute a(t = t + Δt) using equation 3-66, v (t = t + Δt) using equation 3-62 and x (t = t + Δt) using equation 3-63.

Step 4. Repeat steps 2 and 3 until some specified time or until the maximum displacement is reached.

It should be noted that if x (t = 0) and v (t = 0) are zero, then the system will not move as long as F (t = 0) is zero; however, if F (t = 0) is not zero, Equation 3-66 will give an acceleration and motion will start. Thus the system of equation is self-starting and requires no special starting provisions.

The procedure outlined above for an elastic single-degree-of-freedom system can be easily extended to accomodate elastic-plastic behavior. To do so, equation 3-61 is re-written to include the restoring force R which replaces the spring restoring force kx, Equation 3-61 becomes

$$F - R - cv = ma \qquad\qquad 3\text{-}67$$

Substituting equations 3-62 and 3-63 into equation 3-67, the following equation for acceleration is obtained:

$$a_t = \frac{1}{m + \frac{c \Delta t}{2}} \ [F - R - c \ (v_{t-1} + \frac{\Delta t \ a_{t-1}}{2}) \qquad\qquad 3\text{-}68$$

Unlike equation 3-66, equation 3-68 has a non-linear term R, and it depends on the displacement x at time t. Therefore, instead of using the direct integration approach as in the previous case, a predictor-corrector method is

utilized. Briefly, the displacement x at time t is estimated (predicted) and then corrected and covergence of this procedure can be obtained in a single iteration if the value of Δt is small enough. The step-by-step procedure is outlined as follows:

Step 1. At t = 0: Compute a_t (t = t_0) from equation 3-67 and the initial conditions.

Step 2. Increment time: t = t + Δt

Step 3. At t = t + Δt: Set $a_t = a_{t-1}$ (t - 1 = 0, initially)

Step 4. Compute v_t and x_t from equations 3-62 and 3-63

Step 5. Compute R

Step 6. Compute a_t from equation 3-68

Step 7. If you are in the predicting pass, return to Step 4, if in the correcting pass, set $x_{t-1} = x_t$, $v_{t-1} = v_t$, $a_t = a_{t-1}$ and go to Step 2.

3-19.2.1.2 *Acceleration Impulse Extrapolation Method* . Suppose the acceleration of the system is defined by figure 3-45a. The acceleration-impulse extrapolation method assumes that the actual acceleration curve can be replaced by a series of equally spaced impulses occurring at t_0, t_1, t_2, ..., t_n, as shown in figure 3-45b.

The magnitude of the acceleration impulse at t_n is given by

$$I(t_n) = a_n(\Delta t) \qquad\qquad 3-69$$

where t- t_1 - t_0 = t_2 - t_1 = . . . = t_n - t_{n-1}. This is shown in figure 3-45b. Since an impulse is applied at t_n, there is a discontinuity in the value of velocity at t_n. In the time interval from t_n to t_{n-1}, the velocity is constant and the displacement varies linearly with time. The velocity and displacement thus obtained are shown in figures 3-45c and 3-45d.

Suppose t_n^- and t_n^+ indicate the time immediately before and after the application of the impulse at t_n, and let v_n^- and v_n^+ indicate respectively the velocity at t_n^- and t_n^+; these two velocities are related by the following equation:

$$v_n^+ = v_n^- + a_n(\Delta t) \qquad\qquad 3-70$$

The relationship between x_{n-1} and x_n, and between x_n and x_{n+1} are given by:

$$x_n - x_n{-}1 = v_n^-(\Delta t) \qquad\qquad 3-71a$$

$$x_n{+}1 - x_n = v_n^+(\Delta t) \qquad\qquad 3-71b$$

Combining equations 3-70 and 3-71, the three successive displacements are related by:

$$x_{n+1} = 2x_n - x_{n-1} + a_n(\Delta t)^2 \qquad\qquad 3-72$$
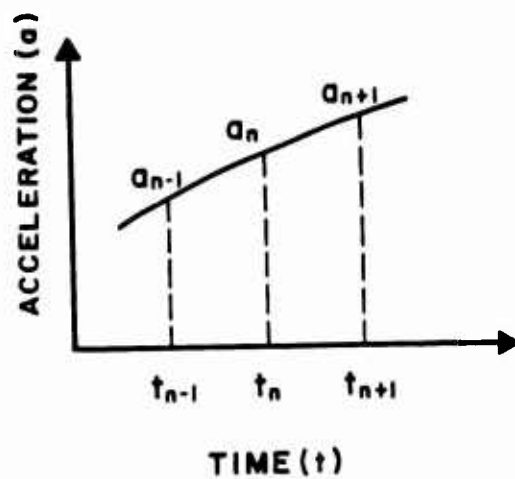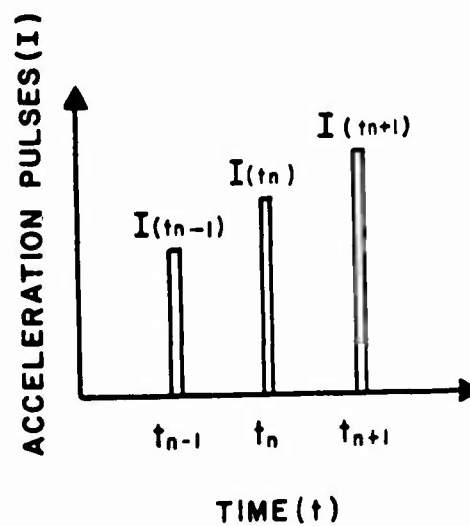
- 86 -
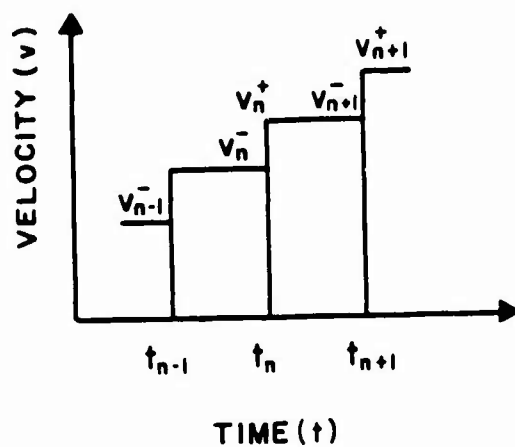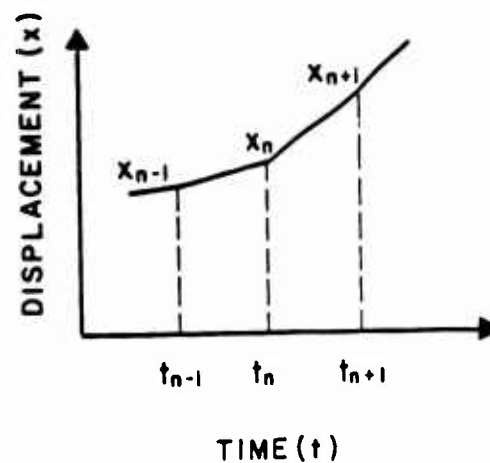
Figure 3-45   Acceleration-impulse extrapolation method

This is the basic recurrence formula for the acceleration impulse extrapolation method. Once the values of x at t_{n-1} and t_n are known, the value at t_{n+1} can be directly computed without resorting to a trial and error procedure.

It is necessary, however, to use a special procedure in the first time interval because, at $t = 0$, no value of x_{n-1} is available. Two different procedures may be used. The first assumes the acceleration varies linearly up to the first time station, in which case, the displacement of the system at that time can be expressed as:

$$x_1 = (1/6)(2a_0 + a_1)(\Delta t)^2 \qquad\qquad 3\text{-}73$$

The second procedure assumes that the acceleration is constant during the first time interval and is equal to the initial value. This assumption results in the following expression for x_1:

$$x_1 = (1/2)a_0(\Delta t)^2 \qquad\qquad 3\text{-}74$$

It should be noted that equation 3-73 has to be solved by trial and error since a_1 depends on x_1. This trial-and-error procedure can be avoided by taking the value of a_1 to be $f(t)/m$ instead of the exact value of $[f(t_1) - R(t_1)]/m$. In figure 3-46a if $a_0' = 0$, a_0 is equal to $a_0'/6$ and in figure 3-46b if a_0 and a_1 are approximately equal to each other, the value $a_0'/2$ may be used for a_0. The recurrence formula is directly applicable for the evaluation of x_2, x_3, ..., x_{n+1} whenever the acceleration is a continuous function. When there is a discontinuity in the acceleration, this equation can still be used but not before some modifications are made to reflect this discontinuity. In figure 3-46a there is a discontinuity at t_4 which occurs at the end of the time interval Δt. Under this condition, the value of a_n used in the numerical procedure is the average value at discontinuity, namely $1/2 (a_4' + a_4'')$ for a_4. In figure 3-46b the discontinuity occurs within time interval, t. The correct value for a_3 in this procedure is:

$$a_3 = (1/2)[a_3 + a_3'' + (a_3' - a_3'') (\Delta t'/\Delta t)^2] \qquad\qquad 3\text{-}75$$

When there are more than two discontinuities, this procedure becomes cumbersome and it is more convenient to replace the given acceleration by a smooth curve. Equation 3-73 must be used if there is zero force (and hence zero acceleration) at zero time, for in no other way can x_1 be determined. If acceleration at $t = 0$ is not zero, equation 3-74 may be used without appreciable error, provided the force does not change greatly in the first interval.

The tedious method of numerical analysis is made somewhat easier if the computation procedure is set up as shown in table 3-14. In the first time interval, the value used for the acceleration, a_0, depends on the forcing function. If the value of the forcing function is zero at time zero, then a_0 is taken as one-sixth of a_1, where a, is the ratio of the value of the forcing function at t, to the mass of the system $[a_0 = f(t_1)/6m]$. When the value of the forcing function is not zero at time zero, and if the values of the forcing function at times t=o and t=t_1 are approximately equal, then a_0 may be taken as $(P_0-R_0)/2$. The recurrence formula (equation 3-72) is used in the other intervals.
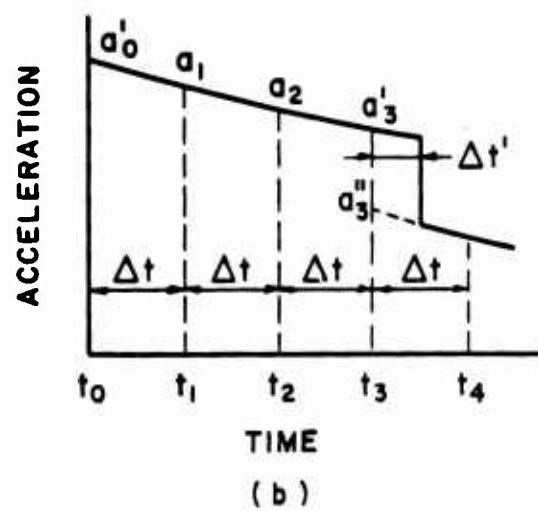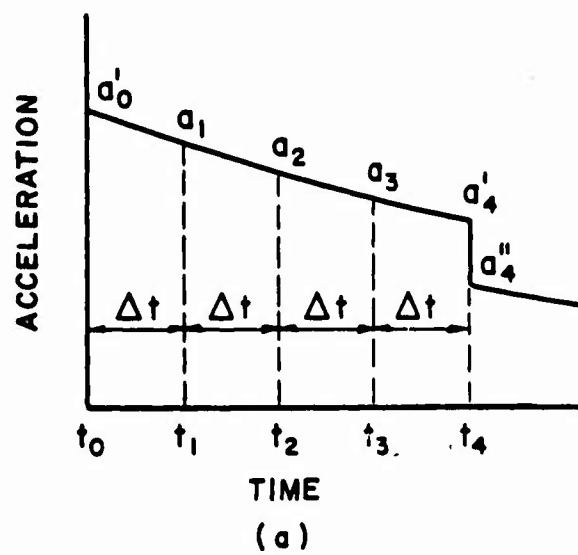
Figure 3-46   Discontinuities in the acceleration curve

Table 3-14 Details of computation by acceleration impulse extrapolation method.

n	t	P_n	R_n	$P_n - R_n$	$a_n = \dfrac{P_n - R_n}{m}$	$a_n(\Delta t)^2$	$2X_n$	X_{n-1}	X_{n+1}
0	0	P_0	R_0	$P_0 - R_0$	a_0	$a_0(\Delta t_1)^2$	O_1	0	X_1
1	Δt_1	P_1	R_1	$P_1 - R_1$	a_1	$a_1(\Delta t_1)^2$	$2X_1$	0	X_2
2	$2(\Delta t_1)$	P_2	R_2	$P_2 - R_2$	a_2	$a_2(\Delta t_1)^2$	$2X_2$	X_1	X_3
• • • • • •									
$j-1$	$(j-1)\Delta t_1$	P_{j-1}	R_{j-1}	$P_{(j-1)} - R_{(j-1)}$	a_{j-1}	$a_{j-1}(\Delta t_1)^2$	$2X_{j-1}$	X_{j-2}	X_j
j	$j\Delta t_1$	P_j	R_j	$P_j - R_j$	a_j	$a_j(\Delta t_1)^2$	$2X_j$	X_{j-1}	X_{j+1}
$j+1$	$j(\Delta t_1)+\Delta_2$	P_{j+1}	R_{j+1}	$P_{(j+1)} - R_{(j+1)}$	a_{j+1}	$a_{j+1}(\Delta t_2)^2$	$2X_{j+1}$	X_{j-1}	X_{j+2}

$P_n = f(t)$

$R_n = f(X_n)$

$X_{n+1} = 2X_n - X_{n-1} + a_n(\Delta t)^2$

$\Delta t_1 = T_N/10$

$\Delta t_2 = 2\Delta t_1$

It may be necessary during the computational procedure, to increase the value of t so as to reduce the number of time intervals. In figure 3-47, for example, the forcing function varies linearly after time j. For the next time station (j + 1)st, the value of Δt_1 can be increased ($\Delta t_2 = 2 \Delta t_1$ for example) without introducing any errors in the computations. In such cases, caution has to be exercised when using the recurrence formula. In table 3-14, the value of Δt changes after the jth step, to $\Delta t_2 = 2 \Delta t_1$. In the (j + 1)st step, x_{n-1} should be the value of x for the (j-1)nd step and x_n will be the value of x_{n+1} for the (j-1)st step.

3-19.2.2 *A Two-Degree-Of-Freedom System* . A two-degree-of-freedom system is shown in figure 3-48 where the coordinates defining the configuration of the system are X_1 and X_2. The equation of motion for each of the two masses can be expressed as follows:

$$F_1 + R_2 - R_1 = M_1 a_1 \qquad \text{3-76a}$$

$$F_2 - R_2 = M_2 a_2 \qquad \text{3-76b}$$

Equation 3-76 can be rewritten as:

$$a_1 = F_1/M_1 + R_2/M_1 - R_1/M_1 \qquad \text{3-77a}$$

$$a_2 = F_2/M_2 - R_2/M_2 \qquad \text{3-77b}$$

The integration procedures described for a single-degree-of-freedom system can also be applied to two-degrees-of-freedom systems. In the average acceleration procedure, if the equations are placed in the same form as equation 3-61, i.e., if the acceleration at time t are written in terms of displacements and velocities at time t - Δt, then two equations are obtained which must be solved simultaneously for a_1 and a_2. In the other numerical integration procedure, the recurrence formula (equation 3-72) applies to each of the two displacements independently.

3-19.2.3 *Damping* . The effects of damping are hardly ever considered in blast design because of the following reasons:

(1) Damping has very little effect on the first peak of response which is usually the only cycle of response that is of interest.
(2) The energy dissipated through plastic deformation is much greater than that dissipated by normal structural damping.
(3) Ignoring damping is a conservative approach.

If damping has to be considered in an analysis, however, it should be expressed as some percentage of critical damping. For free vibration, this is the amount of damping that would remove all vibration from the system and allow it to return to its neutral position. Critical damping is expressed as

$$C_{cr} = 2 \text{ kM} \qquad \text{3-78}$$

where   k = stiffness of the system

M = mass of system
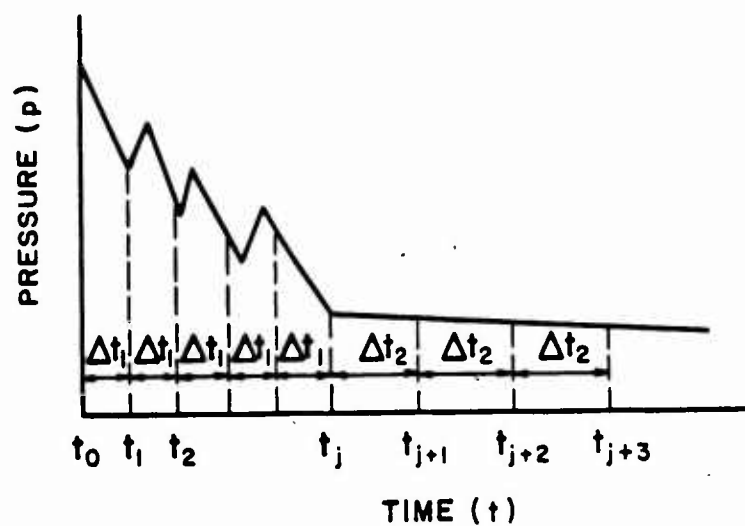
Figure 3-47   Pressure-time function with two different time intervals
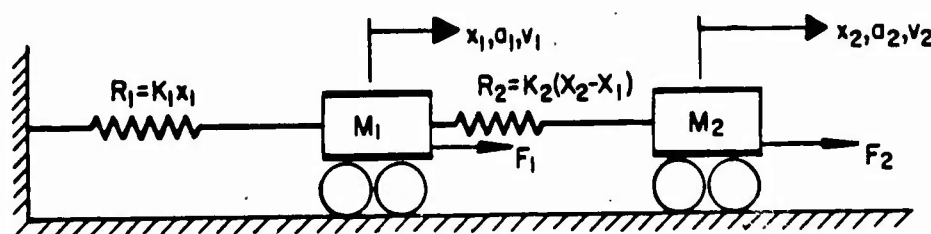
Figure 3-48   A two-degrees-of-freedom system

The damping coefficient, c, in equations 3-61 and 3-67 is expressed as a percentage of critical damping, C_{cr}. For steel structures, c should be taken as 0.05Cr and 0.01 C_{cr} for reinforced concrete structures.

3-19.3 *Design Charts for Idealized Loadings.*

3-19.3.1 *General* . The response of single-degree-of-freedom systems subjected to idealized blast loadings is presented in the form of non-dimensional curves. In order to utilize these response charts, both the blast loads (pressure - time history) and the resistance-deflection curve of the structural system are idealized to linear or bilinear functions. Methods for computing these idealized blast loads are given in Volume II while the methods for computing the resistance-deflection functions as well as converting the actual system to an elastic or elasto-plastic single-degree-of-freedom system have been presented in previous sections of this volume.

The response of a structural system subjected of a dynamic load is defined in terms of its maximum deflection X_m and the time t_m to reach this maximum deflection. The dynamic load is defined by its peak value P and duration T while the single-degree-of-freedom system is defined in terms of its ultimate resistance r_u, elastic deflection X_E and natural period T_N. Response charts relate the dynamic properties of the blast load (P and T) to those of the element (r, X, T_N), that is, X_m/X_E and t_m/T are plotted as a function of r_u/P and T/T_N.

Response charts have been prepared for simplified loads as well as for the more complex bilinear loadings. The simplified loadings include triangular, retangular, step load with finite rise time, triangular with rise time and sinusoidal pulse. The idealized triangular loading is utilized in the analyses of acceptor structures. These structures are subjected to the effects of unconfined explosions, such as free-air or surface bursts or partially confined explosions in donor structures which are fully vented. On the other hand, idealized instantaneously applied or gradually applied flat top loads are usually encountered in the design of roof elements of acceptor structures. These structures are subjected to very long duration loads produced by very large explosive quantities. The triangular loading with a rise time is similar to the previously mentioned triangular load except that it is an equivale.t loading produced by the blast traversing an element. The sinusoidal loadings is usually associated with the vibrational type of load rather than blast induced input. The bilinear loading is utilized in the analysis of containment structures which allow partial venting of an explosion and in the analysis of acceptor structures where reflected pressures clear rapidly around the structure.

The effects of damping have not been included in the preparation of the response charts. In the design of the blast resistant structures, the first peak of response is usually the only cycle of resonse that is of interet since the maximum resistance and deflection is attained in that cycle. Damping has very little effect on this first peak and consequently, neglecting damping has negligible effects on maximum response calculations.

3-19.3.2 *Maximum Response Of Linear Elastic System To Simplified Loads* . To obtain the response of a linear elastic system, it is convenient to consider the concept of the dynamaic load factor. This factor is defined as the ratio of the maximum dynamic deflection to the deflection which would have resulted

from the static application of the peak load P, which is used in specifying the load-time variation. Thus the dynamaic load factor (DLF) is given by:

$$DLF = X_m/X_s \qquad\qquad 3\text{-}79a$$

where X_s = static deflection or, in other words, the displacement produced in the system when the peak load is applied statically.

X_m = maximum dynamic deflection

Since deflections, spring forces, and stresses in an elastic system are all proportional, the dynamic load factor may be applied to any of these to determine the ratio of dynamic to static effects. Therefore, the dynamic load factor may be considered as the ratio of the maximum resistance attained to the peak load or:

$$DLF = r/p \qquad\qquad 3\text{-}79b$$

where r = maximum dynamic resistance
p = peak load used in specifying the load-time variation.

For a linear elastic system subjected to a simplied dynamic load, the maximum response is defined by the dynamic load factor, DLF and maximum response time, t_m. The dynamic load factor and time ratio t_m/T are plotted versus the time ratio T/T_N for a triangular load, rectangular load, step load with finite rise time (T_r), triangular load with rise time, and sinusoidal pulse in figures 3-49 through 3-53.

In many structural problems only the maximum value of the DLF is of interest. For the most prevalent load case, namely, the triangular load as well as the retangular and step load with rise time, the maximum value of the DLF is 2. This immediately indicates that all maximum displacements, forces, and stresses due to the dynamic load are twice the value that would be obtained from a static analysis for the maximum load P.

The above response charts apply for elastic systems. However, the charts can be applied to the entire elasto-plastic range if the actual resistance-deflection curve (two step system, three step system, etc.) is replaced by the equivalent elastic system where the equivalent elastic stiffness K_E and the equivalent elastic deflection X_E are obtained according to previously explained procedures.

In a typical design example, the pressure-time loading is calculated and idealized to one of the simplified loads defined by P and T or T_r. A structural member is assumed and its corresponding dynamic properties are calculated. For a completely elastic response, the values of r_e and T_N are calculated while for a response in the elasto-plastic range, r_u, X_E and T_N are obtained. It should be noted that for a response in the elasto-plastic range, the value of T_N is calculated using the effective mass which is an average of the elastic and elasto-plastic values. Knowing the ratio of T/T_N, the dynamic load factor (DLF) and the time ratio t_m/T can be read from the appropriate figures. The maximum resistance r attained by the structural member is calculated from the DLF and the response time is obtained from the time ratio. If the resistance r is greater than r_e for a completely elastic response in the elasto-plastic range, then the analysis is not valid and the
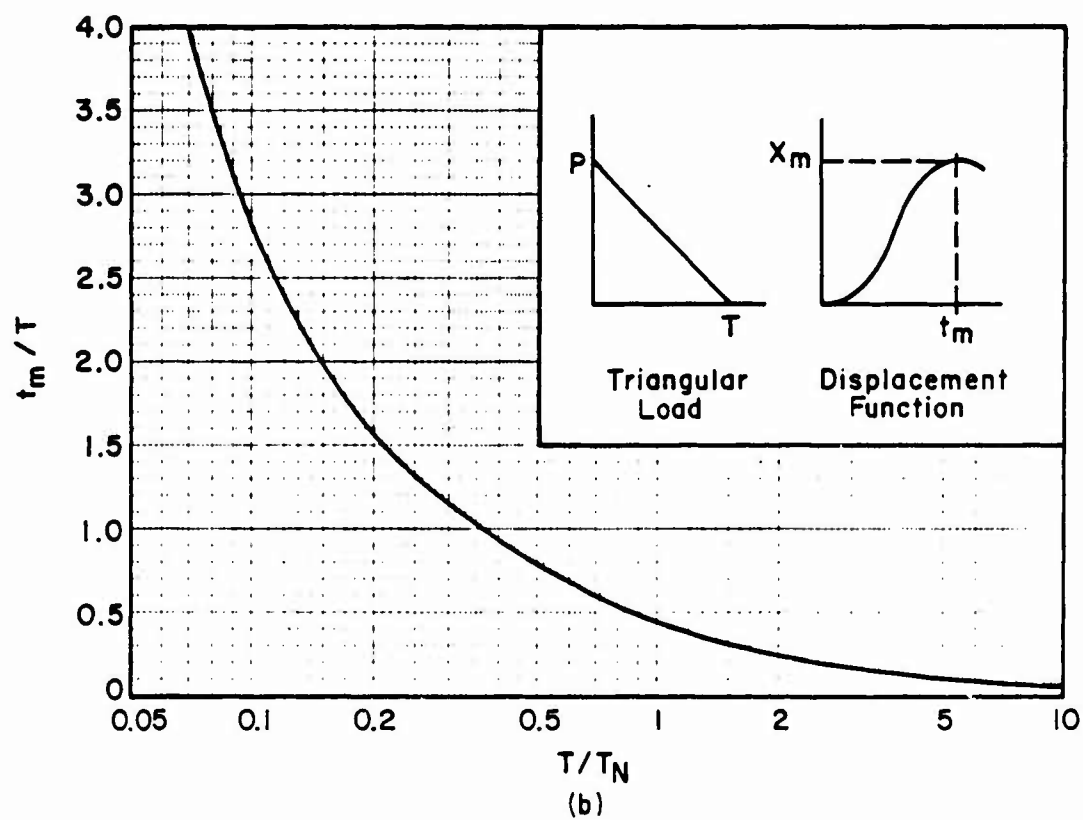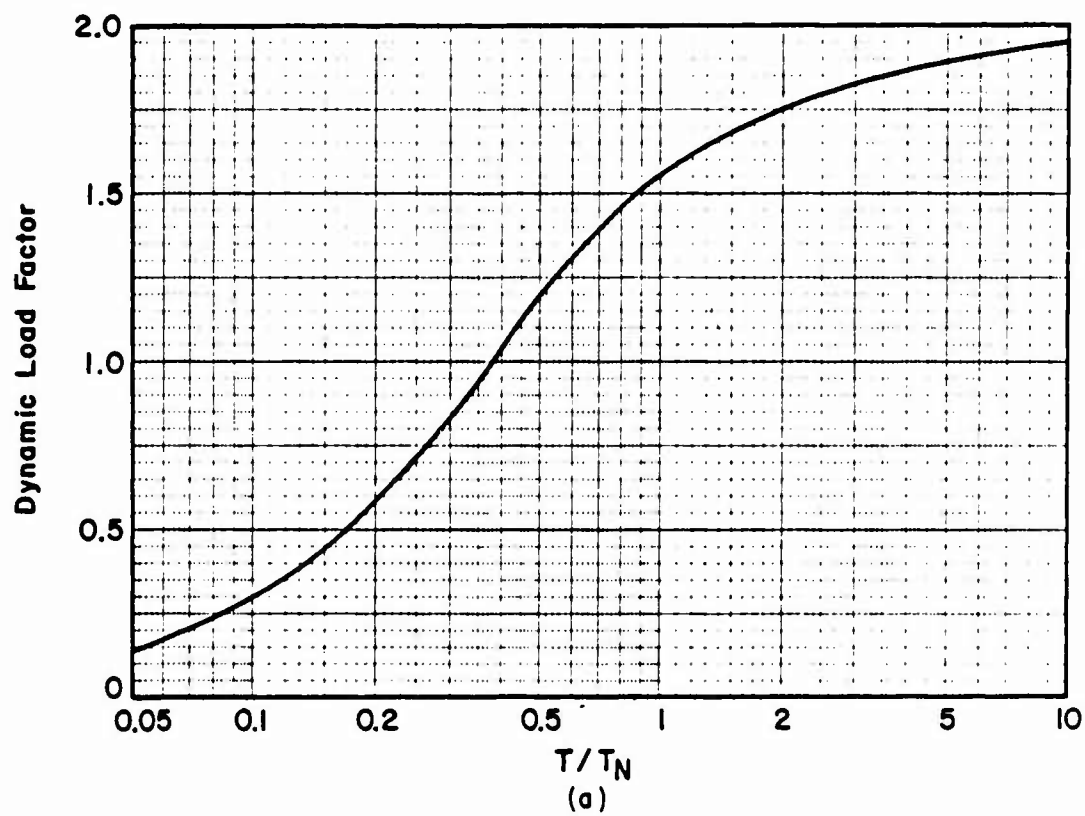
Figure 3-49   Maximum response of elastic one-degree-of-freedom system for triangular load

-96-
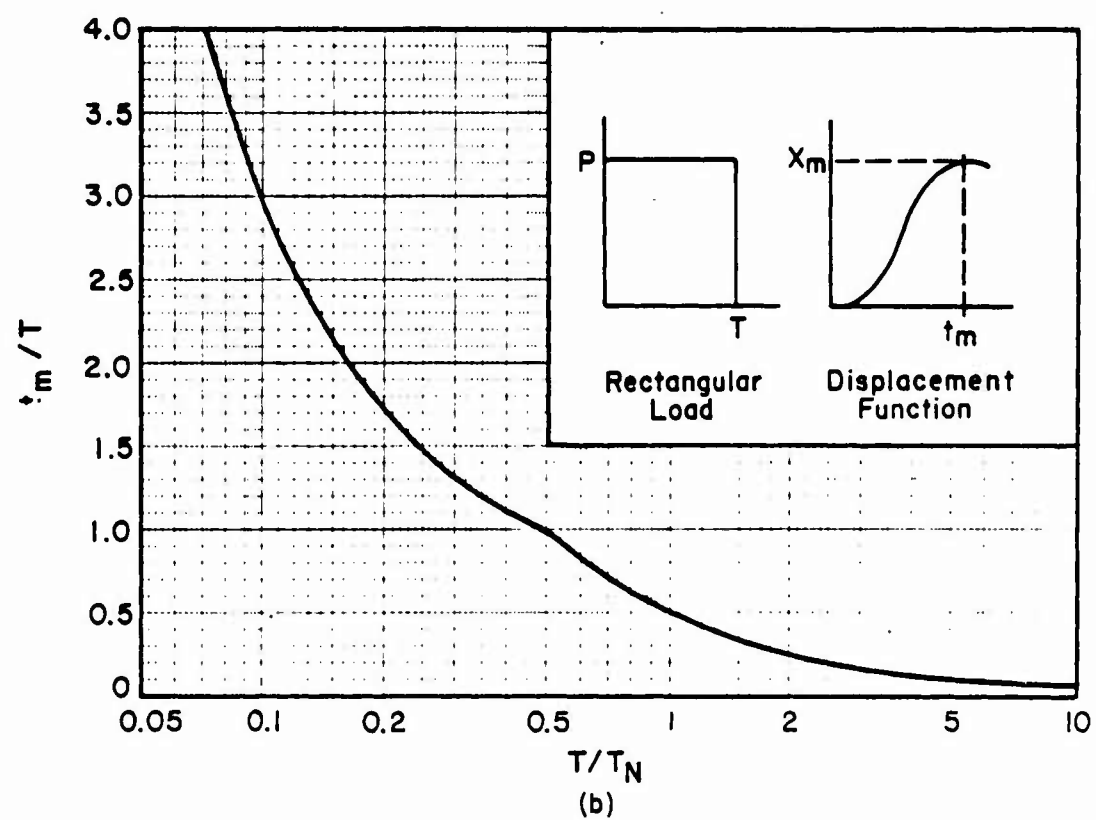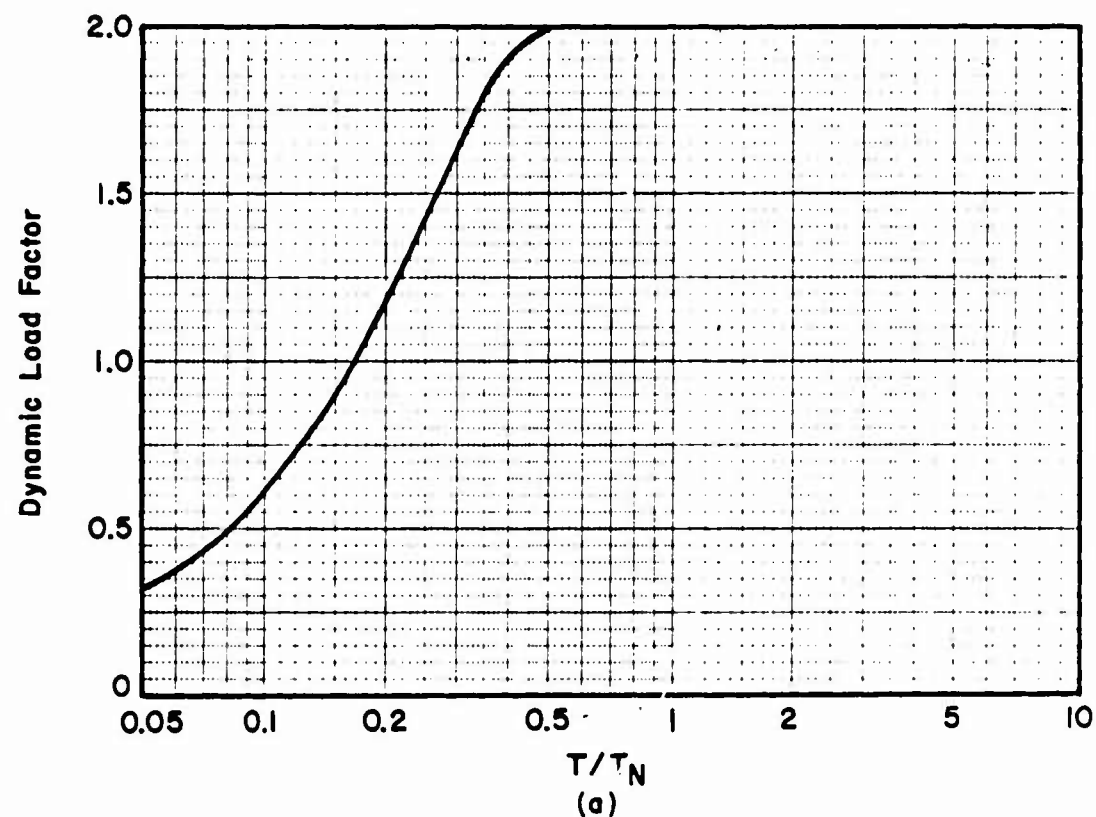
Figure 3-50   Maximum response of elastic, one-degree-of-freedom system for rectangular load
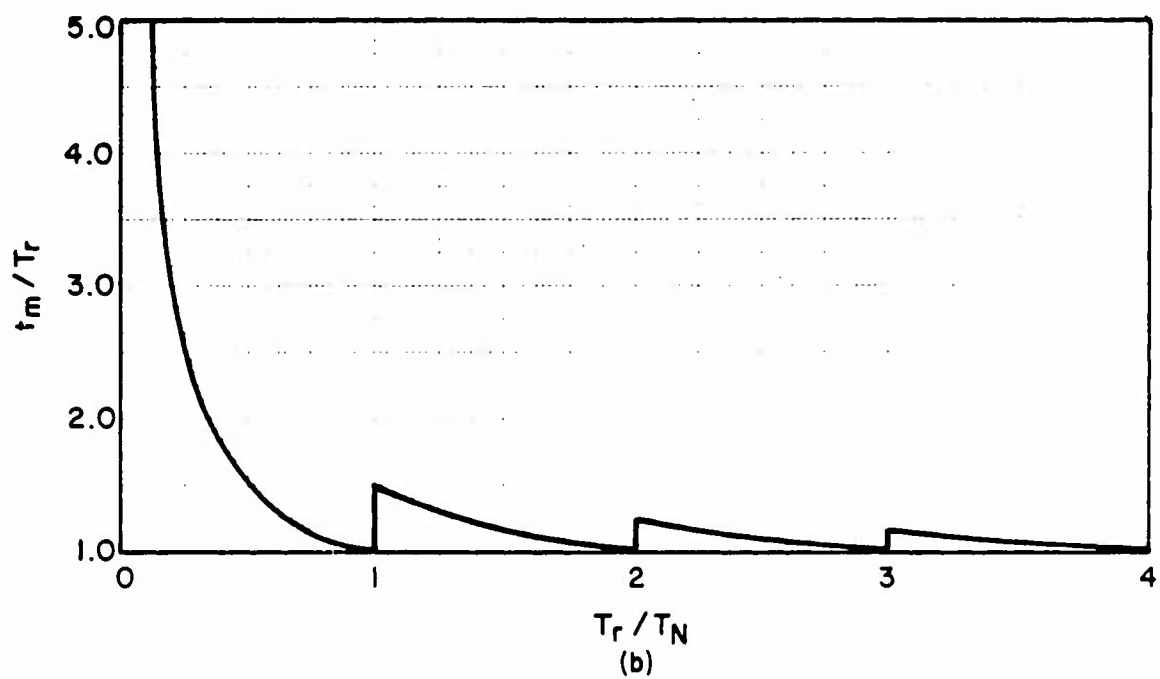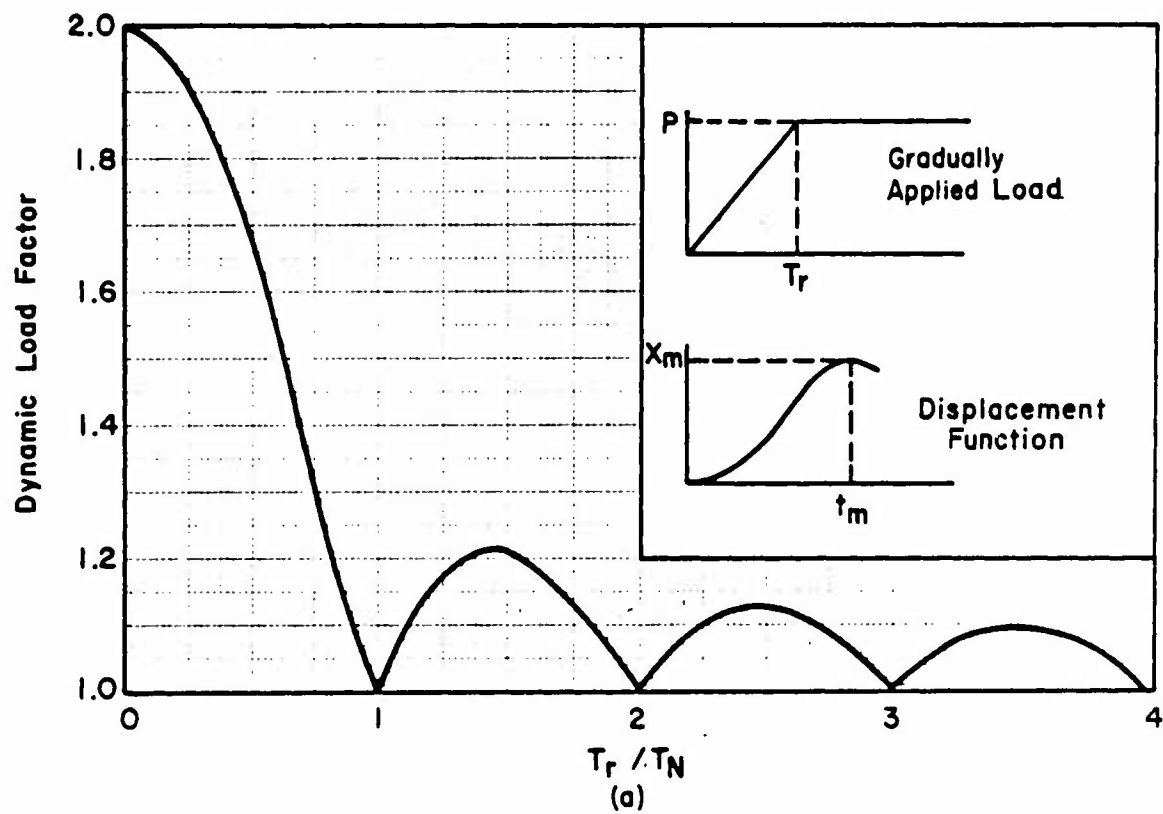
Figure 3-51   Maximum response of elastic, one-degree-of-freedom system for gradually applied load
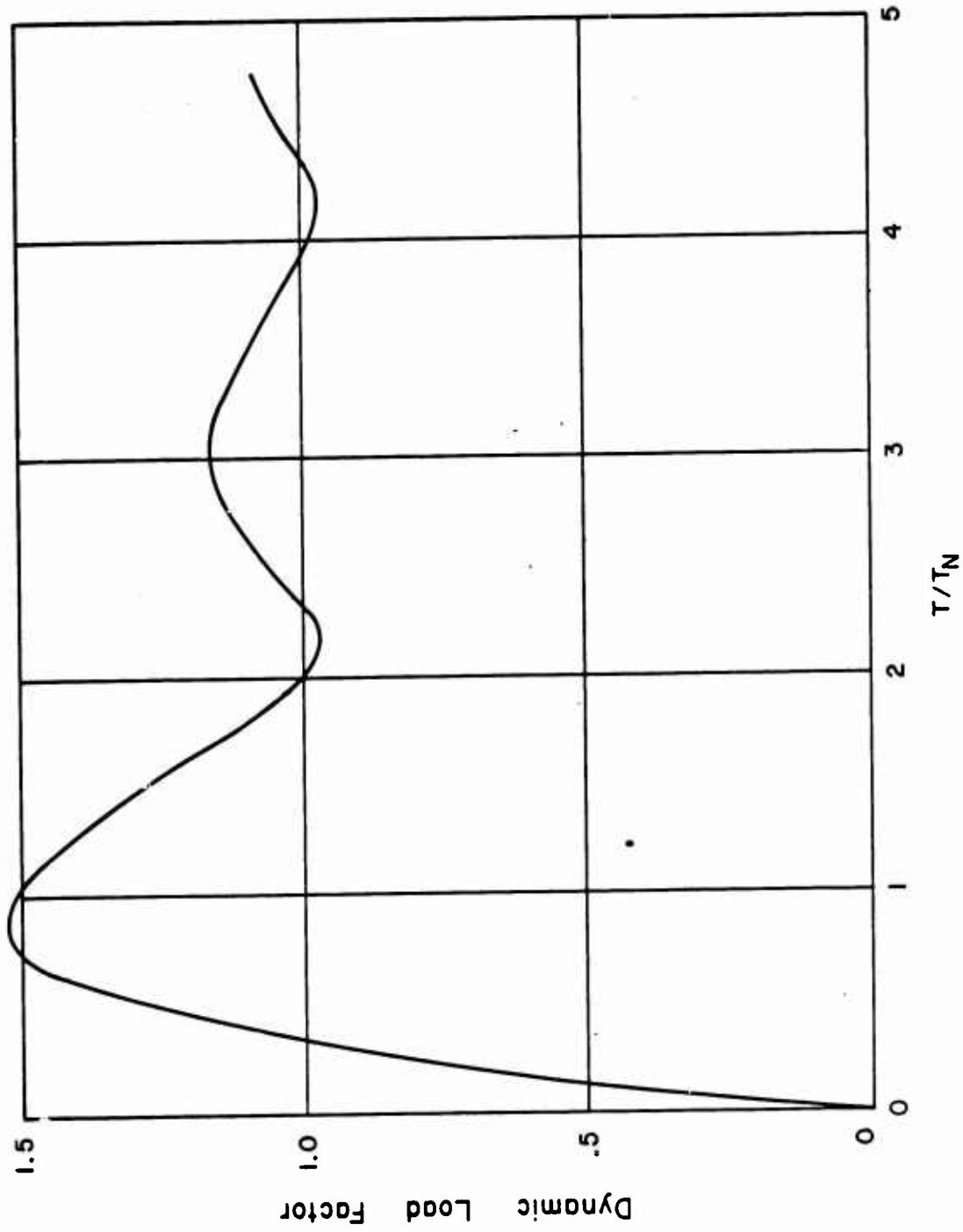
Figure 3-52   Maximum response of elastic one-degree-of-freedom system for triangular pulse load
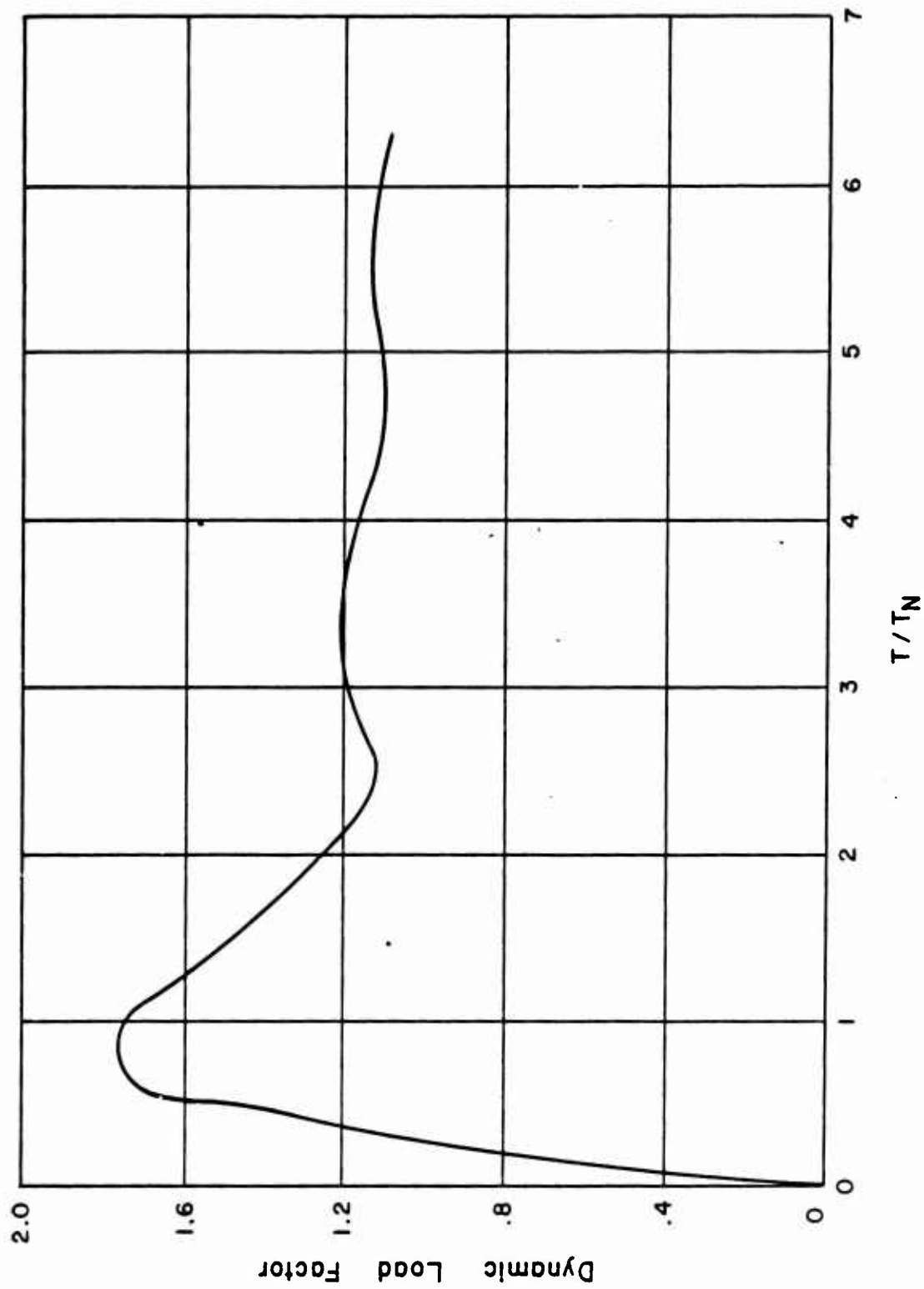
Figure 3-53   Maximum response of elastic one-degree-of-freedom system for sinusoidal pulse load

-100-

procedure is repeated. The maximum deflection is obtained from the resistance r and the stiffness K_e or K_E.

3-19.3.3 *Maximum Plastic Response Of An Elasto-Plastic System To Idealized Loads*. An elasto-plastic system may have an elastic or plastic response depending upon the magnitude of the blast load. If the response is elastic, that is, the member attains a resistance r which is less than its ultimate resistance r_u, then the charts of the preceding section are used. The response charts presented in this section are only for the plastic response of members where the ultimate resistance r_u is attained.

The maximum plastic response of an elasto-plstic system subjected to a blast load is defined by the maximum deflection, X_m it attains and the time, t_m it takes to reach this deflection. The blast load is defined by its peak value P and duration T while the singe-degree-of-freedom system is defined by its ultimate resistance r_u, elastic deflection X_E and natural period T_N. A non-dimensional response chart is constructed by plotting the ductility ratio X_m/X_E and the time ratio t_m/T as a function of r_u/P and T/T_N. Response charts are given for a triangular load, retangular load, step load with finite rise time T_r and triangular load with rise time in figures 3-54 through 3-61. It should be noted that for the step load with finite rise time, the load is defined by the rise time T_r and, consequently, the response curves are plotted using T_r rather than T.

In a typical example, the pressure-time loading is calculated and idealized to one of the simplified loads defined by either P and T or P and T_r. A structural member is assumed and is corresponding dynamic properties (r_u, X_E, T_N) are calculated. Knowing the ratios of r_u/P and T/T_N (or T_r/T_N), the ductility ratio X_m/X_E and the time ratio t_m/T can be read from the appropriate figures. The maximum deflection X_m and response time t_m can readily be calculated. If the ductility ratio X_m/X_E or the maximum deflection X_m and corresponding response time t_m are unsatisfactory, the procedure is repeated.

It should be noted that the value of the natural period of vibration T_N used in conjuntion with the response charts varies according to the magnitude of the ductility ratio X_m/X_E. For small plastic deformations (X_m/X_E less than 5), the calculations of T_N is based on an average of the equivalent elastic and plastic masses. Whereas, for larger plastic deformations (X_m/X_E greater than 5), the equivalent plastic mass is used to obtain T_N.

3-19.3.4 *Maximum Plastic Response Of An Elasto-Plastic System to Idealized Bilinear Loads*. Response charts have been prepared for bilinear loads in much the same manner as for simplified loads. However, four parameters are required to define the bilinear loading rather than two parameters which are required for the simplified loads. These additional parameters greatly increase the number of charts required for the rapid prediction of the dynamic response of an elasto-plastic system. However, the computational procedures remain comparatively simple.
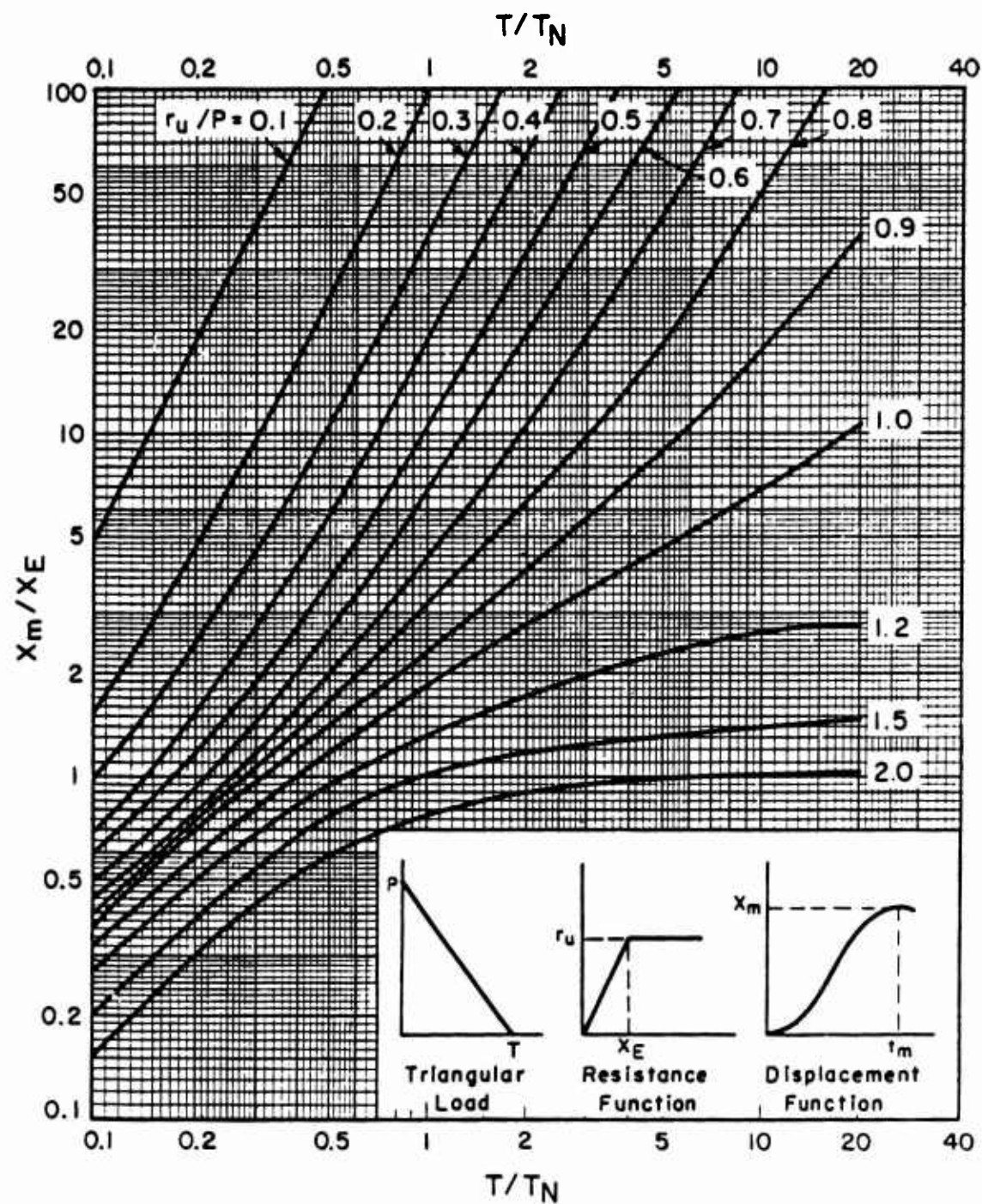
Figure 3-54   Maximum deflection of elasto-plastic, one-degree-of-freedom system for triangular load

-102-
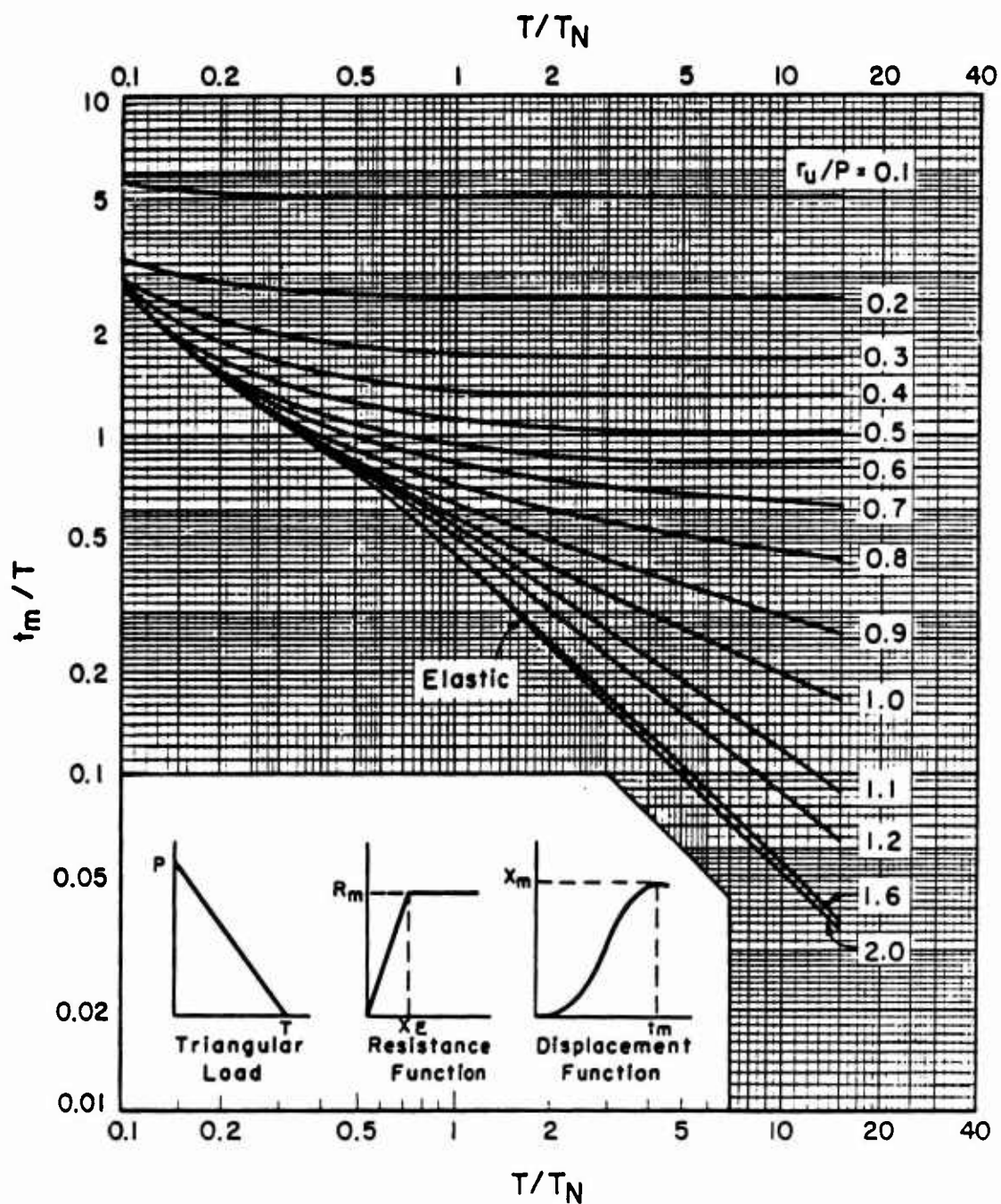
Figure 3-55   Maximum response time of elasto-plastic, one-degree-of-freedom system
for triangular load
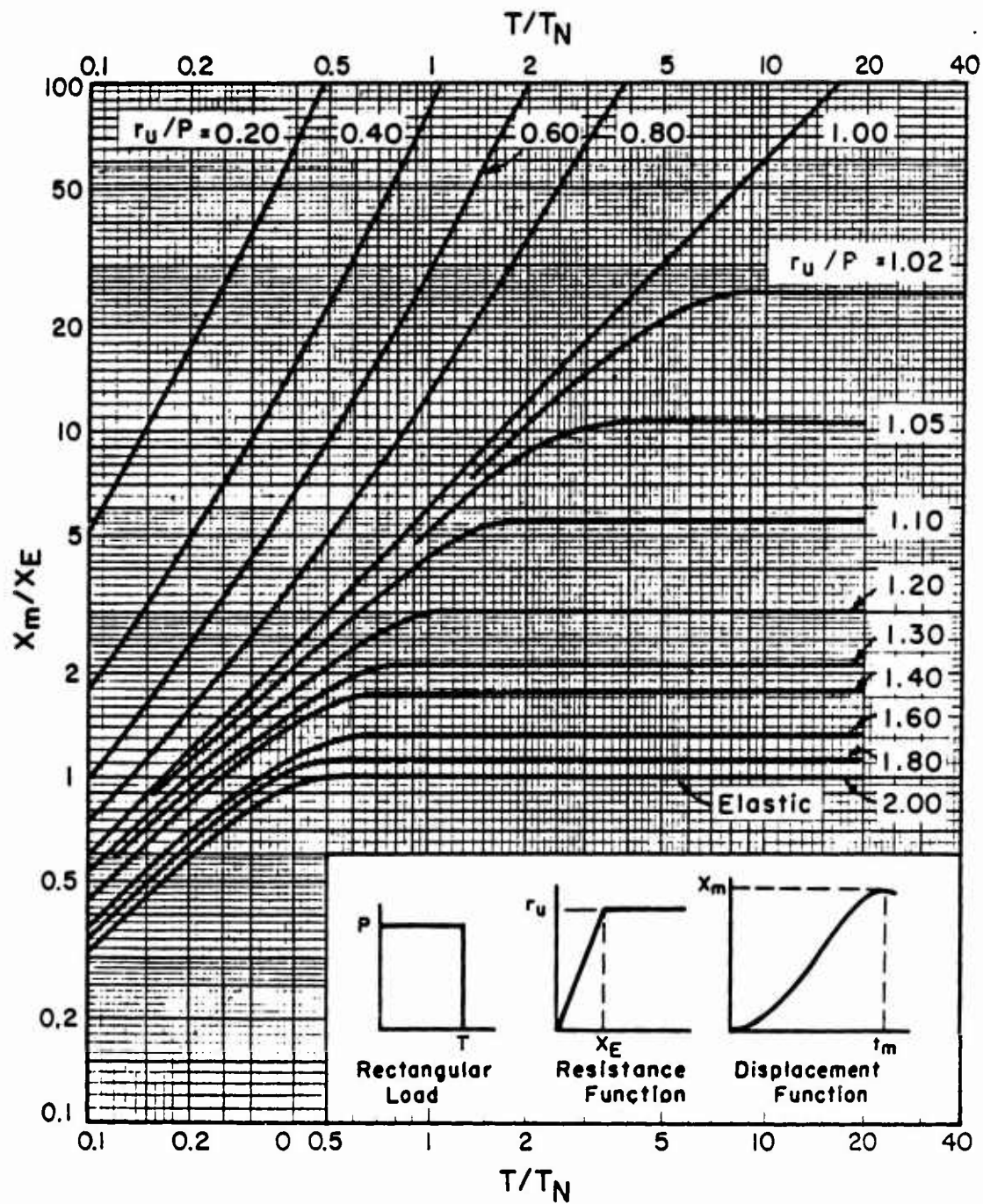
Figure 3-56   Maximum deflection of elasto-plastic, one-degree-of-freedom system for rectangular load

-104-
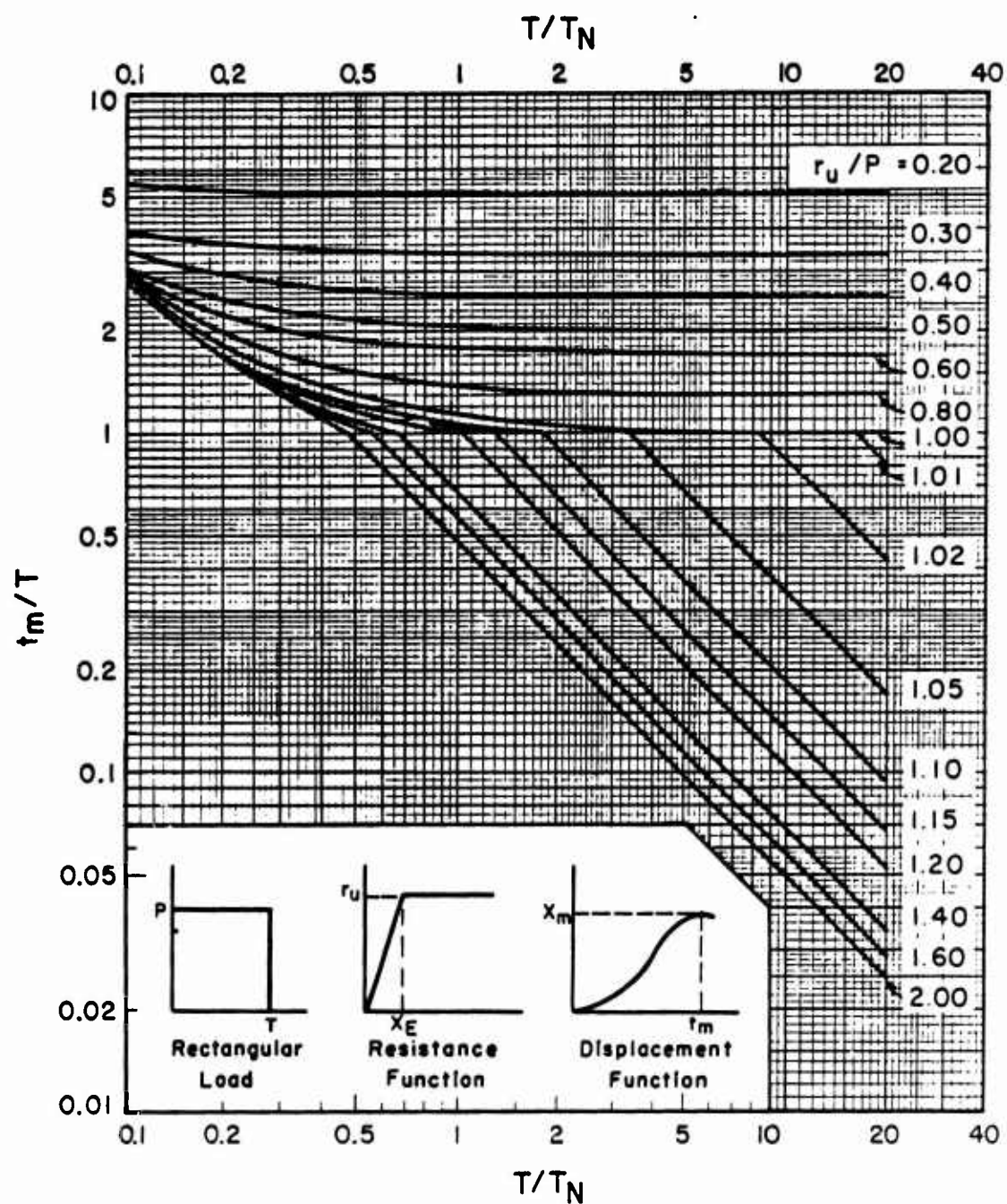
Figure 3-57   Maximum response time of elasto-plastic, one-degree-of-freedom for rectangular load
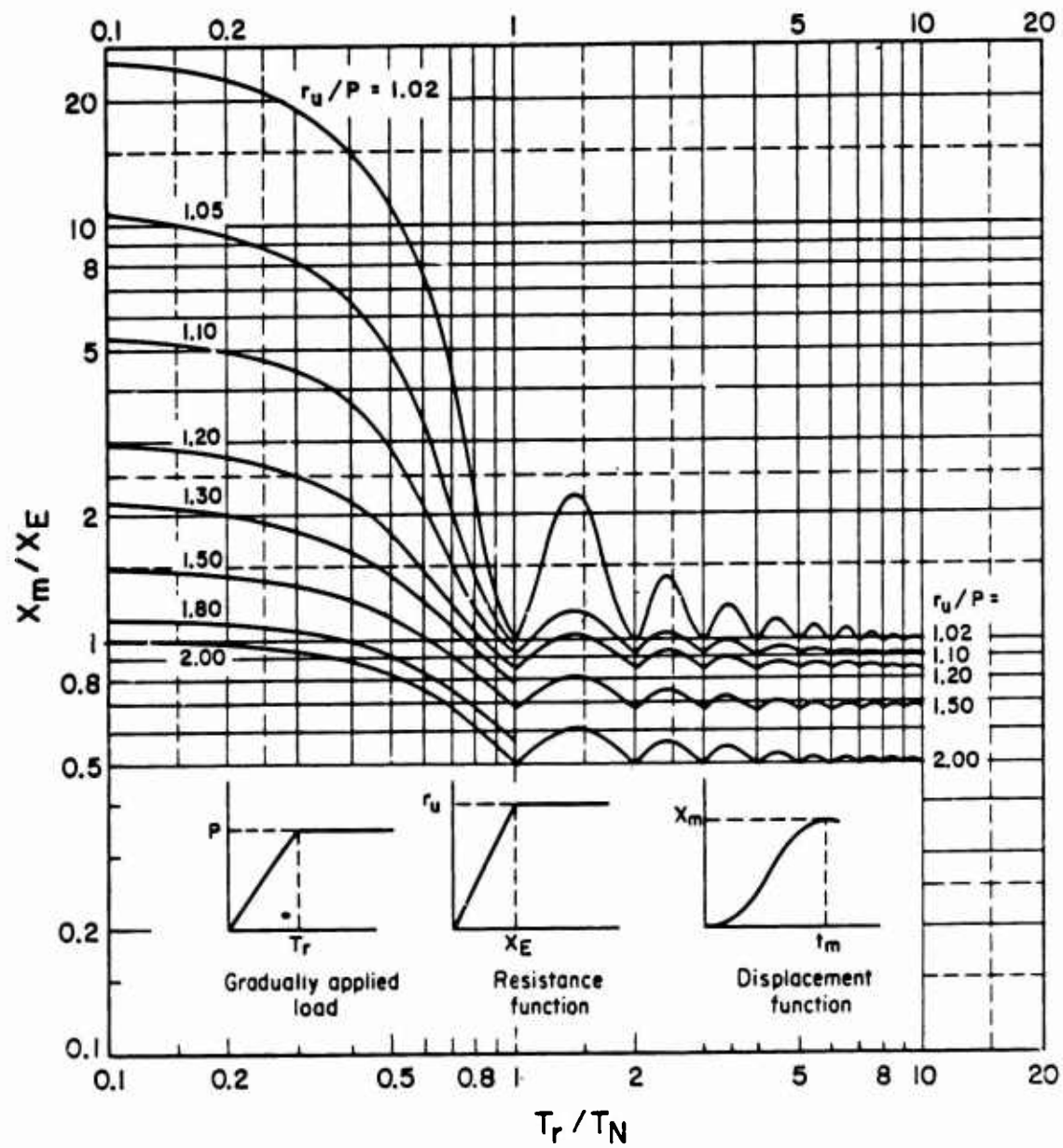
Figure 3-58   Maximum deflection of elasto-plastic, one-degree-of-freedom system
                for gradually applied load
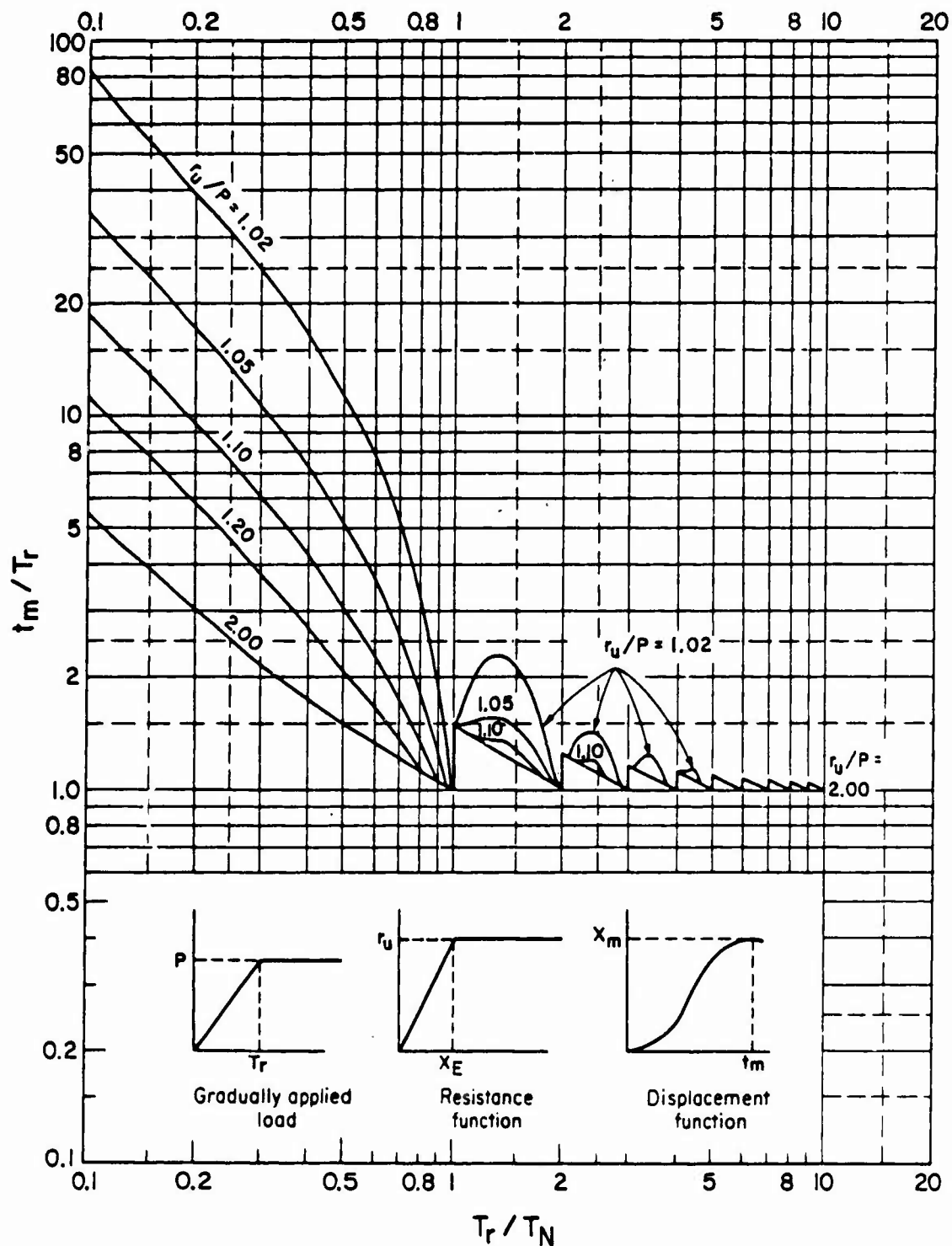
Figure 3-59   Maximum response time of elasto-plastic, one-degree-of-freedom system
for gradually applied load

-107-
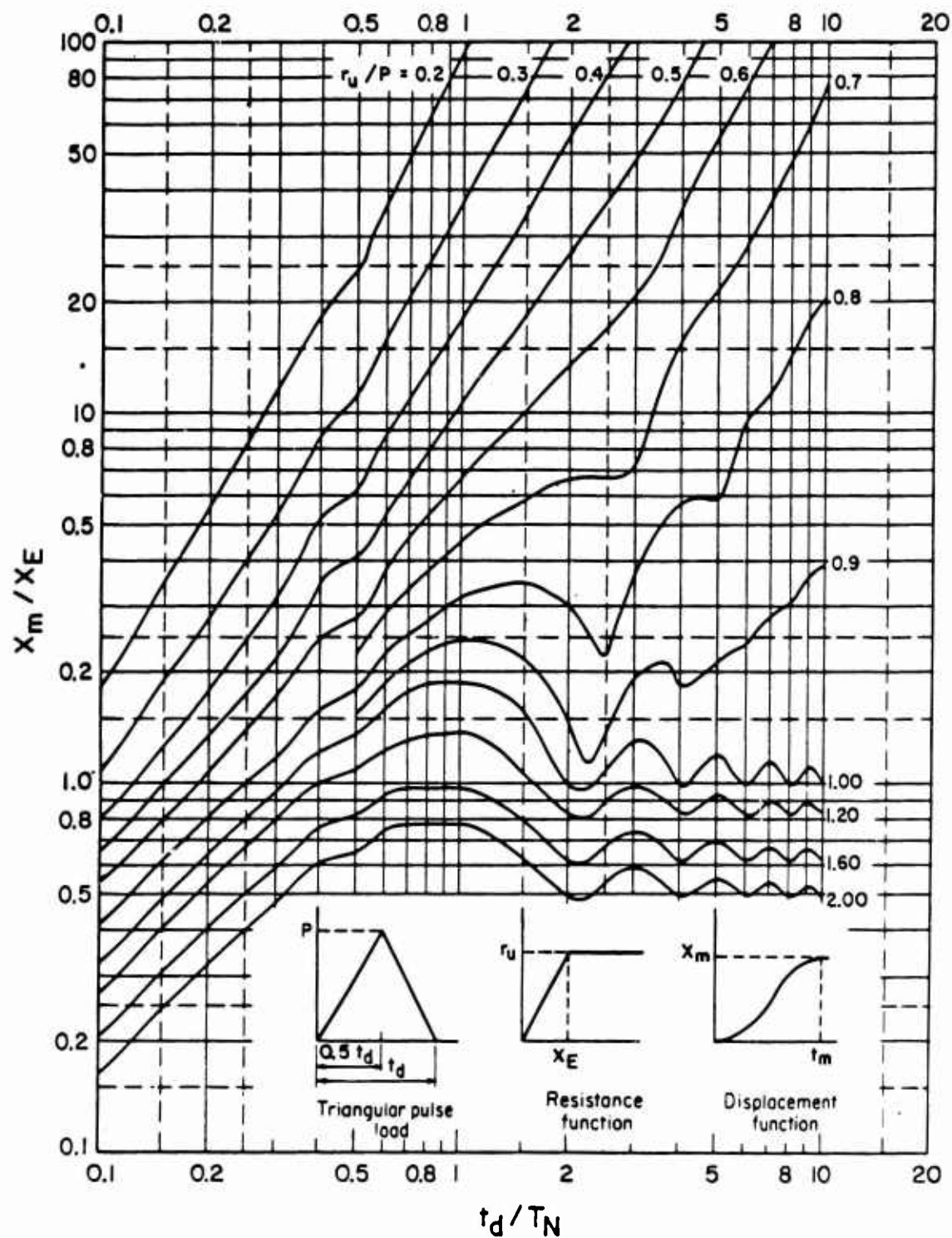
Figure 3-60   Maximum deflection of elasto-plastic, one-degree-of-freedom system for triangular pulse load
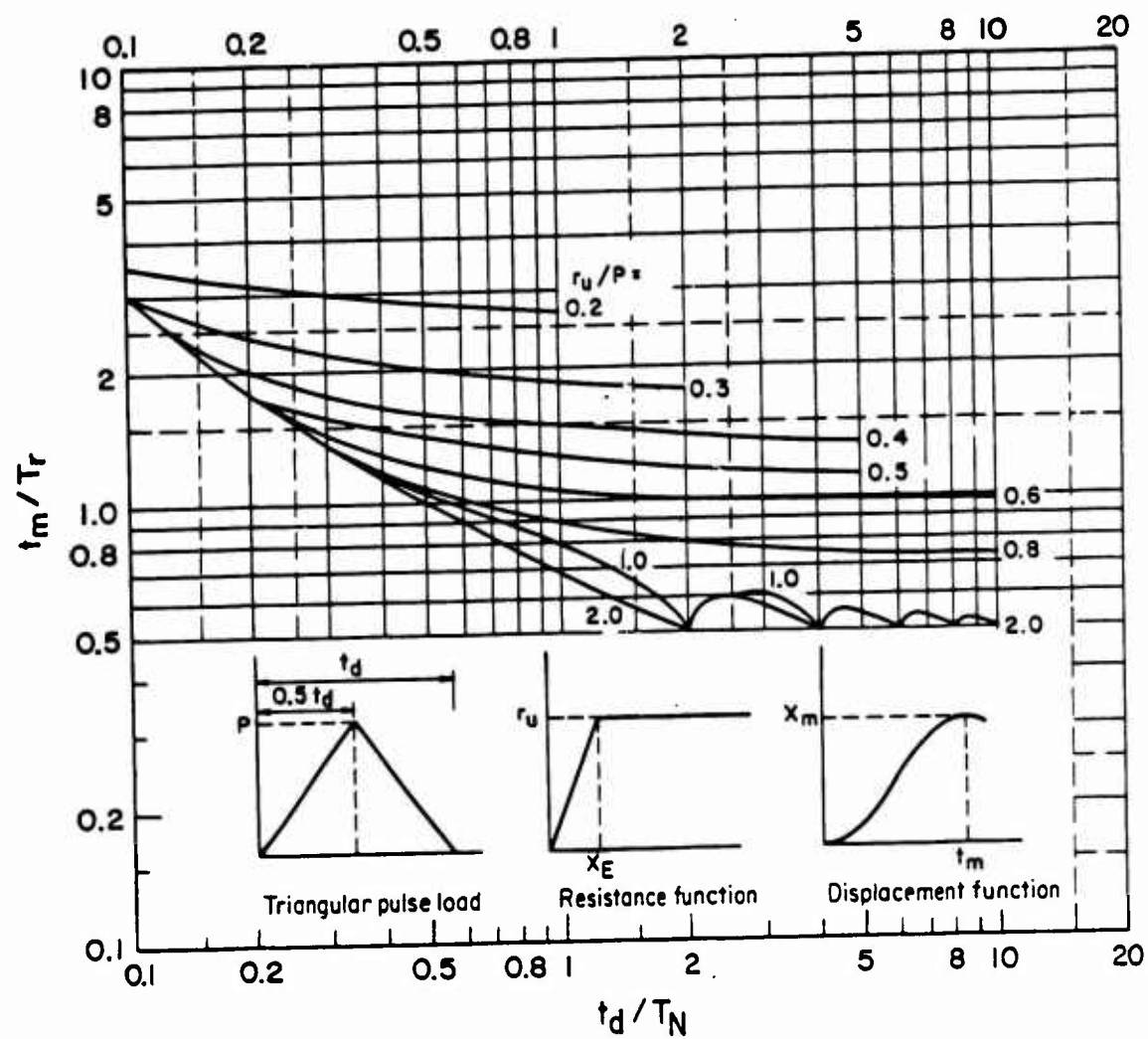
Figure 3-61   Maximum response time of elasto-plastic, one-degree-of-freedom system
for triangular pulse load

A bilinear load is illustrated in figure 3-62c. Four parameters are required to define this load shape, namely:

P = peak pressure of shock load (primary pulse)
C_1P = peak pressure of gas load (secondary pulse)
T = duration of shock load
C_2T = duration of gas load

It can be seen from figure 3-62c that the value of C_1 will always be less than 1 while the value of C_2 will always be greater than 1.

Response charts for the bilinear load are prepared in the same way as the simplified loads except that each chart is prepared for a given value of C_1 and C_2. The ductility ratio X_m/X_E versus T/T_N is plotted on each chart for various values of P/r_u, t_m/T_N and t_E/T (where t_E is the time to reach the maximum elastic deflection X_E). Therefore, each chart contains three families of curves. In addition, each chart contains one, two or three boundaries which are formed by symbols. These boundaries delineate regions of each chart where certain approximations are preferable to chart interpolation. These approximations involve modification of the bilinear load for the various regions. The loads considered for each of the regions are given in figure 3-62 while the boundary for the various regions are defined in figure 3-63.

Numerous response charts are required for bilinear loads. Table 3-15 lists the figure numbers of the response charts prepared for the selected values of C_1 and C_2. These response charts are presented in figures 3-64 through 3-266.

To use the response charts, the first step is to enter table 3-15 with the required values of C_1 and C_2. Locate the points in the table with coordinates C_1 and C_2. The number in the box containing the point is the appropriate figure number to use to solve the problem. If the point is not located in a box having a number, the two or, more frequently, four number bracketing the point are the appropriate figure numbers to use. Interpolation for the required values of C_1 and C_2 must be performed. A graphical and mathematical interpolation proceudre is presented in subsequent sections.

In a typical design, a structural member is assumed and the idealized resistance function defined by r_u, X_E and K_E can be determined along with the natural period. As previously explained for simplified loads; the equivalent mass used to calculated T_N varies according to the amount of plastic deformation. Knowing the ratio of P/r_u and T/T_N, note if the intersection point corresponding to these parameters, is located in region A,B,C or D on the response chart(s) for the required values of C_1 and C_2. The boundaries for these regions are represented by a line of asterisks, solid circles, and solid squares, as illustrated in figure 3-63.

The final step in obtaining the solution depends on which region of the response chart(s) is applicable. These regions were established to reduce the amount of calculations required for a solution by eliminating, where possible, interpolation between charts. Except for one of the four regions, the actual bilinear blast load is replaced by a simplified load. Solution of the response for these simplified loads will predict a solution which is within 10 percent of the exact solution. Of course, the exact solution of the response for the structural member in these three regions can be obtained by using the required response charts and interpolating, where required, between charts.

- 110 -
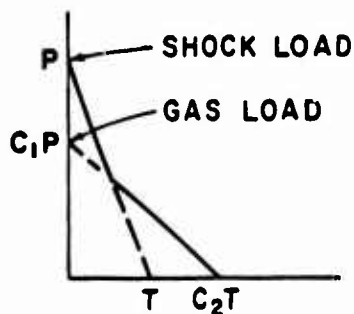
REGION A : NEGLECT CHARTS
USE EQUATIONS 3-80 AND 3-81
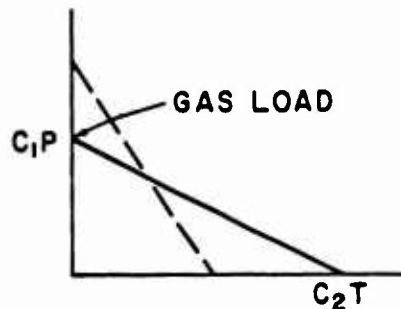
REGION B : NEGLECT SHOCK LOAD
USE FIGURE 3-64 .
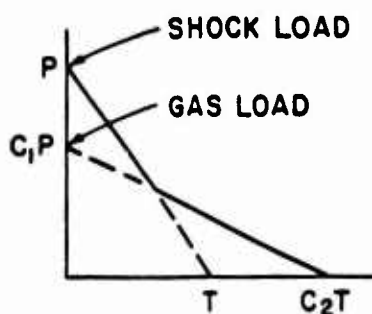
REGION C : BOTH SHOCK AND GAS
LOADS ARE SIGNIFICANT. USE
APPROPRIATE FIGURES AND
INTERPOLATE.
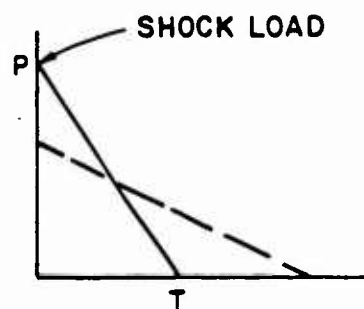
REGION D : NEGLECT GAS LOAD
USE FIGURE 3-64 .

Figure 3-62   Various bilinear triangular loads
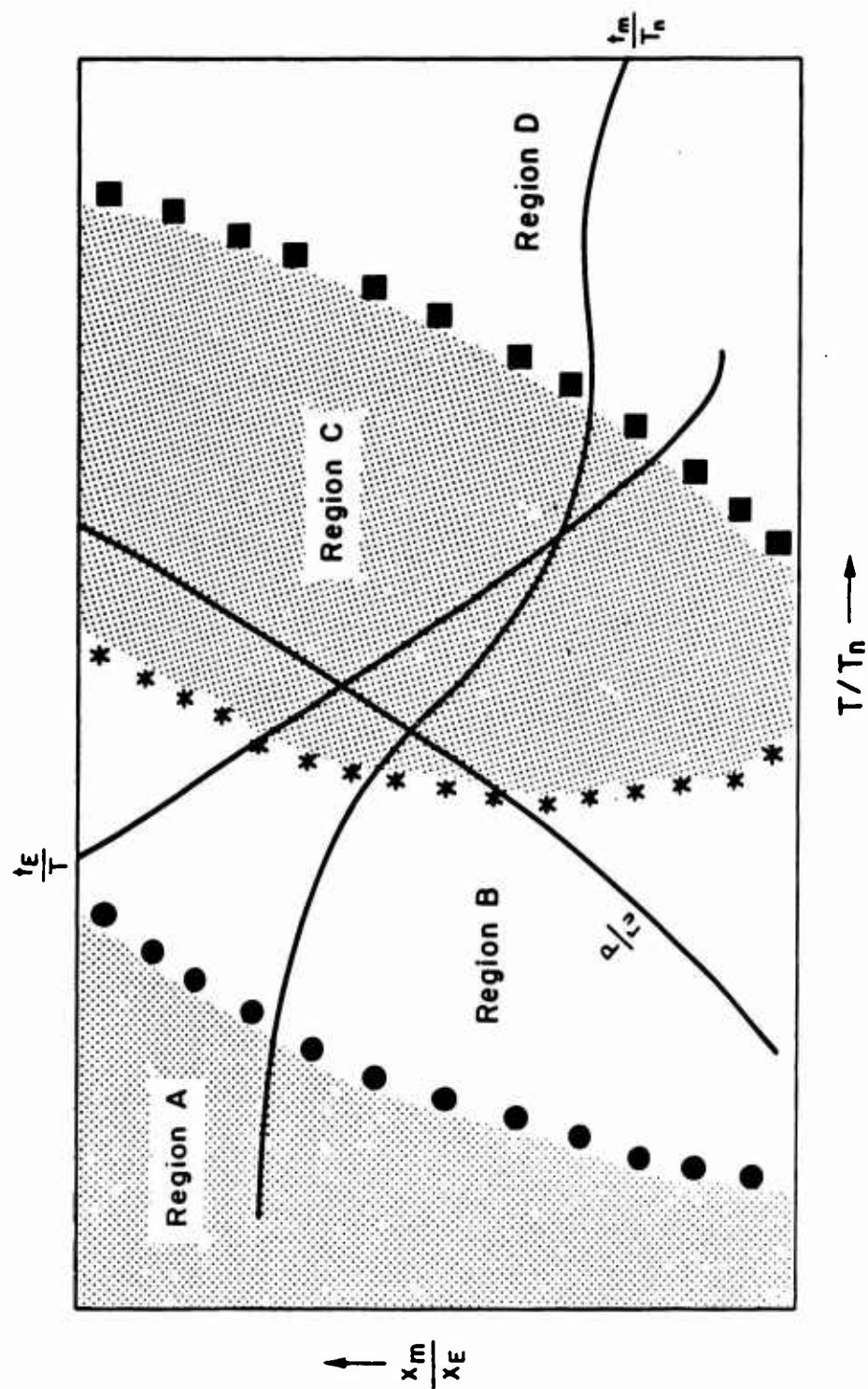
Figure 3-63   Regions of figures 3-54 through 3-266, labeling of axis and curves.

Table 3-15 Figure numbers corresponding to various combinations of C_1 and C_2

C_1 \ C_2	1.00	1.70	3.00	5.50	10.0	30.0	100.	300	1000
1.000	3-64	3-64	3-64	3-64	3-64	3-64	3-64	3-64	3-64
0.909						3-114	3-141	3-173	3-220
0.866						3-115	3-142	3-174	3-221
0.825						3-116	3-143	3-175	3-222
0.787							3-144	3-176	3-223
0.750				3-85	3-99	3-117	3-145	3-177	3-224
0.715						3-118	3-146	3-178	3-225
0.681	3-64	3-65	3-75			3-119	3-147	3-179	3-226
0.648					3-100	3-120	3-148	3-180	3-227
0.619						3-121	3-149	3-181	3-228
0.590							3-150	3-182	3-229
0.562				3-86	3-101	3-122	3-151	3-183	3-230
0.536								3-184	3-231
0.511						3-123	3-152	3-185	3-232
0.487								3-186	3-233
0.464	3-64	3-66	3-76			3-124	3-153	3-187	3-234
0.422				3-87	3-102		3-154	3-188	3-235
0.383						3-125		3-189	3-236
0.365							3-155	3-190	3-237
0.348								3-191	3-238
0.316	3-64	3-67	3-77	3-88	3-103	3-126	3-156	3-192	3-239
0.287								3-193	3-240
0.274							3-157	3-194	3-241
0.261						3-127	3-158	3-195	3-242
0.237				3-89	3-104		3-159	3-196	3-243
0.215	3-64	3-68	3-78			3-128	3-160	3-197	3-244
0.198								3-198	3-245
0.178				3-90	3-105	3-129	3-161	3-199	3-246
0.162								3-200	3-247
0.147	3-64	3-69	3-79			3-130	3-162	3-201	3-248
0.133				3-91	3-106			3-202	3-249
0.121						3-131	3-163	3-203	3-250
0.110								3-204	3-251
0.100	3-64	3-70	3-80	3-92	3-107	3-132	3-164	3-205	3-252
0.091								3-206	3-253
0.083								3-207	3-254
0.075						3-133	3-165	3-208	3-255
0.068				3-93	3-108			3-209	3-256
0.056	3-64	3-71	3-81			3-134	3-166	3-210	3-257
0.046				3-94	3-109			3-211	3-258
0.042						3-135	3-167	3-212	3-259
0.032	3-64	3-72	3-82	3-95	3-110	3-136	3-168	3-213	3-260
0.026						3-137	3-169	3-214	3-261
0.022				3-96	3-111			3-215	3-262
0.018	3-64	3-73	3-83			3-138	3-170	3-216	3-263
0.015				3-97	3-112			3-217	3-264
0.013						3-139	3-171	3-218	3-265
0.010	3-64	3-74	3-84	3-98	3-113	3-140	3-172	3-219	3-266

NOTE: See section on "Accuracy" for the significance of the dotted and solid lines shown in the table

3-19.3.4.1 *Region A* . This region is defined as the area to the left of the solid circles on the response charts. If a chart does not have a line of solid circles, then region A does not exist. Figures 3-221, 3-222 and 3-223 illustrate this case.

In region A the maximum dynamic response depends primarily upon the total impulse in the blast loading (area under the pressure-time curve). The actual pressure-time distribution does not significantly affect the maximum dynamic response because in these regions the durations T and C_2T are small in comparison to the response time, t_m of the structural member. In this region the response charts are not used and a solution is obtained by considering the modified loading shown in figure 3-62a. This load shape yields the following equations:

$$\frac{X_m}{X_E} = \frac{1}{2} + \frac{\pi^2}{2}\left[\left(\frac{P}{r_u}\right)\left(\frac{T}{T_n}\right)F\right]^2 \qquad 3\text{-}80$$

and

$$\frac{t_m}{T_n} = \left(\frac{1}{2}\right)F\left(\frac{P}{r_u}\right)\left(\frac{T}{T_n}\right) \qquad 3\text{-}81$$

where

$$F = C_2 + \frac{C_2(1-C_1)(1-C_2)}{(C_2 - C_1)} \qquad 3\text{-}82$$

3-19.3.4.2 *Region B* . This region is defined as the area in the chart to the left of the asterisks. If a chart has no line of asterisks, then region B does not exist. Figure 3-65 illustrates the case where region B does not exist.

In region B the maximum dynamic response depends primarily upon the gas load which is described by C_1P and C_2T. The shock load described by P and T is neglected. This load condition is shown in figure 3-62b. Therefore the solution is obtained from consideration of a single triangular load. The dynamic response is obtained from figure 3-64 which like figures 3-54 and 3-55 is for a triangular load and will yield the same results. When using figure 3-64 it must be realized that the P and T used in the chart are actually C_1P and C_2T, respectively. In a typical design, enter figure 3-64 with the normalized parameters, C_1P/r_u and C_2T/T_N, and read the solution, X_m/X_E, t_m/T_N, and t_E/C_2T.

Figure 3-63 depicts region B as the area between the line of solid circles and the line of asterisks. It should be understood that the solution technique associated with region B (i.e., neglect the shock load and use figure 3-64) applies everywhere to the left of the line of asterisks, including region A. In other words, two solution techniques are available in region A.

3-19.3.4.3 *Region D* . This region is defined as the area in the charts to the right of the line of solid squares. If a chart has no line of solid squares, then region D does not exist. Figure 3-69 illustrates the case where region D does not exist.

In region D the maximum dynamic response depends primarily upon the shock load which is described by P and T. The gas load described by C_1P and C_2T is neglected. This load condition is shown in figure 3-62d. Therefore, the solution is obtained from consideration of a single triangular load. Similar

- 114 -

to region B, the dynamic response is obtained from figure 3-64 which is for a triangular load. Unlike region B, the parameters, P and T which describe the load are used in the figure. Therefore, in a typical design, enter figure 3-64 with the normalized parameters P/r_u and T/T_N, and read the solution, X_m/X_E, t_m/T_N and t_E/T.

3-19.3.4.4 *Region C* . This is the region in the charts which do not meet the definitions of regions A, B and D. In most charts, region C is the area to the left of the line of solid squares and to the right of the line of asterisks, as illustrated in figure 3-63. Region C does not exist in some charts, such as figure 3-97 which have over lapping regions A and D.

In region C, both the shock and gas load must be considered. Replacement of the actual bilinear load with a simplified load, as done for the other regions, will yield an incorrect solution. Therefore, in this region the response charts must be used. If the required values of C_1 and/or C_2 do not correspond to the response chart values, interpolation between response charts will be required to obtain a solution. In a few cases one or two response charts are needed, however, in general four response charts are required for a solution.

3-19.3.4.5 *Response Chart Interpolation* . Interpolation between four response charts will usually be required for region C. For regions A, B, or D, if conditions warrant an exact solution rather than the approximate solution usually used in these regions, interpolation between charts may be required. Either a graphical or mathematical interpolation procedure may be employed. The method selected depends upon personal choice. A brief description of each procedure is presented below and an example of each is given in Appendix A.

Graphical interpolation requires a sheet of log-log graph paper. A convenient size is 2 x 1 cycle with the single-cycle axis representing C_1 and C_2, and the two-cycle axis representing the desired parameter (X_m/X_E, t_m/T_N or t_E/T), called Y for ease of presentation. The appropriate figures to be used for a solution are obtained form table 3-15 for the required values of C_1 and C_2. The procedure will illustrate the interpolation between four figures since this is by far the usual case. For the values of P/r_u and T/T_N corresponding to the structural system selected, determine the desired parameter Y for each of the four figures. Organize a table in the same format as table 3-16 and enter each figure number and corresponding value of C_1, C_2 and Y.

Table 3-16 Response Chart Interpolation

Figure Number	C_1	C_2	Desired Parameter
1	C_{11} C_1	C_{21} C_{21}	Y_1 $\Big\}\,Y_a$
2	C_{12} C_1	$C_{22} = C_{21}$ C_2	Y_2 $\Big\}\,Y$
3	C_{13} C_1	C_{23} C_{23}	Y_3 $\Big\}\,Y_b$
4	C_{14}	$C_{24} = C_{23}$	Y_4

In the table, C_{11} and C_{21} are the values of C_1 and C_2, respectively, from figure 1. Likewise, C_{12} and C_{22} are the values of C_1 and C_2, respectively, from figure 2, etc. The symbol Y_1, is the desired parameter, such as X_m/X_E, which is read from figure 1. The symbol Y_2 is the value read from figure 2, etc. The interpolation is first performed for the required value of C_1 and then for the required value of C_2. That is, with C_{21} constant, graphically interpolate on the log-log paper between points (Y_1, C_{11}) and (Y_2, C_{12}) to find Y_a corresponding to C_1 and C_{21}, as shown on figure 3-267. Similarly, with C_{23} constant, graphically interpolate between (Y_3, C_{13}) and (Y_4, C_{14}) to find Y_b corresponding to C_1 and C_{23}, also shown in figure 3-267. The values of Y_a and Y_b are recorded in table 3-16. Finally, with C_1 constant, graphically interpolate on the log-log paper between (Y_a, C_{21}) and (Y_b, C_{23}) to find Y corresponding to the required C_1 and C_2, as shown on figure 3-267. The values of Y is the solution. Since there are three parameters to define the response of a structural, namely, X_m/X_E, t_m/T_N and t_E/T, the interpolation procedure is repeated three times, once for each parameter.

Mathematical interpolation requires the same initial steps as graphical interpolation. That is, the appropriate figures to be used for a solution are obtained from table 3-15 and the required parameters are determined and entered into table 3-16. Logarithmic equations are used to obtain the values of Y_a, Y_b and Y. The value of $\ln Y_a$ is obtained from:

$$\ln Y_a = \ln Y_1 + \frac{\ln(Y_2/Y_1)\ln(C_1/C_{11})}{\ln(C_{12}/C_{11})} \qquad \text{3-83}$$

and the value of $\ln Y_b$ is obtained from:

$$\ln Y_b = \ln Y_3 + \frac{\ln(Y_4/Y_3)\ln(C_1/C_{13})}{\ln(C_{14}/C_{13})} \qquad \text{3-84}$$

Using the values of $\ln Y_a$ and $\ln Y_b$; the value of $\ln Y$ is obtained from:

$$\ln Y = \ln Y_a + \frac{(\ln Y_b - \ln Y_a)\ln(C_2/C_{21})}{\ln(C_{23}/C_{21})} \qquad \text{3-85}$$

The desired parameter Y is then obtained from:

$$Y = e^{\ln Y} \qquad \text{3-86a}$$

The above equations use natural logarithms. Common logarithms can be used to solve the above equations and then solve for Y using:

$$Y = 10^{\log Y} \qquad \text{3-86b}$$

It should be noted that if C_2 is represented by a response chart, then only two charts will be involved, and only equation 3-83 will apply.

3-19.3.4.6 *Accuracy*. The prediction error is less than 10 percent for the approximate solutions obtained in regions A, B and D. This is true provided the recommended procedures are employed, that is , the actual load is replaced

by the approximate loads as shown on figure 3-62 and the solution is obtained using the equations provided for region A and using figure 3-64 for regions B and D.

Exact solutions are obtained from the response charts if the required values of C_1 and C_2 correspond to those given in the charts. This is true for all four regions. Errors result from interpolation between the response charts. The prediction error in X_m/X_E for region C, where interpolation between charts is required, is less than 10 percent provided response charts bounded by the dashed or solid lines on table 3-15 are not used. The prediction error in X_m/X_E will range from 55 to 100 percent for solutions in region C, if the point (C_1, C_2) lies in the area bounded by the solid line in table 3-15, and will range from 10 to 55 percent for the area bounded by the dashed line. If the solution involves charts from both sides of either the dashed or solid lines, the prediction error will range from 10 to 55 percent. The large interpolation error for these charts result from the big change in X_m/X_E for a small change in P/r_u which is peculiar to this chart.

It should be noted that the large errors described above will always be on the high side, that is, the predicted value of X_m/X_E will always be greater than the exact value. Hence, a conservative design will always result. In addition, it should be noted that the prediction error in t_m/T_N is about half the error in X_m/X_E.

While the errors produced from interpolation between the charts in table 3-15 bounded by the dashed and solid lines is large, the area in which they apply is small. As can be seen, region C is rather small on these charts. It is for points in this small area where interpolation must be performed. For the remaining areas (A, B and D), the approximate solutions may be used rather than interpolation. These approximate solutions will result in a error of less than 10 percent.

Solutions involving $0.920 < C_1 < 1.00$ and $C_2 > 100$ can result in very large errors if interpolating procedures are employed. In this region, the dynamic response is primarily due to the gas load. Therefore, figure 3-64 is used to obtain X_m/X_E for the gas load. However, this value is too low and should be increased by 20 percent. The value of t_m/T_N corresponding to the increased value of X_m/X_E is then obtained from figure 3-64.

3-19.3.5 *Determination of Rebound* . In the design of elements which respond to the pressure only and pressure-time relationship, the element must be designed to resist the negative deflection or rebound which can occur after maximum positive deflection has been reached. The ratio of the required unit rebound resistance to the ultimate unit resistance r/r_u, such that the element will remain elastic during rebound is presented in figure 3-268 for a single-degree-of-freedom system subjected to a triangular loading function. Entering with ratios X_m/X_E and t/T_N previously determined for design, the required unit rebound resistance r- can be read in terms of the originally designed ultimate unit resistance r_u. To obtain the rebound resistance for an element subjected to another form of load other than the triangular loading function, a time-history analysis such as the one described in Section 3-19 has to be performed.

Figure 3-64a Maximum response of elasto-plastic, one-degree-of-freedom system for bilinear-triangular pulse (C_1 = 1.000, C_2 = 1.0)

TIME OF MAXIMUM DEFLECTION TO FUNDAMENTAL PERIOD, t_m/T_N

TIME OF YIELD TO LOAD DURATION, t_E/T

MAXIMUM DEFLECTION TO YIELD DEFLECTION, X_m/X_E

LOAD DURATION TO FUNDAMENTAL PERIOD, T/T_N

Figure 3-64b   Maximum response of elasto-plastic, one-degree-of-freedom system for bilinear-triangular pulse ($C_1 = 1.000$, $C_2 = 1.0$) (cont.)

$P/r_u = 0.60$

Figure 3-65 Maximum response of elasto-plastic, one-degree-of-freedom system for bilinear-triangular pulse ($C_1 = 0.681$, $C_2 = 1.7$)
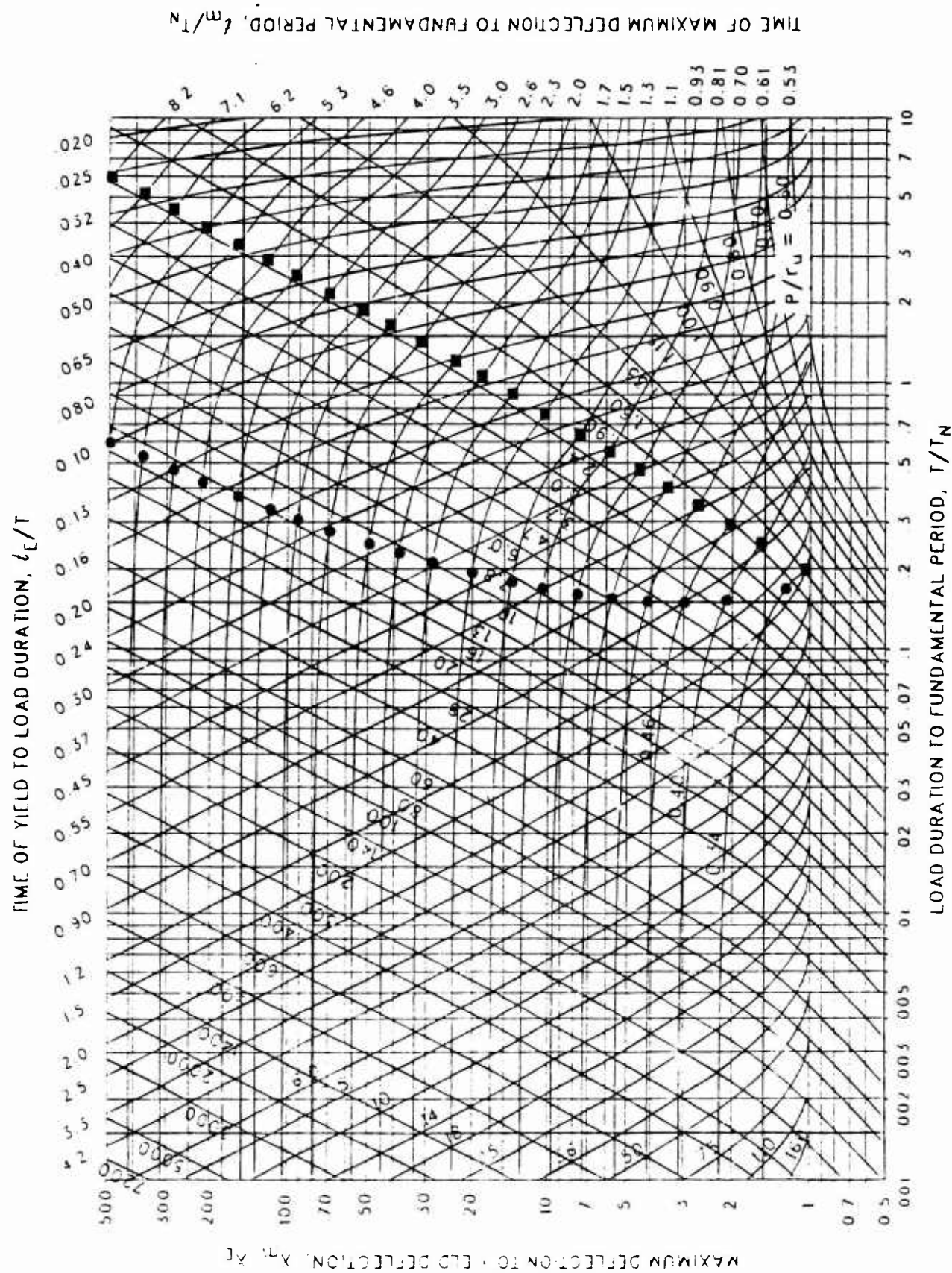
Figure 3-66 Maximum response of elasto-plastic, one-degree-of-freedom system for bilinear-triangular pulse ($C_1 = 0.464$, $C_2 = 1.7$)

-121-

Figure 3-67 Maximum response of elasto-plastic, one-degree-of-freedom system for bilinear-triangular pulse ($C_1 = 0.316$, $C_2 = 1.7$)

-122-

Figure 3-68   Maximum response of elasto-plastic, one-degree-of-freedom
system for bilinear-triangular pulse ($C_1 = 1.215$, $C_2 = 1.7$)

Figure 3-69   Maximum response of elasto-plastic, one-degree-of-freedom system for bilinear-triangular pulse ($C_1 = 0.147$, $C_2 = 1.7$)

TIME OF MAXIMUM DEFLECTION TO FUNDAMENTAL PERIOD, t_m/T_N

TIME OF YIELD TO LOAD DURATION, t_E/T

MAXIMUM DEFLECTION TO YIELD DEFLECTION, x_m/x_E

LOAD DURATION TO FUNDAMENTAL PERIOD, T/T_N

Figure 3-70   Maximum response of elasto-plastic, one-degree-of-freedom system for bilinear-triangular pulse ($C_1 = 0.100$, $C_2 = 1.7$)

Figure 3-71   Maximum response of elasto-plastic, one-degree-of-freedom system for bilinear-triangular pulse ($C_1 = 0.056$, $C_2 = 1.7$)

-126-

Figure 3-72   Maximum response of elasto-plastic, one-degree-of-freedom system for bilinear-triangular pulse ($C_1 = 0.032$, $C_2 = 1.7$)

-127-

Figure 3-73   Maximum response of elasto-plastic, one-degree-of-freedom
system for bilinear-triangular pulse ($C_1 = 0.018$, $C_2 = 1.7$)

Figure 3-74 Maximum response of elasto-plastic, one-degree-of-freedom system for bilinear-triangular pulse ($C_1 = 0.010$, $C_2 = 1.7$)

-129-

Figure 3-75 Maximum response of elasto-plastic, one-degree-of-freedom system for bilinear-triangular pulse ($C_1 = 0.681$, $C_2 = 3.0$)

-130-

Figure 3-76   Maximum response of elasto-plastic, one-degree-of-freedom system for bilinear-triangular pulse (C_1 = 0.464, C_2 = 3.0)

-131-

Figure 3-77   Maximum response of elasto-plastic, one-degree-of-freedom
system for bilinear-triangular pulse ($C_1 = 0.3\dot{1}5$, $C_2 = 3.0$)

-132-

Figure 3-78   Maximum response of elasto-plastic, one-degree-of-freedom
system for bilinear-triangular pulse (C_1 = 1.215, C_2 = 3.0)

Figure 3-79   Maximum response of elasto-plastic, one-degree-of-freedom system for bilinear-triangular pulse ($C_1 = 0.147$, $C_2 = 3.0$)

-134-

Figure 3-80   Maximum response of elasto-plastic, one-degree-of-freedom
system for bilinear-triangular pulse ($C_1 = 0.100$, $C_2 = 3.0$)

Figure 3-81   Maximum response of elasto-plastic, one-degree-of-freedom system for bilinear-triangular pulse ($C_1 = 0.056$, $C_2 = 3.0$)

Figure 3-82   Maximum response of elasto-plastic, one-degree-of-freedom
system for bilinear-triangular pulse ($C_1 = 0.032$, $C_2 = 3.0$)

-137-

Figure 3-83   Maximum response of elasto-plastic, one-degree-of-freedom system for bilinear-triangular pulse ($C_1 = 0.018$, $C_2 = 3.0$)

Figure 3-84 Maximum response of elasto-plastic, one-degree-of-freedom system for bilinear-triangular pulse ($C_1 = 0.010$, $C_2 = 3.0$)

-139-

Figure 3-85   Maximum response of elasto-plastic, one-degree-of-freedom
system for bilinear-triangular pulse ($C_1 = 0.750$, $C_2 = 5.5$)

-140-

Figure 3-86   Maximum response of elasto-plastic, one-degree-of-freedom system for bilinear-triangular pulse (C_1 = 0.562, C_2 = 5.5)

Figure 3-87   Maximum response of elasto-plastic, one-degree-of-freedom
system for bilinear-triangular pulse ($C_1 = 0.422$, $C_2 = 5.5$)

Figure 3-88 Maximum response of elasto-plastic, one-degree-of-freedom system for bilinear-triangular pulse ($C_1 = 0.316$, $C_2 = 5.5$)

-143-

Figure 3-89   Maximum response of elasto-plastic, one-degree-of-freedom
system for bilinear-triangular pulse ($C_1 = 0.237$, $C_2 = 5.5$)

-144-

Figure 3-90   Maximum response of elasto-plastic, one-degree-of-freedom system for bilinear-triangular pulse ($C_1 = 0.178$, $C_2 = 5.5$)

Figure 3-91   Maximum response of elasto-plastic, one-degree-of-freedom system for bilinear-triangular pulse ($C_1 = 0.133$, $C_2 = 5.5$)

TIME OF MAXIMUM DEFLECTION TO FUNDAMENTAL PERIOD, t_m/T_N

Figure 3-92 Maximum response of elasto-plastic, one-degree-of-freedom system for bilinear-triangular pulse ($C_1 = 0.100$, $C_2 = 5.5$)

LOAD DURATION TO FUNDAMENTAL PERIOD, T/T_N

TIME OF YIELD TO LOAD DURATION, t_E/T

MAXIMUM DEFLECTION TO YIELD DEFLECTION, x_m/x_E

-147

Figure 3-93   Maximum response of elasto-plastic, one-degree-of-freedom system for bilinear-triangular pulse ($C_1 = 0.068$, $C_2 = 5.5$)

-148-

TIME OF MAXIMUM DEFLECTION TO FUNDAMENTAL PERIOD, t_m/T_N

TIME OF YIELD TO LOAD DURATION, t_E/T

LOAD DURATION TO FUNDAMENTAL PERIOD, T/T_N

MAXIMUM DEFLECTION TO YIELD DEFLECTION, x_m/x_E

Figure 3-94   Maximum response of elasto-plastic, one-degree-of-freedom
system for bilinear-triangular pulse ($C_1 = 0.046$, $C_2 = 5.5$)

-149-

Figure 3-95   Maximum response of elasto-plastic, one-degree-of-freedom system for bilinear-triangular pulse ($C_1 = 0.032$, $C_2 = 5.5$)

-150-

Figure 3-96   Maximum response of elasto-plastic, one-degree-of-freedom
system for bilinear-triangular pulse ($C_1 = 0.022$, $C_2 = 5.5$)

-151-

Figure 3-97 Maximum response of elasto-plastic, one-degree-of-freedom system for bilinear-triangular pulse ($C_1 = 0.015$, $C_2 = 6$)

Figure 3-98   Maximum response of elasto-plastic, one-degree-of-freedom system for bilinear-triangular pulse ($C_1 = 0.010$, $C_2 = 6$)

Figure 3-99 Maximum response of elasto-plastic, one-degree-of-freedom system for bilinear-triangular pulse (C_1 = 0.750, C_2 = 10)

Figure 3-100   Maximum response of elasto-plastic, one-degree-of-freedom system for bilinear-triangular pulse ($C_1 = 0.648$, $C_2 = 10$)

-155-

Figure 3-101   Maximum response of elasto-plastic, one-degree-of-freedom system for bilinear-triangular pulse ($C_1 = 0.562$, $C_2 = 10$)

Figure 3-102   Maximum response of elasto-plastic, one-degree-of-freedom
system for bilinear-triangular pulse ($C_1 = 0.422$, $C_2 = 10$)

Figure 3-103 Maximum response of elasto-plastic, one-degree-of-freedom system for bilinear-triangular pulse ($C_1 = 0.316$, $C_2 = 10$)

Figure 3-104 Maximum response of elasto-plastic, one-degree-of-freedom system for bilinear-triangular pulse ($C_1 = 0.237$, $C_2 = 10$)

Figure 3-105   Maximum response of elasto-plastic, one-degree-of-freedom
system for bilinear-triangular pulse (C_1 = 0.178, C_2 = 10)

Figure 3-106   Maximum response of elasto-plastic, one-degree-of-freedom system for bilinear-triangular pulse ($C_1 = 0.133$, $C_2 = 10$)

Figure 3-107   Maximum response of elasto-plastic, one-degree-of-freedom system for bilinear-triangular pulse ($C_1 = 0.100$, $C_2 = 10$)

Figure 3-108   Maximum response of elasto-plastic, one-degree-of-freedom
system for bilinear-triangular pulse ($C_1 = 0.068$, $C_2 = 10$)

Figure 3-109   Maximum response of elasto-plastic, one-degree-of-freedom system for bilinear-triangular pulse ($C_1 = 0.046$, $C_2 = 10$)

-164-

Figure 3-110   Maximum response of elasto-plastic, one-degree-of-freedom system for bilinear-triangular pulse ($C_1 = 0.032$, $C_2 = 10$)

Figure 3-111 Maximum response of elasto-plastic, one-degree-of-freedom system for bilinear-triangular pulse ($C_1 = 0.022$, $C_2 = 10$)

-166-

Figure 3-112   Maximum response of elasto-plastic, one-degree-of-freedom
system for bilinear-triangular pulse ($C_1 = 0.015$, $C_2 = 10$)
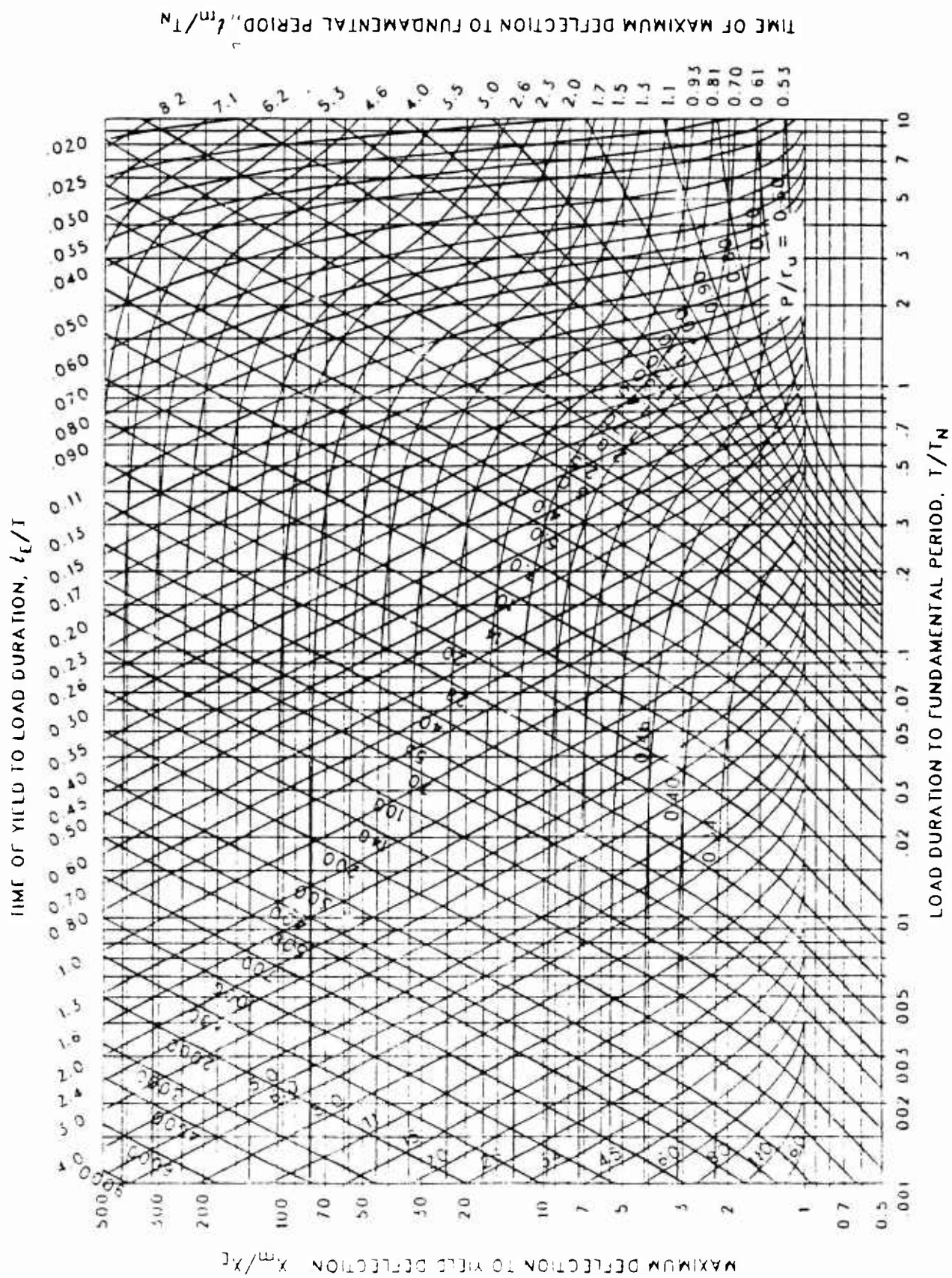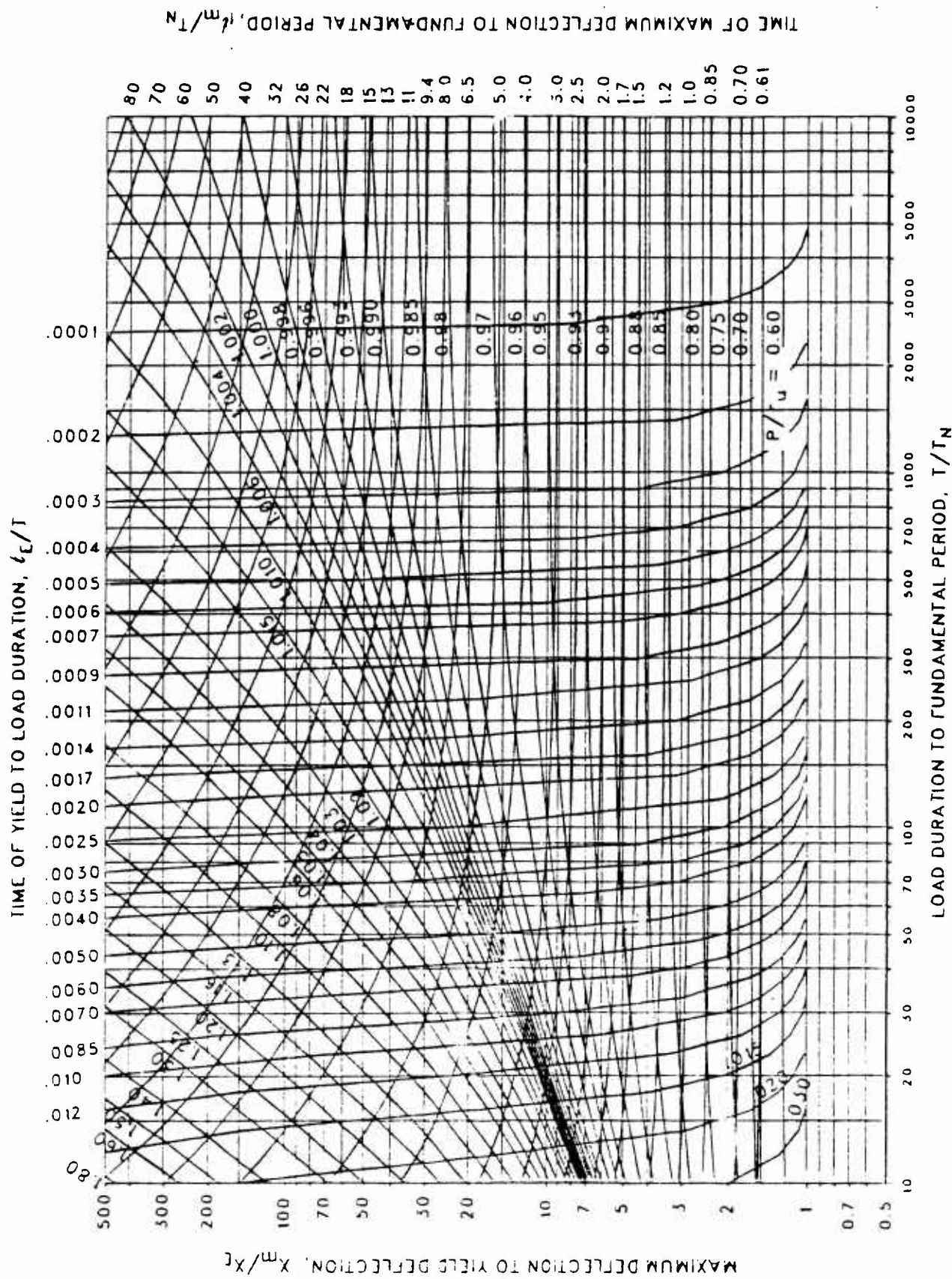
-167-

Figure 3-113 Maximum response of elasto-plastic, one-degree-of-freedom system for bilinear-triangular pulse ($C_1 = 0.010$, $C_2 = 10$)

-168-

Figure 3-114   Maximum response of elasto-plastic, one-degree-of-freedom system for bilinear-triangular pulse ($C_1 = 0.909$, $C_2 = 30$)
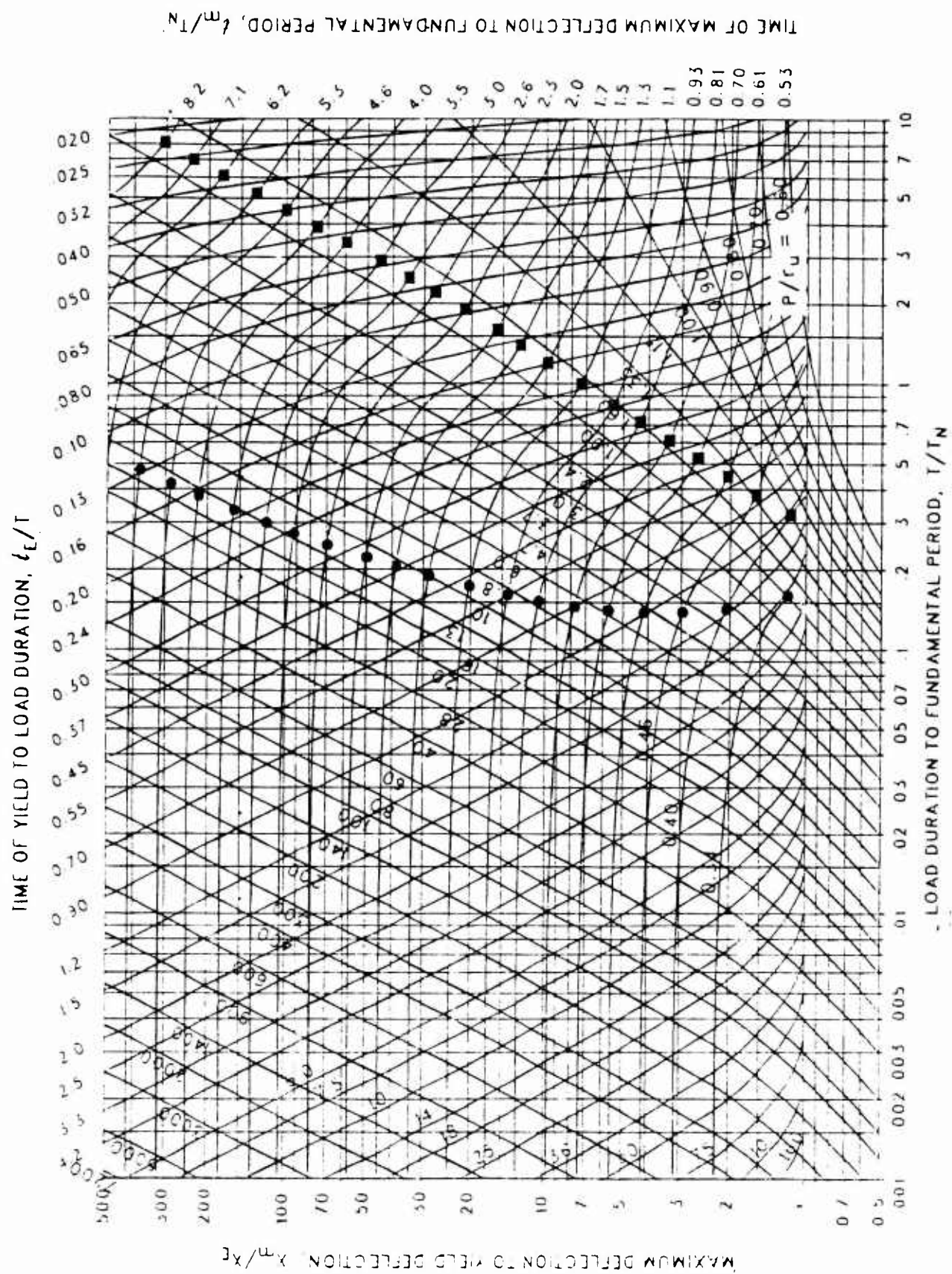
-169-

Figure 3-115   Maximum response of elasto-plastic, one-degree-of-freedom
system for bilinear-triangular pulse (C_1 = 0.866, C_2 = 30)

-170-

Figure 3-116 Maximum response of elasto-plastic, one-degree-of-freedom
system for bilinear-triangular pulse ($C_1 = 0.825$, $C_2 = 30$)

TIME OF MAXIMUM DEFLECTION TO FUNDAMENTAL PERIOD, t_m/T_N

TIME OF YIELD TO LOAD DURATION, t_E/T

LOAD DURATION TO FUNDAMENTAL PERIOD, T/T_N

MAXIMUM DEFLECTION TO YIELD DEFLECTION x_m/x_E

Figure 3-117 Maximum response of elasto-plastic, one-degree-of-freedom system for bilinear-triangular pulse ($C_1 = 0.750$, $C_2 = 30$)

-172-
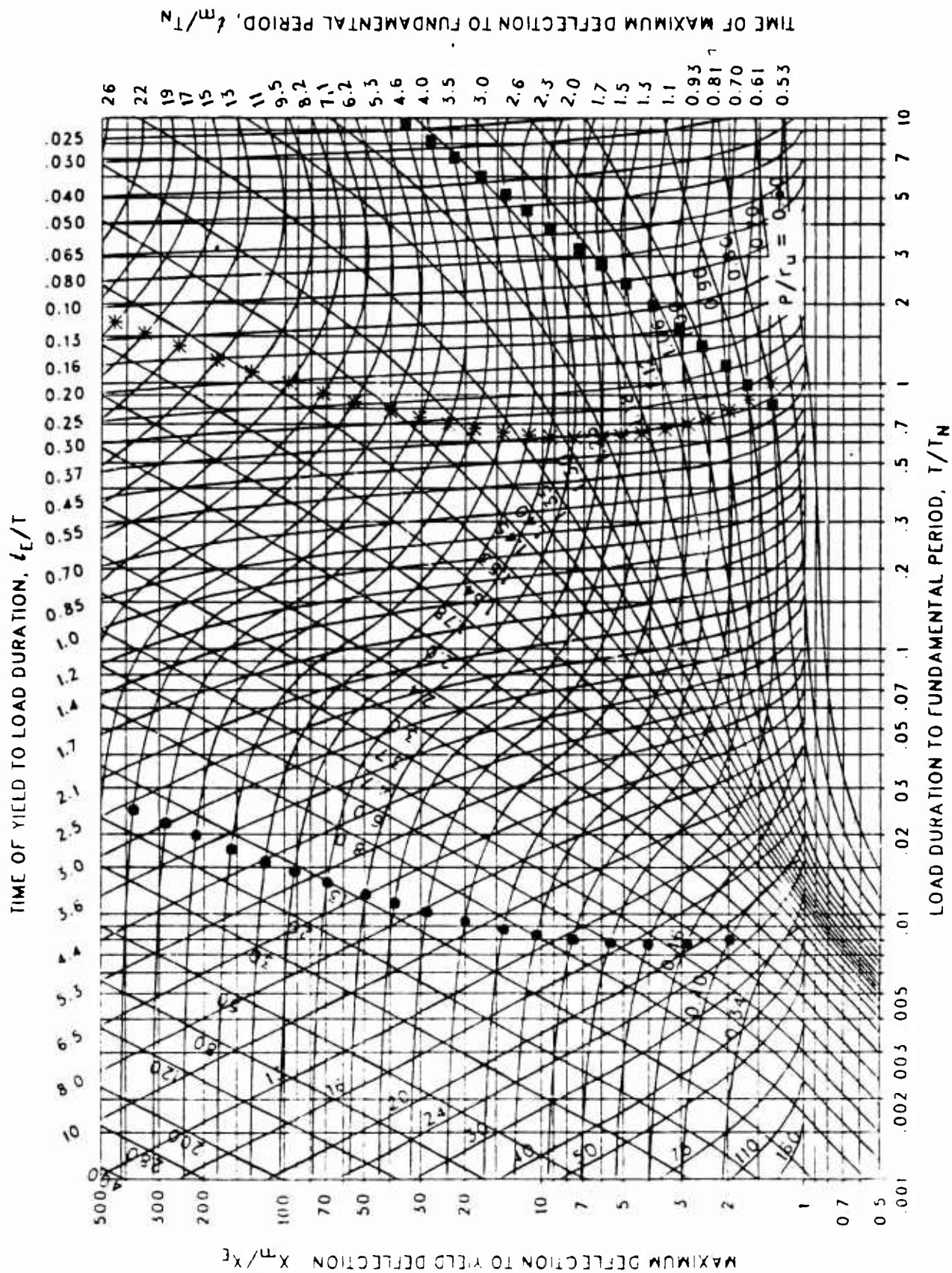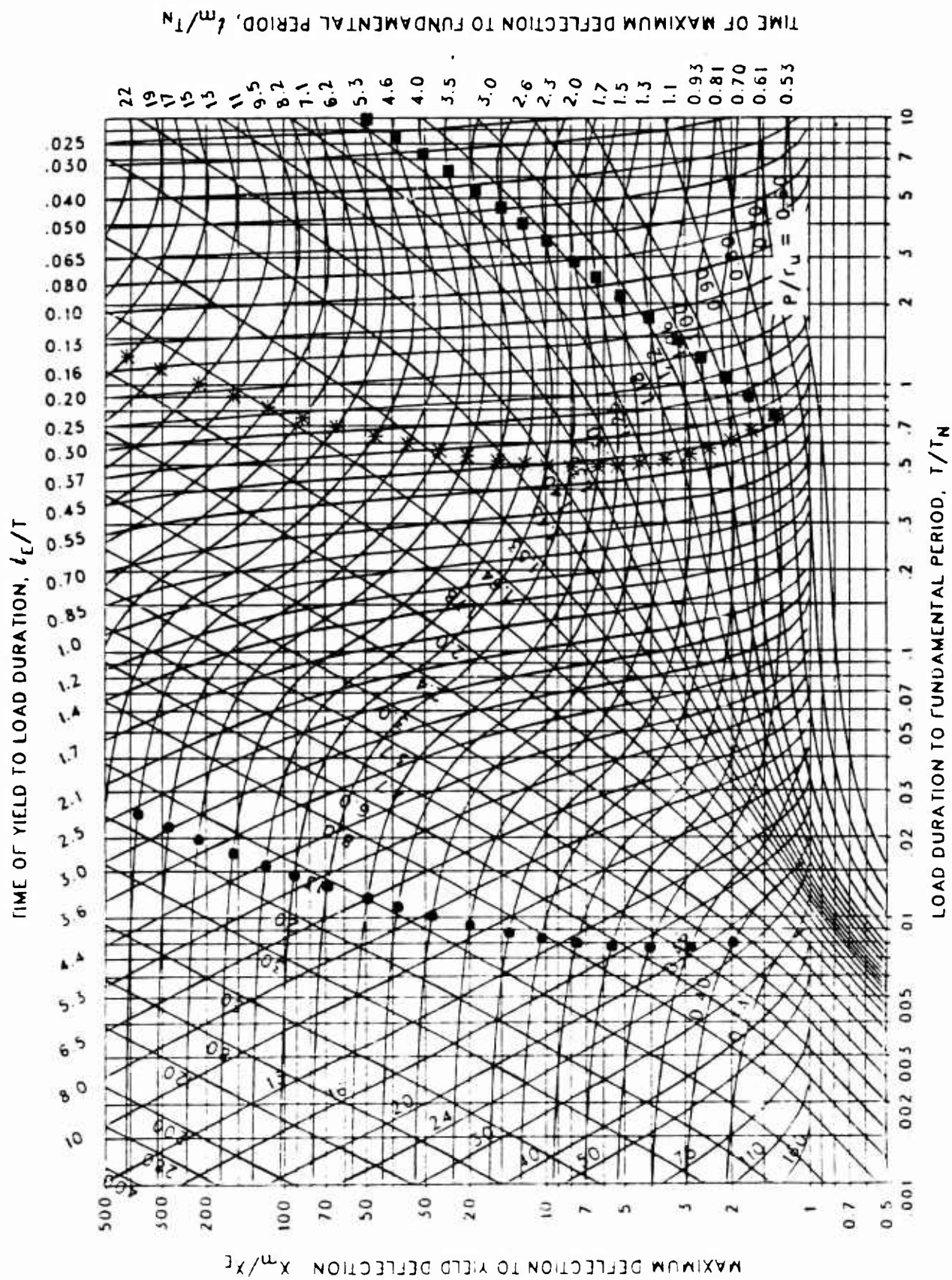
Figure 3-118   Maximum response of elasto-plastic, one-degree-of-freedom system for bilinear-triangular pulse ($C_1 = 0.715$, $C_2 = 30$)
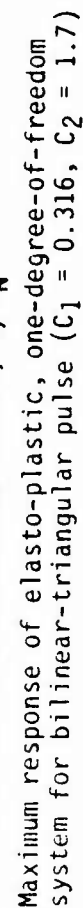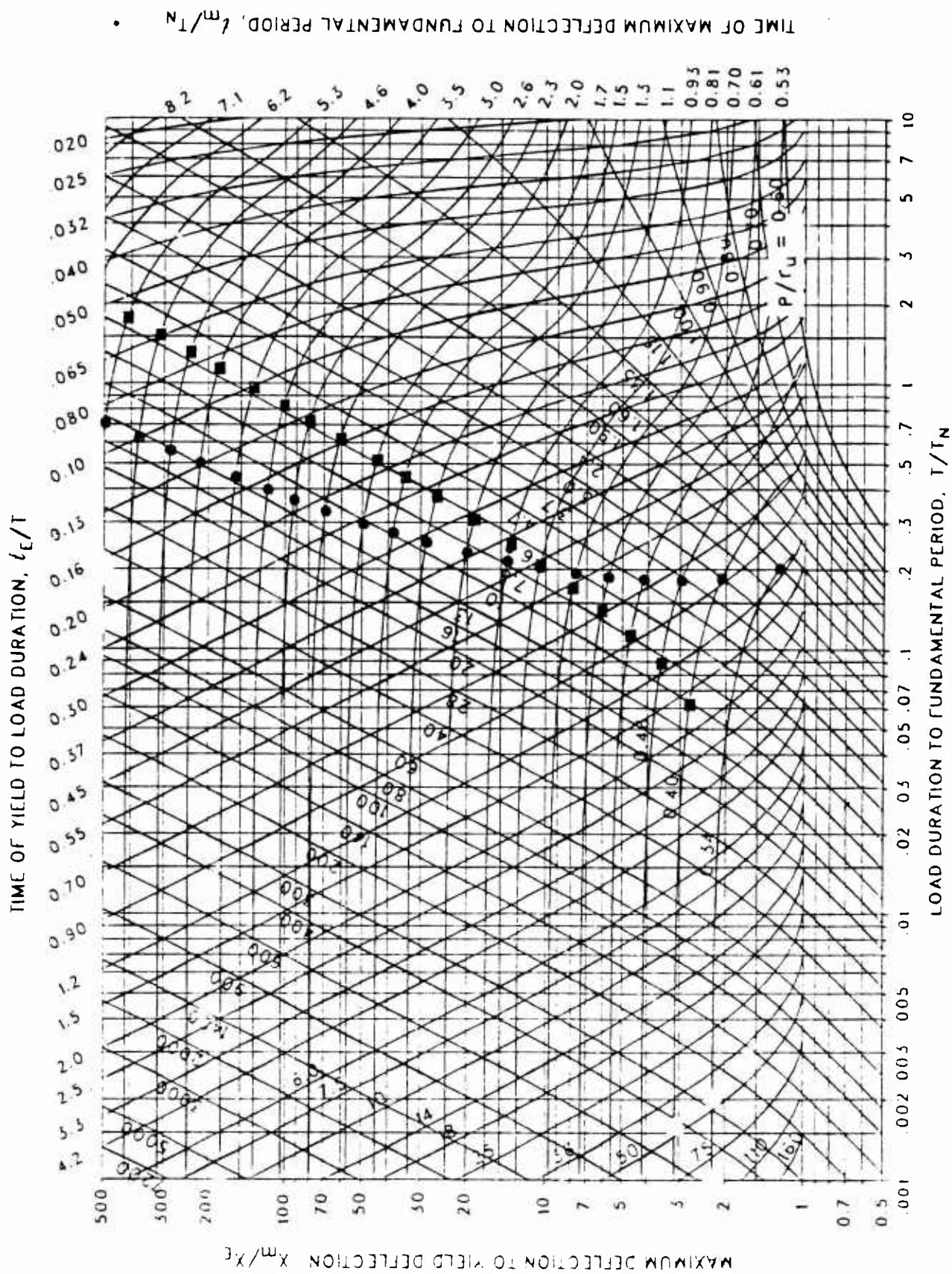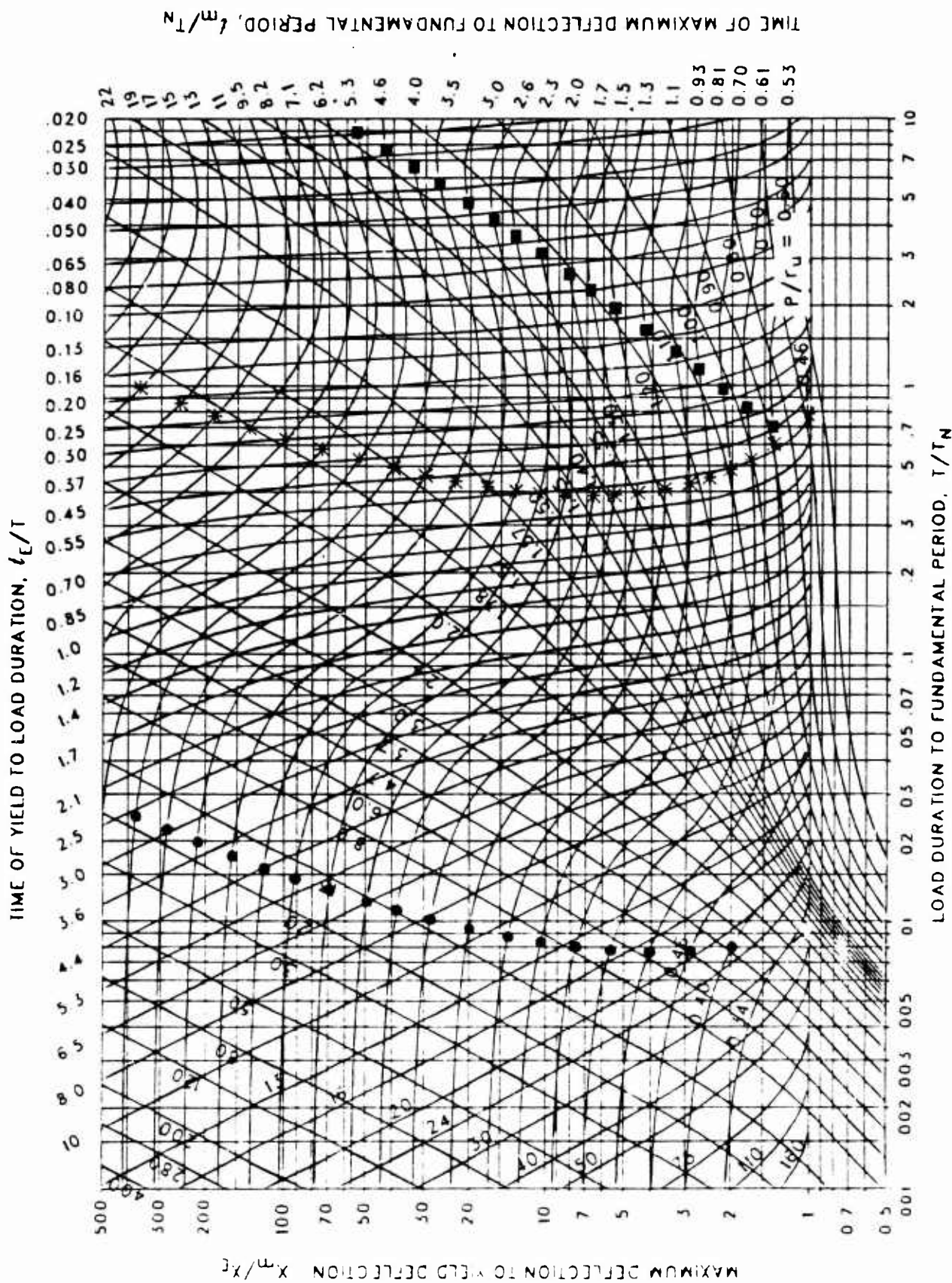
Figure 3-119   Maximum response of elastc-plastic, one-degree-of-freedom
system for bilinear-triangular pulse ($C_1 = 0.681$, $C_2 = 30$)

Figure 3-120   Maximum response of elasto-plastic, one-degree-of-freedom system for bilinear-triangular pulse ($C_1 = 0.648$, $C_2 = 30$)
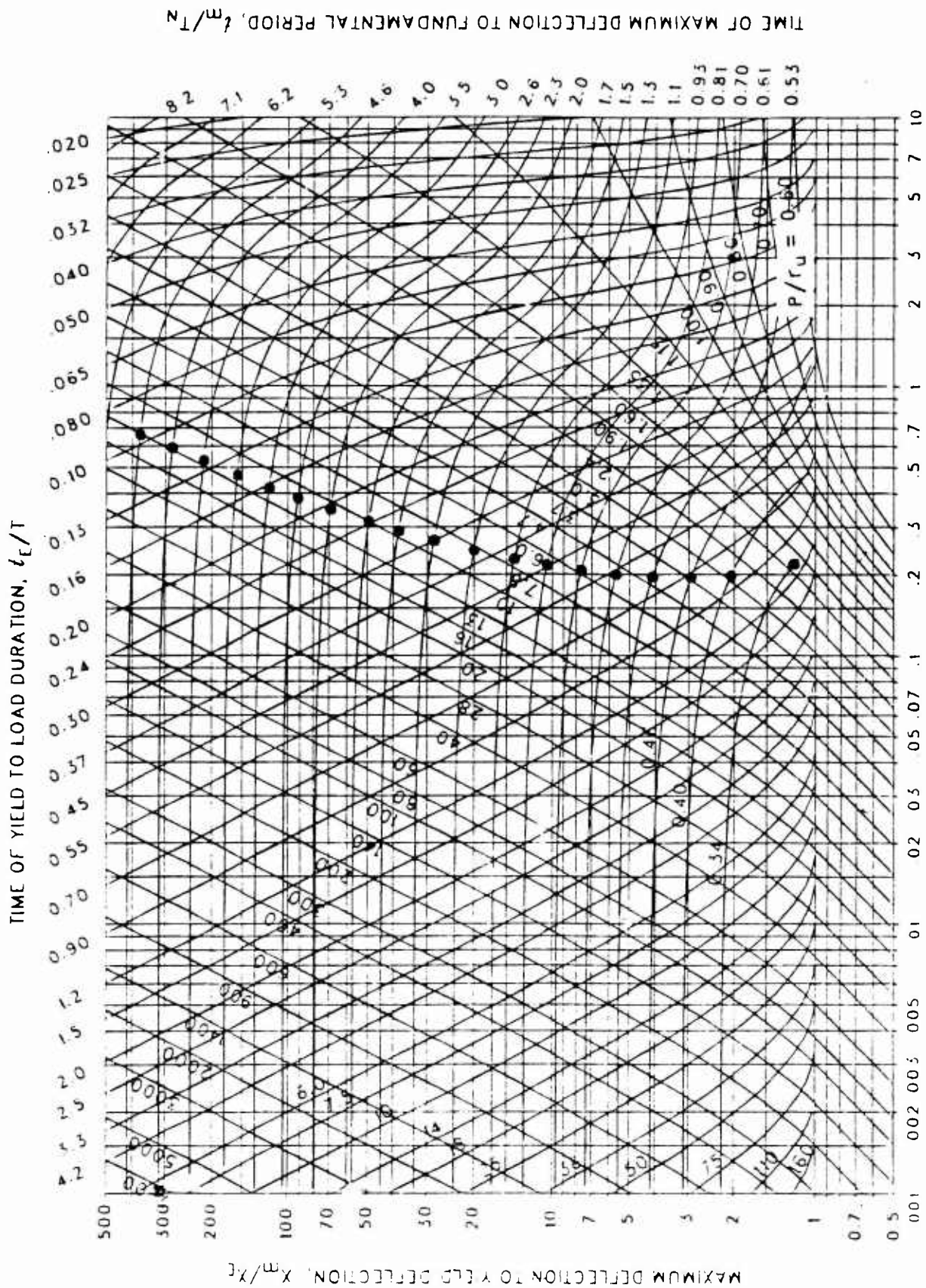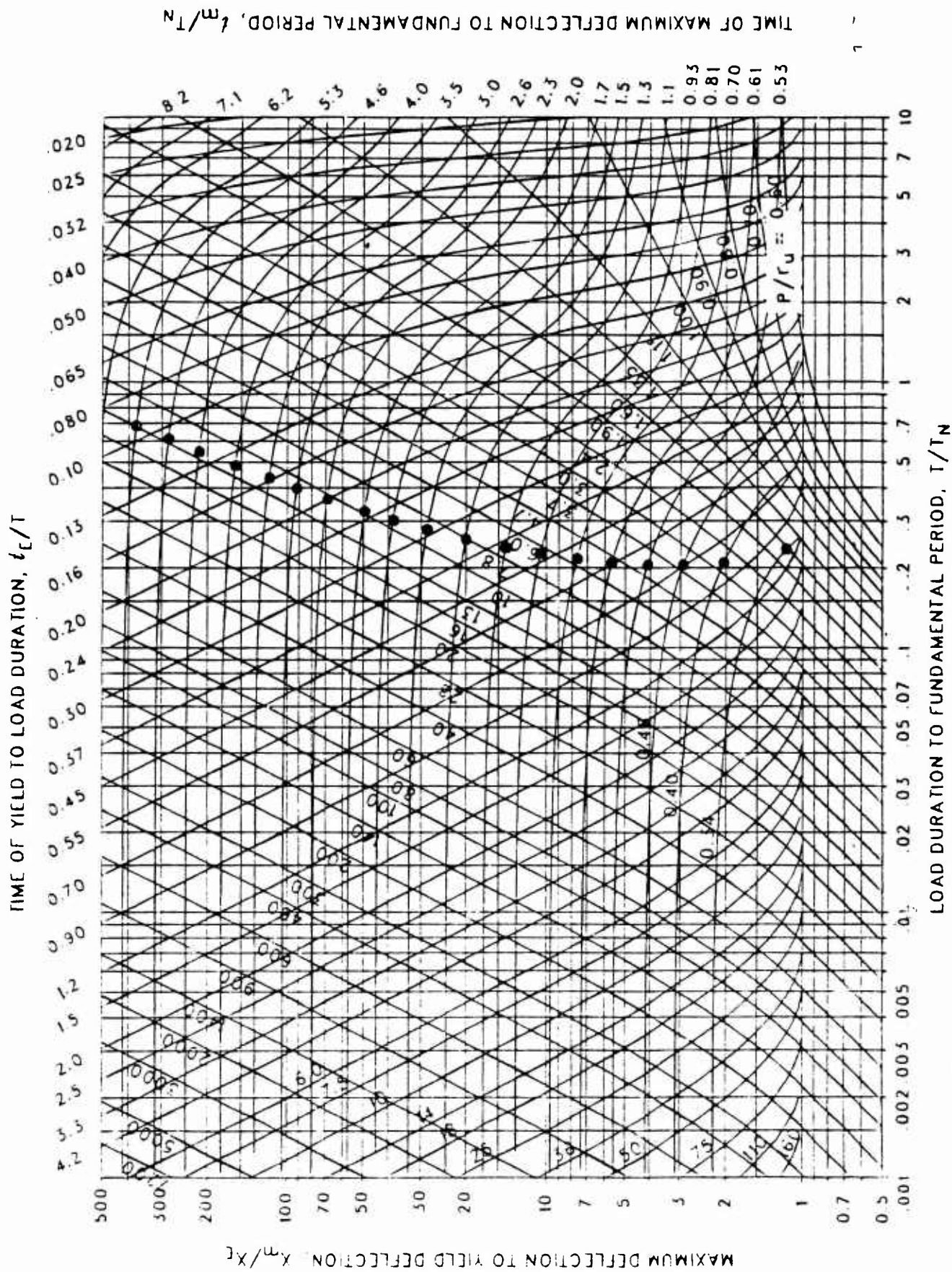
-175-

Figure 3-121   Maximum response of elasto-plastic, one-degree-of-freedom
system for bilinear-triangular pulse ($C_1 = 0.619$, $C_2 = 30$)

Figure 3-122 Maximum response of elasto-plastic, one-degree-of-freedom system for bilinear-triangular pulse ($C_1 = 0.562$, $C_2 = 30$)

Figure 3-123   Maximum response of elasto-plastic, one-degree-of-freedom
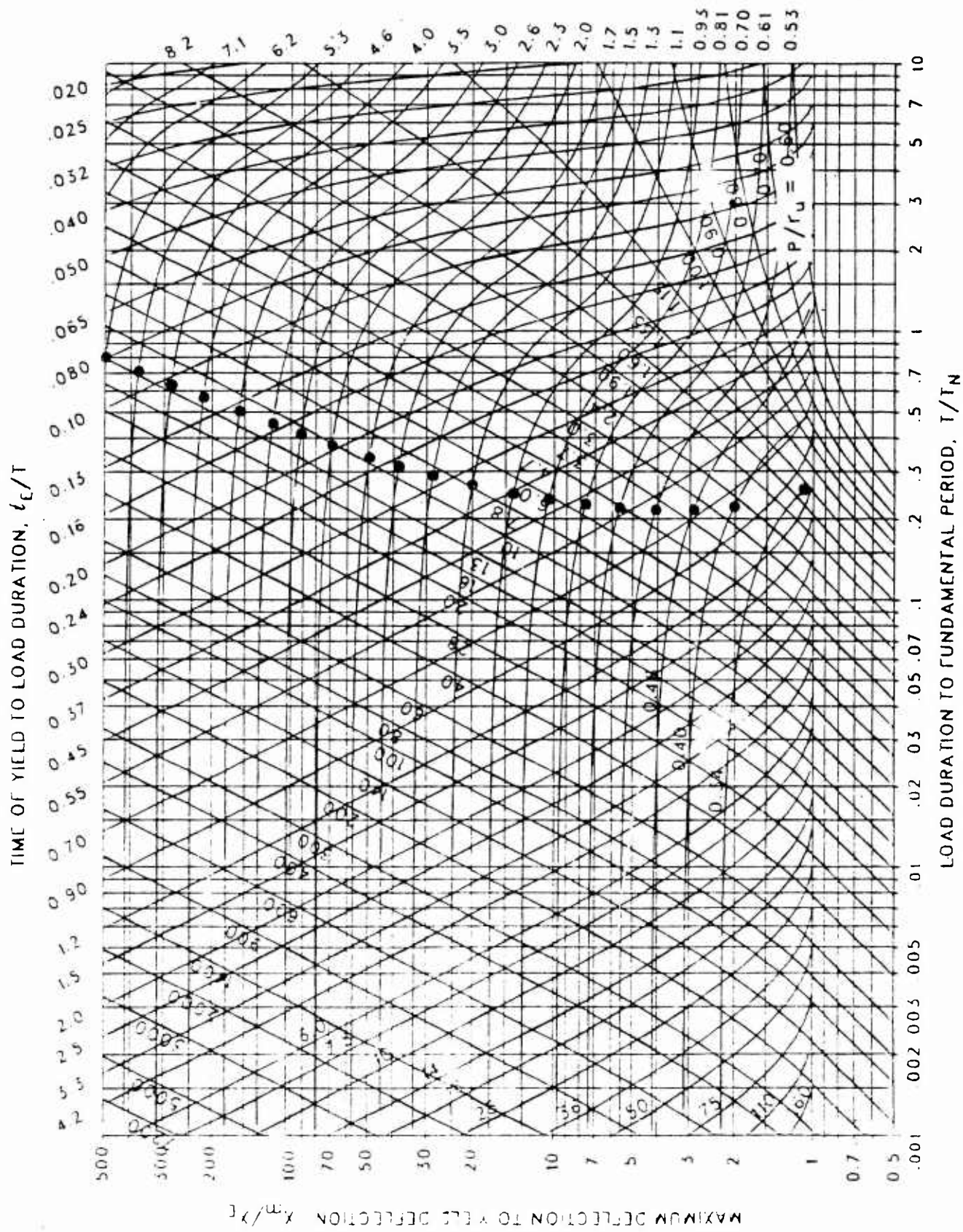system for bilinear-triangular pulse ($C_1 = 0.511$, $C_2 = 30$)

Figure 3-124   Maximum response of elasto-plastic, one-degree-of-freedom
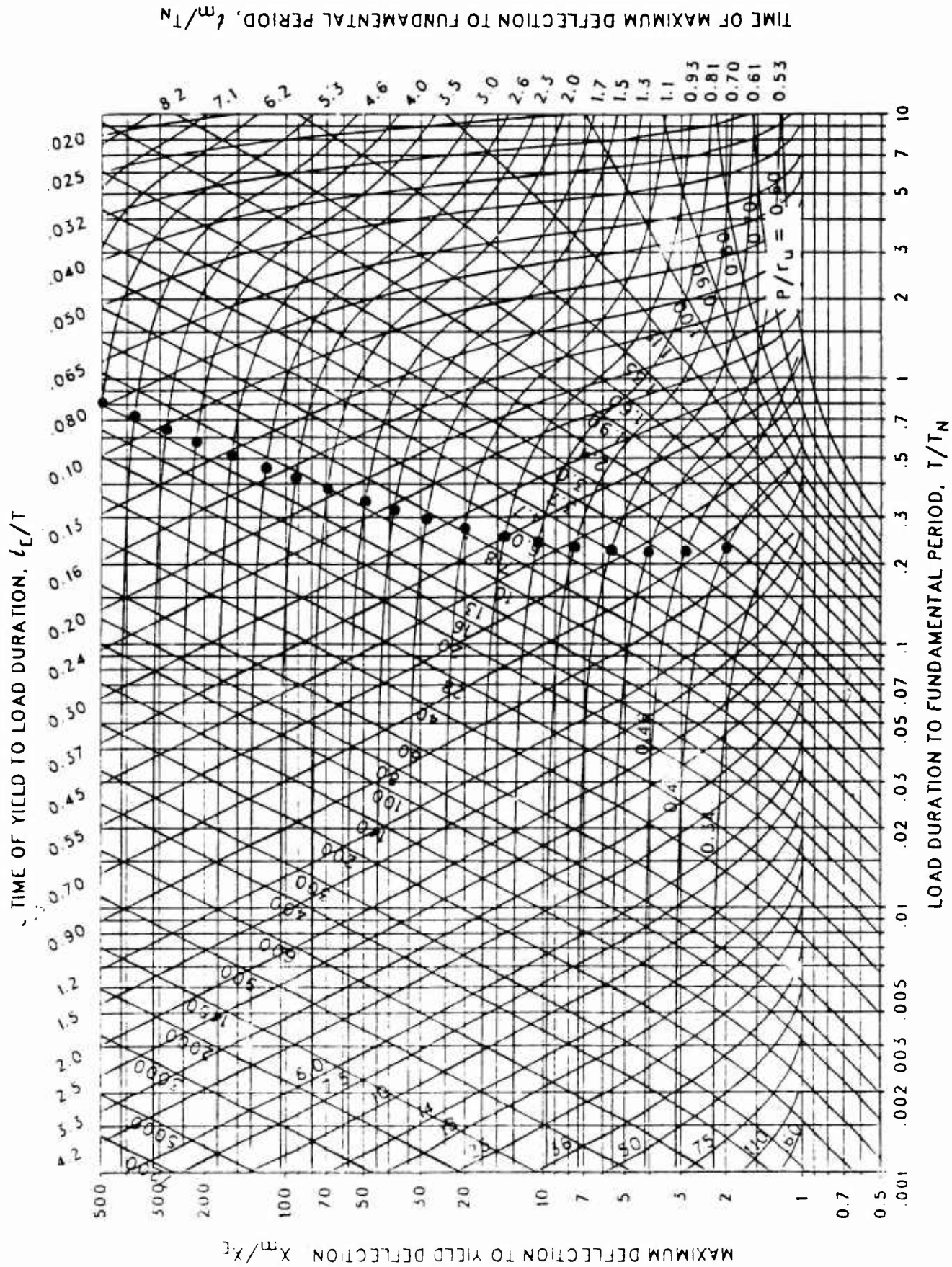system for bilinear-triangular pulse ($C_1 = 0.464$, $C_2 = 30$)

-179-

Figure 3-125   Maximum response of elasto-plastic, one-degree-of-freedom system for bilinear-triangular pulse (C_1 = 0.383, C_2 = 30)

-180-

Figure 3-126   Maximum response of elasto-plastic, one-degree-of-freedom system for bilinear-triangular pulse ($C_1 = 0.316$, $C_2 = 30$)

-181-

Figure 3-127   Maximum response of elasto-plastic, one-degree-of-freedom
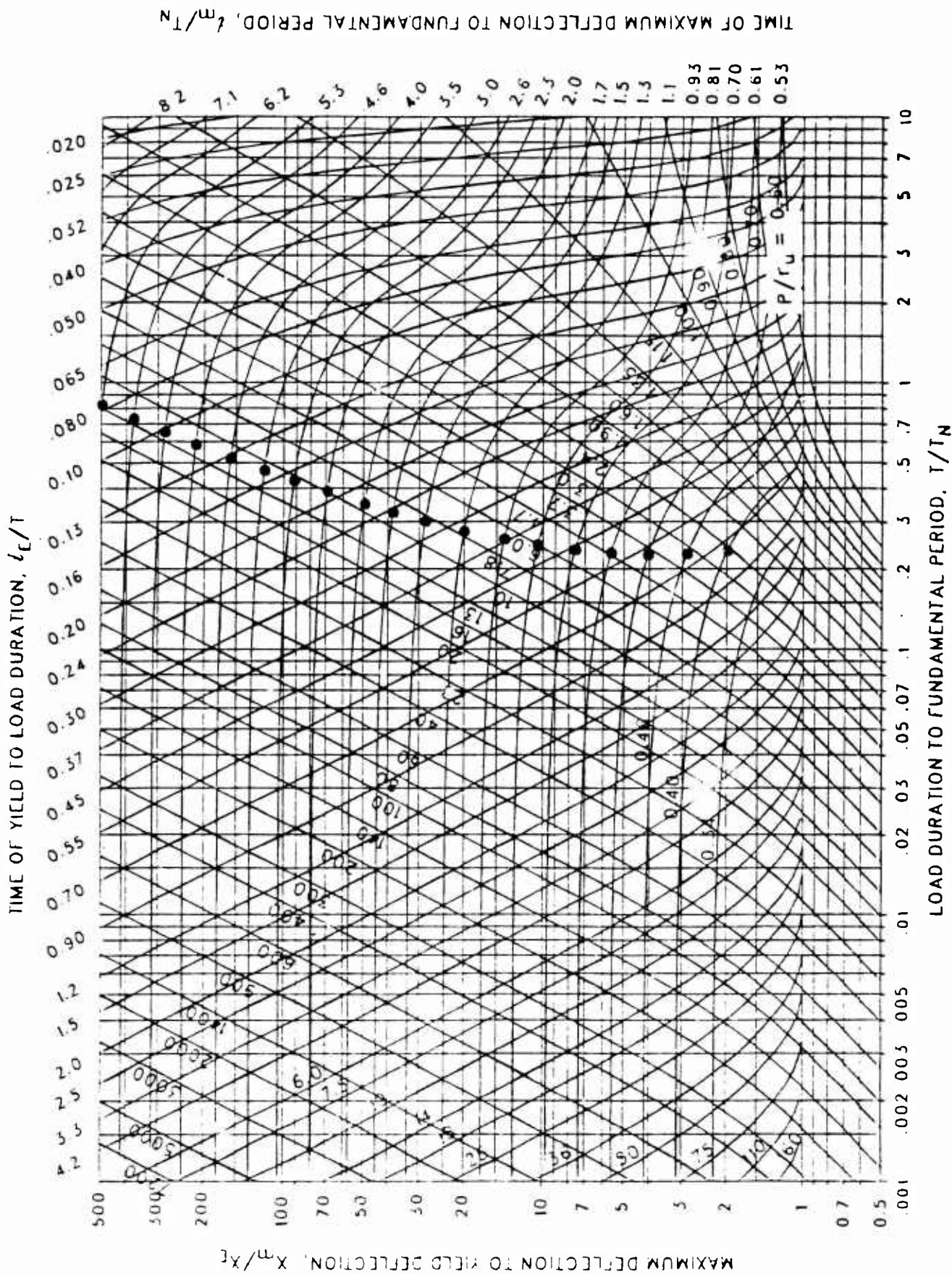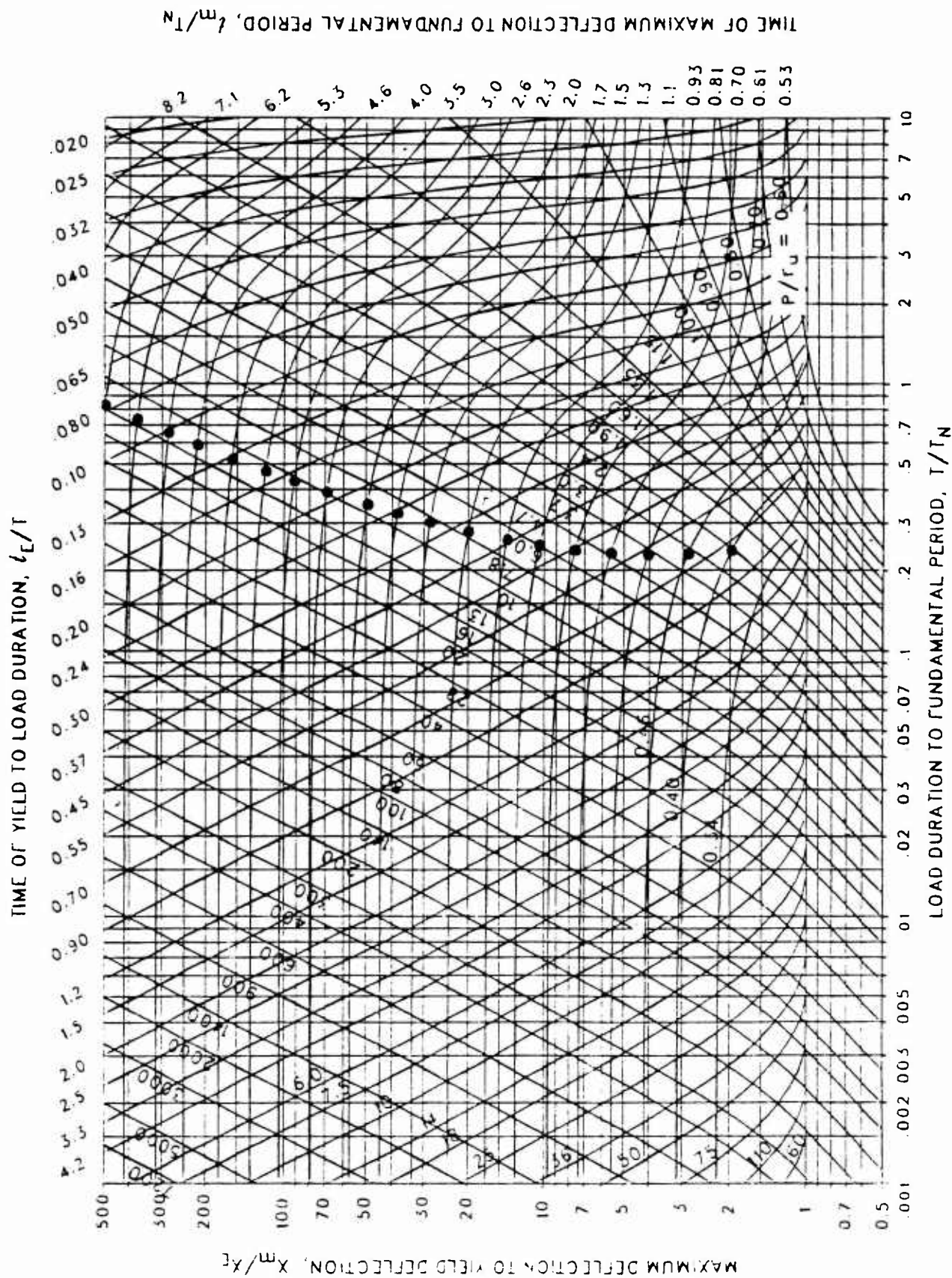system for bilinear-triangular pulse ($C_1 = 0.261$, $C_2 = 30$)

-182-

Figure 3-128   Maximum response of elasto-plastic, one-degree-of-freedom system for bilinear-triangular pulse ($C_1 = 0.215$, $C_2 = 30$)

Figure 3-129 Maximum response of elasto-plastic, one-degree-of-freedom system for bilinear-triangular pulse (C_1 = 0.178, C_2 = 30)
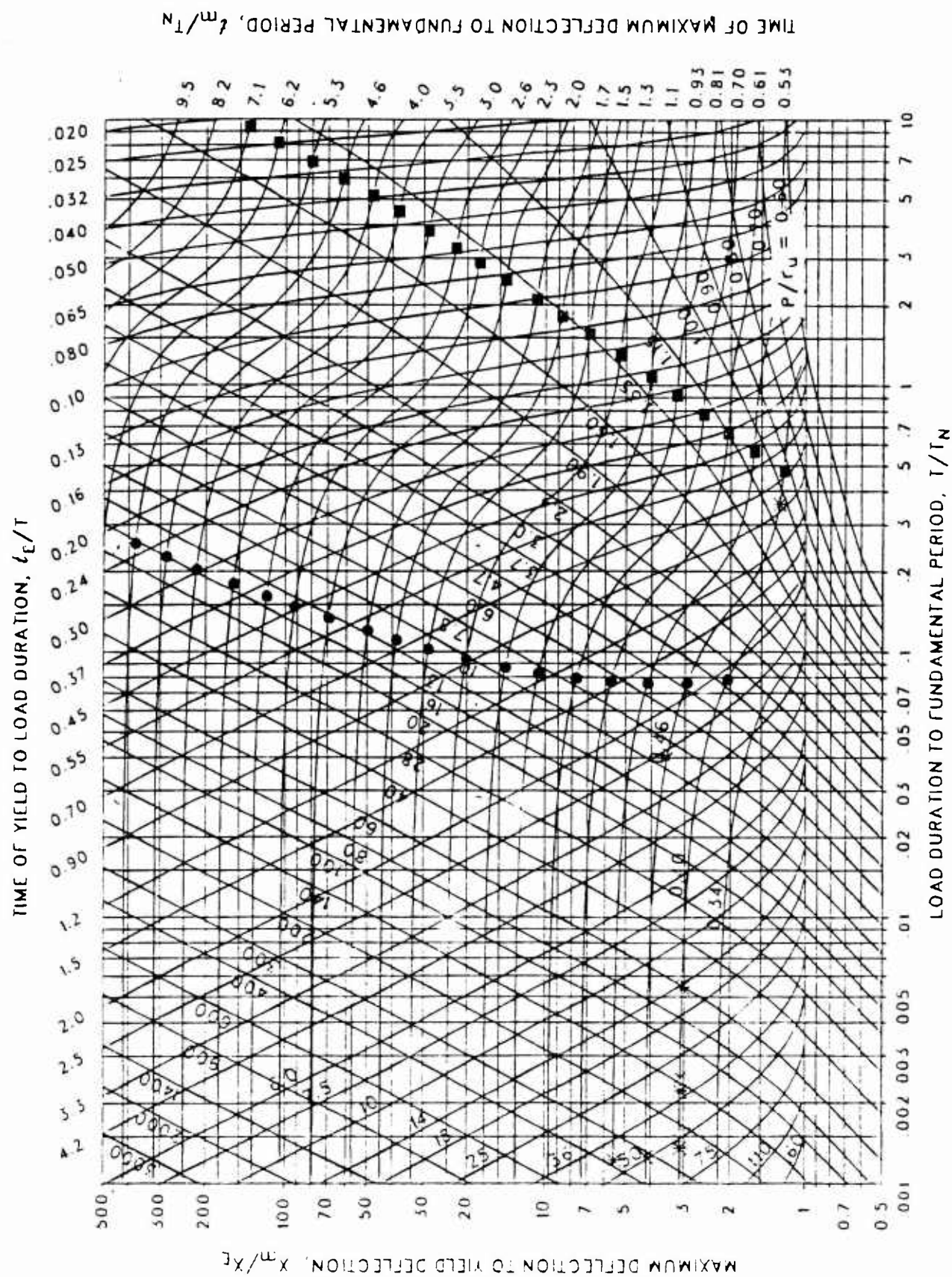
-184-

Figure 3-130   Maximum response of elasto-plastic, one-degree-of-freedom system for bilinear-triangular pulse ($C_1 = 0.147$, $C_2 = 30$)

Figure 3-131   Maximum response of elasto-plastic, one-degree-of-freedom system for bilinear-triangular pulse ($C_1 = 0.121$, $C_2 = 30$)
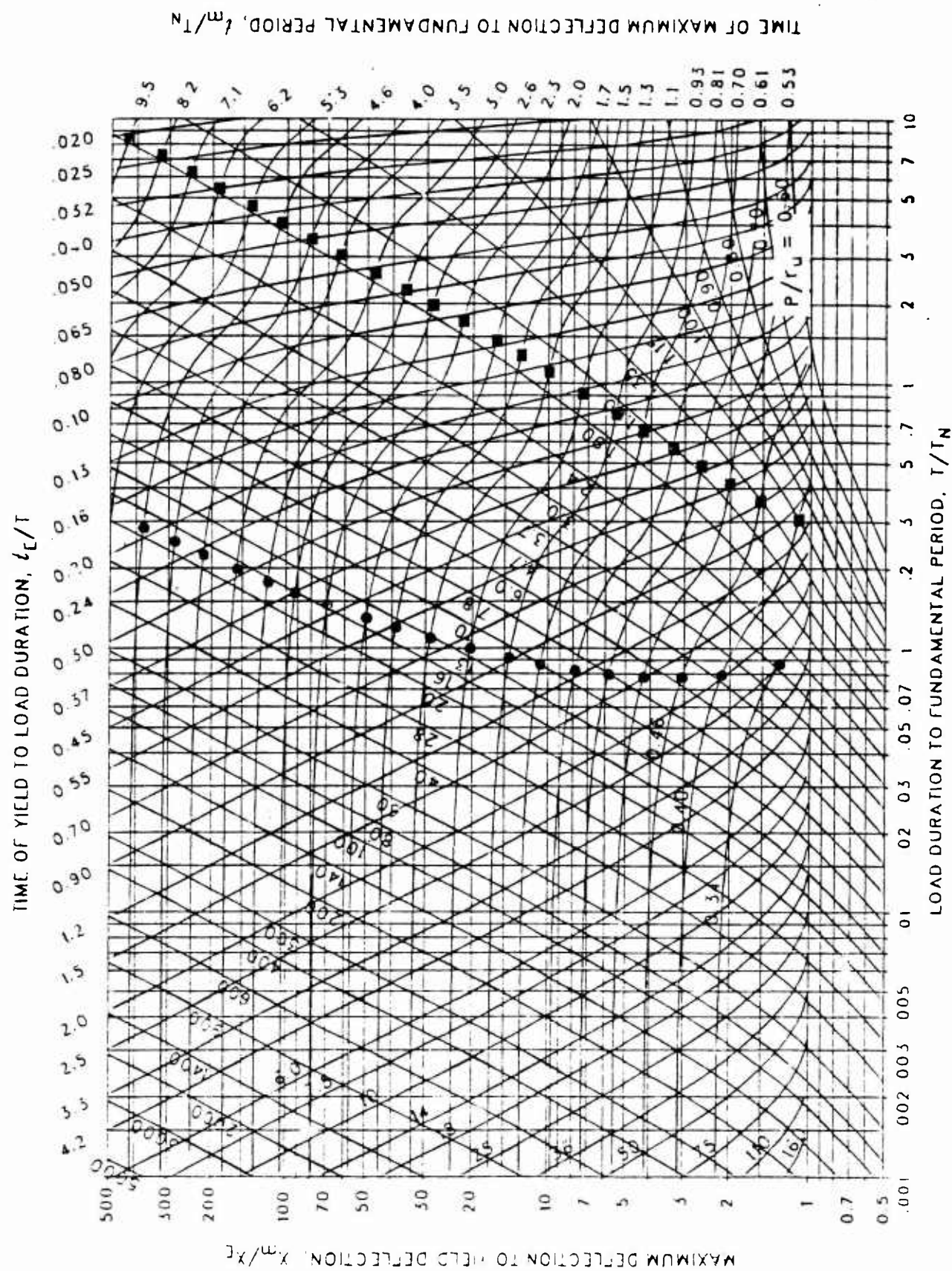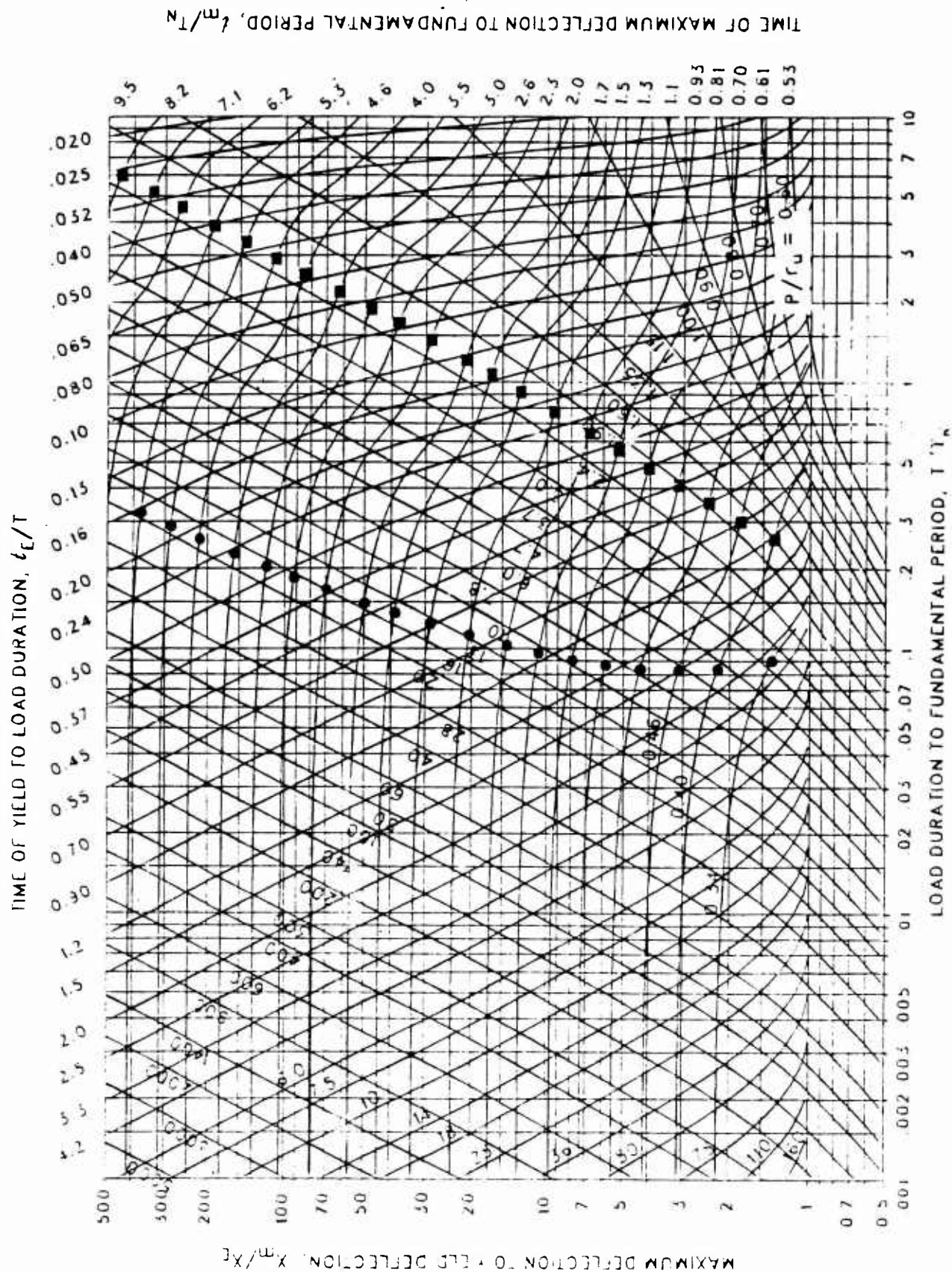
-186-

Figure 3-132   Maximum response of elasto-plastic, one-degree-of-freedom
system for bilinear-triangular pulse ($C_1 = 0.100$, $C_2 = 30$)

-187-

Figure 3-133   Maximum response of elasto-plastic, one-degree-of-freedom system for bilinear-triangular pulse ($C_1 = 0.075$, $C_2 = 30$)
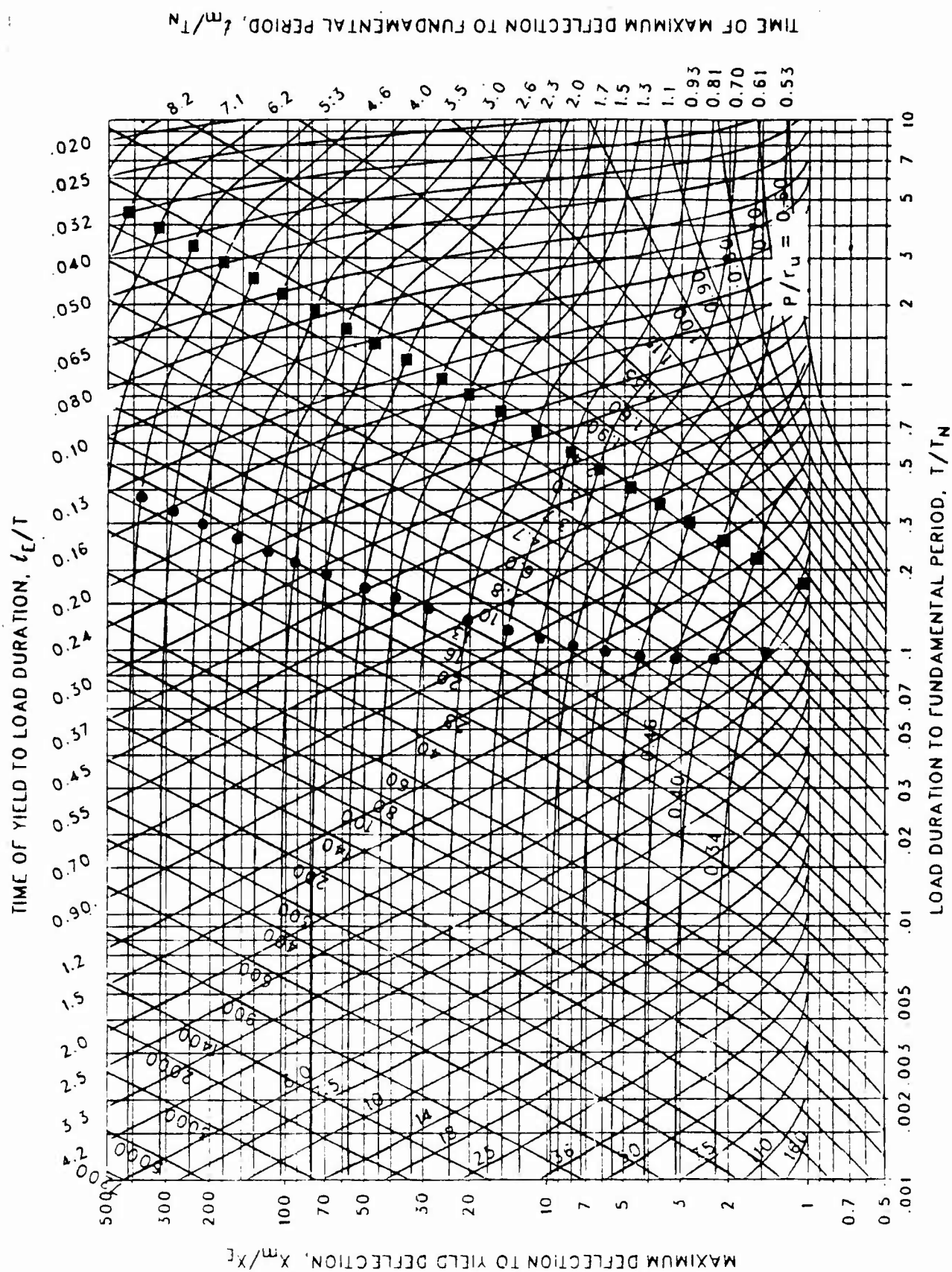
-188-

Figure 3-134   Maximum response of elasto-plastic, one-degree-of-freedom system for bilinear-triangular pulse ($C_1 = 0.056$, $C_2 = 30$)

-189-

Figure 3-135   Maximum response of elasto-plastic, one-degree-of-freedom
system for bilinear-triangular pulse ($C_1 = 0.042$, $C_2 = 30$)

Figure 3-136   Maximum response of elasto-plastic, one-degree-of-freedom system for bilinear-triangular pulse ($C_1 = 0.032$, $C_2 = 30$)

Figure 3-137   Maximum response of elasto-plastic, one-degree-of-freedom system for bilinear-triangular pulse ($C_1 = 0.026$, $C_2 = 30$)
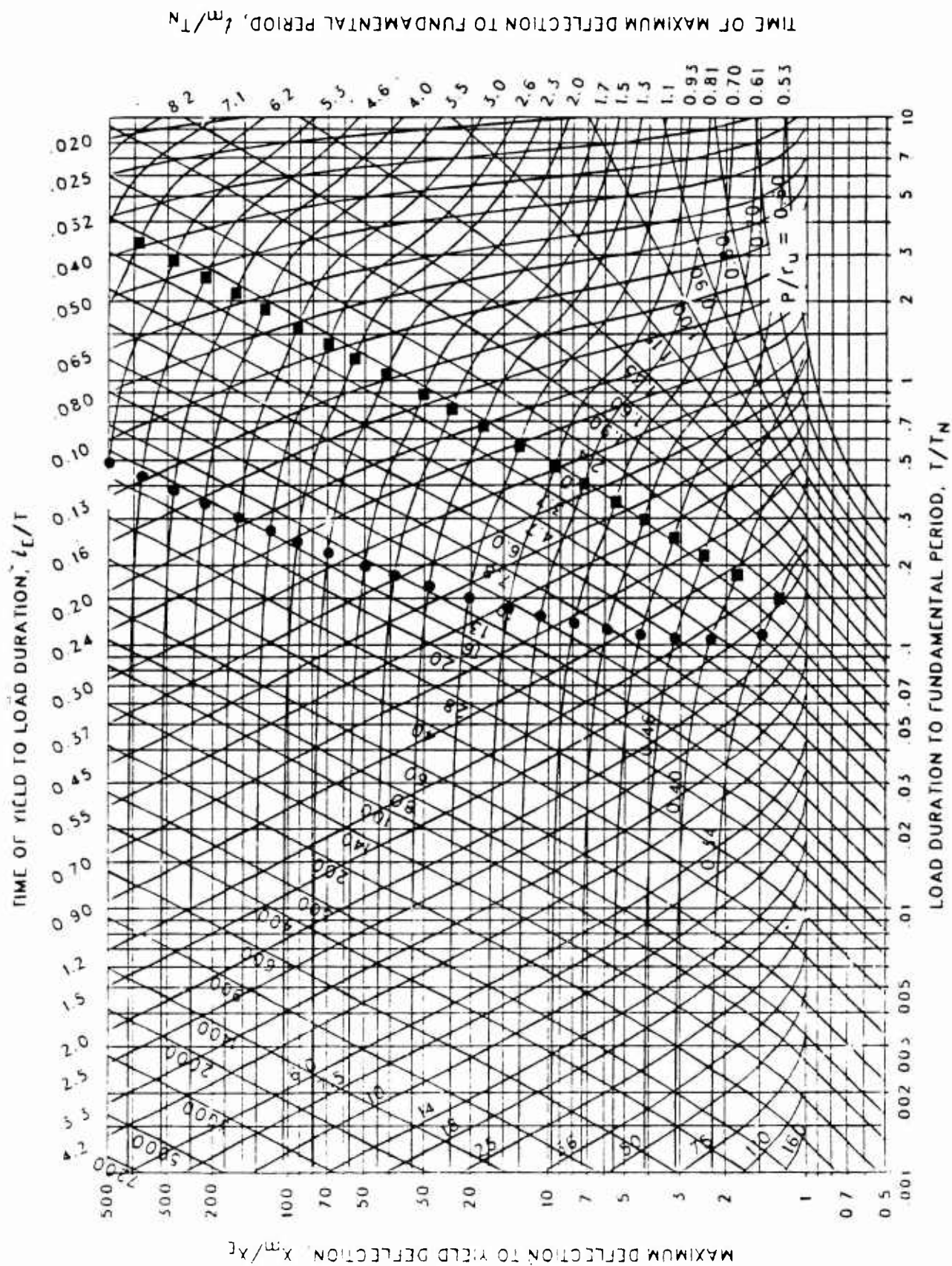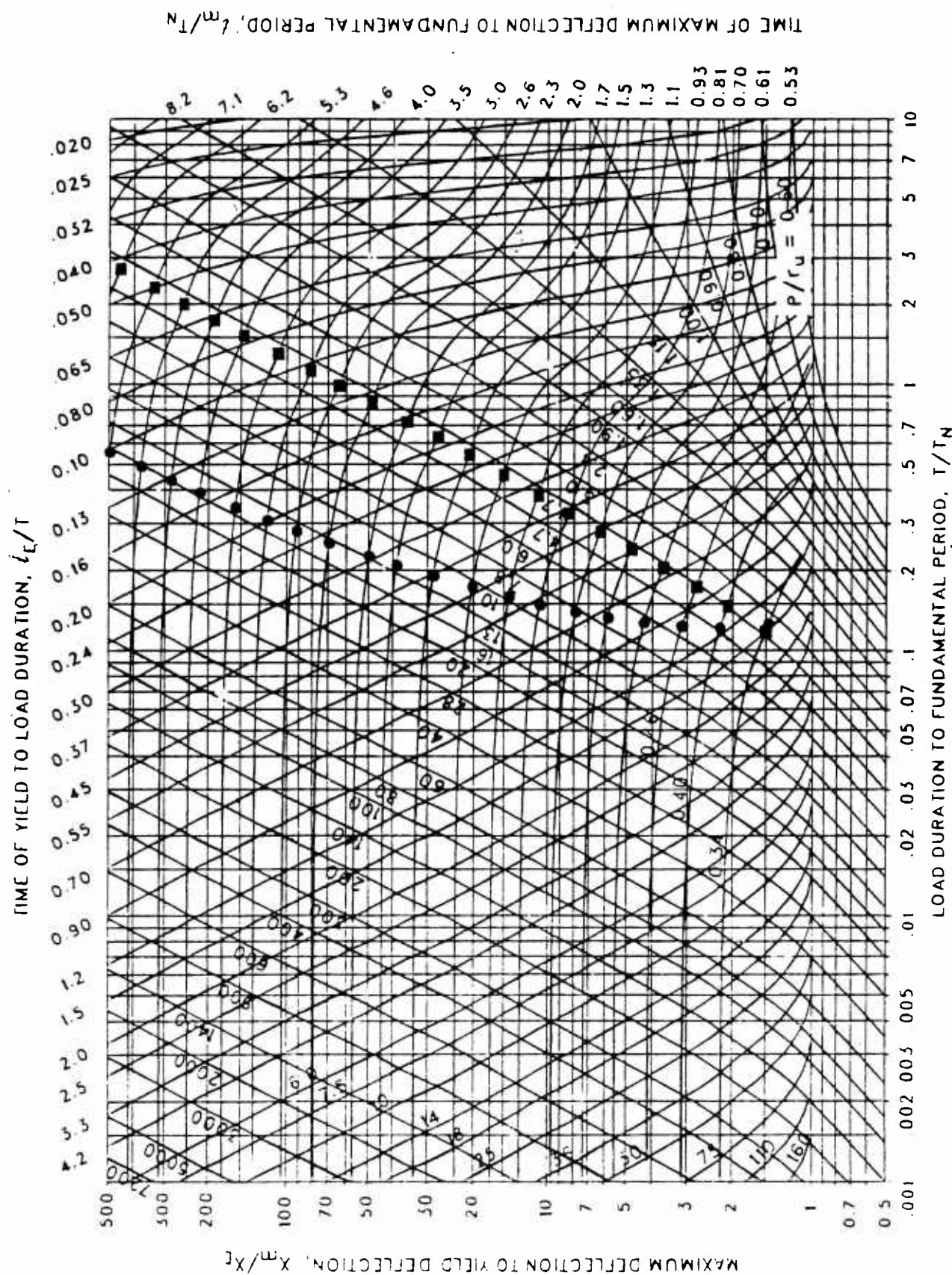
Figure 3-138   Maximum response of elasto-plastic, one-degree-of-freedom system for bilinear-triangular pulse ($C_1 = 0.018$, $C_2 = 30$)
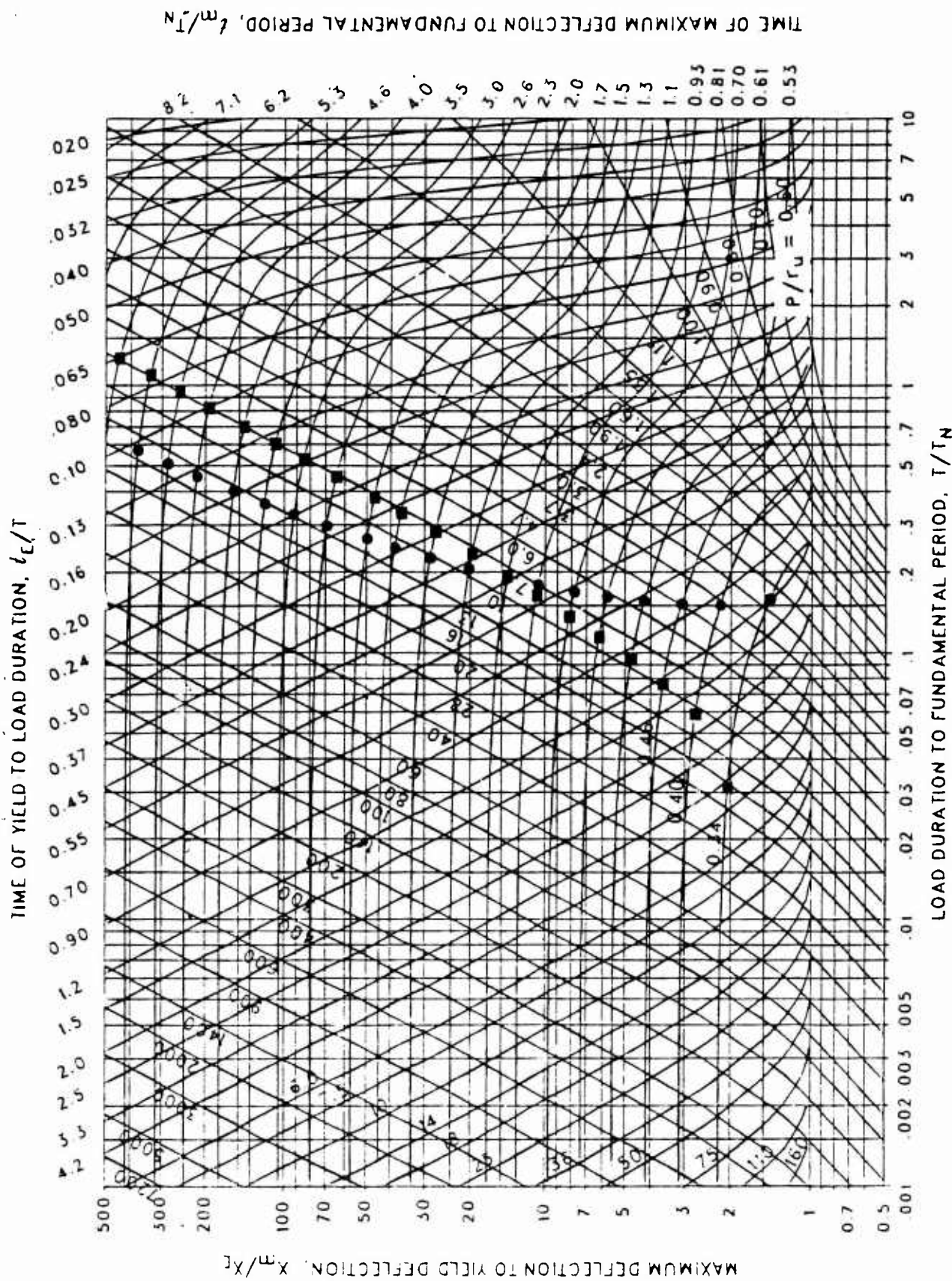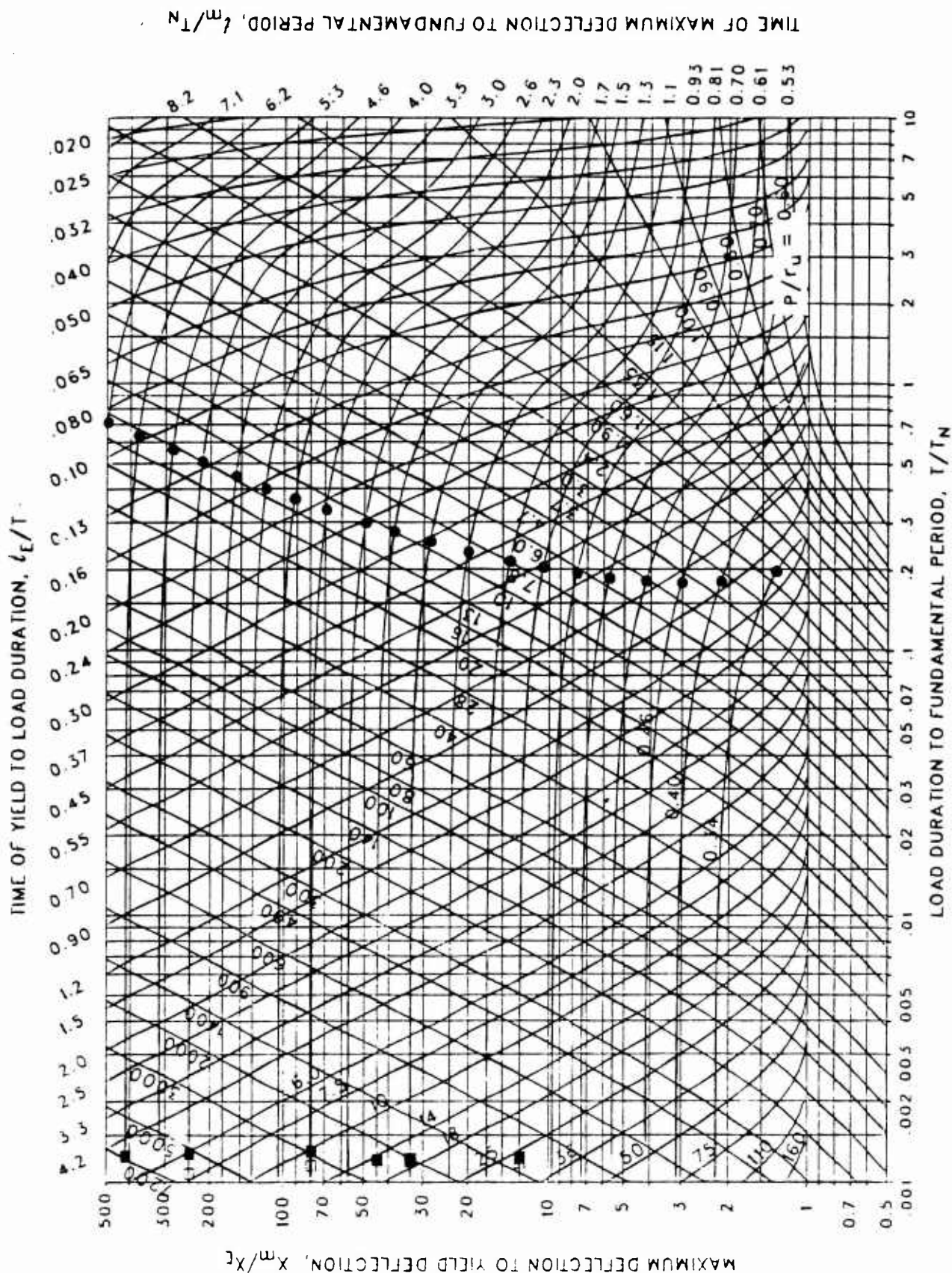
-193-

Figure 3-139   Maximum response of elasto-plastic, one-degree-of-freedom system for bilinear-triangular pulse ($C_1 = 0.013$, $C_2 = 30$)
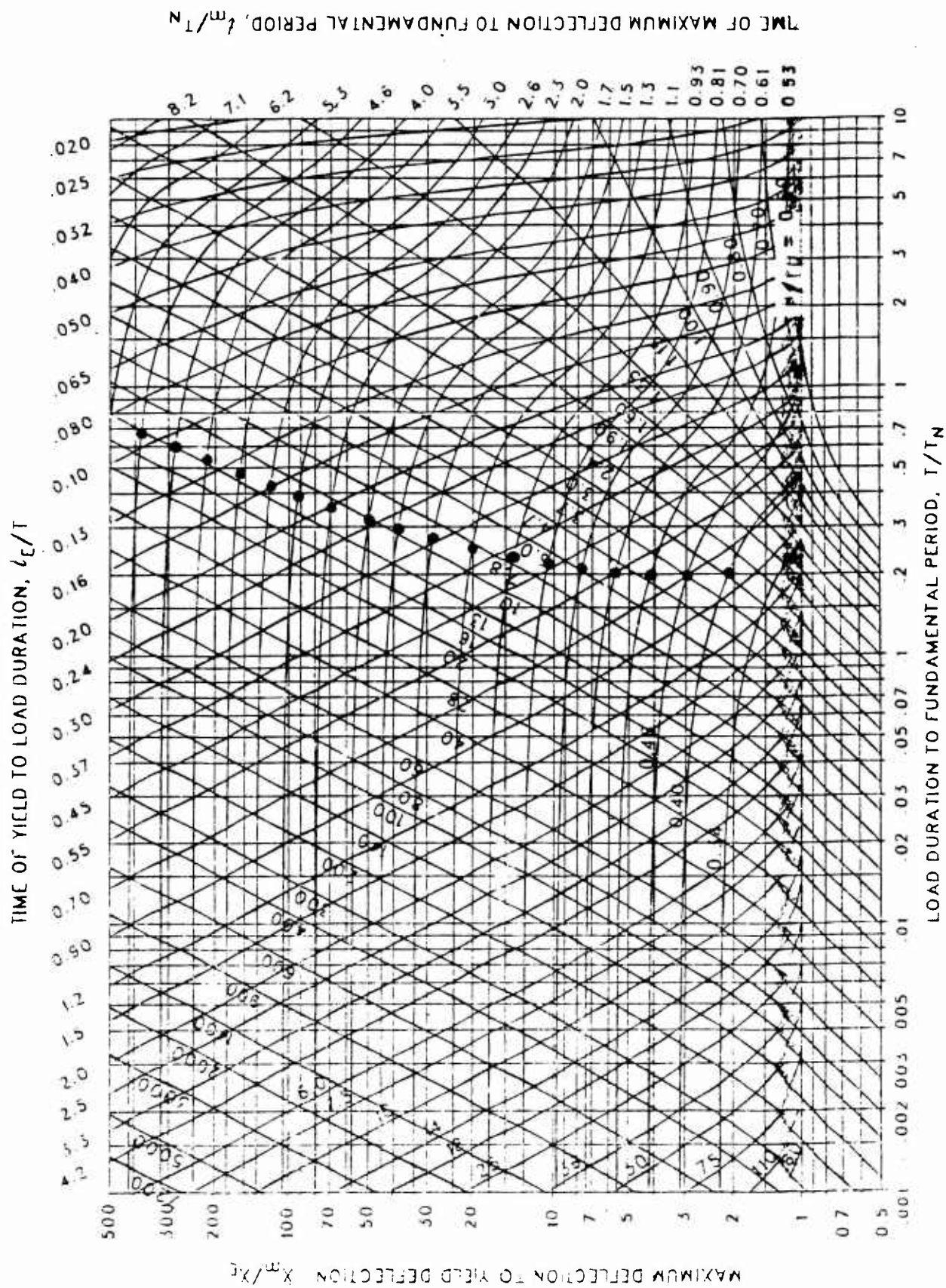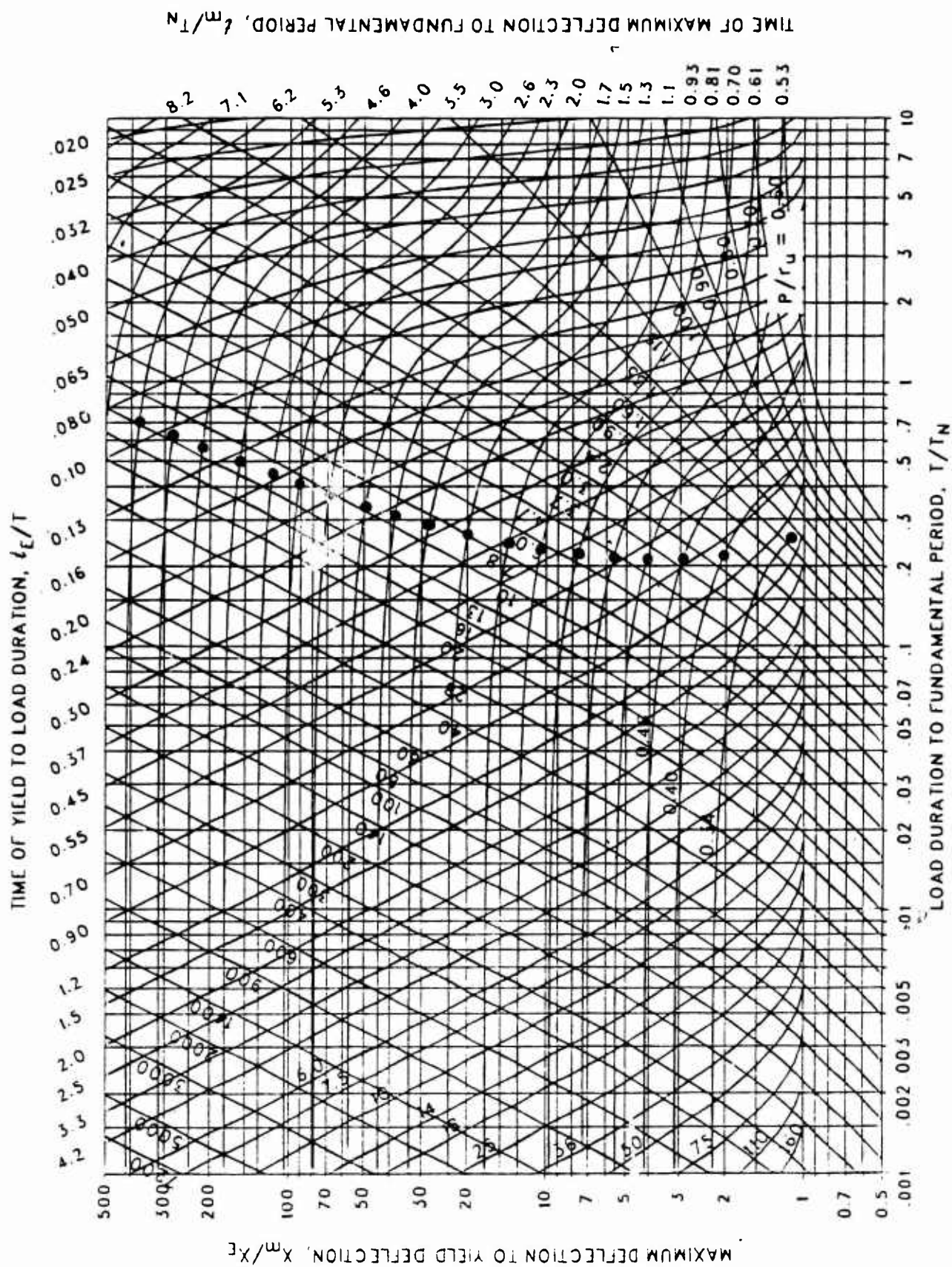
-194-

Figure 3-140   Maximum response of elasto-plastic, one-degree-of-freedom system for bilinear-triangular pulse ($C_1 = 0.010$, $C_2 = 30$)

-195-

Figure 3-141 Maximum response of elasto-plastic, one-degree-of-freedom system for bilinear-triangular pulse ($C_1 = 0.909$, $C_2 = 100.$)

-196-

Figure 3-142   Maximum response of elasto-plastic, one-degree-of-freedom
system for bilinear-triangular pulse ($C_1 = 0.866$, $C_2 = 100.$)

-197-

Figure 3-143   Maximum response of elasto-plastic, one-degree-of-freedom
system for bilinear-triangular pulse ($C_1 = 0.825$, $C_2 = 100.$)

-198-

TIME OF MAXIMUM DEFLECTION TO FUNDAMENTAL PERIOD, t_m/T_N

TIME OF YIELD TO LOAD DURATION, t_E/T

MAXIMUM DEFLECTION TO YIELD DEFLECTION, X_m/X_E

LOAD DURATION TO FUNDAMENTAL PERIOD, T/T_N

Figure 3-144   Maximum response of elasto-plastic, one-degree-of-freedom system for bilinear-triangular pulse ($C_1 = 0.787$, $C_2 = 100.$)
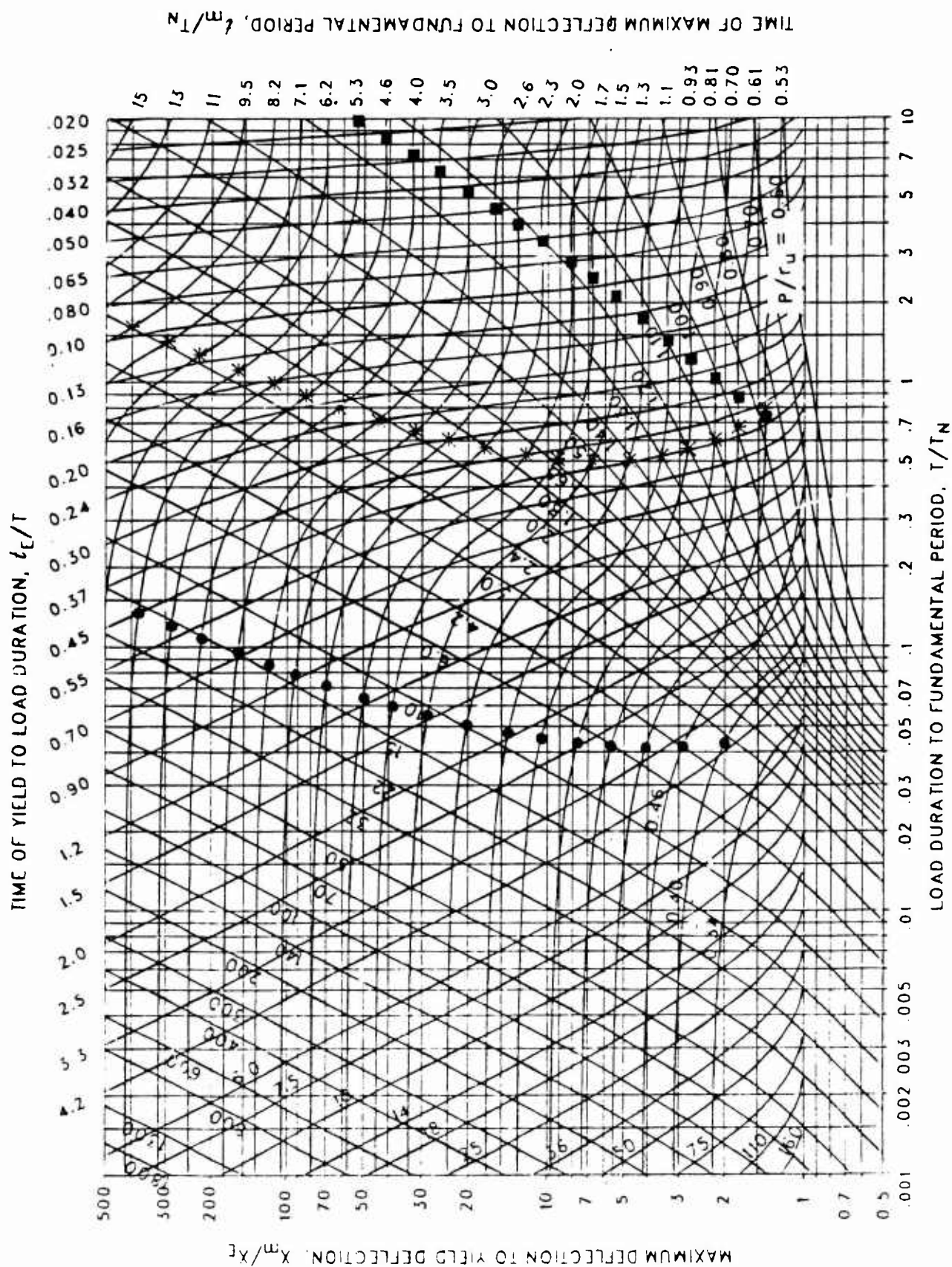
Figure 3-145   Maximum response of elasto-plastic, one-degree-of-freedom
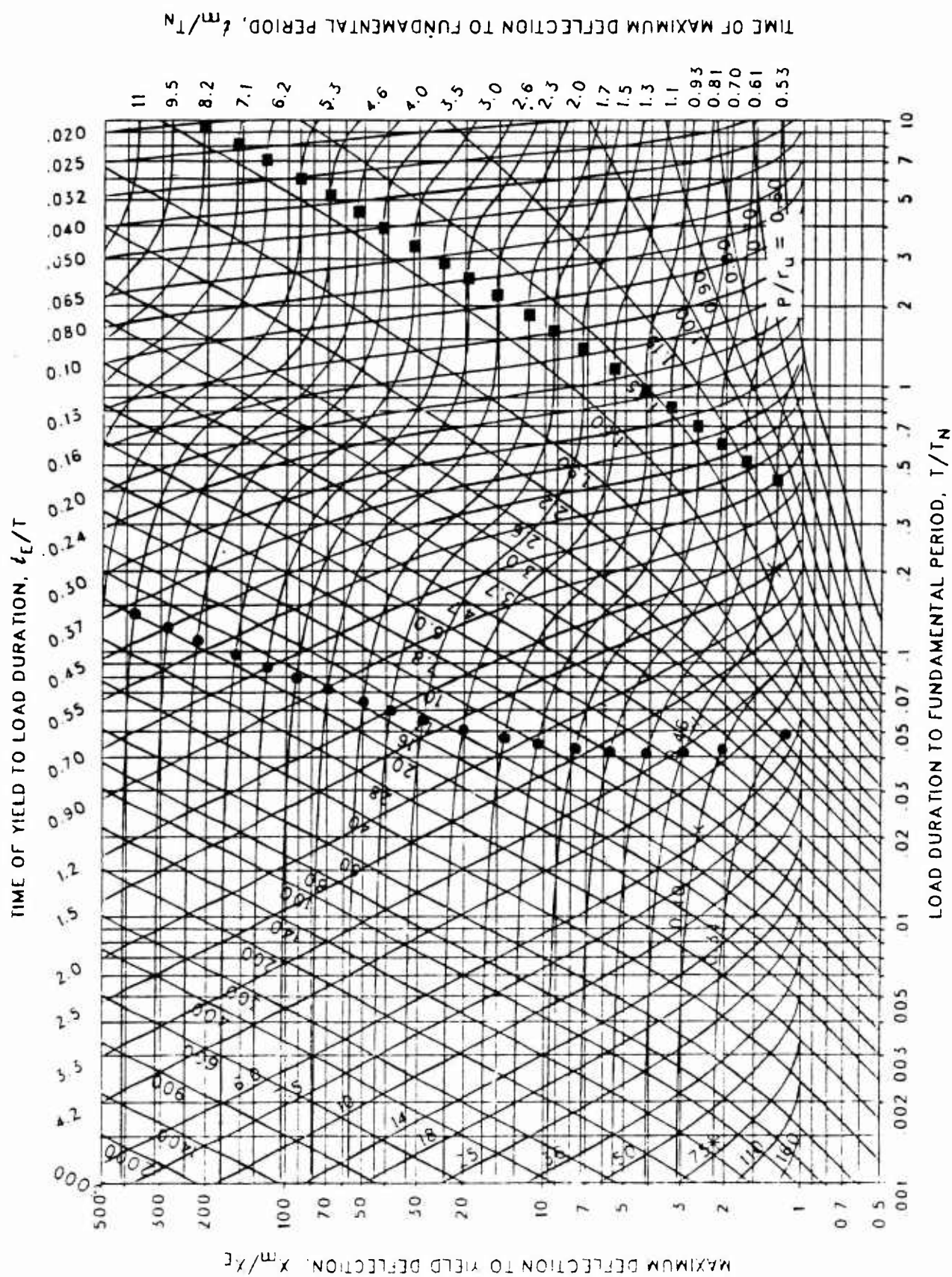system for bilinear-triangular pulse ($C_1 = 0.750$, $C_2 = 100.$)

Figure 3-146   Maximum response of elasto-plastic, one-degree-of-freedom system for bilinear-triangular pulse ($C_1 = 0.715$, $C_2 = 100.$)
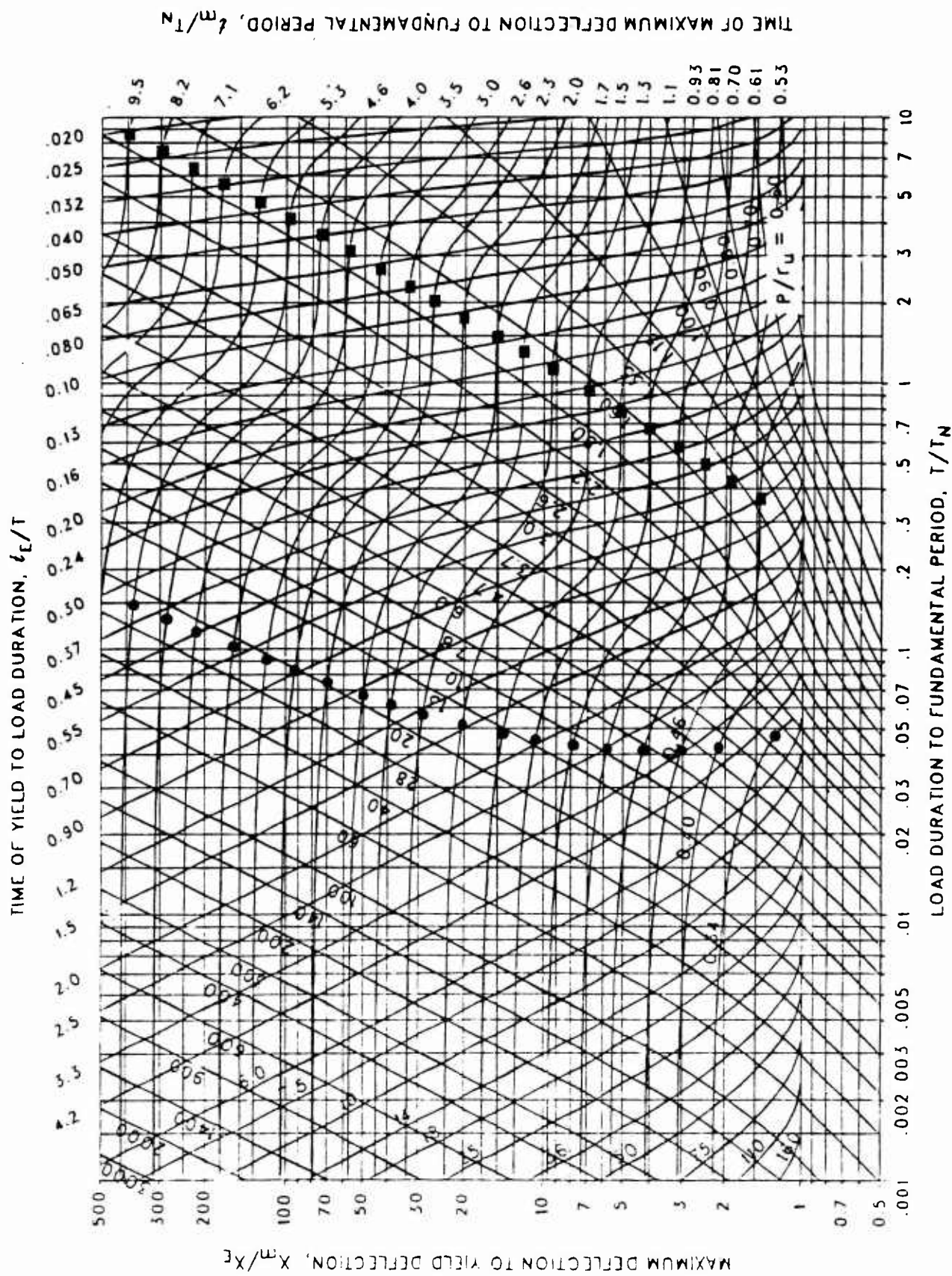
Figure 3-147 Maximum response of elasto-plastic, one-degree-of-freedom system for bilinear-triangular pulse ($C_1 = 0.681$, $C_2 = 100.$)

Figure 3-148   Maximum response of elasto-plastic, one-degree-of-freedom system for bilinear-triangular pulse ($C_1 = 0.648$, $C_2 = 100.$)
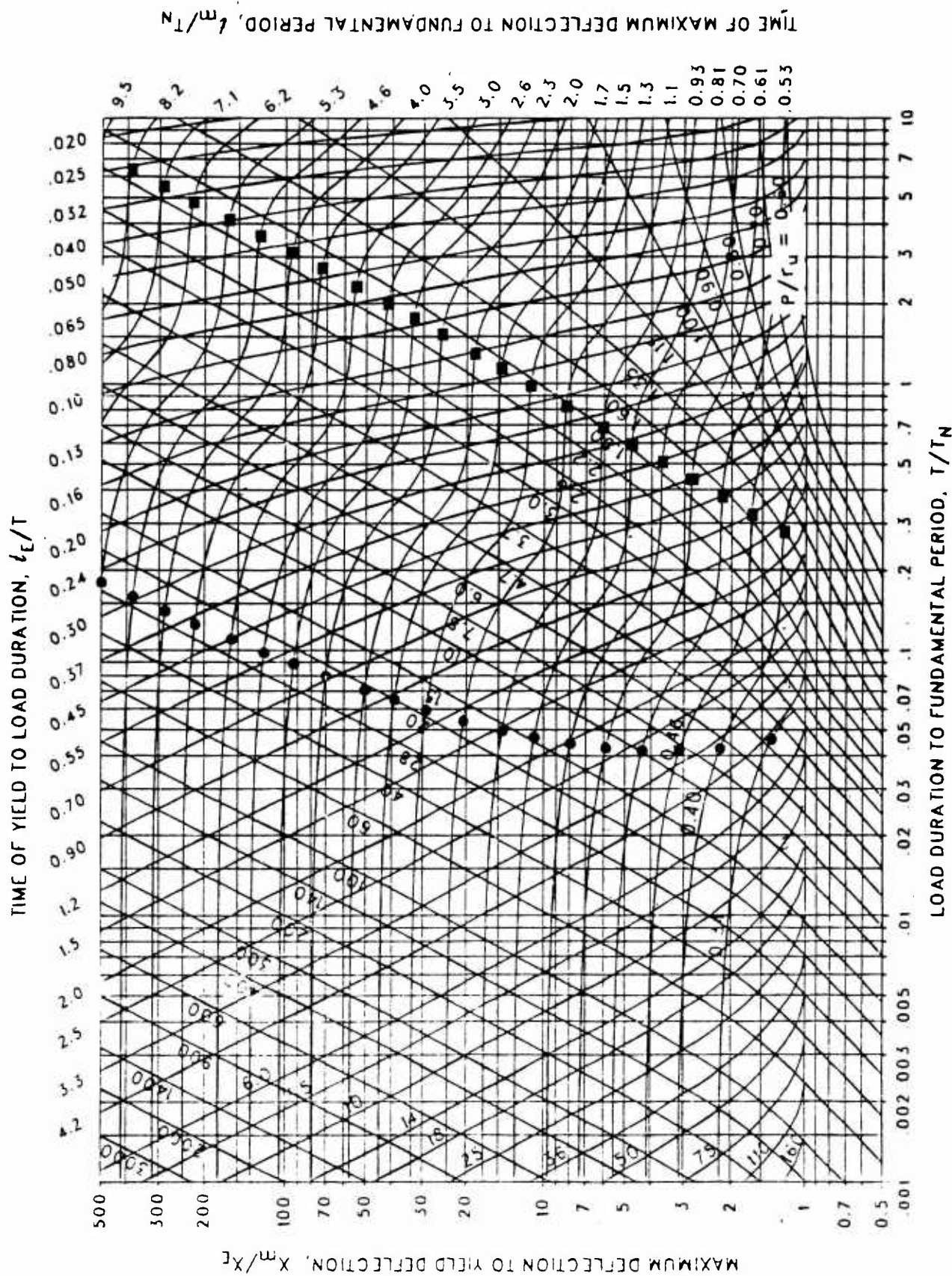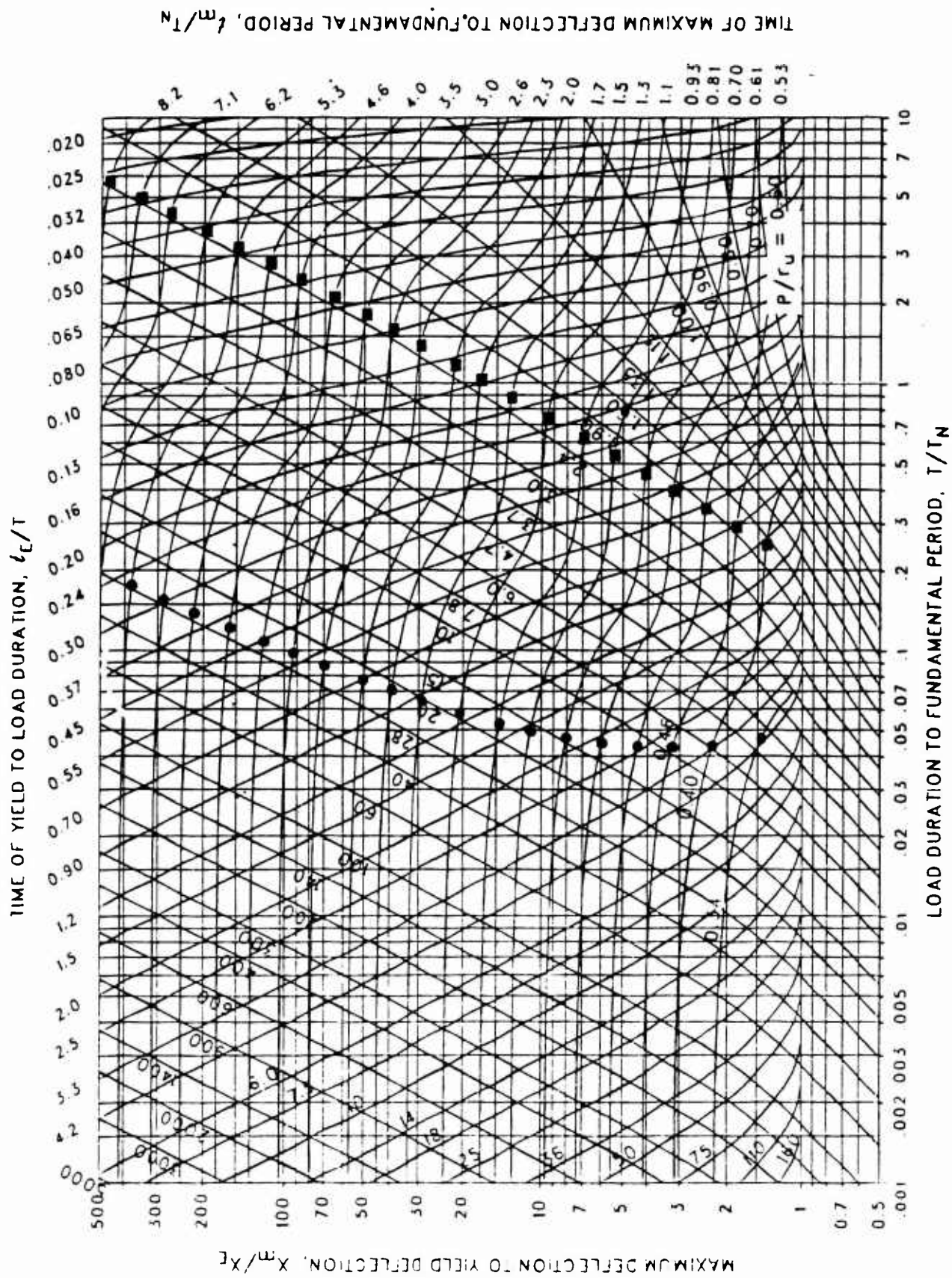
-203-

Figure 3-149 Maximum response of elasto-plastic, one-degree-of-freedom system for bilinear-triangular pulse ($C_1 = 0.619$, $C_2 = 100$.)

Figure 3-150   Maximum response of elasto-plastic, one-degree-of-freedom
system for bilinear-triangular pulse (C_1 = 0.590, C_2 = 100.)

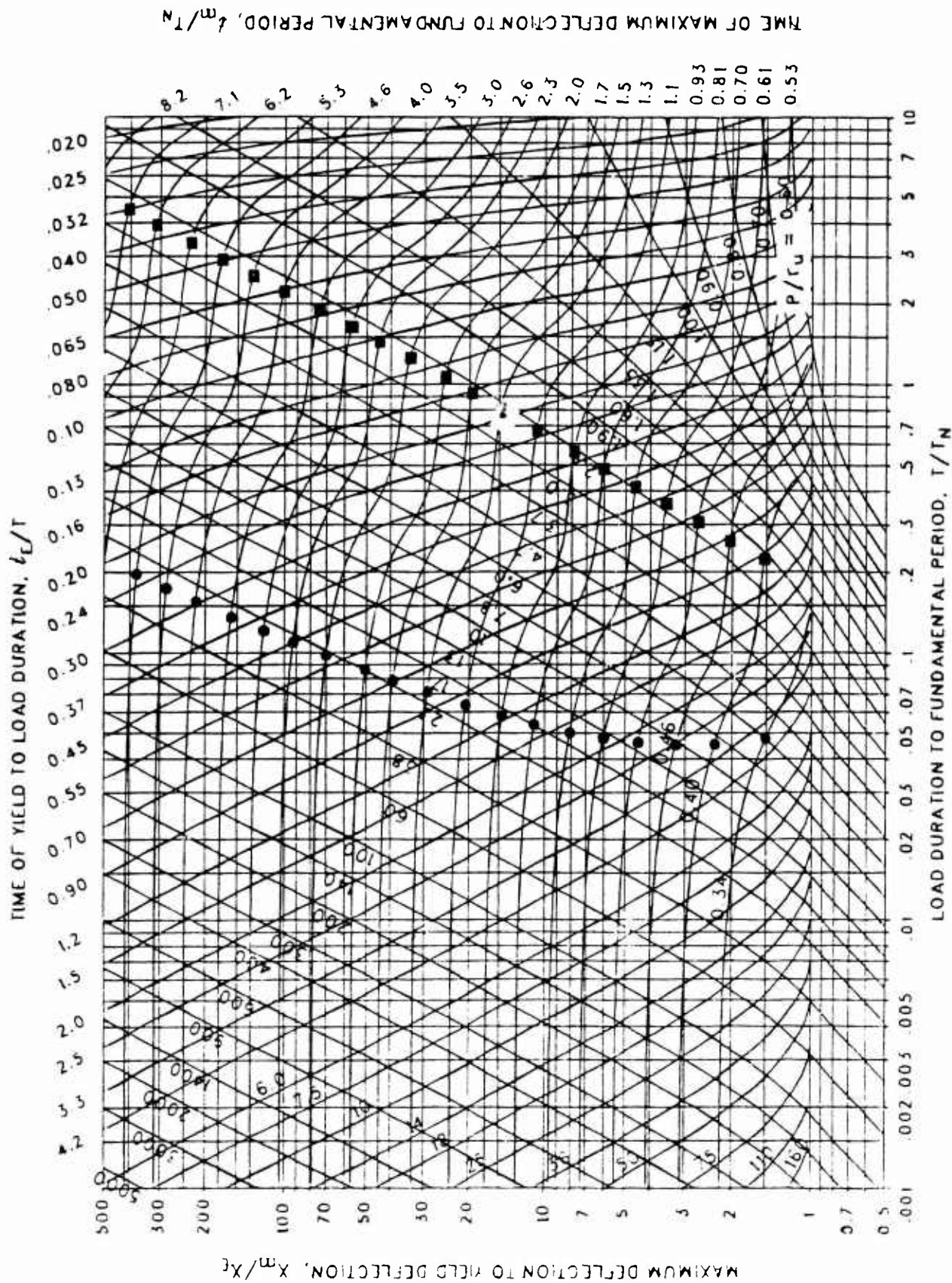Figure 3-151   Maximum response of elasto-plastic, one-degree-of-freedom system for bilinear-triangular pulse ($C_1 = 0.562$, $C_2 = 100.$)

Figure 3-152 Maximum response of elasto-plastic, one-degree-of-freedom system for bilinear-triangular pulse ($C_1 = 0.511$, $C_2 = 100$.)
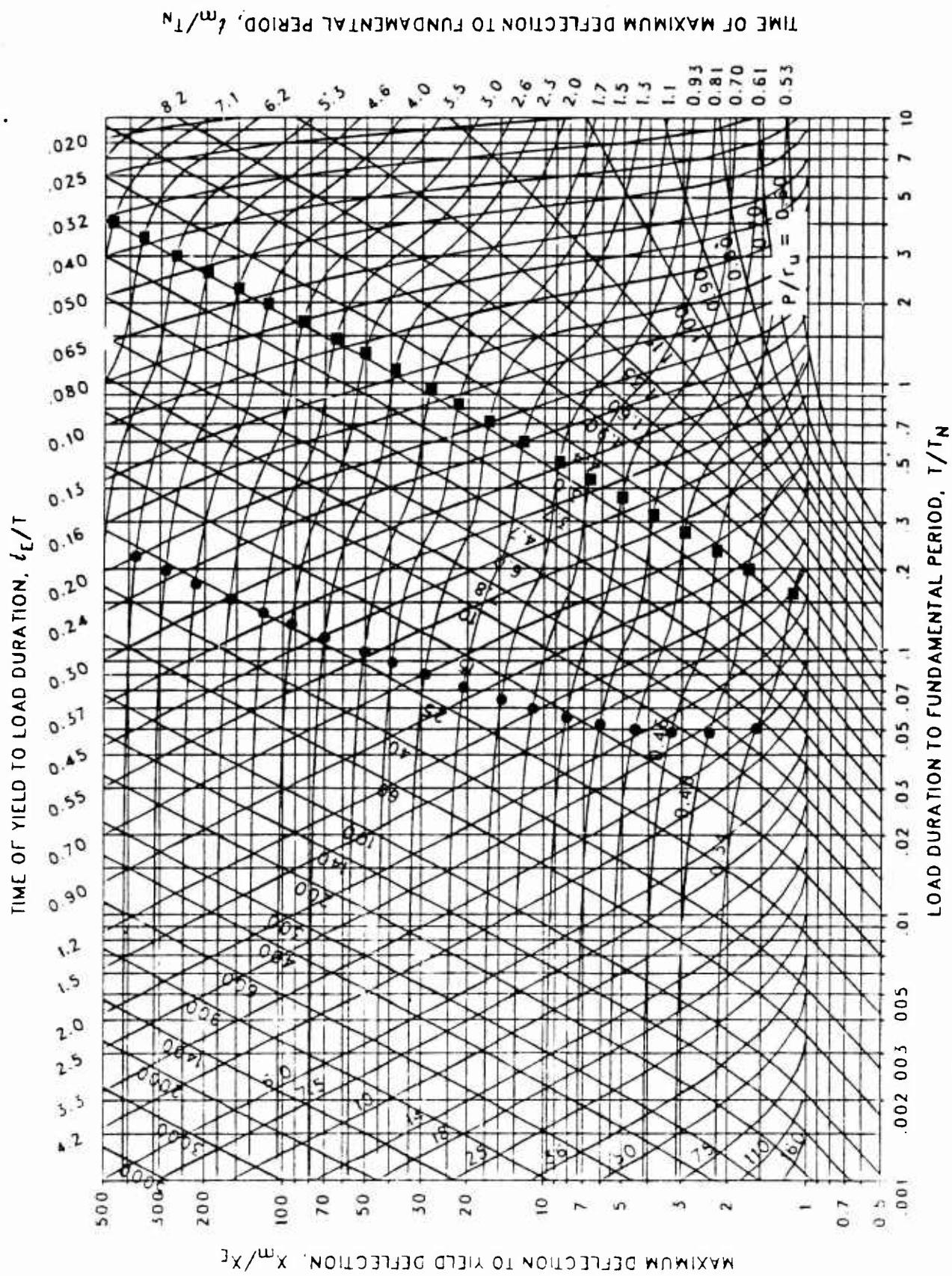
Figure 3-153   Maximum response of elasto-plastic, one-degree-of-freedom system for bilinear-triangular pulse ($C_1 = 0.464$, $C_2 = 100.$)

Figure 3-154 Maximum response of elasto-plastic, one-degree-of-freedom system for bilinear-triangular pulse ($C_1 = 0.422$, $C_2 = 100.$)
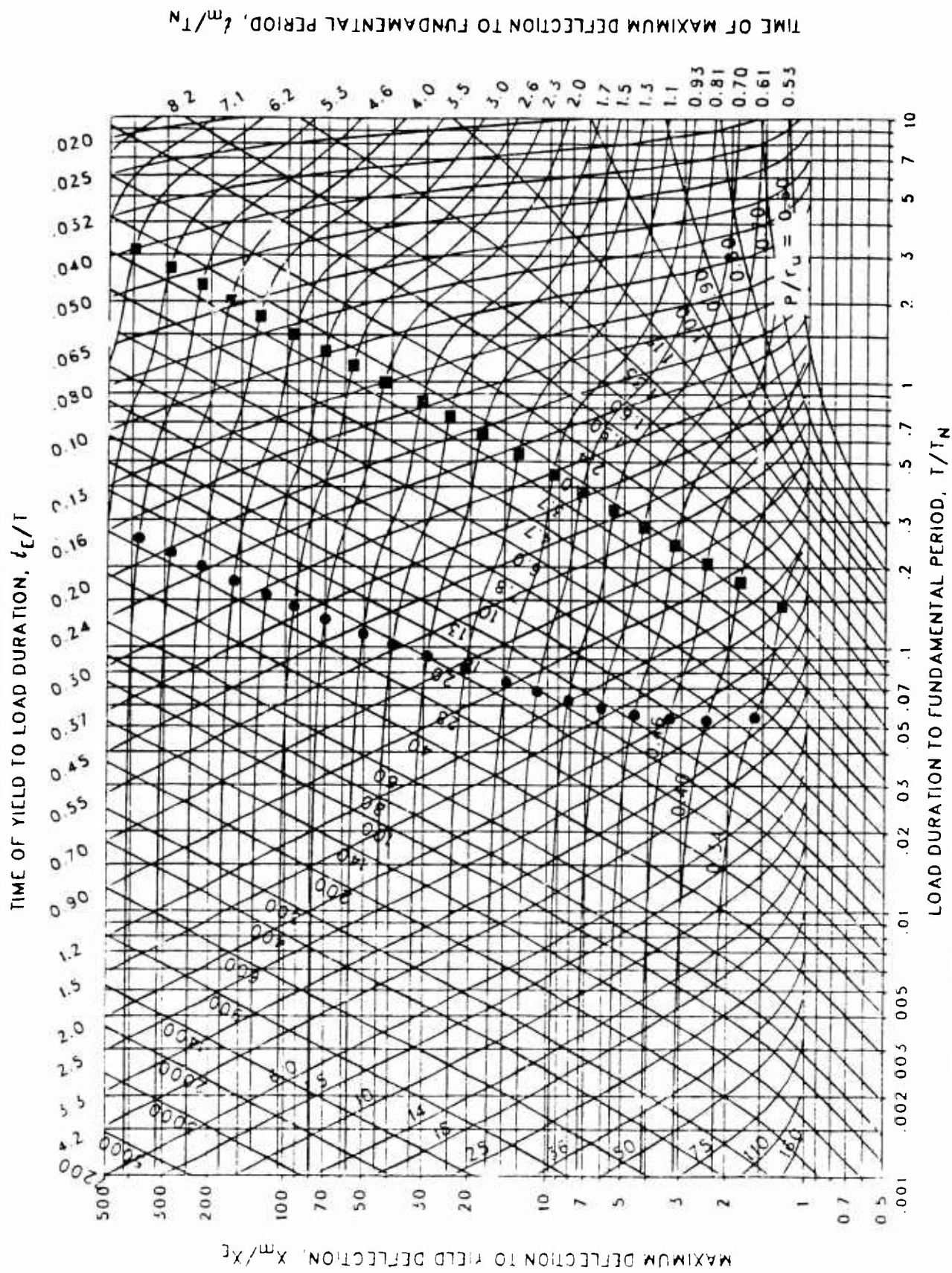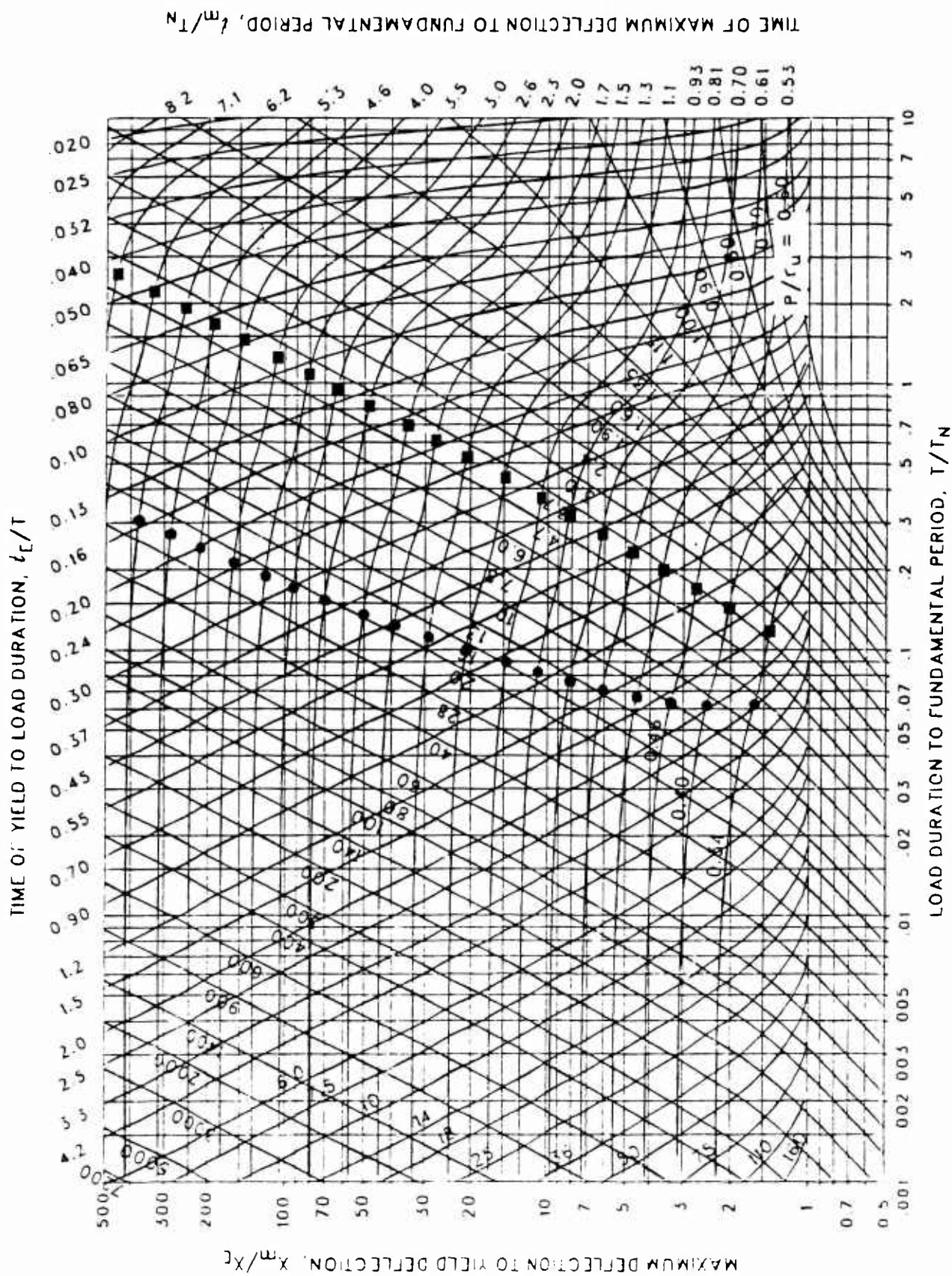
-209-

Figure 3-155 Maximum response of elasto-plastic, one-degree-of-freedom
system for bilinear-triangular pulse ($C_1 = 0.365$, $C_2 = 100.$)

Figure 3-156   Maximum response of elasto-plastic, one-degree-of-freedom system for bilinear-triangular pulse (C_1 = 0.316, C_2 = 100.)

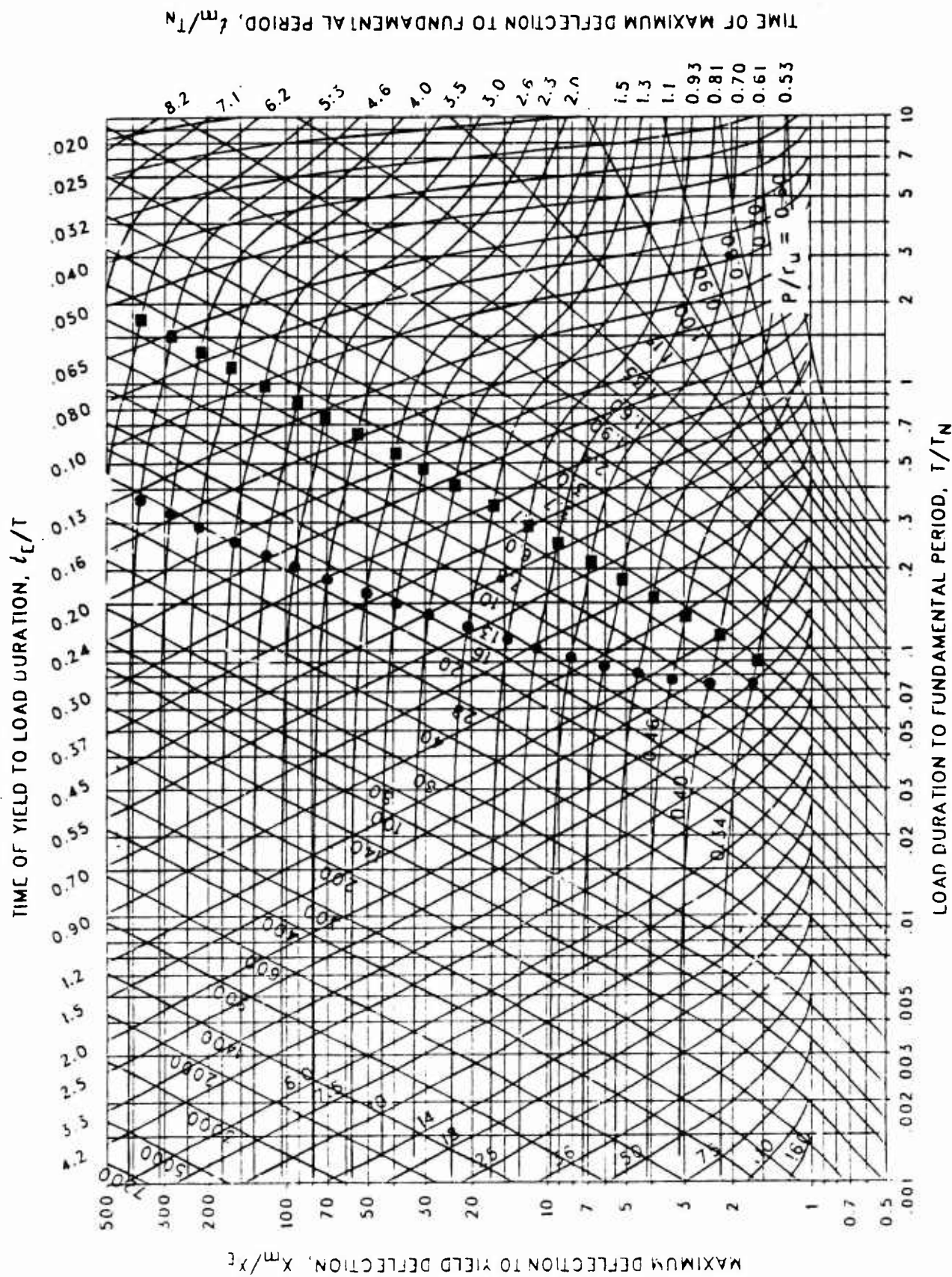Figure 3-157 Maximum response of elasto-plastic, one-degree-of-freedom system for bilinear-triangular pulse ($C_1 = 0.274$, $C_2 = 100$.)

Figure 3-158   Maximum response of elasto-plastic, one-degree-of-freedom system for bilinear-triangular pulse ($C_1 = 0.261$, $C_2 = 100.$)
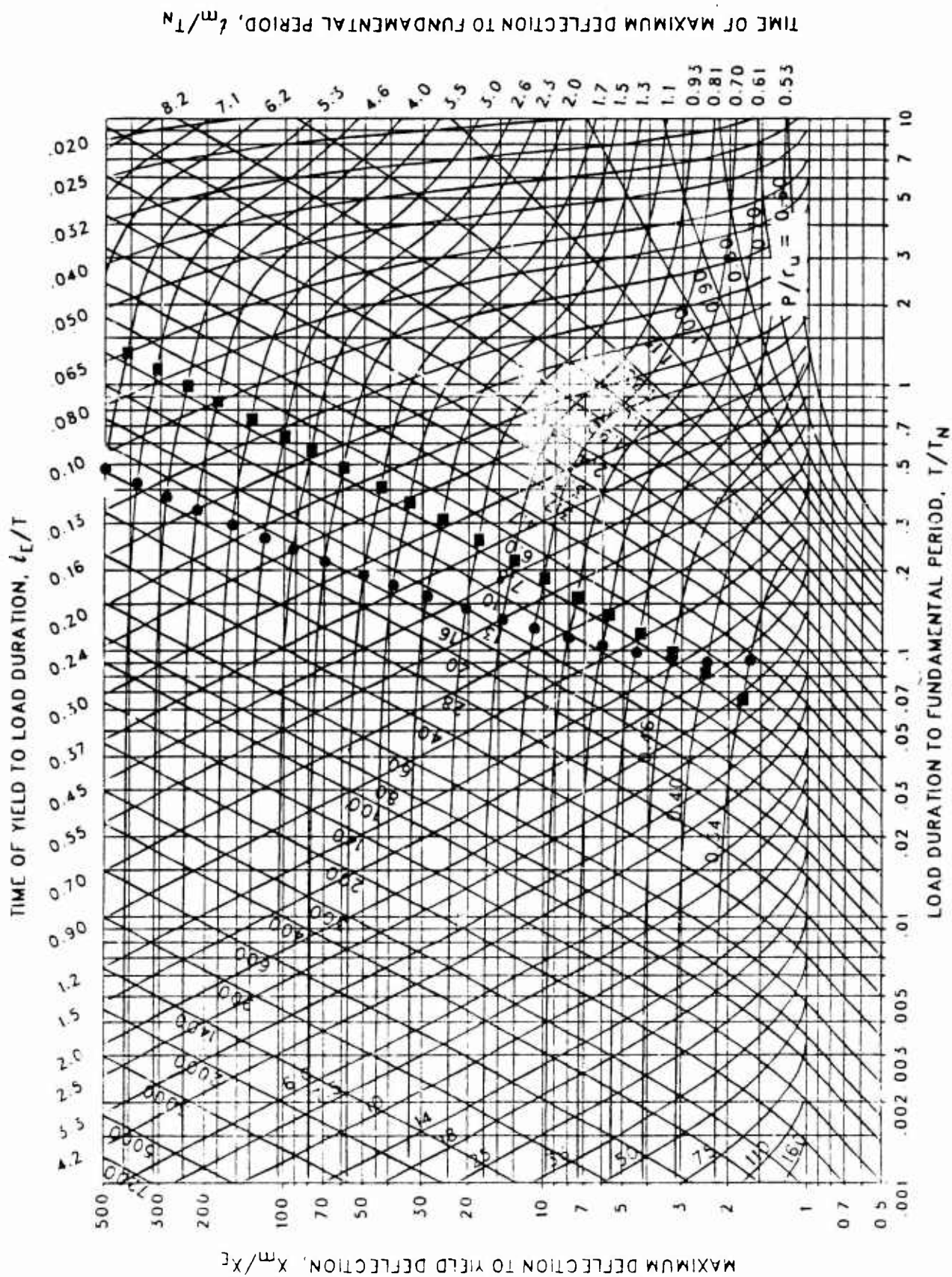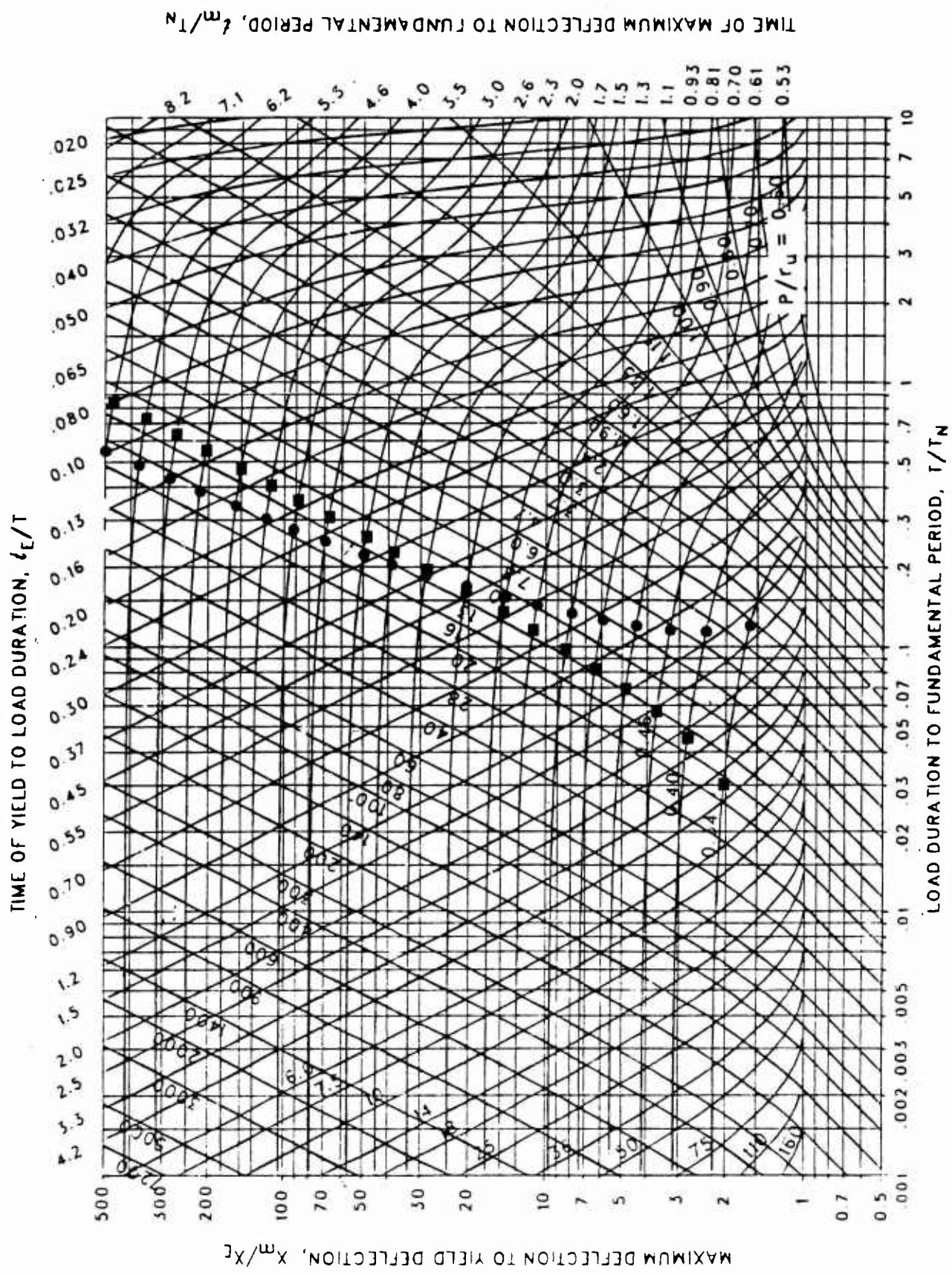
-213-

Figure 3-159   Maximum response of elasto-plastic, one-degree-of-freedom
system for bilinear-triangular pulse ($C_1 = 0.237$, $C_2 = 100.$)

Figure 3-160   Maximum response of elasto-plastic, one-degree-of-freedom
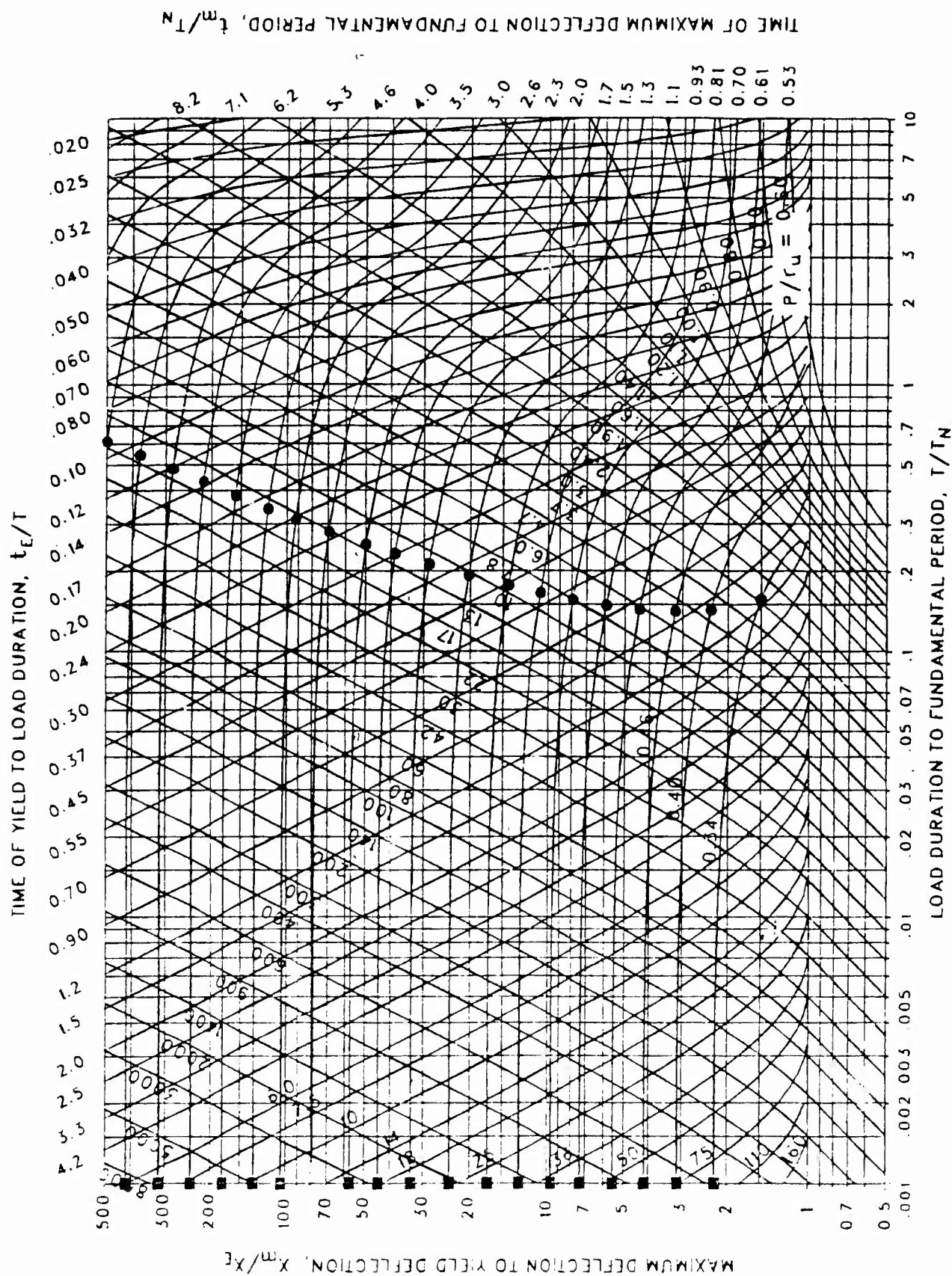system for bilinear-triangular pulse ($C_1 = 0.215$, $C_2 = 100.$)

-215-

Figure 3-161   Maximum response of elasto-plastic, one-degree-of-freedom system for bilinear-triangular pulse ($C_1 = 0.178$, $C_2 = 100$.)

Figure 3-162   Maximum response of elasto-plastic, one-degree-of-freedom system for bilinear-triangular pulse ($C_1 = 0.147$, $C_2 = 100.$)
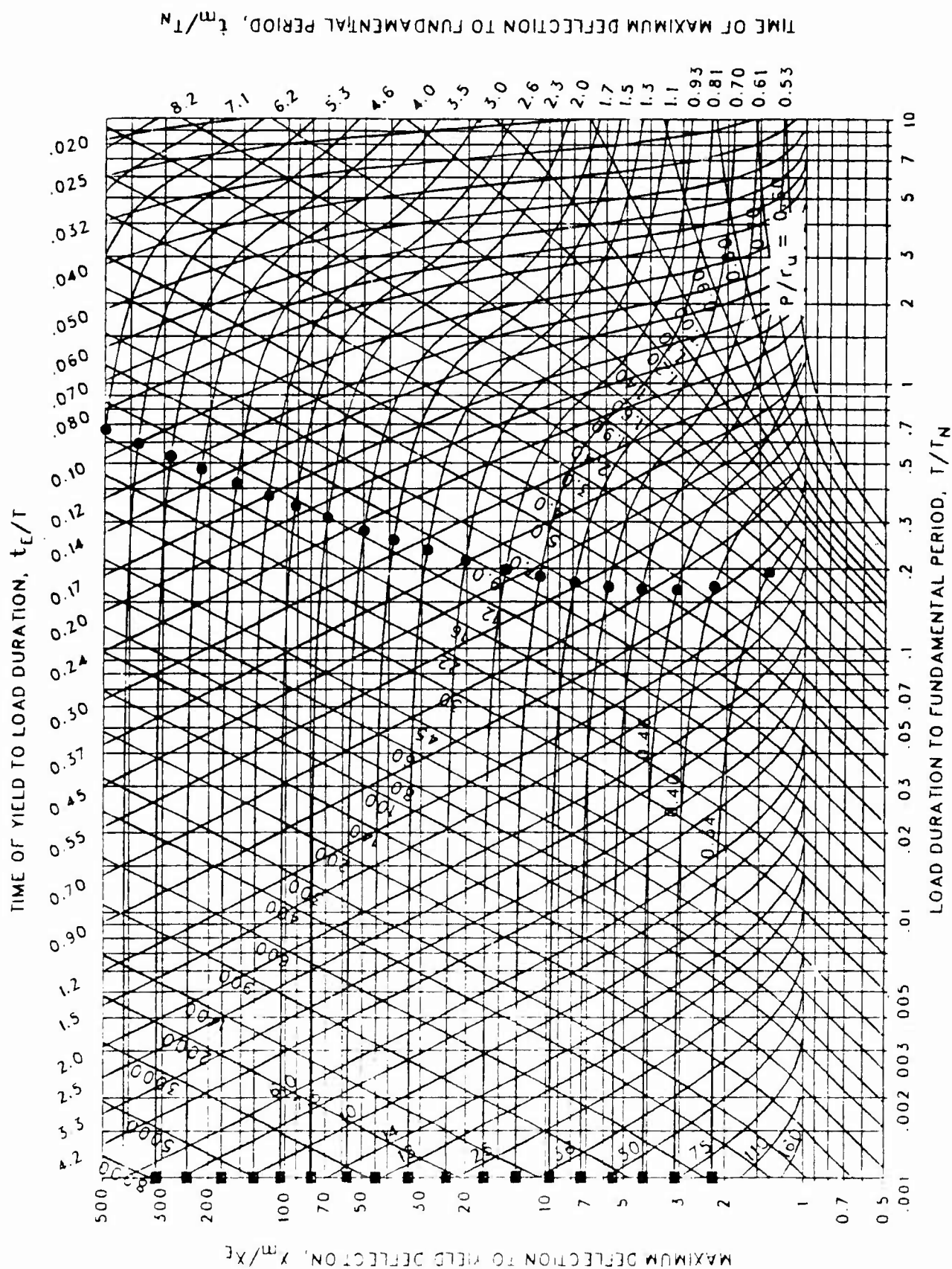
-217-

Figure 3-163   Maximum response of elasto-plastic, one-degree-of-freedom
system for bilinear-triangular pulse ($C_1 = 0.121$, $C_2 = 100.$)

-218-

Figure 5-164 Maximum response of elasto-plastic, one-degree-of-freedom system for bilinear-triangular pulse ($C_1 = 0.100$, $C_2 = 100.$)
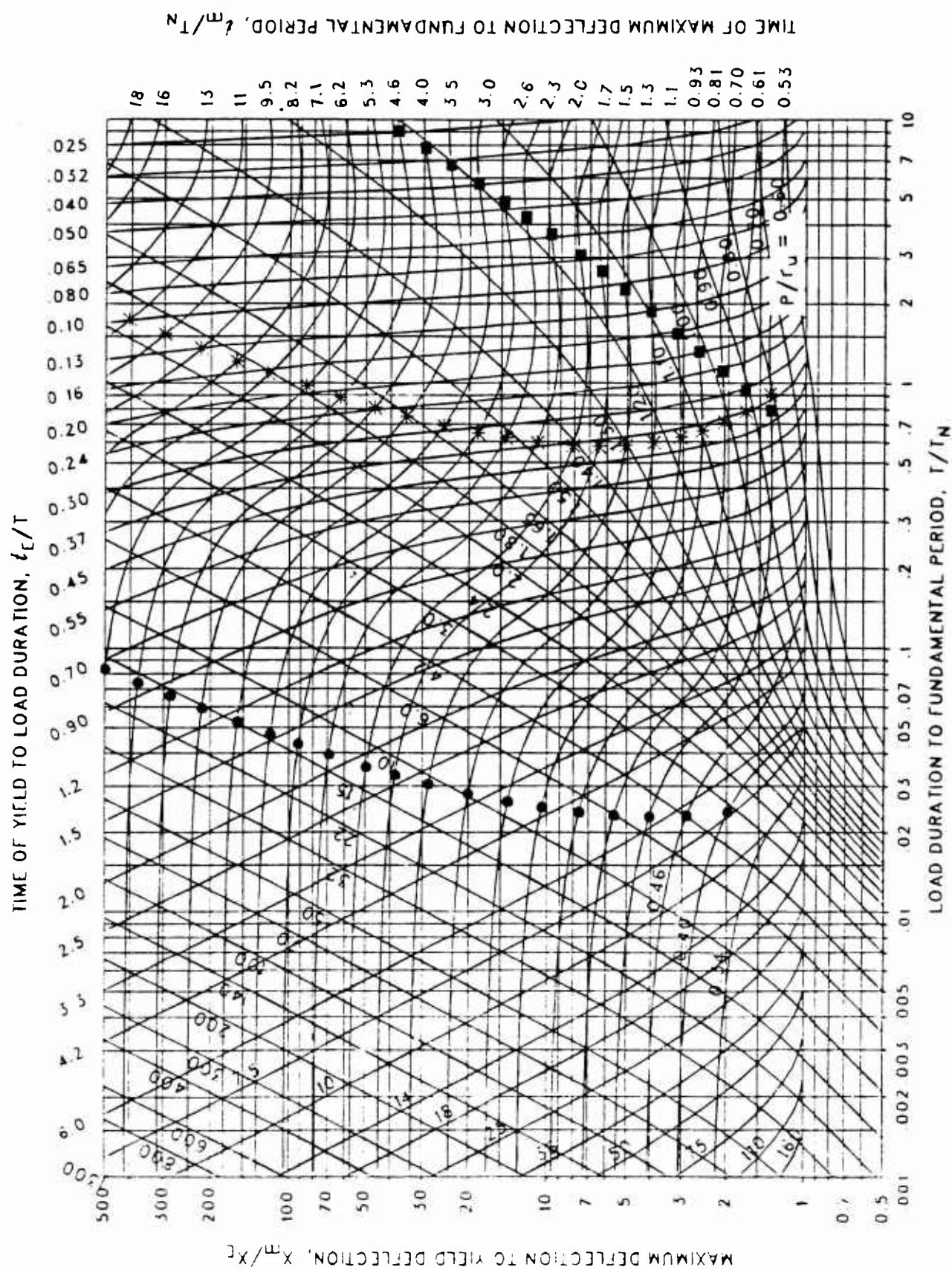
Figure 3-16b Maximum response of elasto-plastic, one-degree-of-freedom system for bilinear-triangular pulse ($C_1 = 0.075$, $C_2 = 100.$)
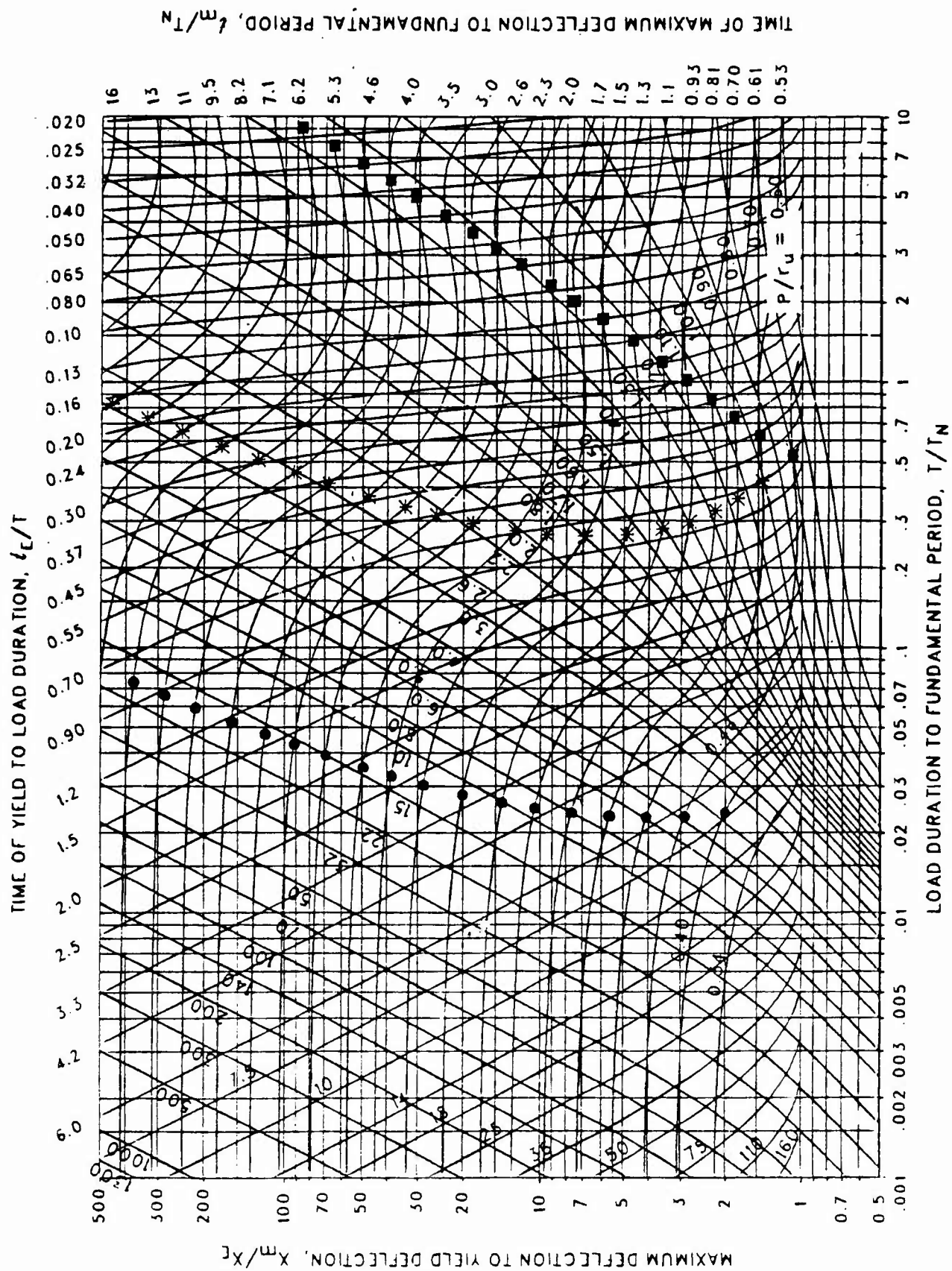
Figure 3-166 Maximum response of elasto-plastic, one-degree-of-freedom system for bilinear-triangular pulse ($C_1 = 0.056$, $C_2 = 100.$)

Figure 3-167 Maximum response of elasto-plastic, one-degree-of-freedom system for bilinear-triangular pulse ($C_1 = 0.042$, $C_2 = 100$.)

Figure 3-168   Maximum response of elasto-plastic, one-degree-of-freedom
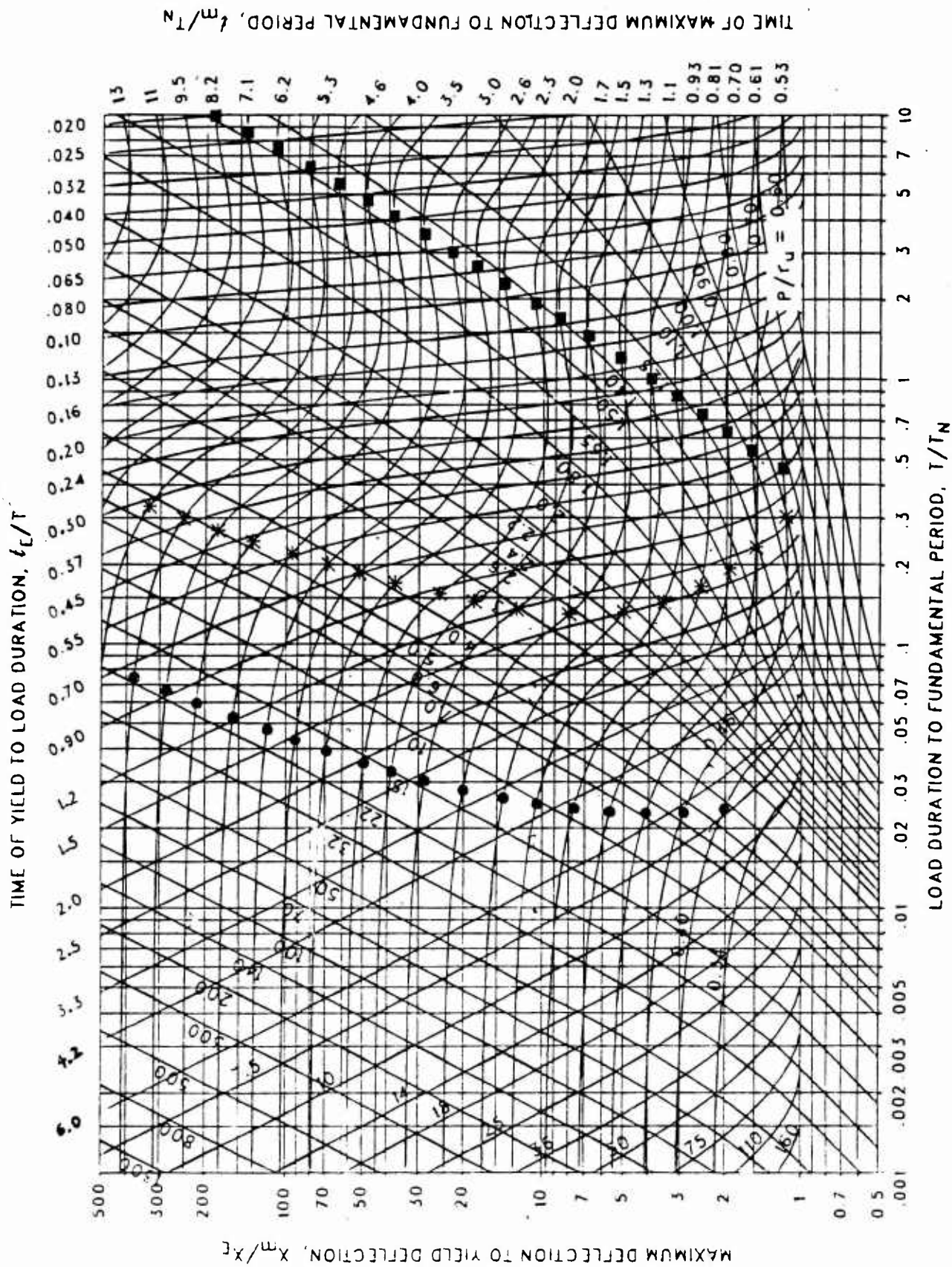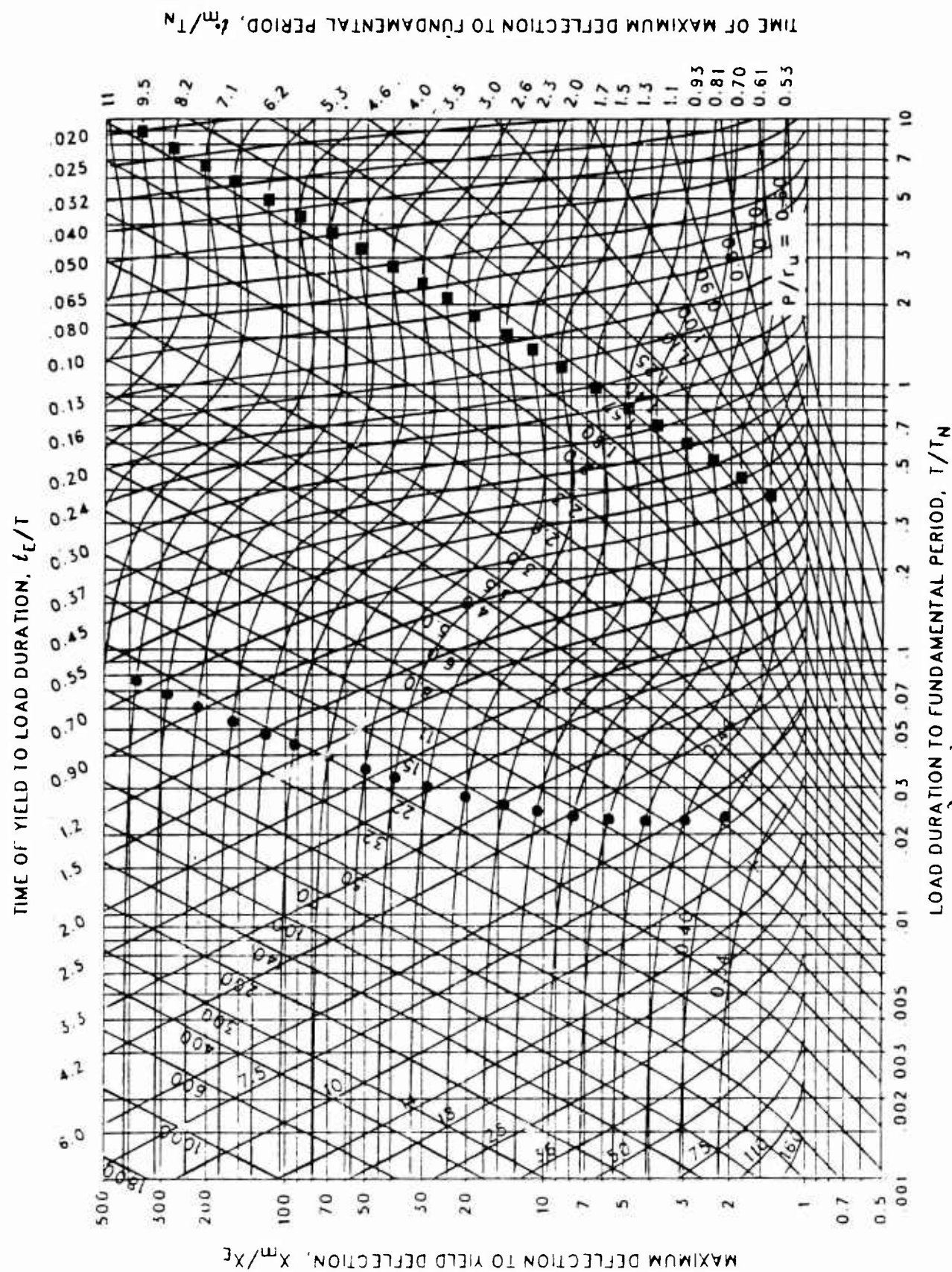system for bilinear-triangular pulse ($C_1 = 0.032$, $C_2 = 100.$)

-223-

Figure 3-169 Maximum response of elasto-plastic, one-degree-of-freedom system for bilinear-triangular pulse ($C_1 = 0.026$, $C_2 = 100.$)
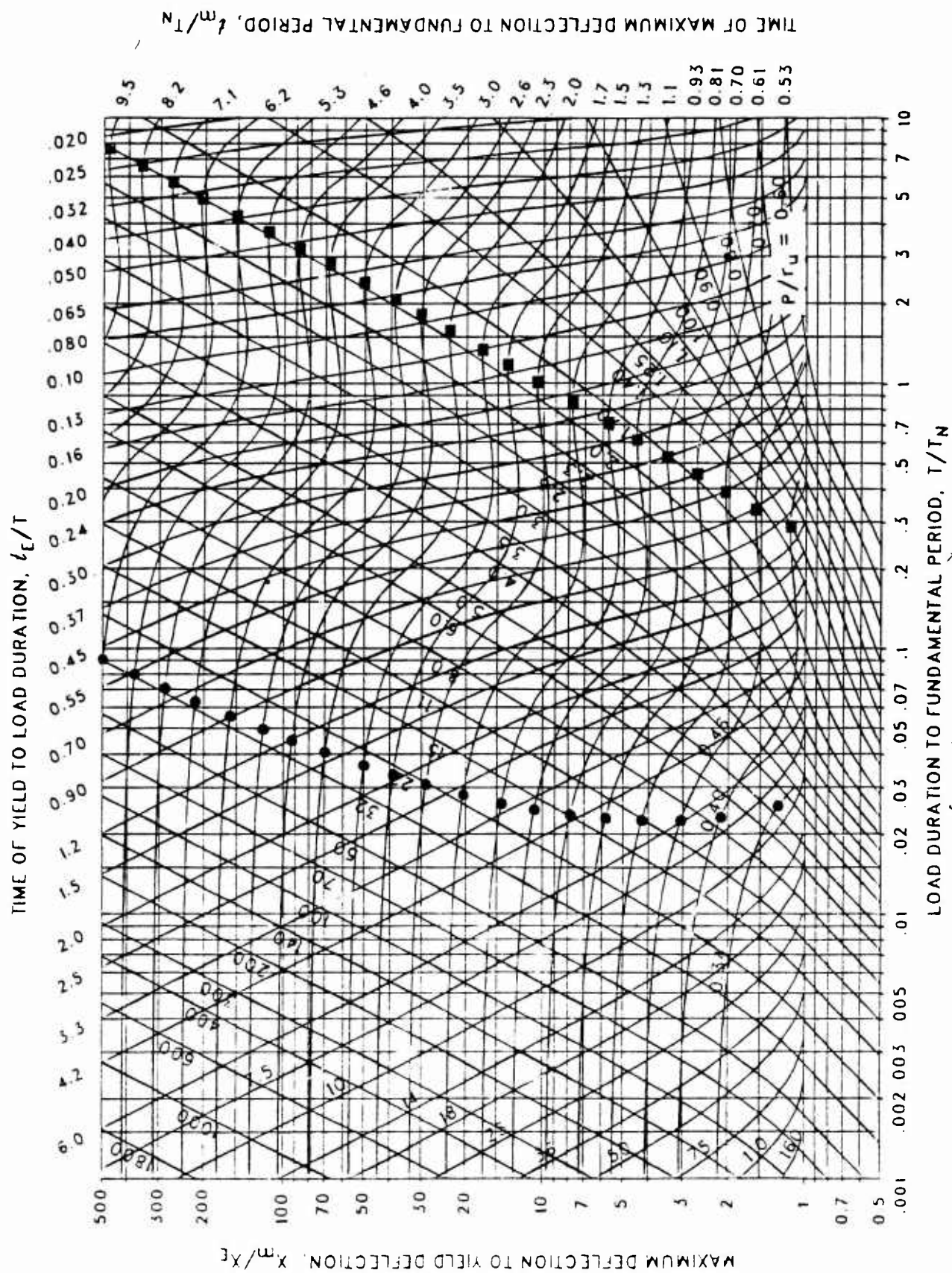
-224-

Figure 3-170 Maximum response of elasto-plastic, one-degree-of-freedom system for bilinear-triangular pulse ($C_1 = 0.018$, $C_2 = 100$.)

Figure 3-171   Maximum response of elasto-plastic, one-degree-of-freedom system for bilinear-triangular pulse ($C_1 = 0.013$, $C_2 = 100.$)
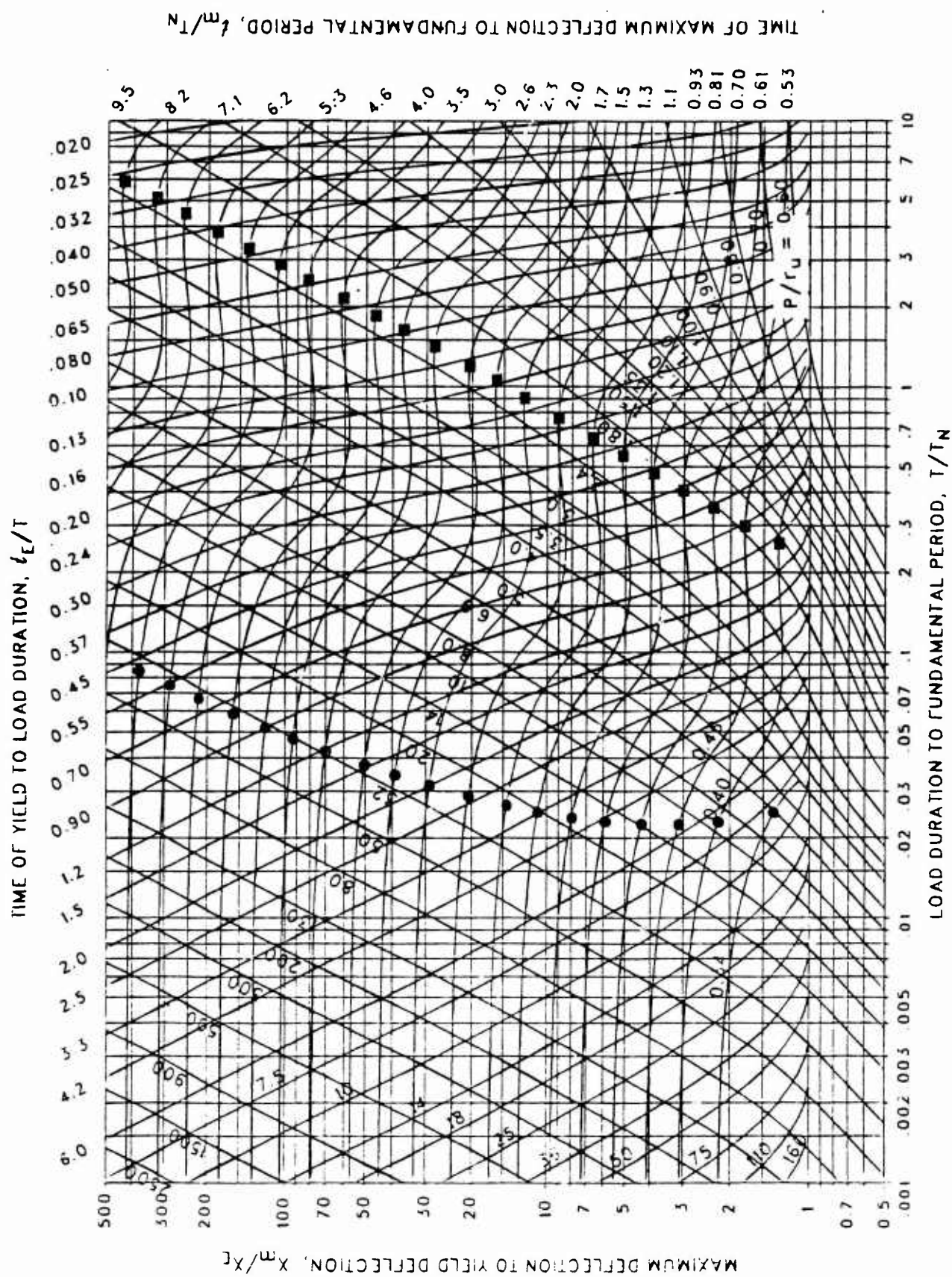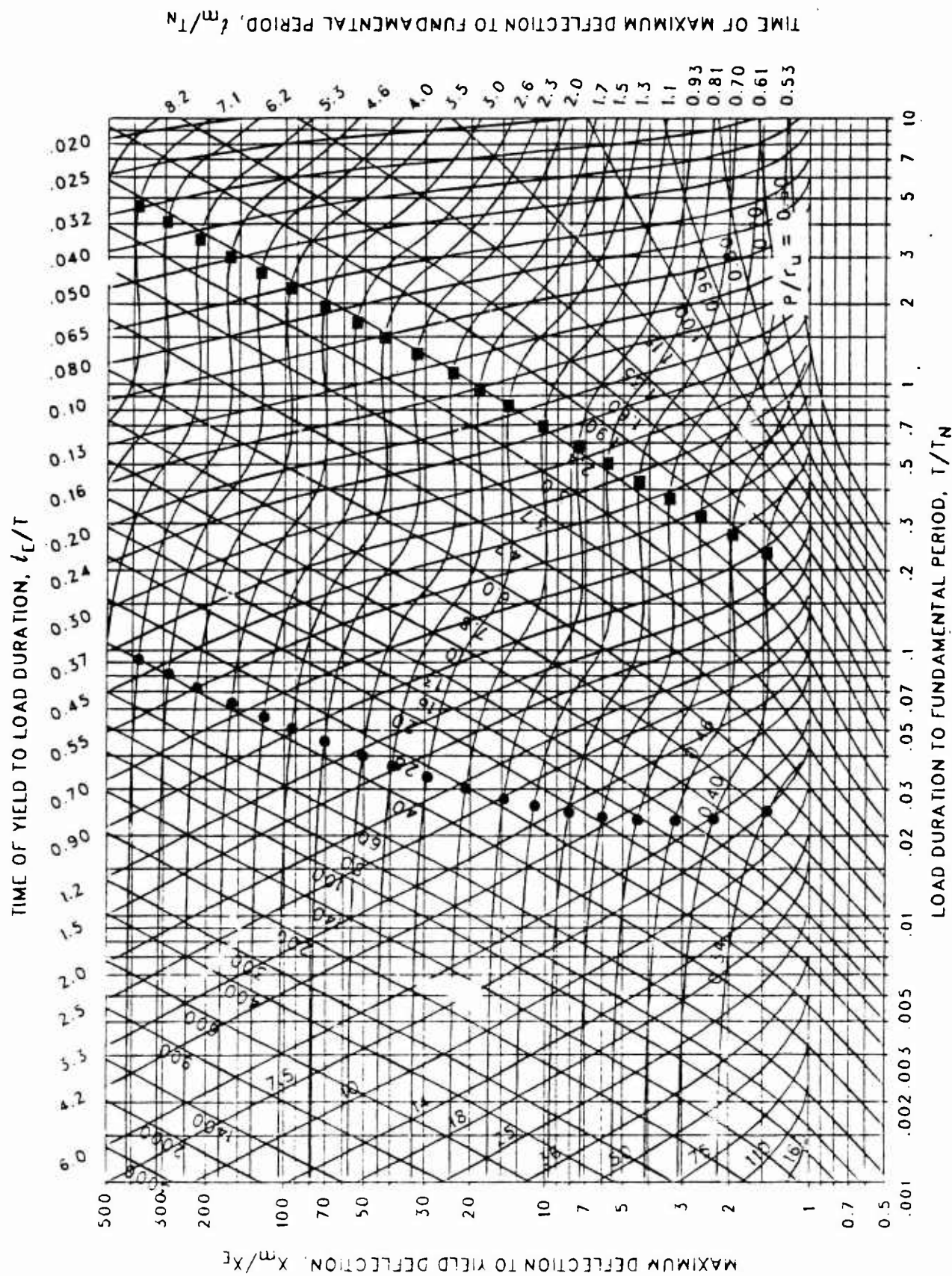
-226-

Figure 3-172   Maximum response of elasto-plastic, one-degree-of-freedom
system for bilinear-triangular pulse (C_1 = 0.010, C_2 = 100.)

Figure 3-173 Maximum response of elasto-plastic, one-degree-of-freedom system for bilinear-triangular pulse (C_1 · 0.909, C_2 = 300.)
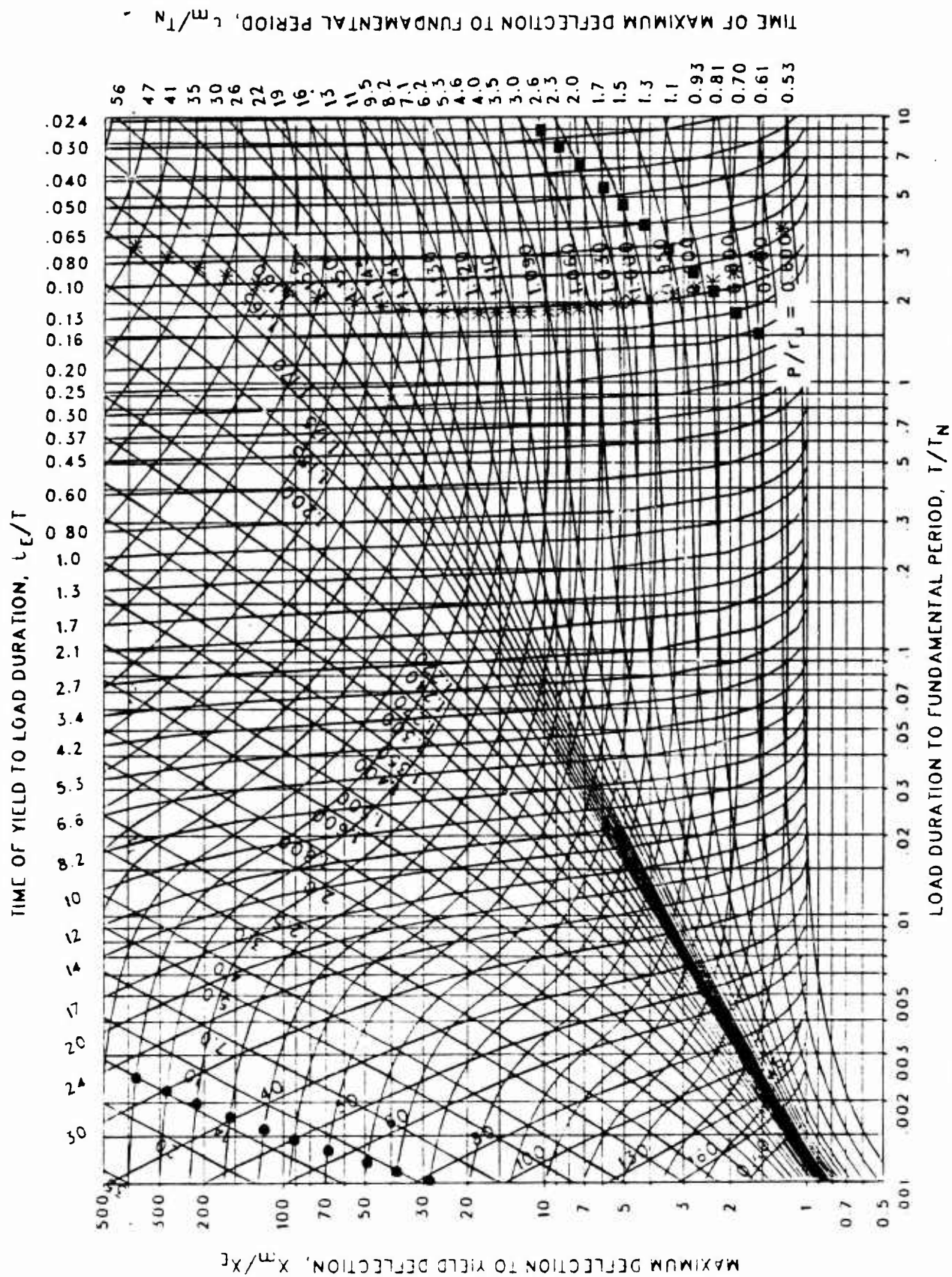
Figure 3-174   Maximum response of elasto-plastic, one-degree-of-freedom system for bilinear-triangular pulse ($C_1 = 0.866$, $C_2 = 300$.)

-229-
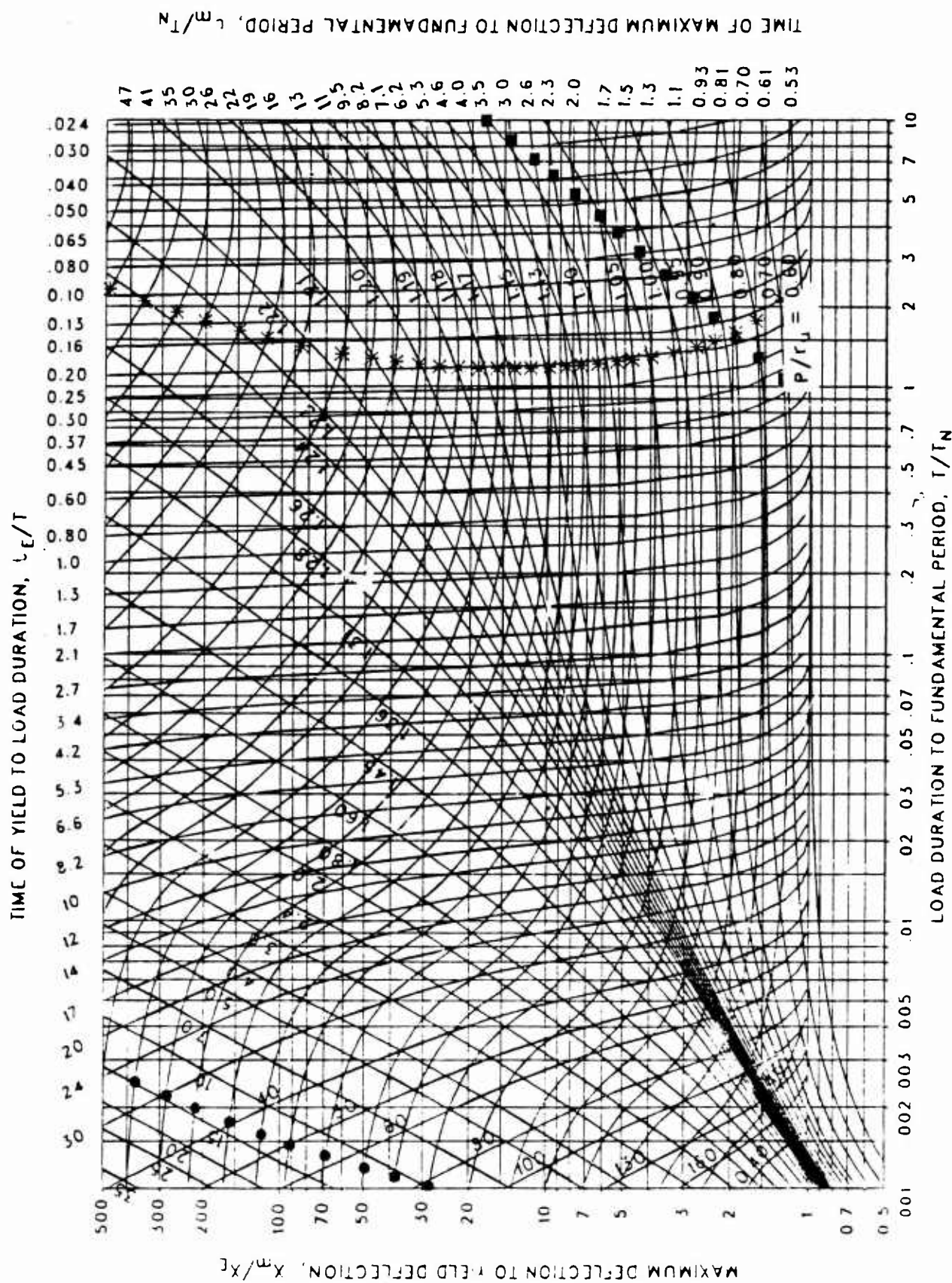
Figure 3-175 Maximum response of elasto-plastic, one-degree-of-freedom system for bilinear-triangular pulse ($C_1 = 0.825$, $C_2 = 300.$)
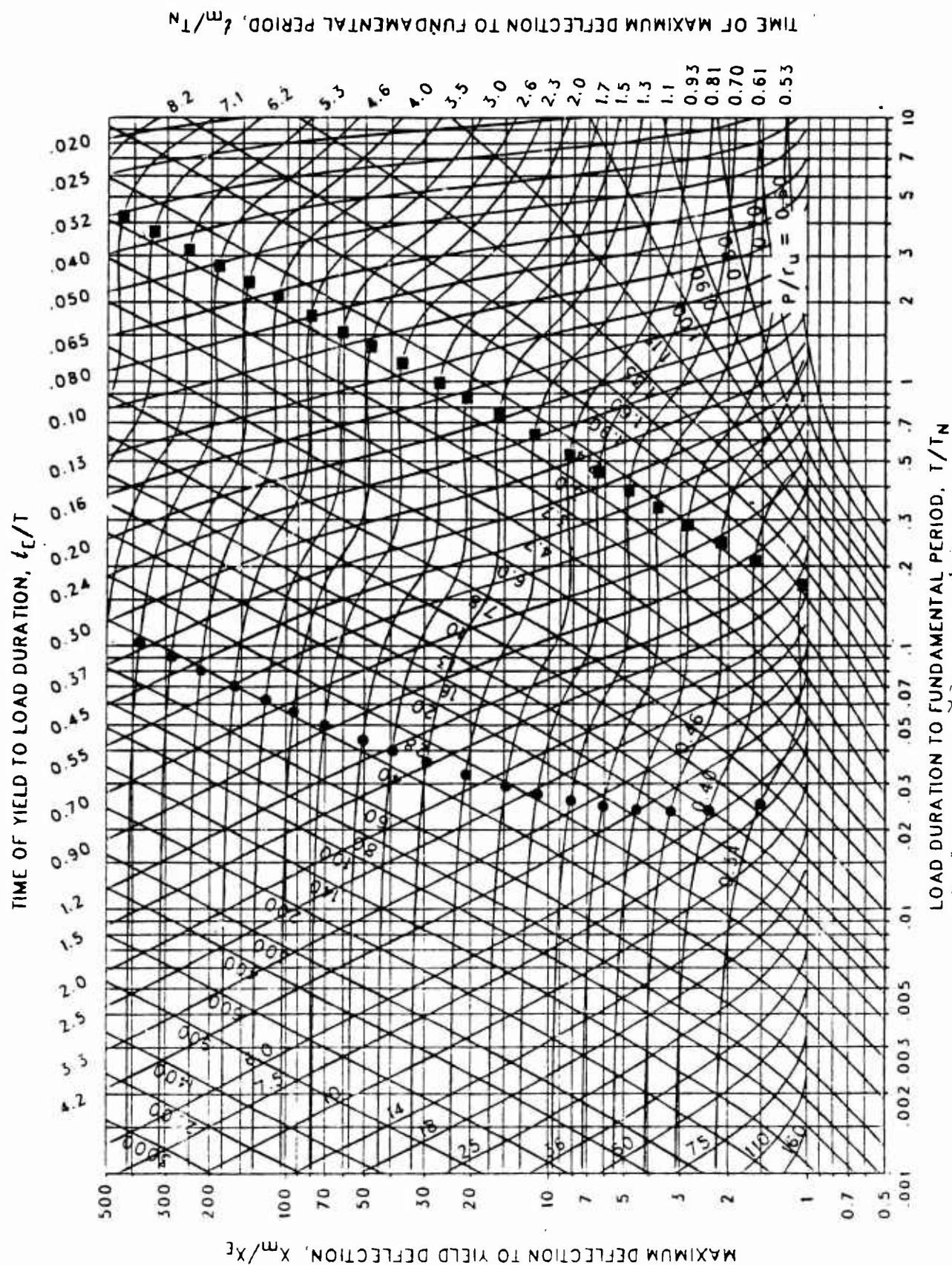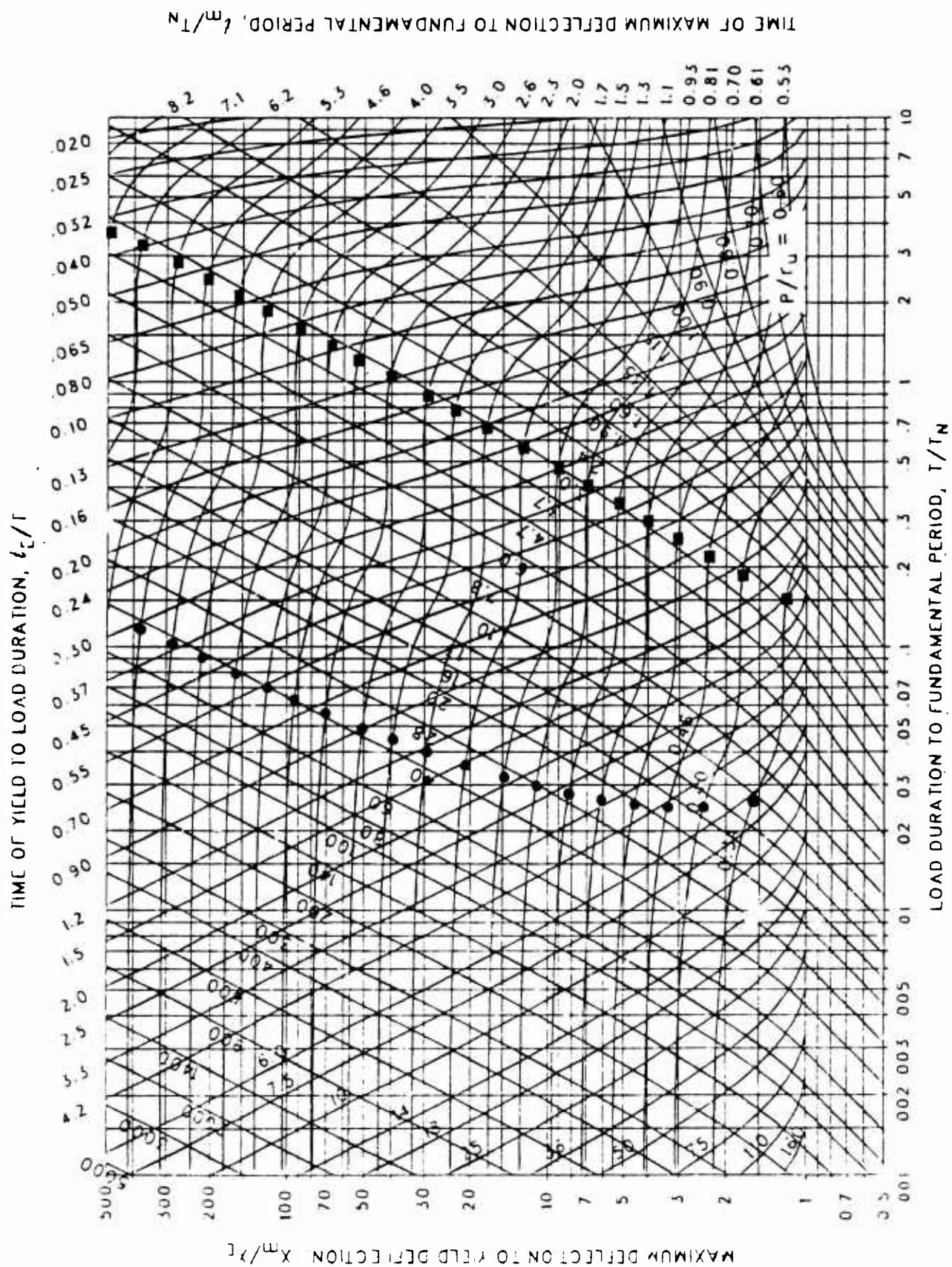
-230-
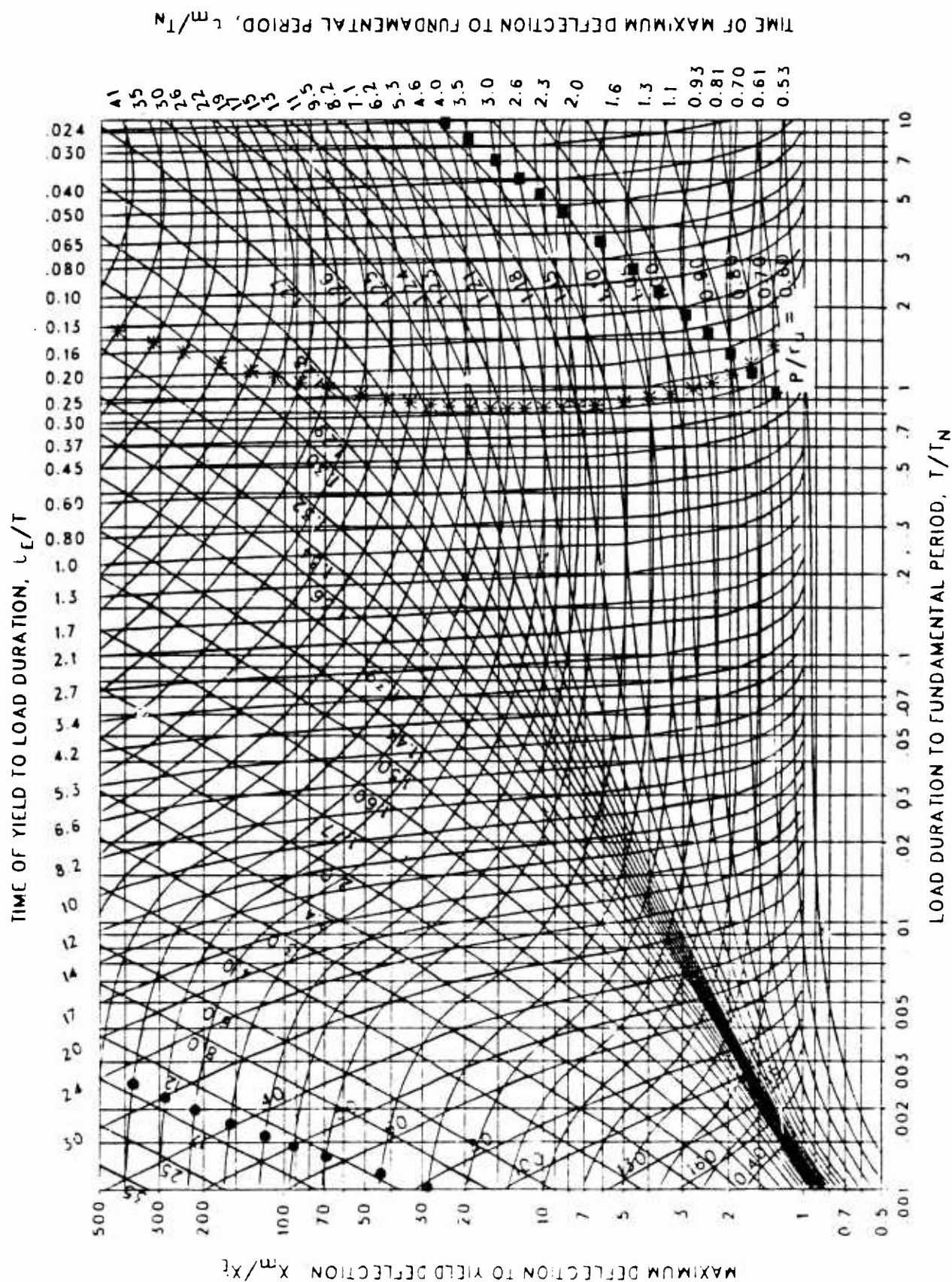
Figure 3-176   Maximum response of elasto-plastic, one-degree-of-freedom system for bilinear-triangular pulse ($C_1 = 0.787$, $C_2 = 300$.)

Figure 3-177 Maximum response of elasto-plastic, one-degree-of-freedom system for bilinear-triangular pulse ($C_1 = 0.750$, $C_2 = 300$.)
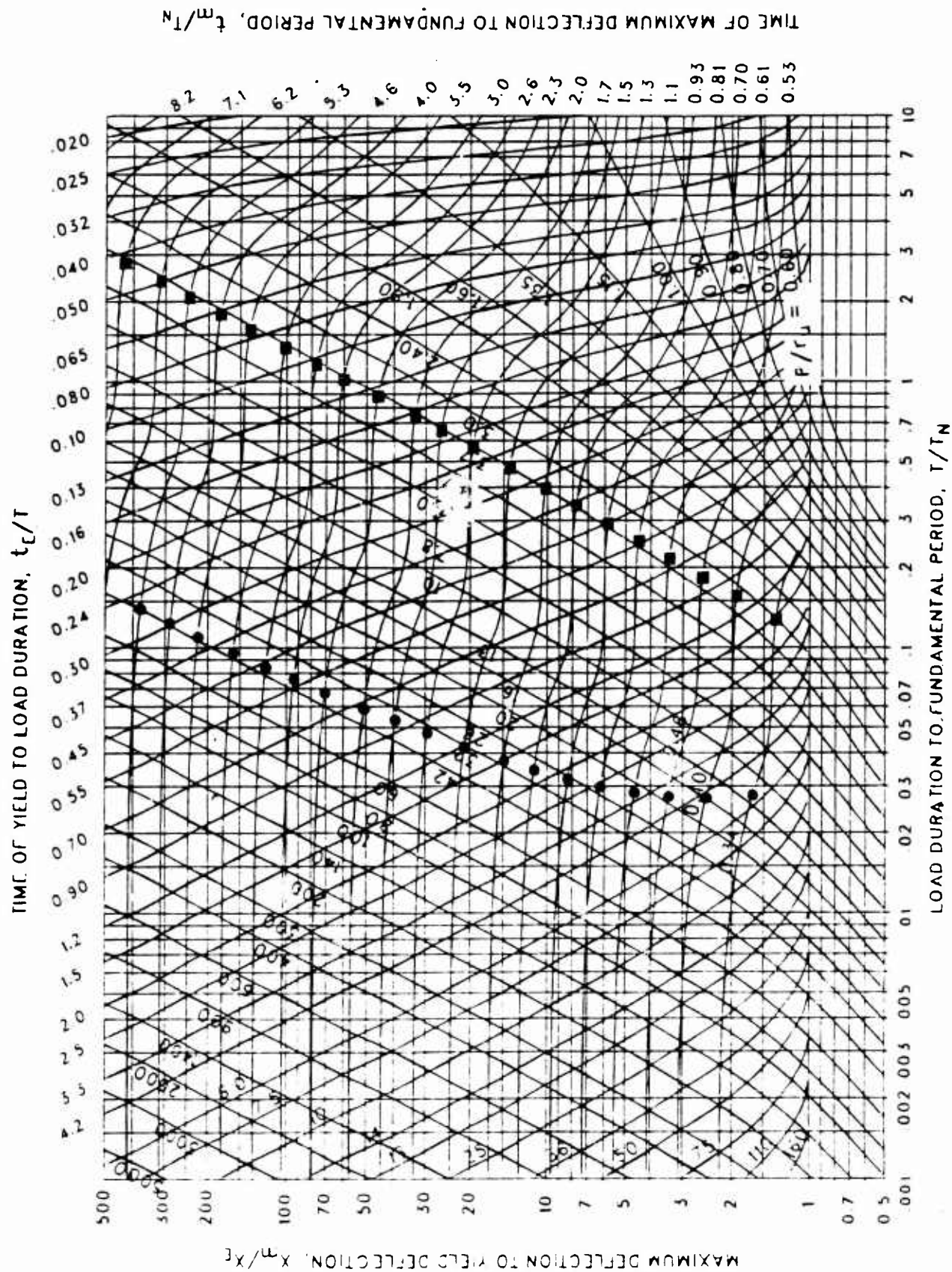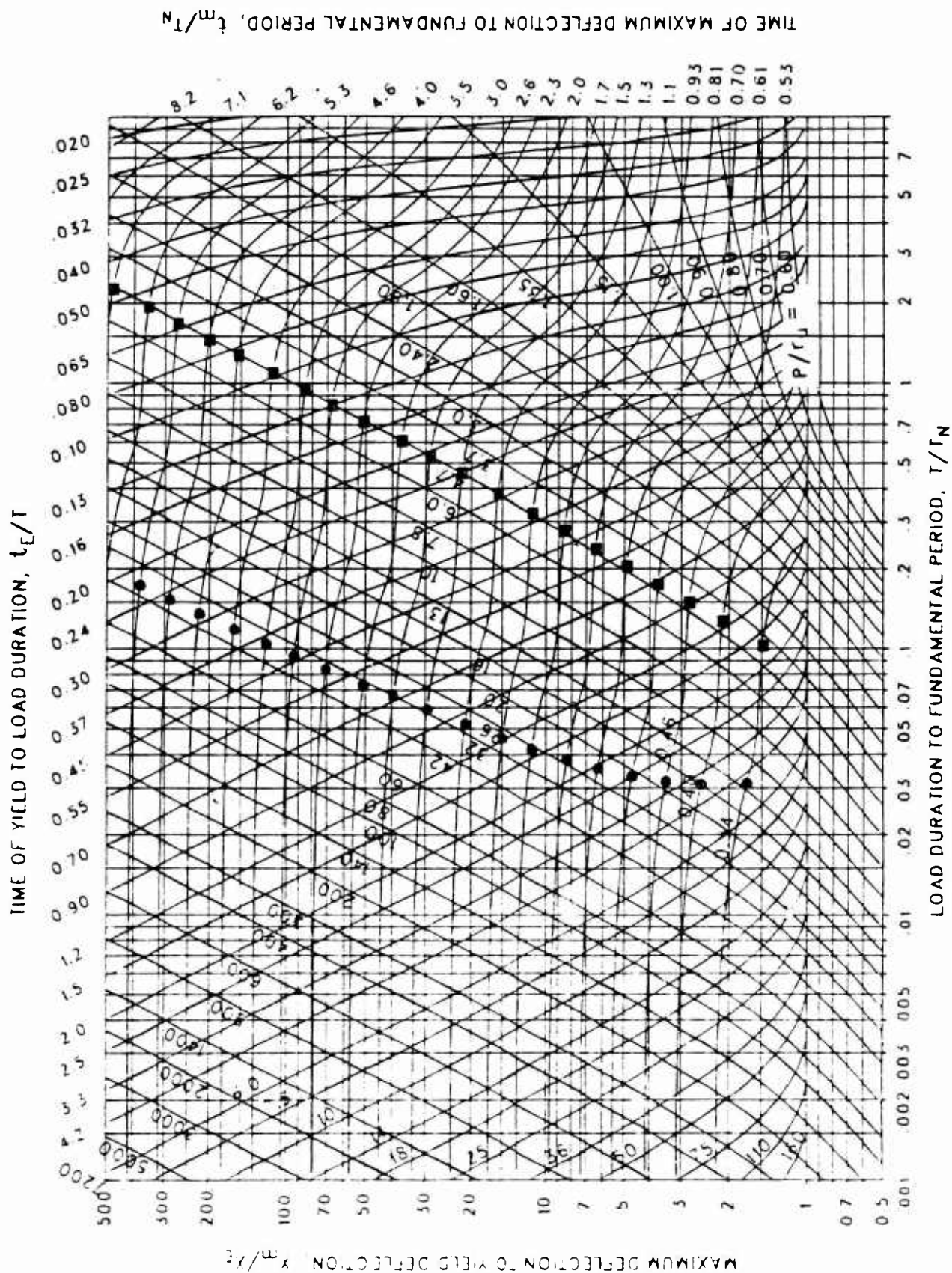
-232-
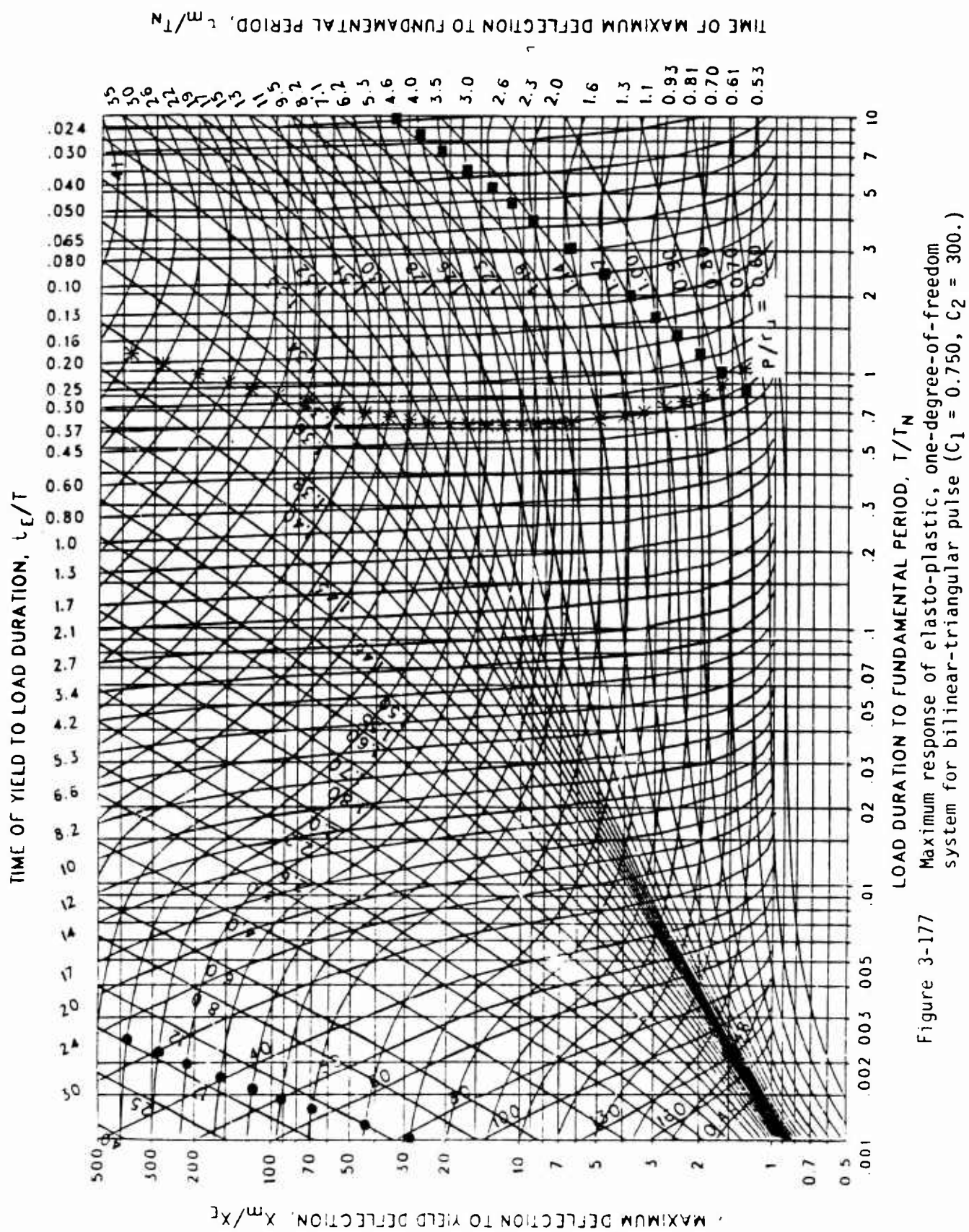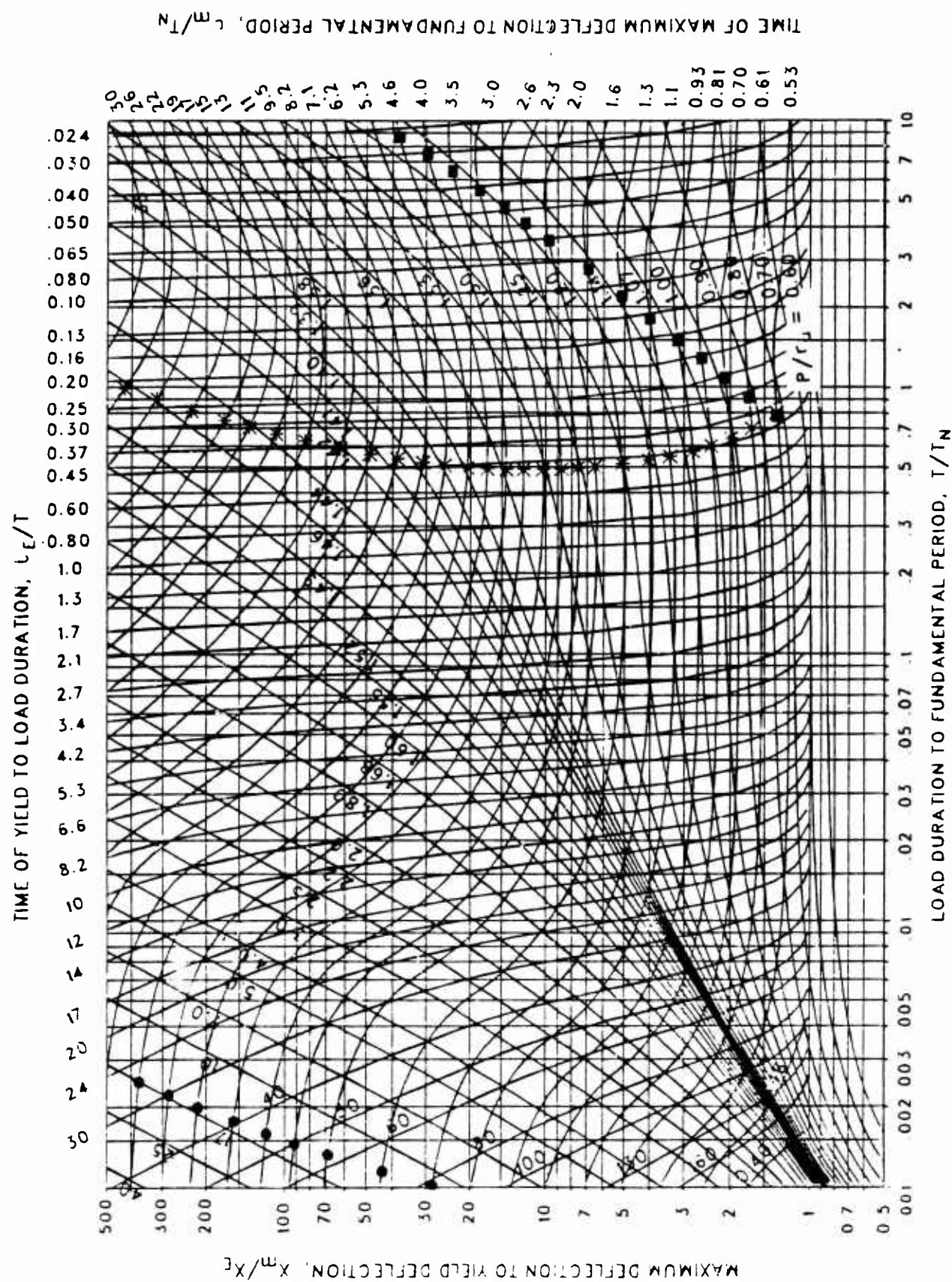
Figure 3-178   Maximum response of elasto-plastic, one-degree-of-freedom system for bilinear-triangular pulse ($C_1 = 0.715$, $C_2 = 300.$)

-233-

TIME OF MAXIMUM DEFLECTION TO FUNDAMENTAL PERIOD, τ_m/T_N

TIME OF YIELD TO LOAD DURATION, t_E/T

LOAD DURATION TO FUNDAMENTAL PERIOD, T/T_N

MAXIMUM DEFLECTION TO YIELD DEFLECTION, x_m/x_E

Figure 3-179   Maximum response of elasto-plastic, one-degree-of-freedom system for bilinear-triangular pulse ($C_1 = 0.681$, $C_2 = 300.$)
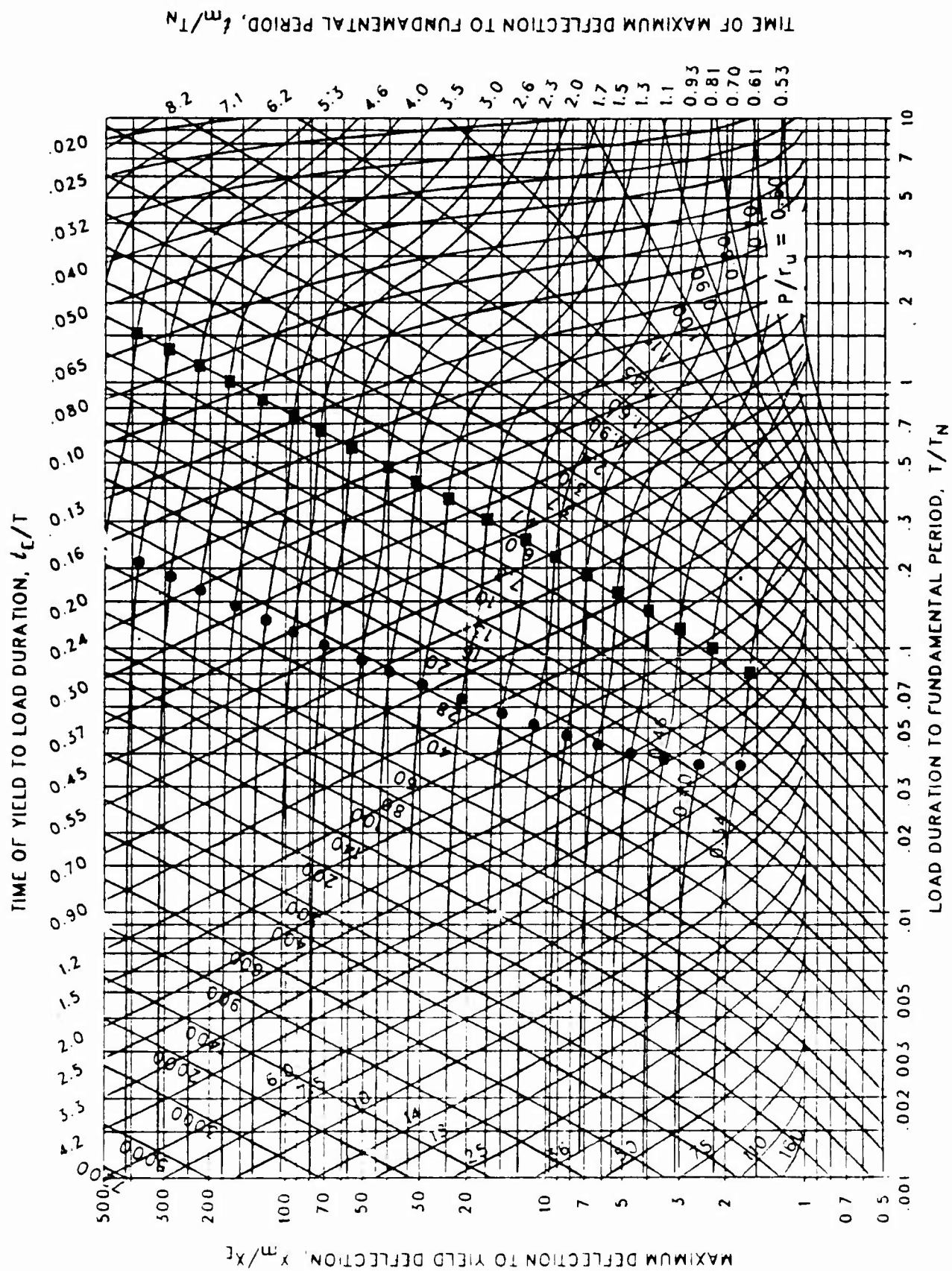
-234-
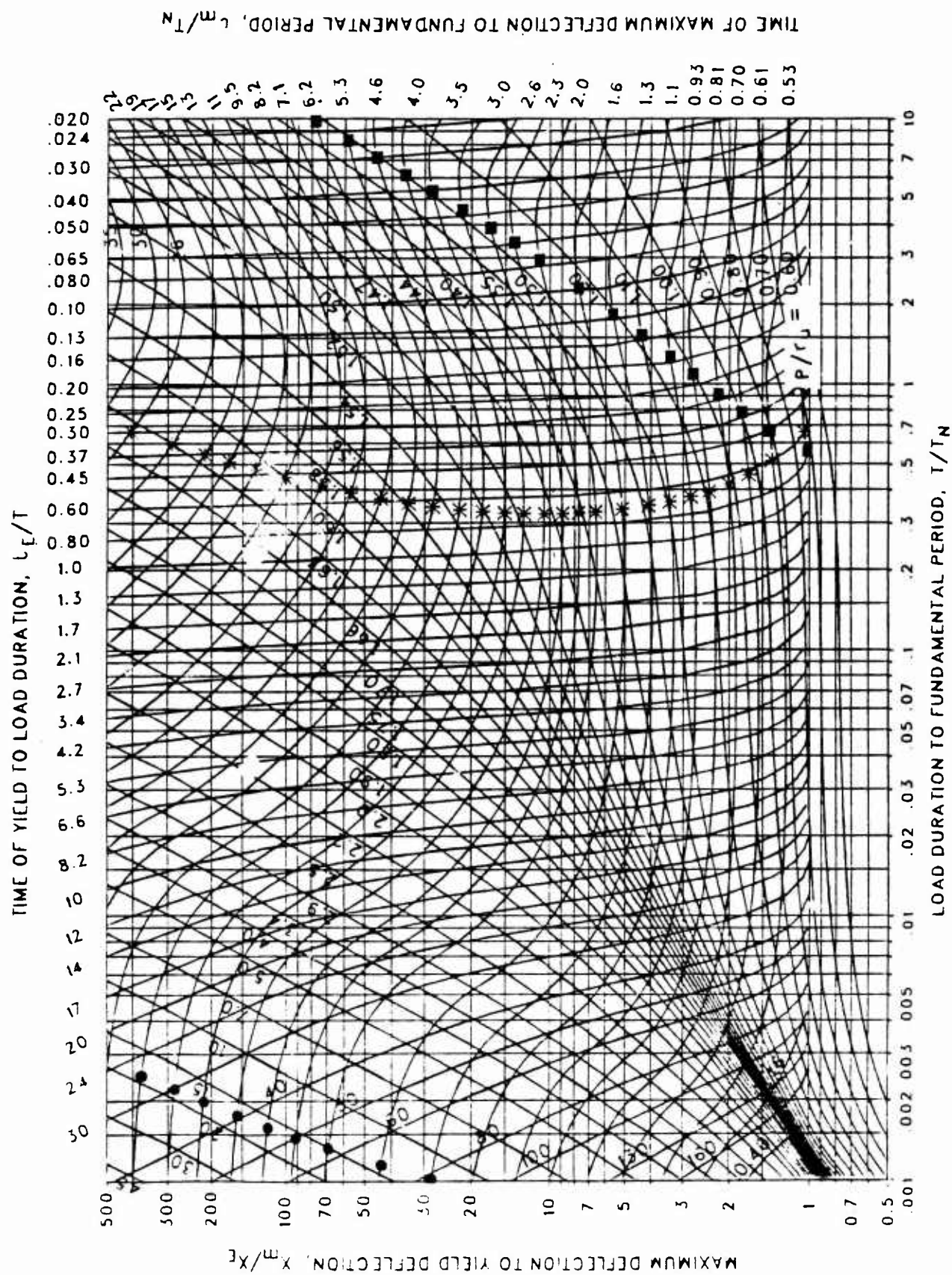
Figure 3-180   Maximum response of elasto-plastic, one-degree-of-freedom system for bilinear-triangular pulse ($C_1 = 0.648$, $C_2 = 300.$)
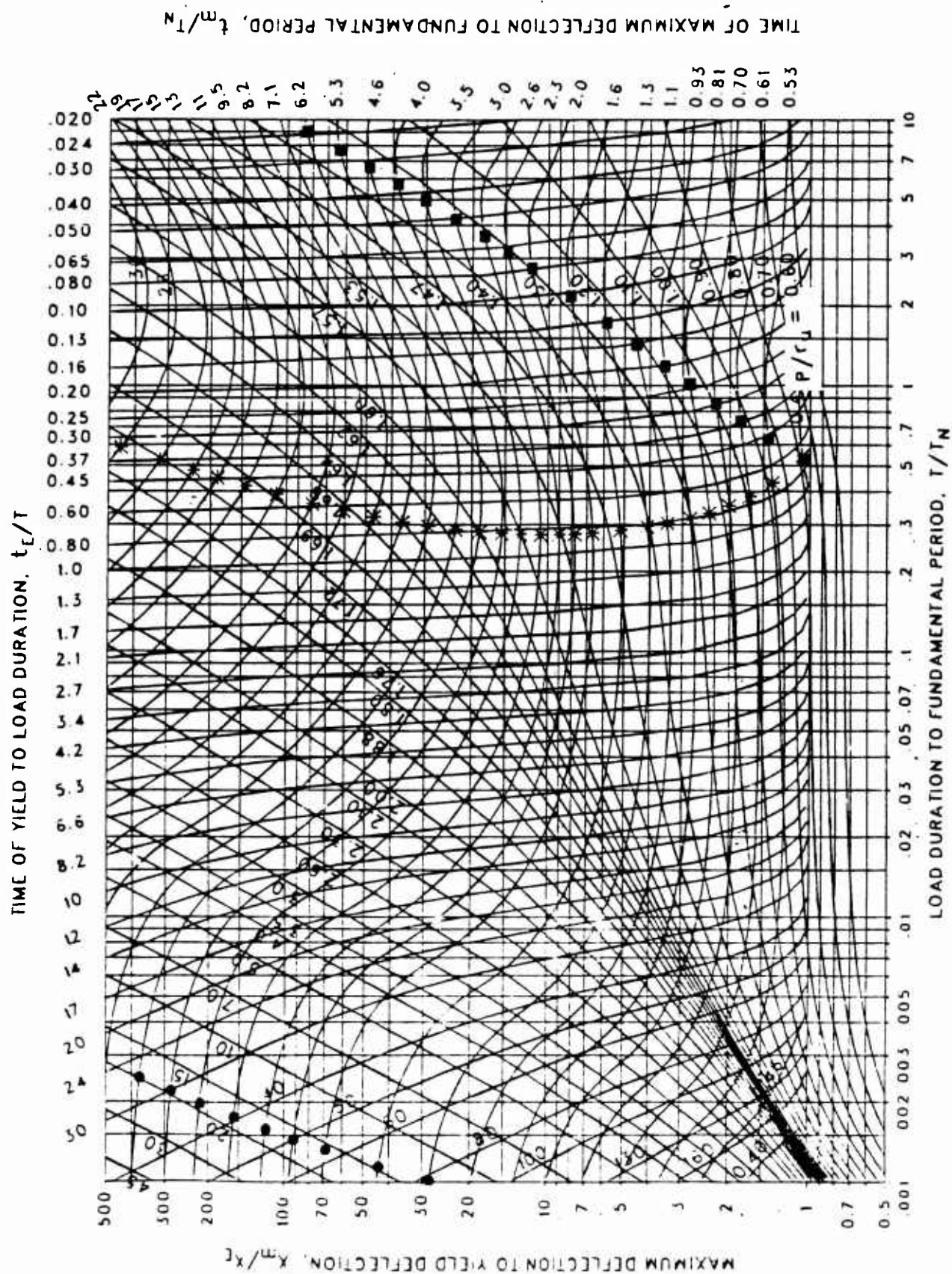
Figure 3-181 Maximum response of elasto-plastic, one-degree-of-freedom system for bilinear-triangular pulse ($C_1 = 0.619$, $C_2 = 300.$)
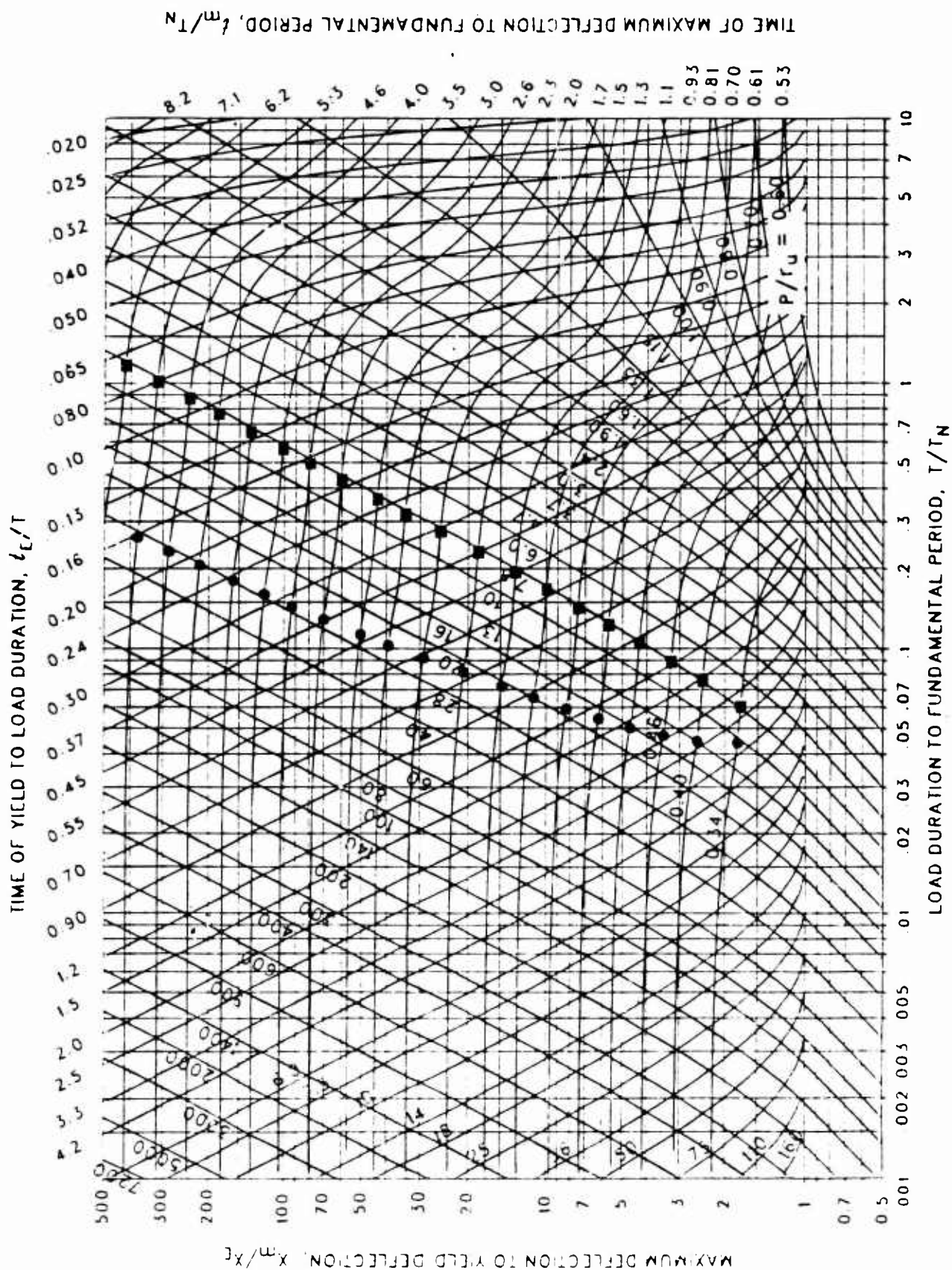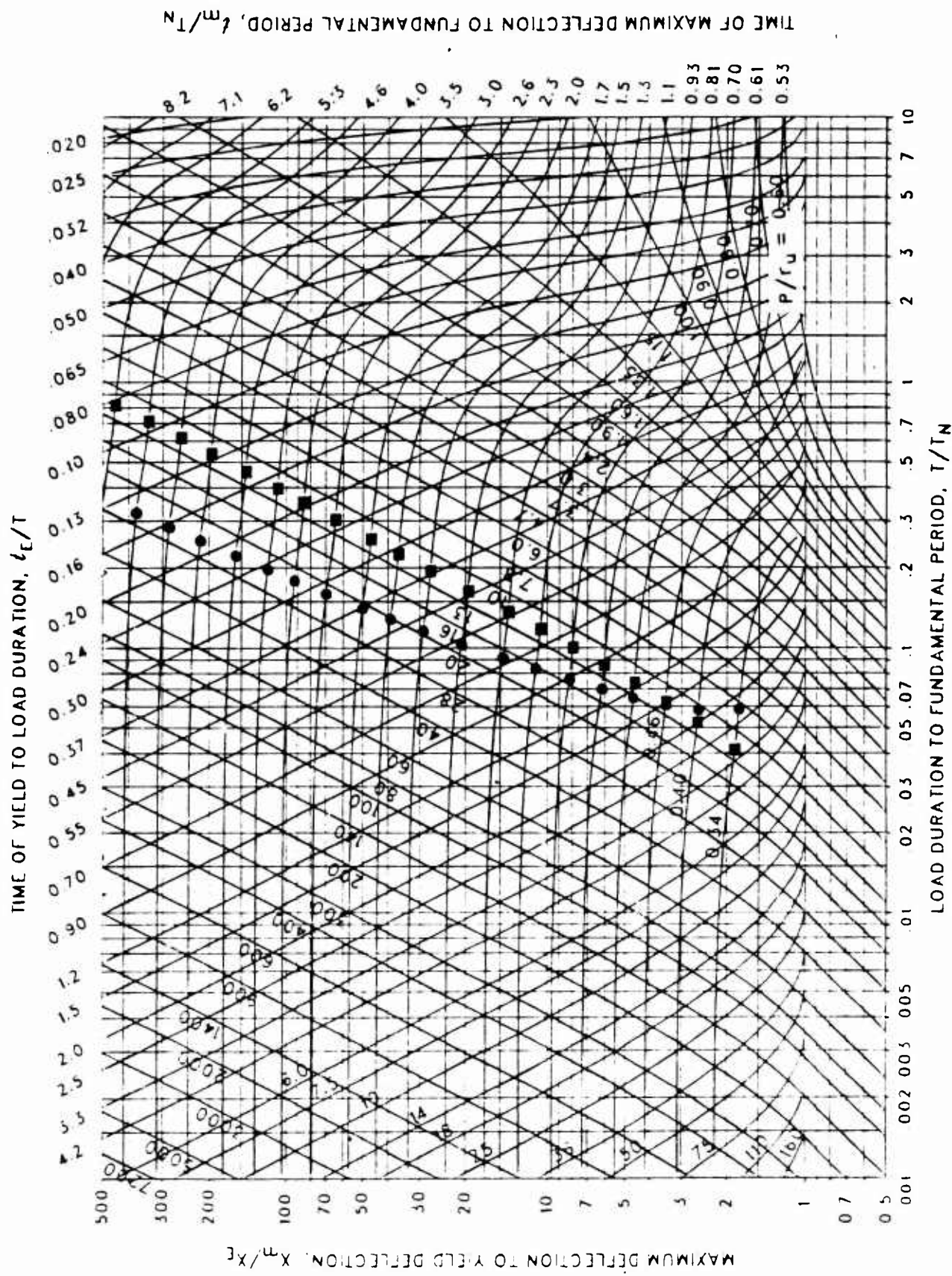
-236-
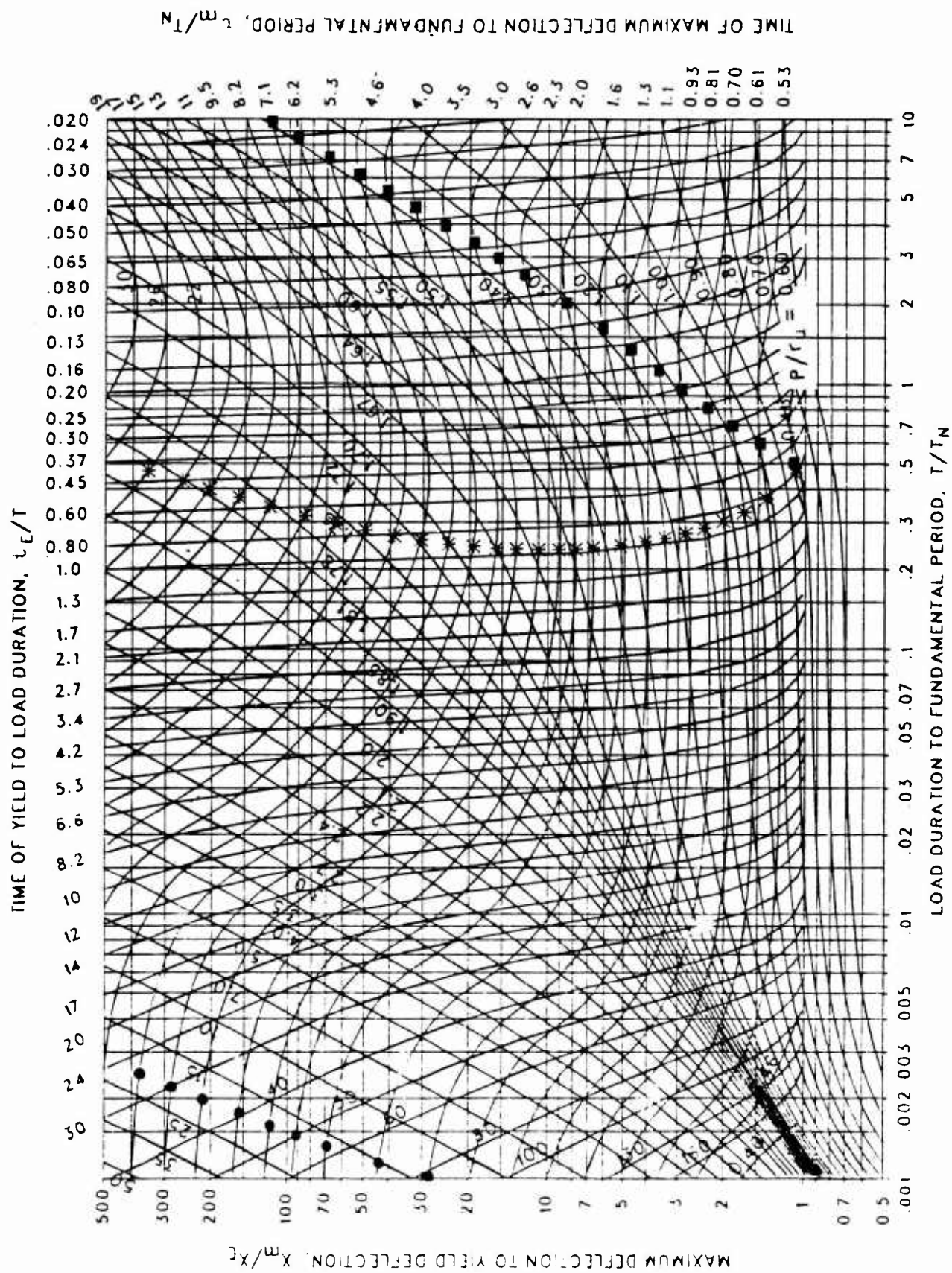
Figure 3-182   Maximum response of elasto-plastic, one-degree-of-freedom
system for bilinear-triangular pulse ($C_1 = 0.590$, $C_2 = 300.$)

-237-
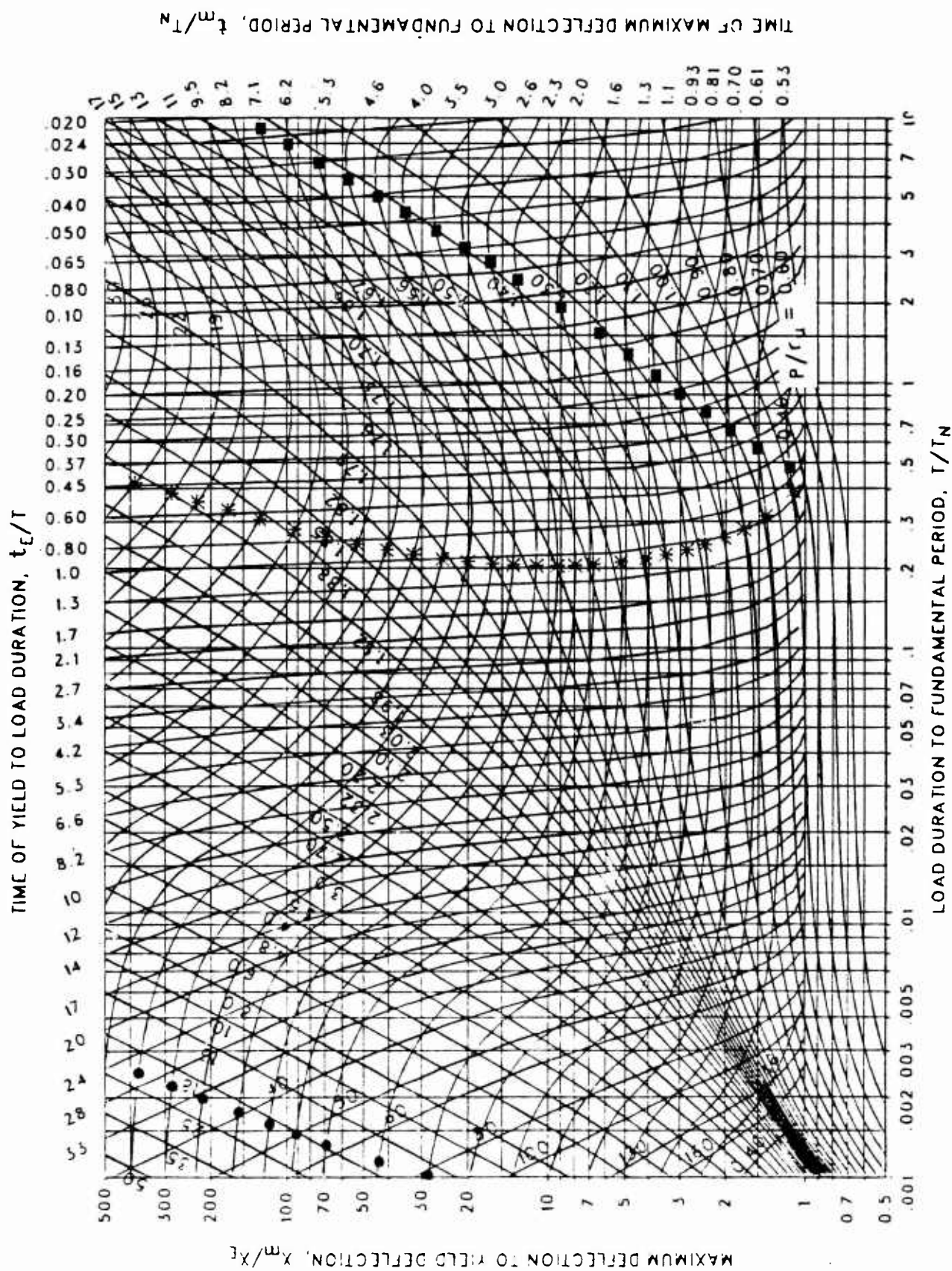
Figure 3-183   Maximum response of elasto-plastic, one-degree-of-freedom system for bilinear-triangular pulse ($C_1 = 0.562$, $C_2 = 300$.)

-238-
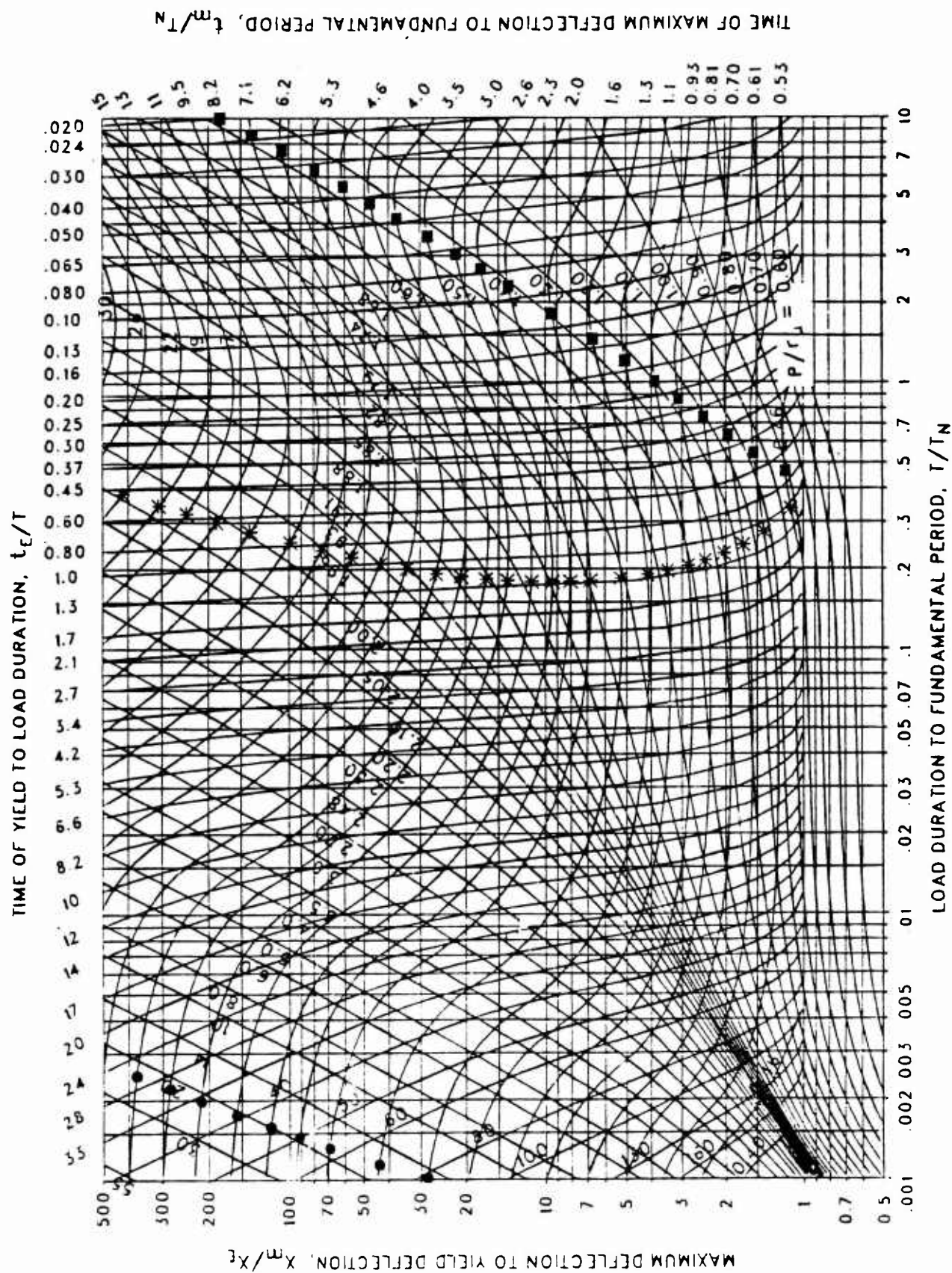
Figure 3-184 Maximum response of elasto-plastic, one-degree-of-freedom system for bilinear-triangular pulse ($C_1 = 0.536$, $C_2 = 300.$)

-239-
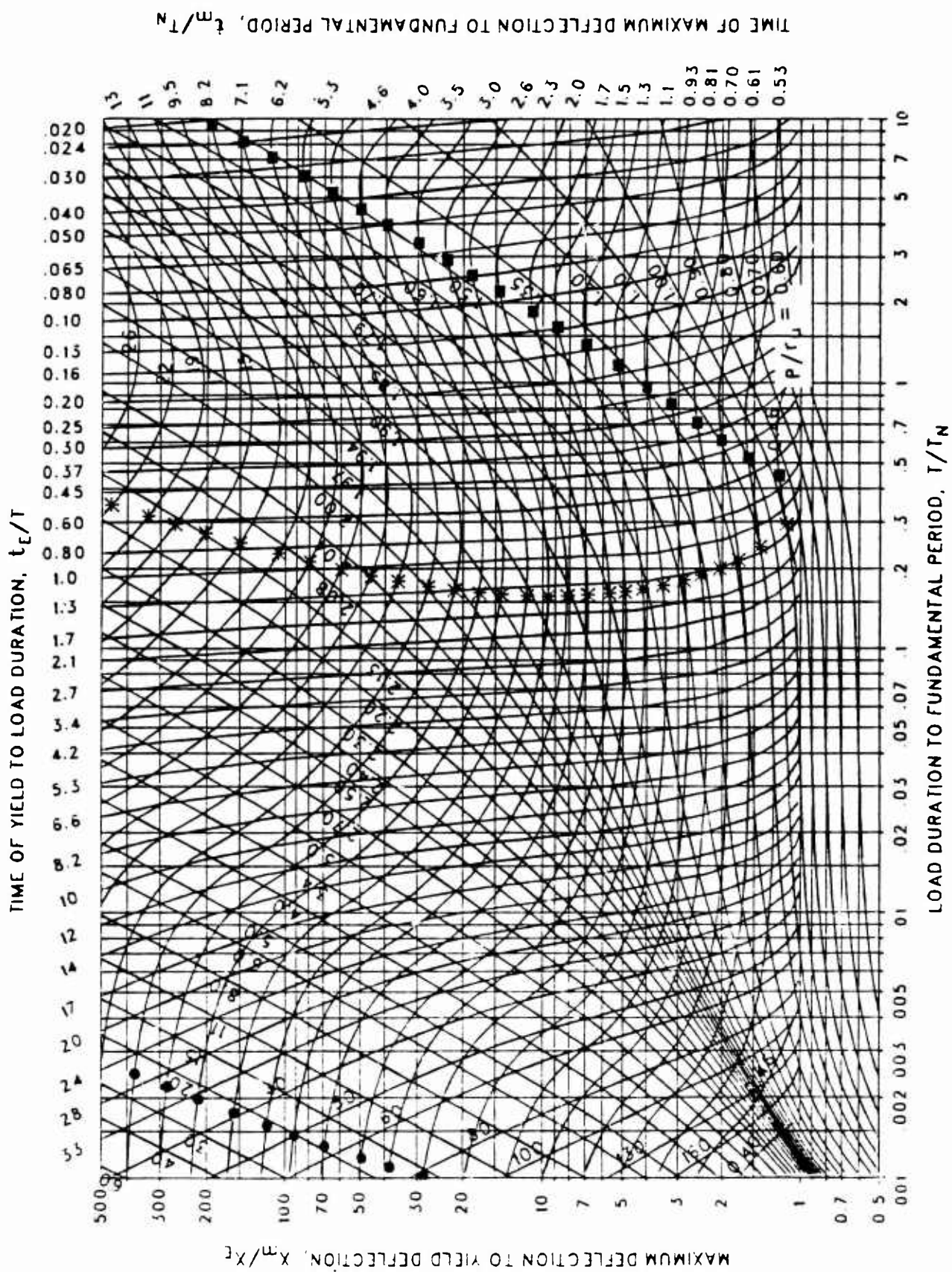
Figure 3-185   Maximum response of elasto-plastic, one-degree-of-freedom system for bilinear-triangular pulse ($C_1 = 0.511$, $C_2 = 300.$)
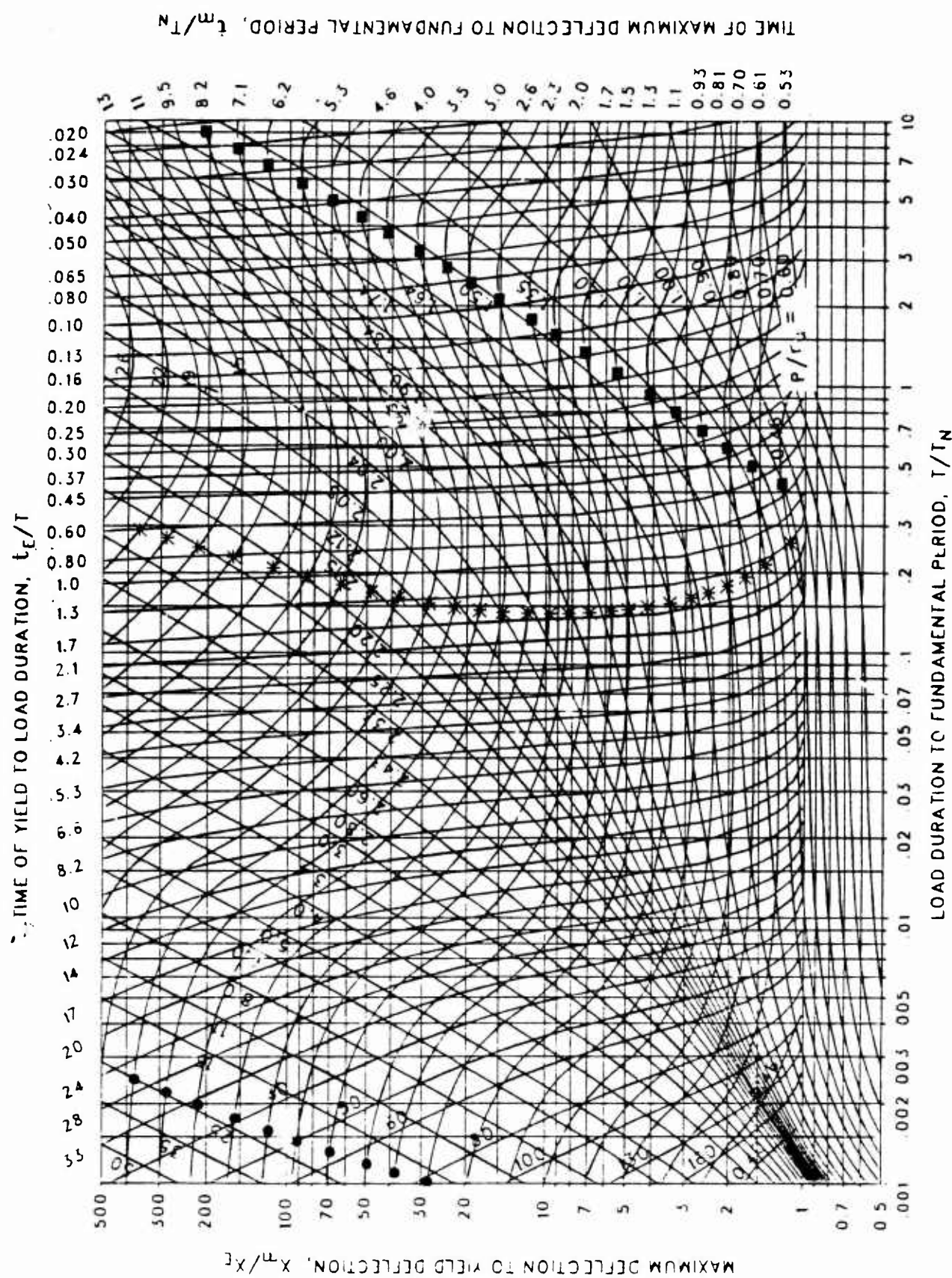
Figure 3-186   Maximum response of elasto-plastic, one-degree-of-freedom
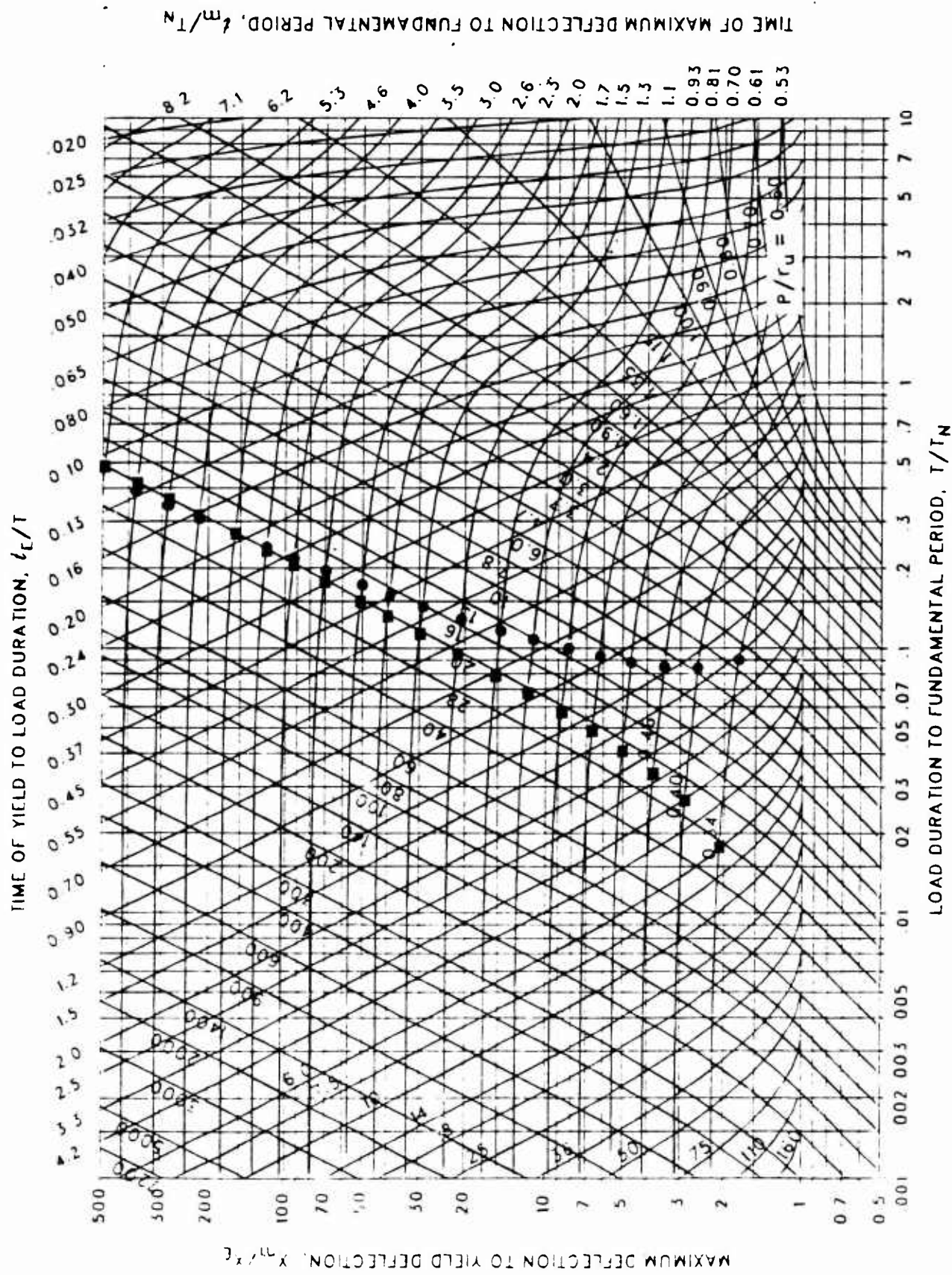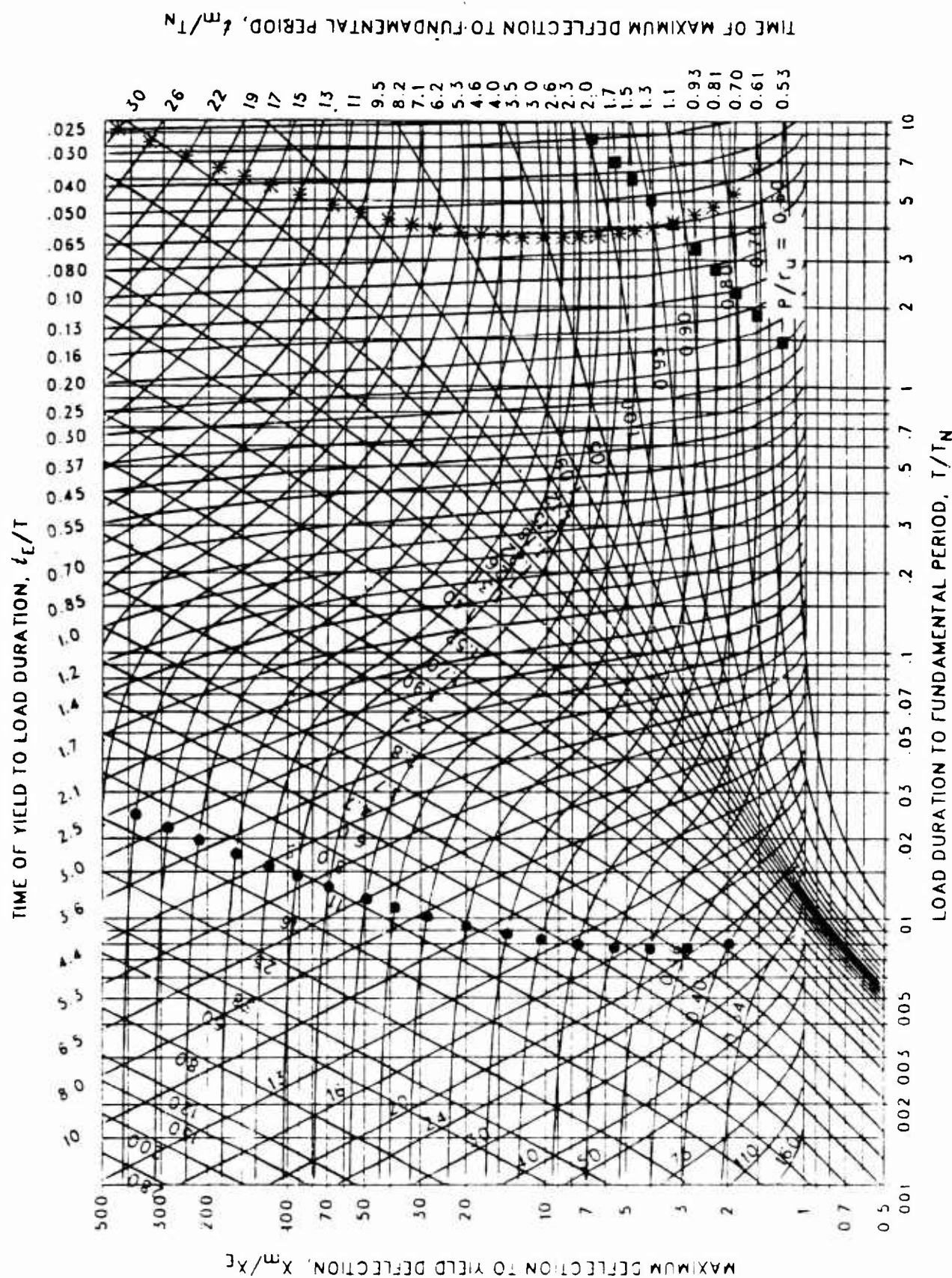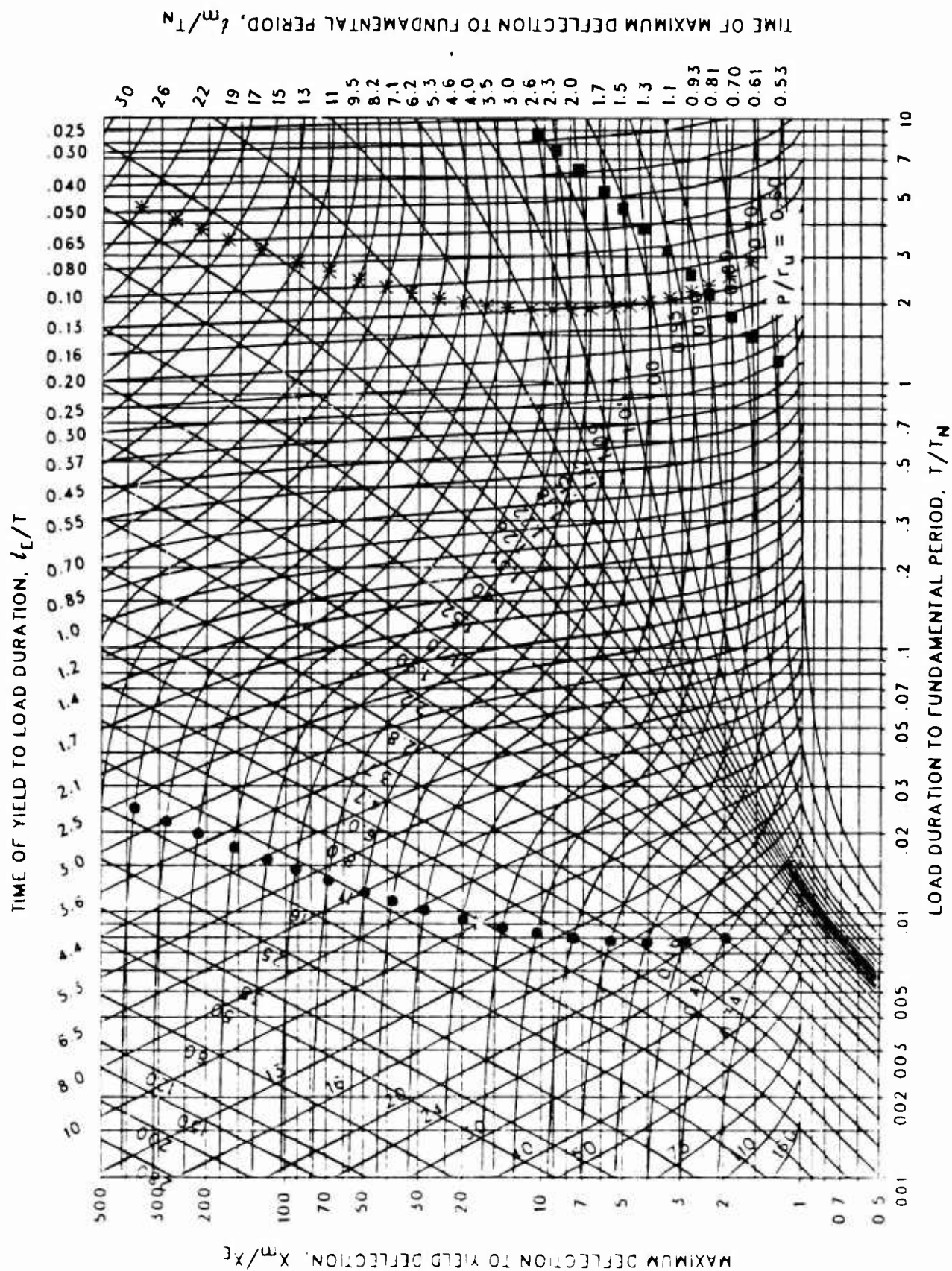system for bilinear-triangular pulse ($C_1 = 0.487$, $C_2 = 300.$)
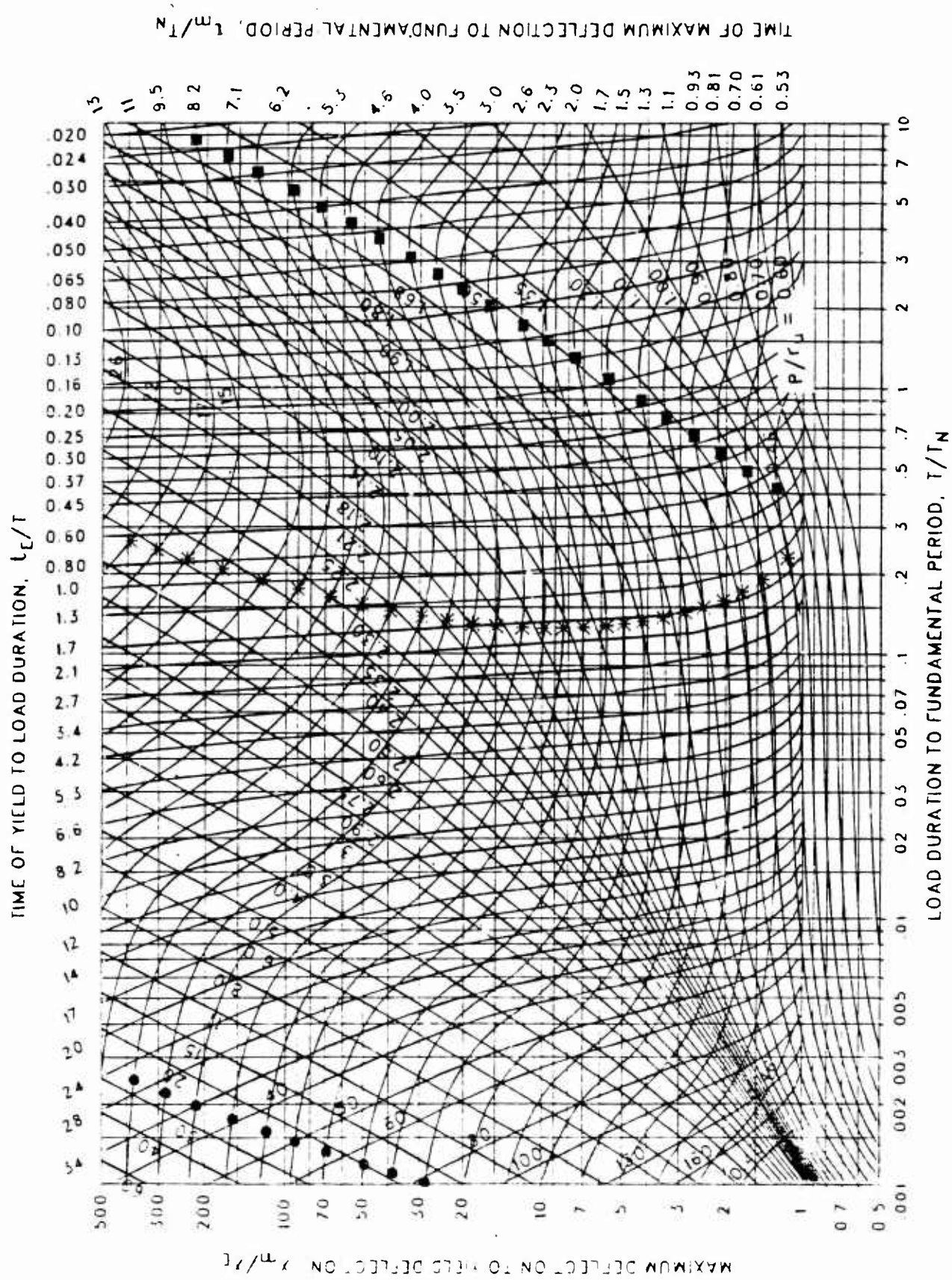
Figure 3-187   Maximum response of elasto-plastic, one-degree-of-freedom system for bilinear-triangular pulse ($C_1 = 0.464$, $C_2 = 300.$)
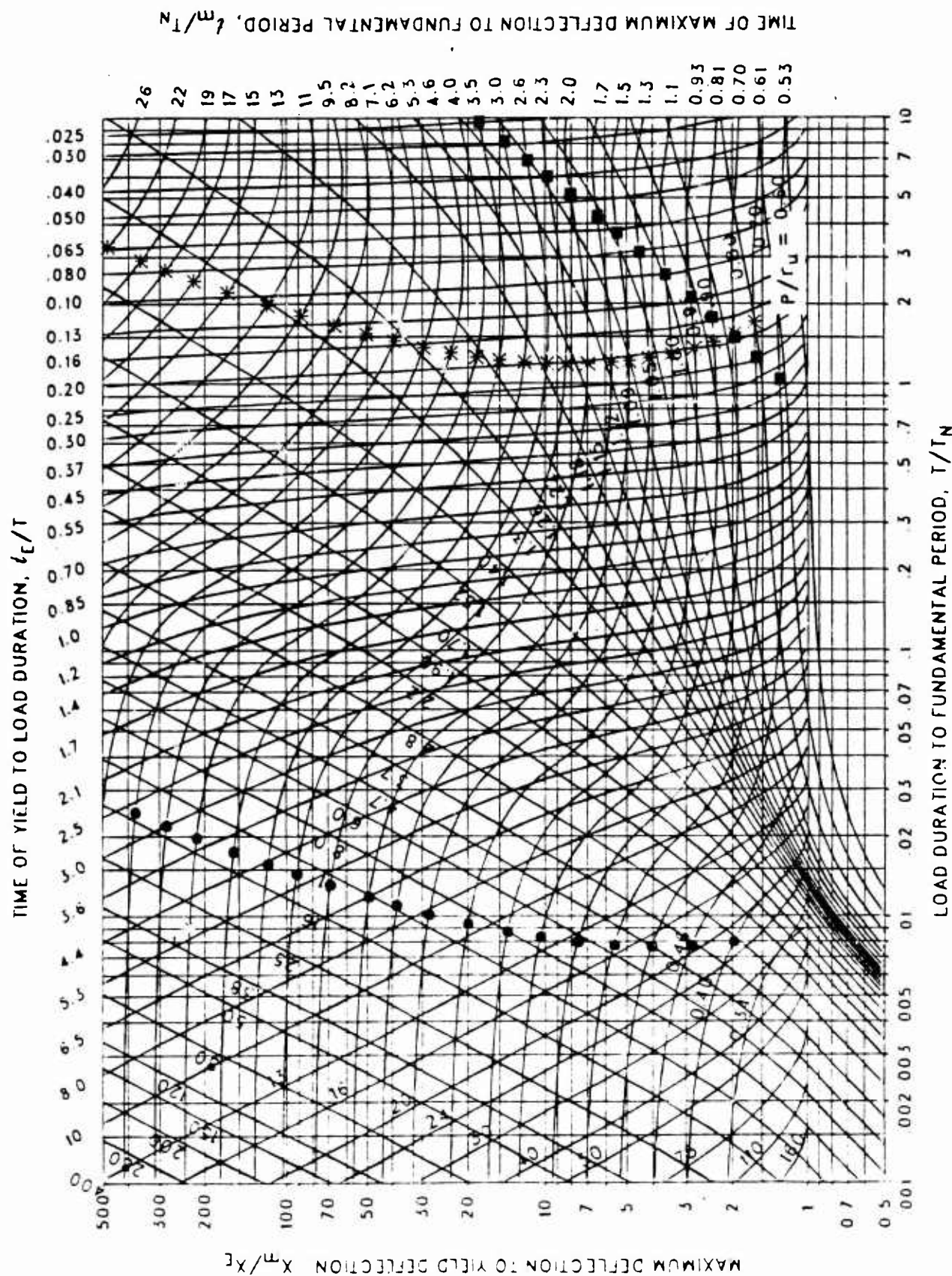
-242-
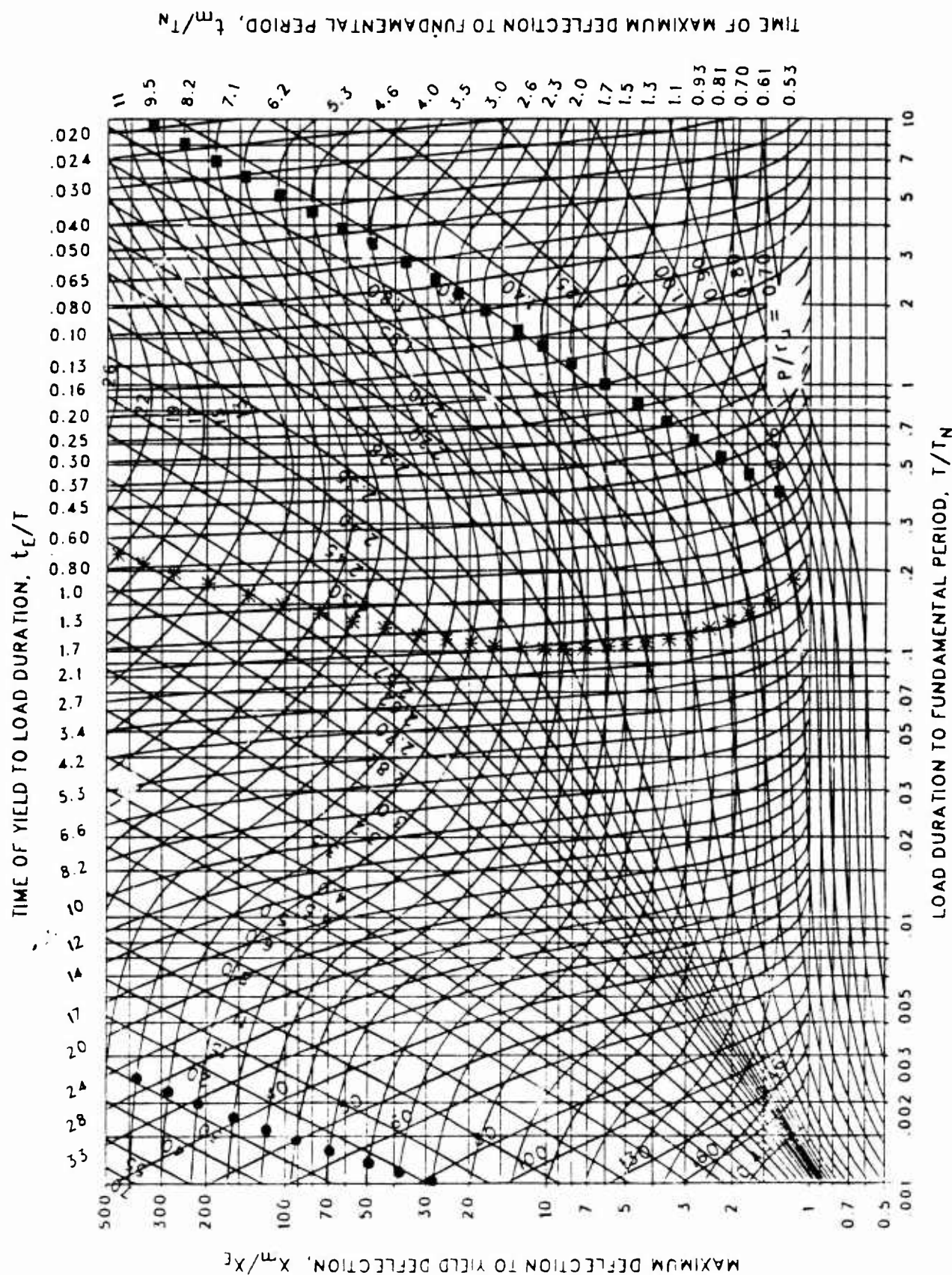
Figure 3-188   Maximum response of elasto-plastic, one-degree-of-freedom system for bilinear-triangular pulse ($C_1 = 0.422$, $C_2 = 300$.)

-243-
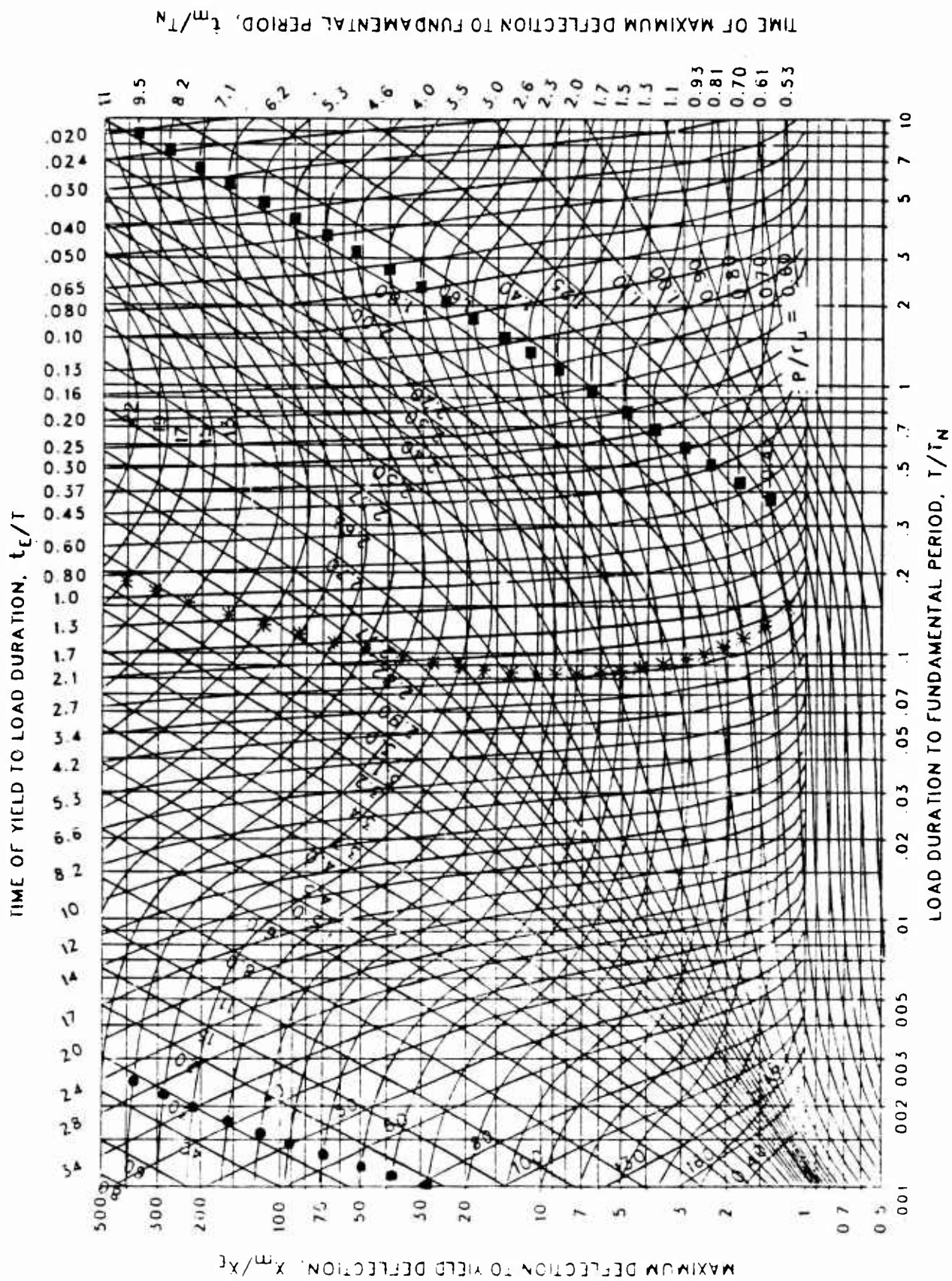
Figure 3-189   Maximum response of elasto-plastic, one-degree-of-freedom
system for bilinear-triangular pulse ($C_1 = 0.383$, $C_2 = 300.$)

-244-
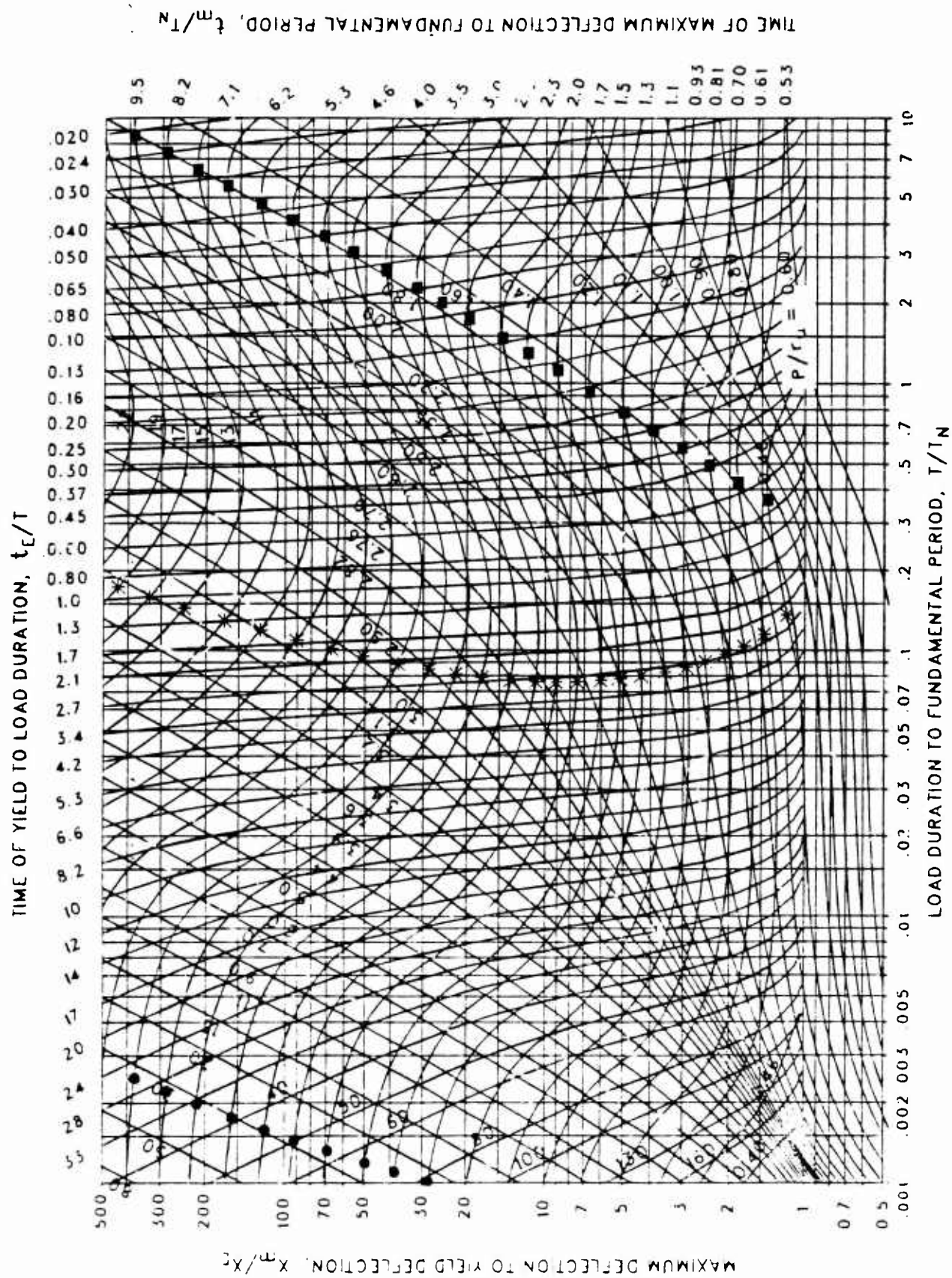
Figure 3-190   Maximum response of elasto-plastic, one-degree-of-freedom system for bilinear-triangular pulse ($C_1 = 0.365$, $C_2 = 300.$)
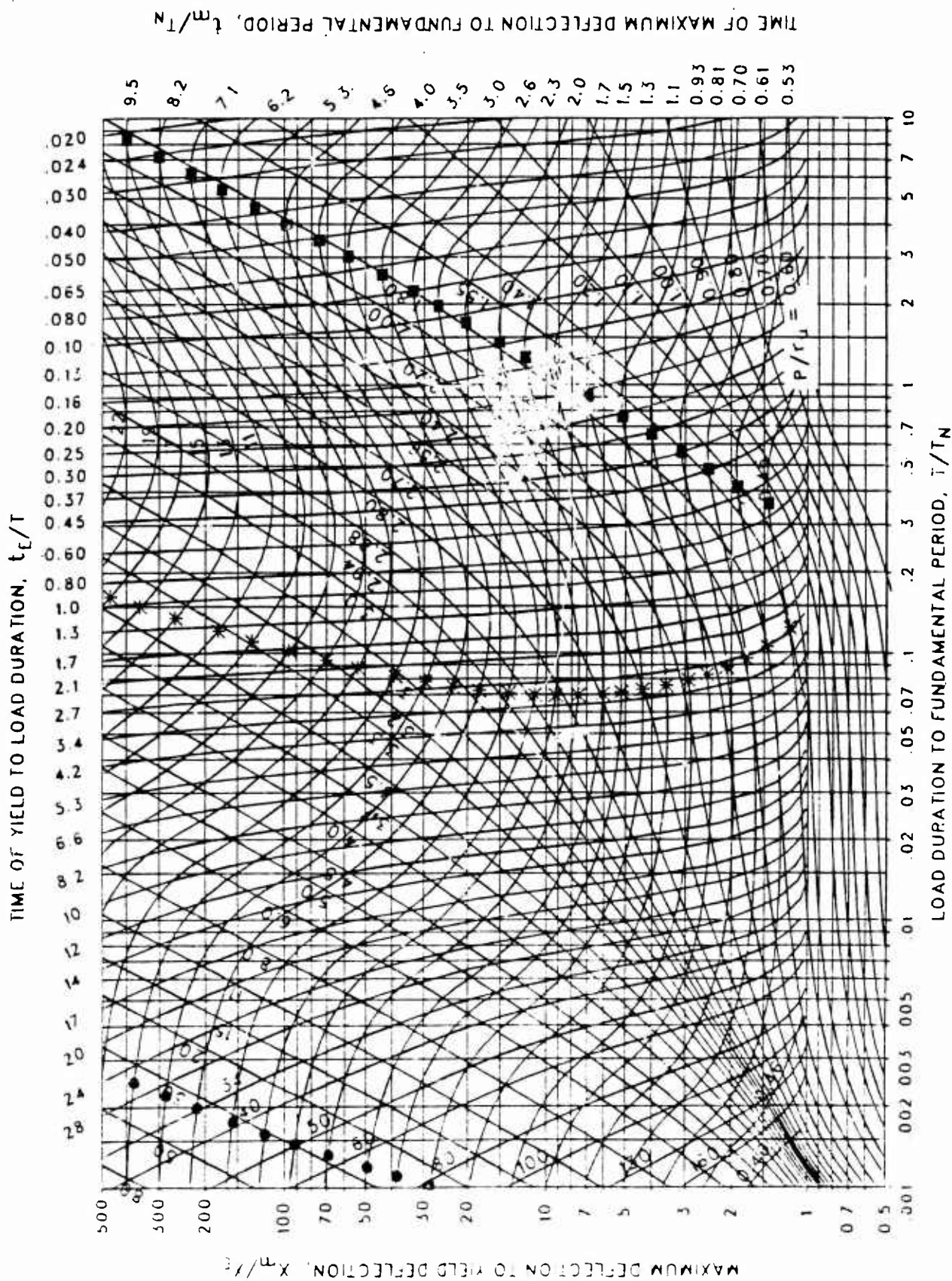
Figure 3-191   Maximum response of elasto-plastic, one-degree-of-freedom system for bilinear-triangular pulse ($C_1 = 0.348$, $C_2 = 300$.)

TIME OF MAXIMUM DEFLECTION TO FUNDAMENTAL PERIOD, t_m/T_N

TIME OF YIELD TO LOAD DURATION, t_E/T

LOAD DURATION TO FUNDAMENTAL PERIOD, T/T_N

MAXIMUM DEFLECTION TO YIELD DEFLECTION, x_m/x_E
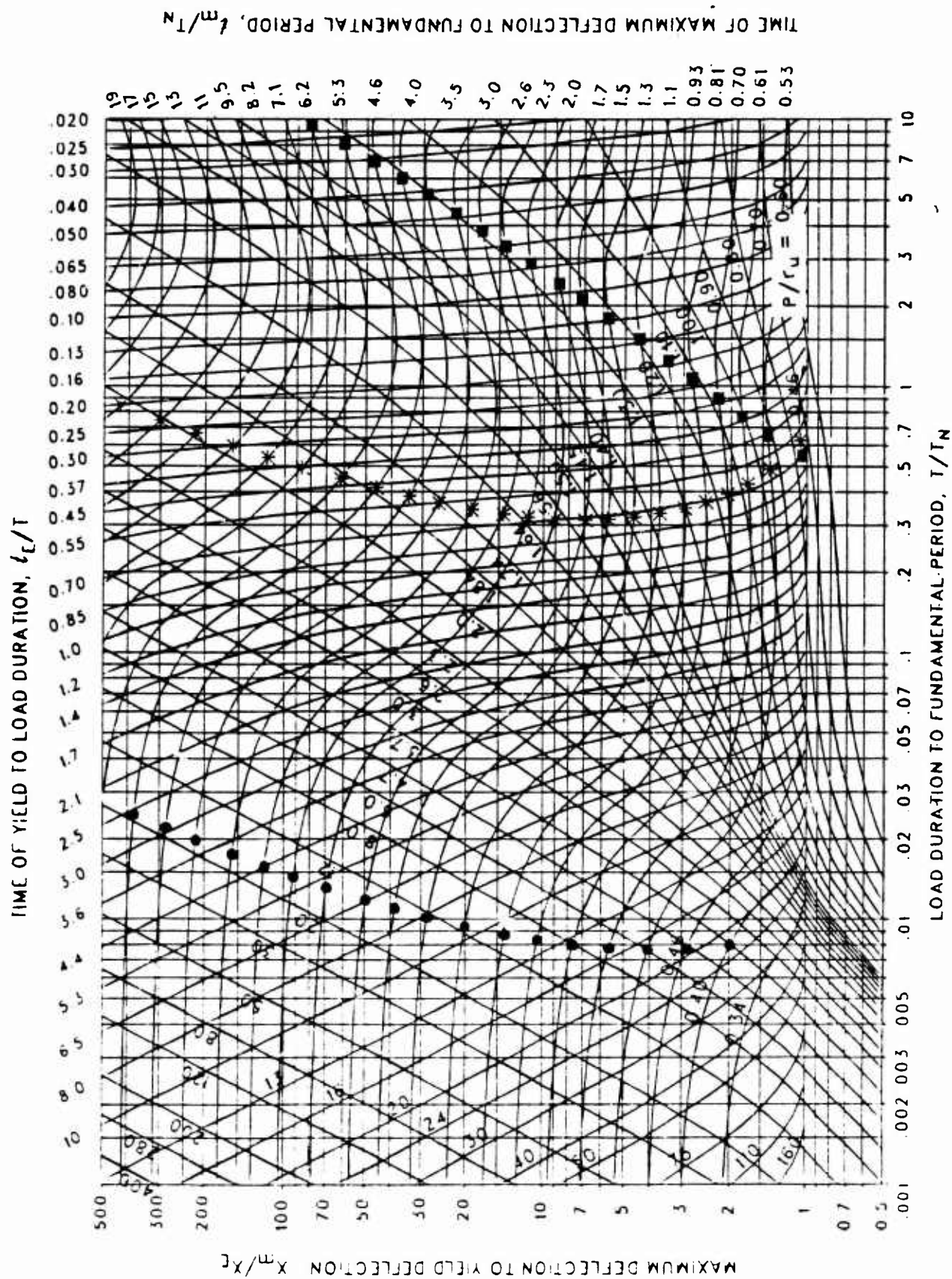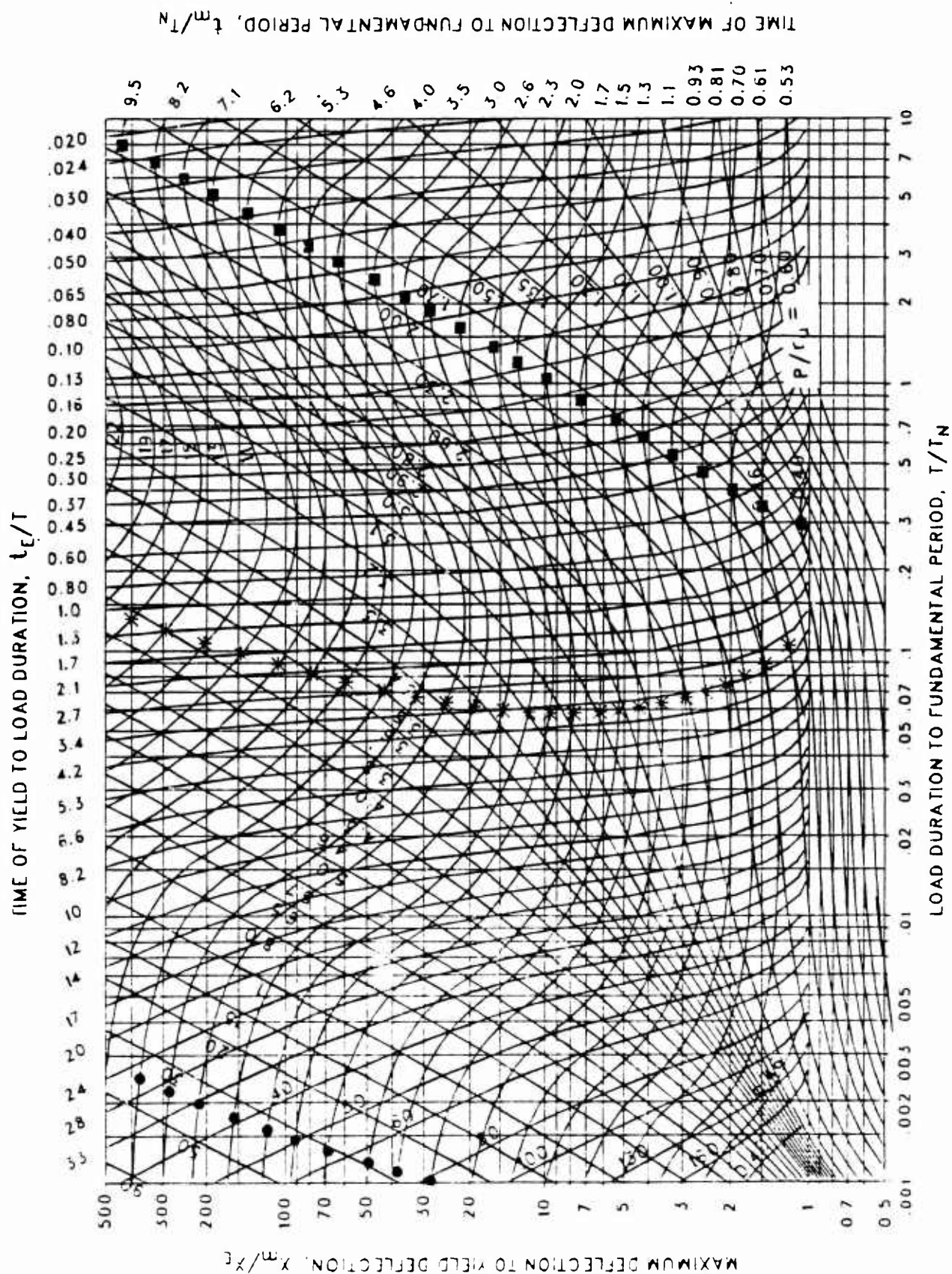
Figure 3-192   Maximum response of elasto-plastic, one-degree-of-freedom
system for bilinear-triangular pulse ($C_1 = 0.316$, $C_2 = 300$.)

-247-
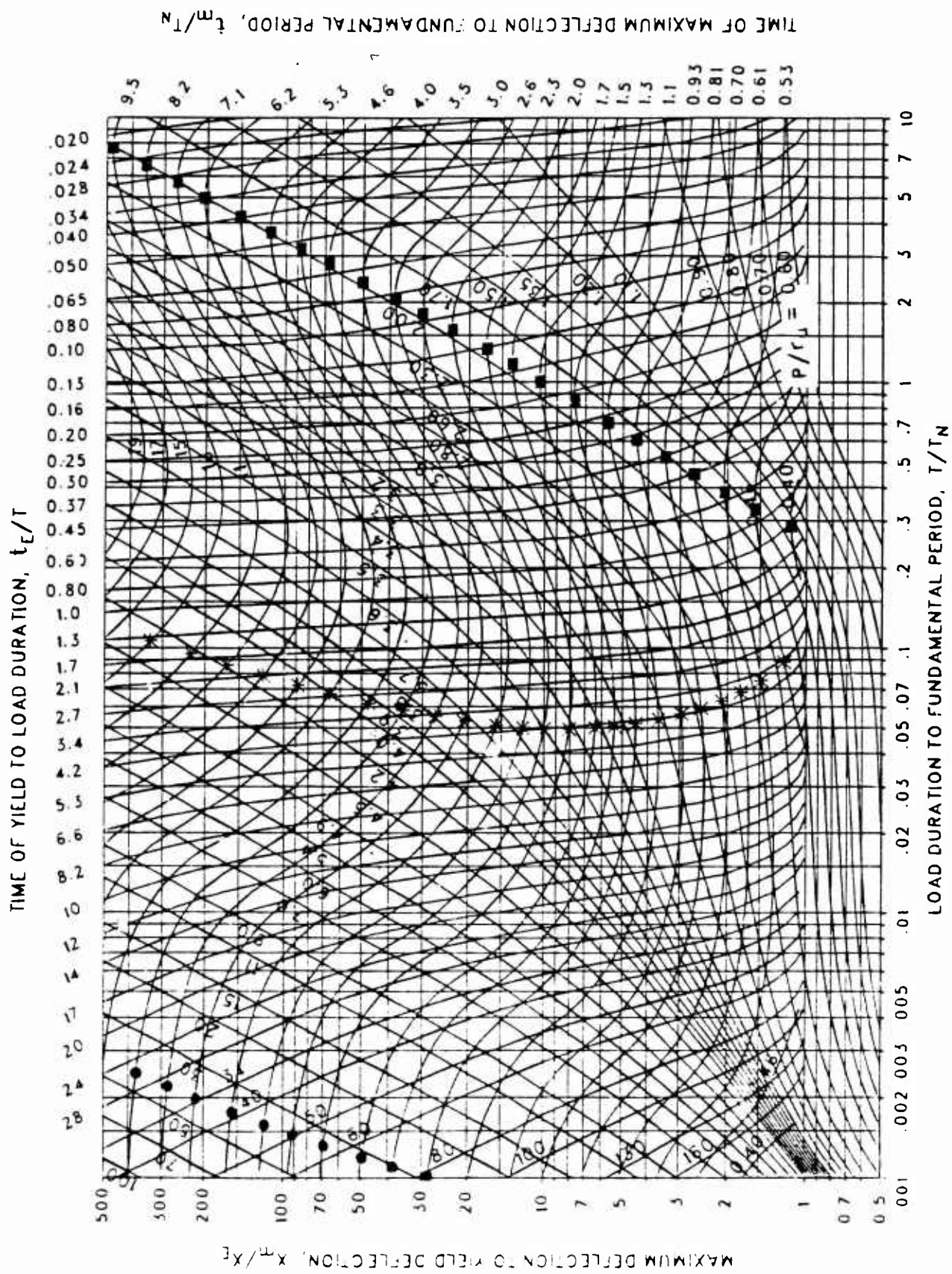
Figure 3-193   Maximum response of elasto-plastic, one-degree-of-freedom
system for bilinear-triangular pulse ($C_1 = 0.287$, $C_2 = 300.$)

-248-
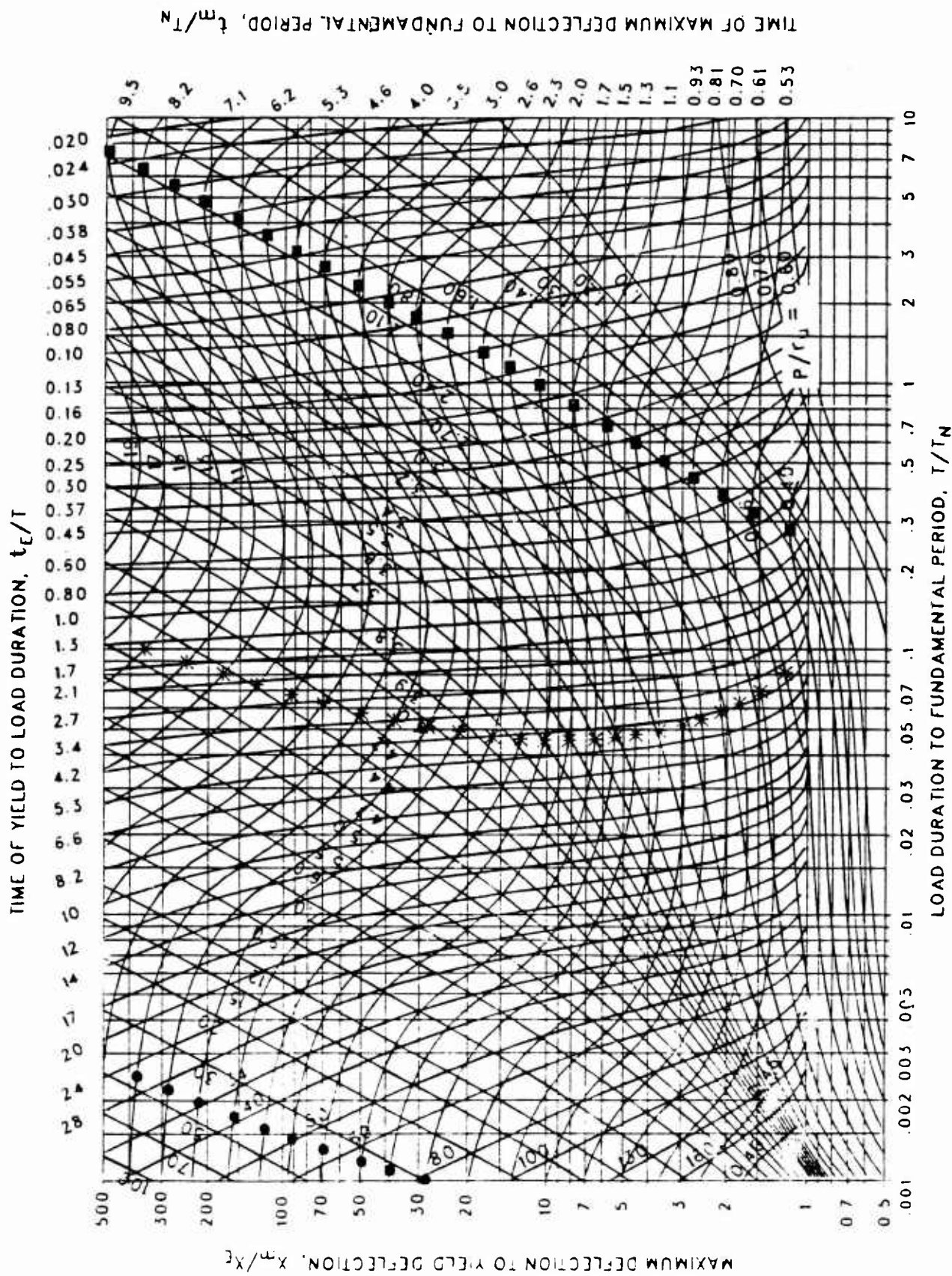
Figure 3-194   Maximum response of elasto-plastic, one-degree-of-freedom system for bilinear-triangular pulse ($C_1 = 0.274$, $C_2 = 300.$)

Figure 3-195   Maximum response of elasto-plastic, one-degree-of-freedom system for bilinear-triangular pulse ($C_1 = 0.261$, $C_2 = 300$.)
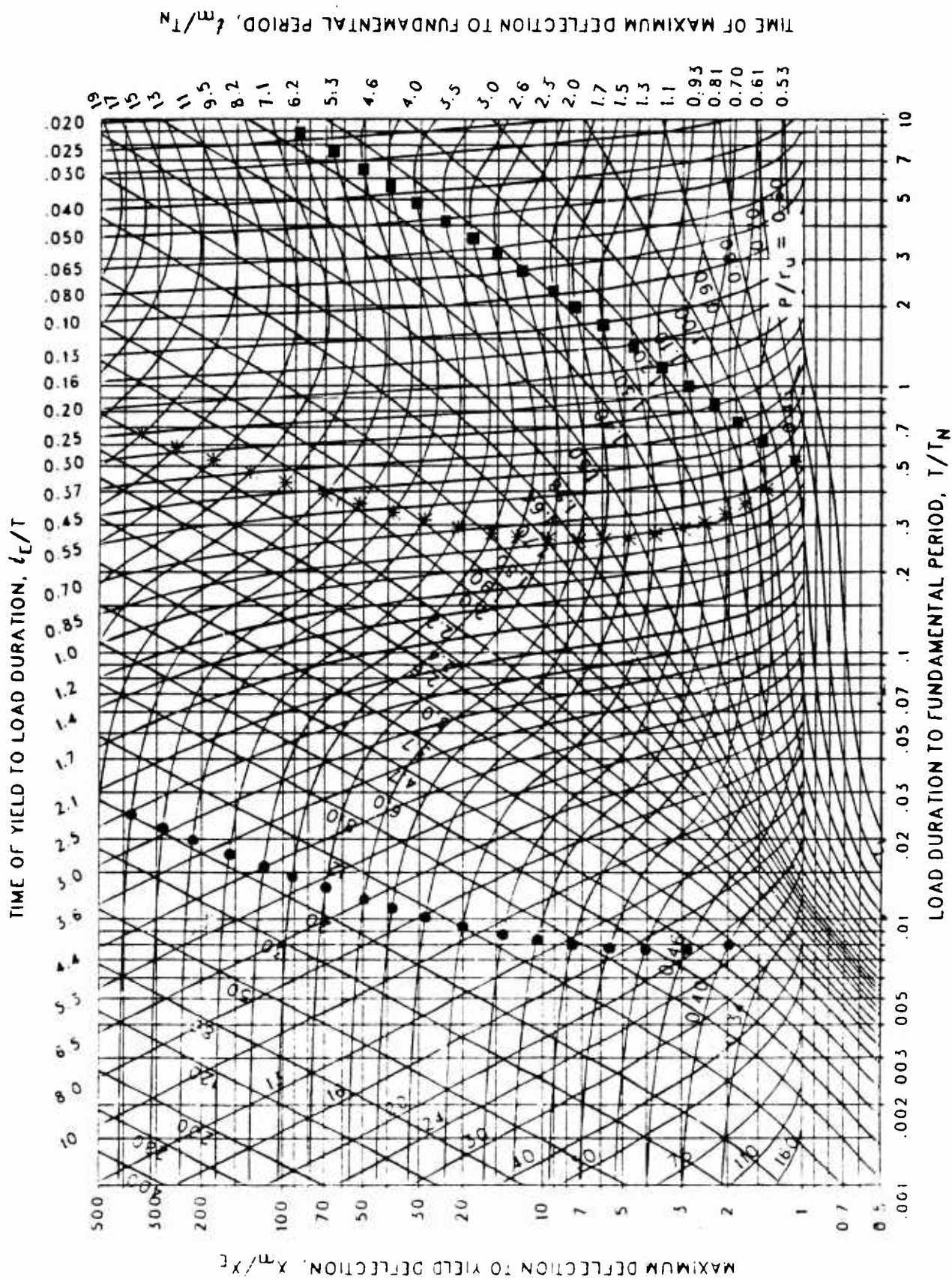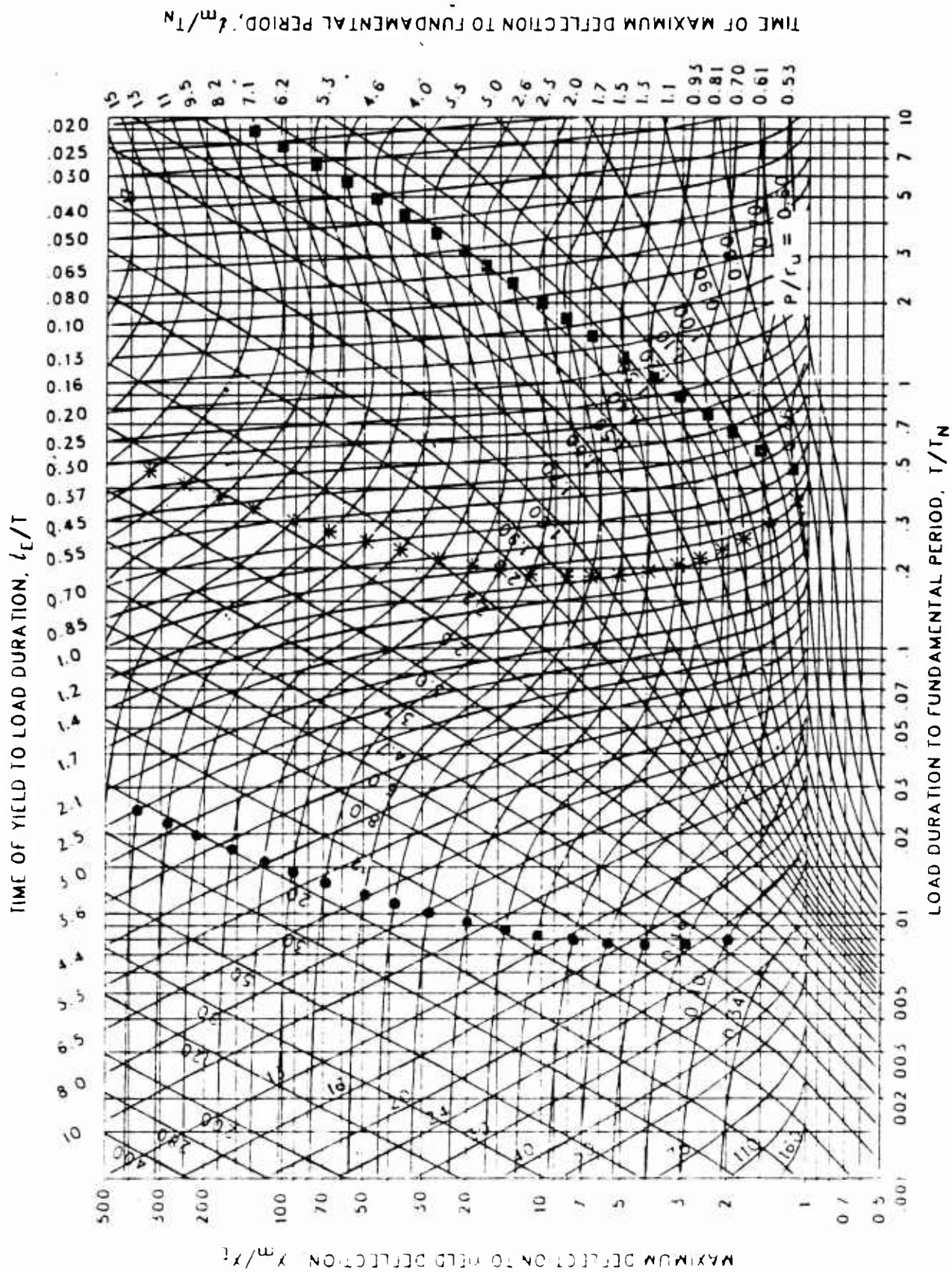
-250-
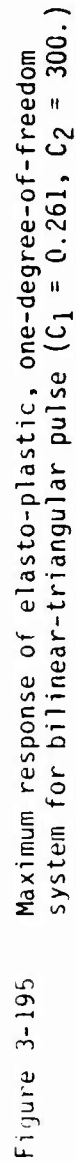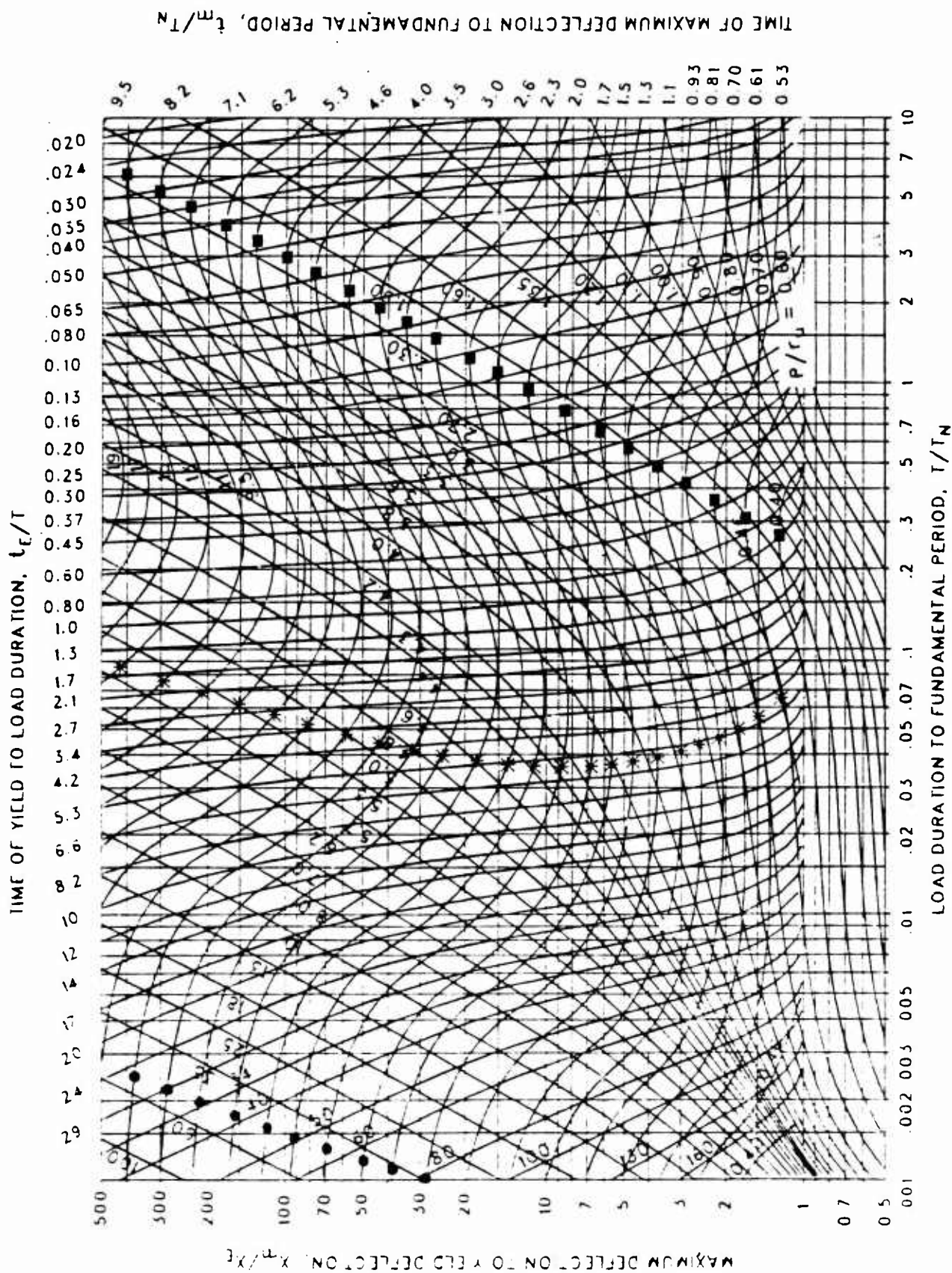
Figure 3-196   Maximum response of elasto-plastic, one-degree-of-freedom system for bilinear-triangular pulse ($C_1 = 0.237$, $C_2 = 300$.)
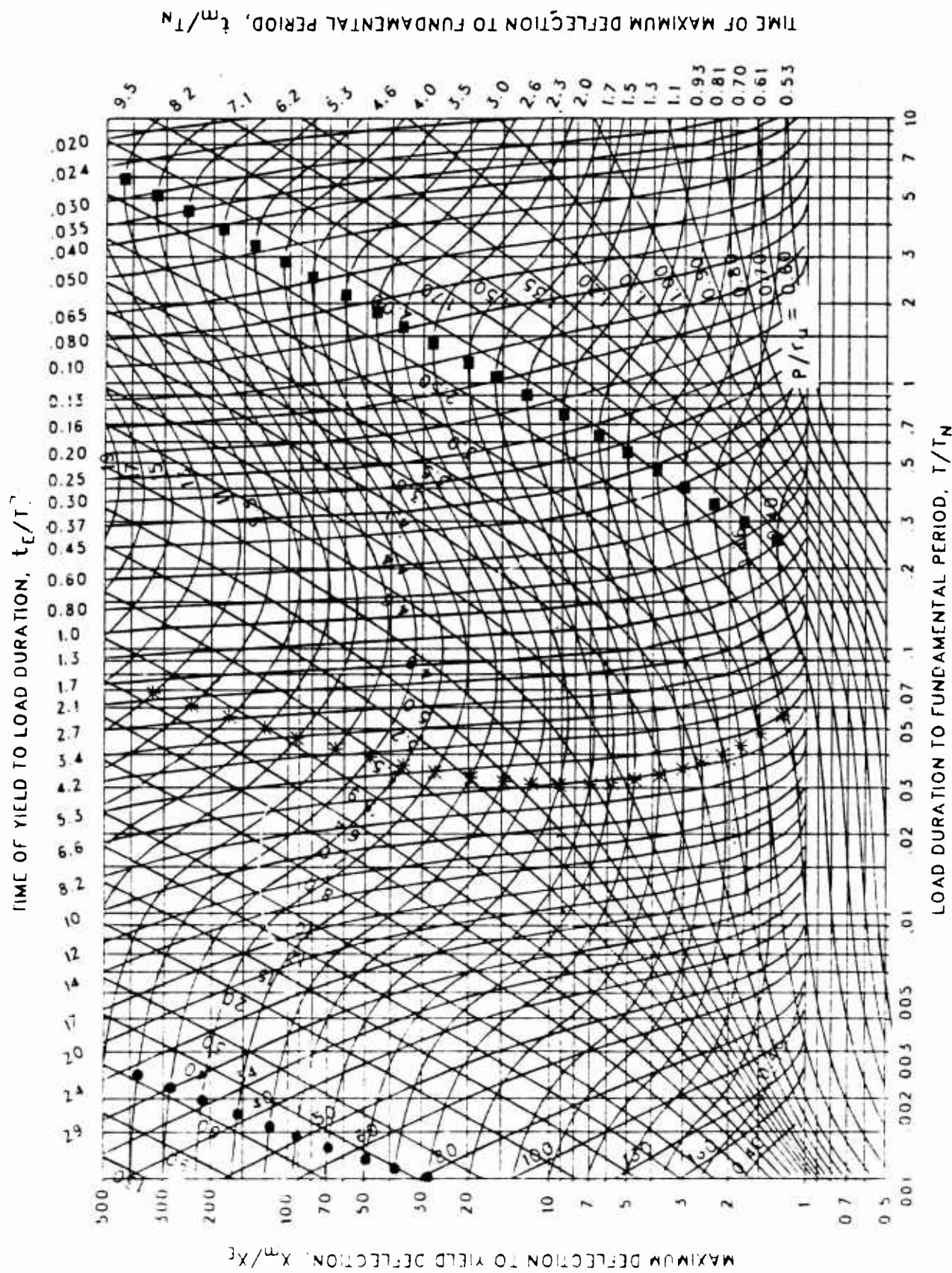
Figure 3-197   Maximum response of elasto-plastic, one-degree-of-freedom system for bilinear-triangular pulse ($C_1 = 0.215$, $C_2 = 300$.)
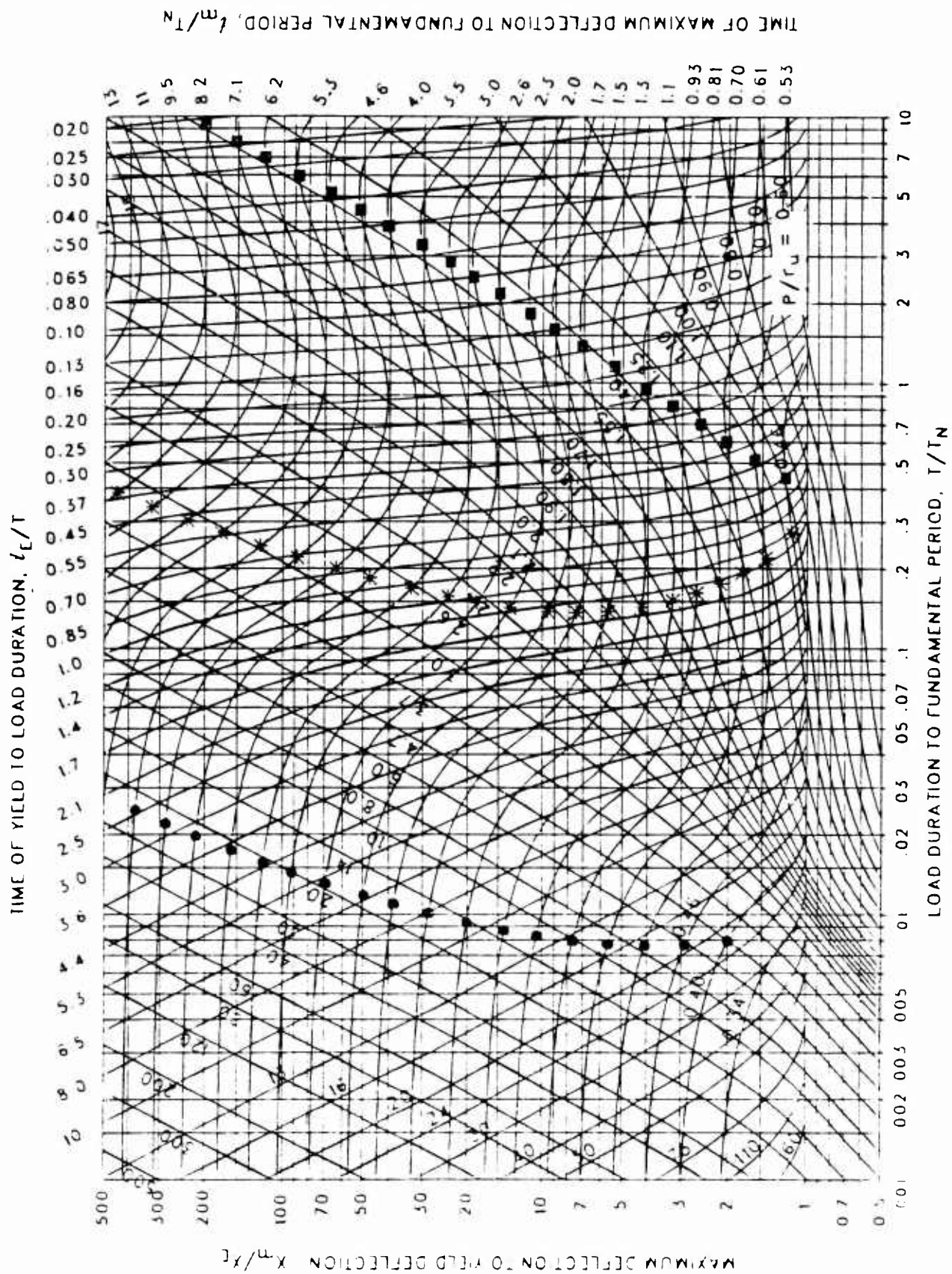
-252-
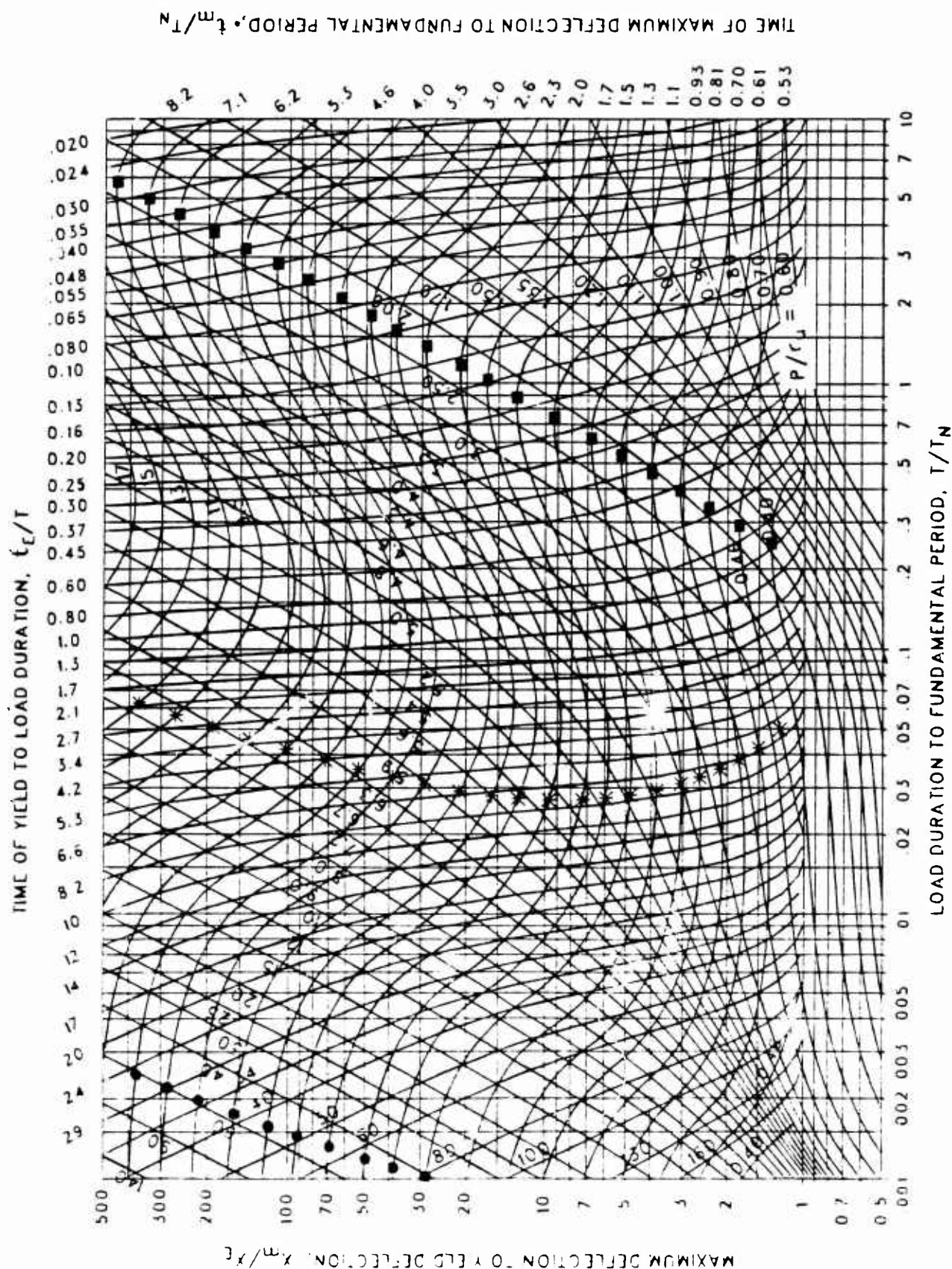
Figure 3-198   Maximum response of elasto-plastic, one-degree-of-freedom system for bilinear-triangular pulse (C_1 = 0.198, C_2 = 300.)
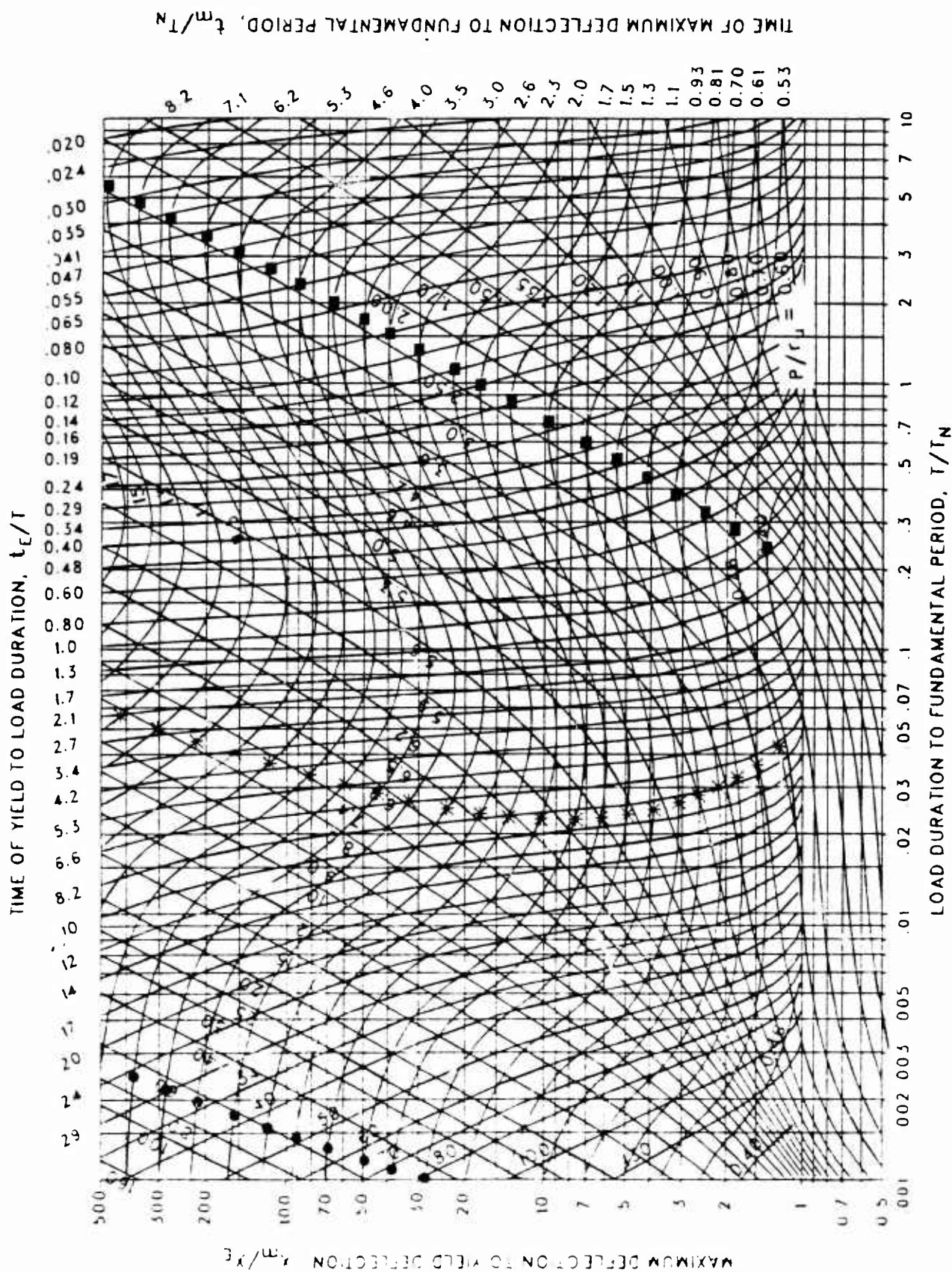
Figure 3-199   Maximum response of elasto-plastic, one-degree-of-freedom
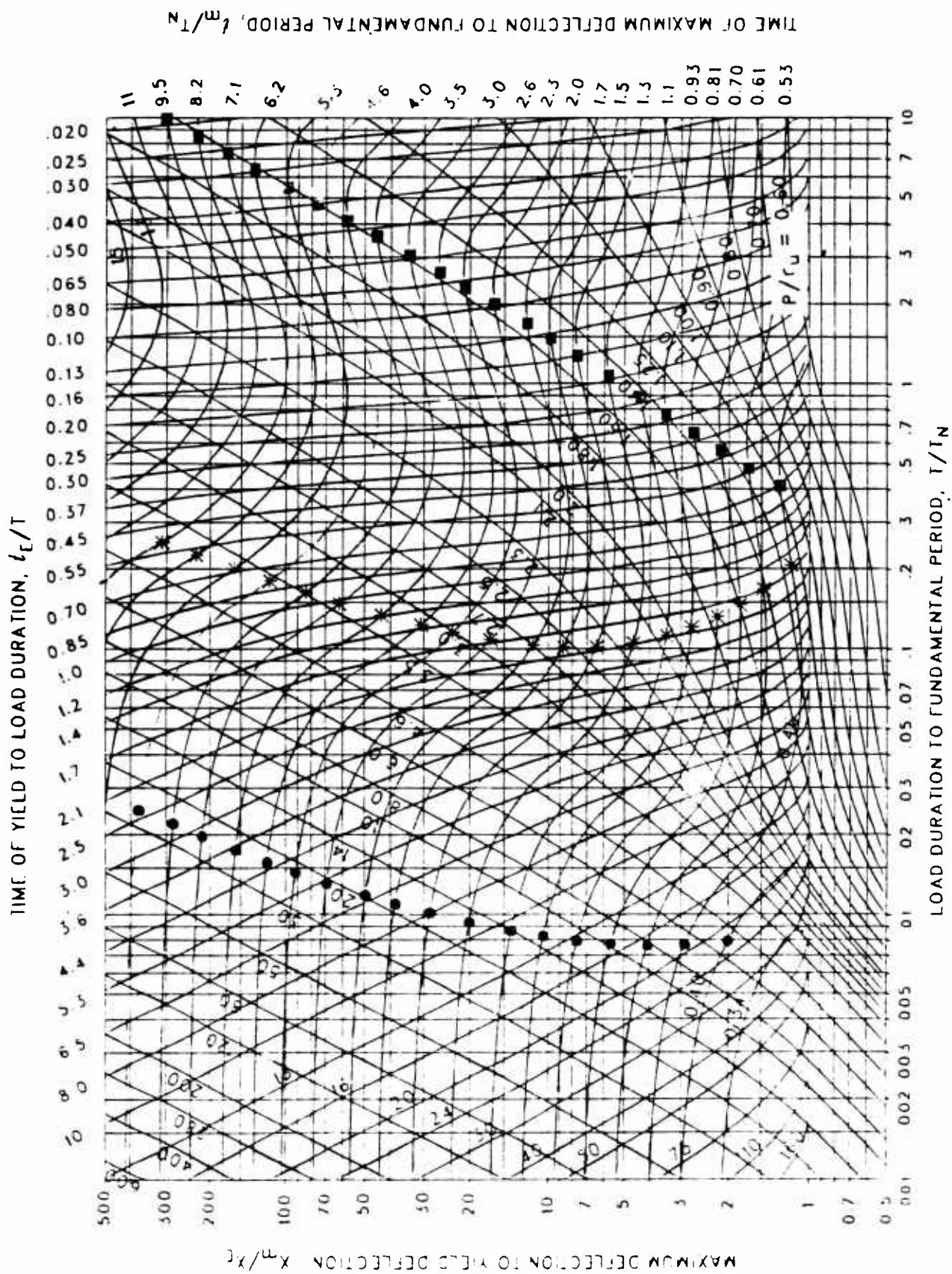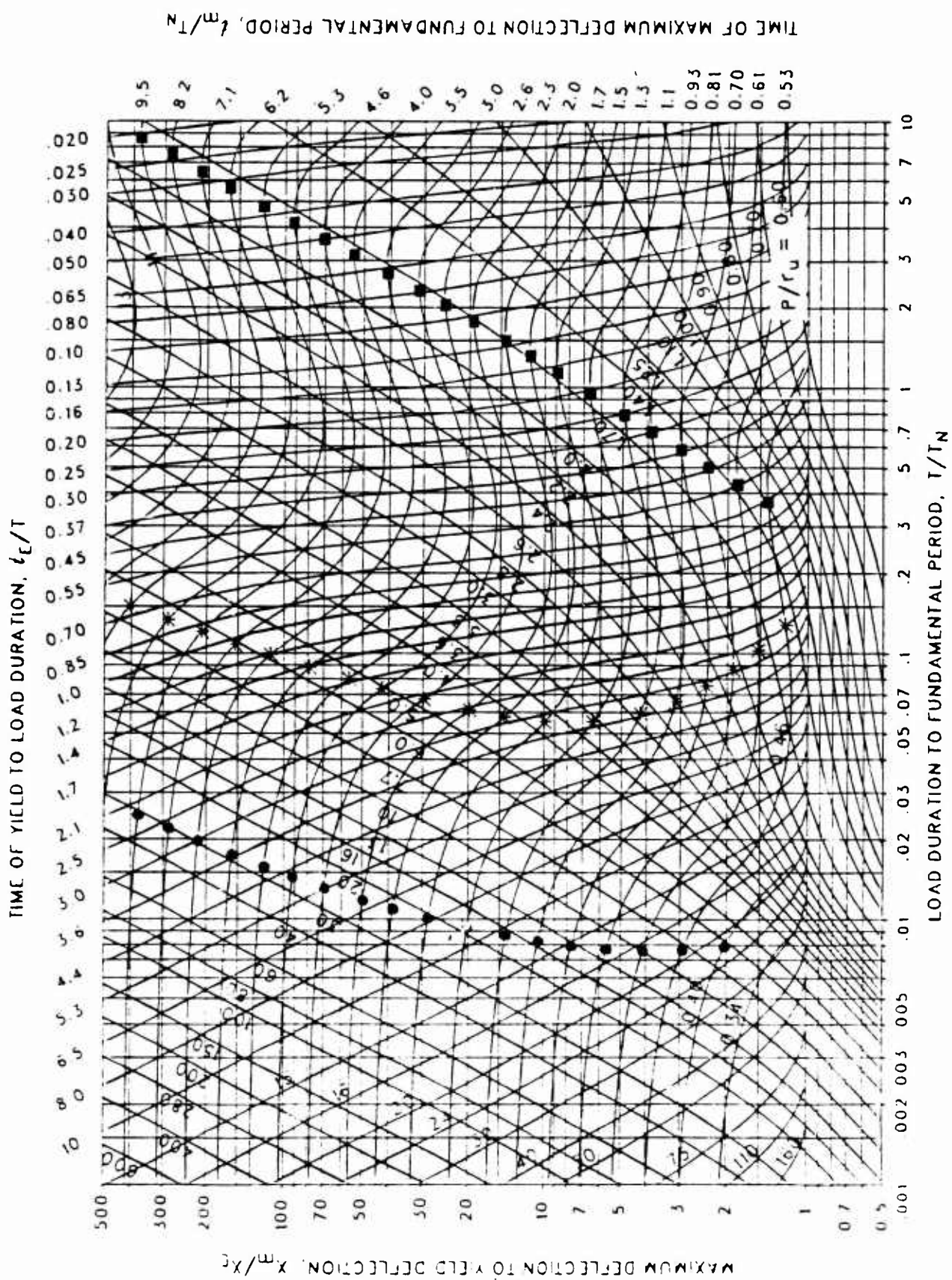system for bilinear-triangular pulse (C_1 = 0.178, C_2 = 300.)

-254-
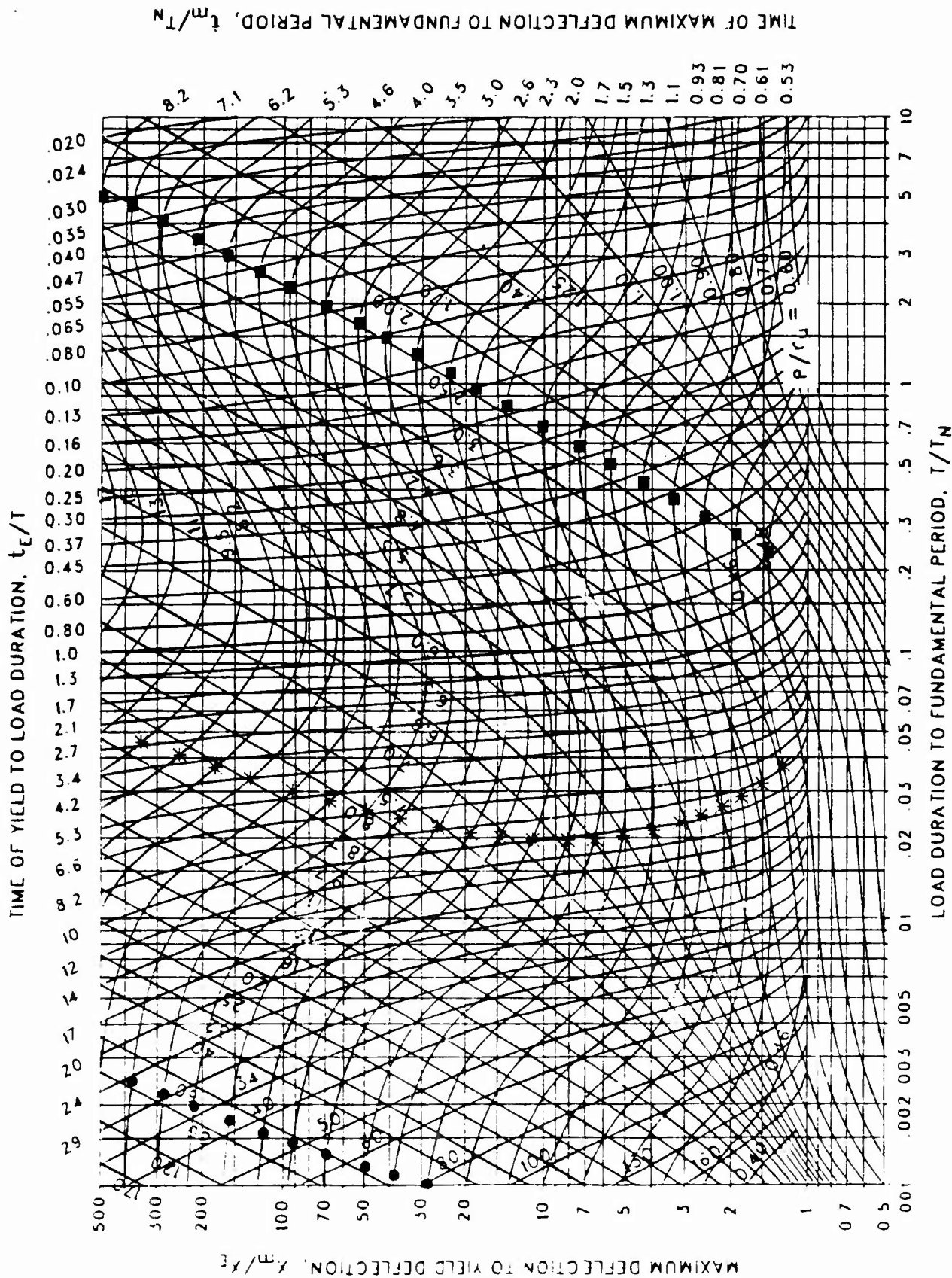
Figure 3-200 Maximum response of elasto-plastic, one-degree-of-freedom system for bilinear-triangular pulse (C_1 = 0.162, C_2 = 300.)

-255-
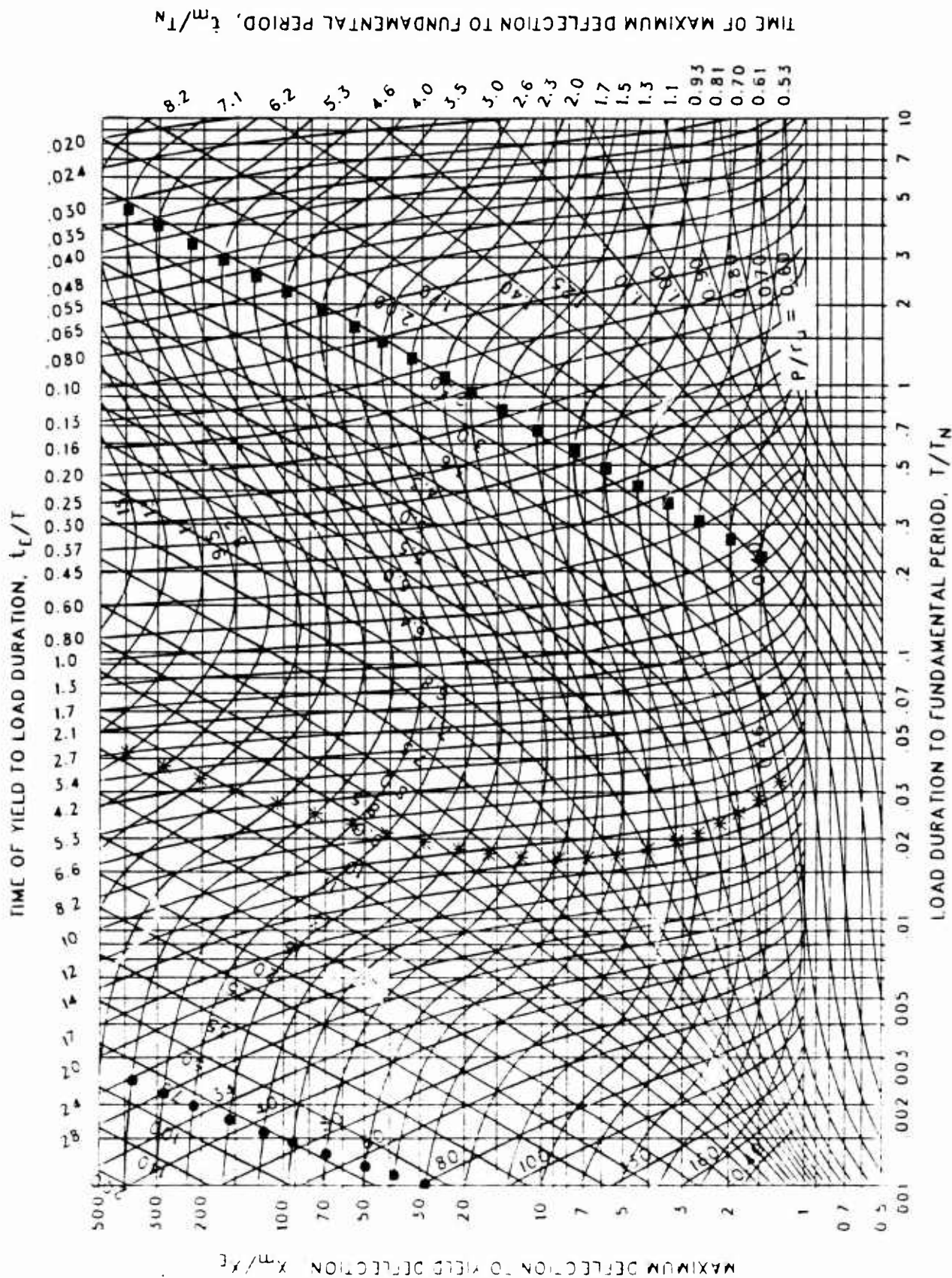
Figure 3-2(1)   Maximum response of elasto-plastic, one-degree-of-freedom system for bilinear-triangular pulse ($C_1 = 0.147$, $C_2 = 300.$)

-256-
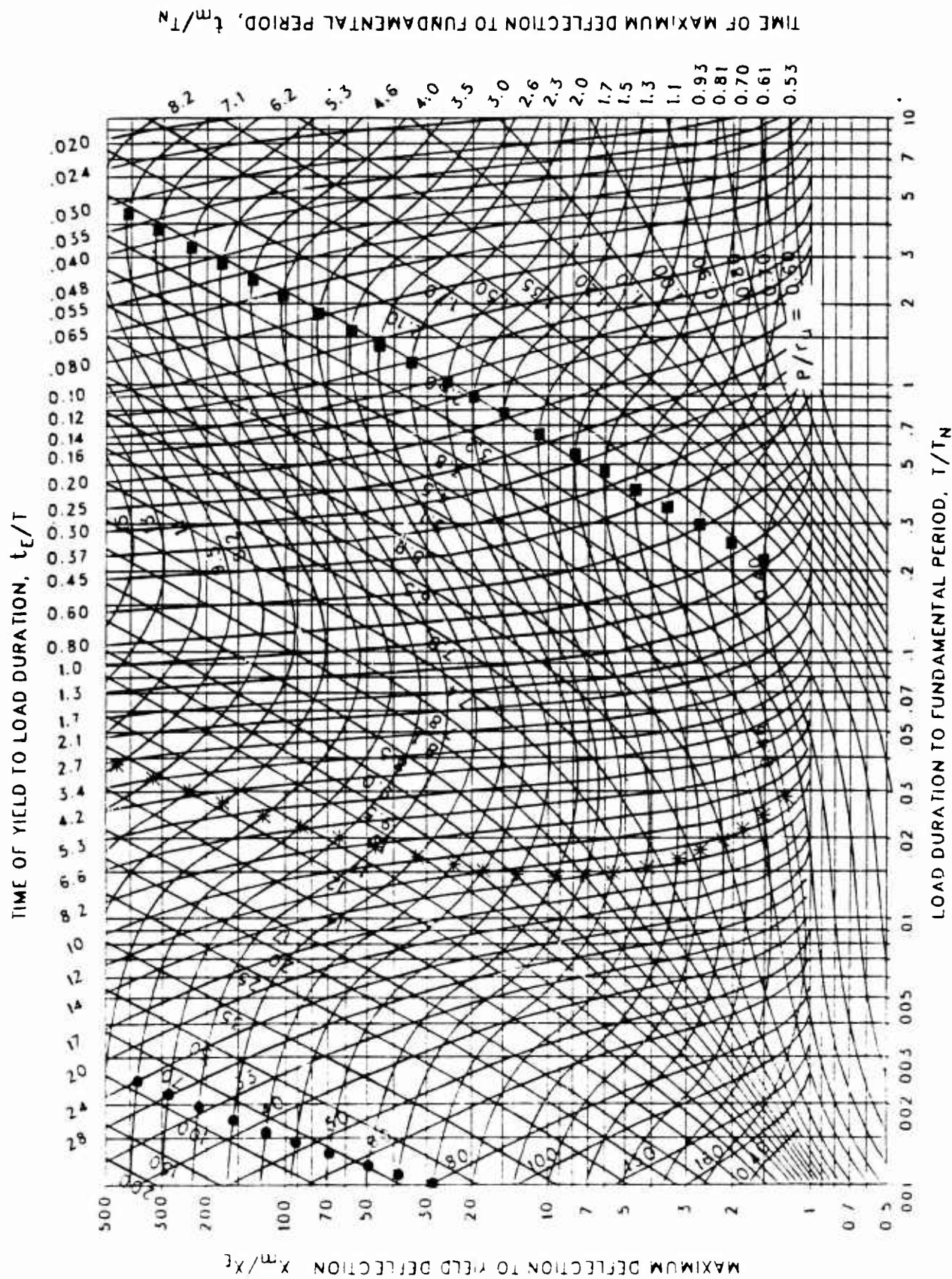
Figure 3-202   Maximum response of elasto-plastic, one-degree-of-freedom
system for bilinear-triangular pulse ($C_1 = 0.133$, $C_2 = 300.$)
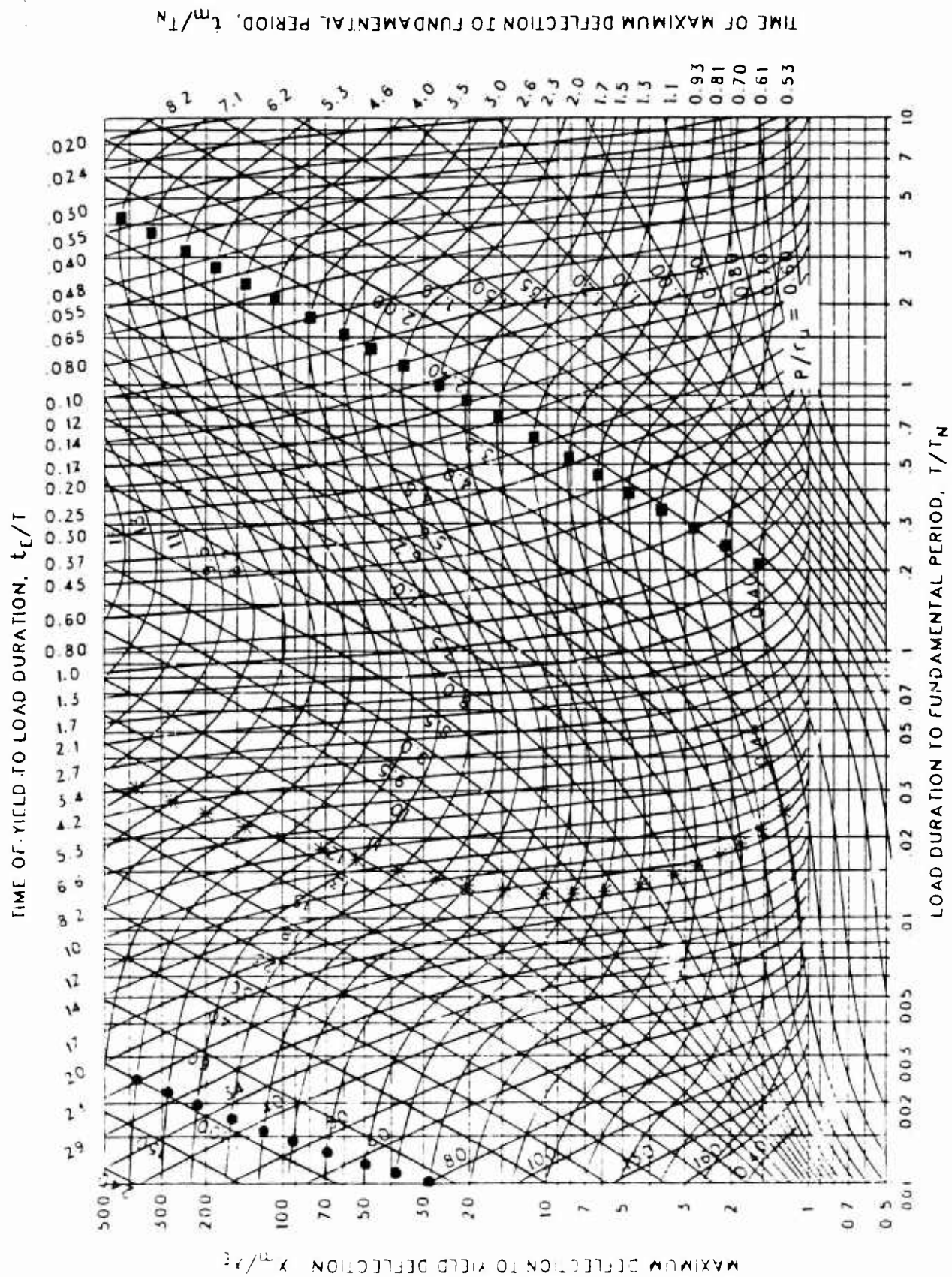
Figure 3-203　Maximum response of elasto-plastic, one-degree-of-freedom system for bilinear-triangular pulse ($C_1 = 0.121$, $C_2 = 300.$)
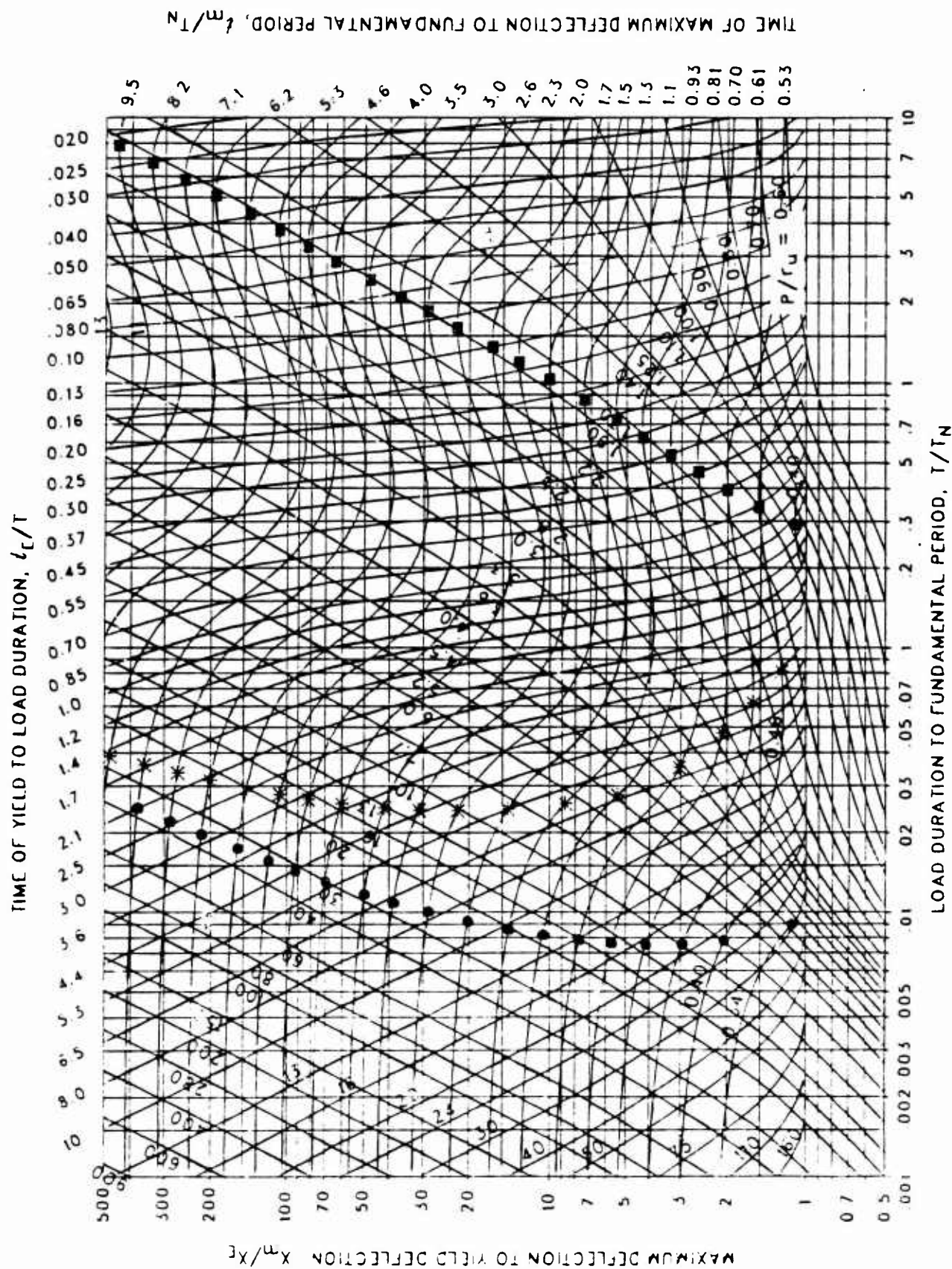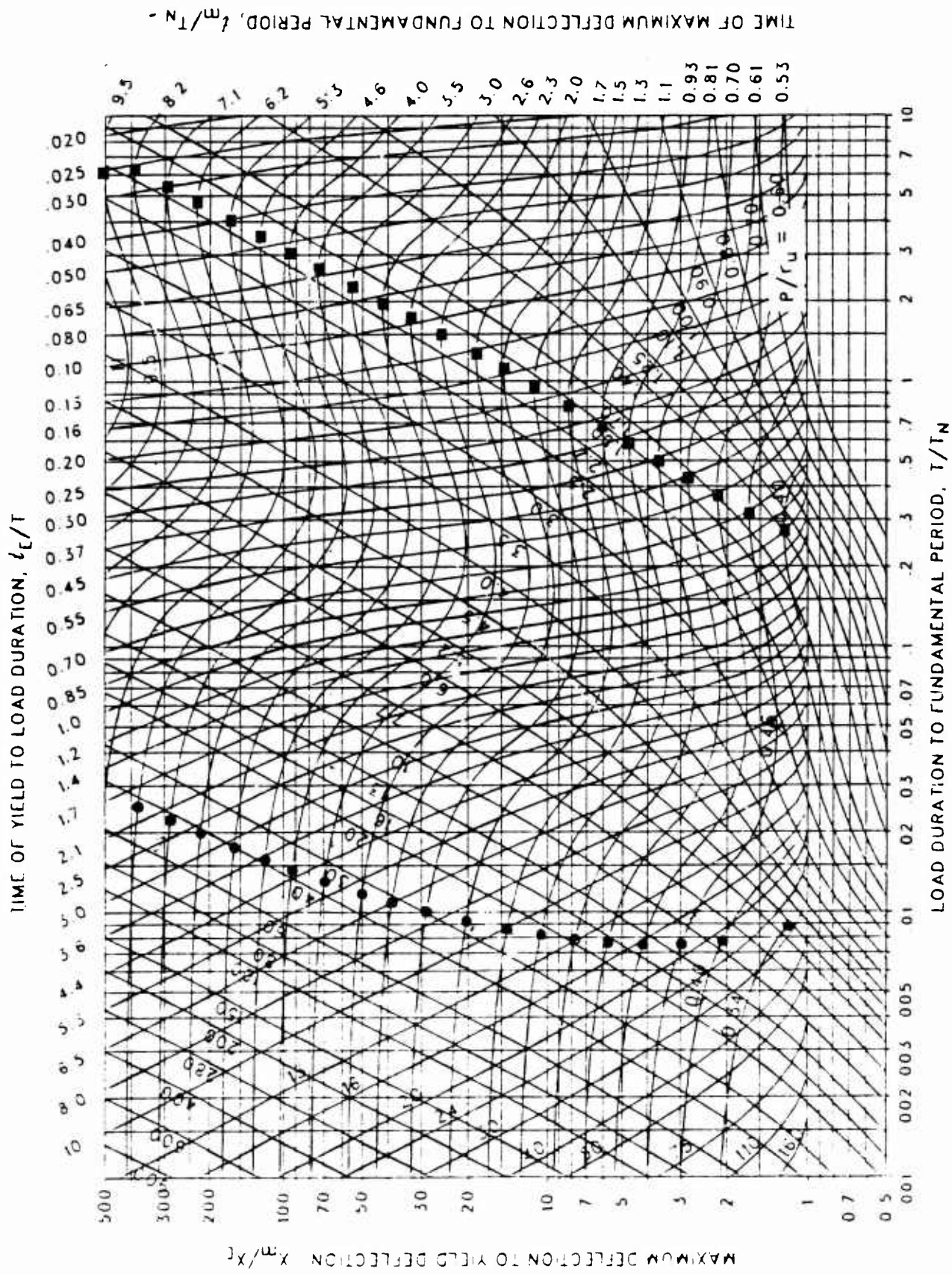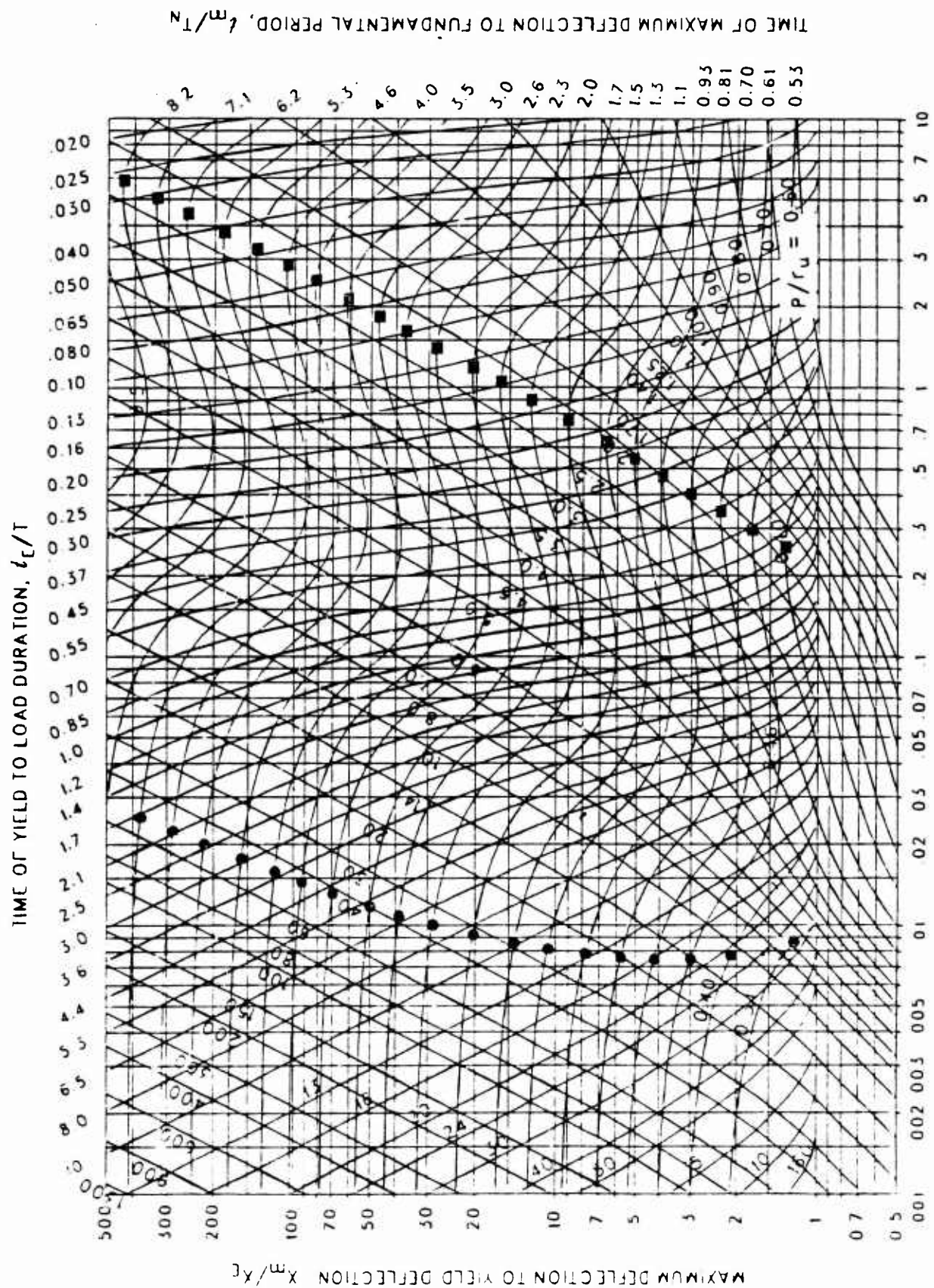
-258-
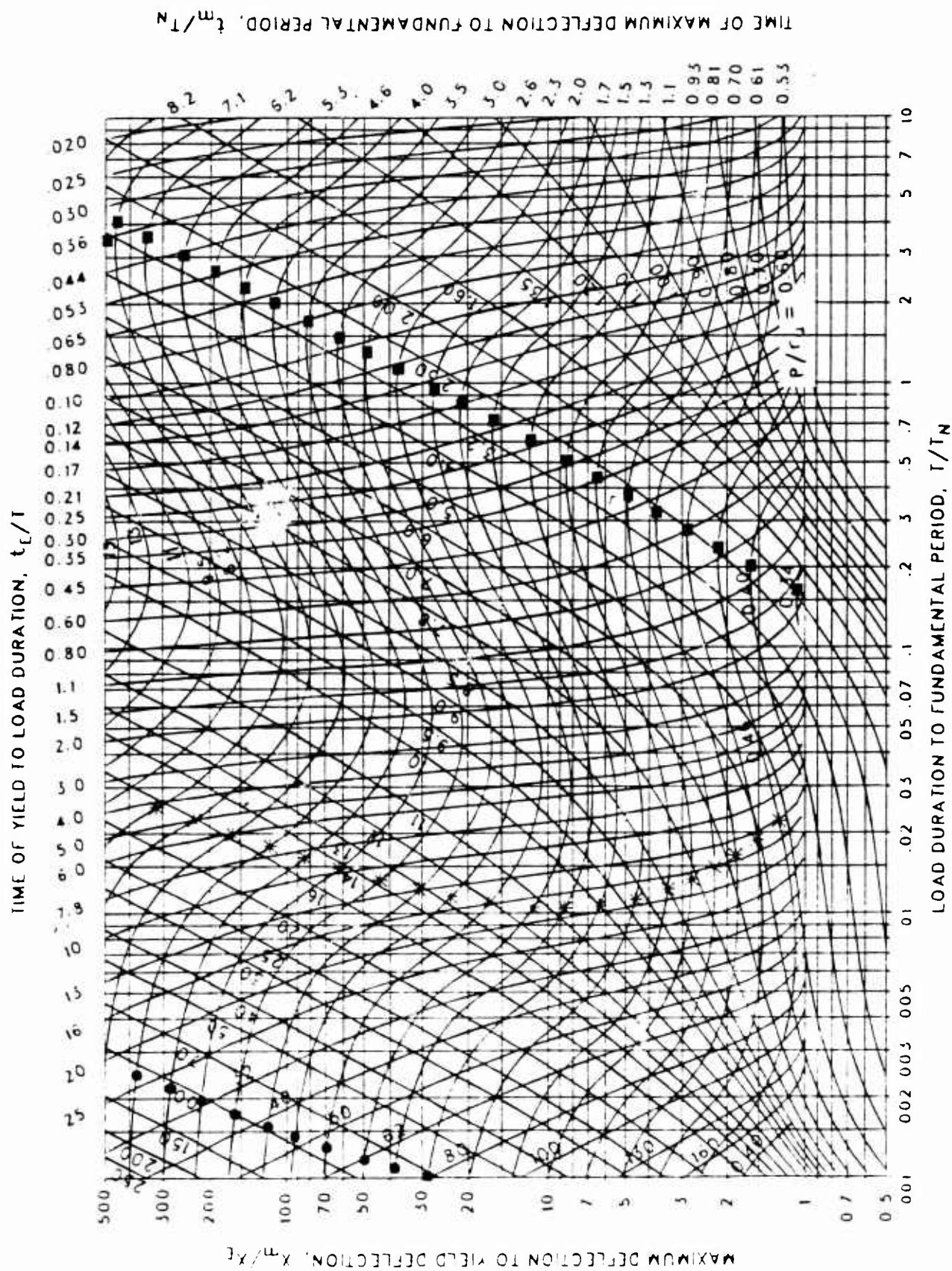
Figure 3-204 Maximum response of elasto-plastic, one-degree-of-freedom
system for bilinear-triangular pulse (C_1 = 0.110, C_2 = 300.)
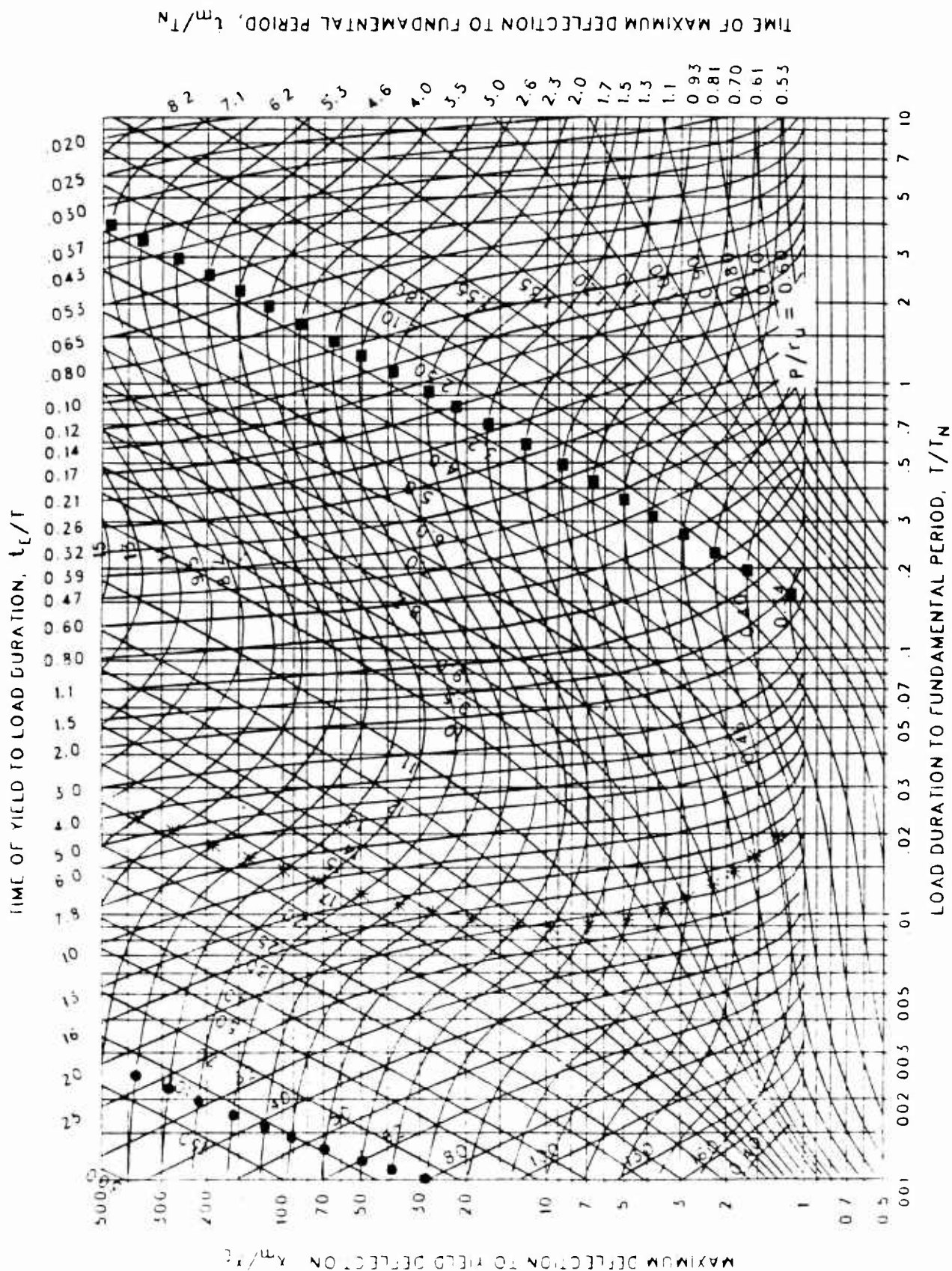
Figure 3-205   Maximum response of elasto-plastic, one-degree-of-freedom
system for bilinear-triangular pulse ($C_1 = 0.100$, $C_2 = 300.$)
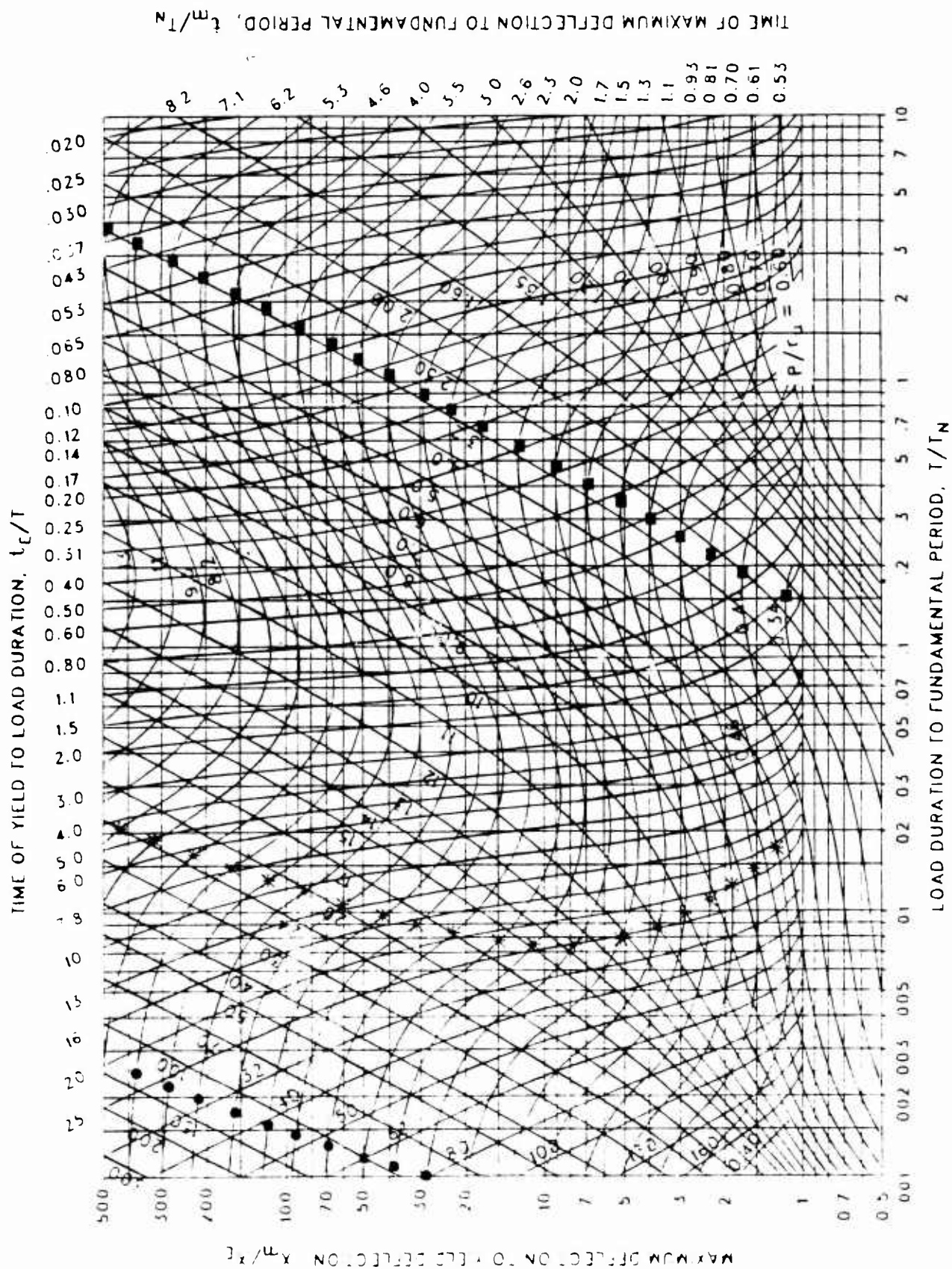
Figure 3-20b Maximum response of elasto-plastic, one-degree-of-freedom system for bilinear-triangular pulse ($C_1 = 0.091$, $C_2 = 300.$)
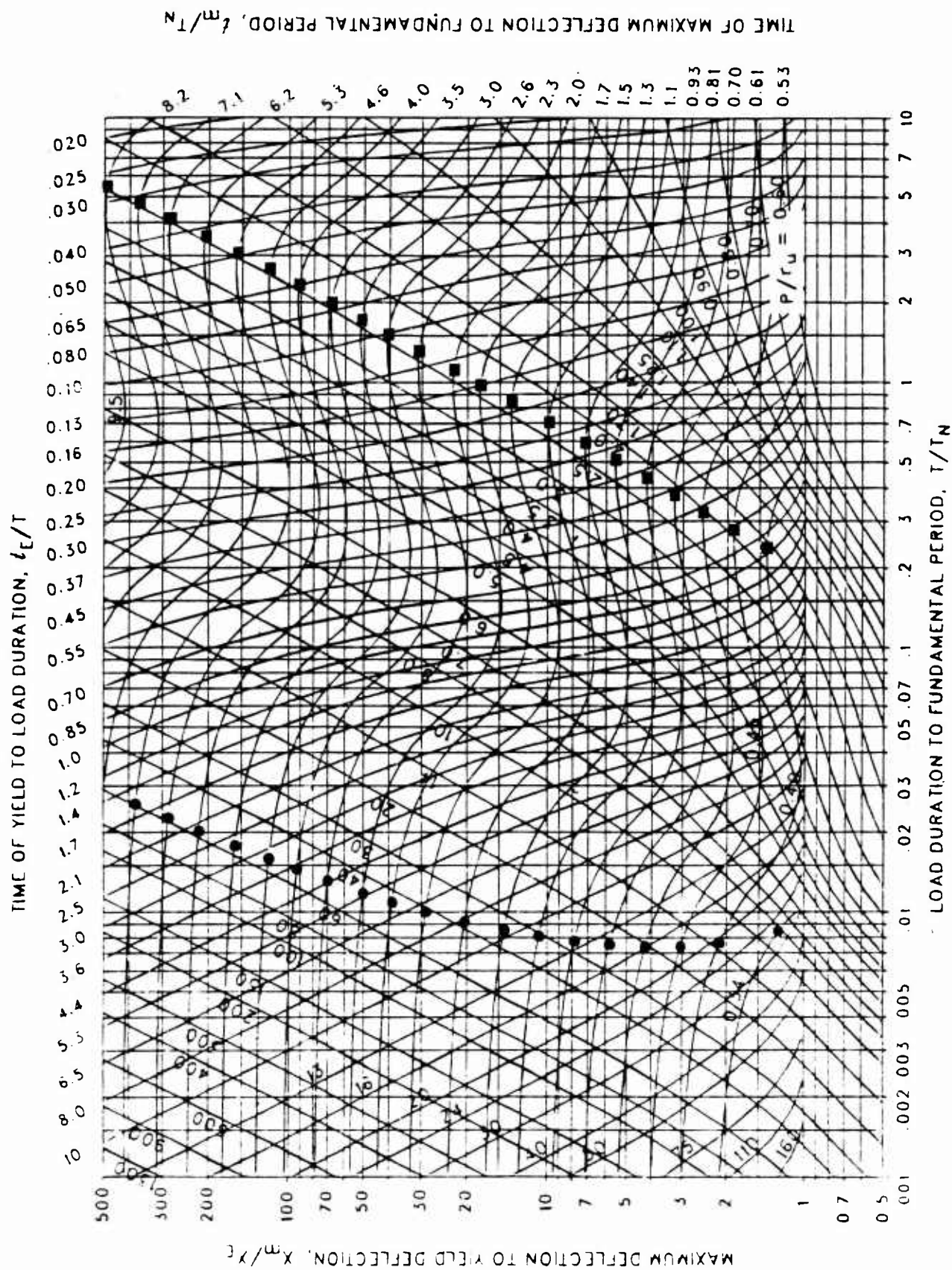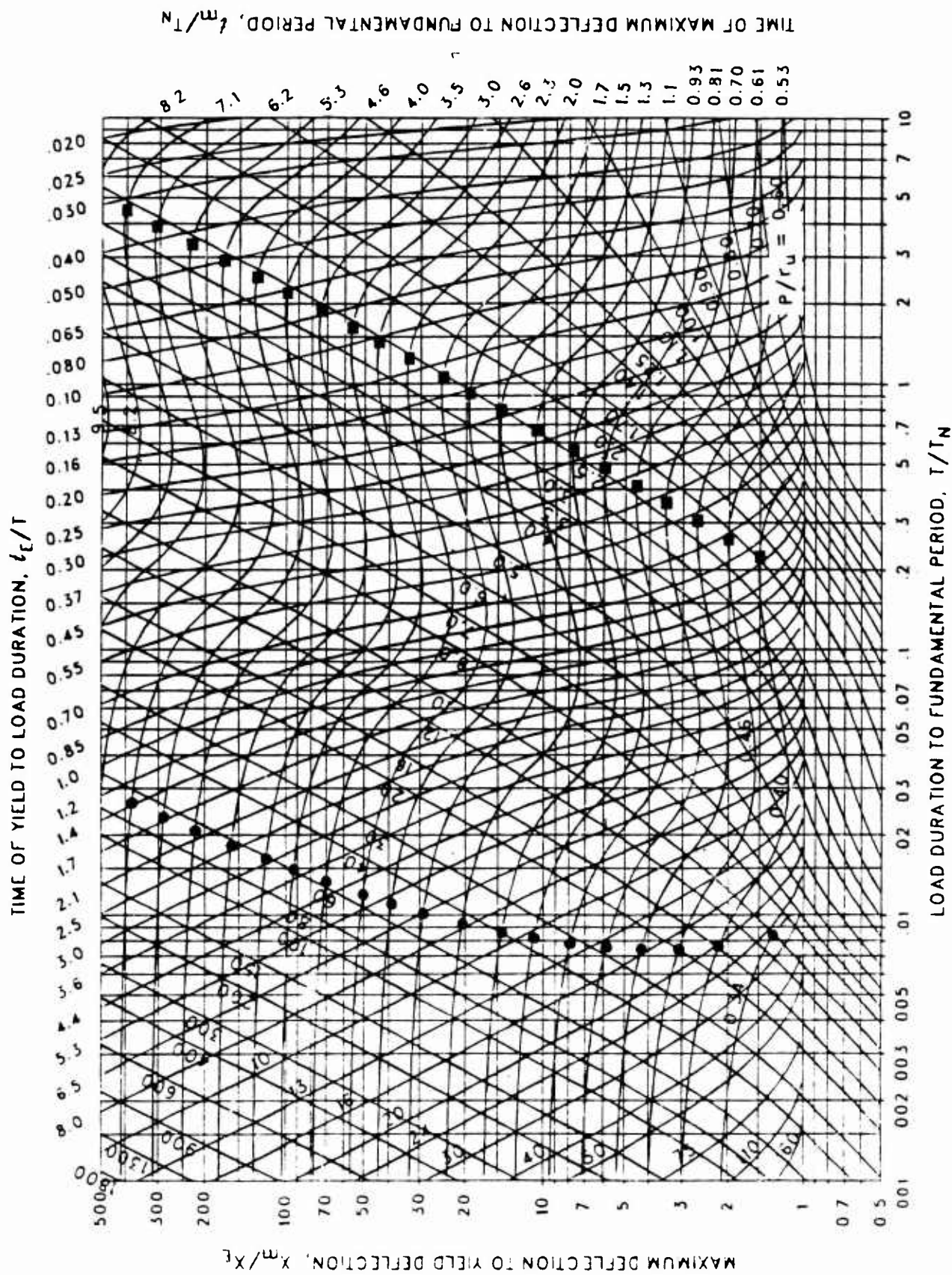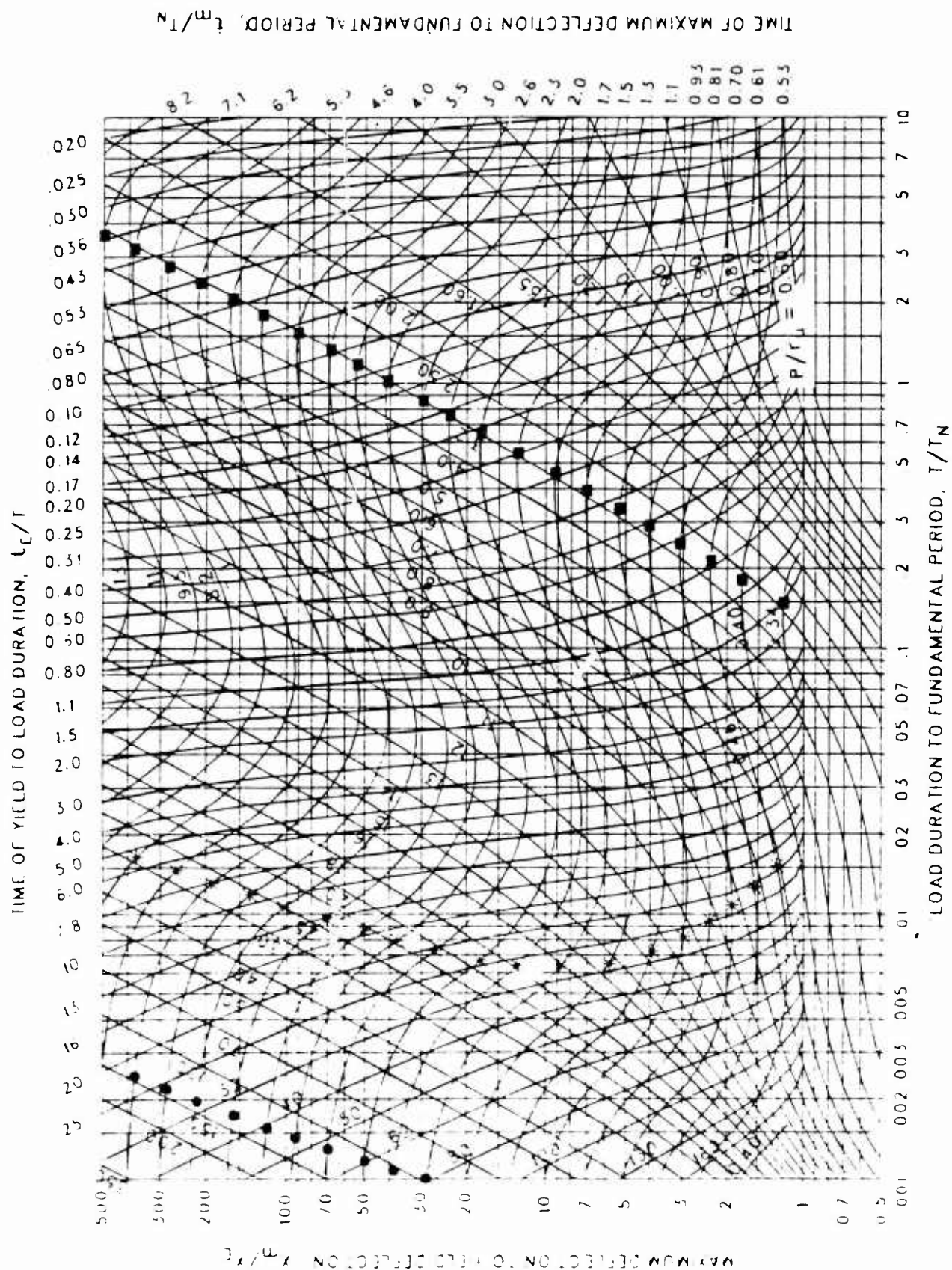
Figure 3-207   Maximum response of elasto-plastic, one-degree-of-freedom system for bilinear-triangular pulse ($C_1 = 0.083$, $C_2 = 300.$)
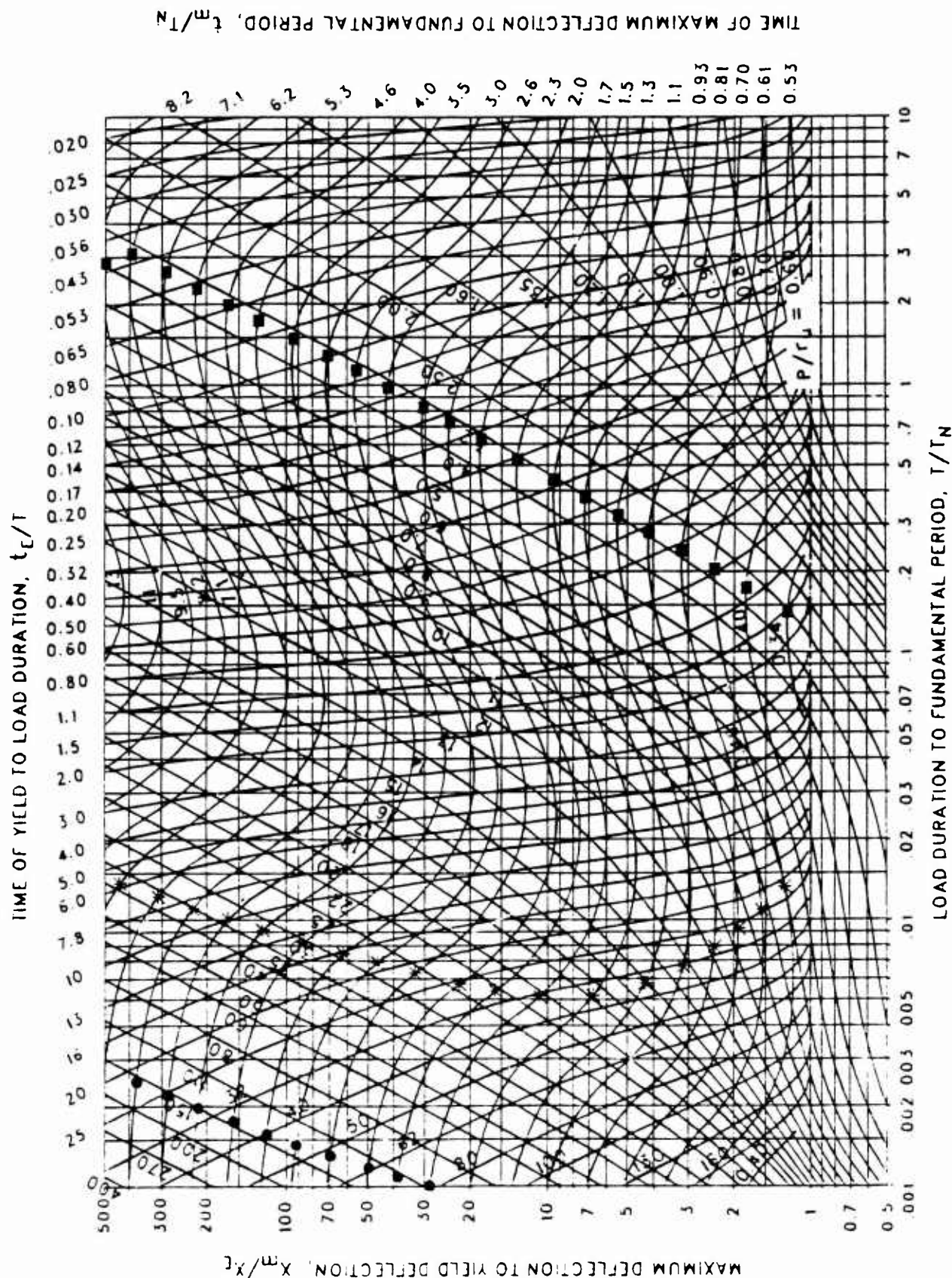
Figure 3-208   Maximum response of elasto-plastic, one-degree-of-freedom system for bilinear-triangular pulse ($C_1 = 0.075$, $C_2 = 300.$)
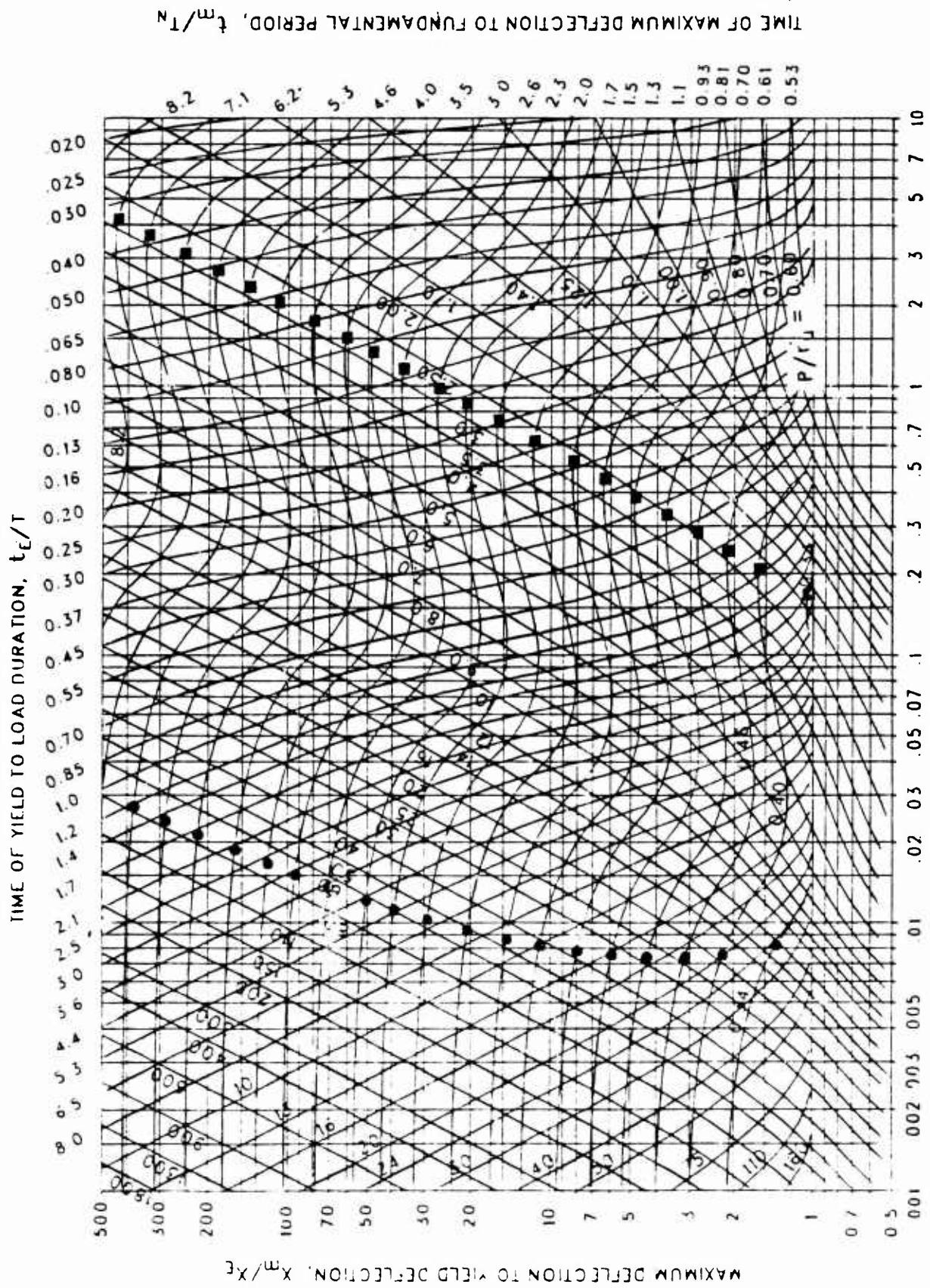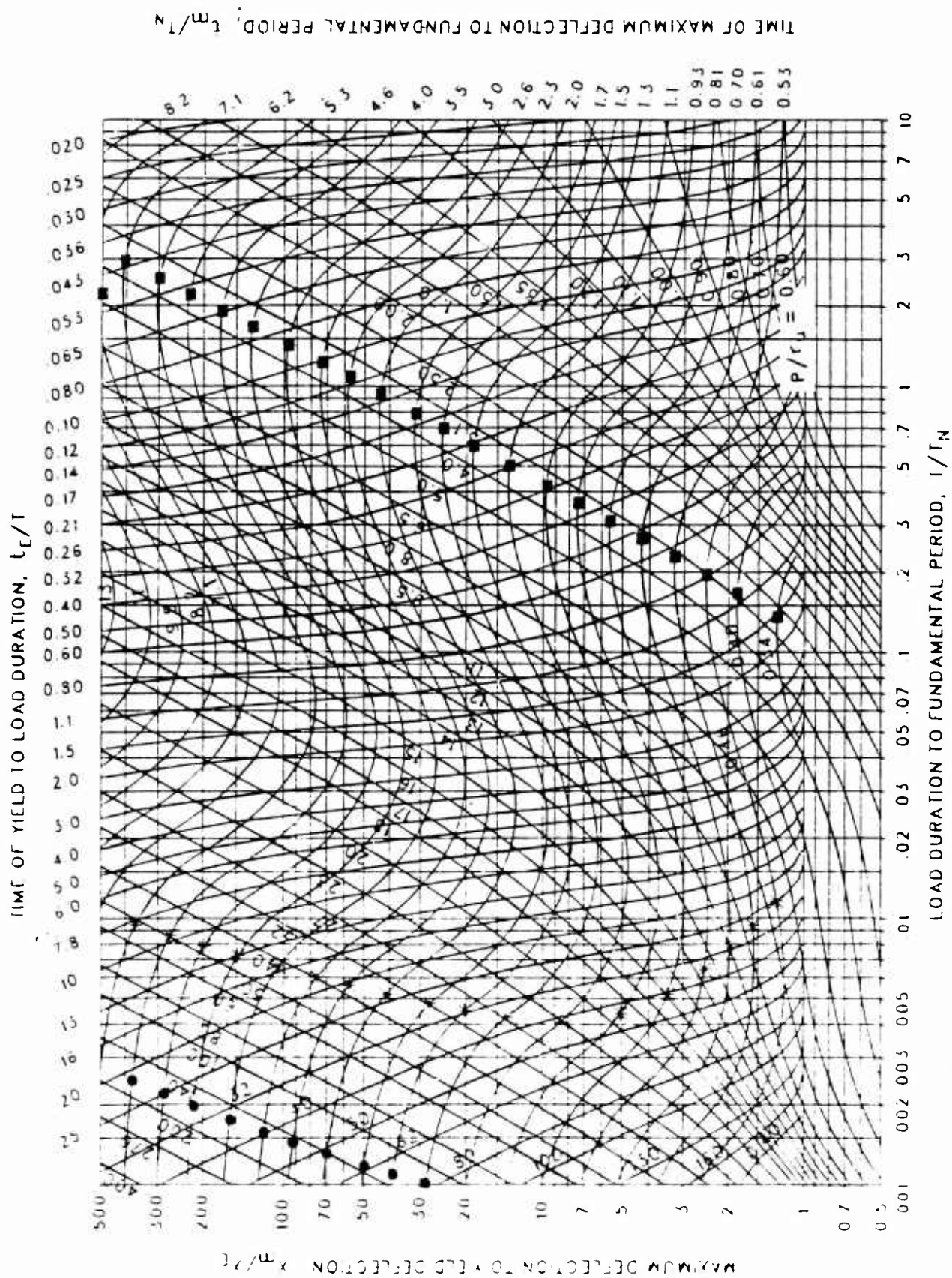
Figure 3-209 Maximum response of elasto-plastic, one-degree-of-freedom system for bilinear-triangular pulse ($C_1 = 0.068$, $C_2 = 300.$)

TIME OF MAXIMUM DEFLECTION TO FUNDAMENTAL PERIOD, t_m/T_N

TIME OF YIELD TO LOAD DURATION, t_E/T

LOAD DURATION TO FUNDAMENTAL PERIOD, $1/T_N$

MAXIMUM DEFLECTION TO YIELD DEFLECTION, x_m/x_E
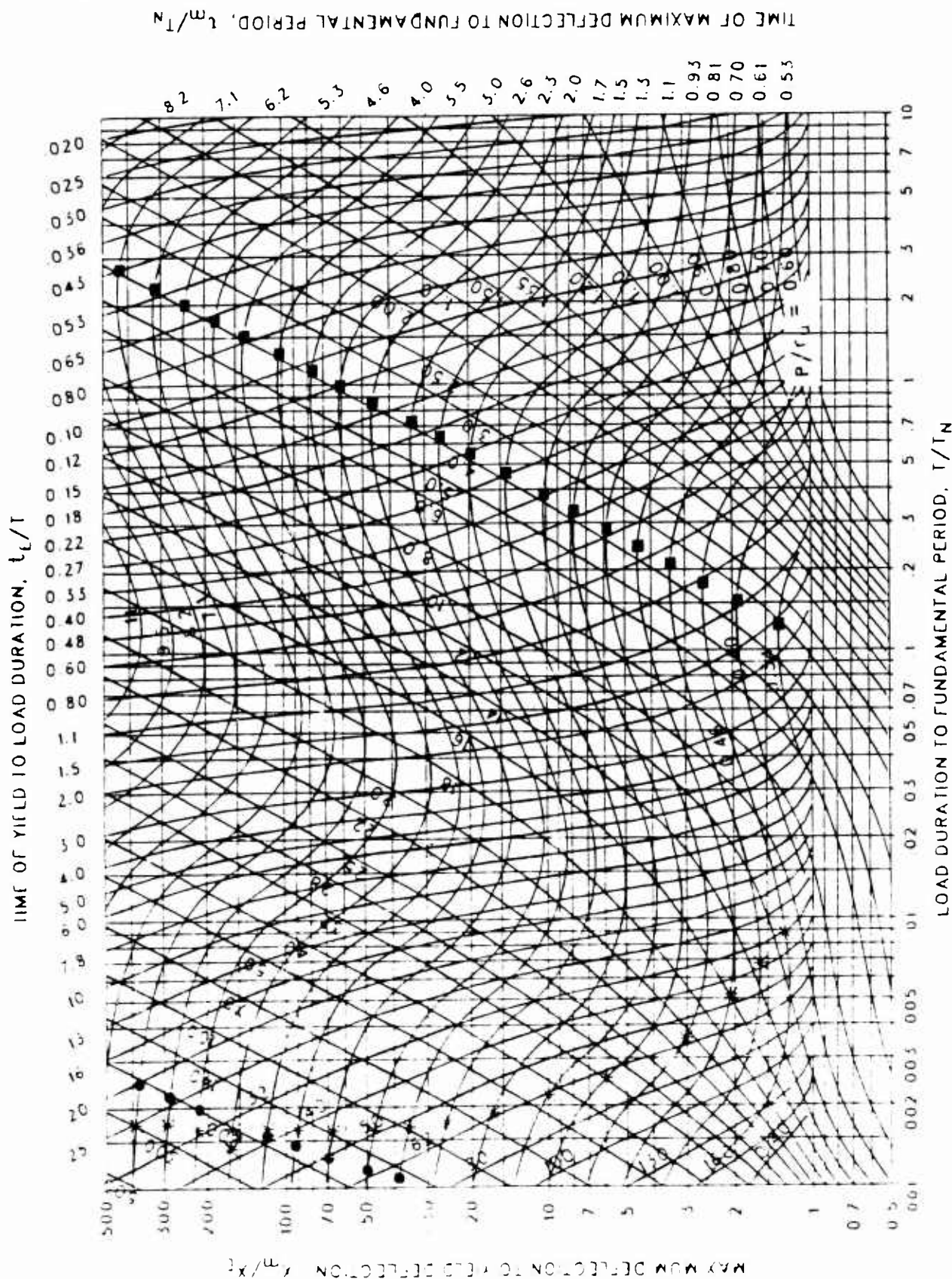
Figure 3-210 Maximum response of elasto-plastic, one-degree-of-freedom system for bilinear-triangular pulse ($C_1 = 0.056$, $C_2 = 30u$.)
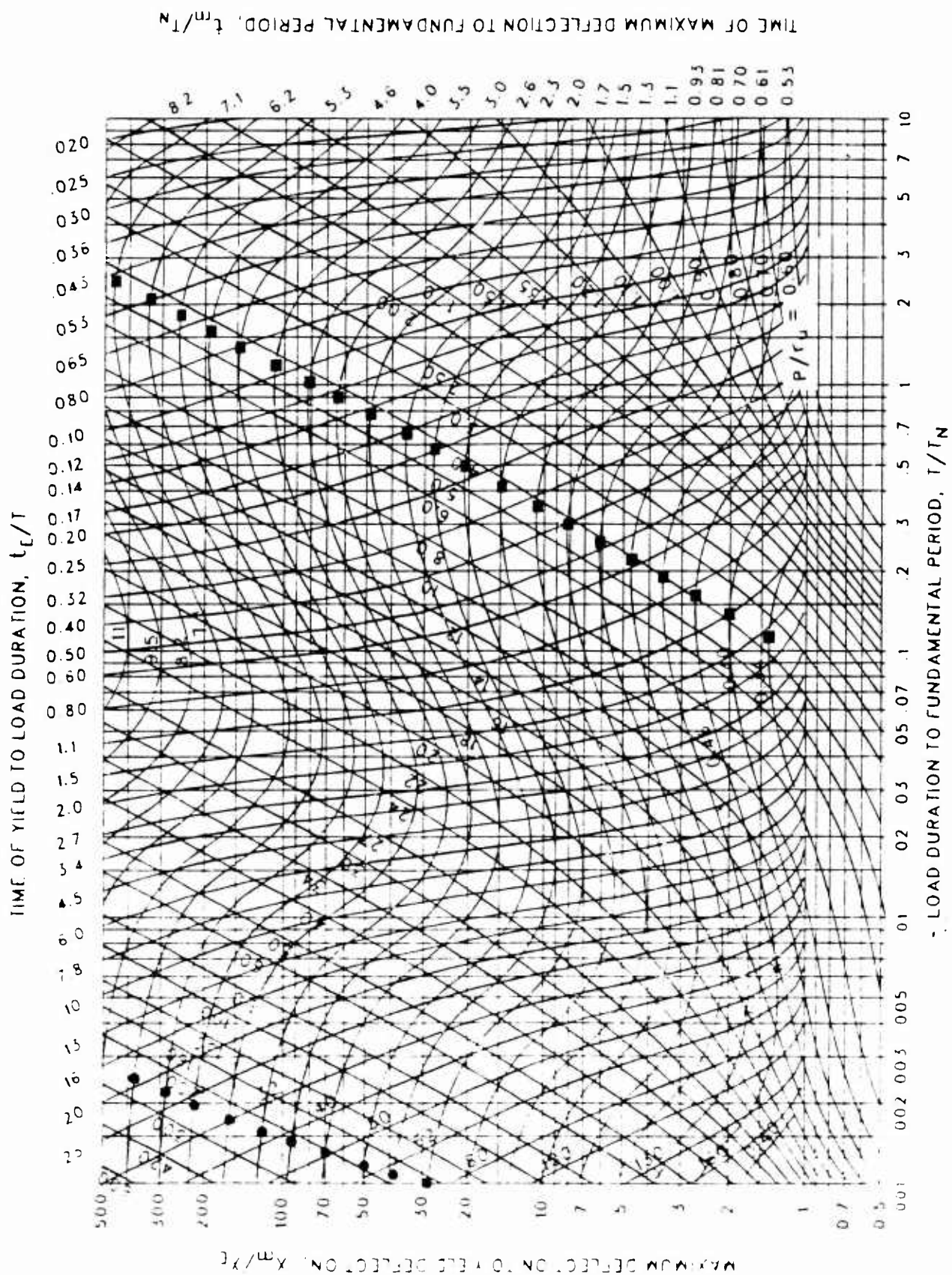
Figure 3-211 Maximum response of elasto-plastic, one-degree-of-freedom system for bilinear-triangular pulse ($C_1 = 0.046$, $C_2 = 300$.)
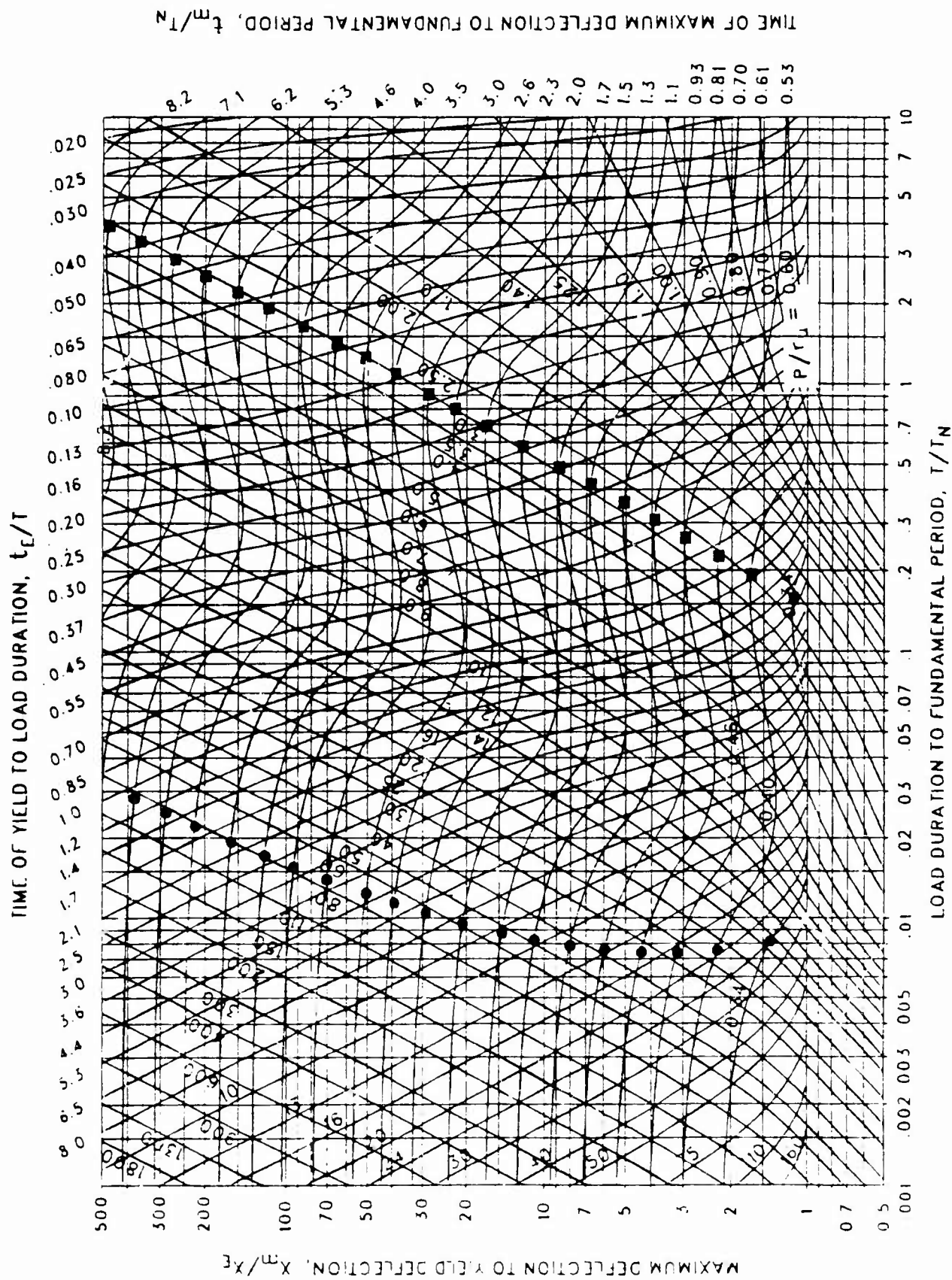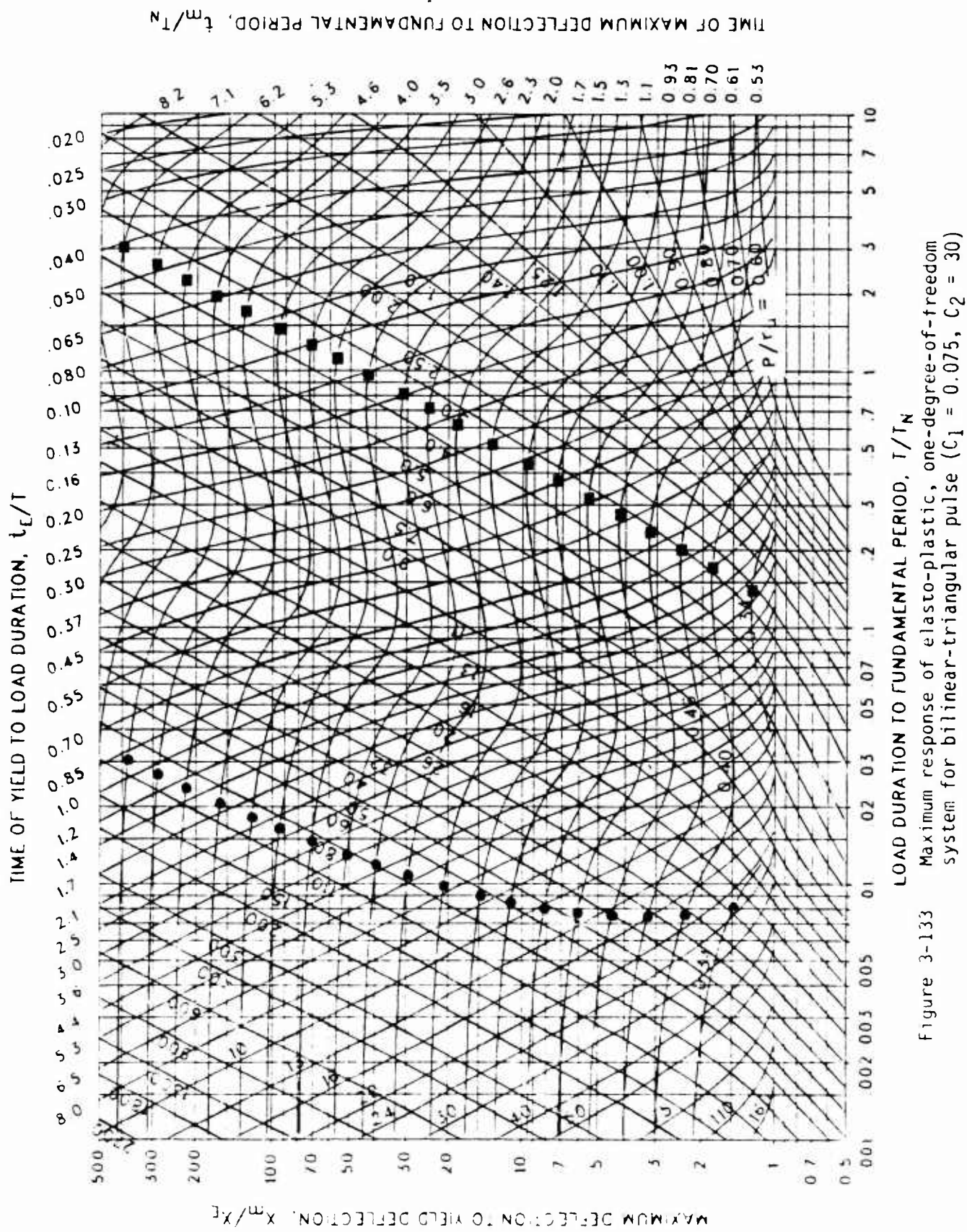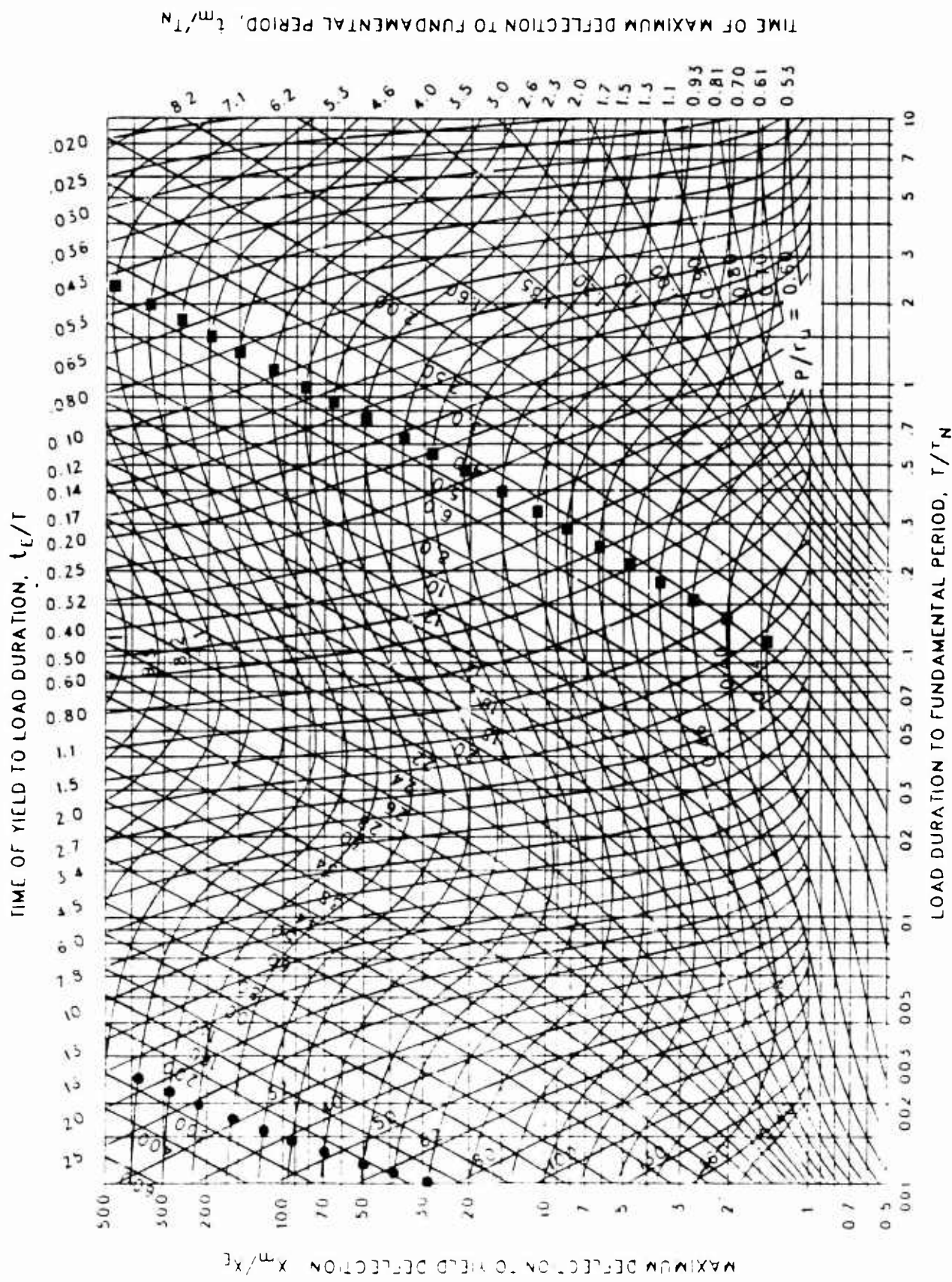
Figure 3-212   Maximum response of elasto-plastic, one-degree-of-freedom system for bilinear-triangular pulse ($C_1 = 0.042$, $C_2 = 300.$)
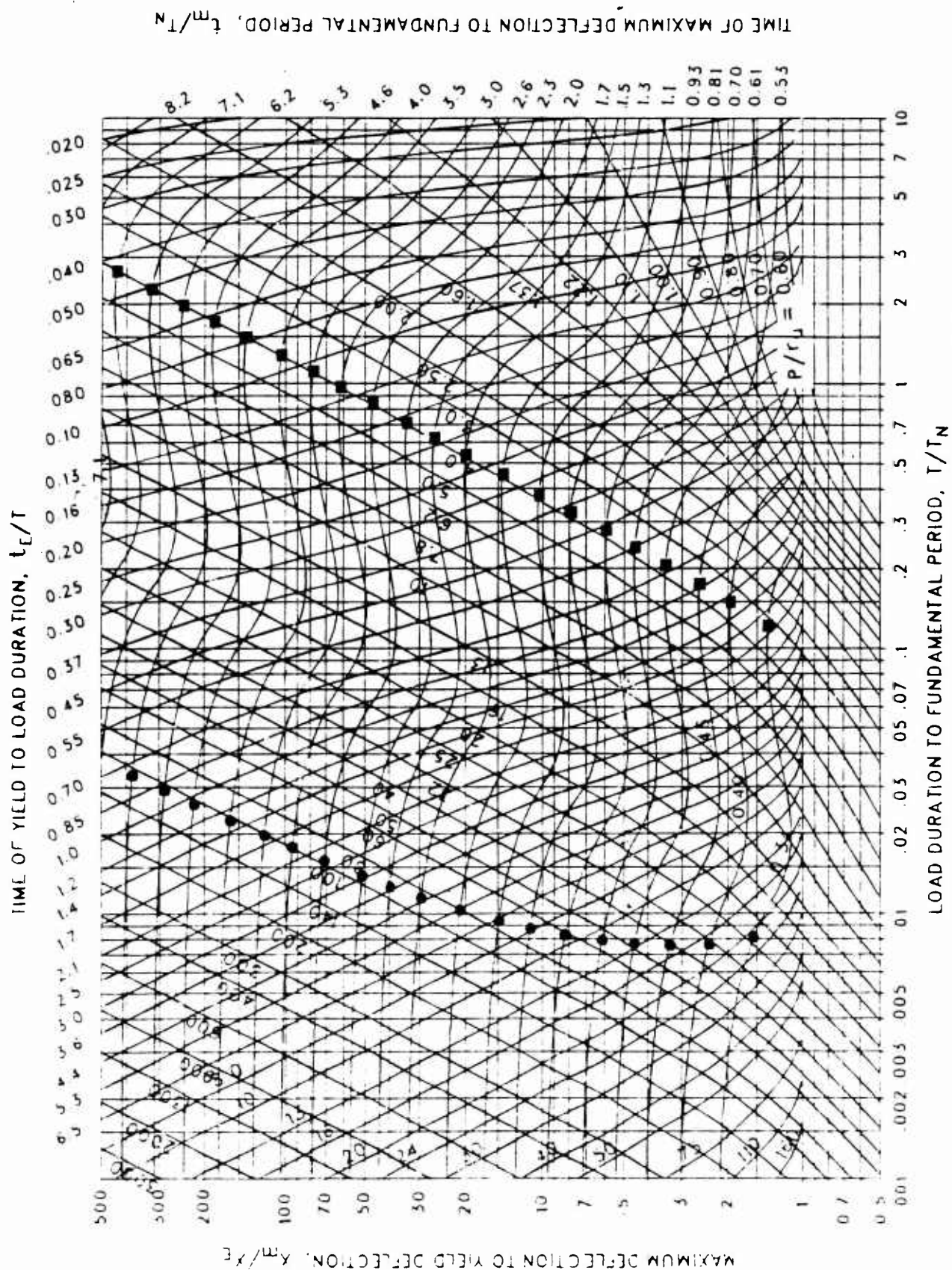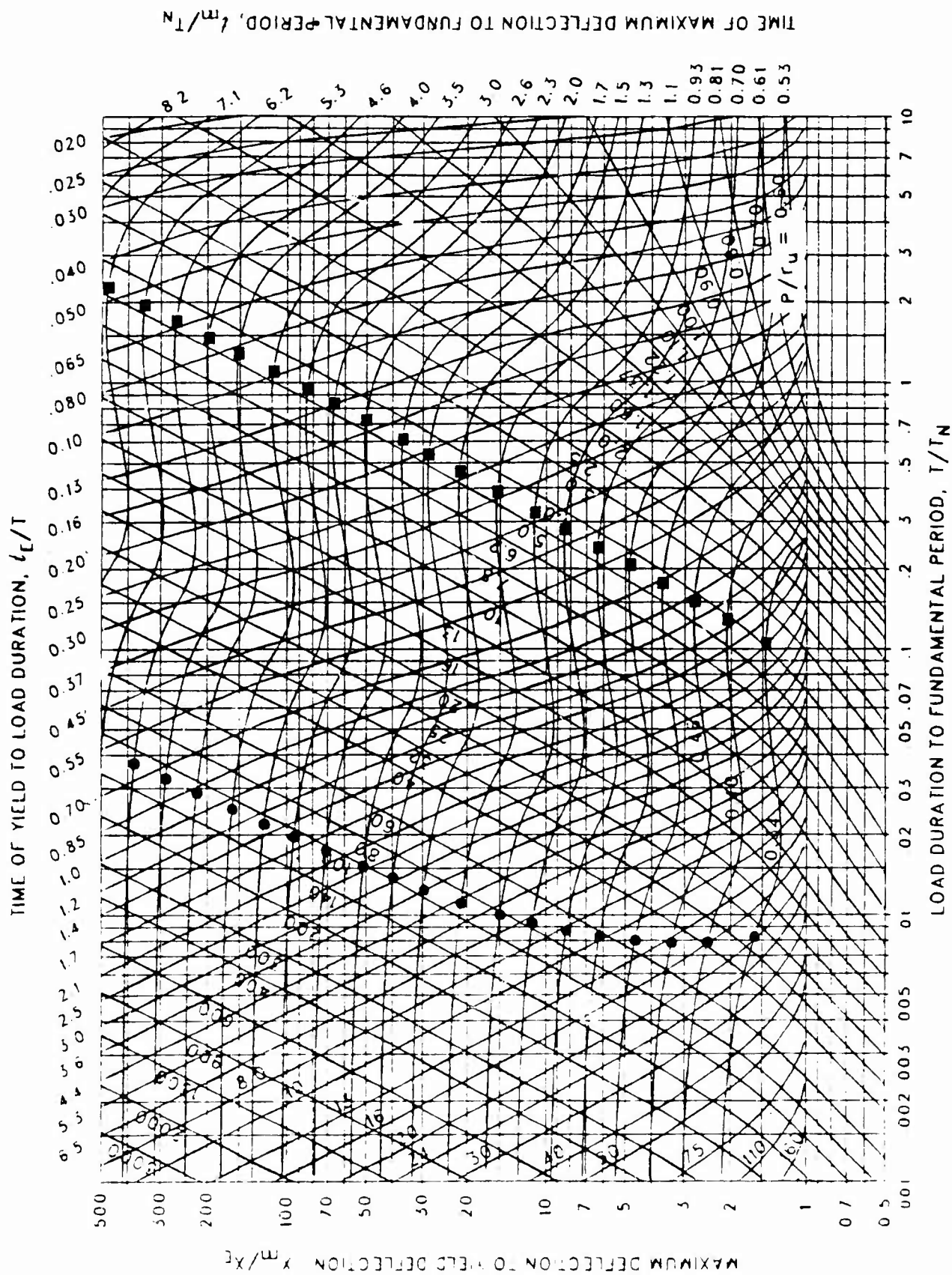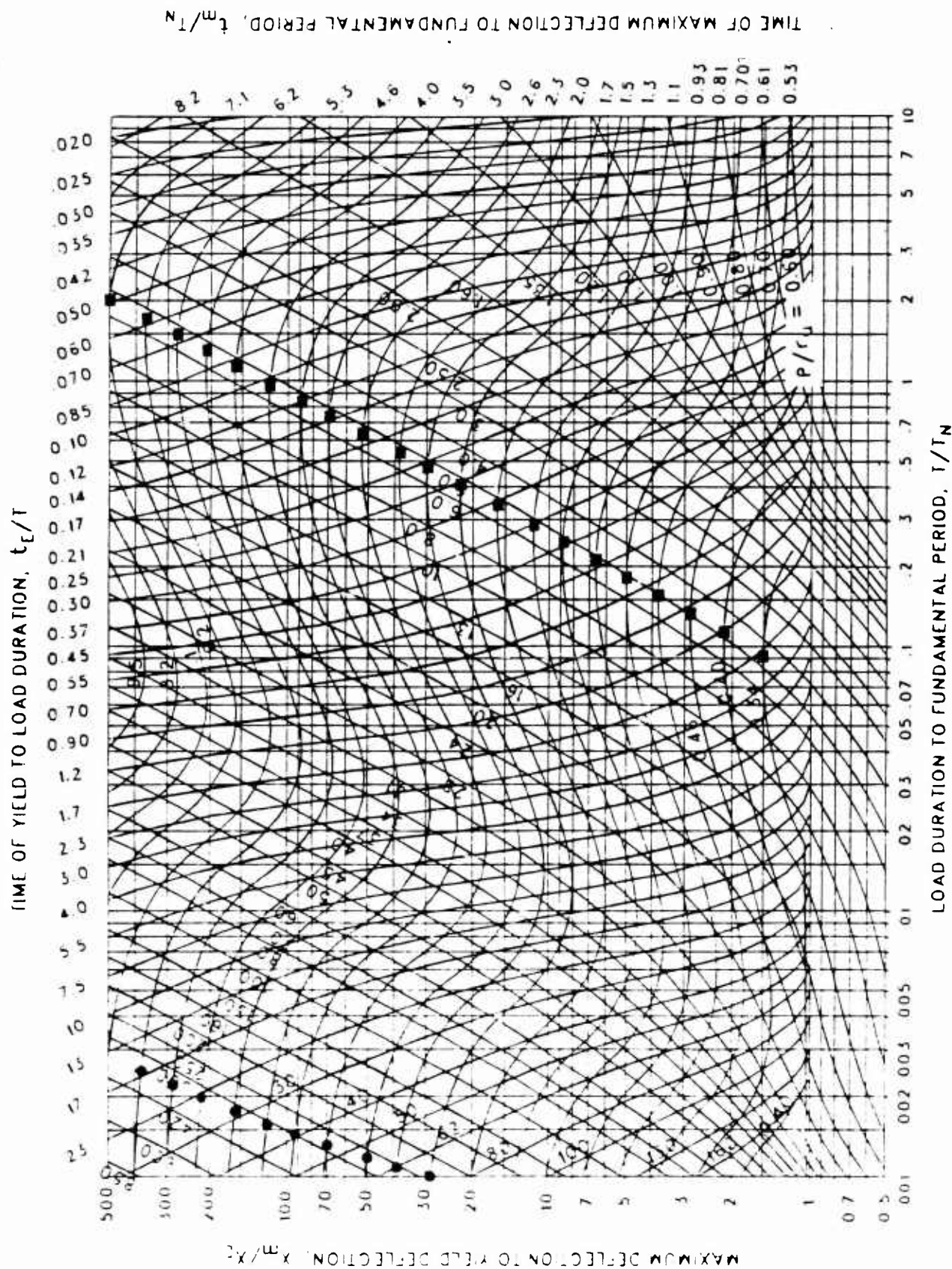
Figure 3-213   Maximum response of elasto-plastic, one-degree-of-freedom system for bilinear-triangular pulse (C_1 = 0.032, C_2 = 300.)
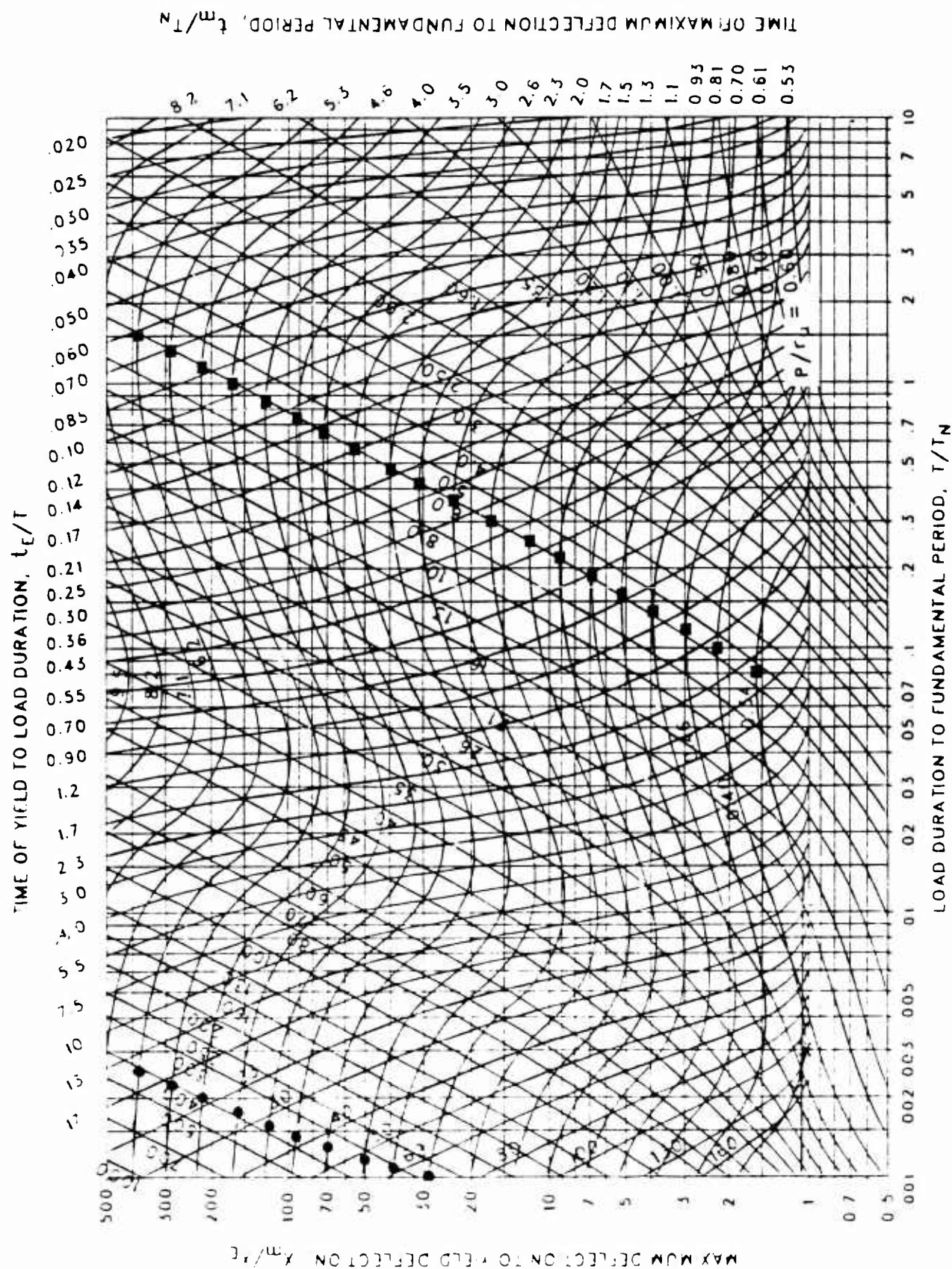
Figure 3-214   Maximum response of elasto-plastic, one-degree-of-freedom system for bilinear-triangular pulse ($C_1 = 0.026$, $C_2 = 300.$)
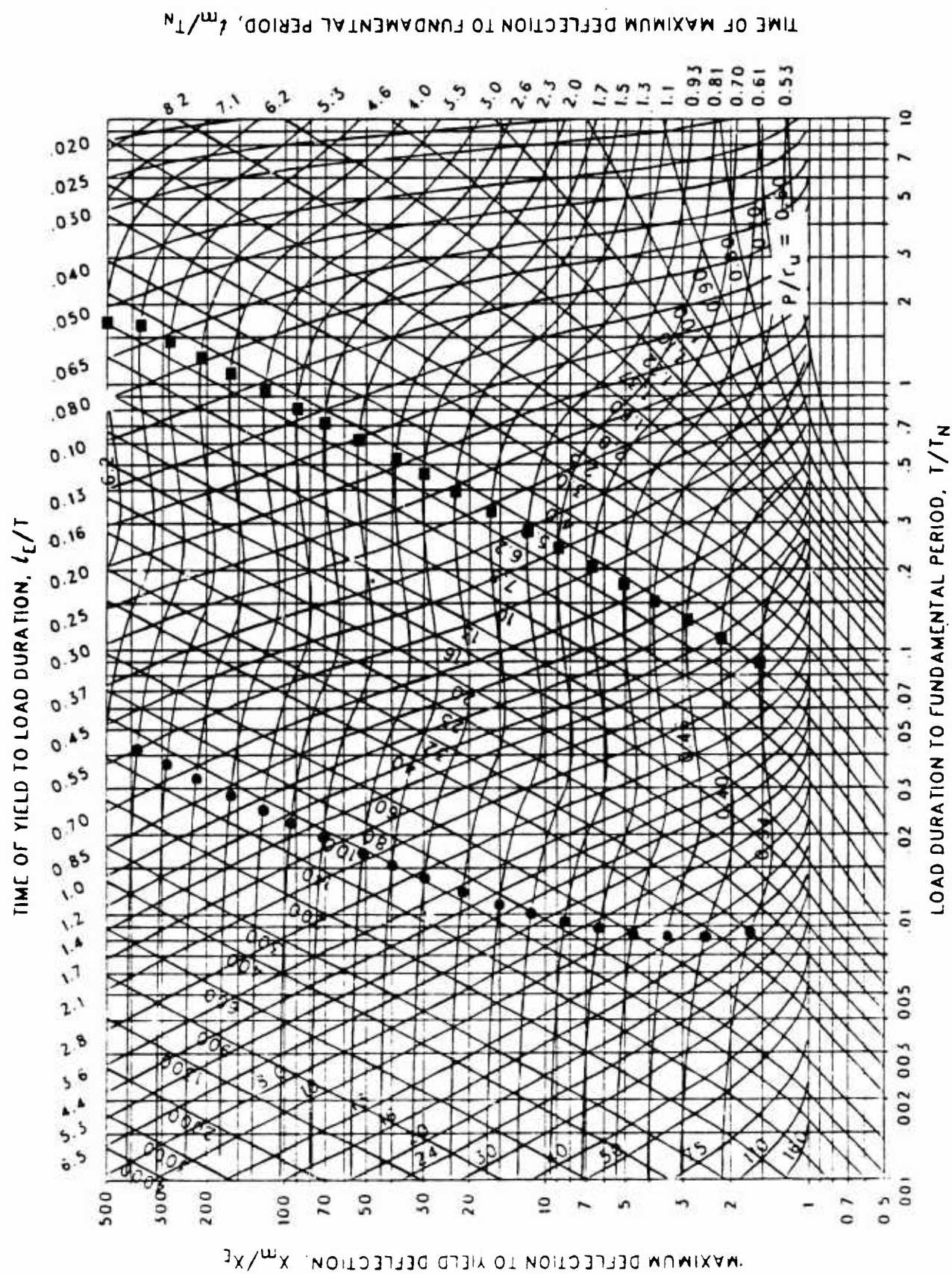
-269-
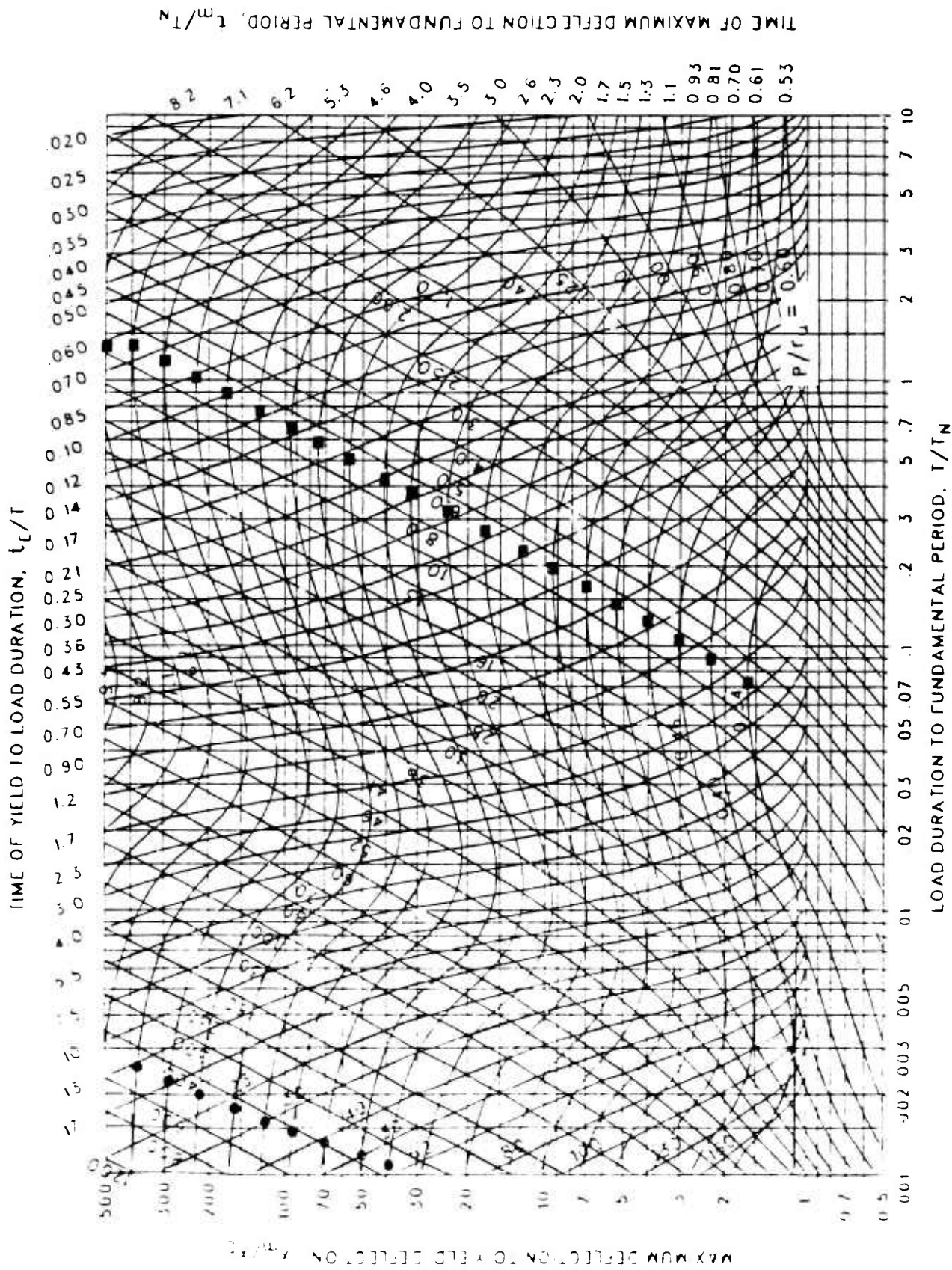
Figure 3-215   Maximum response of elasto-plastic, one-degree-of-freedom system for bilinear-triangular pulse ($C_1 = 0.022$, $C_2 = 300.$)

-270-
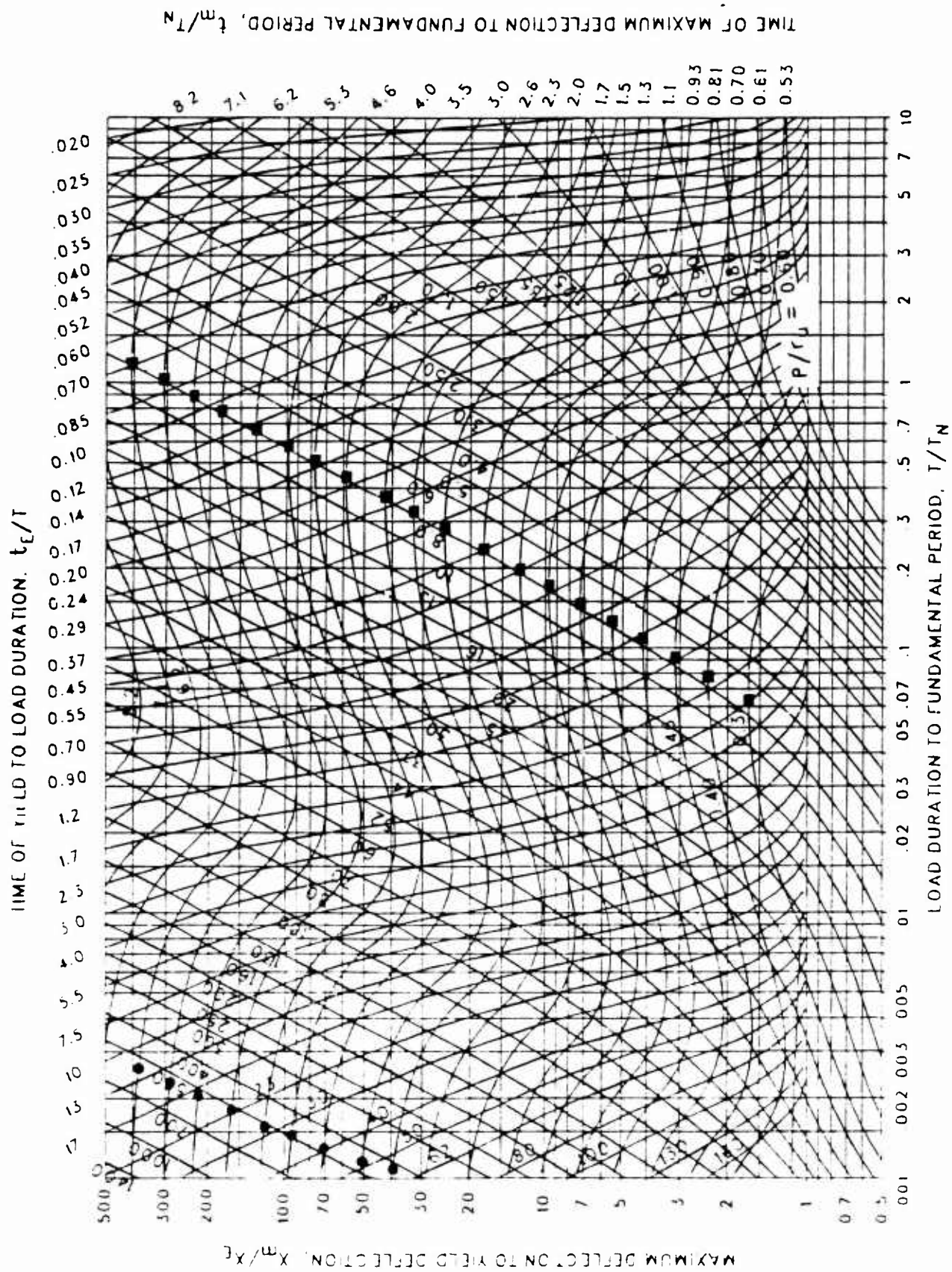
Figure 3-21b   Maximum response of elasto-plastic, one-degree-of-freedom
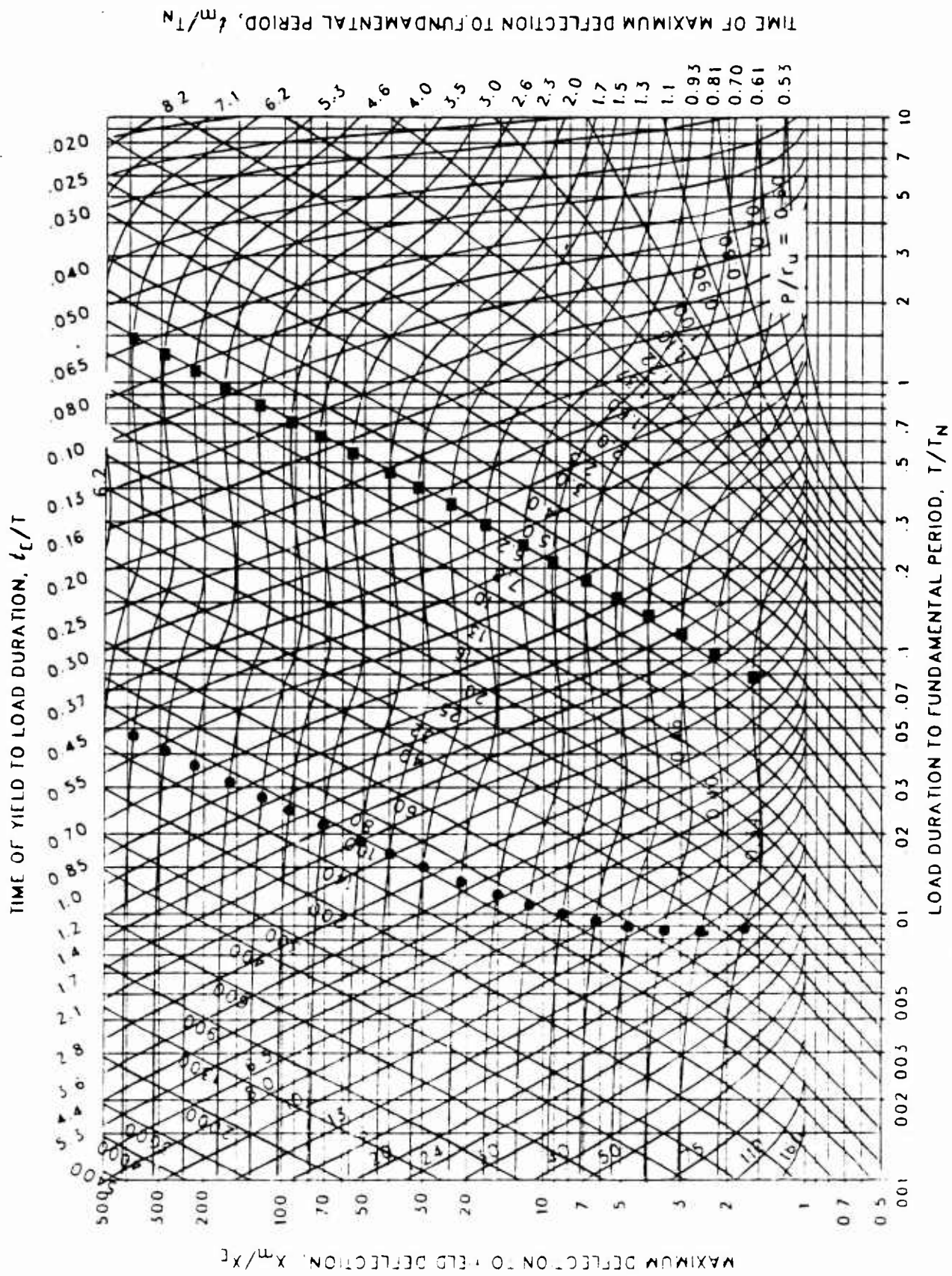system for bilinear-triangular pulse ($C_1 = 0.018$, $C_2 = 300.$)
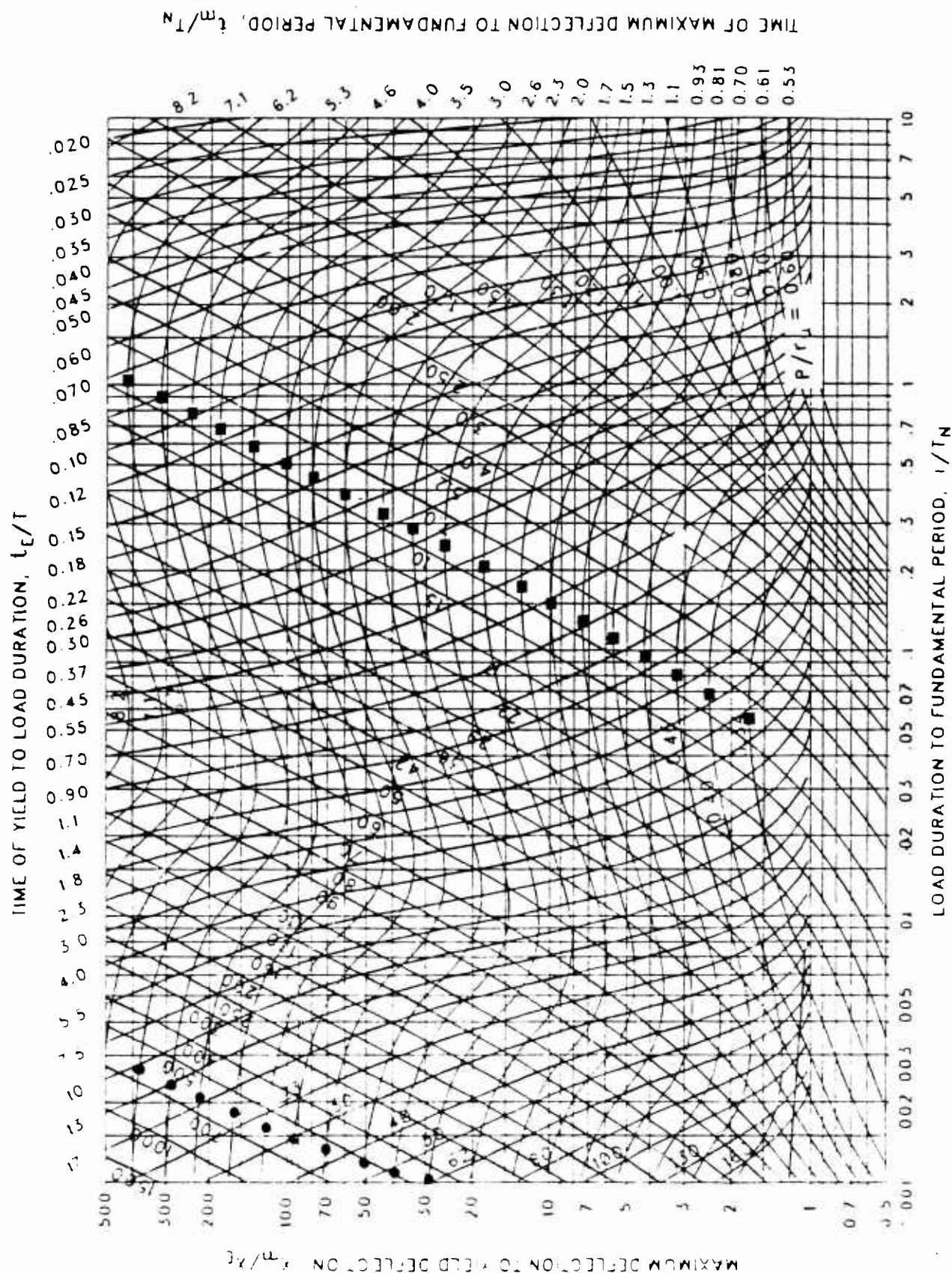
Figure 3-217. Maximum response of elasto-plastic, one-degree-of-freedom system for bilinear-triangular pulse ($C_1 = 0.015$, $C_2 = 300.$)
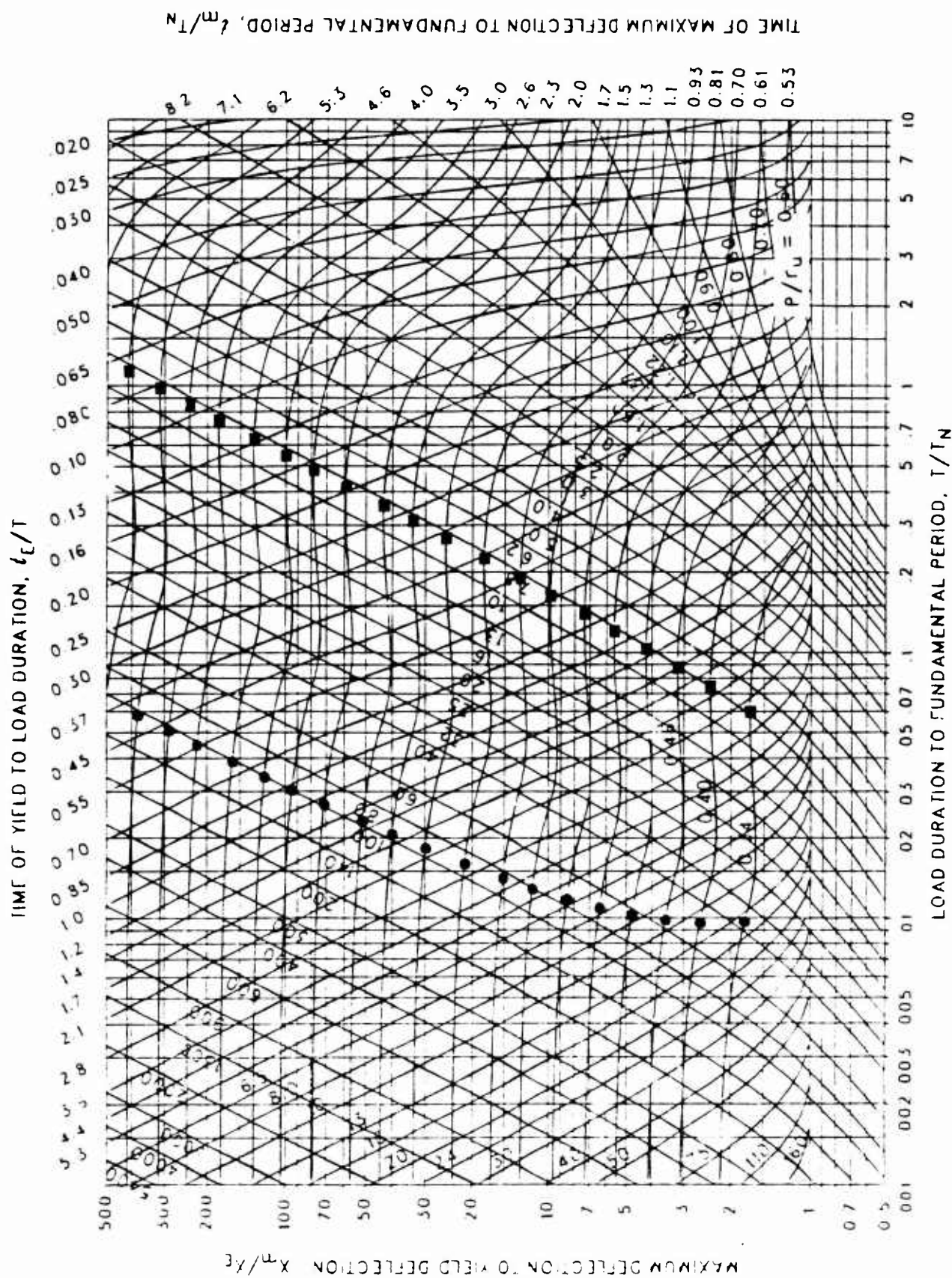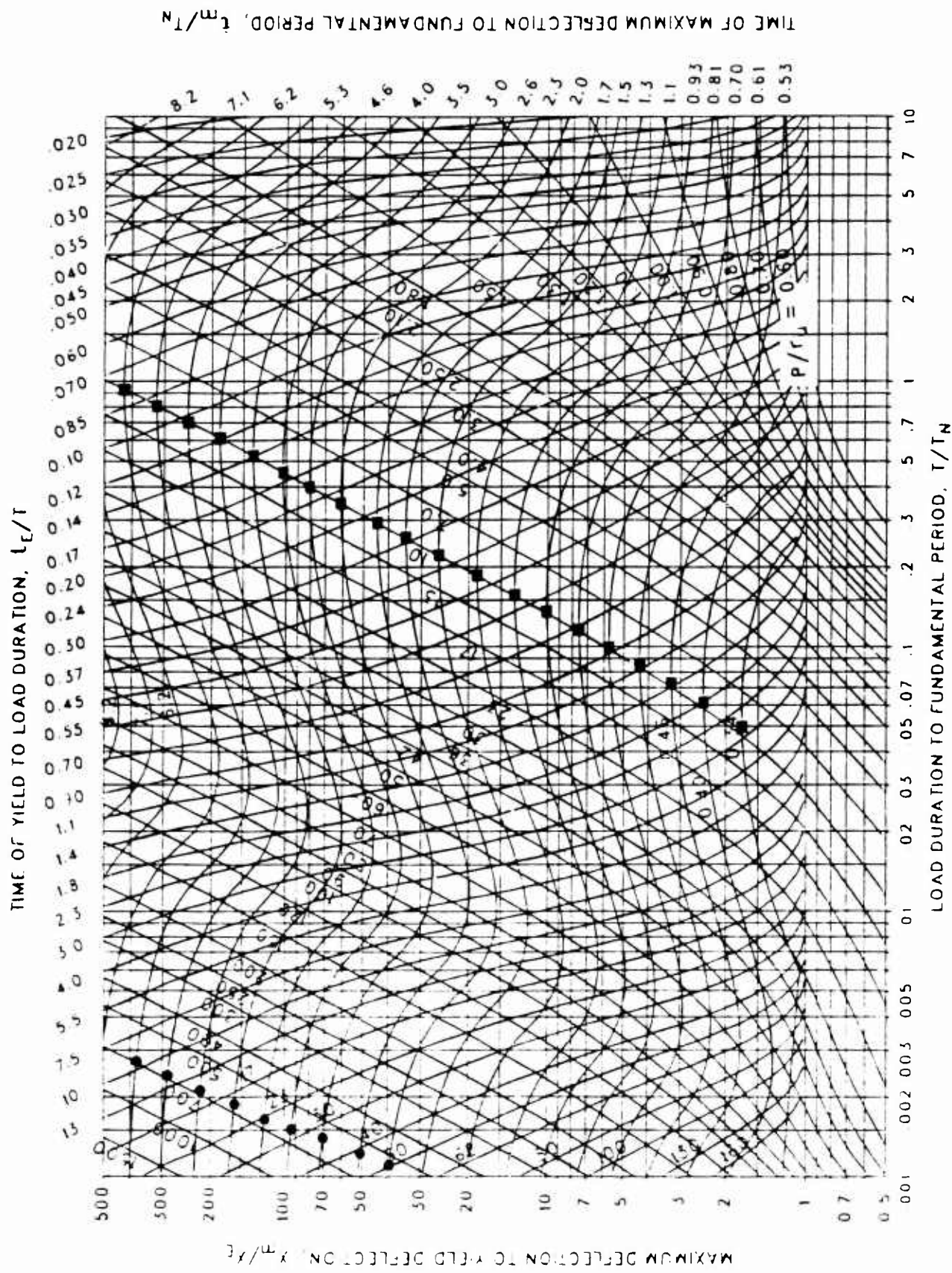
Figure 3-218   Maximum response of elasto-plastic, one-degree-of-freedom
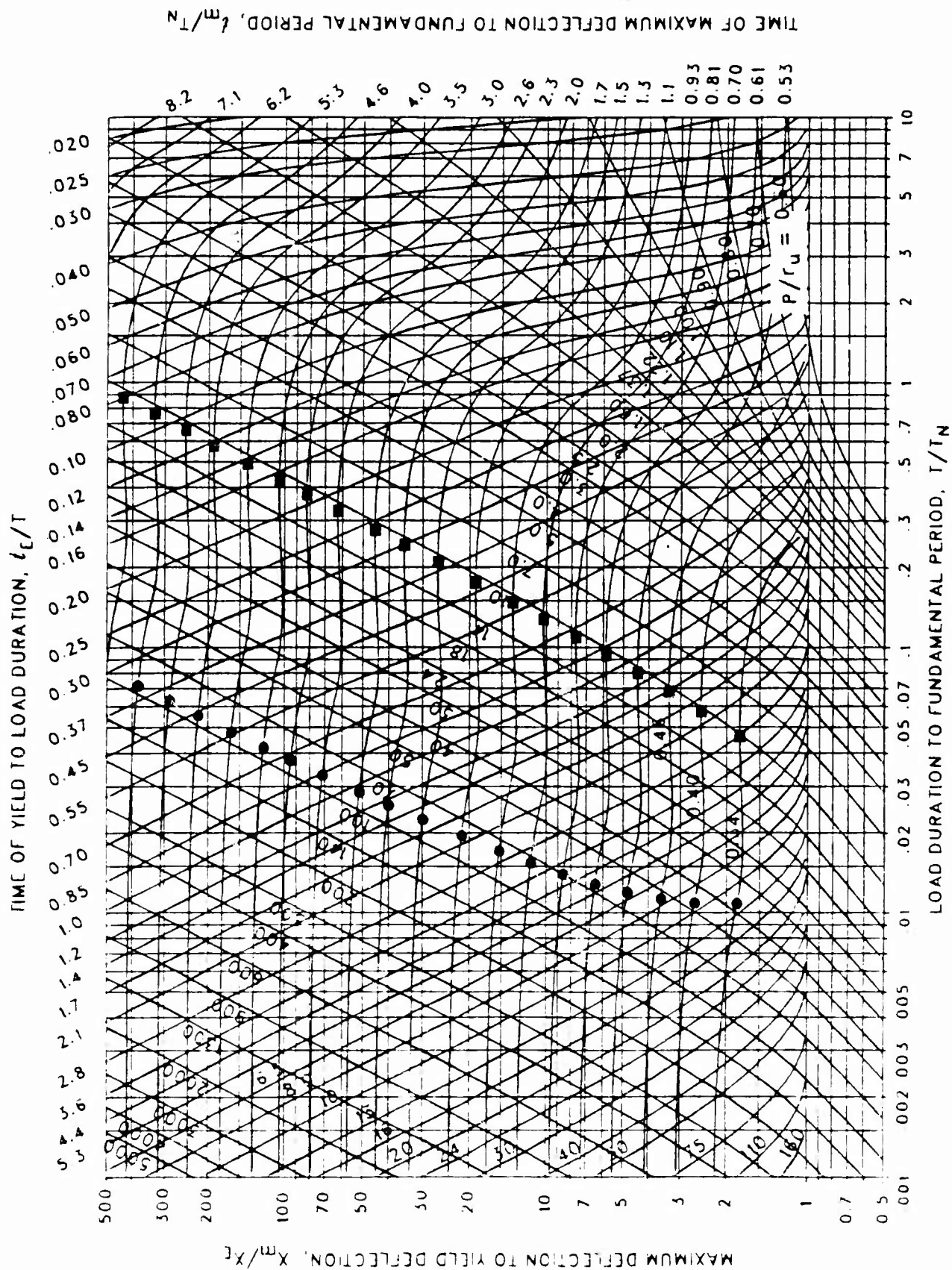system for bilinear-triangular pulse (C_1 = 0.013, C_2 = 300.)

-273-
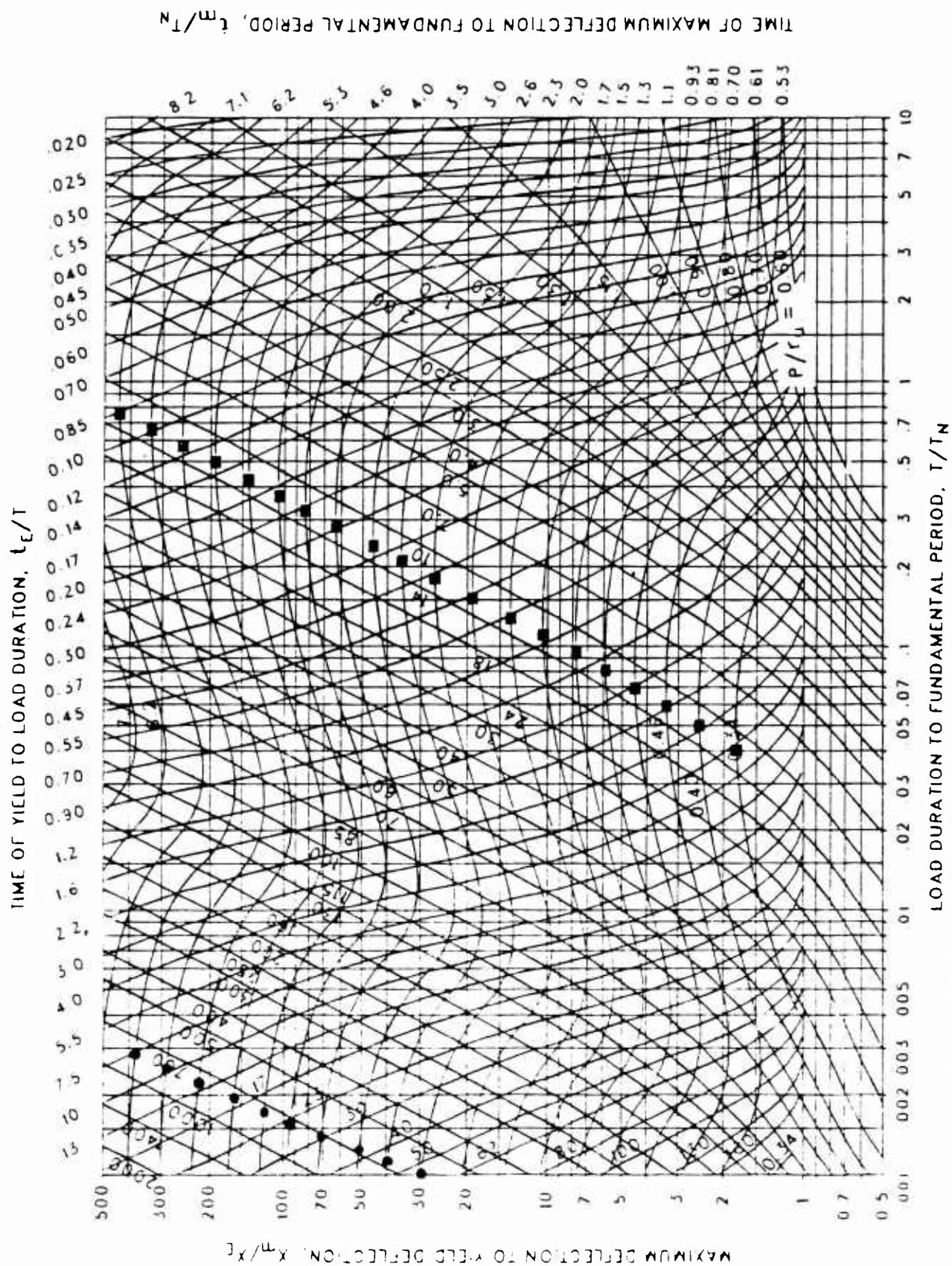
Figure 3-219   Maximum response of elasto-plastic, one-degree-of-freedom system for bilinear-triangular pulse ($C_1 = 0.010$, $C_2 = 300$.)

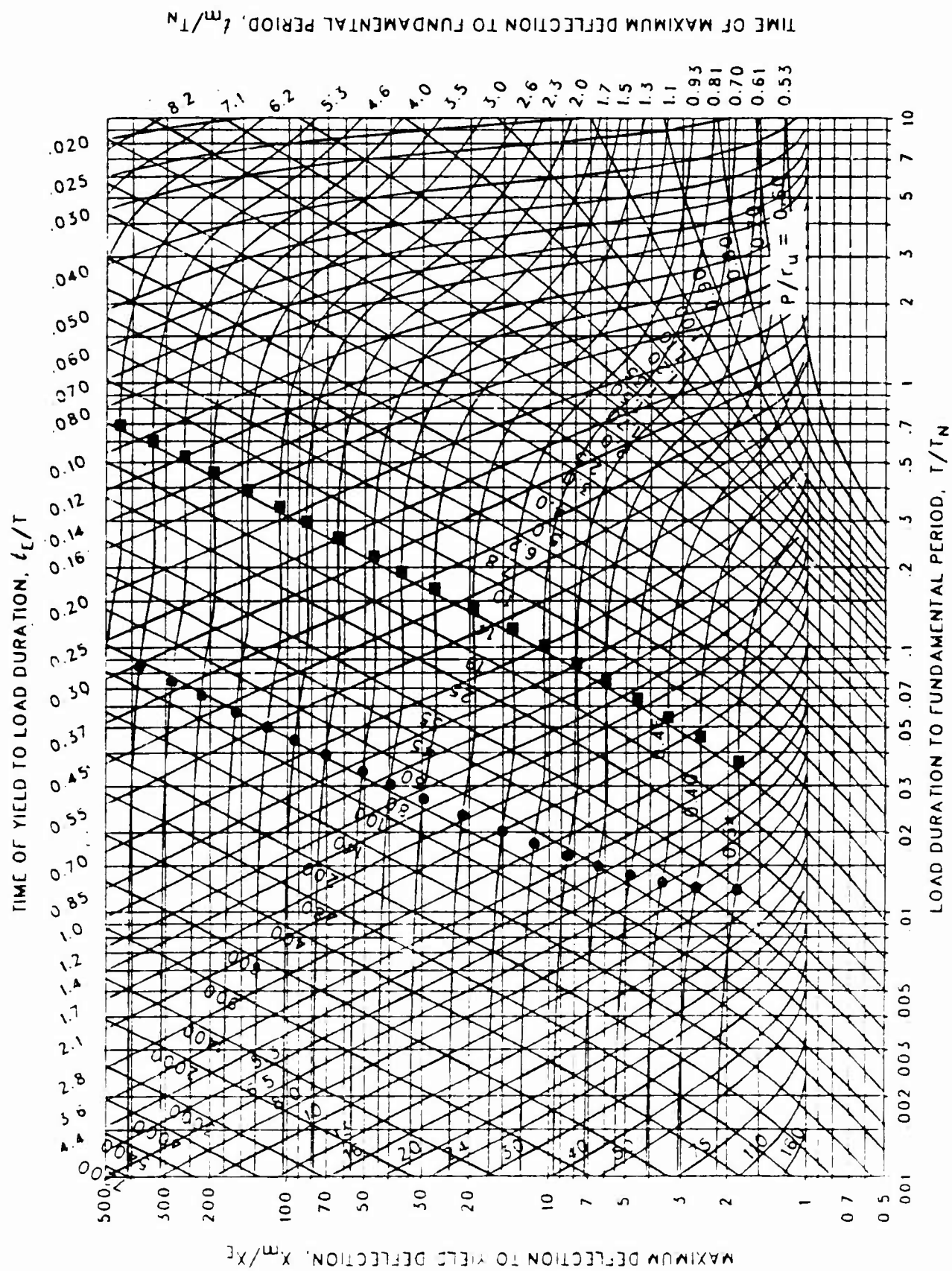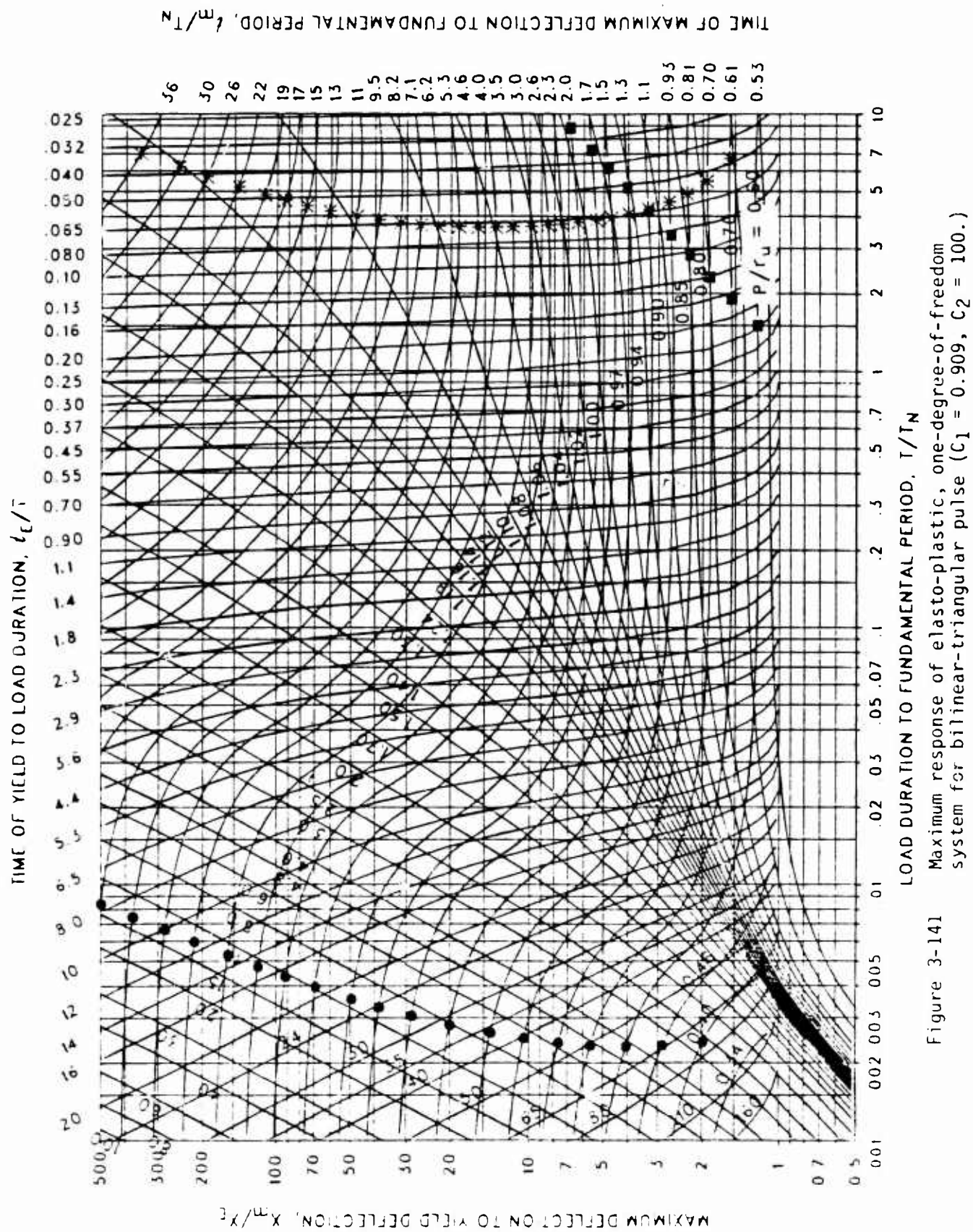TIME OF MAXIMUM DEFLECTION TO FUNDAMENTAL PERIOD, t_m/T_N
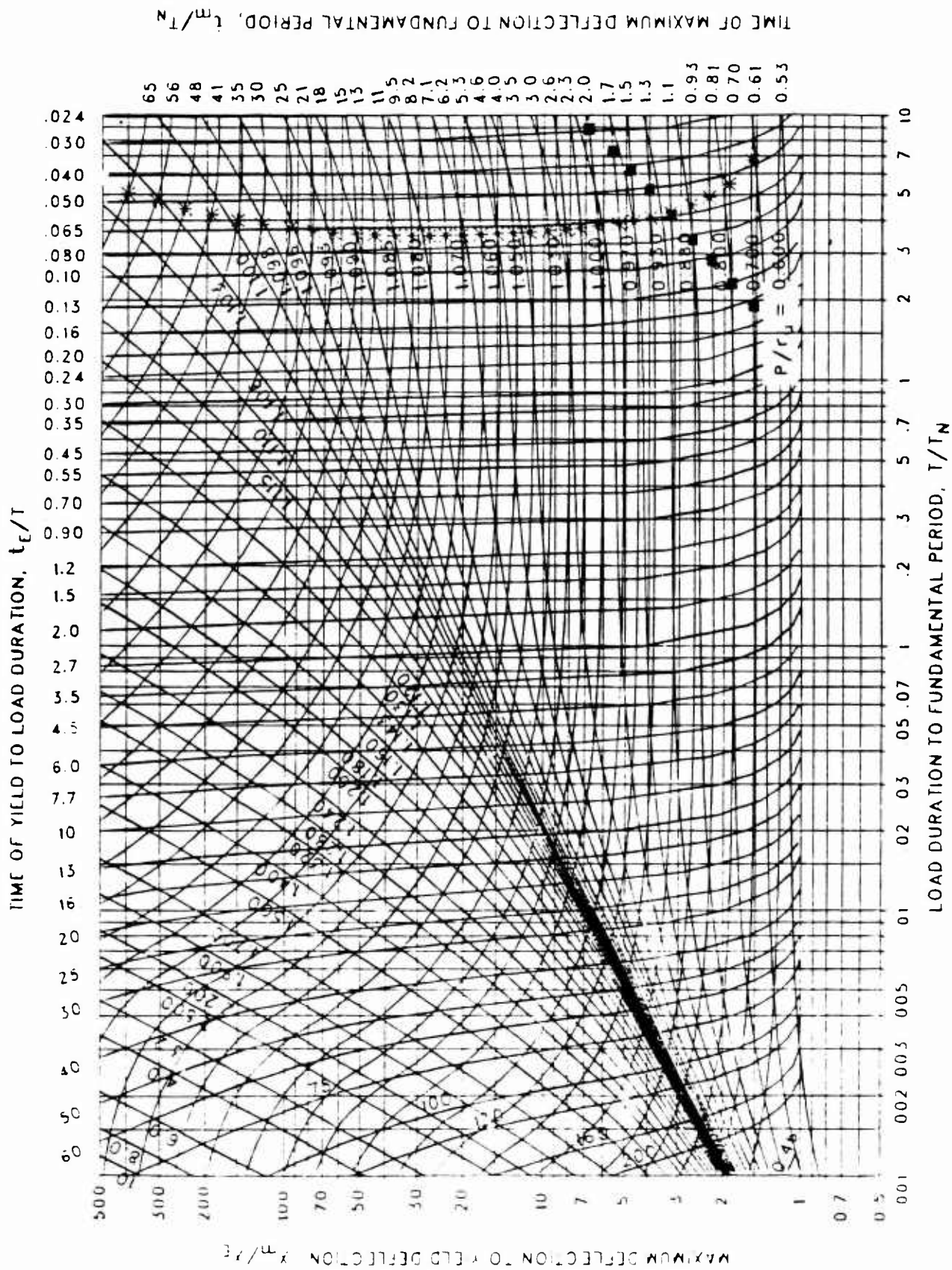
Figure 3-220   Maximum response of elasto-plastic, one-degree-of-freedom
system for bilinear-triangular pulse ($C_1 = 0.909$, $C_2 = 1000.$)
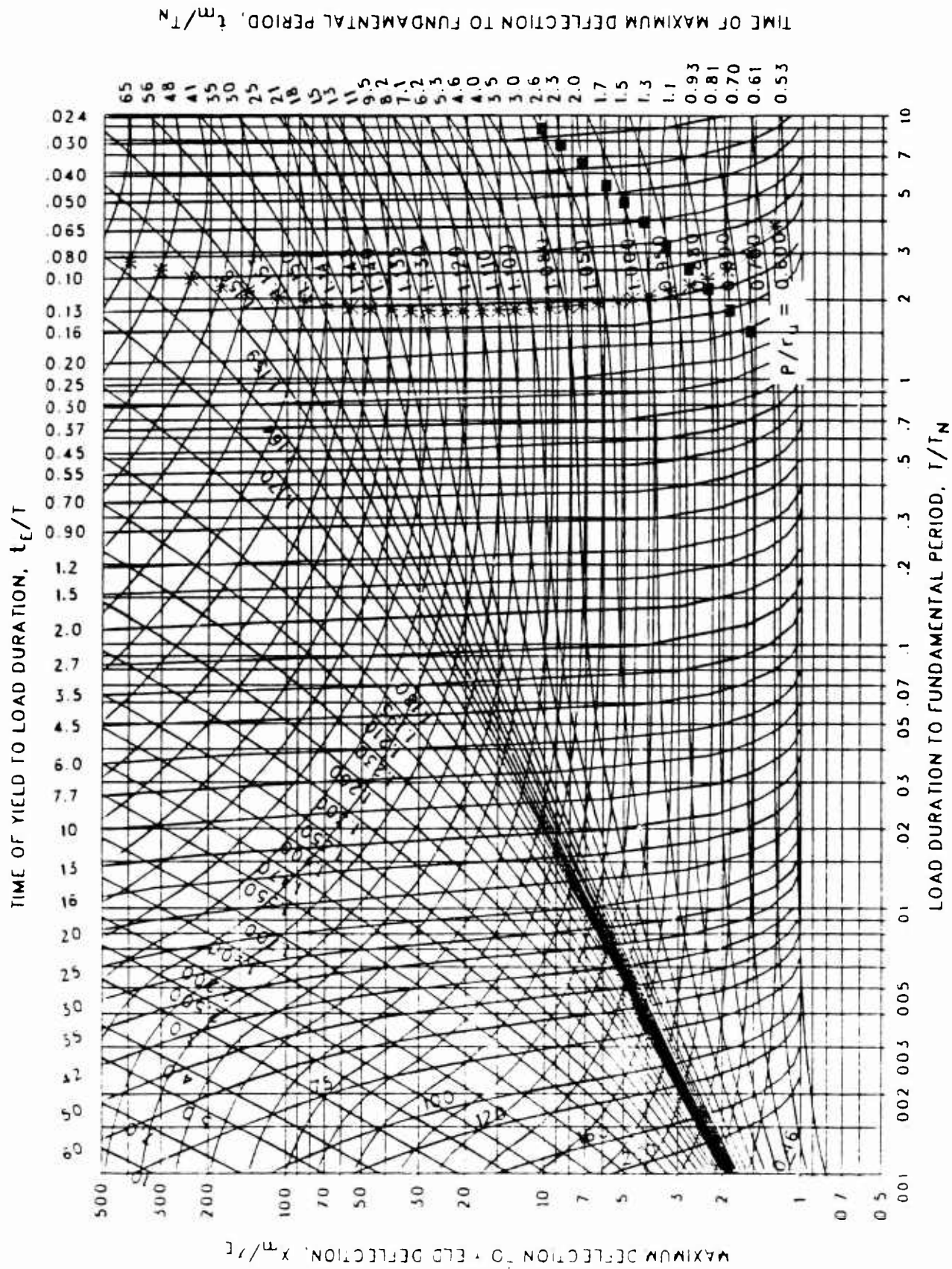
Figure 3-221   Maximum response of elasto-plastic, one-degree-of-freedom
system for bilinear-triangular pulse ($C_1 = 0.866$, $C_2 = 1000.$)
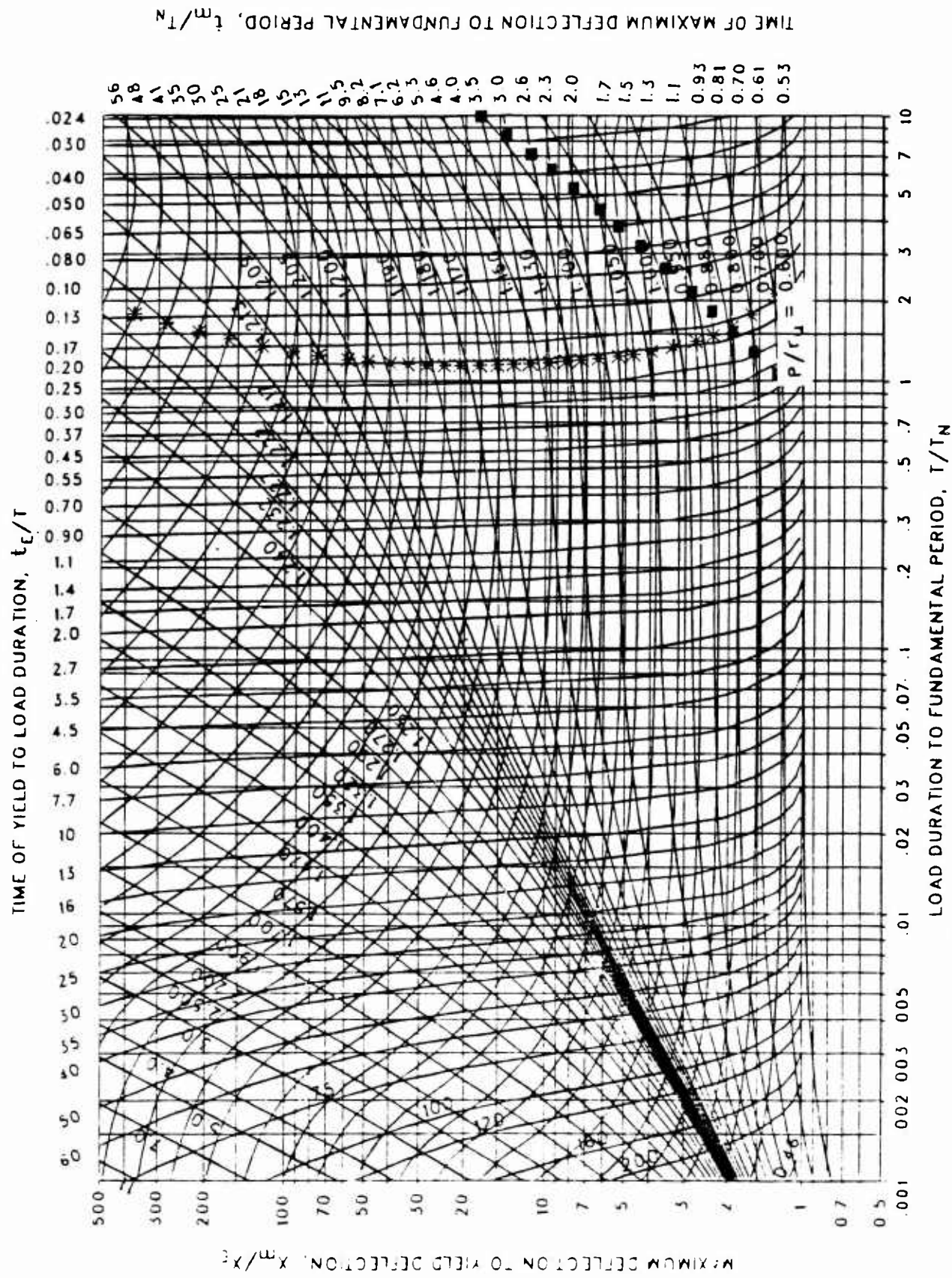
Figure 3-222 — Maximum response of elasto-plastic, one-degree-of-freedom system for bilinear-triangular pulse ($C_1 = 0.825$, $C_2 = 1000.$)
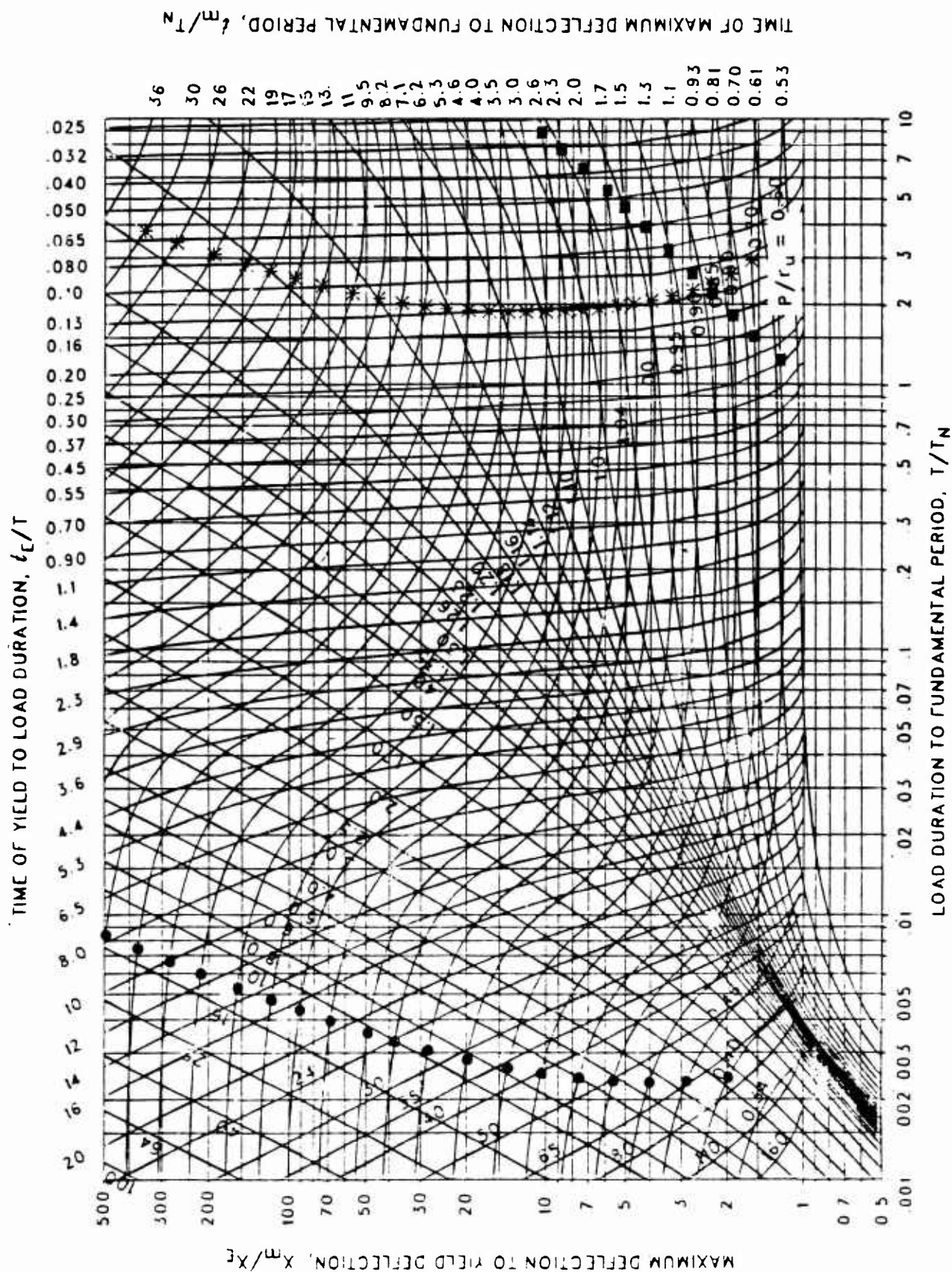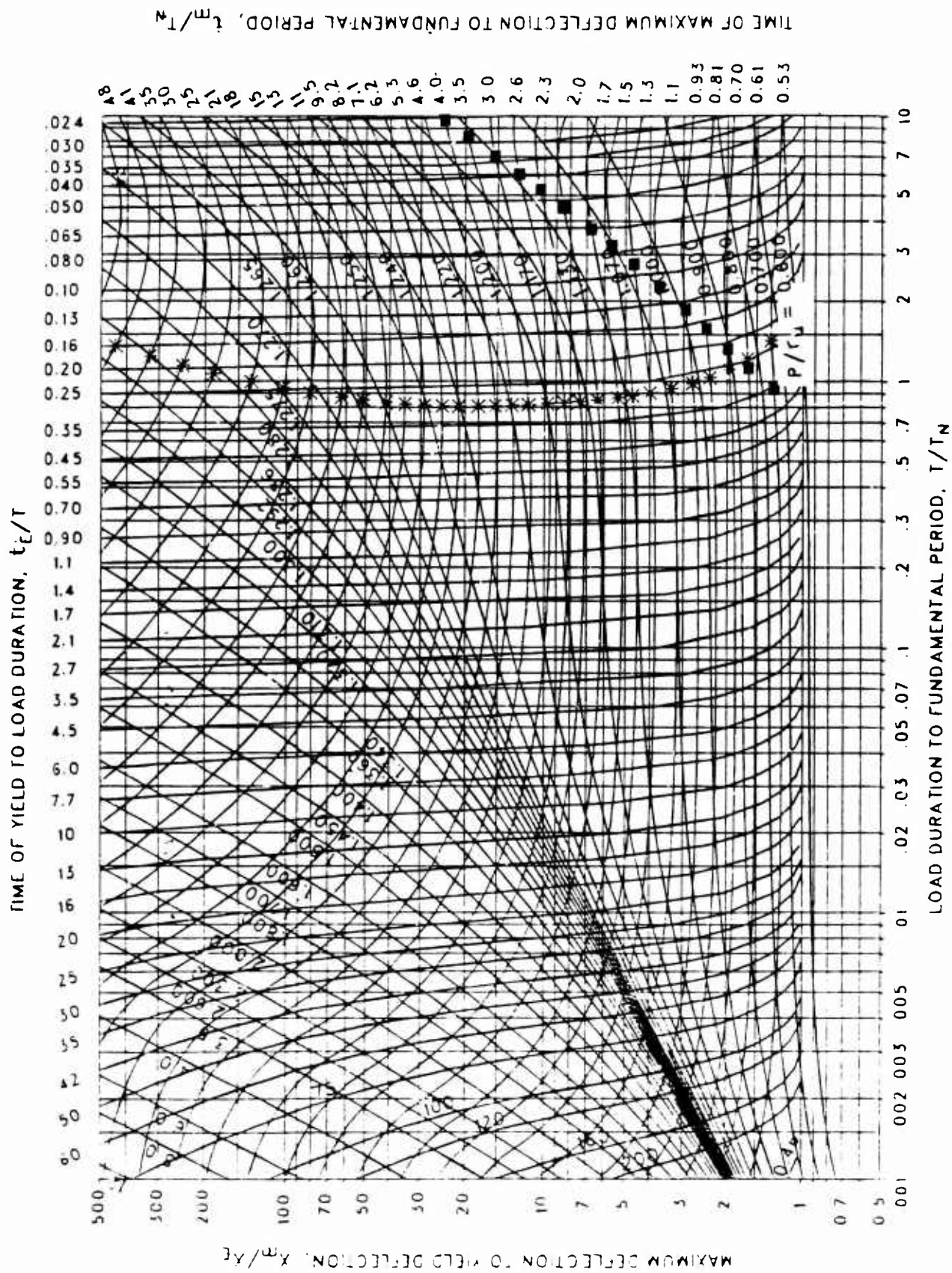
Figure 3-223   Maximum response of elasto-plastic, one-degree-of-freedom
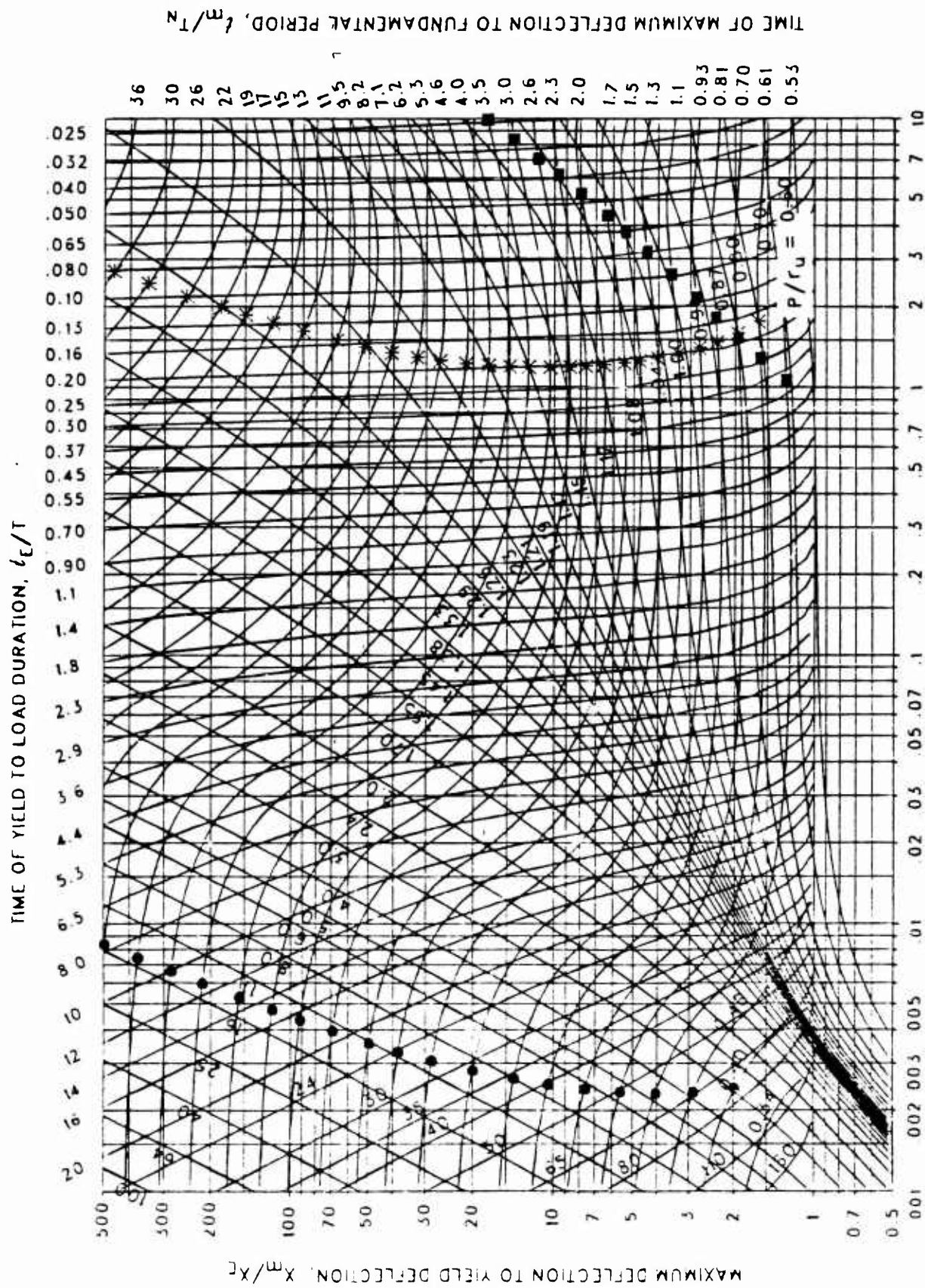system for bilinear-triangular pulse ($C_1 = 0.787$, $C_2 = 1000.$)
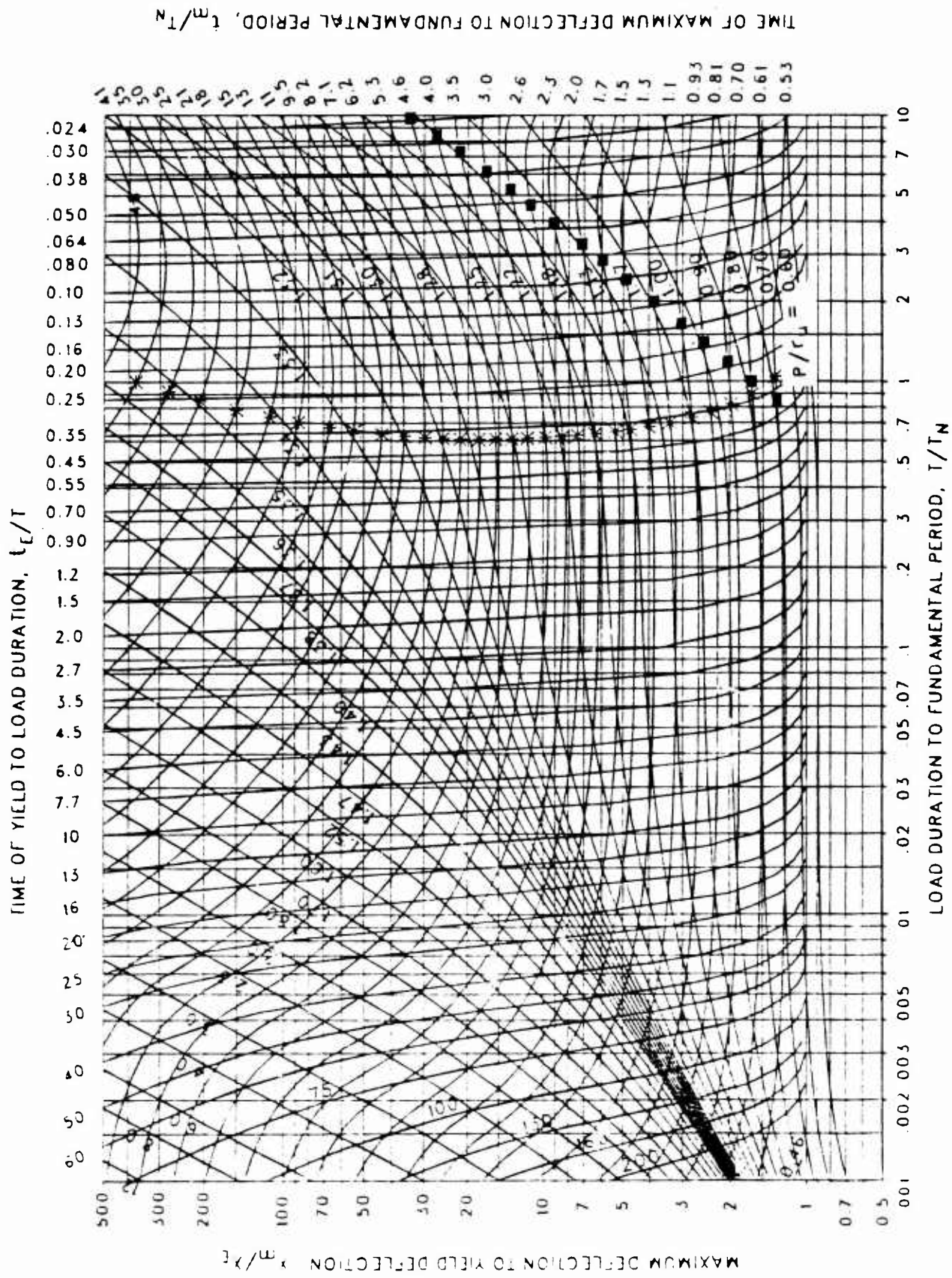
Figure 3-224   Maximum response of elasto-plastic, one-degree-of-freedom
system for bilinear-triangular pulse ($C_1 = 0.750$, $C_2 = 1000.$)
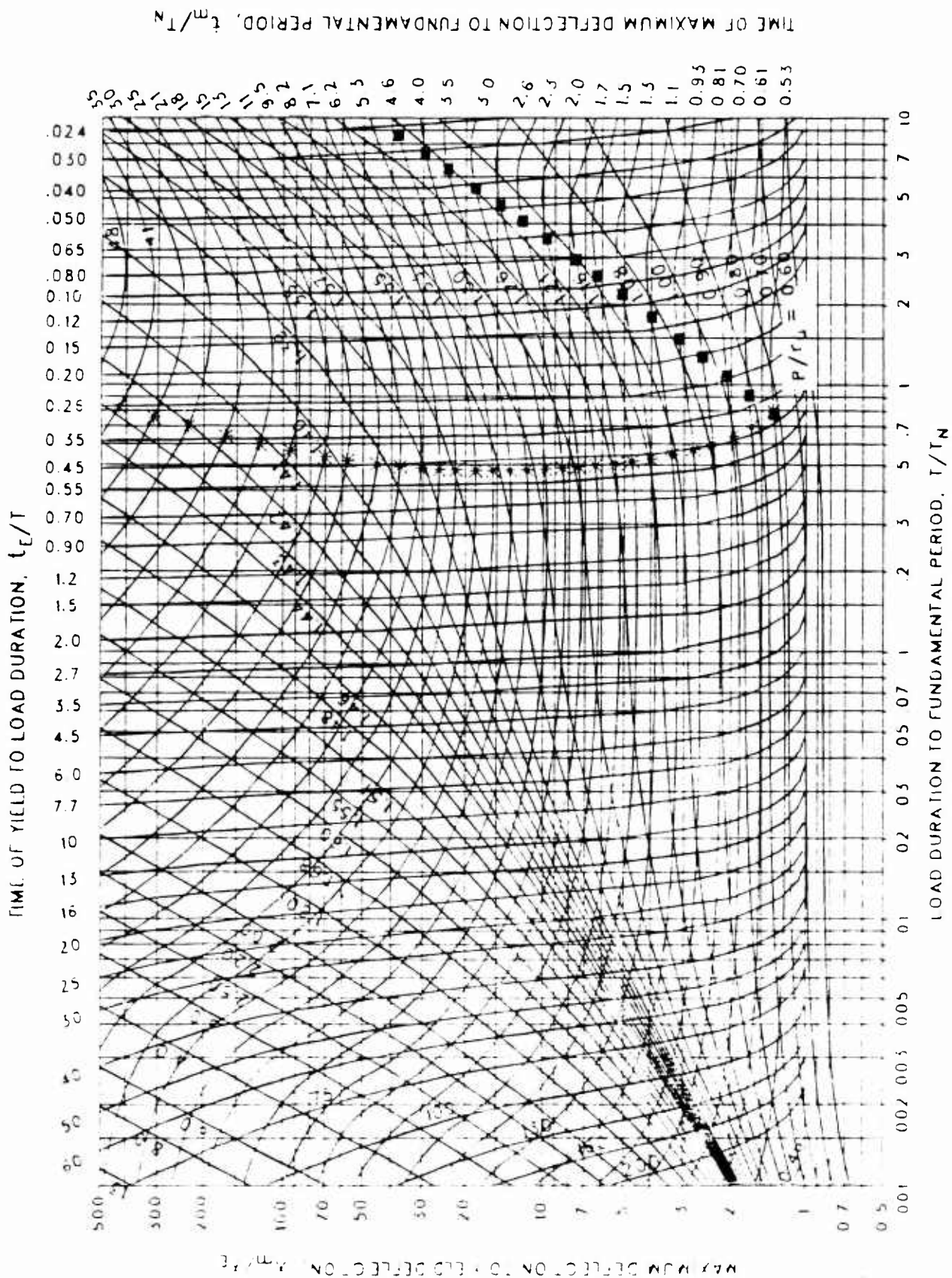
Figure 3-225   Maximum response of elasto-plastic, one-degree-of-freedom
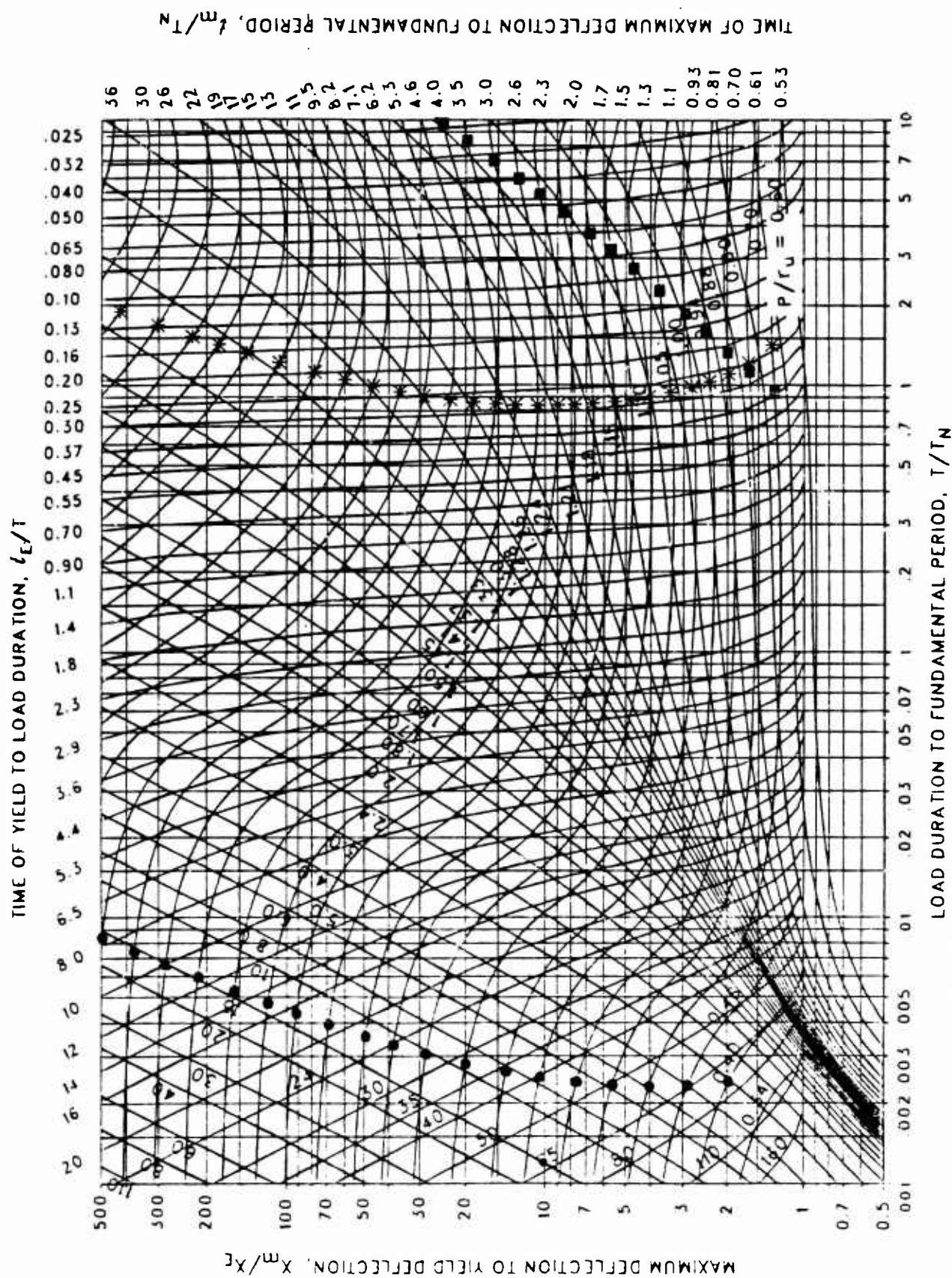system for bilinear-triangular pulse ($C_1 = 0.715$, $C_2 = 1000.$)

Figure 3-22b   Maximum response of elasto-plastic, one-degree-of-freedom system for bilinear-triangular pulse ($C_1 = 0.681$, $C_2 = 1000.$)
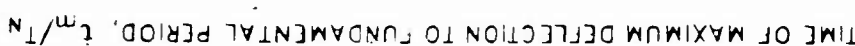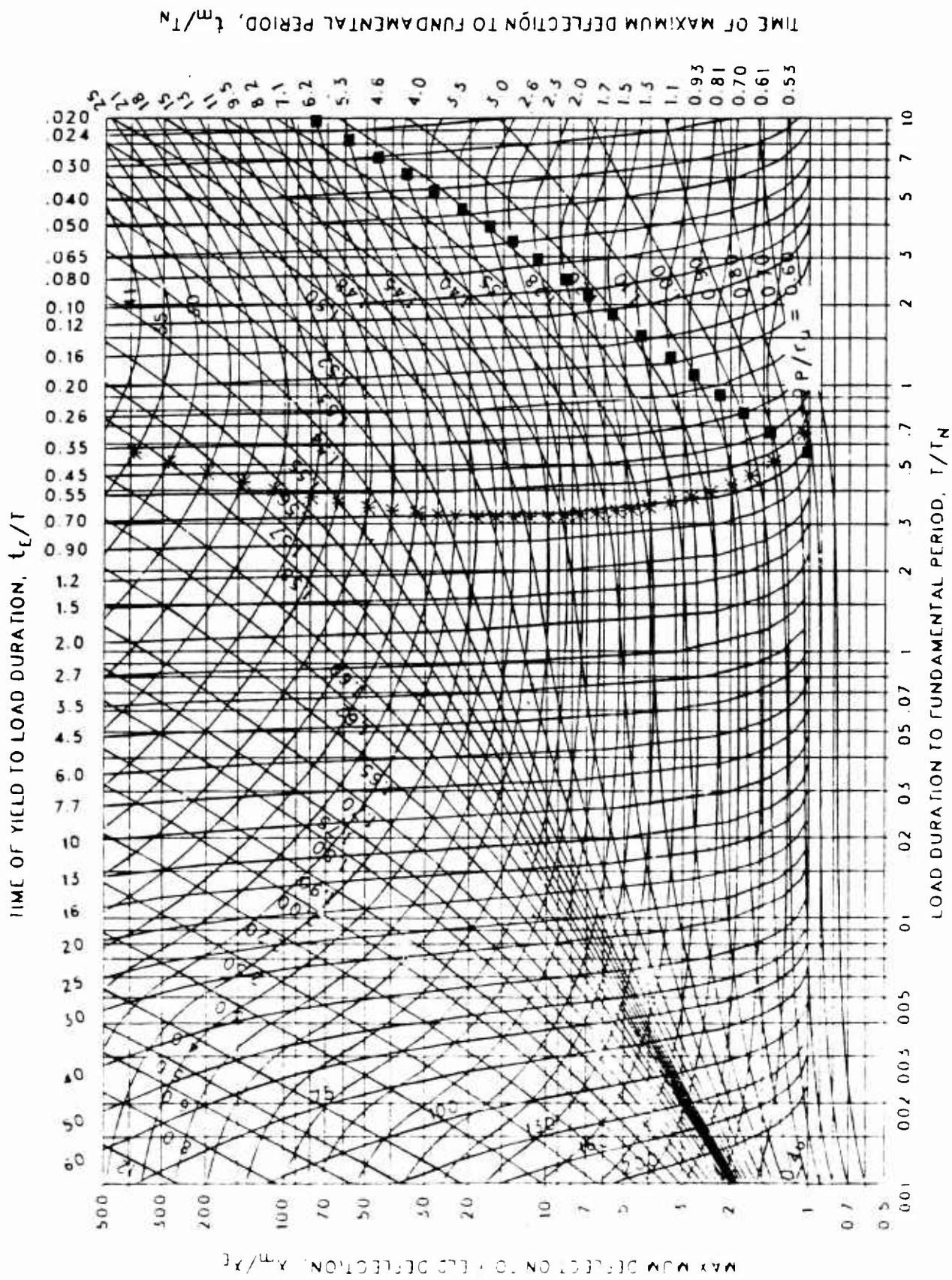
Figure 3-227 Maximum response of elasto-plastic, one-degree-of-freedom system for bilinear-triangular pulse ($C_1 = 0.648$, $C_2 = 1000$.)
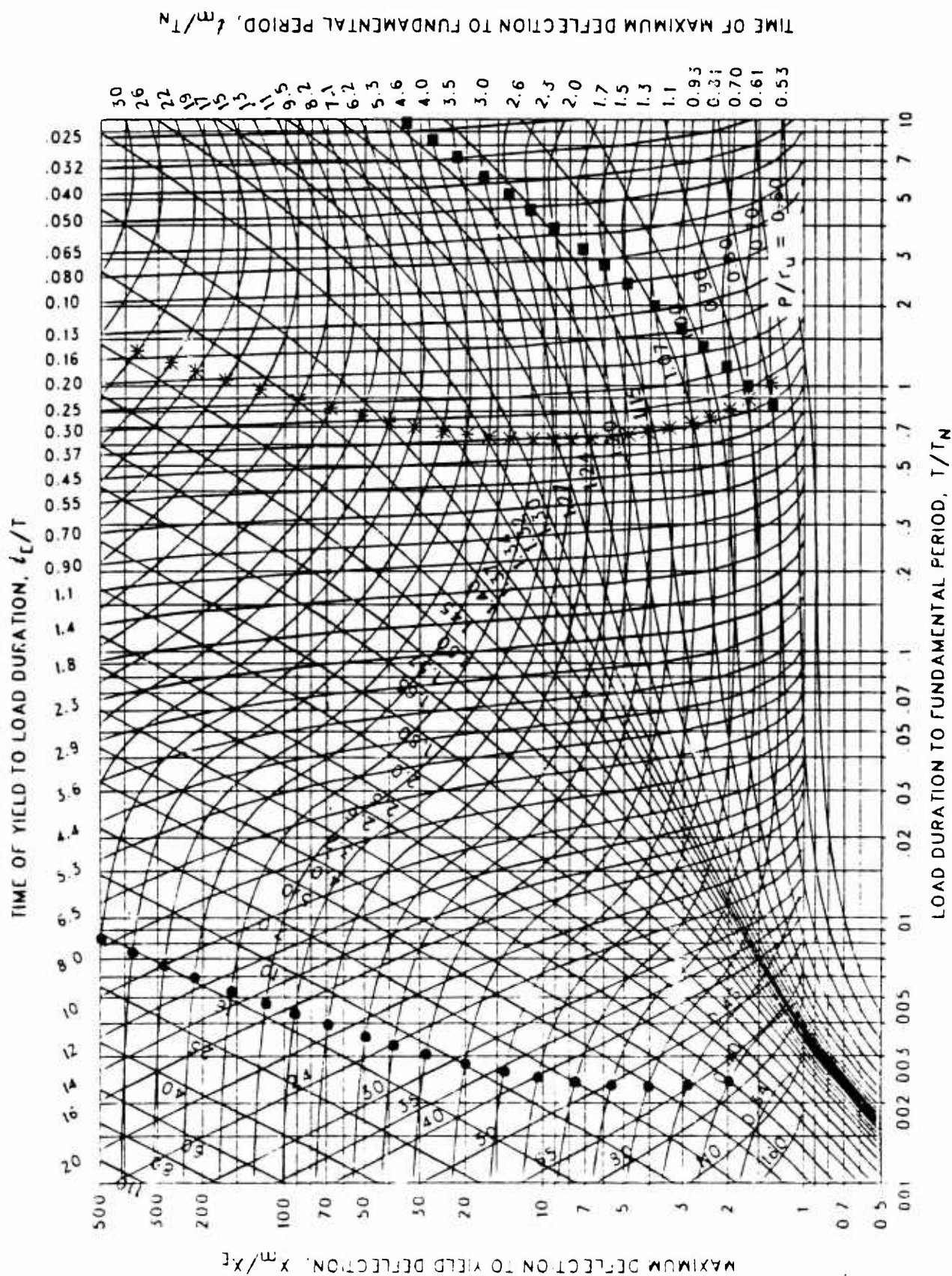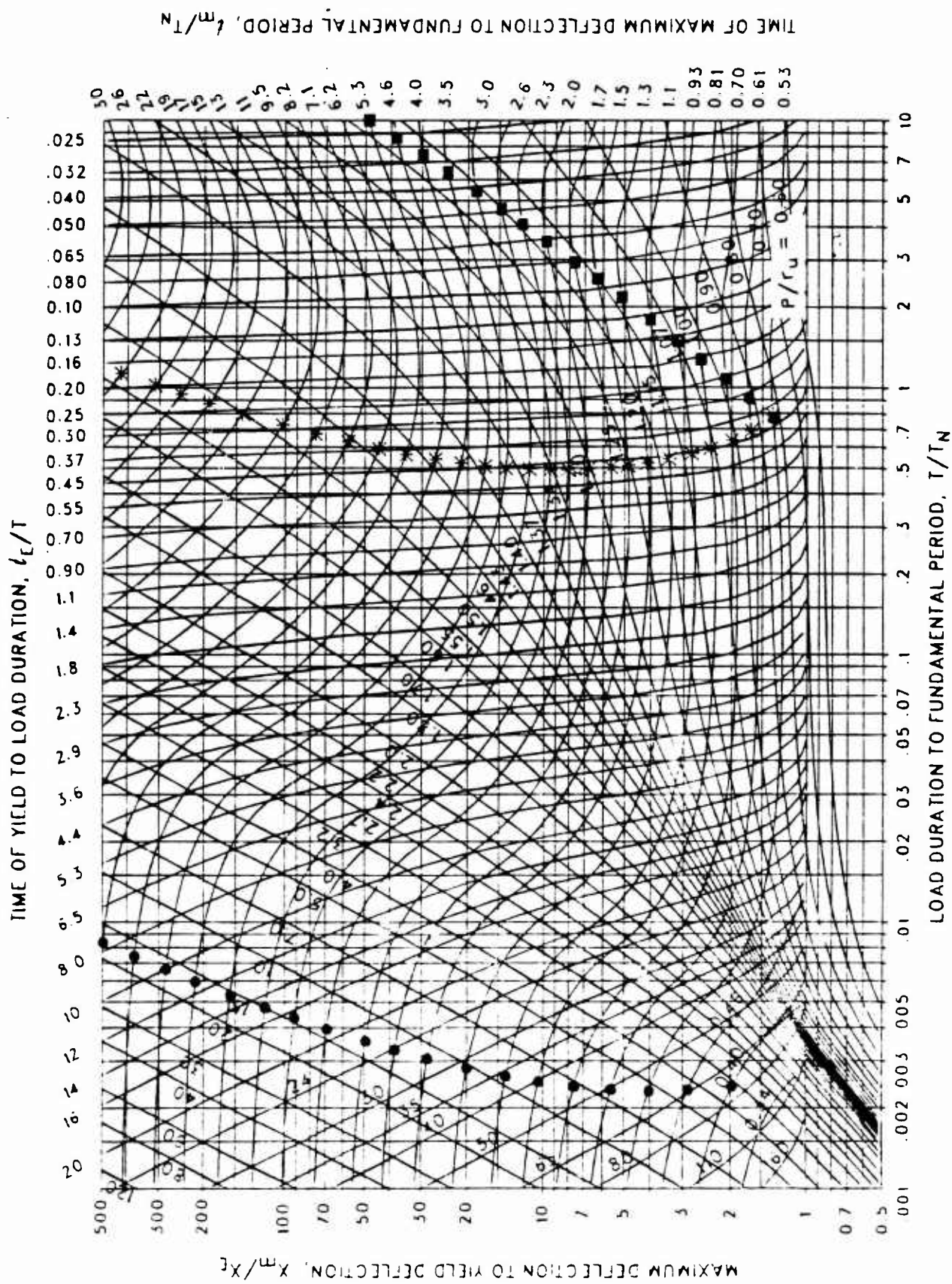
-282-
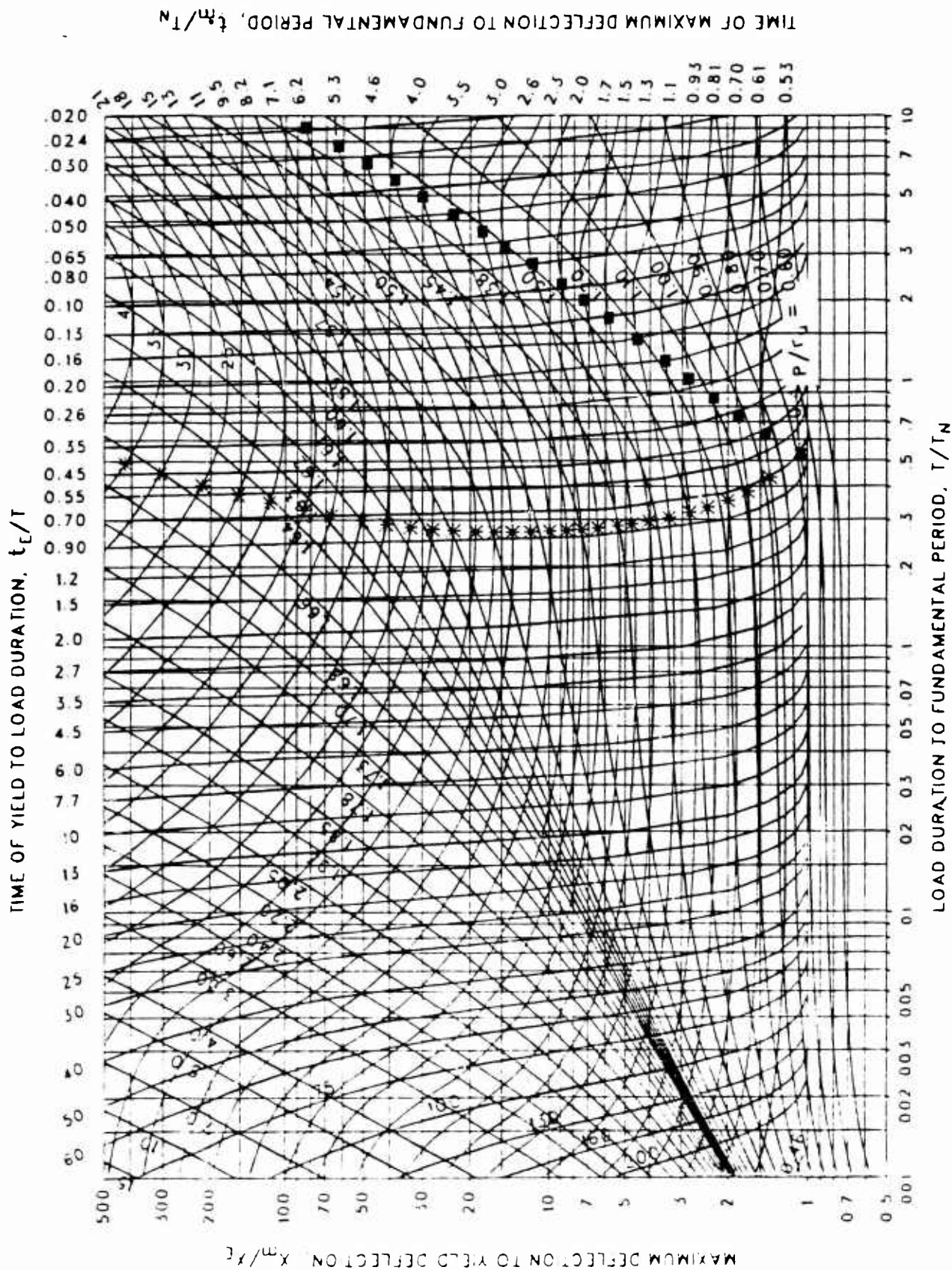
Figure 3-228 Maximum response of elasto-plastic, one-degree-of-freedom system for bilinear-triangular pulse ($C_1 = 0.619$, $C_2 = 1000.$)
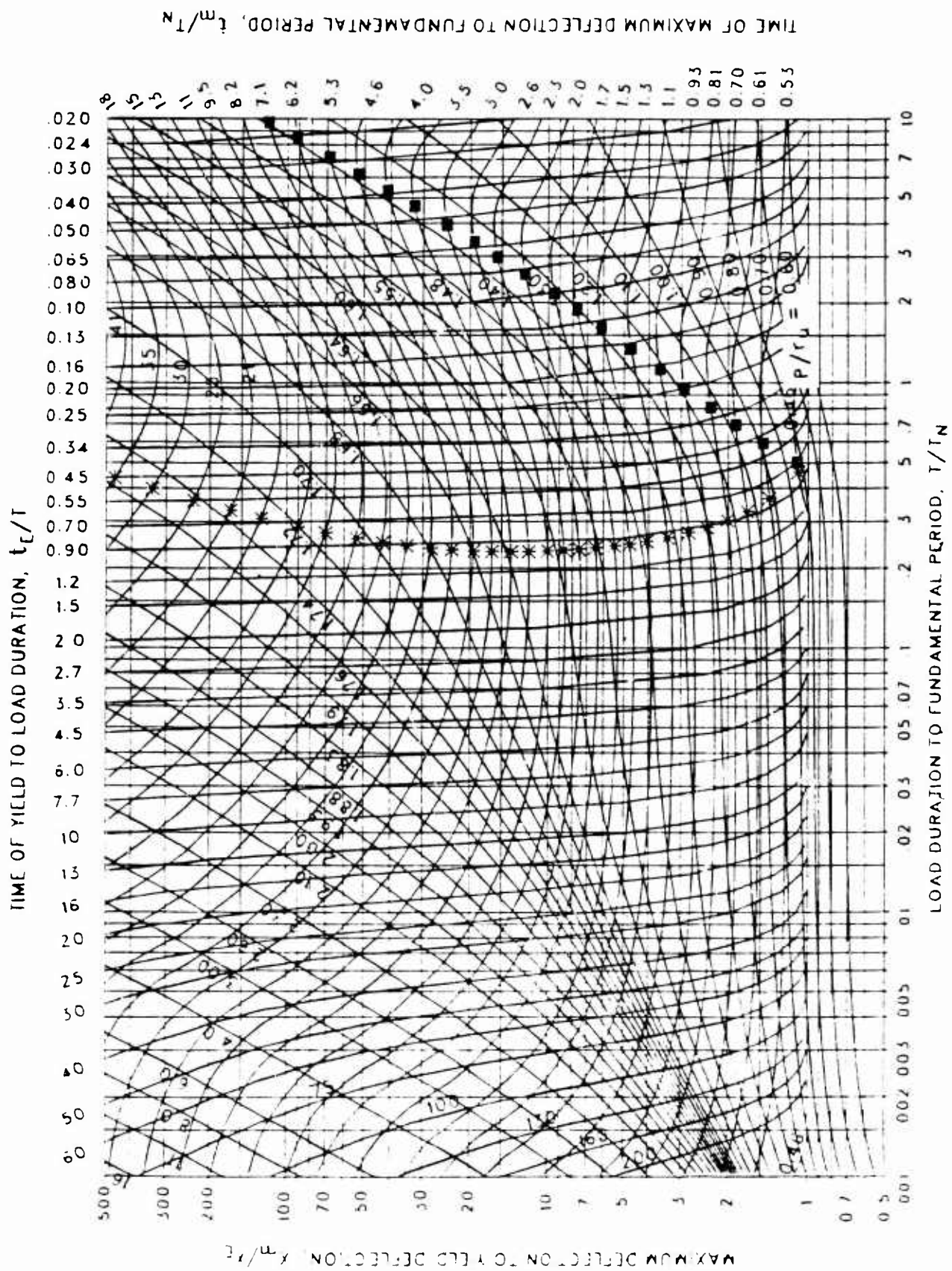
Figure 3-229   Maximum response of elasto-plastic, one-degree-of-freedom system for bilinear-triangular pulse (C_1 = 0.590, C_2 = 1000.)
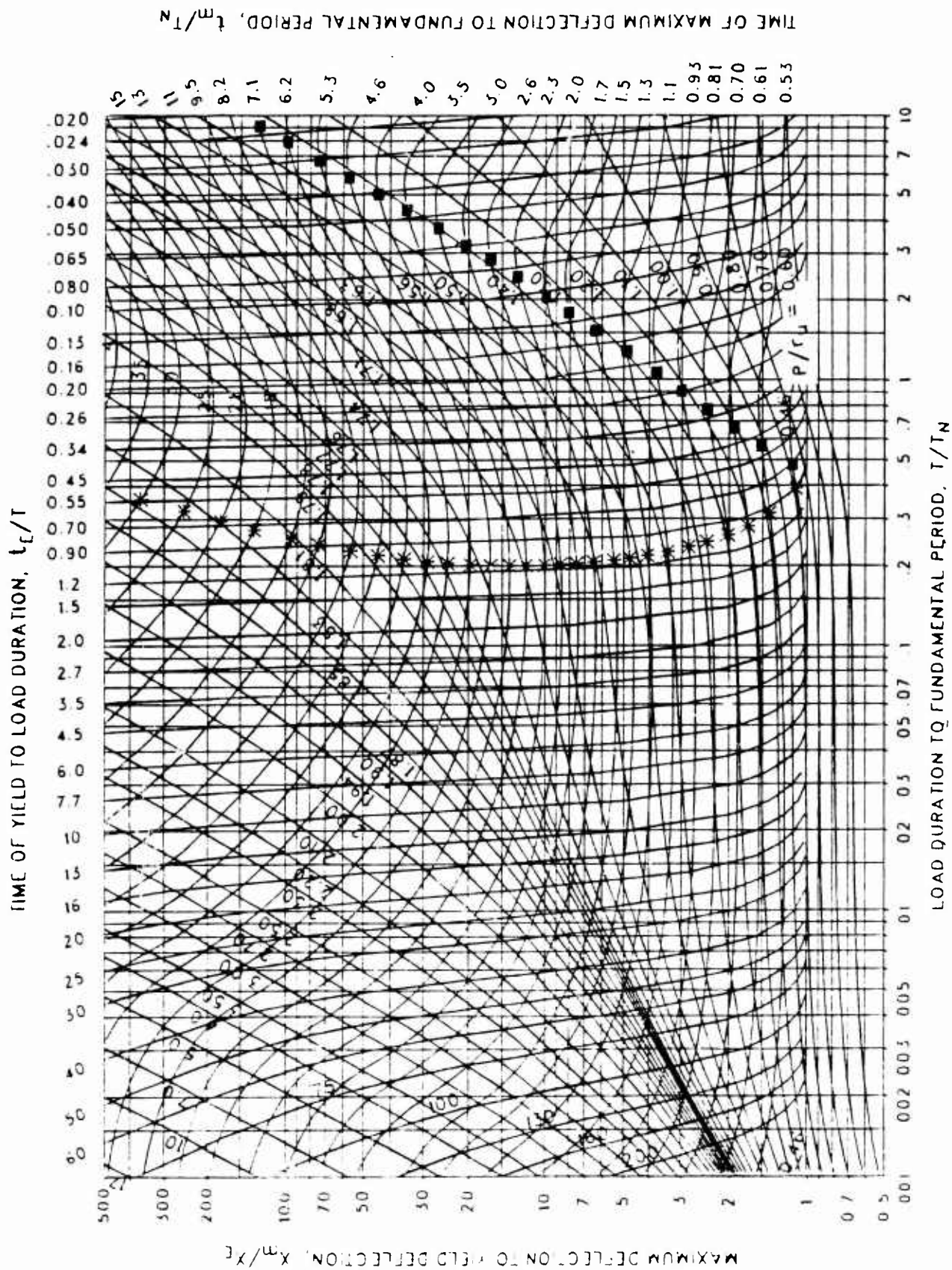
Figure 3-230 Maximum response of elasto-plastic, one-degree-of-freedom system for bilinear-triangular pulse (C_1 = 0.562, C_2 = 1000.)
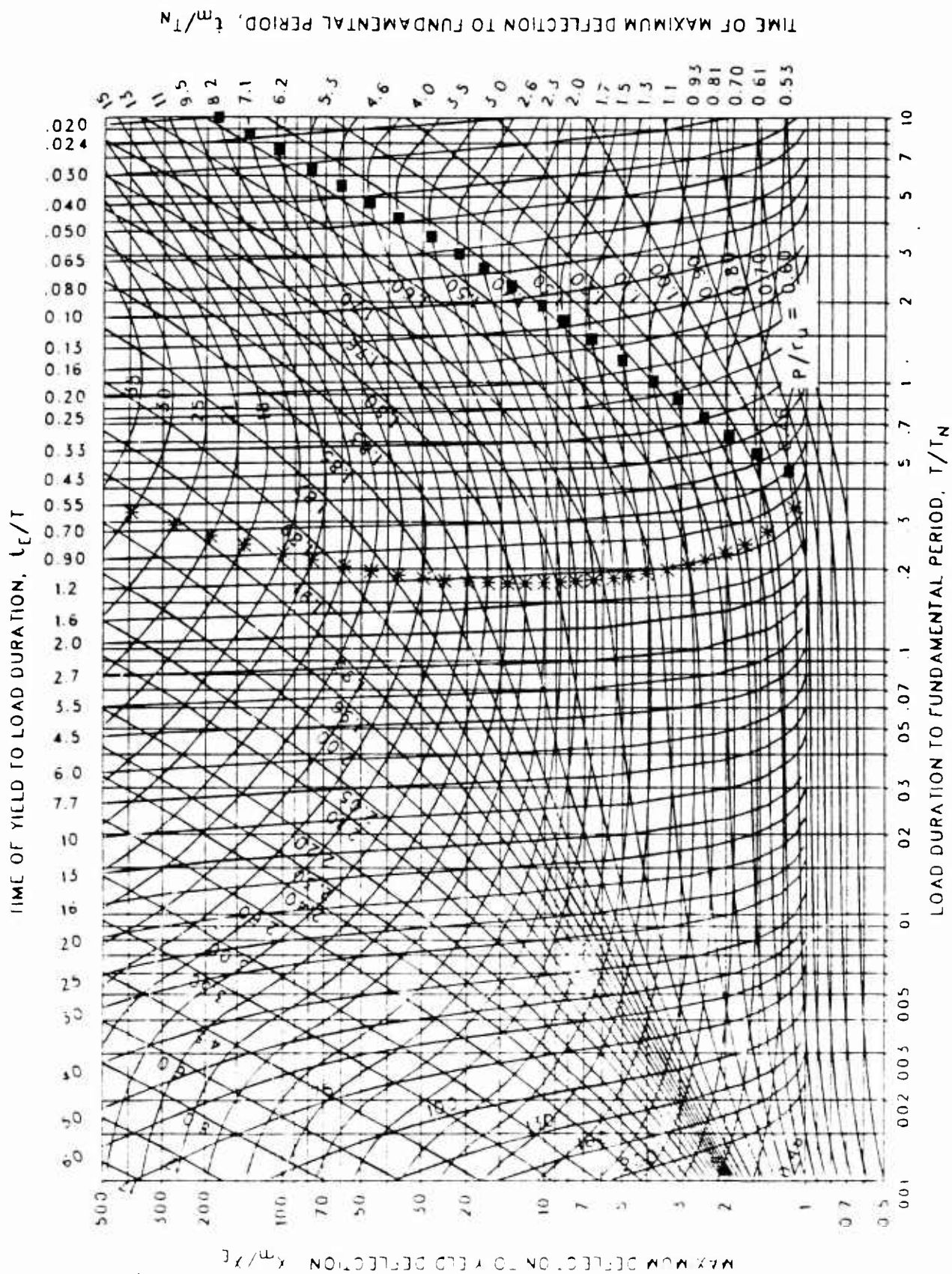
Figure 3-231 Maximum response of elasto-plastic, one-degree-of-freedom system for bilinear-triangular pulse ($C_1 = 0.536$, $C_2 = 1000.$)
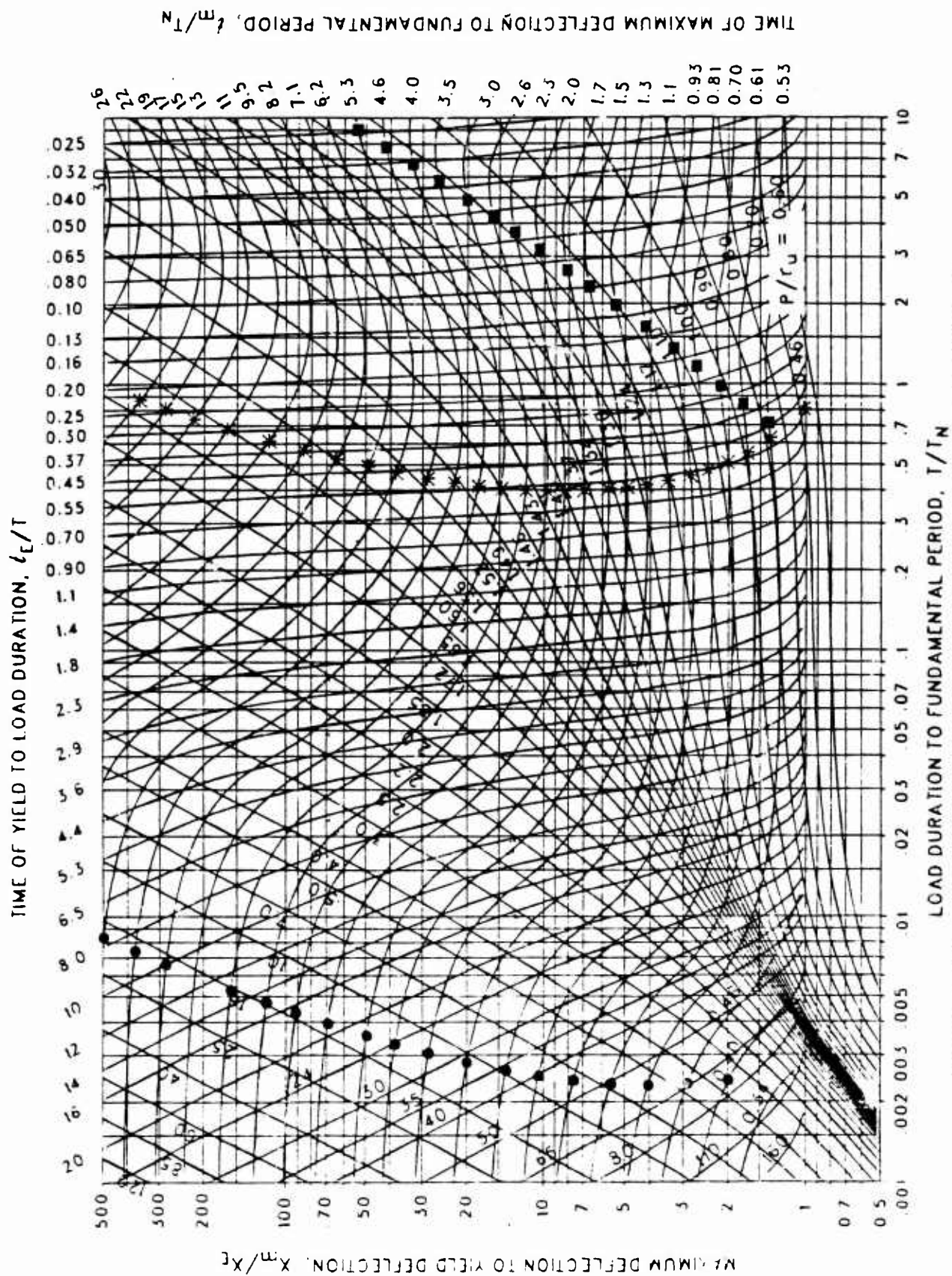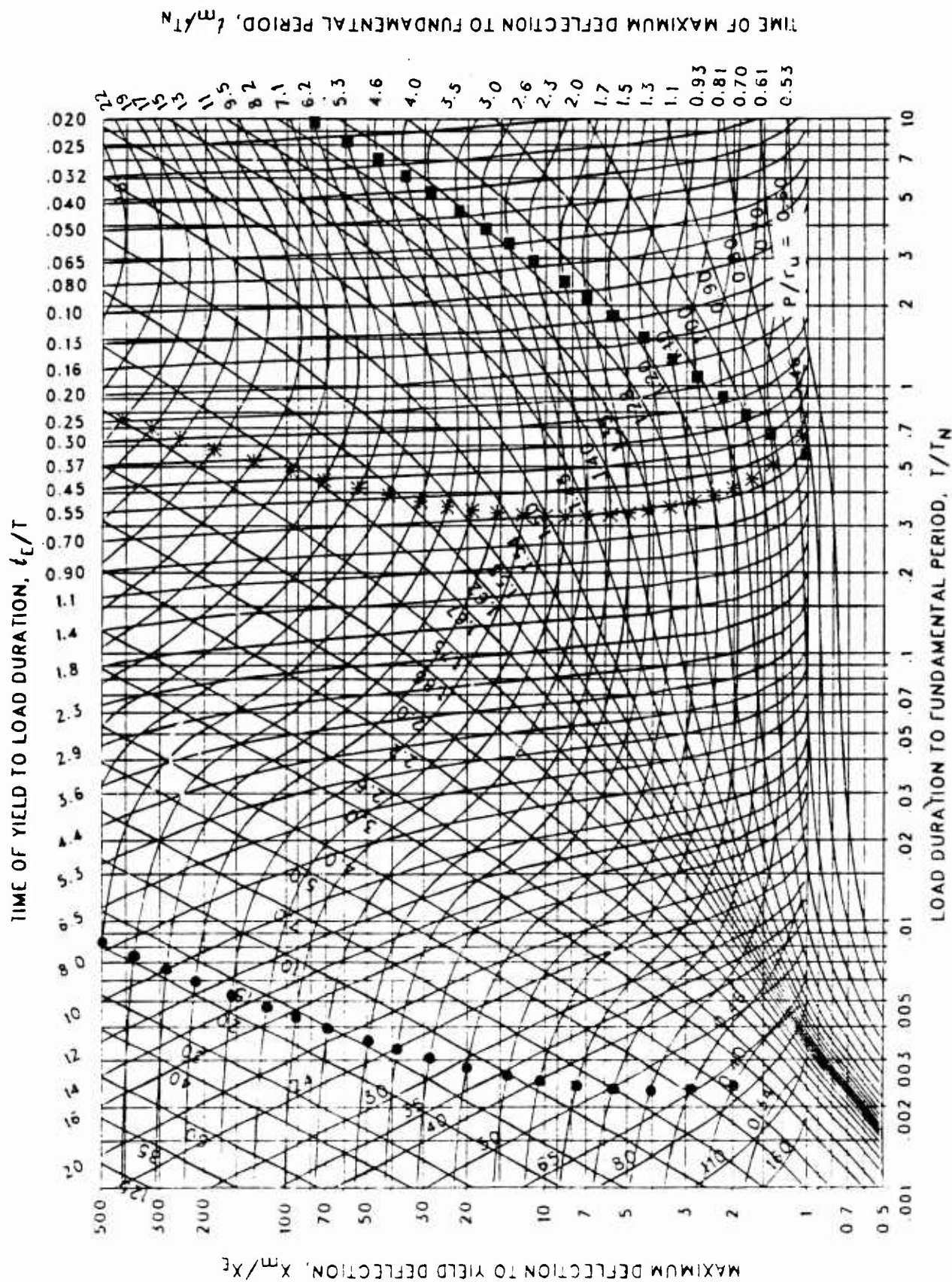
-286-
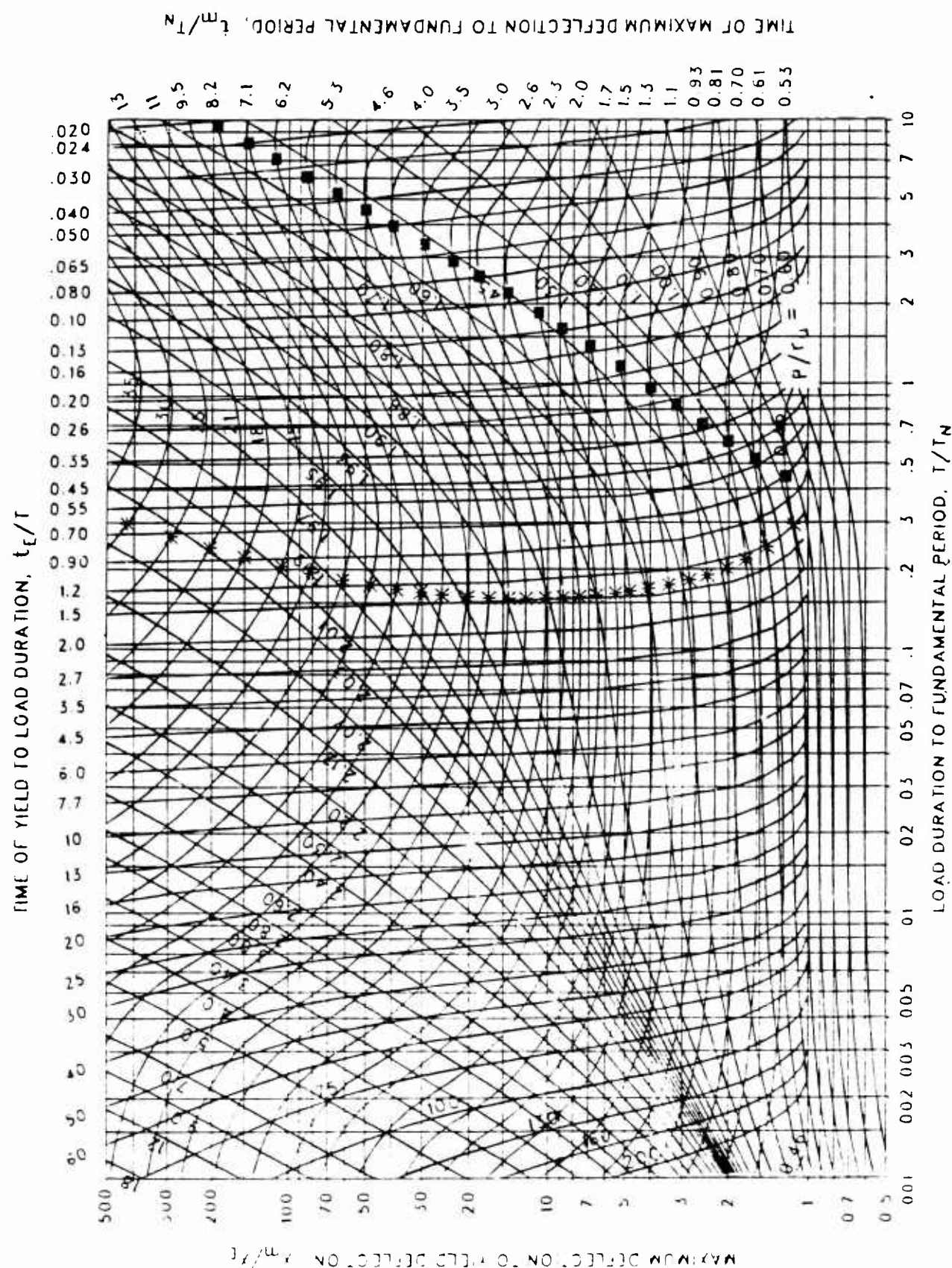
Figure 3-232 Maximum response of elasto-plastic, one-degree-of-freedom system for bilinear-triangular pulse ($C_1 = 0.511$, $C_2 = 1000.$)
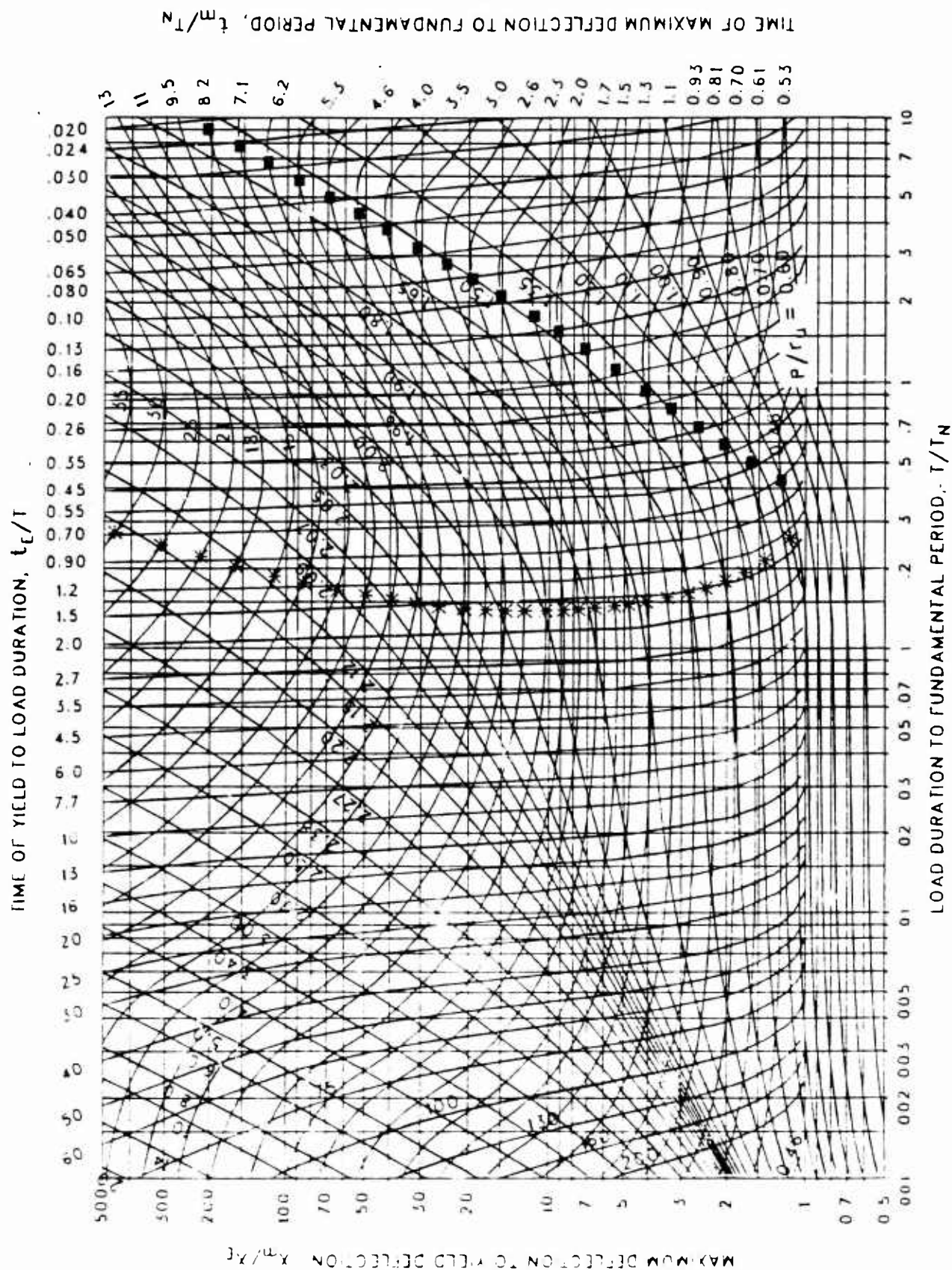
Figure 3-233   Maximum response of elasto-plastic, one-degree-of-freedom system for bilinear-triangular pulse (C_1 = 0.487, C_2 = 1000.)
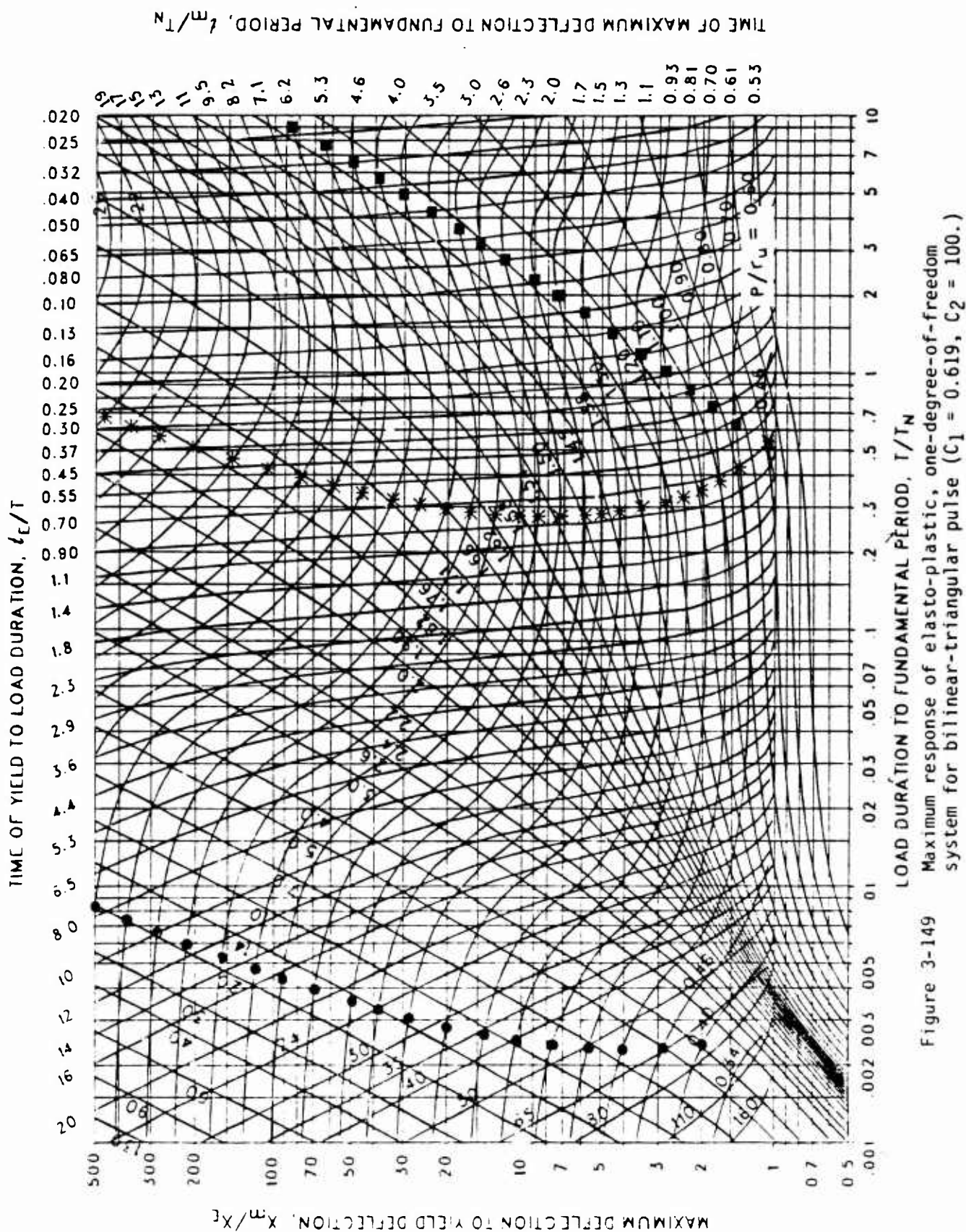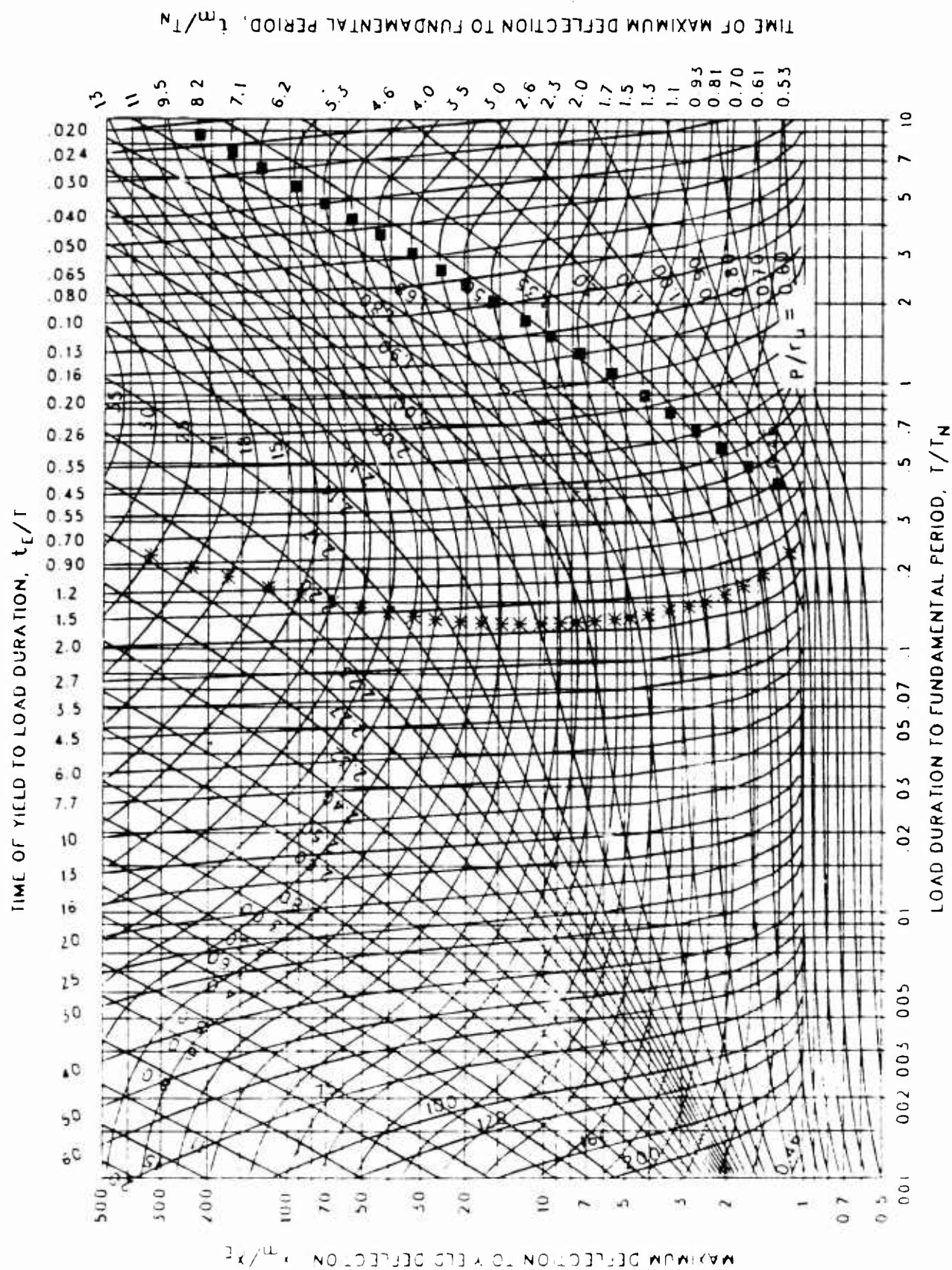
Figure 3-234   Maximum response of elasto-plastic, one-degree-of-freedom
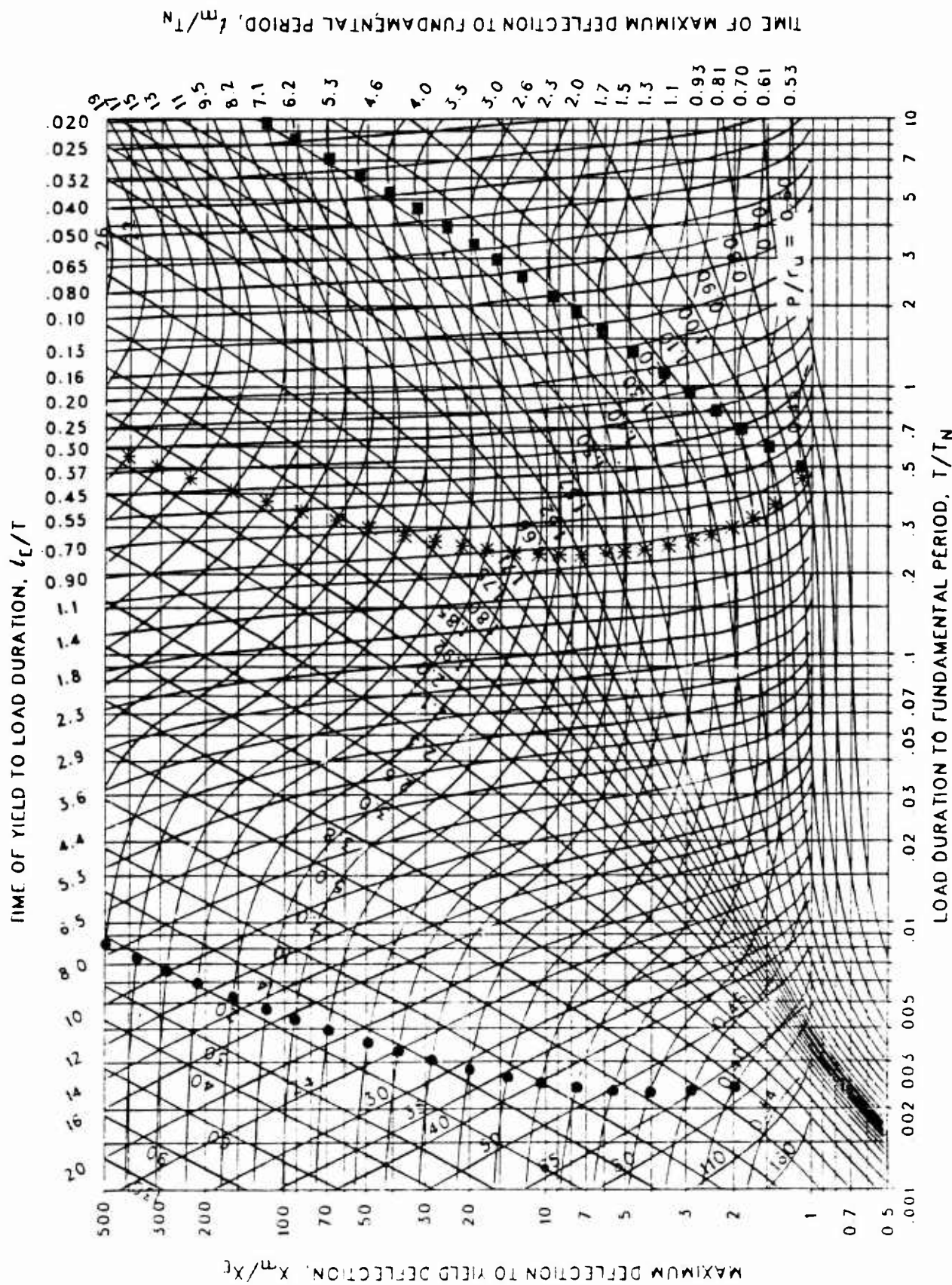system for bilinear-triangular pulse (C_1 = 0.464, C_2 = 1000.)
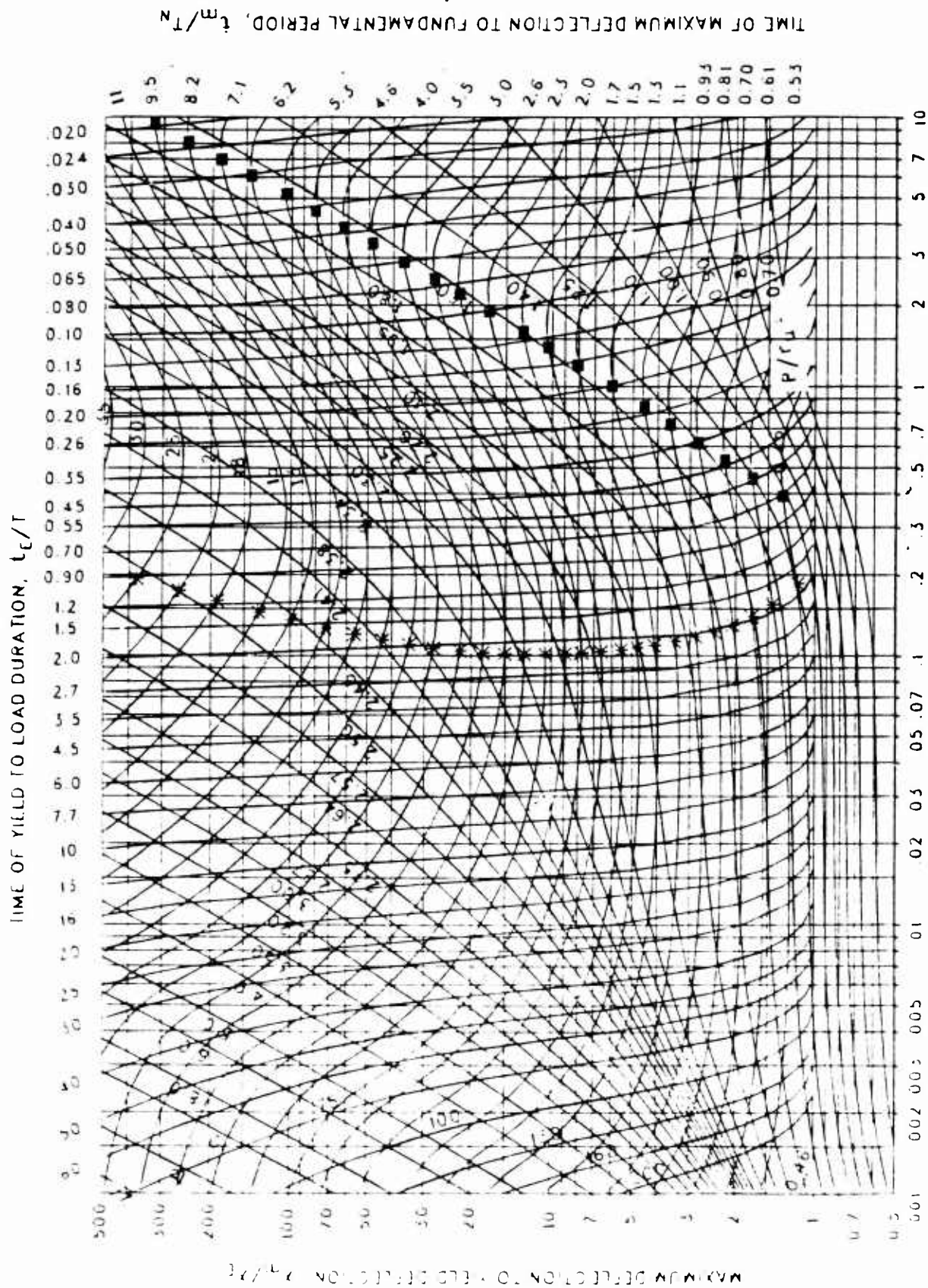
Figure 3-235   Maximum response of elasto-plastic, one-degree-of-freedom
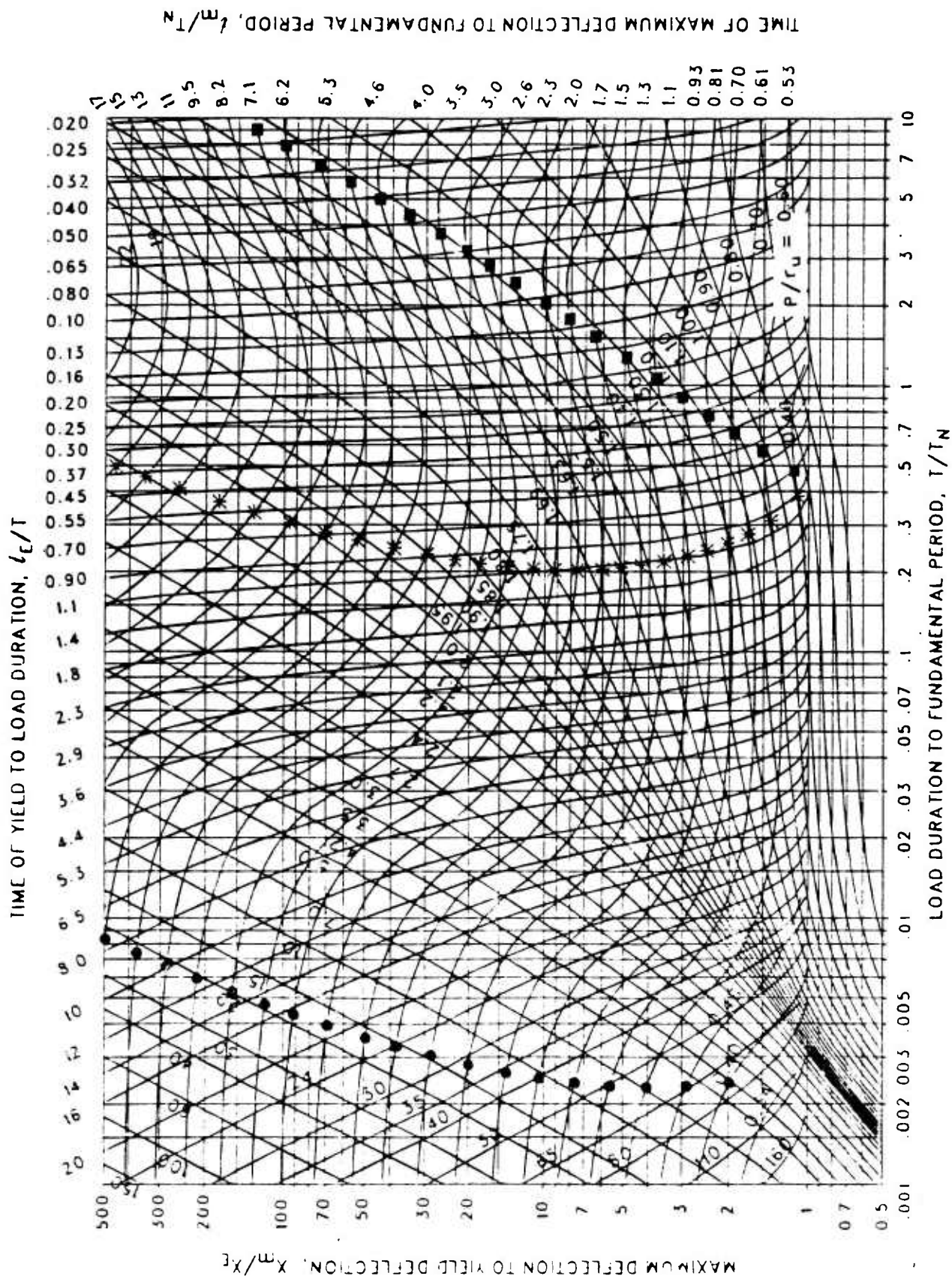system for bilinear-triangular pulse ($C_1 = 0.422$, $C_2 = 1000.$)

-290-
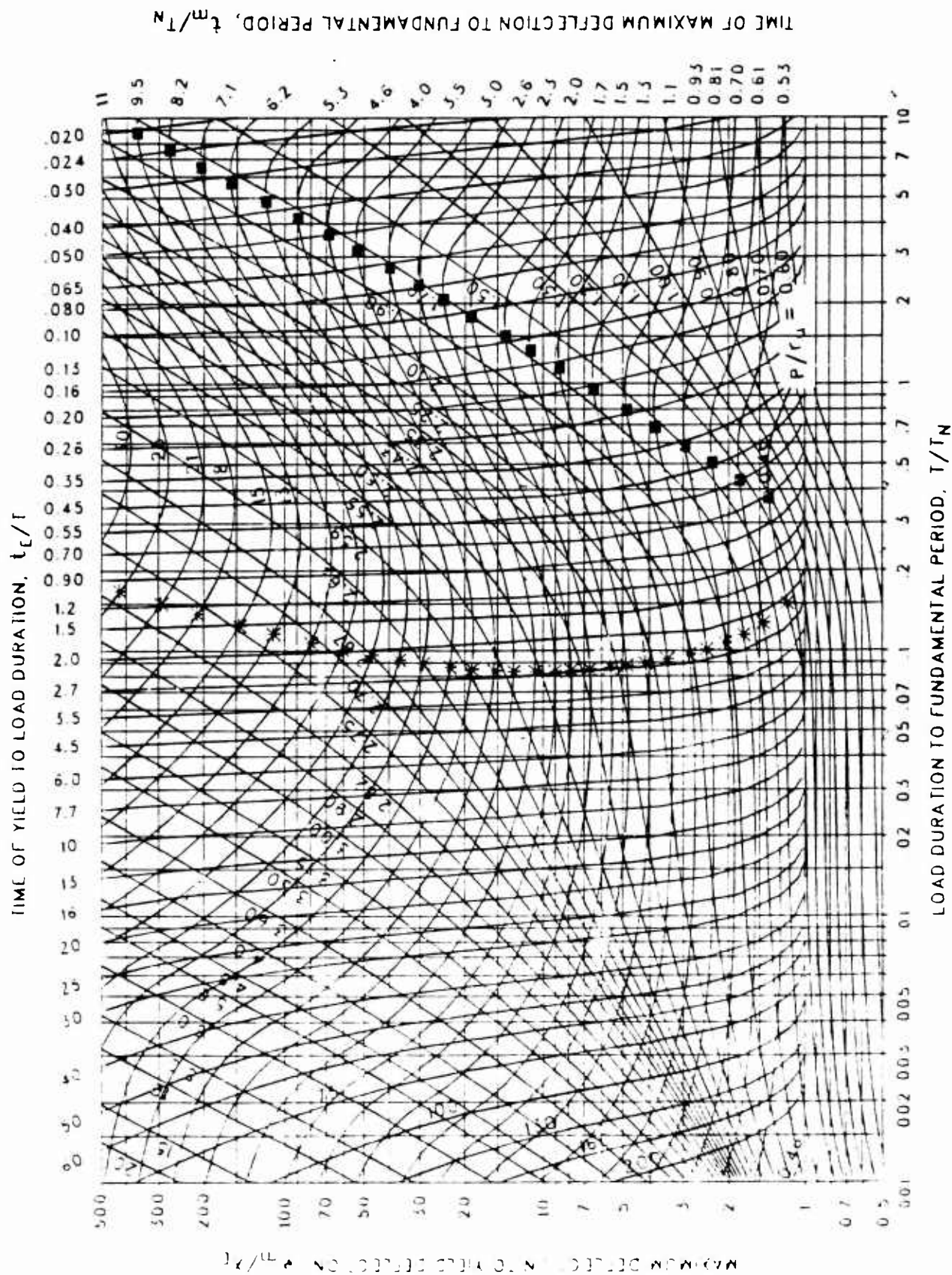
Figure 3-236 Maximum response of elasto-plastic, one-degree-of-freedom system for bilinear-triangular pulse ($C_1 = 0.383$, $C_2 = 1000$.)
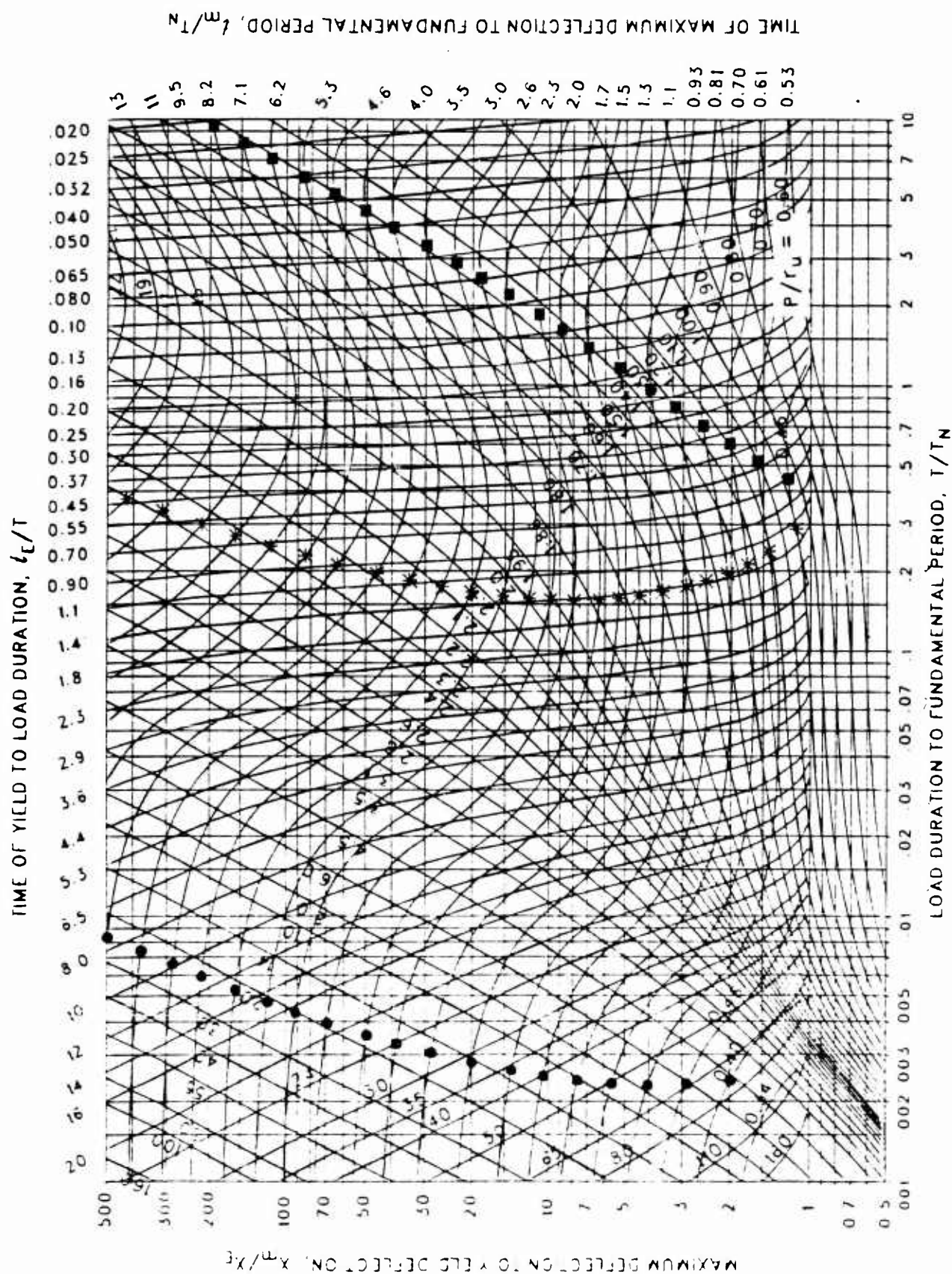
-291-
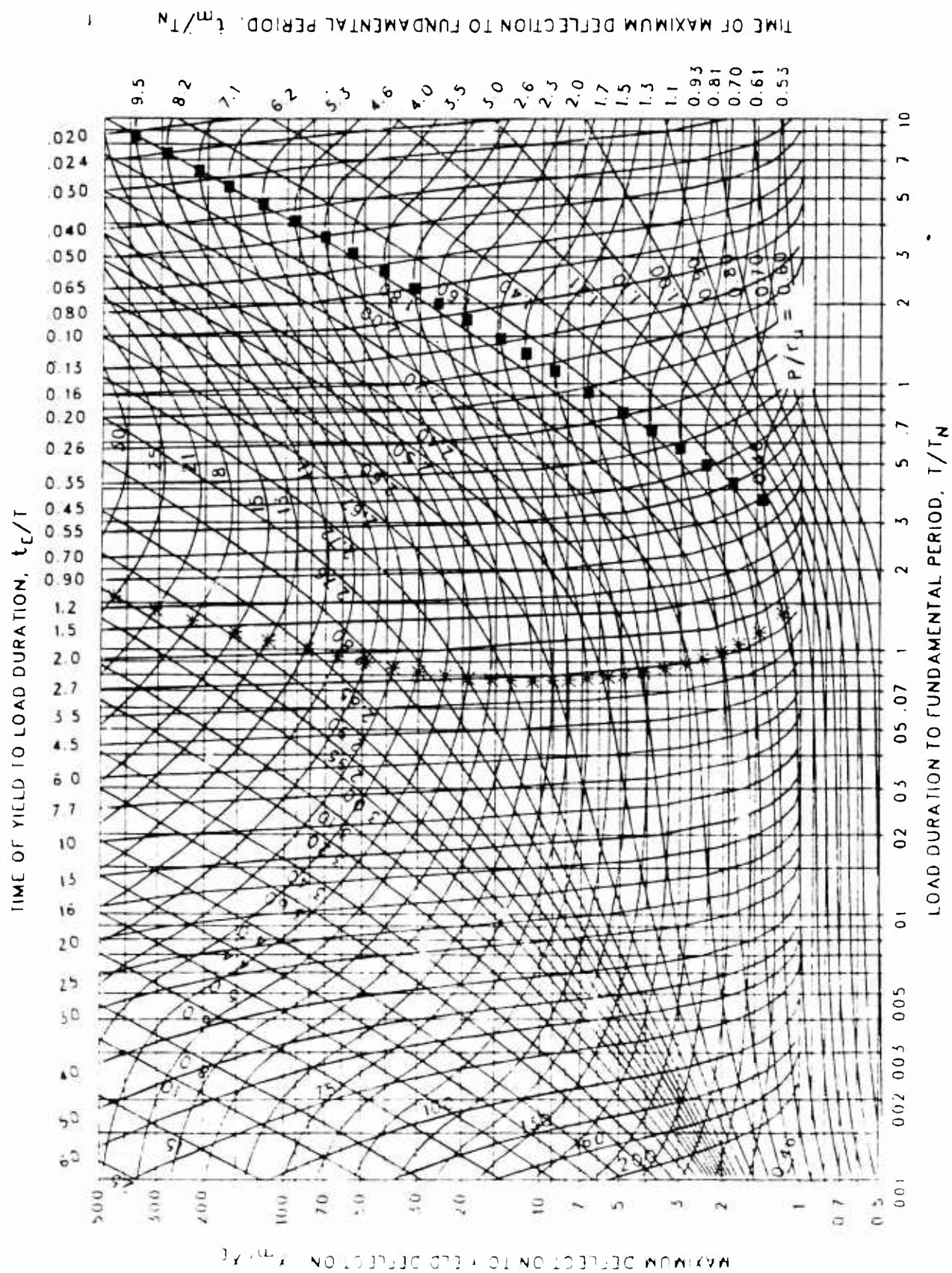
Figure 5-237   Maximum response of elasto-plastic, one-degree-of-freedom system for bilinear-triangular pulse ($C_1 = 0.365$, $C_2 = 1000.$)
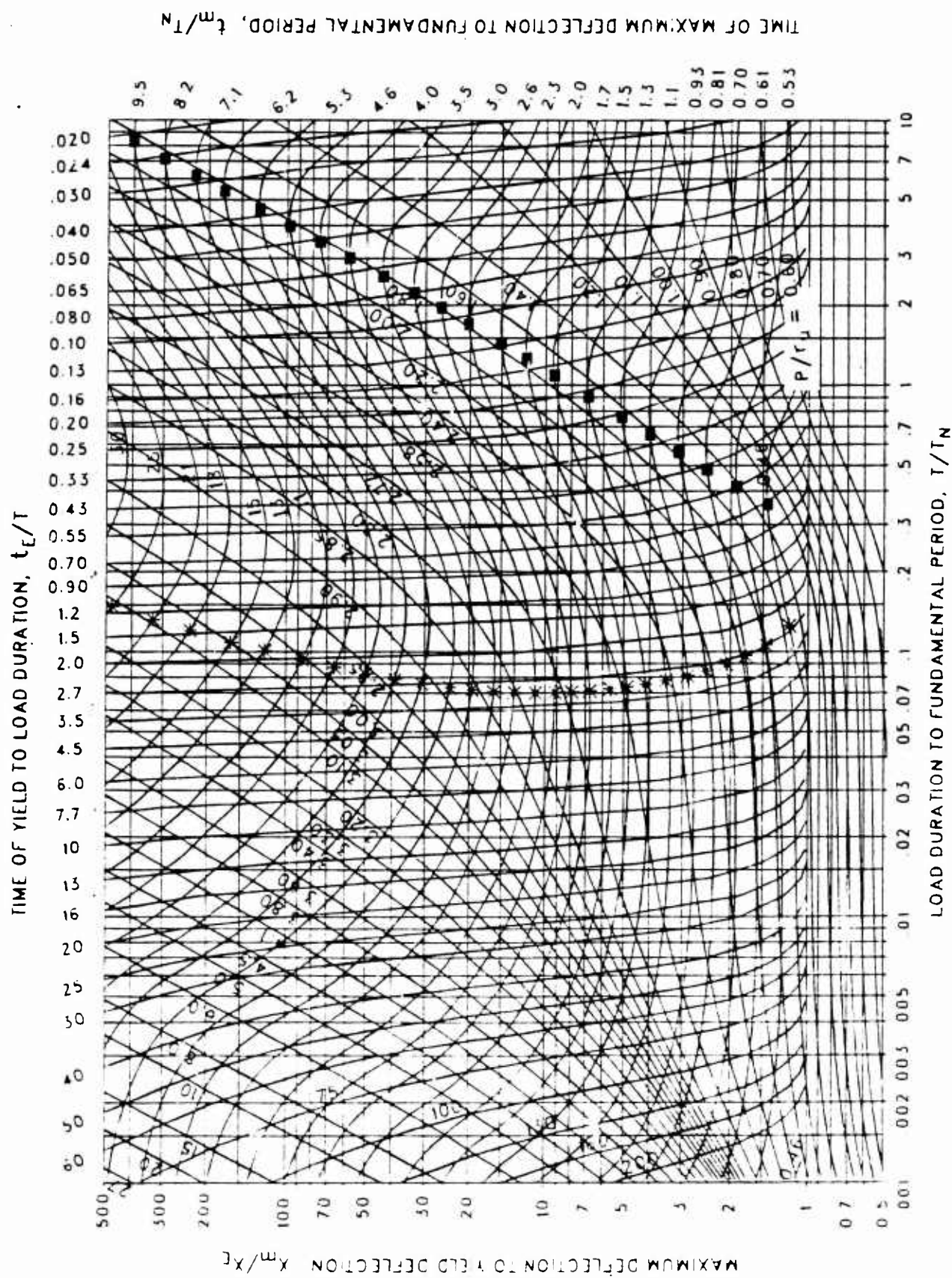
Figure 3-238 Maximum response of elasto-plastic, one-degree-of-freedom system for bilinear-triangular pulse ($C_1 = 0.348$, $C_2 = 1000.$)
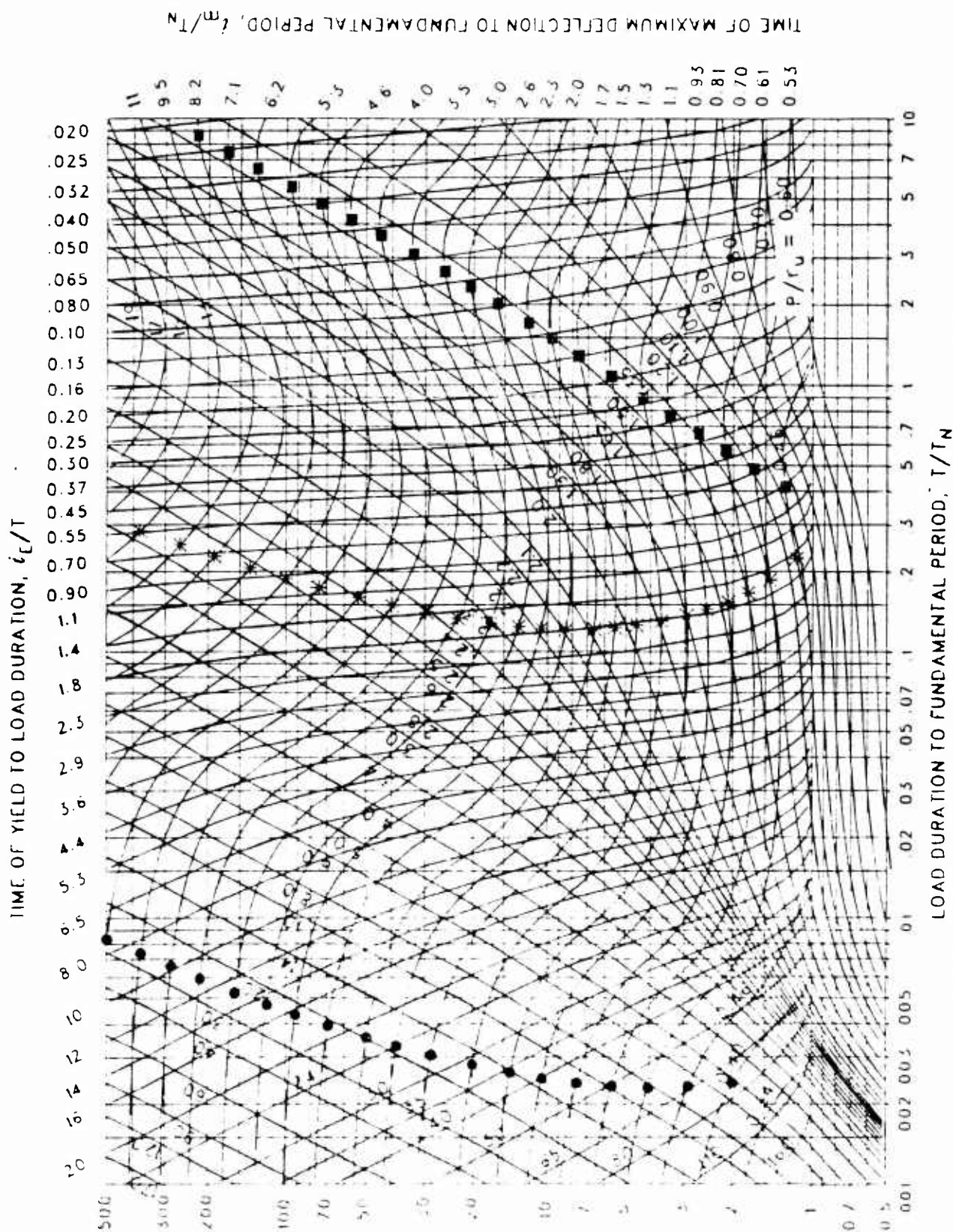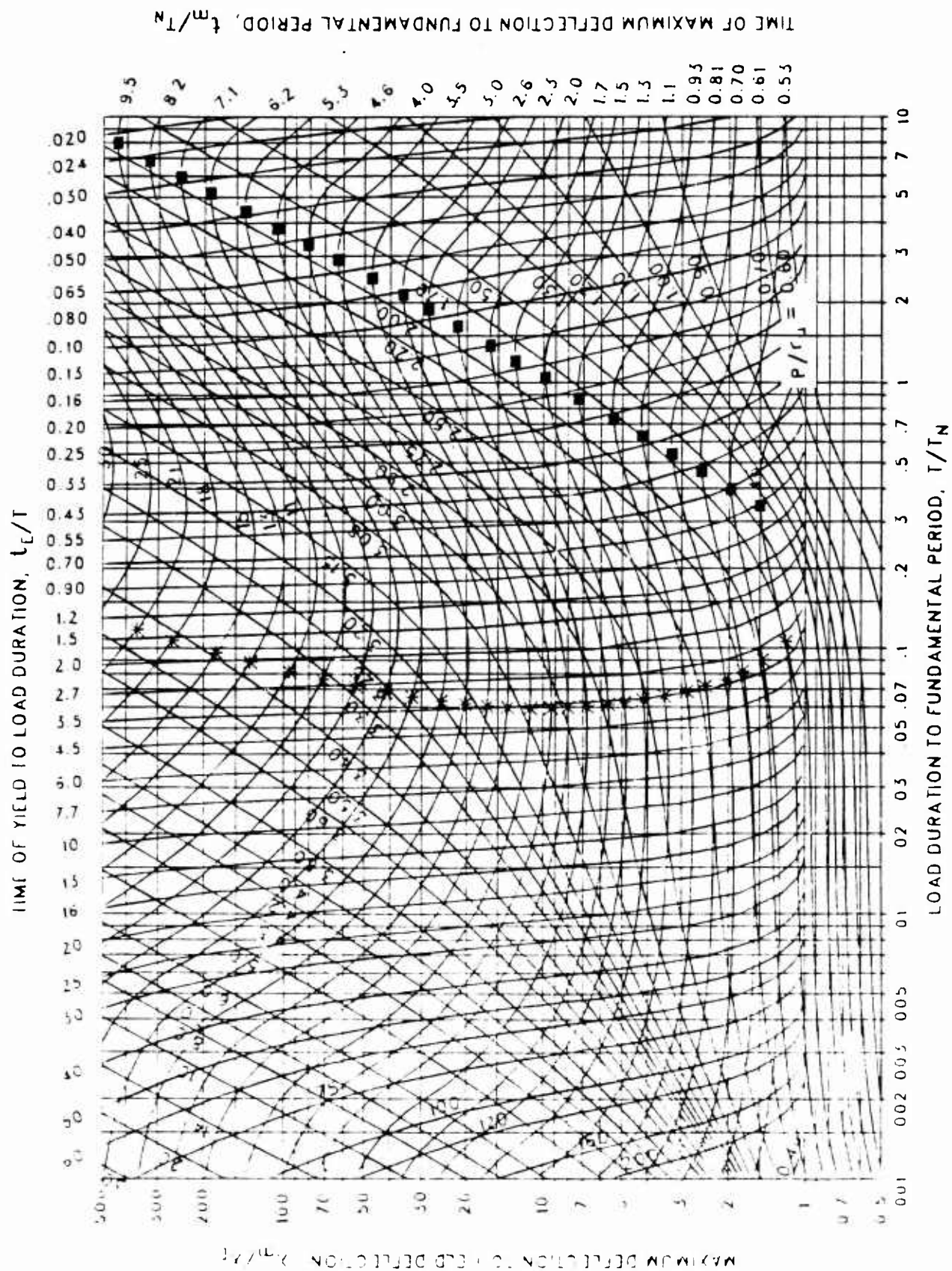
Figure 3-239   Maximum response of elasto-plastic, one-degree-of-freedom
              system for bilinear-triangular pulse (C_1 = 0.316, C_2 = 1000.)
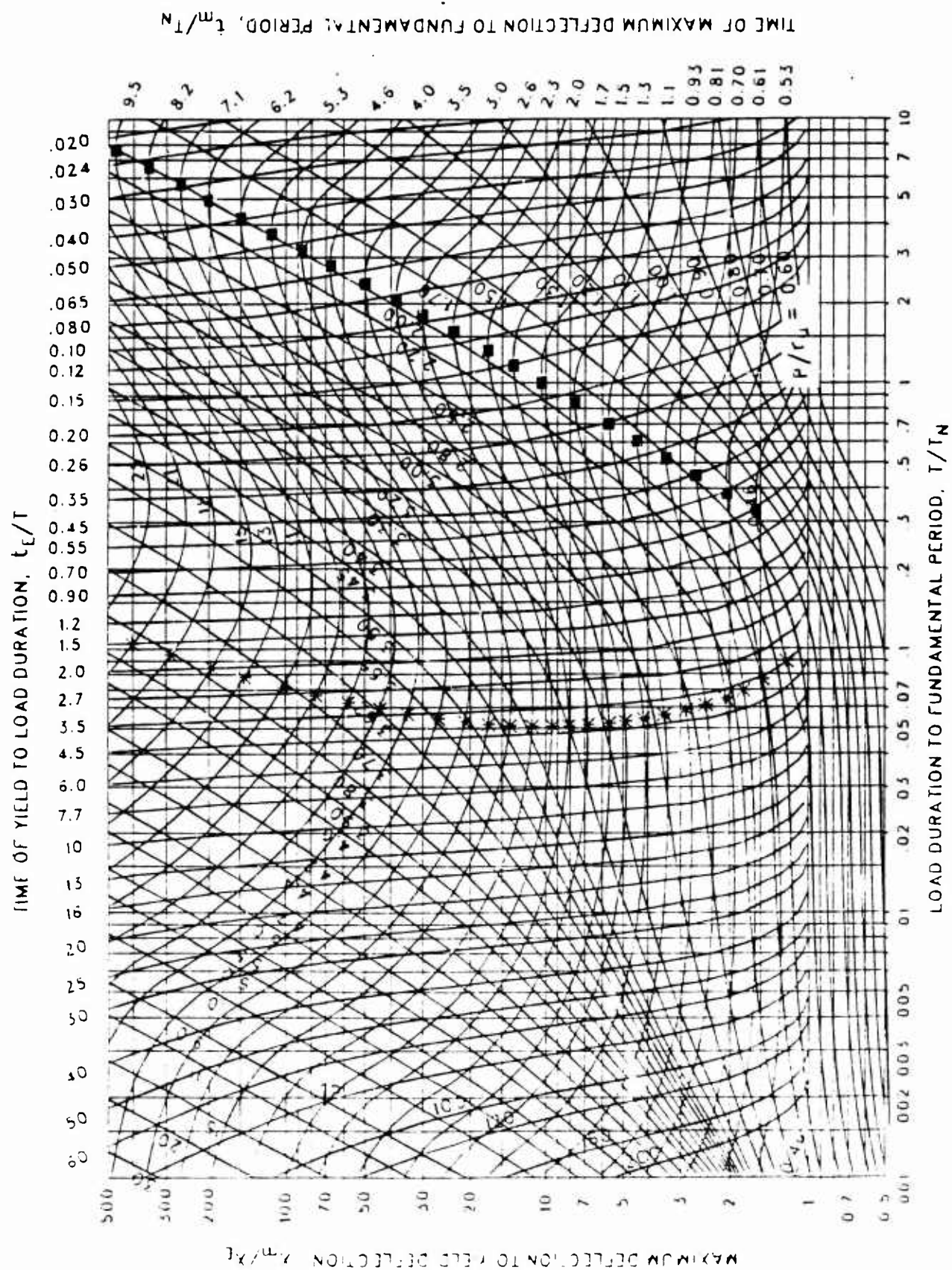
Figure 3-240 Maximum response of elasto-plastic, one-degree-of-freedom system for bilinear-triangular pulse ($C_1 = 0.287$, $C_2 = 1000.$)
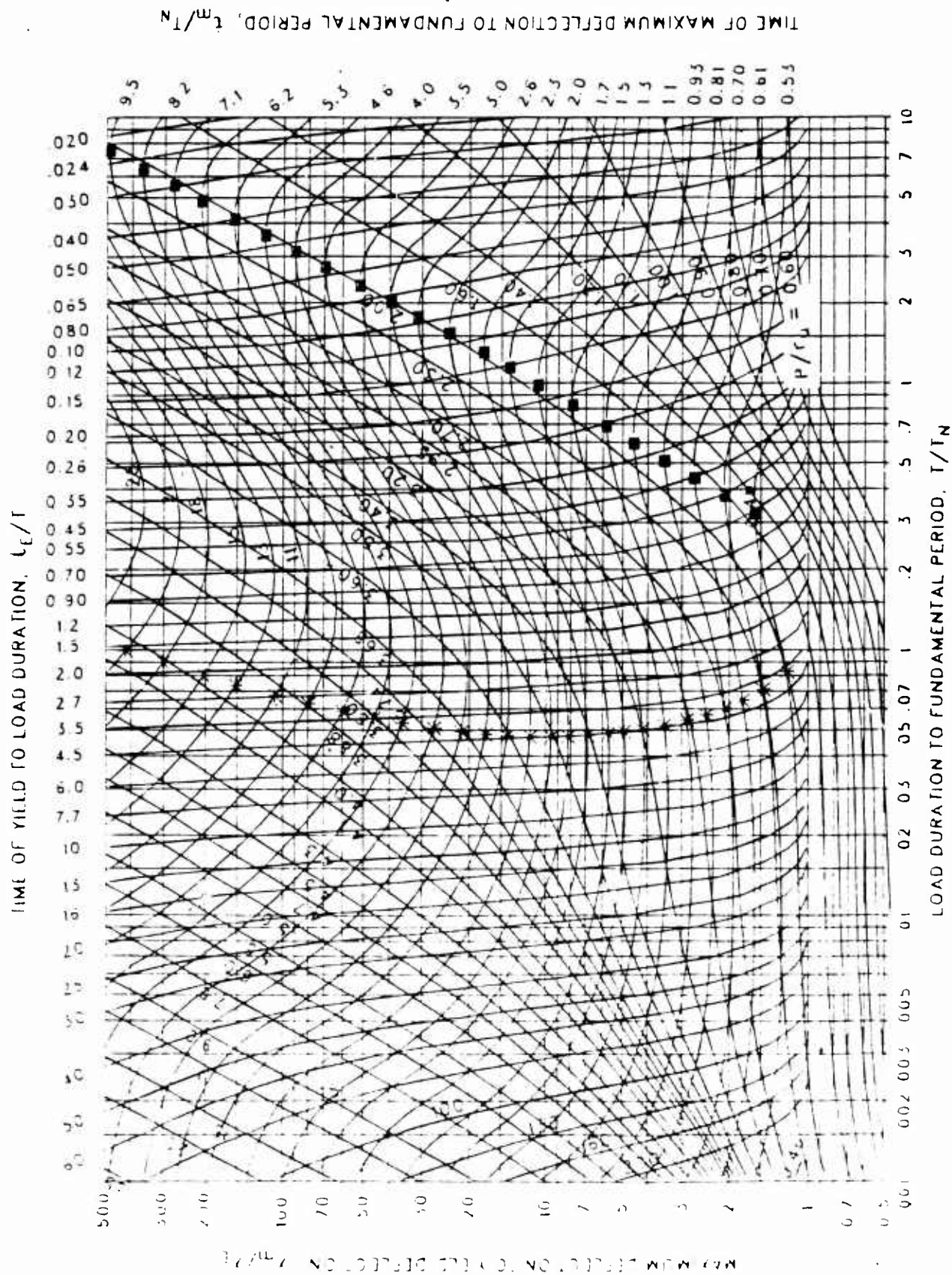
Figure 3-241 Maximum response of elasto-plastic, one-degree-of-freedom system for bilinear-triangular pulse ($C_1 = 0.274$, $C_2 = 1000.$)
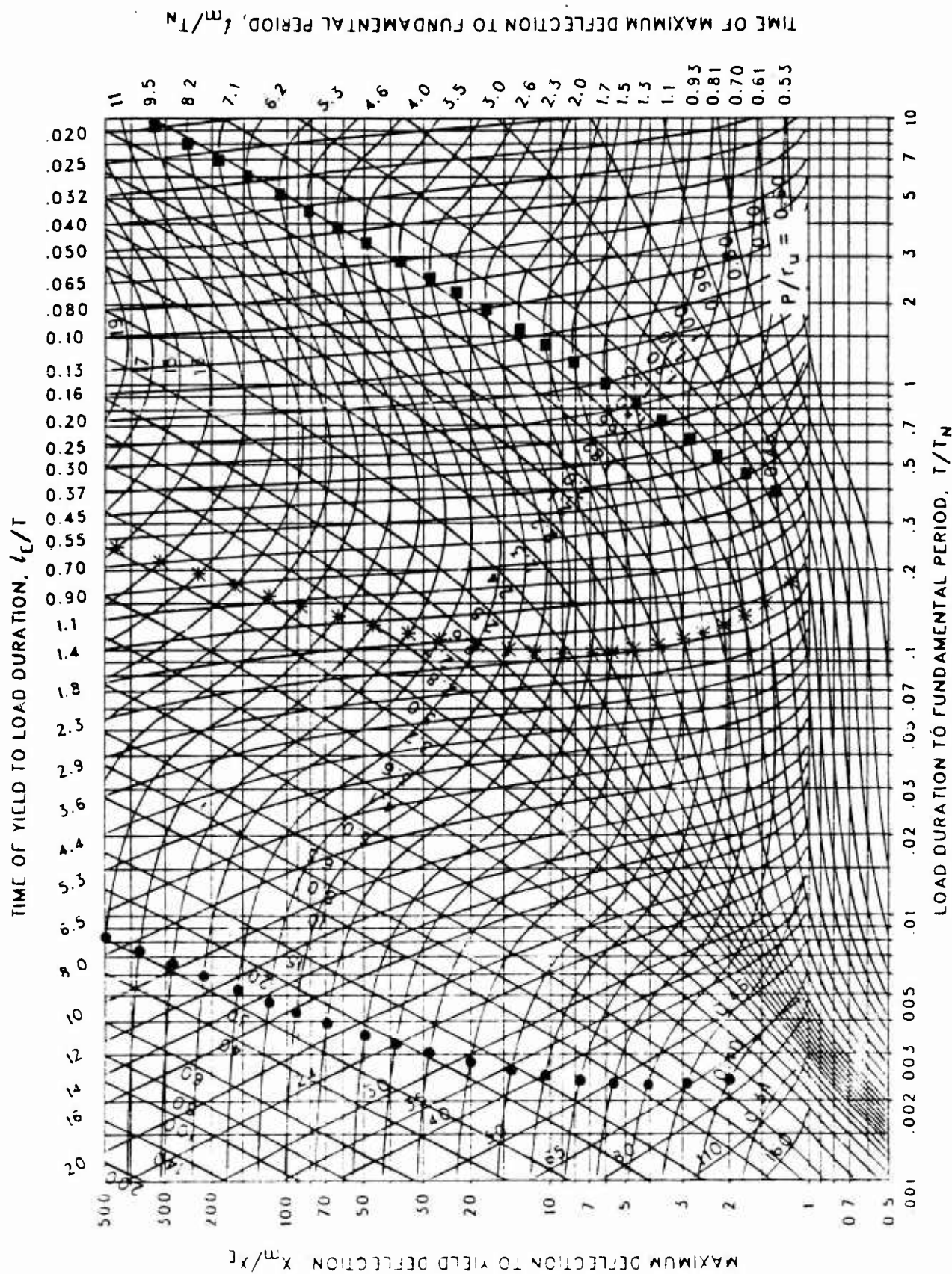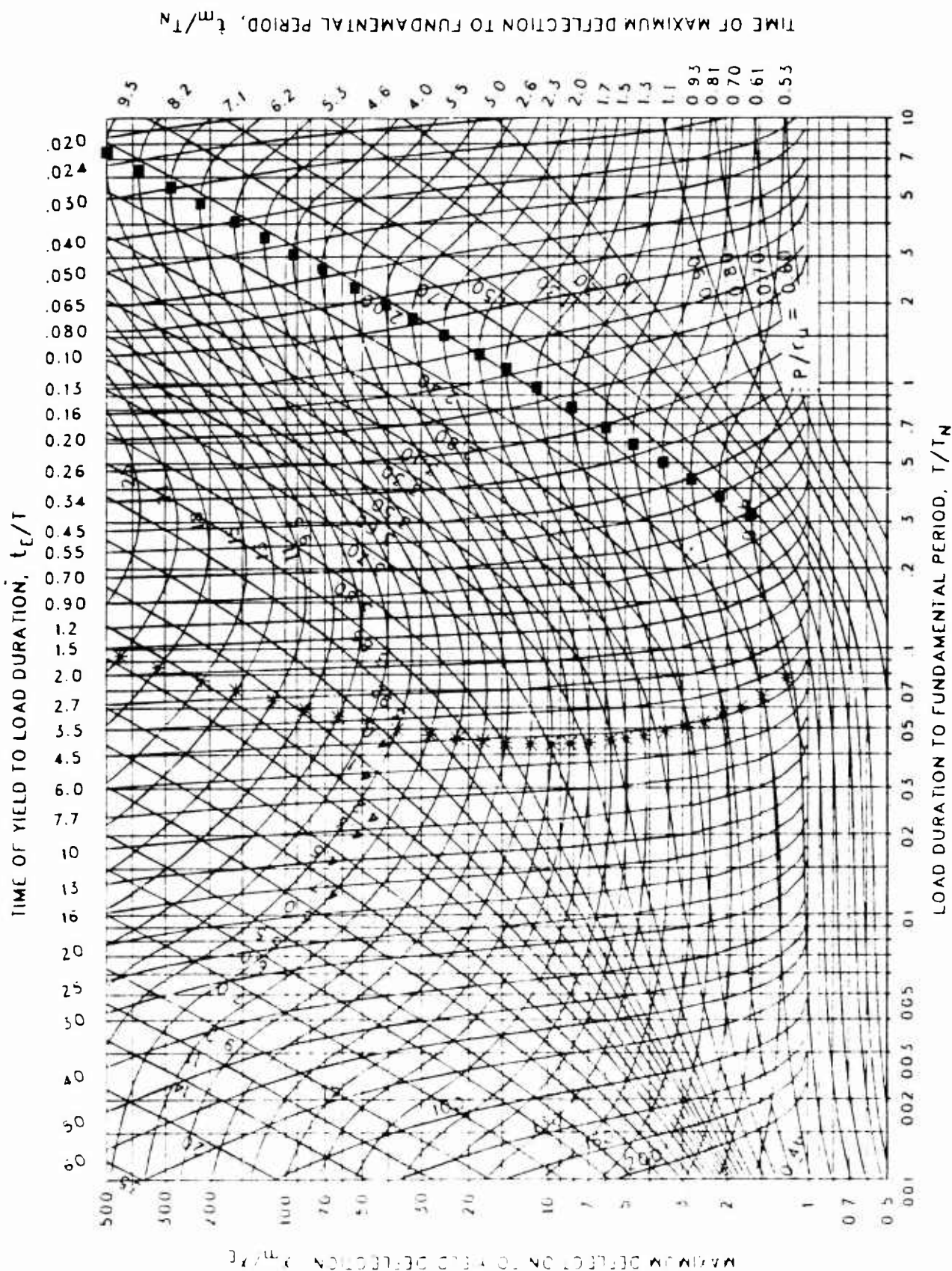
Figure 5-242   Maximum response of elasto-plastic, one-degree-of-freedom
system for bilinear-triangular pulse (C_1 = 0.261, C_2 = 1000.)
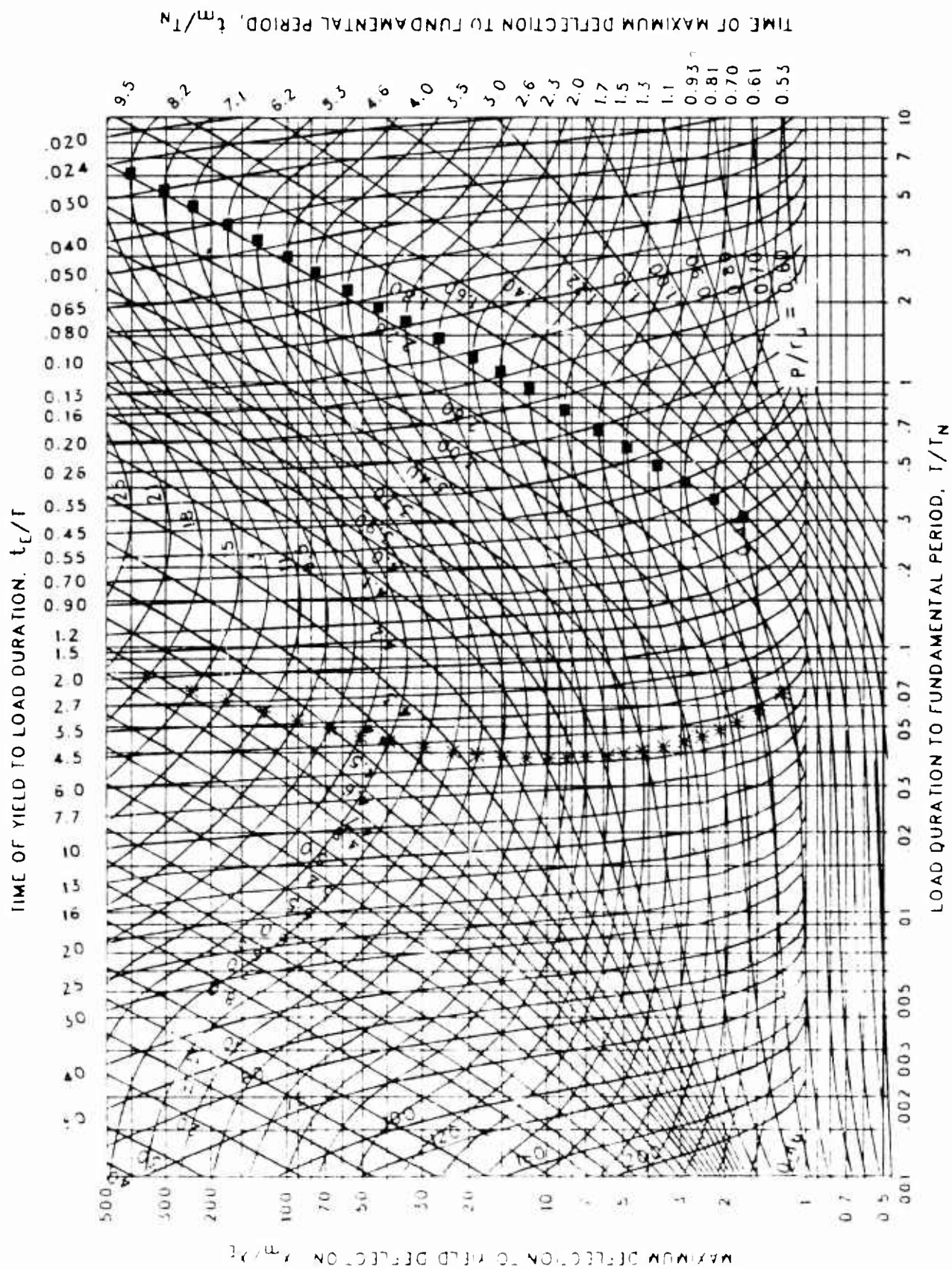
Figure 3-243 Maximum response of elasto-plastic, one-degree-of-freedom system for bilinear-triangular pulse ($C_1 = 0.237$, $C_2 = 1000$.)
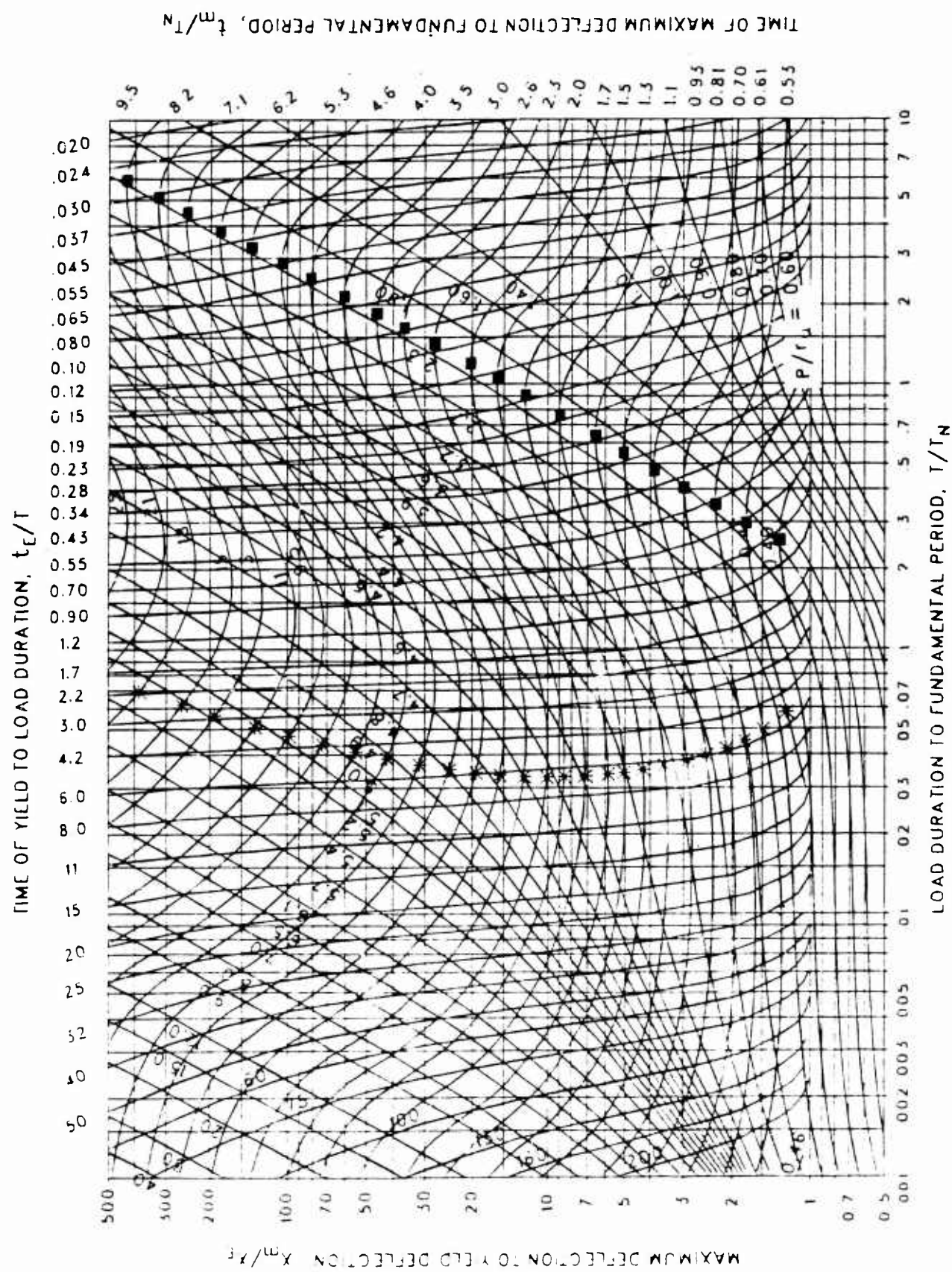
Figure 3-244   Maximum response of elasto-plastic, one-degree-of-freedom
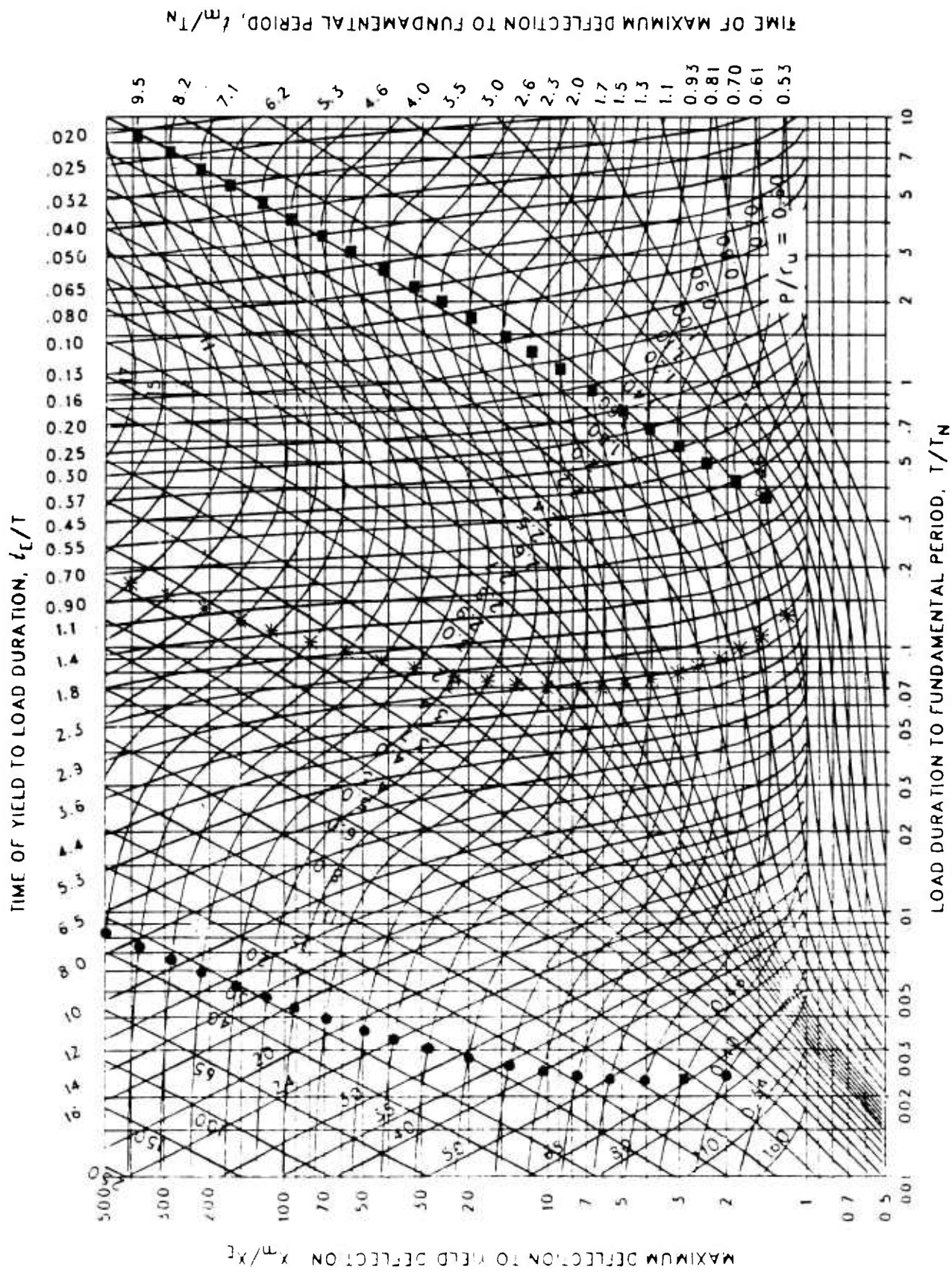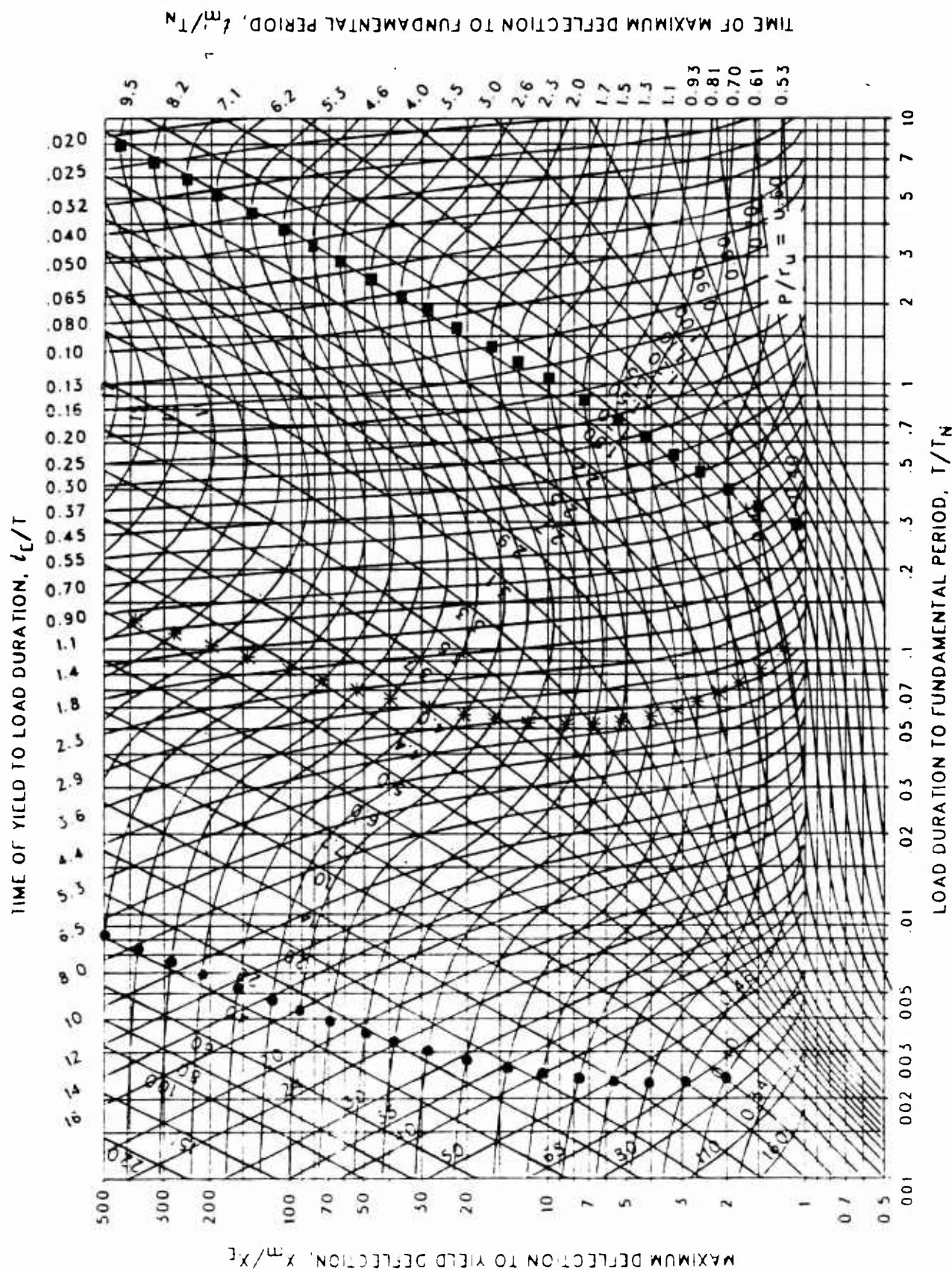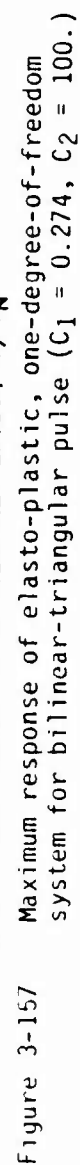system for bilinear-triangular pulse ($C_1 = 0.215$, $C_2 = 1000$.)
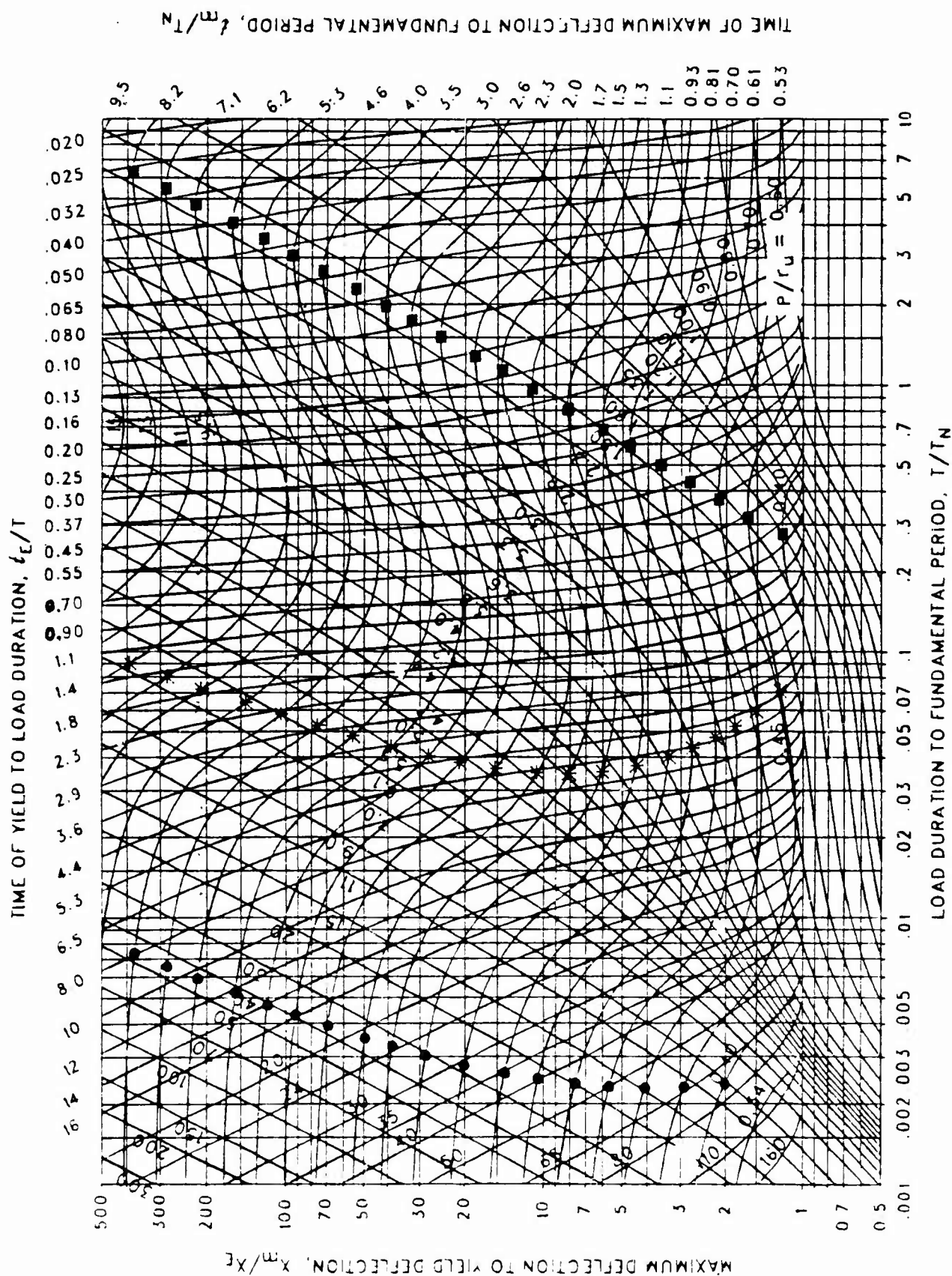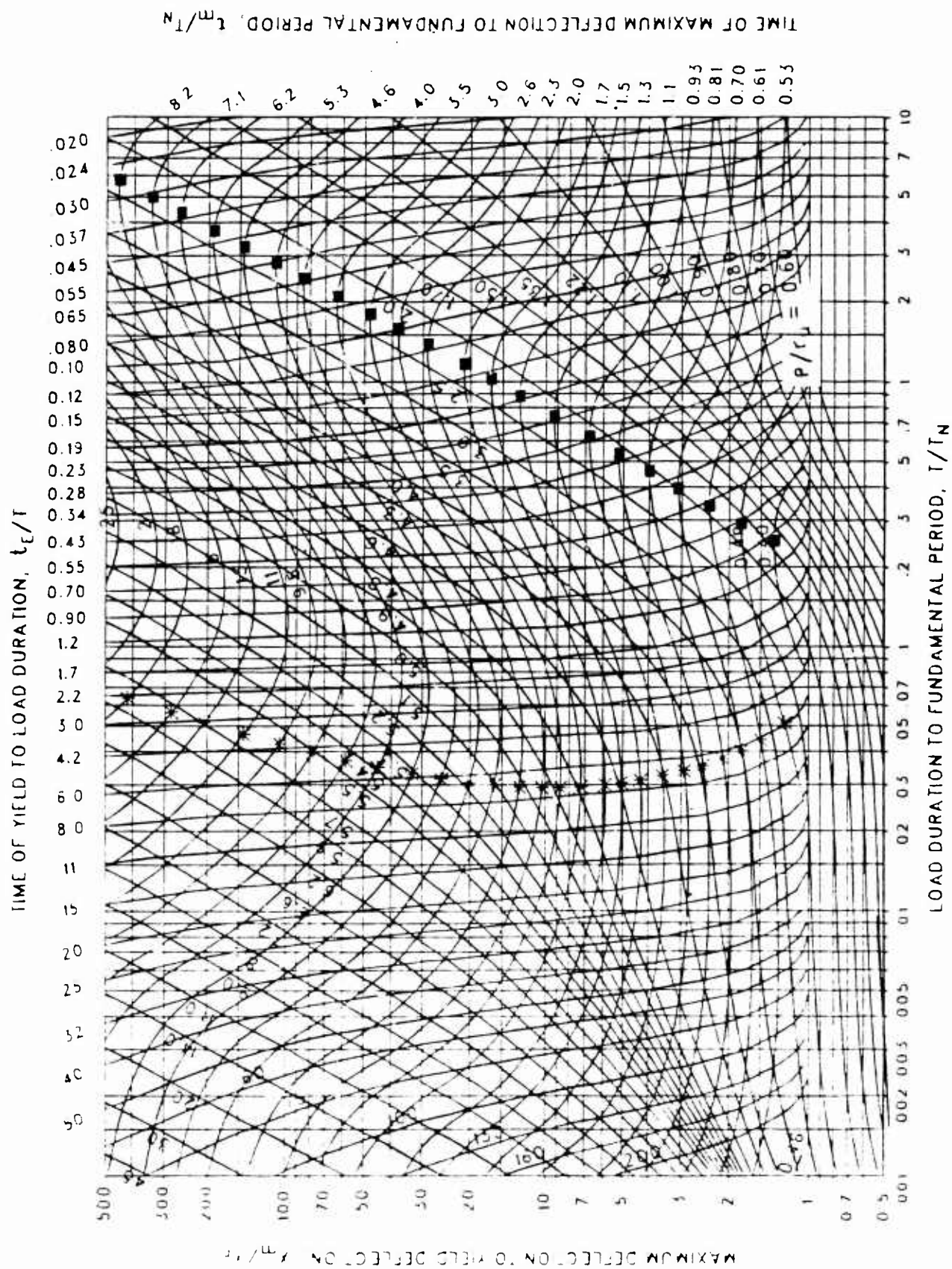
Figure 3-245   Maximum response of elasto-plastic, one-degree-of-freedom
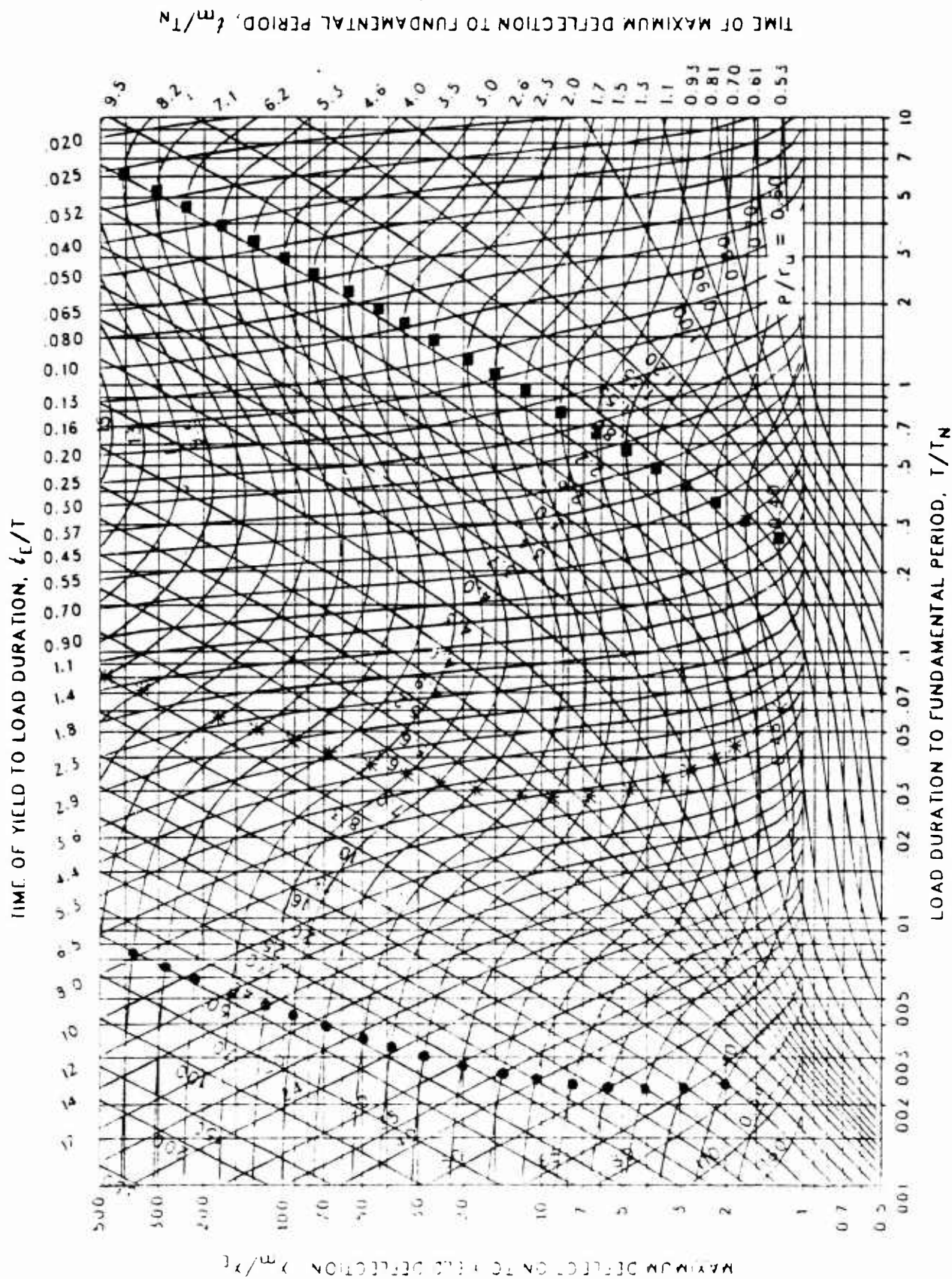system for bilinear-triangular pulse ($C_1 = 0.198$, $C_2 = 1000.$)
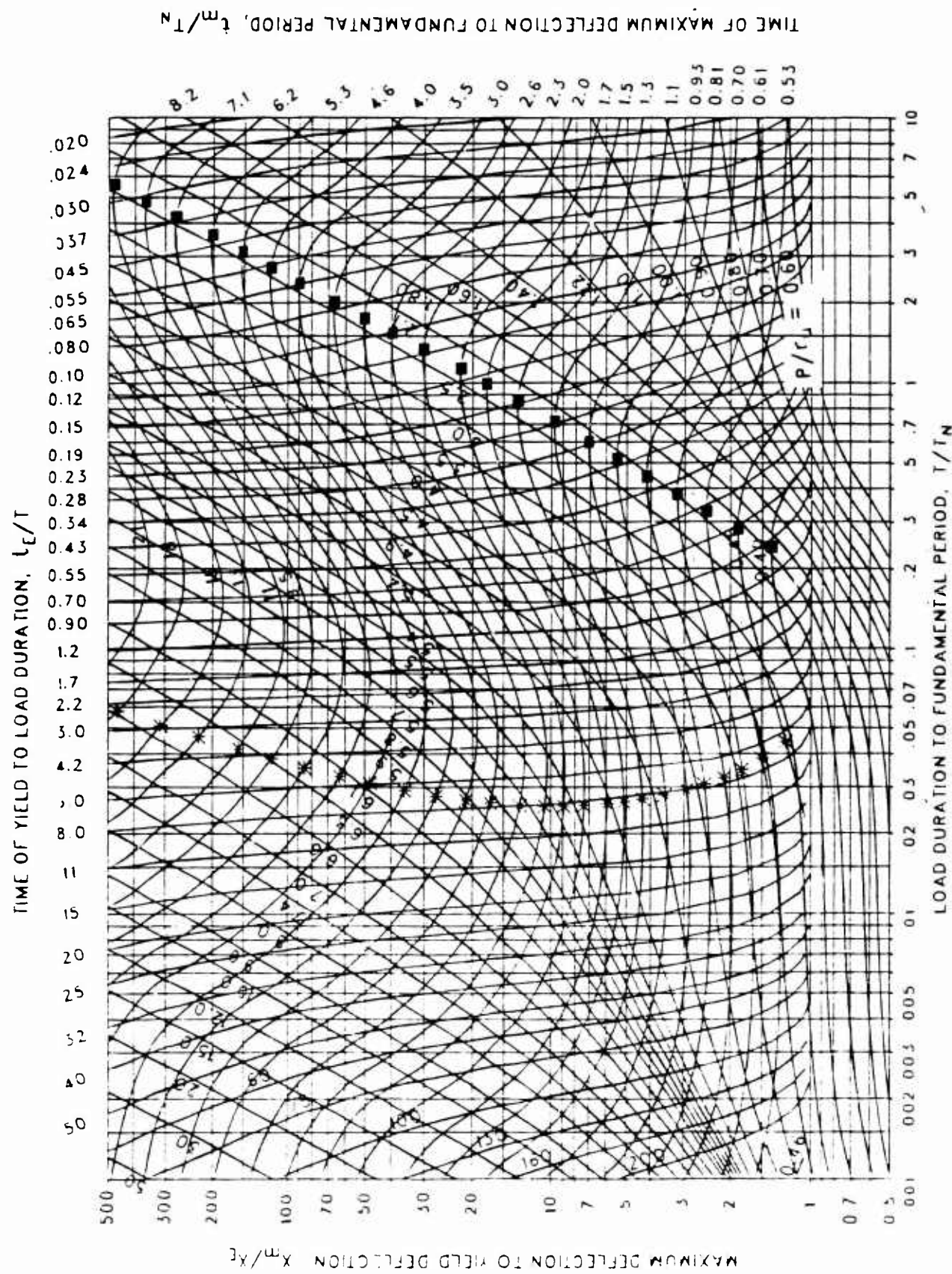
Figure 3-246   Maximum response of elasto-plastic, one-degree-of-freedom system for bilinear-triangular pulse ($C_1 = 0.178$, $C_2 = 1000.$)

TIME OF MAXIMUM DEFLECTION TO FUNDAMENTAL PERIOD, t_m/T_N

LOAD DURATION TO FUNDAMENTAL PERIOD, T/T_N
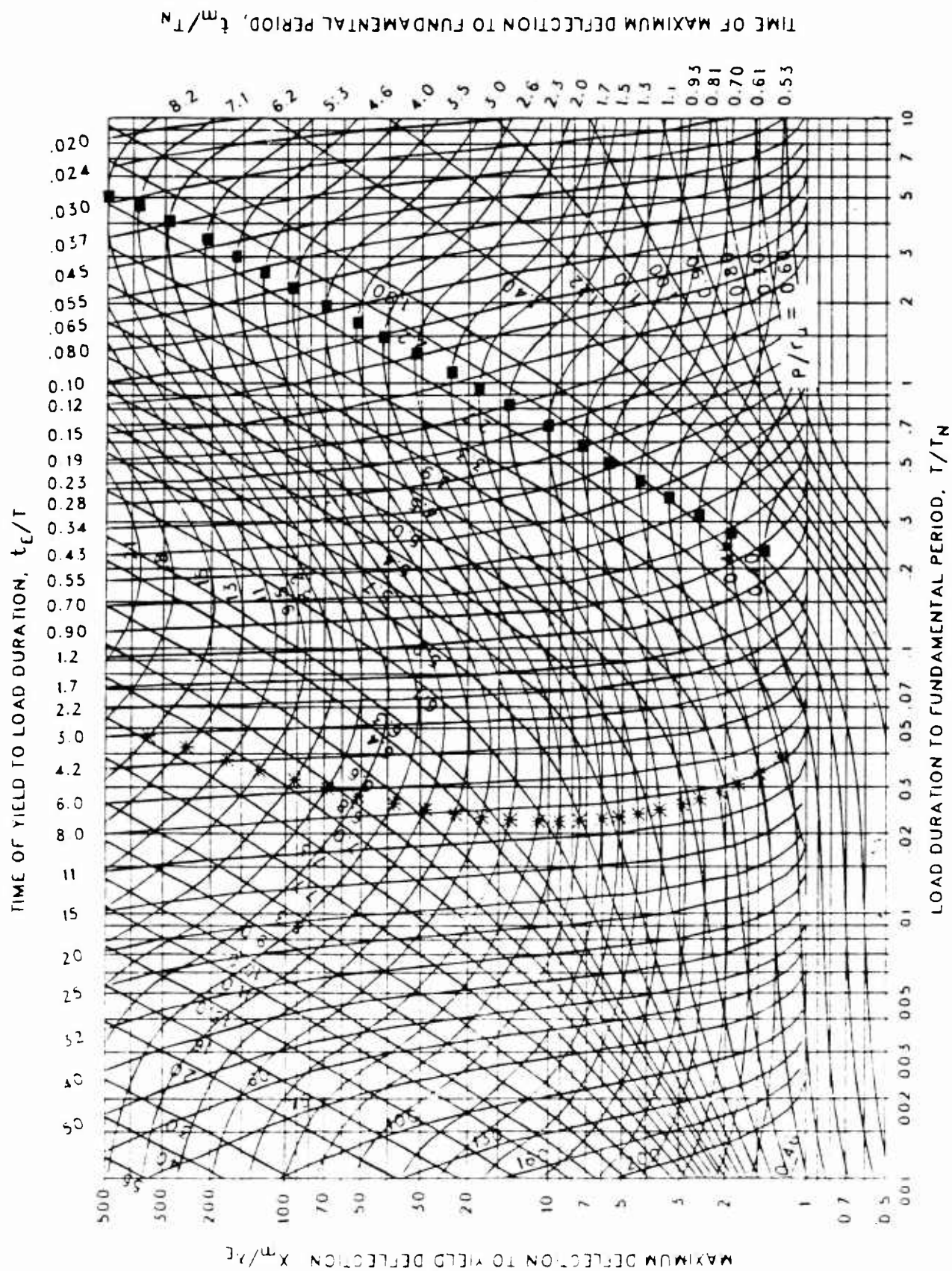
Figure 3-247   Maximum response of elasto-plastic, one-degree-of-freedom
system for bilinear-triangular pulse ($C_1 = 0.162$, $C_2 = 1000.$)

TIME OF YIELD TO LOAD DURATION, t_E/T

MAXIMUM DEFLECTION TO YIELD DEFLECTION X_m/x_E
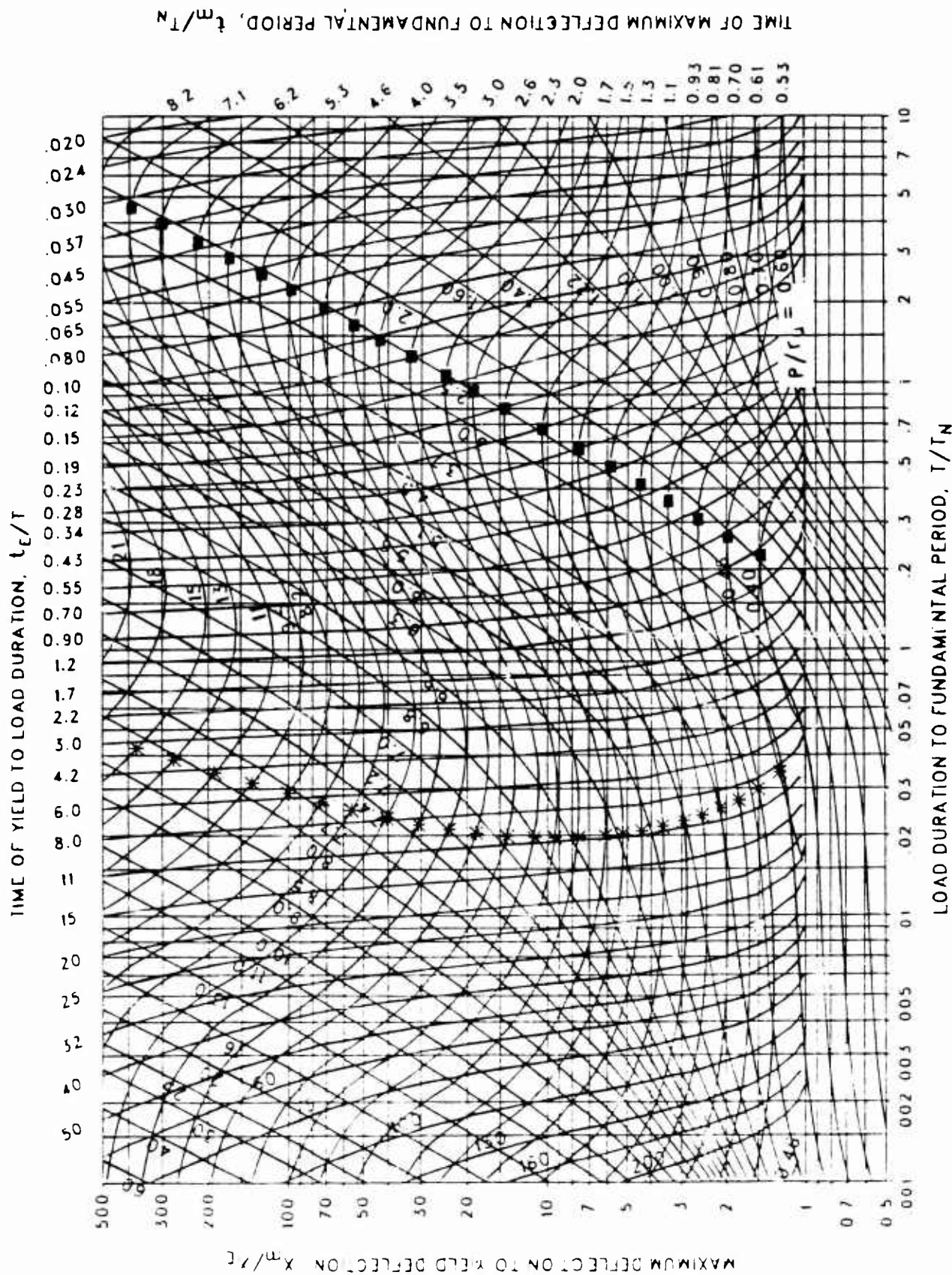
Figure 3-248   Maximum response of elastic-plastic, one-degree-of-freedom system for bilinear-triangular pulse ($C_1 = 0.147$, $C_2 = 1000.$)

-303-
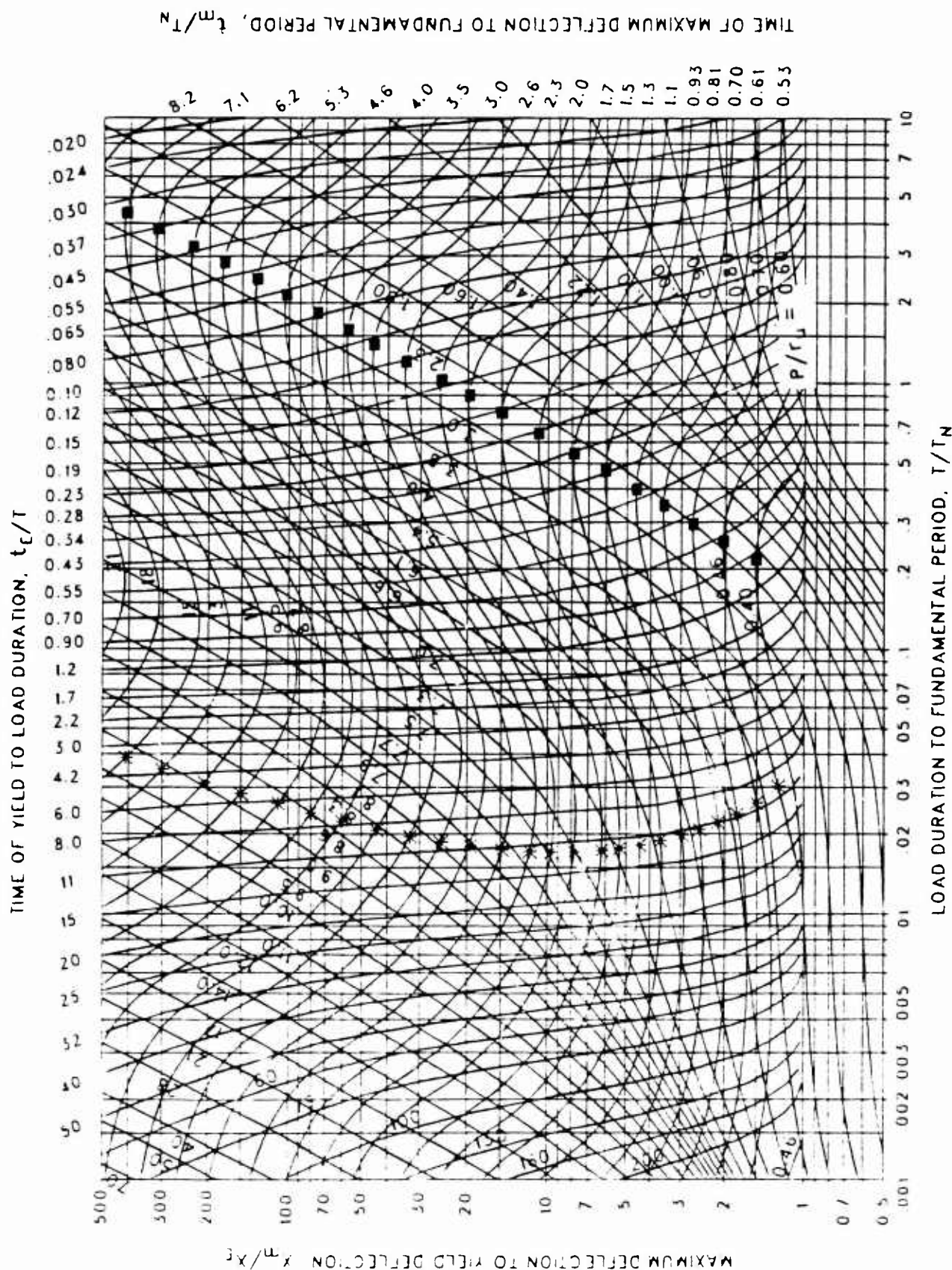
Figure 3-249   Maximum response of elasto-plastic, one-degree-of-freedom
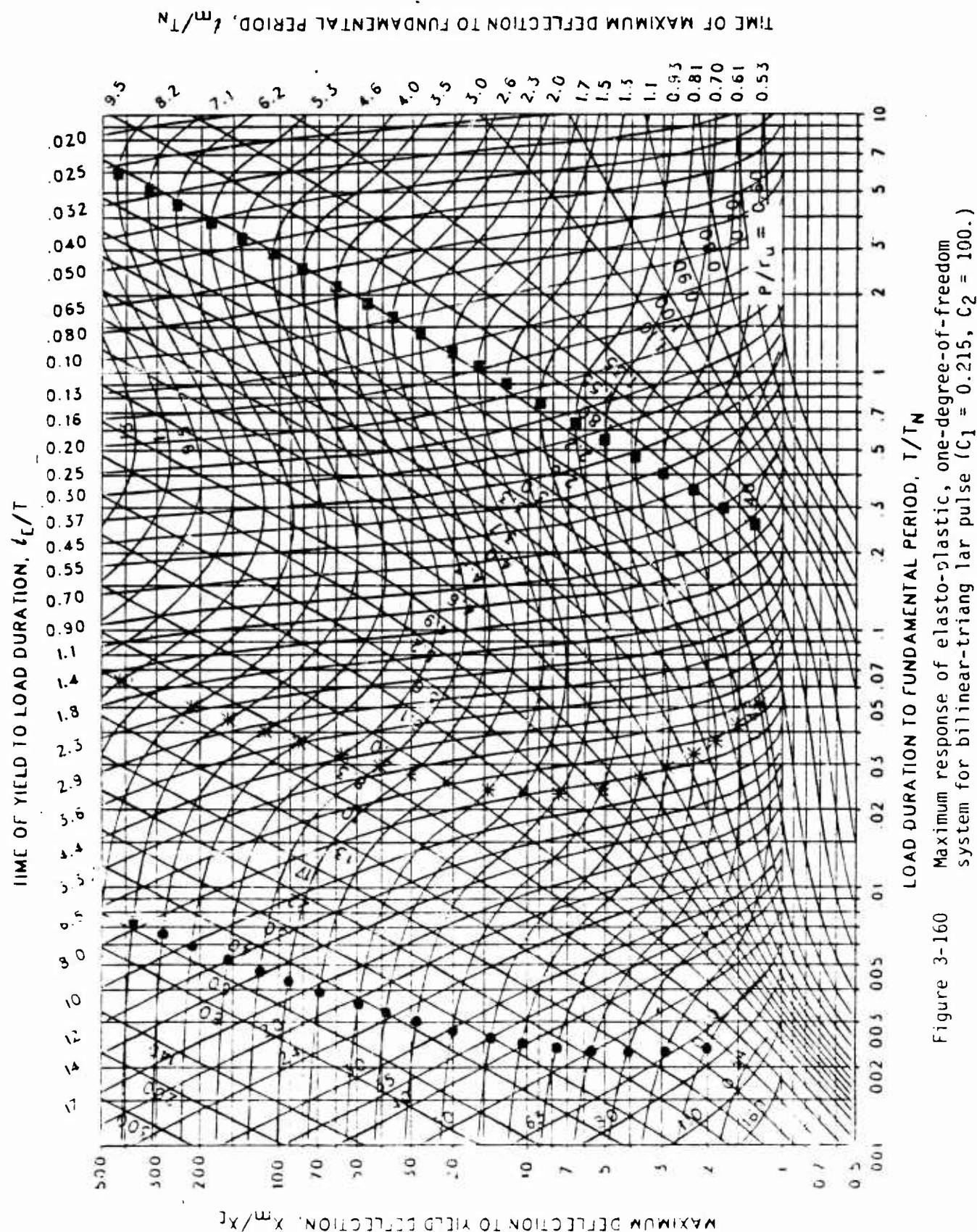system for bilinear-triangular pulse ($C_1 = 0.133$, $C_2 = 1000.$)

-304-
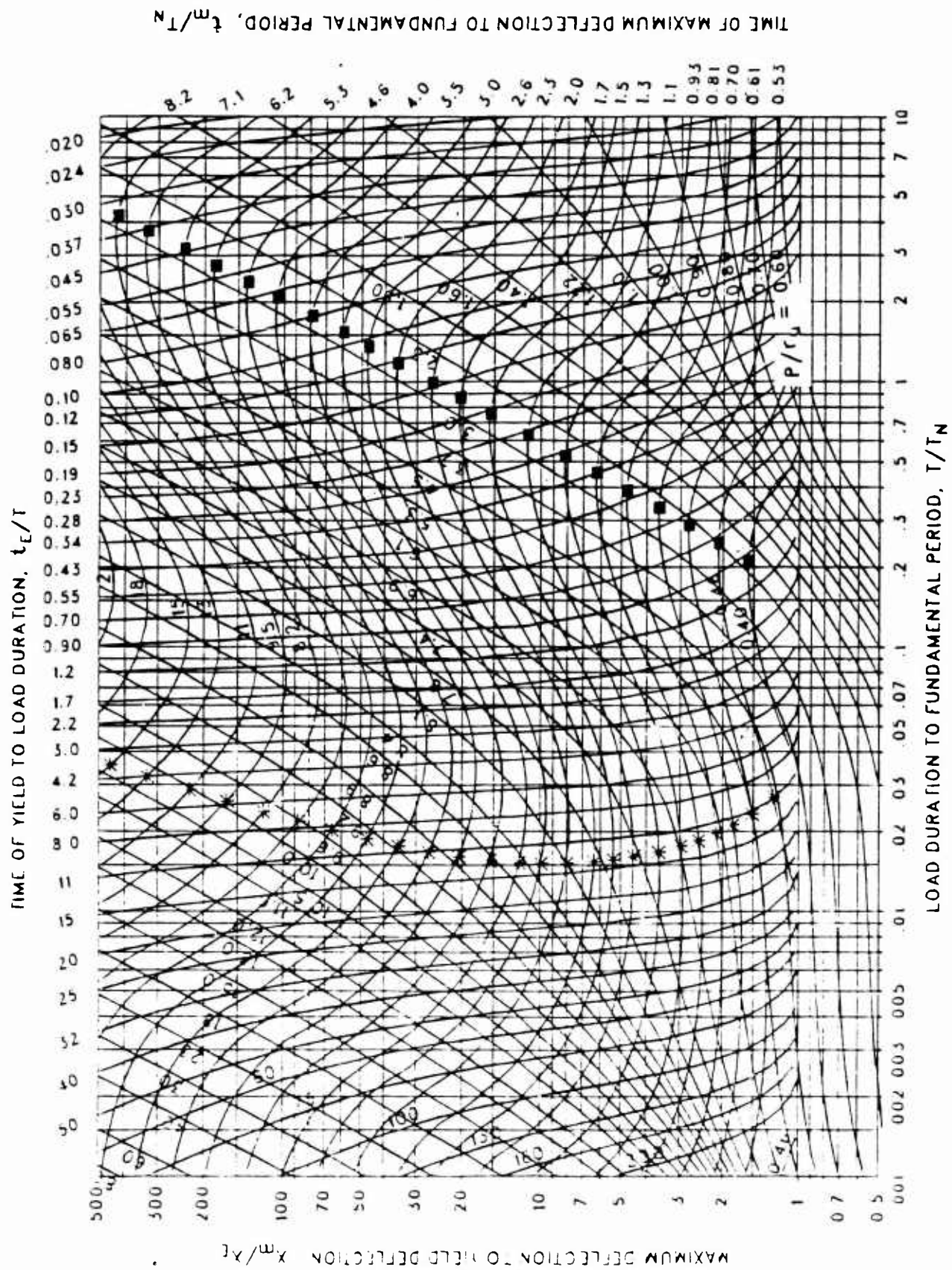
Figure 3-250 Maximum response of elasto-plastic, one-degree-of-freedom system for bilinear-triangular pulse ($C_1 = 0.121$, $C_2 = 1000.$)
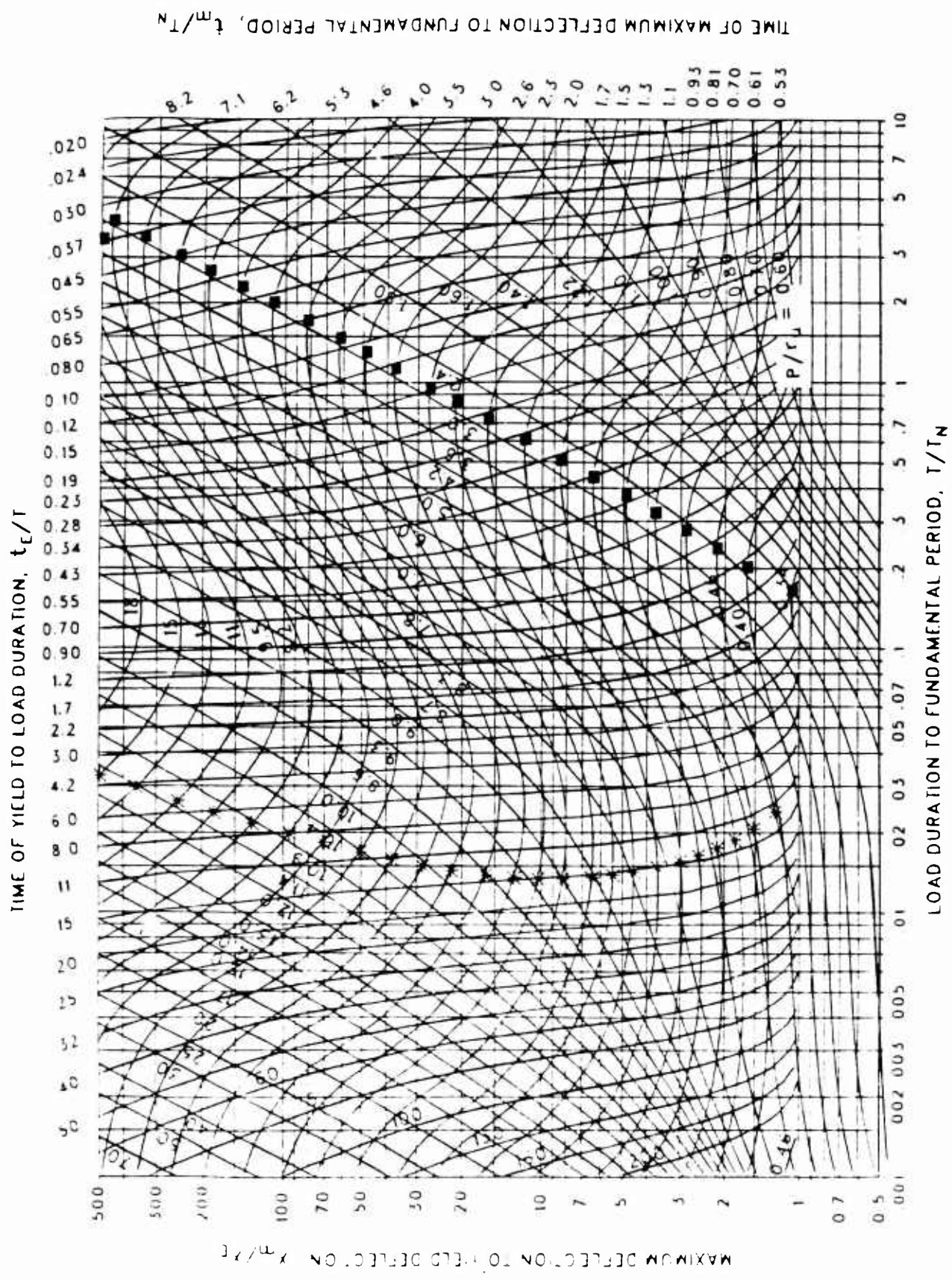
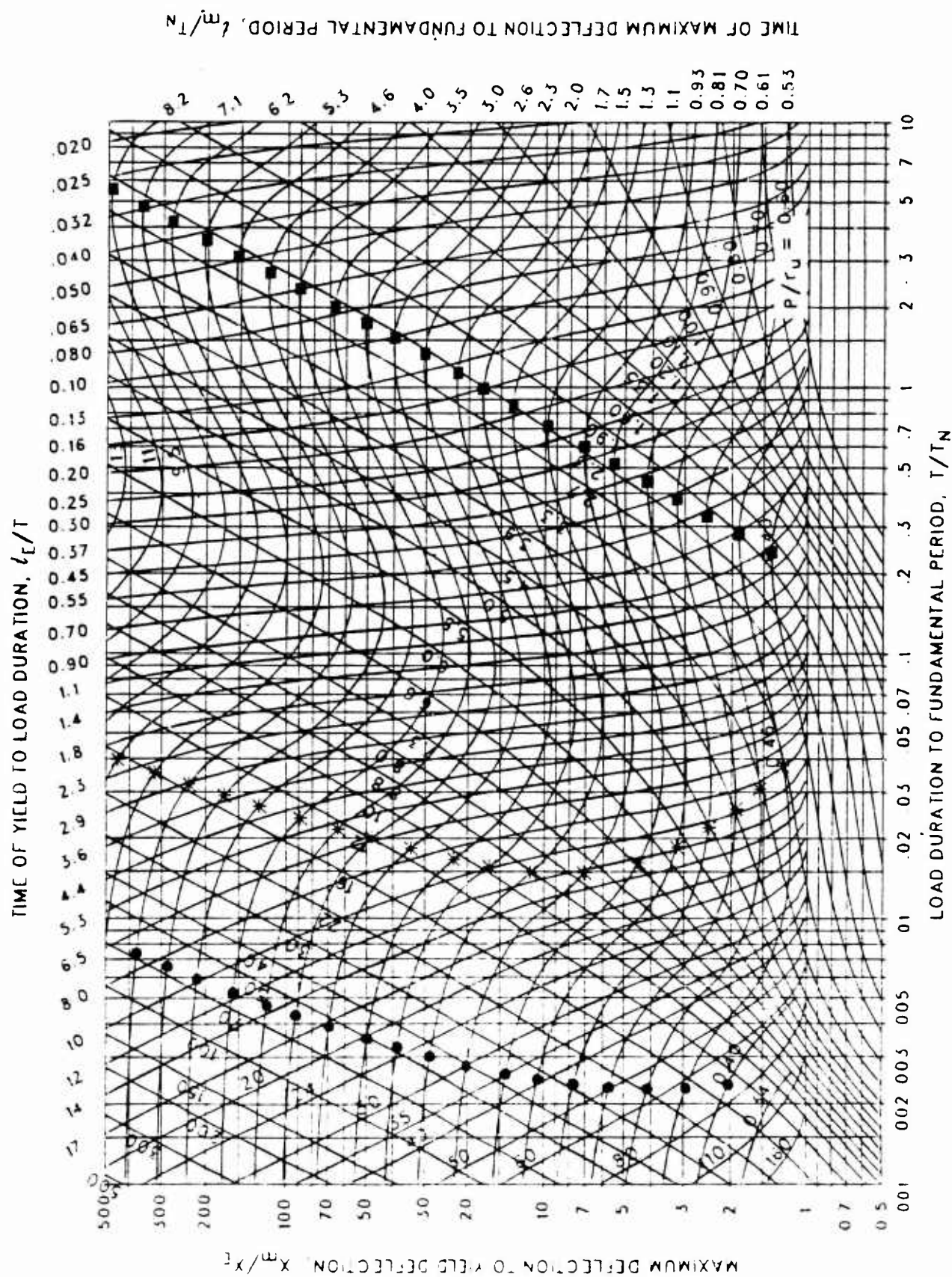Figure 3-251 Maximum response of elasto-plastic, one-degree-of-freedom system for bilinear-triangular pulse ($C_1 = 0.110$, $C_2 = 1000.$)
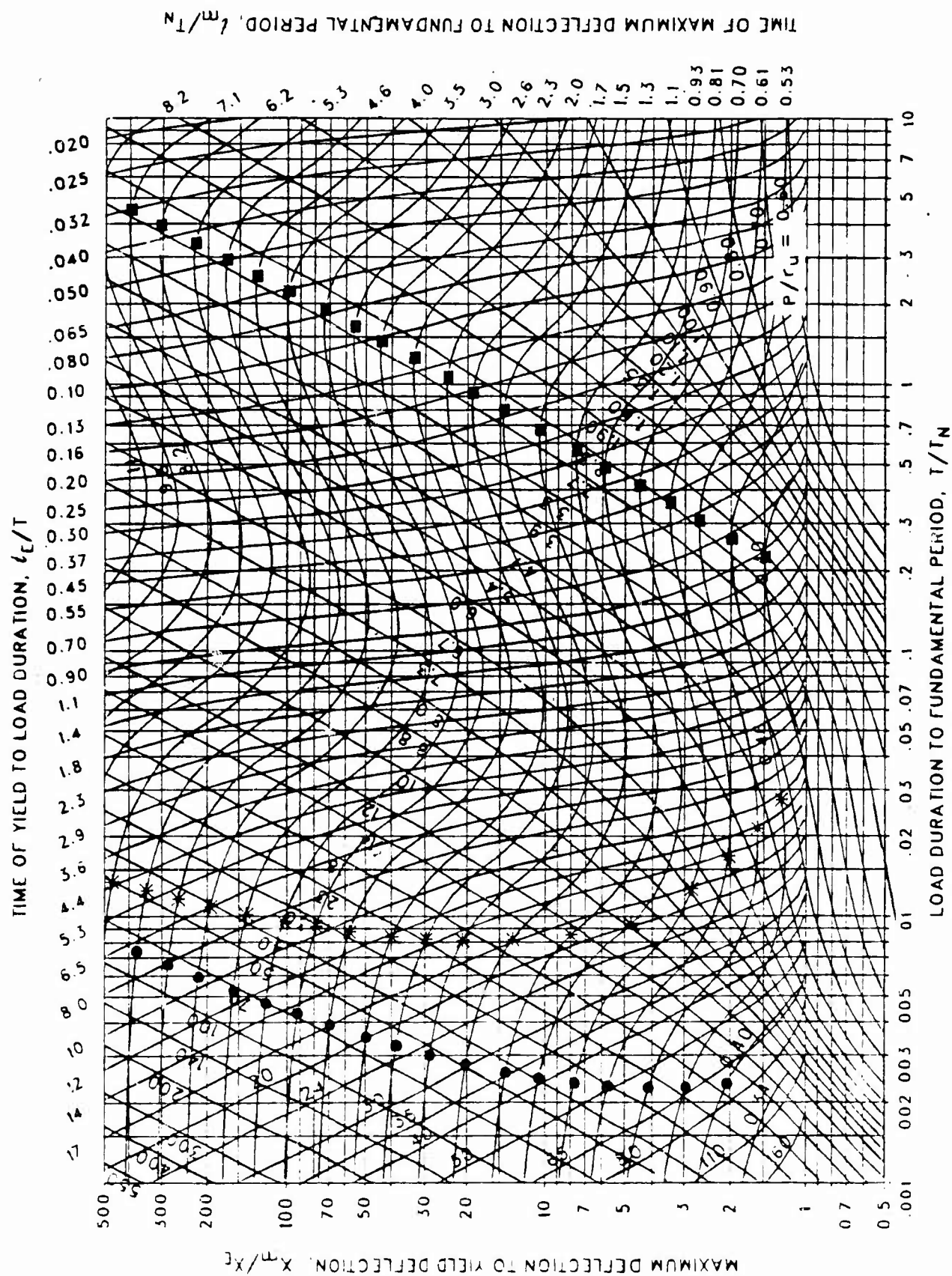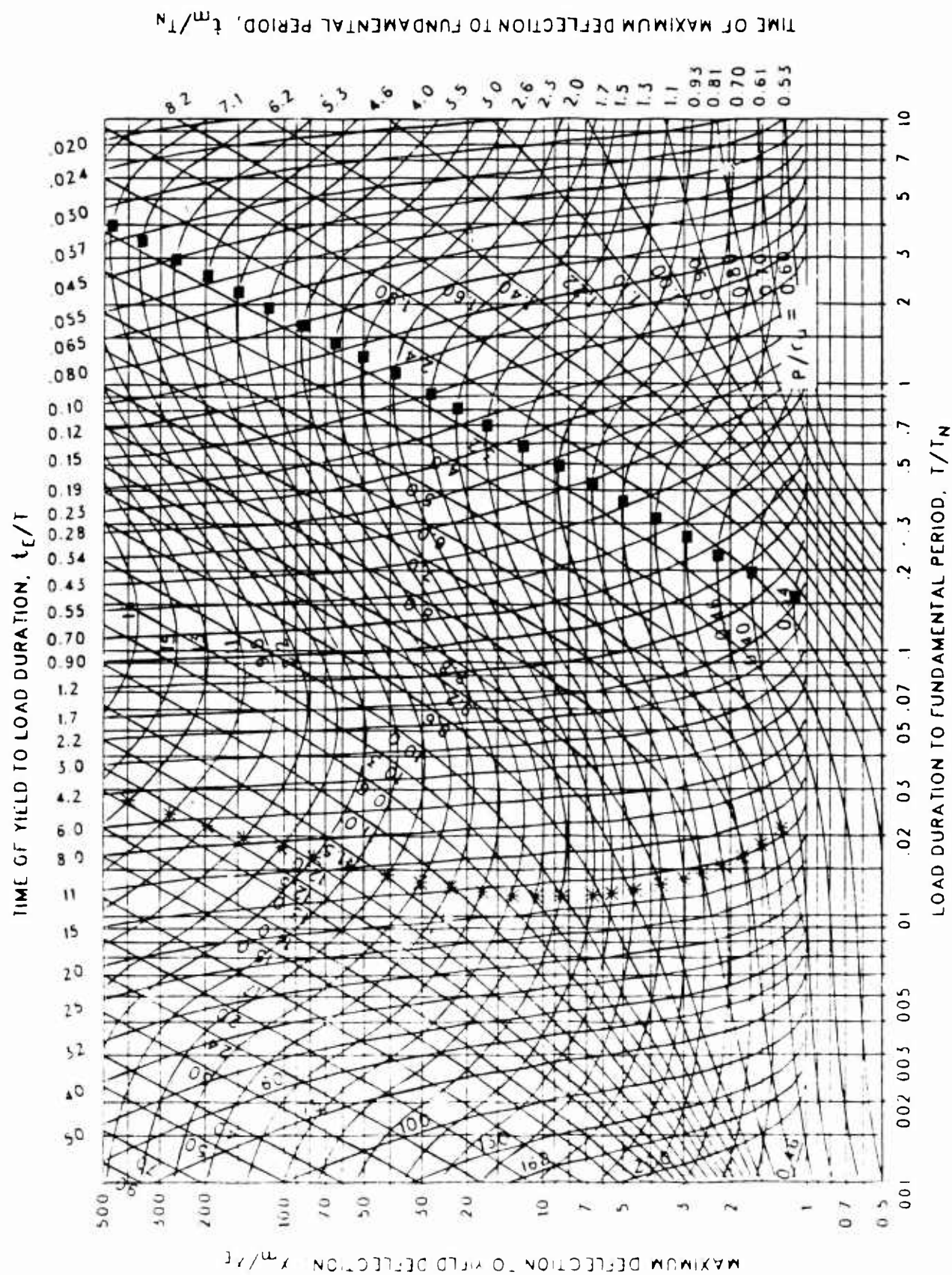
Figure 3-252   Maximum response of elasto-plastic, one-degree-of-freedom
system for bilinear-triangular pulse ($C_1 = 0.100$, $C_2 = 1000.$)
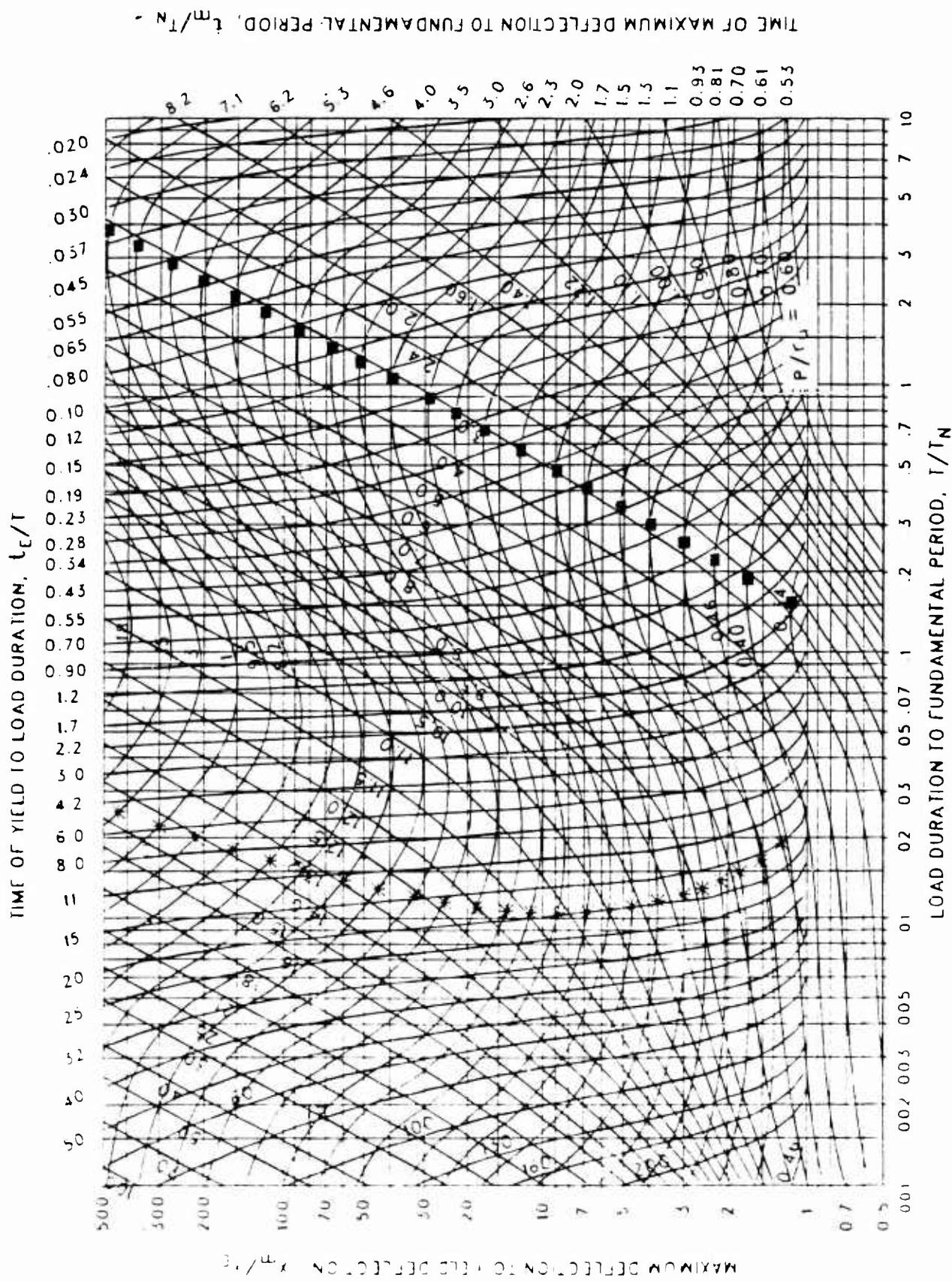
Figure 3-253   Maximum response of elasto-plastic, one-degree-of-freedom system for bilinear-triangular pulse ($C_1 = 0.091$, $C_2 = 1000.$)
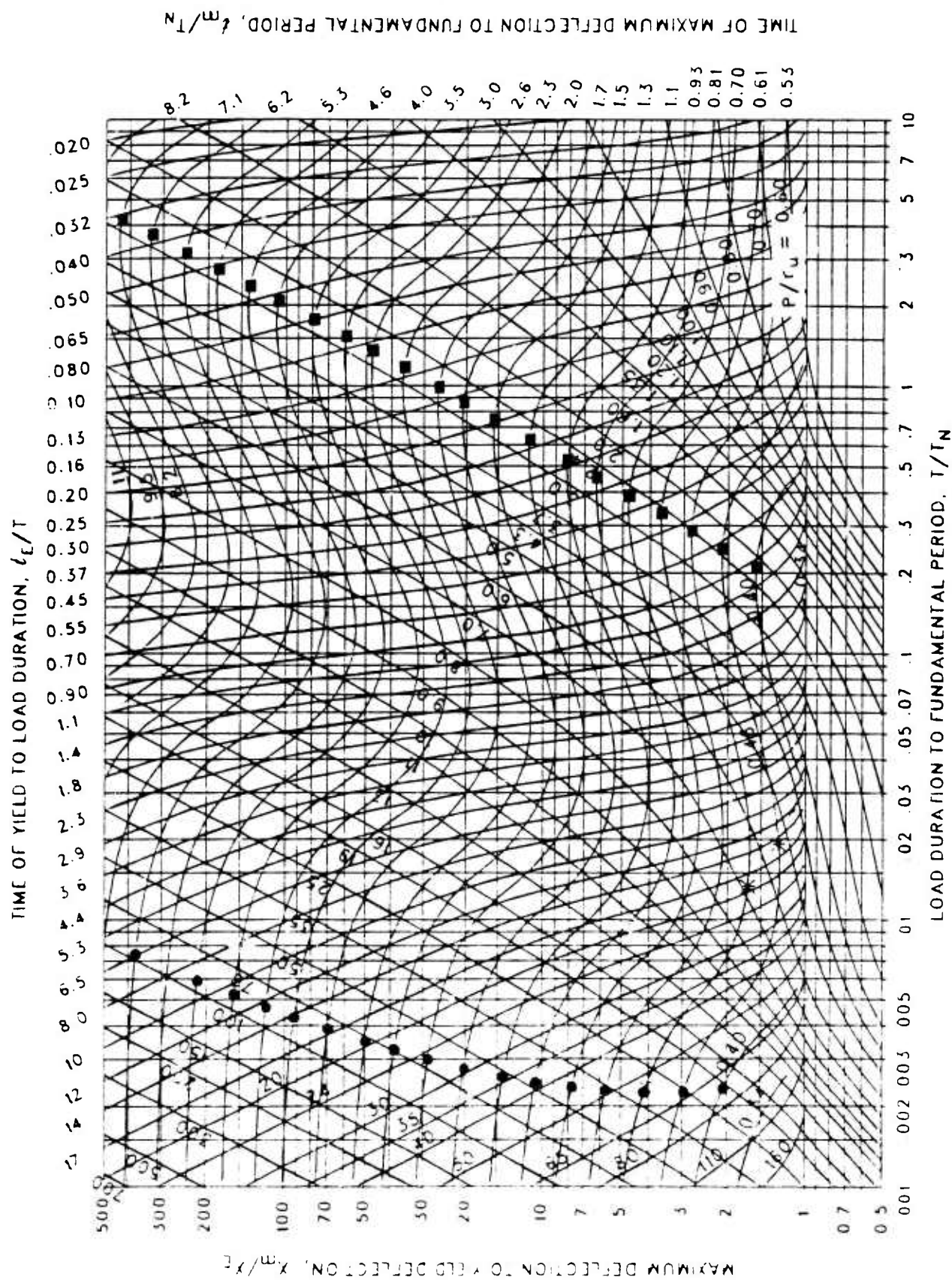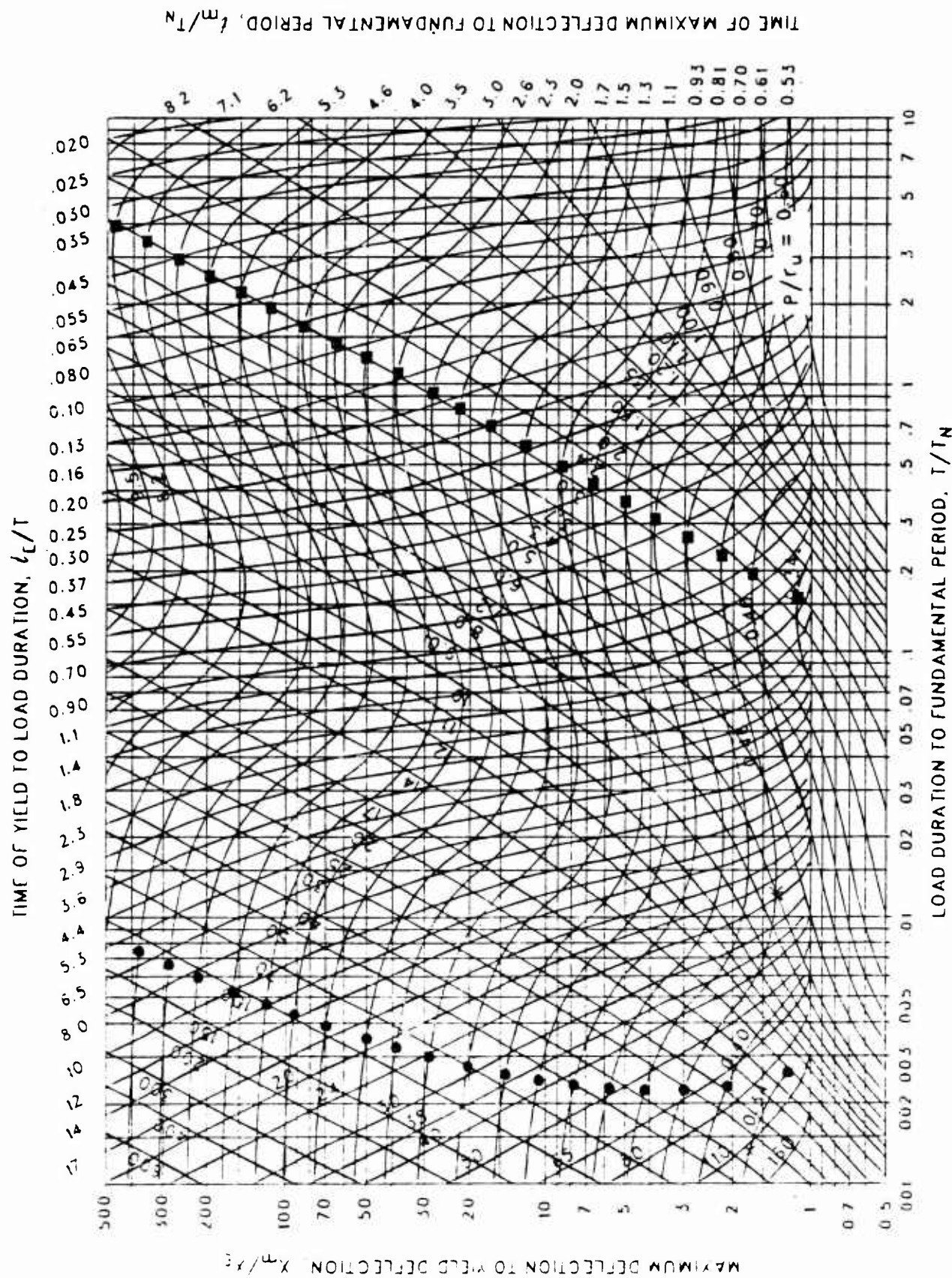
Figure 3-254   Maximum response of elasto-plastic, one-degree-of-freedom system for bilinear-triangular pulse ($C_1 = 0.083$, $C_2 = 1000.$)
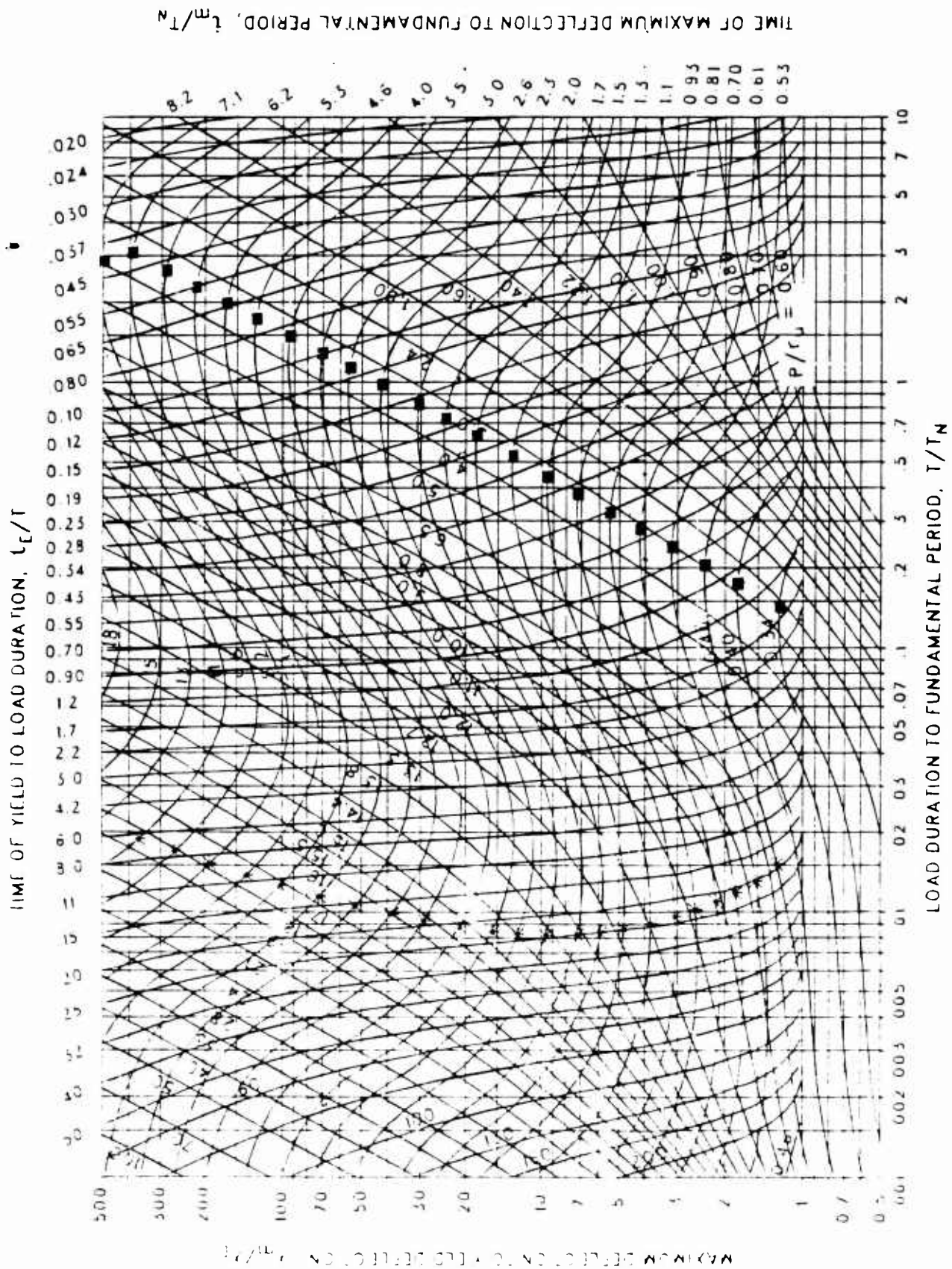
Figure 3-255 Maximum response of elasto-plastic, one-degree-of-freedom system for bilinear-triangular pulse ($C_1 = 0.075$, $C_2 = 1000.$)

-310-
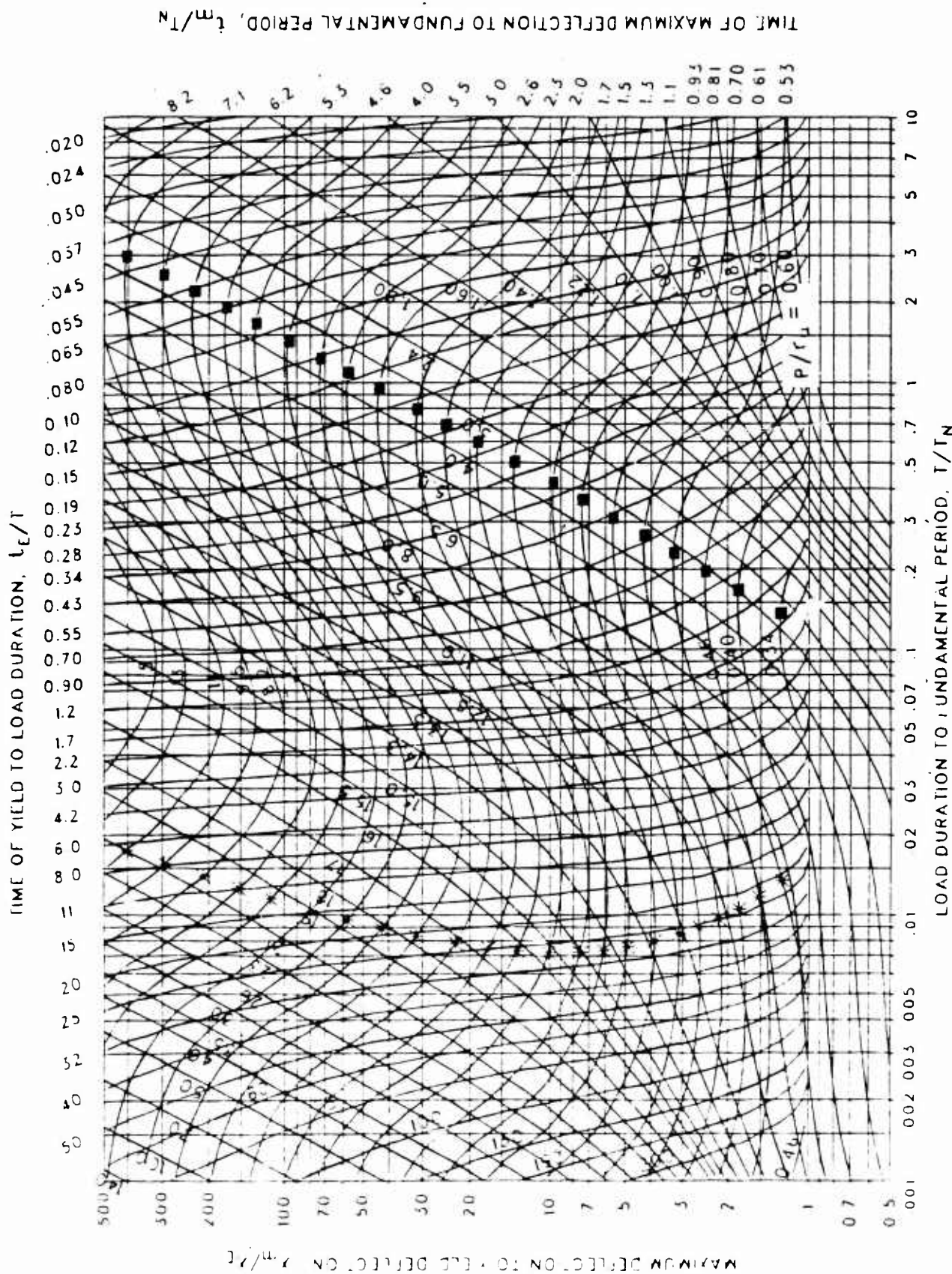
Figure 3-256 Maximum response of elasto-plastic, one-degree-of-freedom system for bilinear-triangular pulse ($C_1 = 0.068$, $C_2 = 1000.$)
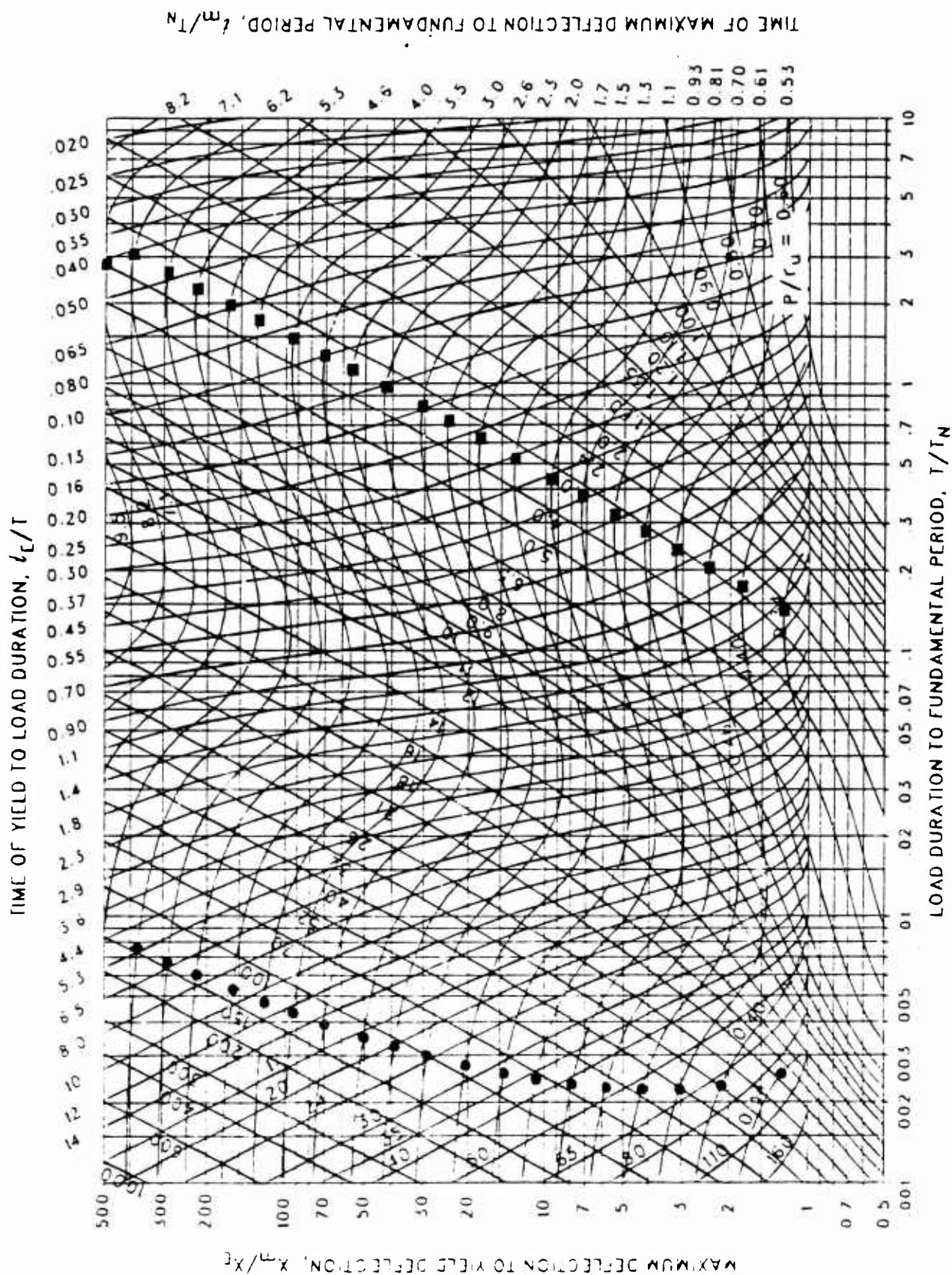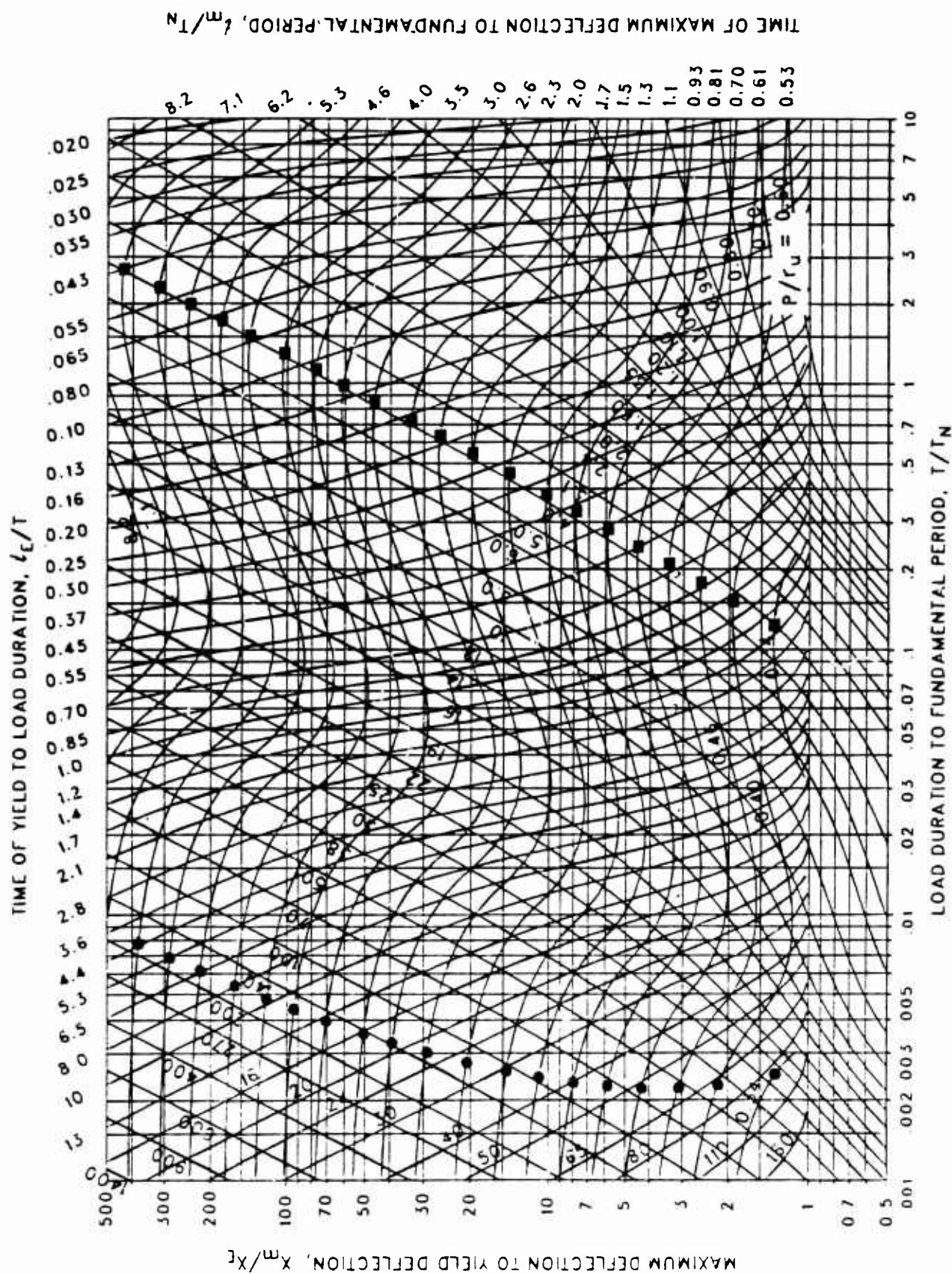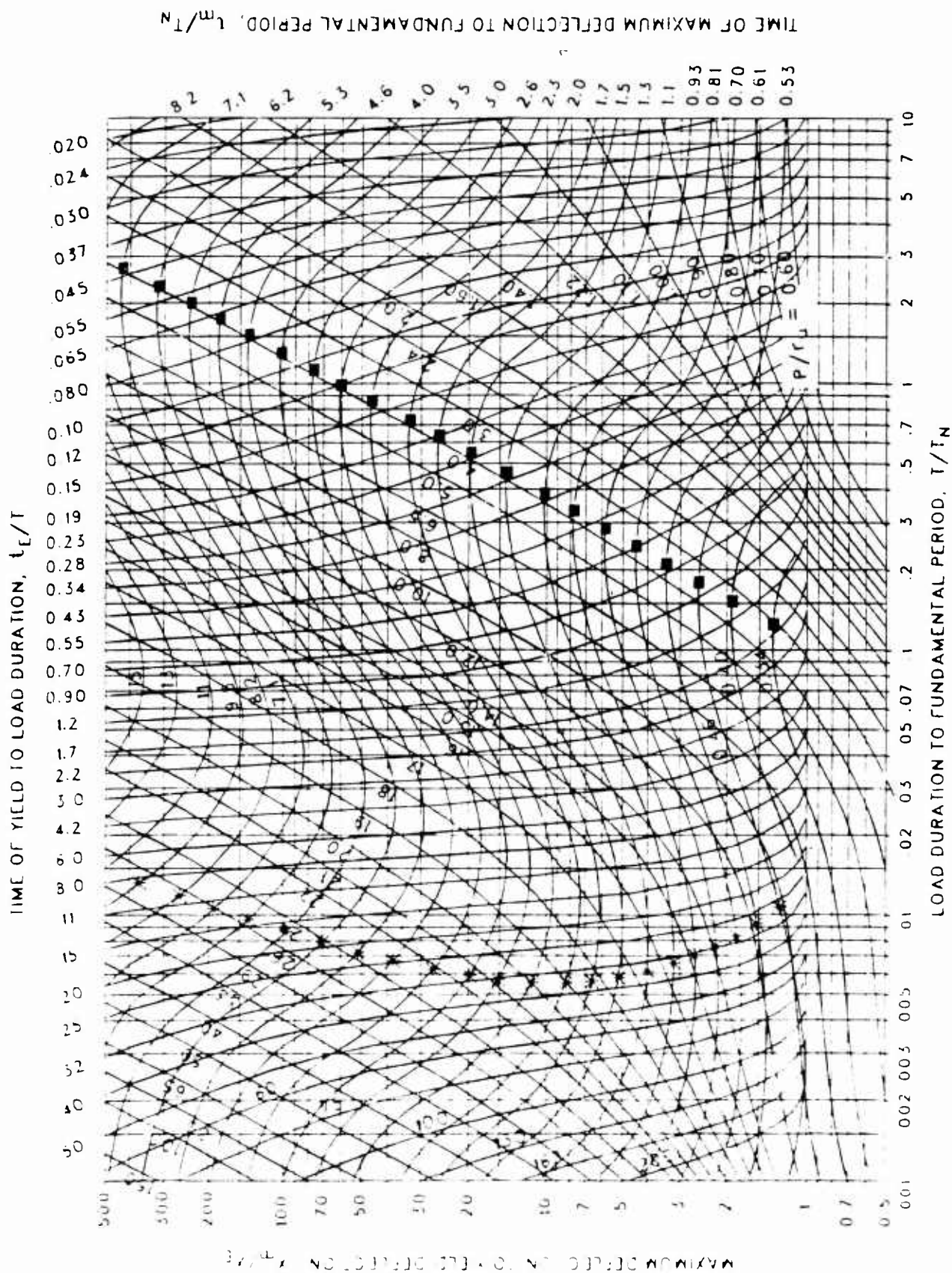
Figure 3-257   Maximum response of elasto-plastic, one-degree-of-freedom
system for bilinear-triangular pulse ($C_1 = 0.056$, $C_2 = 1000.$)
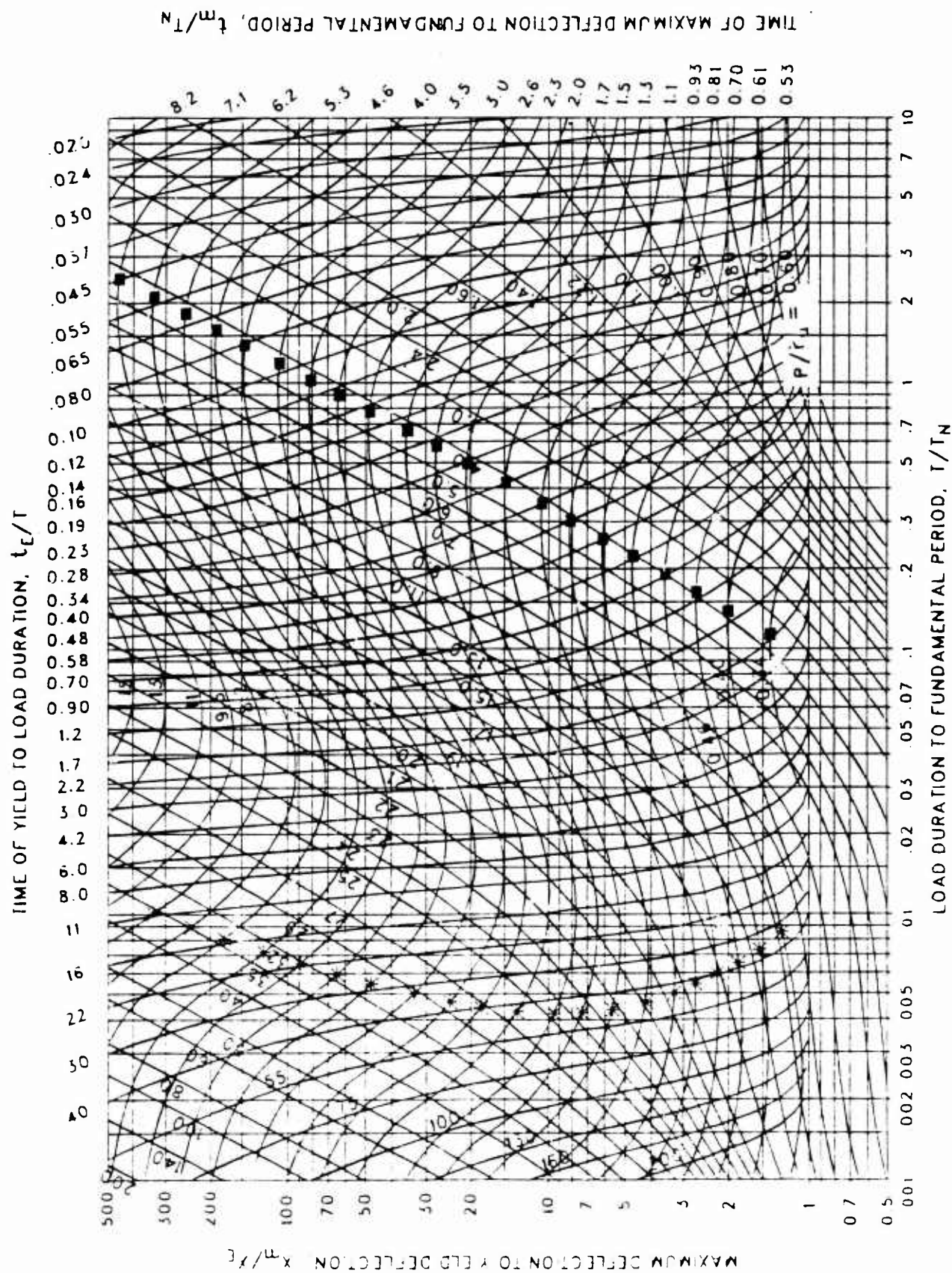
Figure 3-258   Maximum response of elasto-plastic, one-degree-of-freedom
system for bilinear-triangular pulse ($C_1 = 0.046$, $C_2 = 1000.$)
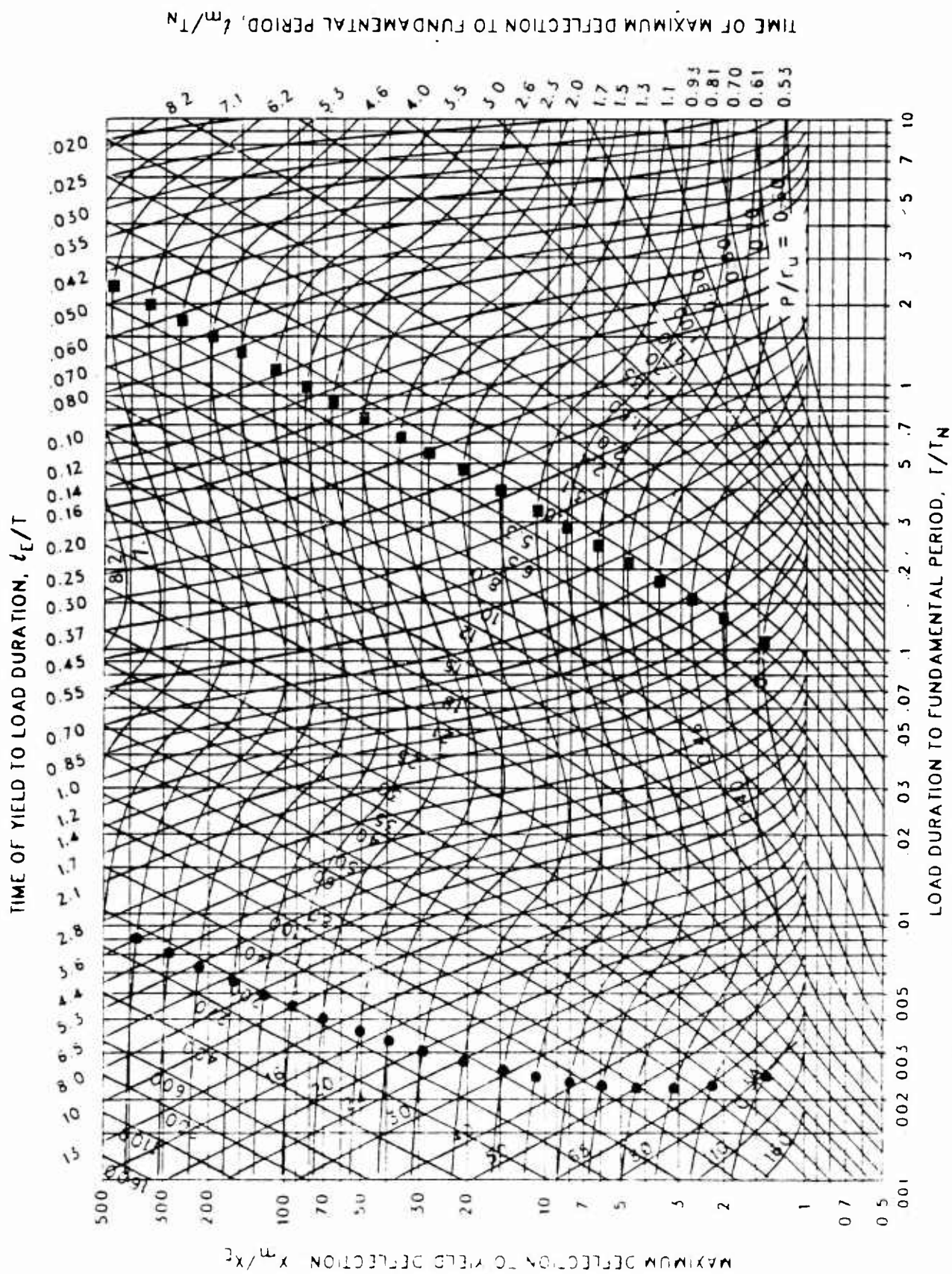
-313-
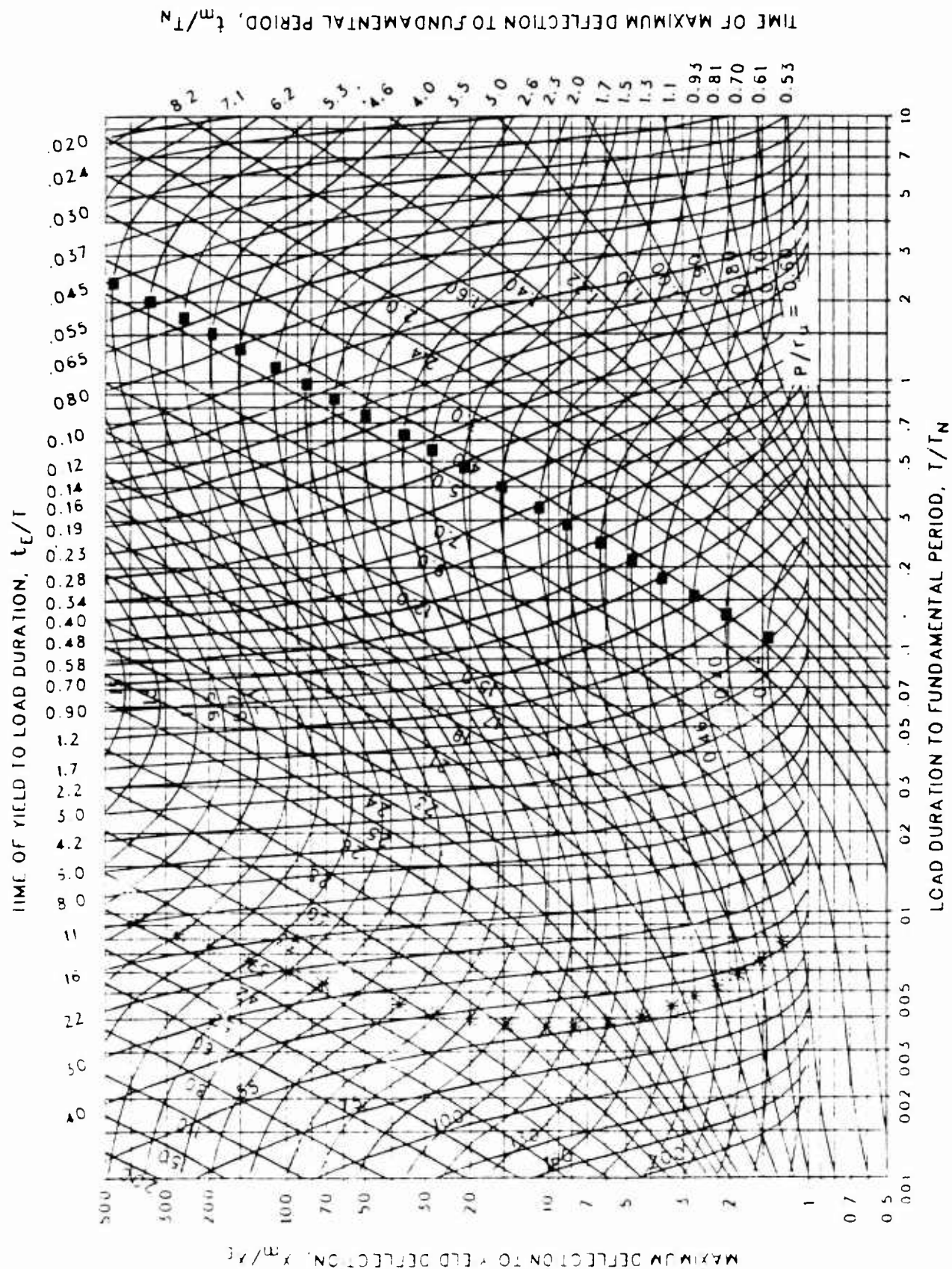
Figure 3-259   Maximum response of elasto-plastic, one-degree-of-freedom system for bilinear-triangular pulse ($C_1 = 0.042$, $C_2 = 1000.$)
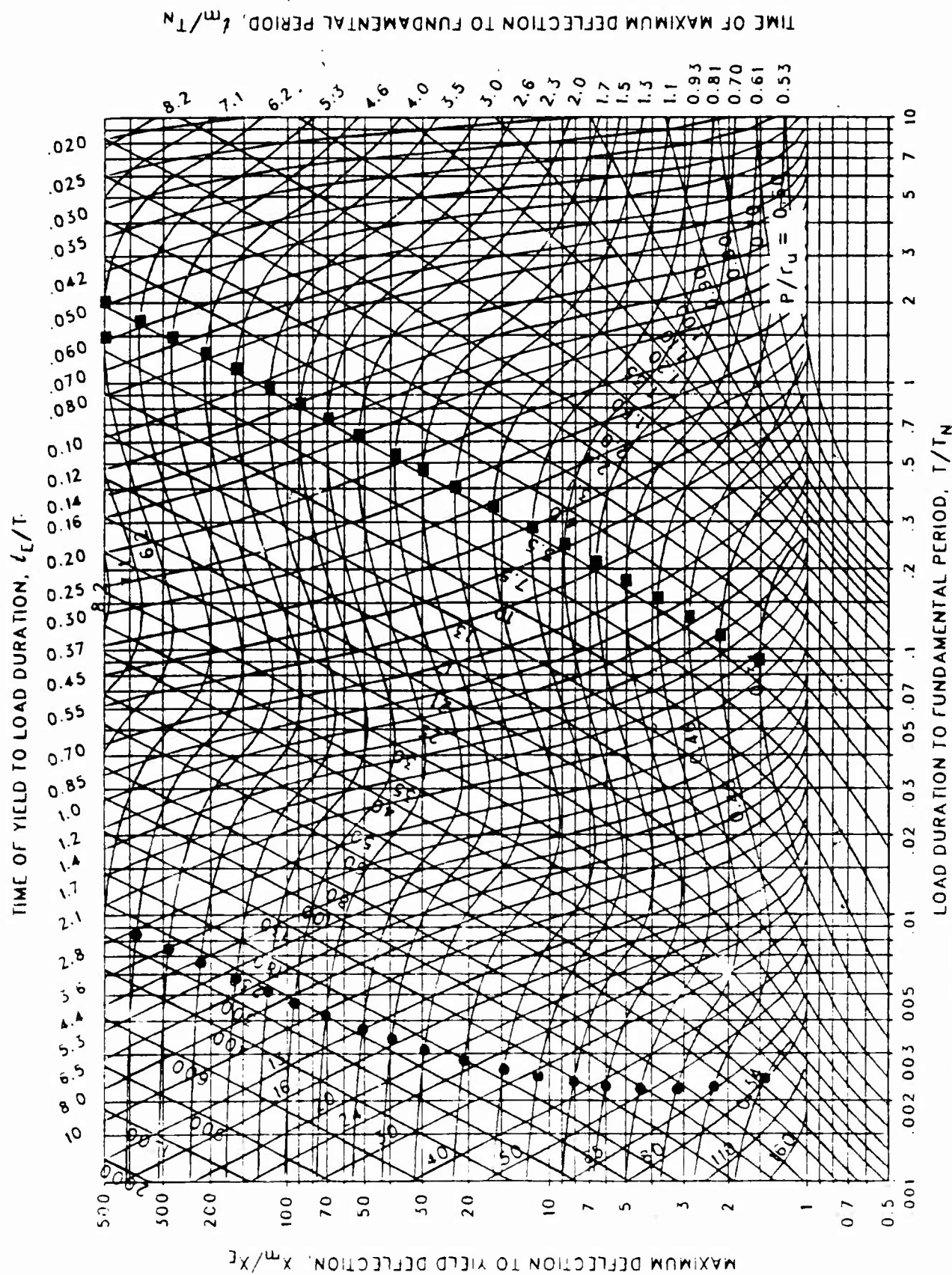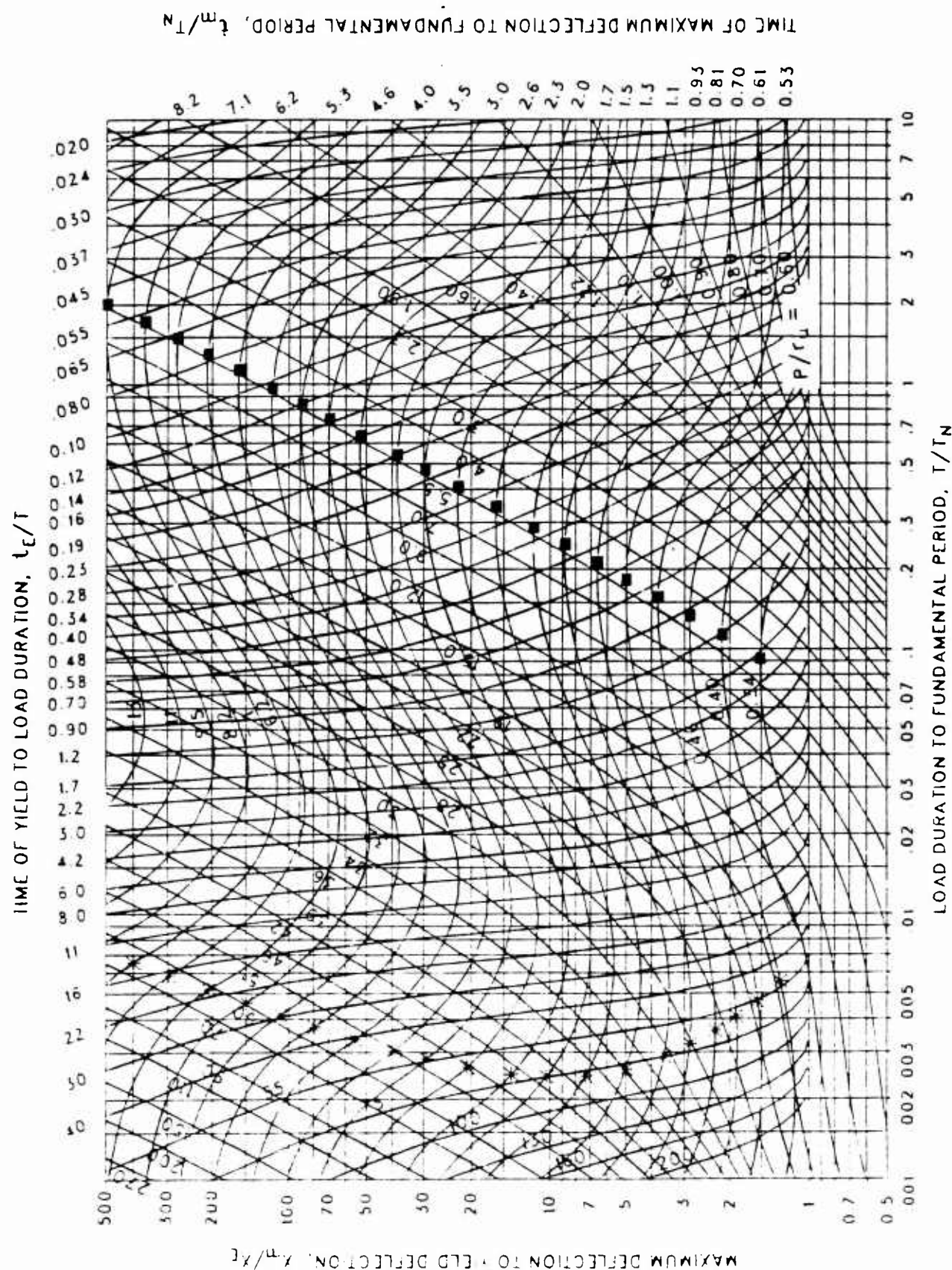
Figure 3-260   Maximum response of elasto-plastic, one-degree-of-freedom
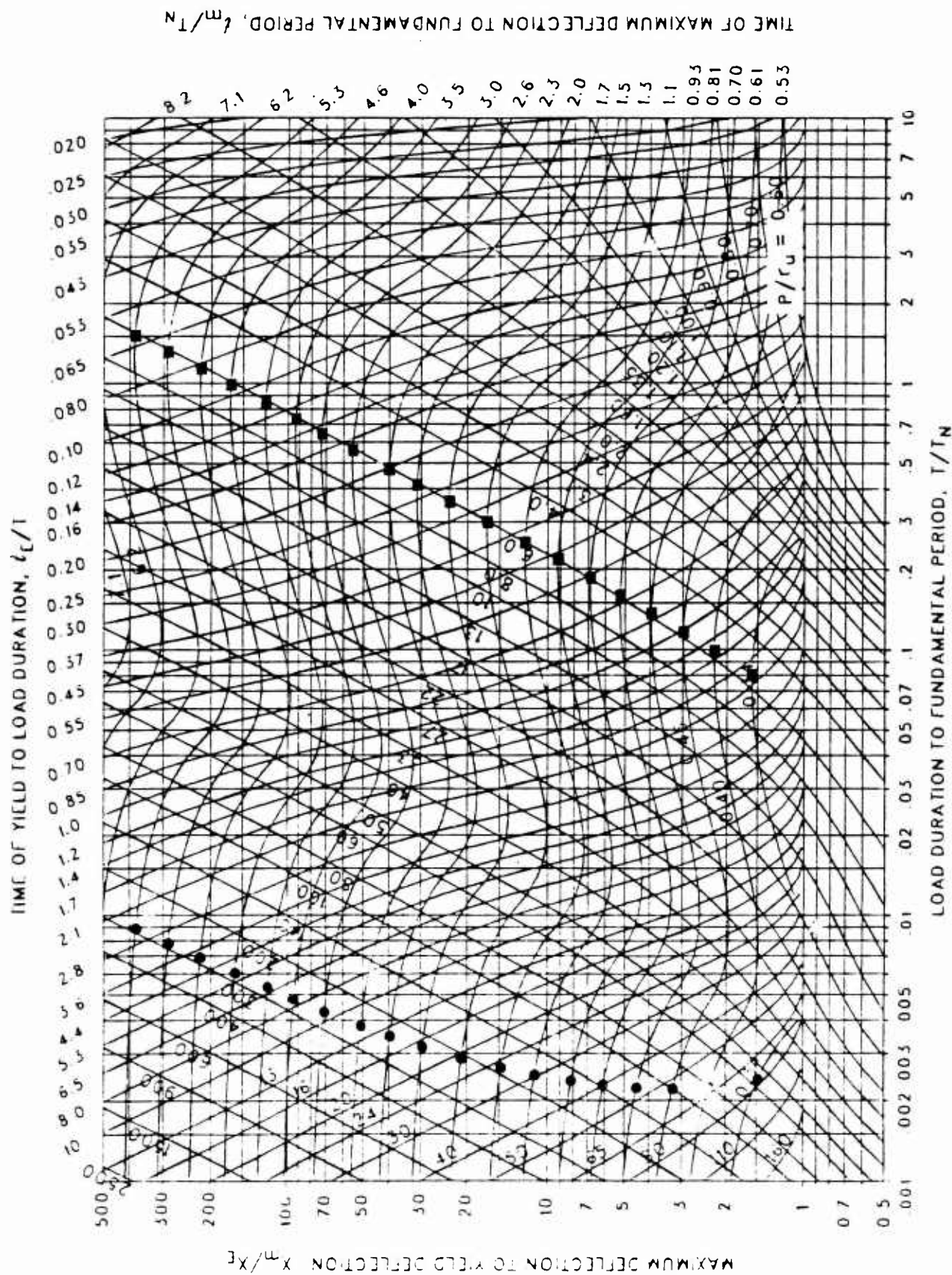system for bilinear-triangular pulse ($C_1 = 0.032$, $C_2 = 1000.$)
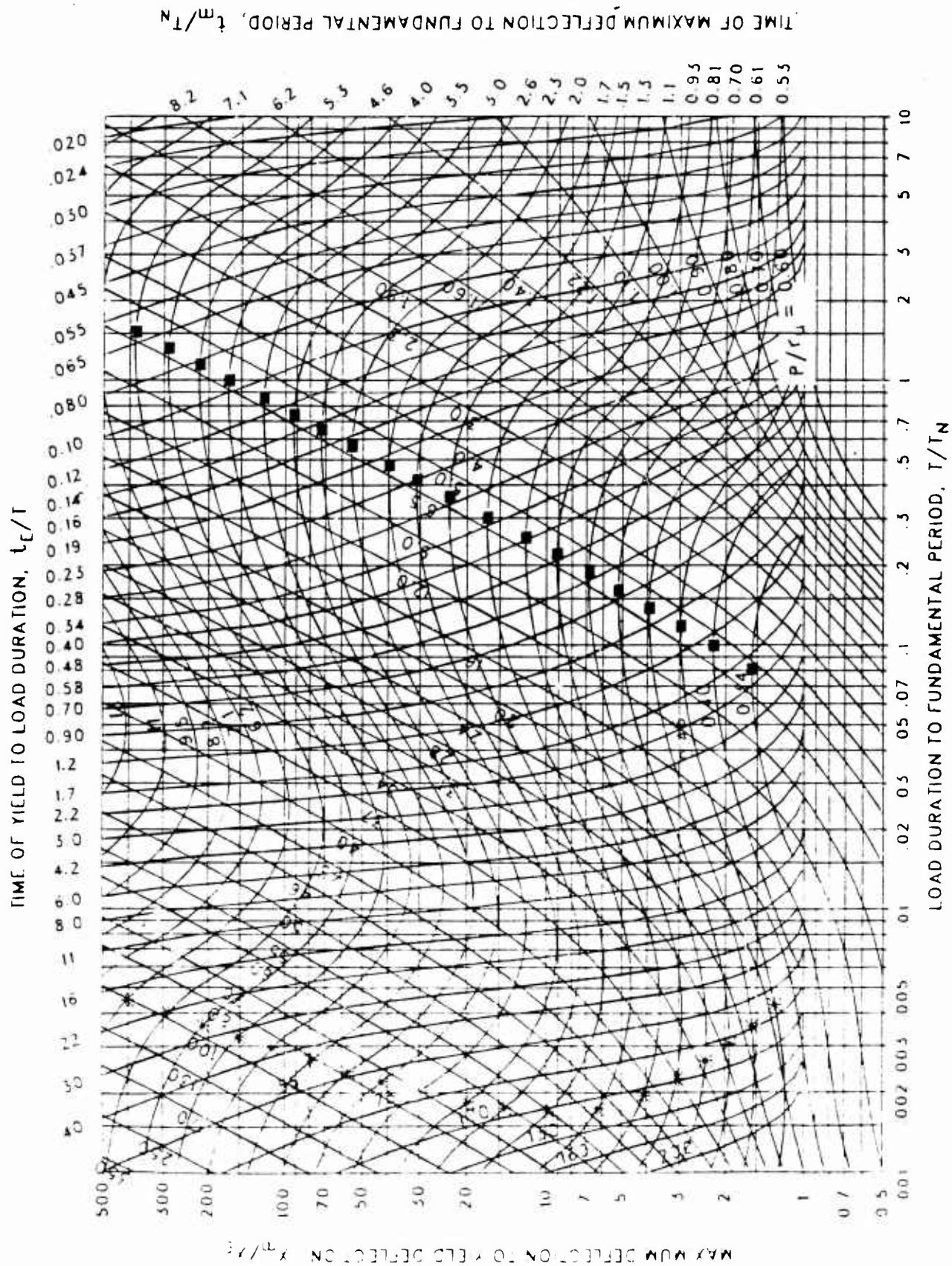
Figure 3-261   Maximum response of elasto-plastic, one-degree-of-freedom
system for bilinear-triangular pulse ($C_1 = 0.026$, $C_2 = 1000.$)

-316-
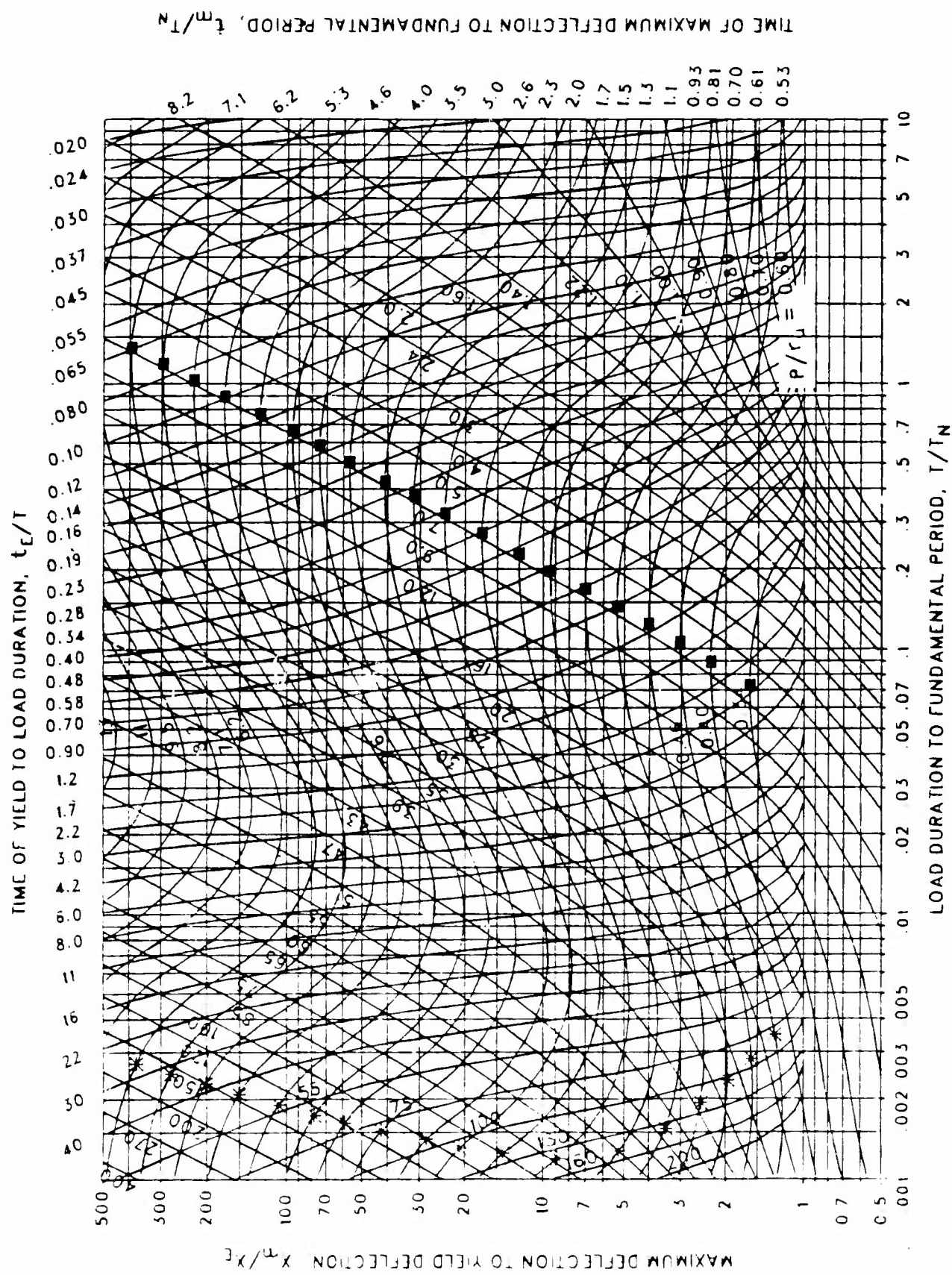
Figure 3-262   Maximum response of elasto-plastic, one-degree-of-freedom
system for bilinear-triangular pulse ($C_1 = 0.022$, $C_2 = 1000.$)

-317-
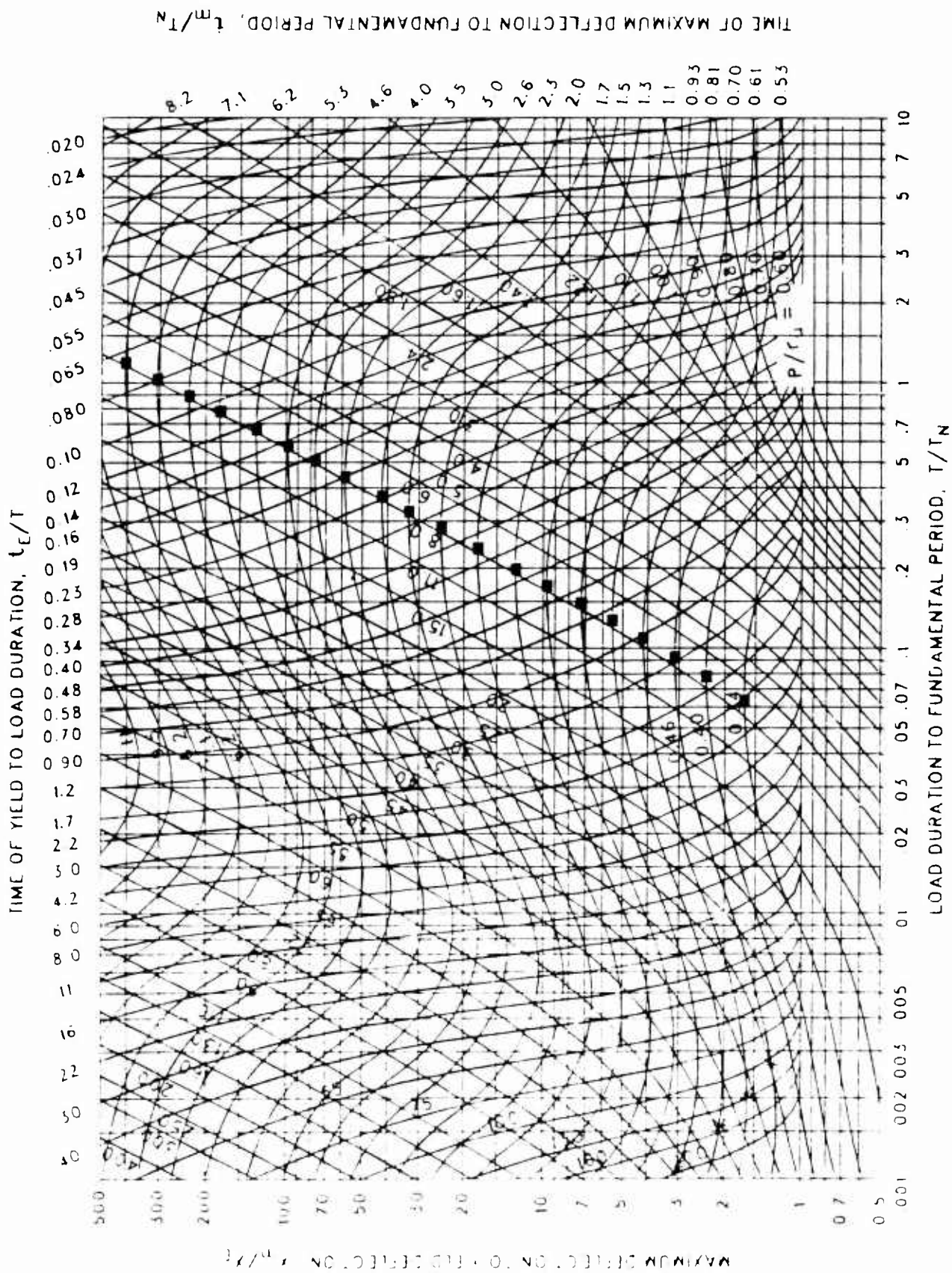
Figure 3-263 Maximum response of elasto-plastic, one-degree-of-freedom system for bilinear-triangular pulse ($C_1 = 0.018$, $C_2 = 1000.$)
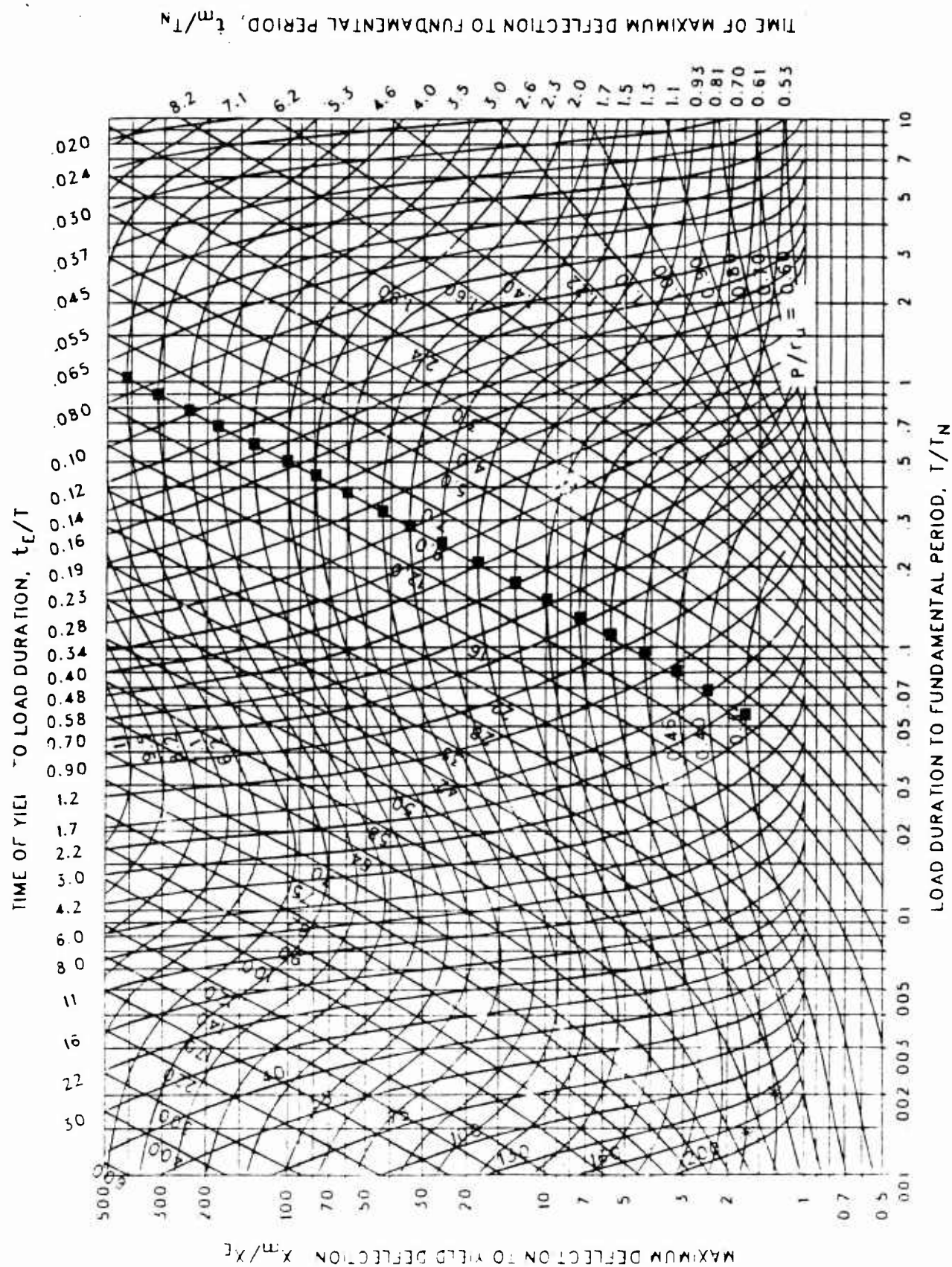
Figure 3-264   Maximum response of elasto-plastic, one-degree-of-freedom system for bilinear-triangular pulse (C_1 = 0.015, C_2 = 1000.)
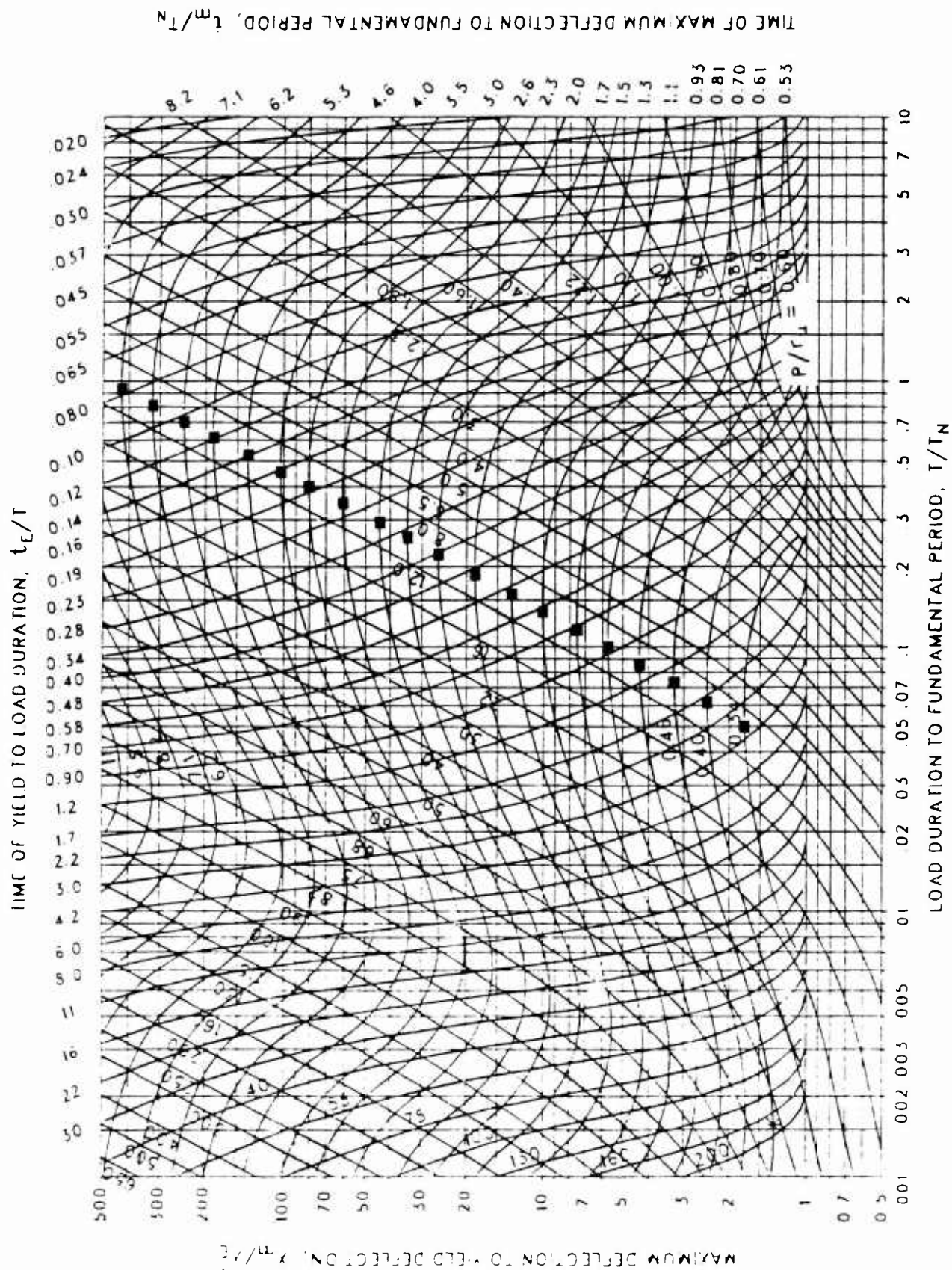
Figure 3-265   Maximum response of elasto-plastic, one-degree-of-freedom
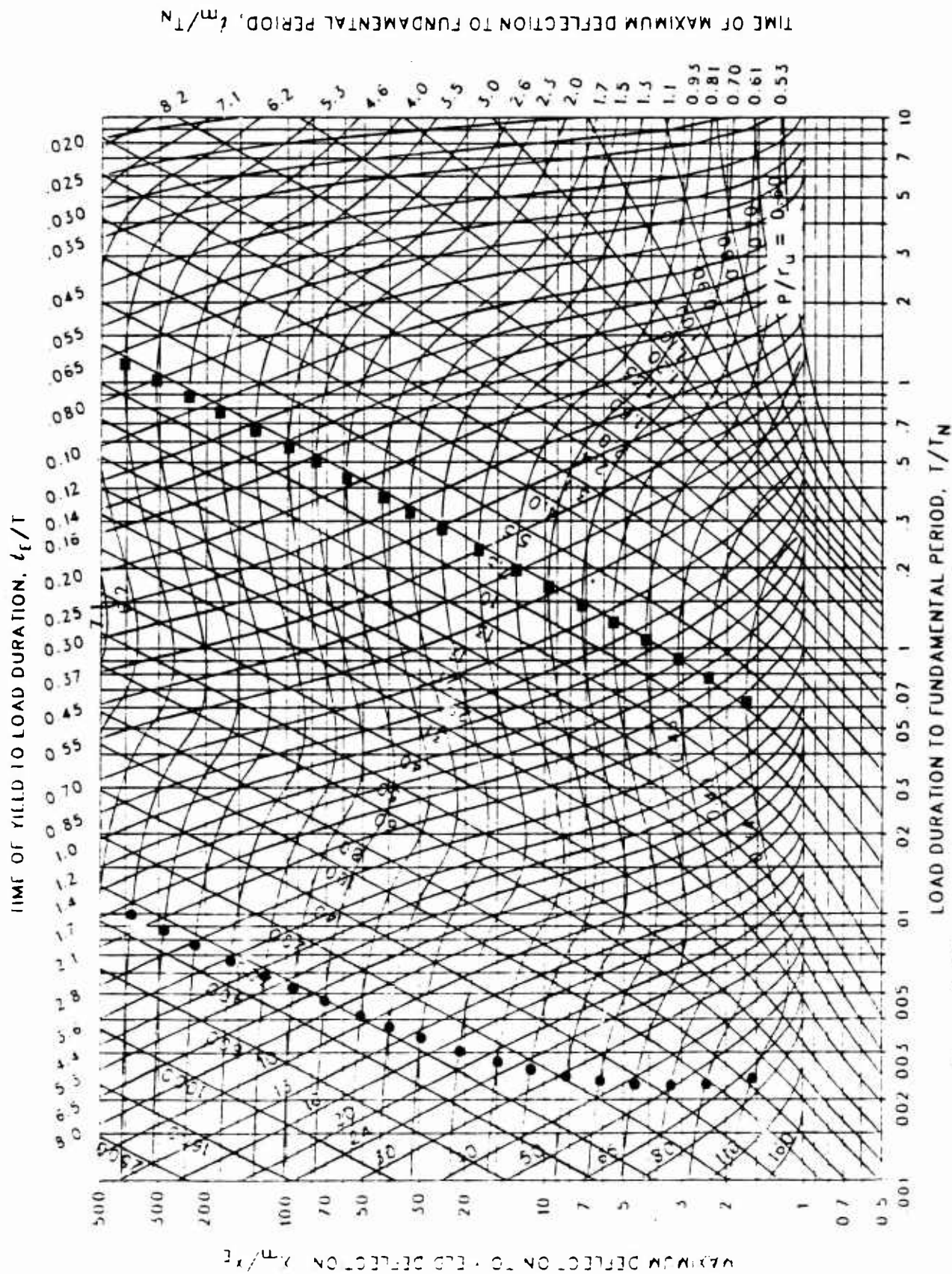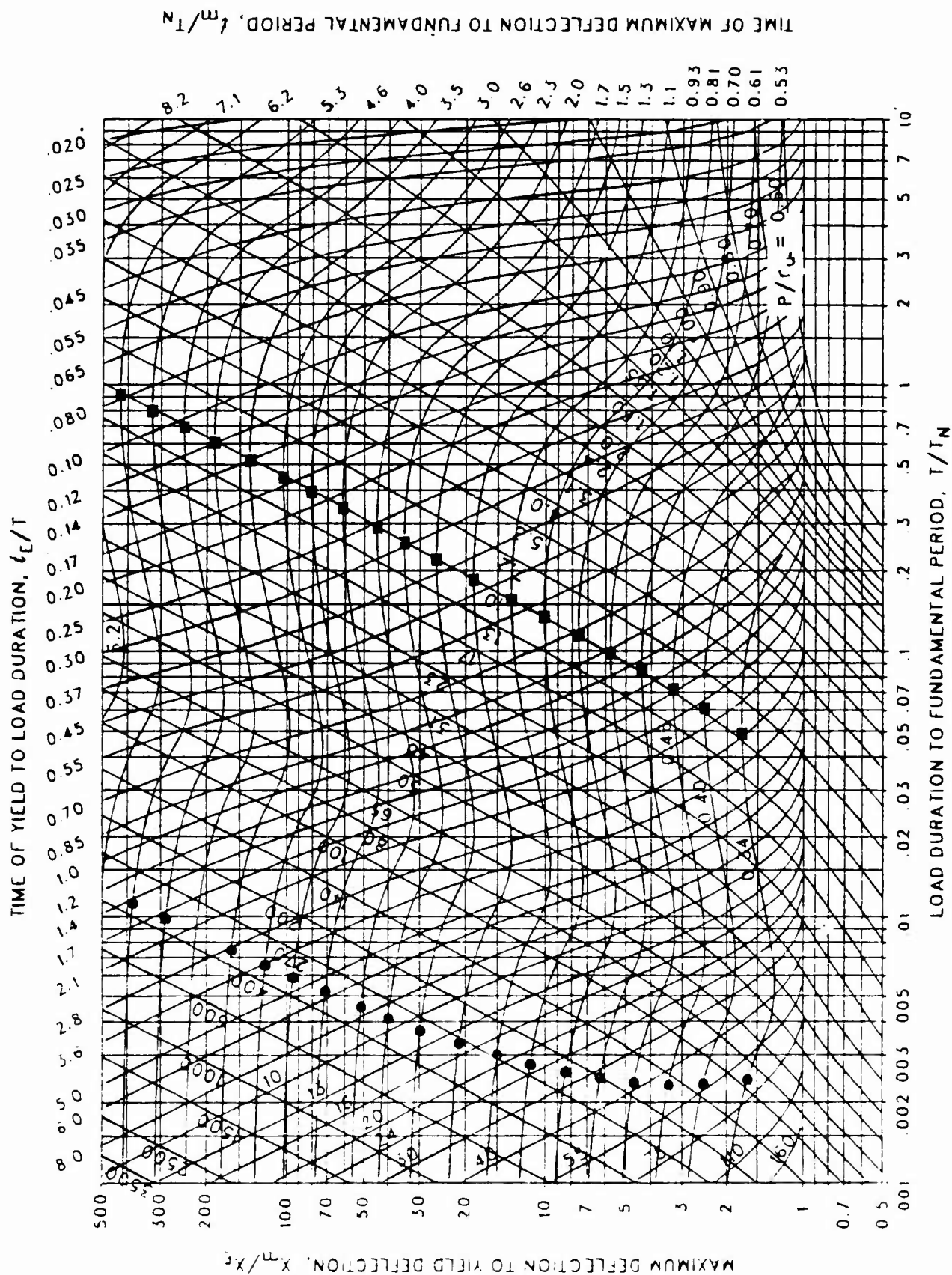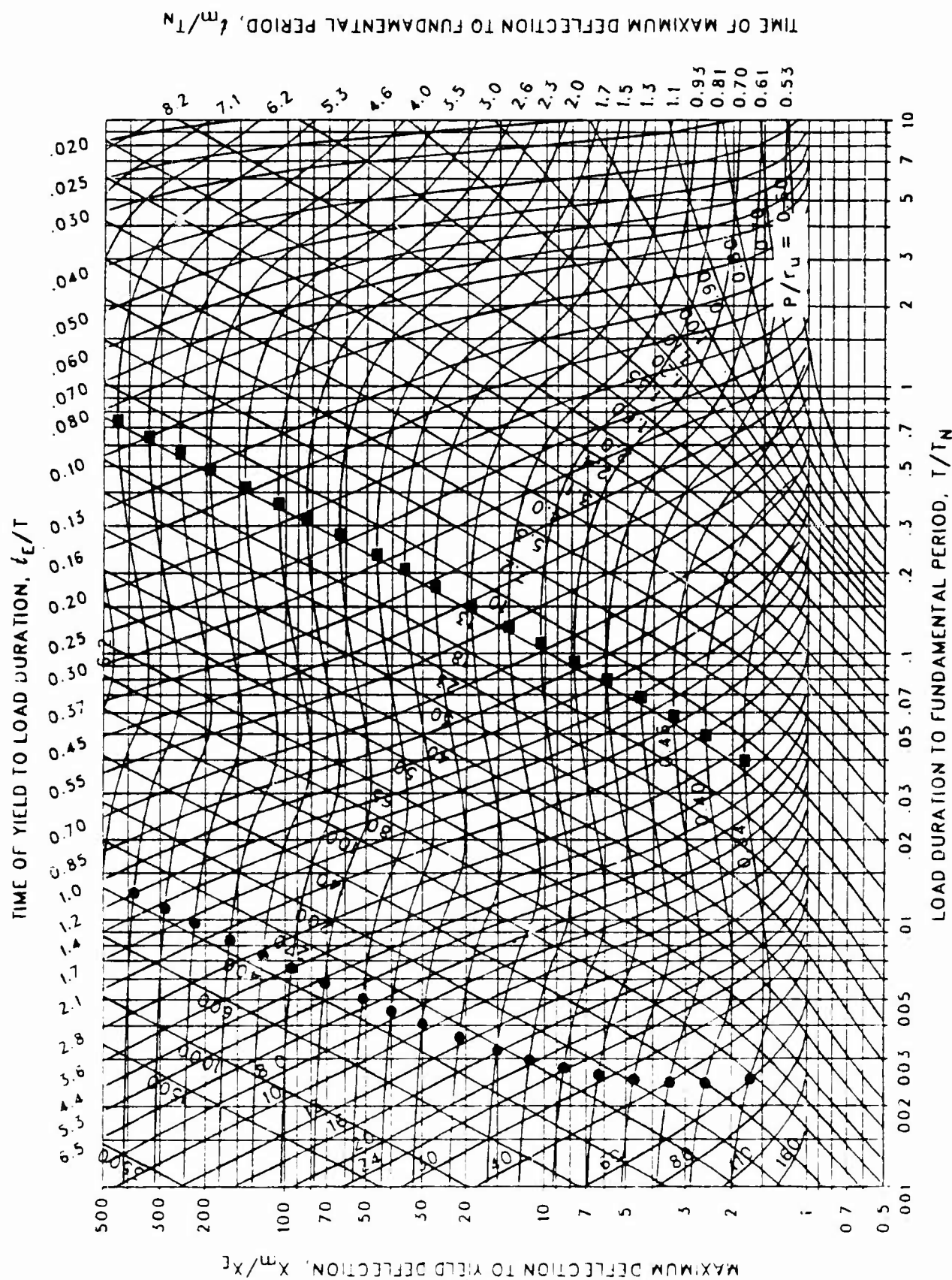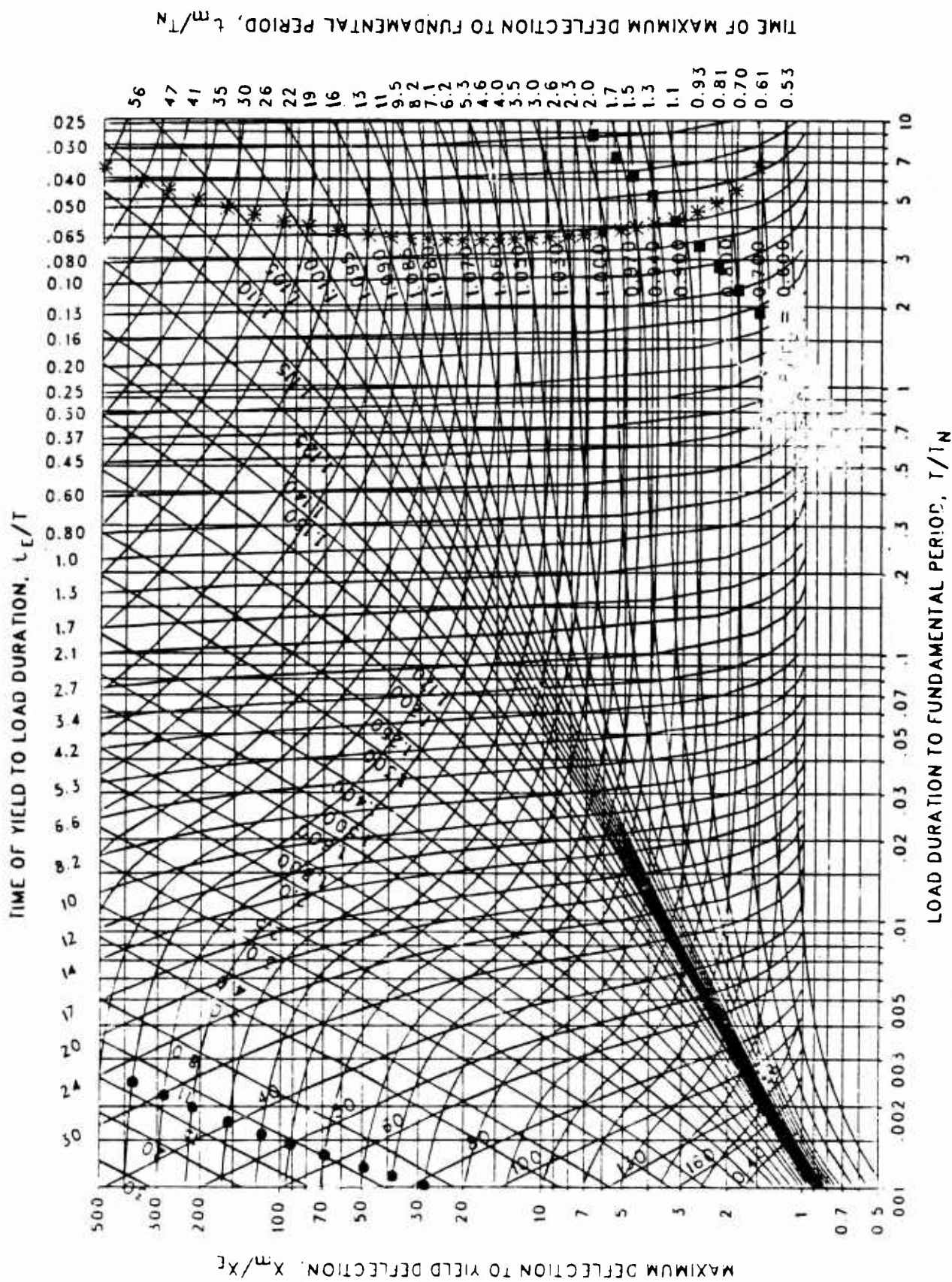system for bilinear-triangular pulse ($C_1 = 0.013$, $C_2 = 1000$.)
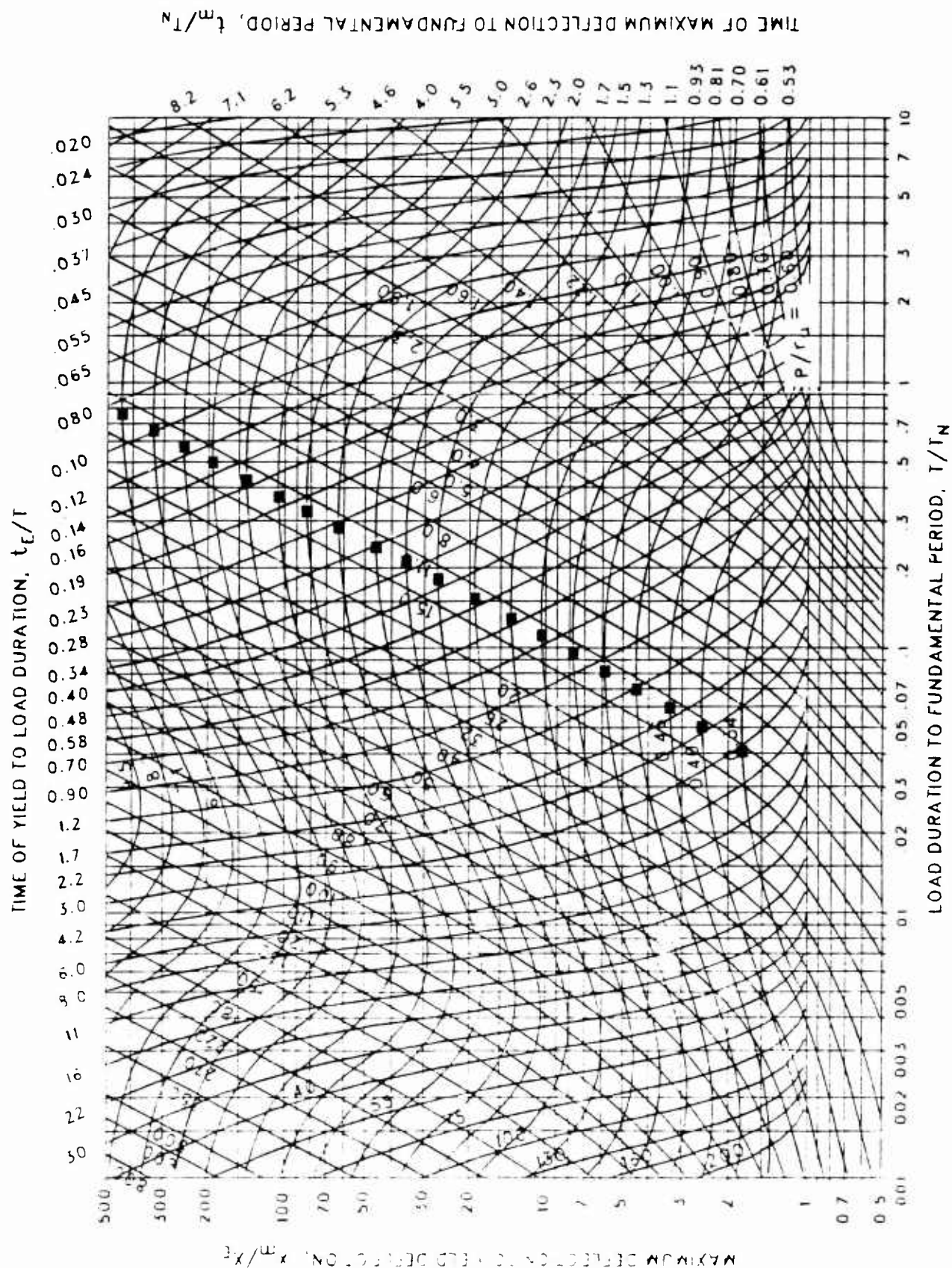
Figure 3-266   Maximum response of elasto-plastic, one-degree-of-freedom system for bilinear-triangular pulse (C_1 = 0.010, C_2 = 1000.)
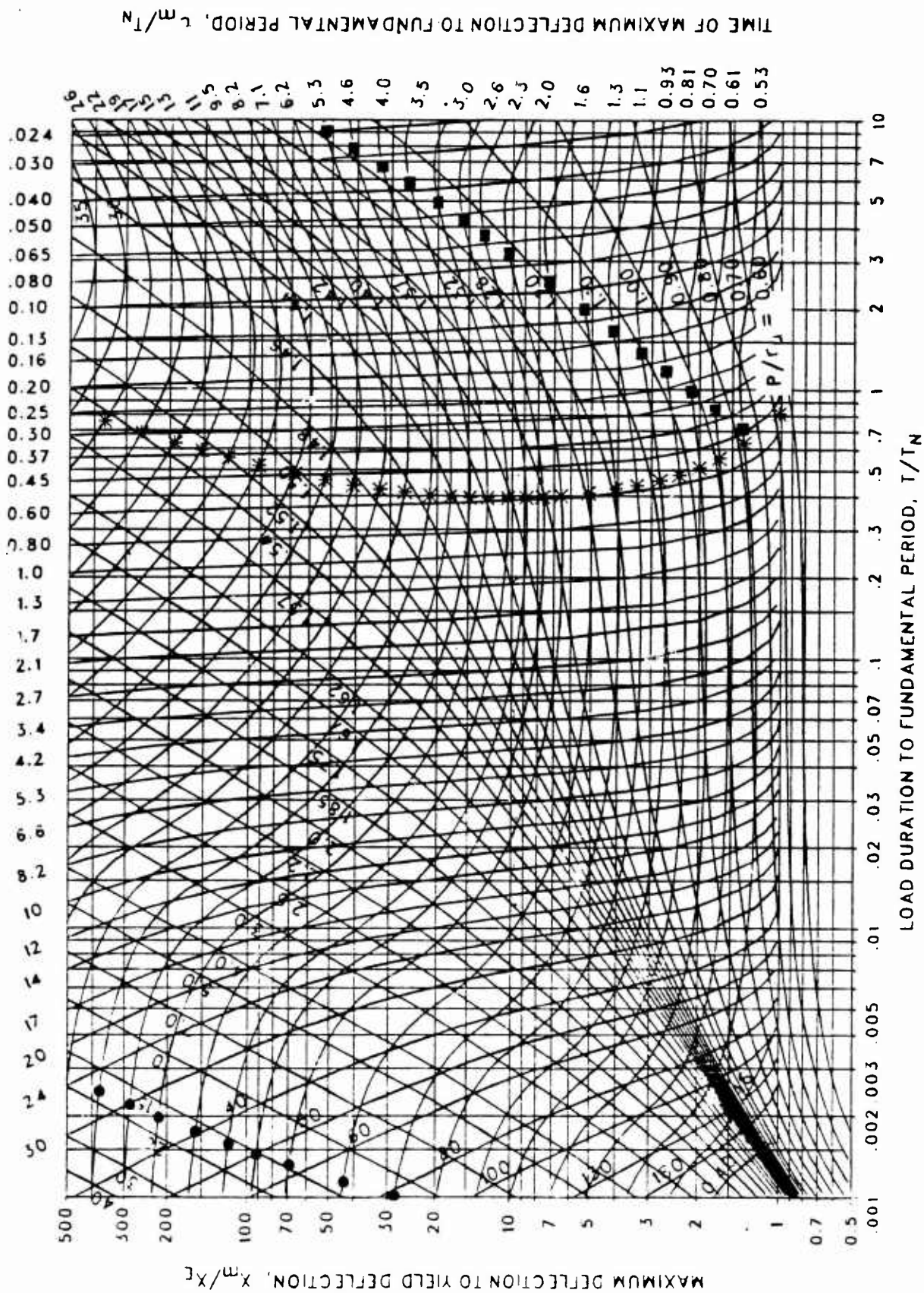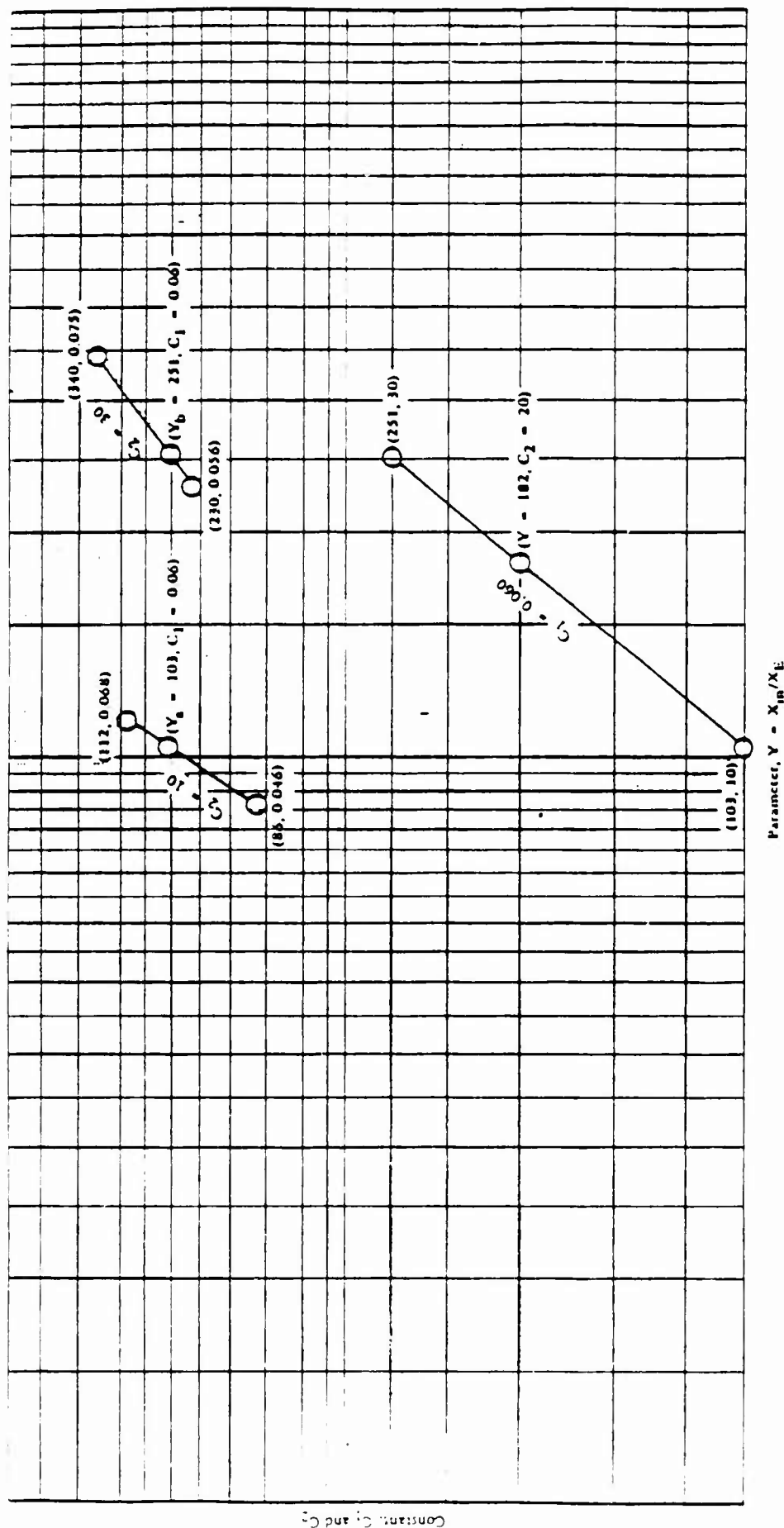
Figure 3-267   Graphical interpolation
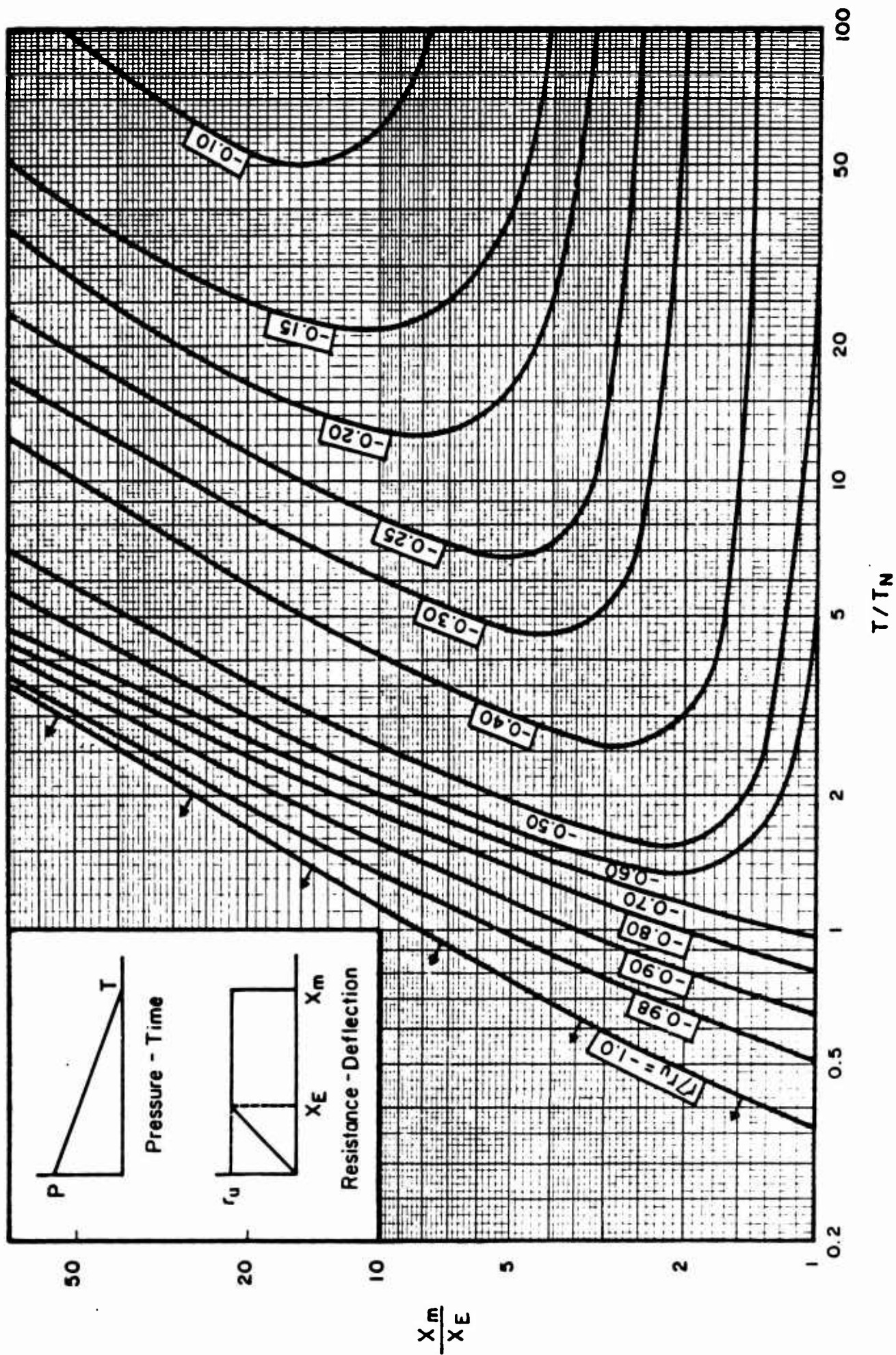
Figure 3-268   Elastic rebound of simple spring-mass system

It may be noted that if the loading is applied in a relatively short time compared to the natural period of vibration of the system, the required rebound resistance can be equal to the resistance in the initial design direction. When the loading is applied for a relatively long time, the maximum deflection is reached when the positive forces are still large and the rebound resistance is reduced.

3-20   Elements Which Respond to Impulse

3-20.1   *General Equations For Maximum Response*

When an element responds to the impulse, the maximum response depends upon the area under the pressure time curve (impulse of blast loading). The magnitude and time variation of the pressure are not important. The response charts presented in Section 3-19, which are based on pressure-time relationship are therefore not required for these problems. Instead, the element resistance required to limit the maximum deflection to a specific value is obtained through the use of a semigraphical method of analysis.

Consider the pressure-time and resistance-time functions shown in figure 3-269. The resistance curve depicted s for a two-way element with a resistance-deflection function having ..-t-ultimate range. From Newton's equation of motion it can be shown that .e sumation of the areas (considering area A as positive and area B as negati... .. i the load-time curves up to any time t_a divided by the corresponding .... rive masses is equal to the instantaneous velocity of that time:

$$v_a = \int_0^{t_a} \frac{(f-r)dt}{m_e} \qquad\qquad 3\text{-}87$$

The displacement at time t_a is found by multiplying each differential area divided by the appropriate effective mass by its distance to t_a and summing the values algebraically:

$$X_a = \int_0^{t_a} \frac{(f-r)}{m_e} (t_a - t)dt \qquad\qquad 3\text{-}88$$

In each range the mass is the effective plastic mass:

Time Interval	Resistance	Effective Mass
$0 \le t \le t_1$	r_u	$m_u = (K_{LM})_u m$
$t_1 \le t \le t_m$	r_{up}	$m_{up} = (K_{LM})_{up} m$

Time t_1 is the time at which the partial failure deflection X_1 occurs, and time t_m is the time at which maximum deflection X_m is reached ($X_m \lessgtr X_u$).

For an element to be in equilibrium at its maximum deflection, its impulse capacity must be numerically equal to the impulse of the applied blast load. With the use of the foregoing equations, the expressions which define the motion and capacity of elements subjected to impulse type loads, can be defined. These expressions are presented for both large and limited deflection

- 324 -
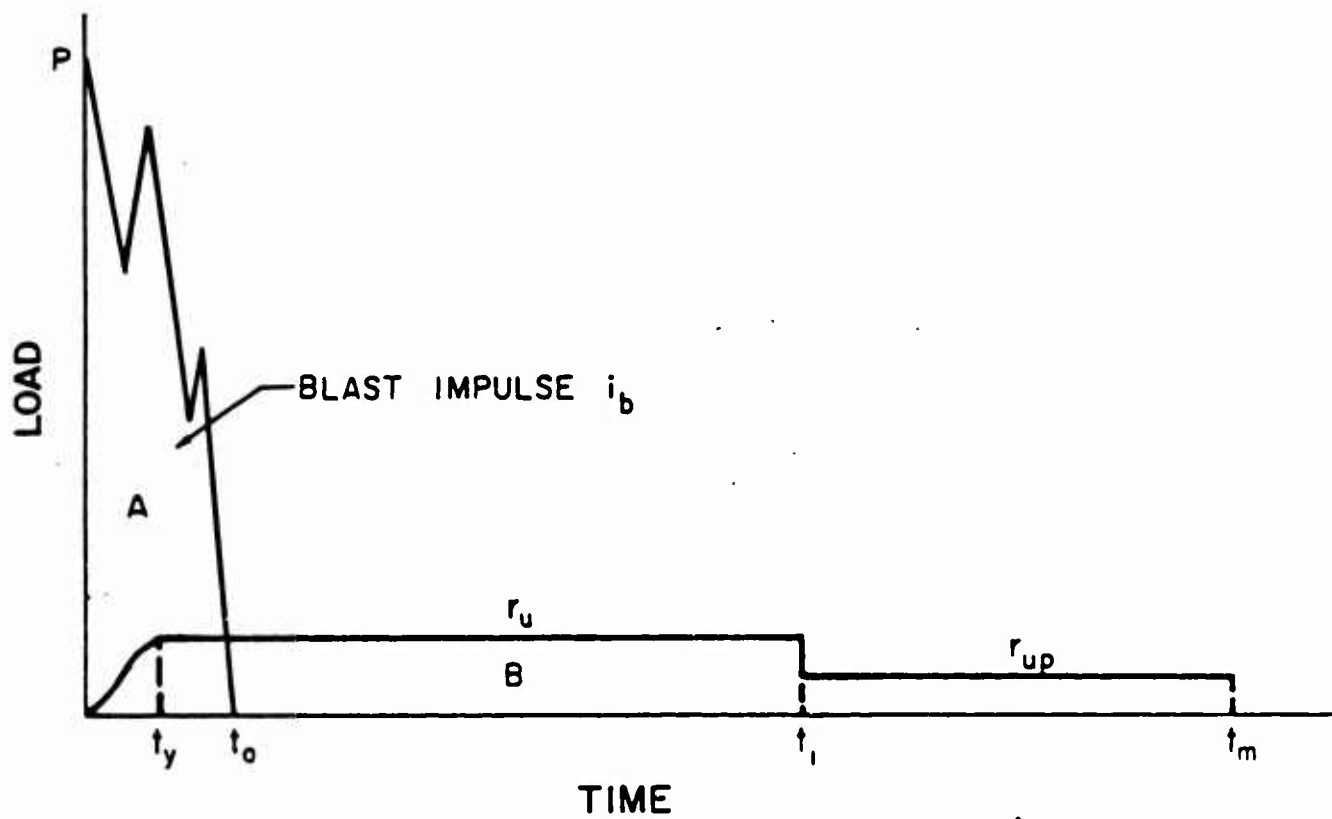
Figure 3-269   Pressure-time and resistance-time curves for elements which
               respond to impulse

criteria. This criteria varies for the different materials used in protective design. The criteria for each material is obtained from the volume that describes the design procedures for that material.

Case 1 - large deflections. Utilizing equation 3-88 and by taking moments of the areas under the pressure-time and resistance-time curves (fig. 3-_59) about time t_m, assuming that the unit blast impulse i_b is applied instantaneously at time $t=0$, and that time to reach yield t_y is also close to zero the expression for the maximum deflection is

$$X_m = \frac{i_b t_m}{m_u} - \frac{r_u t_1 (t_m - t_1/2)}{m_u} - \frac{r_{up}(t_m - t_1)}{2m_{up}} \ (t_m - t_1) \qquad 3-89$$

If moments of the areas are taken about t_1, then the deflection at partial failure X_1, is

$$X_1 = \frac{i_b t_1}{m_u} - \frac{r_u t_1^2}{2m_u} \qquad 3-90$$

Using equation 3-87 and summing the areas of t_m and recognizing that the instantaneous velocity at t_m equals zero.

$$\frac{i_b}{m_u} - \frac{r_u t_1}{m_u} - \frac{r_{up}(t_m - t_1)}{m_{up}} = 0 \qquad 3-91$$

Solution of the above three simultaneous equations is accomplished by solving equation 3-91 for t_m and substituting this expression into equation 3-89, and solving equation 3-90 for t_1 and substituting this expression into the modified equation 3-89. After continuing and rearranging terms, the general response equation becomes

$$\frac{i_b^2}{2m_u} = r_u X_1 + \frac{m_u}{m_{up}} r_{up} (X_m - X_1) \qquad 3-92$$

The left side of this equation is simply the initial kinetic energy resulting from the applied blast impulse and the right side is the modified potential energy of the element. The modification is required since the above analysis requires the use of two equivalent dynamic systems (before and after time t_1). The modification factor m_u/m_{up} equates the two dynamic systems. If the effective mass in each range was the same, m_u/m_{up} would equal one and the right side of the expression would be $r_u X_m$ which is the potential energy.

For one-way elements which do not exhibit the post-ultimate resistance range, or for two-way panels where the maximum deflection X_m is less than X_1, equation 3-92 becomes

$$\frac{i_b^2}{2m_u} = r_u X_m \qquad 3-93$$

The above solutions are valid only for what is considered large deflection design since the variation of resistance with deflection in the elasto-plastic range has been ignored. This limitation is based on the assumption that the time to reach yield t_y and the duration of the impulse t_o are small in comparison to t_m.

Case 2 - limited deflections. For elements which respond to the impulse with limited deflections where the time to reach maximum deflection t_m is greater than three times the duration t_0 of the load, but where the support rotations are equal to or less than the established criteria, the elasto-plastic range behavior of the element must be accounted for in determining the overall response of the element to the applied blast load. For this case, equation 3-92 becomes

$$\frac{i_b^2}{2m_a} = \frac{r_u X_E}{2} + \frac{m_a}{m_u} \; r_u(X_m - X_E) \qquad\qquad 3\text{-}94$$

where m_a is the average of the effective elastic and plastic masses and X_E the equivalent deflection.

When the response time t_m of an element is less than three times the load duration t_0, the element will respond to the pressure pulse rather than to the impulse alone. In this case the response of the element may be obtained through the use of a response chart considering a fictitious pressure pulse as outlined in Volume II. However, if the element's maximum deflection is greater than given in the response charts (ductility ration X_m/X_E greater than 100), the response of the element may be obtained through use of the semigraphical method of analysis as outlined in this paragraph considering the fictitious pressure pulse. It should be noted that the resistance time relationship used in the analysis to express the element's response should include the elasto-plastic region.

3-20.2 *Determination of Time to Reach Maximum Deflection*

The time t_m for each of the cases covered previously can be determined by applying equations 3-87 and 3-88 to the particular problem. The resulting equations are as follows:

Case 1 - large deflections.

A. $X_1 < X_m \leq X_u$

$$t_m = \frac{i_b}{r_u} + \left(\frac{m_{up}}{m_u r_{up}} - \frac{1}{r_u}\right) \sqrt{i_b^2 - 2m_u r_u X_1} \qquad\qquad 3\text{-}95$$

B. $X_m \leq X_1$

$$t_m = i_b/r_u \qquad\qquad 3\text{-}96$$

Case 2 - limited deflections.

Since the variation of resistance with time is not known in the elasto-plastic range, t_m can only be determined approximately by assuming a linear variation of resistance with time.

$$t_m \text{ (approx)} = \frac{i_b}{r_u} \left(3 - \frac{m_u}{2m_a}\right) + \frac{1}{r_u} \left(\frac{m_u}{2m_a} - 1\right) \sqrt{9i_b^2 - 6m_a r_u X_E} \qquad\qquad 3\text{-}97$$

- 327 -

APPENDIX 3A

ILLUSTRATIVE EXAMPLES

Problem 3A-1(A)   Ultimate Unit Resistance

Problem: Determine the ultimate unit resistance of a two-way structural element using (1) general solution and (2) charts.

Procedure: Part (a) - General Solution

Step 1.   Establish design parameters.

Step 2.   Assume yield line locations in terms of x and/or y considering support conditions, presence of openings, etc.

Step 3.   Determine negative and positive moment capacities of sections crossed by assumed yield lines.

Step 4.   Establish distribution of moments across negative and assumed yield lines, considering corner effects and those of openings.

Step 5.   Determine the ultimate unit resistance for each sector in terms of x and/or y considerting free body diagram of the sectors (fig. 3-3). Summation of the moments about the axis of rotation (support) of the sector yields equation 3-3.

Step 6.   Equate the ultimate unit resistance of the sectors and solve for the yield line location x and/or y.

Step 7.   With known yield line location, solve for ultimate unit resistance of the element, using equations obtained in Step 6.

Note: For complex problems (three or more different sectors), the solution for the ultimate unit resistance is most easily accomplished through a trial-and-error procedure by determining r_u for each sector for a given (assumed) yield line location and adjusting the yield lines until the several values of r_u agree to within a few percent.

Procedure: Part (b) - Chart Solution

Step 1.   Same as in step 1 of part a.

Step 2.   Same as in step 2 of part a.

Step 3.   Determine the negative and positive ultimate moment capacities in vertical and horizontal directions.

331

Step 4.   For given support conditions (and value of x_2/x_1 in the case of an element with three edges supported and fourth free), use the appropriate chart (figs. 3-4 through 3-20) to obtain yield line location ratios x/L or y/H for value of quantity abtained in step 4. Then calculate x or y.

Step 5.   Using the appropriate equation from table 3-2, determine the ultimate unit resistance of the element.

Example 3A-1   Ultimate Resistance

Required: Ultimate unit resistance of two-way structural steel element shown below using (1) general solution and (2) charts.
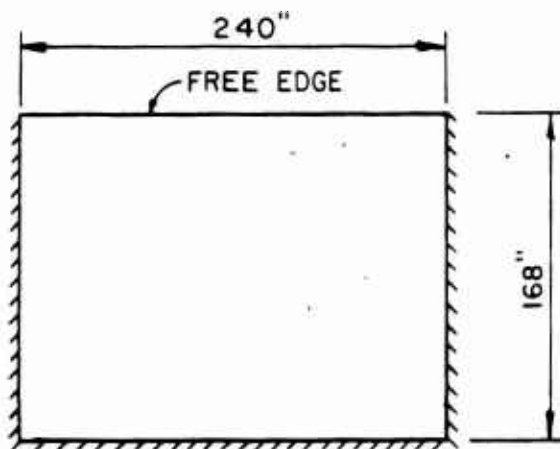
Figure 3A - 1

(Solution: Part (a) - General Solution)

Step 1.   Given:

(a) L = 240 in   H = 168 in
(b) Fixed on three sides and free at the fourth

Step 2.   Assume yield line location (fig. 3A - 2)

Step 3.   The negative and positive moment capacities in both the horizontal and vertical directions are determined from the properties of the material. For this example, it will be assumed that the moment capacities are equal to M = 20,000 in-lbs/in.

240

120

168

y

II

I

168-$\frac{y}{2}$

$\frac{y}{2}$

60   120   60

AT NEGATIVE
YIELD LINE

$\frac{2}{3}M_{HN}$

M_{HN}

AT POSITIVE
YIELD LINE

$\frac{2}{3}M_{HP}$

M_{HP}

M_{VN}

$\frac{2}{3}M_{VN}$

AT NEGATIVE
YIELD LINE

M_{VP}

$\frac{2}{3}M_{VP}$

AT POSITIVE
YIELD LINE
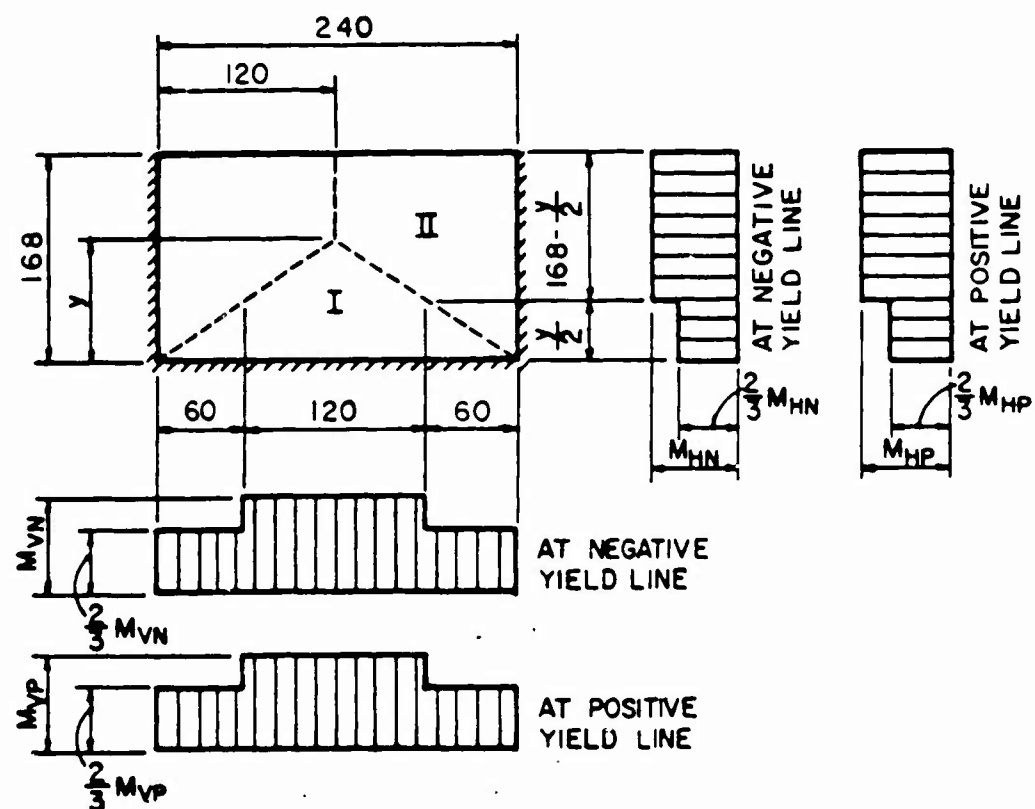
a) ASSUMED YIELD LINES AND DISTRIBUTION OF MOMENTS

y

I

240

C_I

R_I

ΣM_{VN} ΣM_{VP}

R_I

y

168-y

y

II

168

120

C_{II}

R_{II}

ΣM_{HP} ΣM_{HN}

R_{II}

120
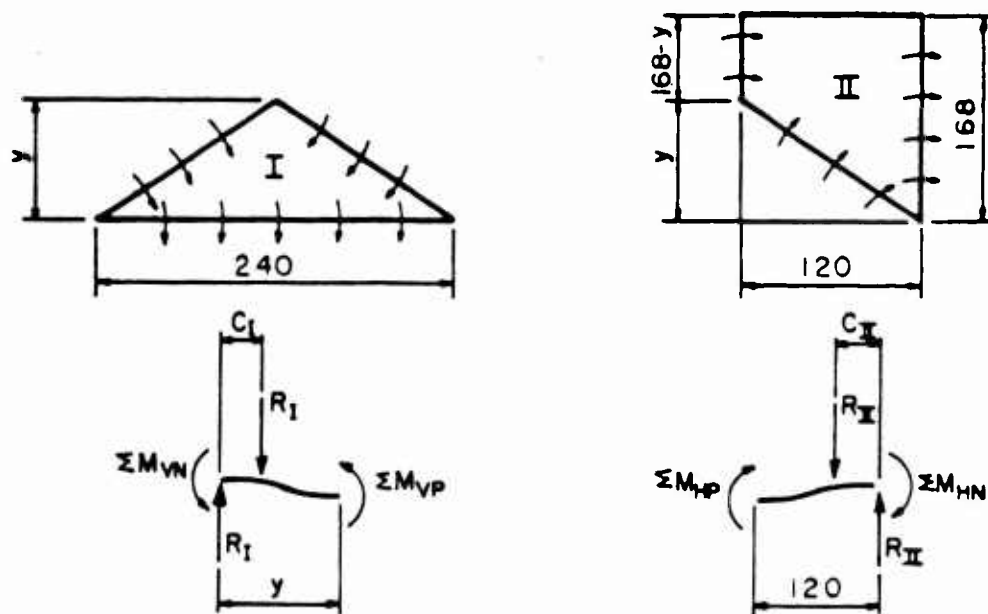
b) FREE-BODY DIAGRAMS FOR INDIVIDUAL SECTORS

Figure   3A - 2

333

$$M_{HN} = M_{HP} = M_{VN} = M_{VP} = 20{,}000 \text{ in lbs/in.}$$

Step 4. For distribution of moments across negative and assumed positive lines, see figure 3A - 2(a).

Step 5. The ultimate unit resistance of each sector is obtained by taking the summation of the moments about its axis of rotation (supports) so that

$$\Sigma M_N + \quad \Sigma M_P = R_c = r_u A_c$$

a. Sector I (fig. 5A - 2)

$$\Sigma M_{VN} + \Sigma M_{VP} = 120(20{,}000) + 2(2/3)(20{,}000)(60) + \\ 120(20{,}000) + 2(2/3)(20{,}000)(60)$$

$$= 8.0 \times 10^6 \text{ in-lbs.}$$

$$r_u A_c = r_u \left[\frac{240(y)}{2} \right] \left[\frac{y}{3} \right] = 40 \ r_u y^2$$

therefore,

$$r_u = 400(20{,}000)/40y^2 = 0.2 \times 10^6/y^2$$

b. Sector II (fig. 3A - 2)

$$\Sigma M_{HN} + \Sigma M_{HP} = (168-y/2)(20{,}000) + 2/3(20{,}000)(y/2) + \\ (20{,}000)(168-y/2) + 2/3(20{,}000)(y/2)$$

$$= 336(20{,}000) - y/3(20{,}000)$$

$$r_u Ac = r_u \left[\frac{120(168+168-y)}{2} \right] \left[\frac{120[168+2(168-y)]}{3} \right]/(168+168-y)$$

$$= 4{,}800 r_u(252-y)$$

therefore,

$$r_u = \frac{336(20{,}000) - y/3(20{,}000)}{4800 \ (252-y)}$$

Step 6. Equate the ultimate unit resistance of the sectors.

$$\frac{10(20{,}000)}{y^2} = \frac{336(20{,}000) - y/3(20{,}000)}{4800(252-y)}$$

Simplifying:

$$y^3 - 1008y^2 - 144000y + 36288000 = 0$$

and the desired root is: $y = 137.6$ ins.

334

Step 7.   The ultimate unit resistance is obtained by substituting the value of y into either equation obtained in step 5, both of which yield:

$$r_u = (20,000)/(137.6)^2 = 10.6 \text{ psi}$$

Solution: Part (b) - Chart Solution

Note:

Element conforms to the requirements of section 3-8 since it is fixed on three sides and free on the remaining side and has uniform thickness in the horizontal and vertical directions.

Step 1.   Same as step 1 in part a.

Step 2.   For illustrative purposes, a different yield pattern (fig. 3A-3) will be assumed.
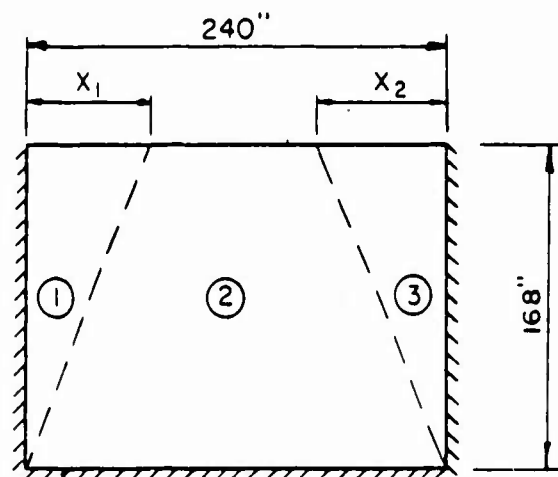
Figure 3A - 3

Step 3.   For ultimate moment capacities, see step 3 of part a

Step 4.   For three sides fixed and the fourth free, calculate the parameter.

$$X_2/X_1 = [(M_{HN3} + M_{HP})/(M_{HN1} + M_{HP})]^{1/2} = [(20,000)(2)/(20,000)(2)]^{1/2} = 1.0$$

From figure 3-11, $(X_2/X_1 = 1.0)$ calculate the parameters:

$$L/H[M_{VP}/(M_{HN1} + M_{HP})] = 240/168[20,000/(2)(20,000)]^{1/2} = 1.01$$

335

and

$$\frac{M_{VP}}{M_{VN2}} = \frac{20,000}{20,000} = 1.0$$

Read yield line location

X₁/L exceeds the maximum possible value of 0.5 therefore, assumed yield line pattern is wrong. Assume alternate yield line pattern as shown in figure 3A-2.

From figure 3-16 calculate the following parameters:

$$\frac{L}{H} = \frac{(M_{VN3} + M_{VP})^{1/2}}{(M_{HN2}+M_{HP})^{1/2} + (M_{HN1}+M_{HP})^{1/2}}$$

$$= \frac{240}{168} \left[\frac{(20,000+20,000)^{1/2}}{(20,000+20,000)^{1/2} + (20,000+20,000)^{1/2}}\right] = 0.71$$

and

$$X/L = [(M_{HN1} + M_{HP})/(M_{HN2} + M_{HP})]^{1/2} / 1+[(M_{HN1} + M_{HP})/(M_{HN2} + M_{HP})]^{1/2}$$

$$= [40,000/40,000]^{1/2} / 1+[40,000/40,000]^{1/2} = 1/2$$

From figure 3-16 read of yield line location:

y/H = 0.82; y = 0.8(168) = 137.6 in

X/L = 0.50; X = 0.5(240) = 120.0 in

Step 5.   From table 3-2

NOTE: Both equations given in the table for each edge condition and yield line location, will provide identical values of r_u.

$$r_u = \frac{5(M_{VN}+M_{VP})}{y^2} = \frac{5(20,000+20,000)}{137.6^2} = (0.00055)20,000 = 10.5 \text{ psi}$$

Example 3A-1(B) Ultimate Unit Resistance

Required: Ultimate unit resistance of the element considered in example 3A-1(A) except there is an opening as shown in figure 3A-4.

Figure 3A - 4

Solution:

Step 1. Given:
(a) L = 240"   H = 168"   Two additional free edges are formed due to the presence of the opening.

Step 2. Assumed yield line location is shown in figure 3A-5 (three different sectors are formed).

Step 3. Same as step 3 of Example 3A-1(A), part a.

Figure 3A - 5

337

Step 4. For distribution of moments across negative and assumed positively yield lines see figure 3A-5. (Since opening is located at lower right corner, there is no reduced moment capacity in this area.)

Step 5. The ultimate unit resistance is obtained from:

$$\Sigma M_N + \Sigma M_p = R_c = r_u A c$$

a. Sector 1 (fig. 3A-5)

$$\Sigma M_{HN} + \Sigma M_{HP} = (20,000)(168-y/2) + 2/3(20,000)(y/2) +$$
$$(20,000)(168-y/2) + 2/3(20,000)(y/2)$$
$$= 336(20,000) - y/3(20,000)$$
$$= (336-y/3)(20,000)$$

$$r_u A_c = r_u[x(168+168-y)/2][x(168+2(168-y))/3(168+168-y)]$$

$$= r_u x^2 (252-y)/3$$

therefore,

$$r_u = \frac{(1008-y)(20,000)}{x^2(252-y)}$$

b. Sector II (fig. 5A-5)

$$\Sigma M_{HN} + \Sigma M_{HP} = (20,000)(80) + (20,000)(80)$$
$$= 160(20,000)$$

Note:

The sector is divided into parts a, b, and c so that the centriod may be obtained (see table below).

Portion of Sector	Area (A')	Distance from Centroid to axis of rotation (c')	A'c'
a	$\dfrac{(y-88)(180-x)}{2}$	$\dfrac{(180-x)}{3} + 60 = \dfrac{360-x}{3}$	$\dfrac{(y-88)(180-x)(360-x)}{6}$
b	$(y-88)(60)$	$\dfrac{60}{2}$	$\dfrac{(y-88)(60)^2}{2}$
c	$(168-y)(240-x)$	$\dfrac{(240-x)}{2}$	$\dfrac{(168-y)(240-x)^2}{2}$

338

$$Ac = \Sigma A'c' = \frac{(y-88)(180-x)(360-x)}{6} + \frac{(y-88)(60)^2}{2} + \frac{(168-y)(240-x)^2}{2}$$

$$= \frac{1}{2}\frac{(y-88)}{3}[(180-x)(360-x) + 10800] + (168-y)(240-x)^2$$

$$r_u = \frac{(\Sigma M_{HN} + \Sigma M_{HP})}{Ac}$$

$$= \frac{6,400,000}{\frac{(y-88)}{3}[(180-x)(360-x) + 10,800] + (168-y)(240-x)^2}$$

c. Sector III (fig. 3A-5)

$$\Sigma M_{vn} + \Sigma M_{vp} = (20,000)(180-x/2) + 2/3(20,000)(x/2) +$$
$$(20,000)(180-x/2) + 2/3(20,000)(x/2)$$

$$= 360(20,000) - (20,000)x/3$$

Portion of Sector	Area (A')	Distance from Centroid to axis of rotation (c')	A'c'
a	$\dfrac{(180-x)(y-88)}{2}$	$\dfrac{(y-88)}{3} + 88 = \dfrac{y+176}{3}$	$\dfrac{(180-x)(y-88)(y+176)}{6}$
b	$(180-x)(88)$	$\dfrac{88}{2}$	$\dfrac{(180-x)(88)^2}{2}$
c	$\dfrac{xy}{2}$	$\dfrac{y}{3}$	$\dfrac{xy^2}{6}$

$$Ac = \Sigma A'c' = (y-88)(180-x)(y+176)/6 + (180-x)(88)^2/2 + xy^2/6$$

$$= 1/6 (180-x)[(y-88)(y+176)+23,232] + xy^2$$

$$r_u = \frac{\Sigma M_{HN} + \Sigma M_{HP}}{Ac}$$

$$= \frac{(2160-2x)(20,000)}{(180-x)[(y-88)(y+176)+23,232]+xy^2}$$

Step 6. Due to the complexity of obtaining a direct solution for ultimate unit resistance, a trial-and-error solution will be used (see table below):

339

x	y	r_I	r_{II}	r_{III}
125	130	9.21	7.67	9.33
125	135	9.55	7.92	8.77
125	140	9.92	8.19	8.25
125	145	10.32	8.48	7.78
125	150	10.77	8.79	7.35
130	130	8.52	8.29	9.50
130	135	8.83	8.55	8.92
131	135	8.70	8.68	8.85

Therefore:

$$x = 131 \text{ ins}$$
$$y = 135 \text{ ins}$$
$$r_u = 8.68 \text{ psi}$$

Problem 3A-2 Resistance - Defection Function

Problem: Determine the acutal and equivalent resistance deflection function in the elasto-plastic region for a two-way structural element.

Procedure:

Step 1. Establish design parameters

   a. Geometry of element.
   b. Support conditions

Step 2. Determine ultimate positive and negative moment capacities.

Step 3. Determine static properties:

   a. Moduls of elasticity for the element.
   b. Moment of inertia of the element.

Step 4. Establish points of interest and their ultimate moment capacities (fig. 3-23)

Step 5. Compute properties at first yield.

   a. Location of first yield
   b. Resistance at first yield r_e
   c. Moments at remaining points consistent with r_e
   d. Maximum deflection at first yield.

Step 6. Compute properties at second yield

   a. Remaining moment capacity at other points
   b. Location of second yield.
   c. Change in unit resistance r between first and second yield.
   d. Unit resistance at second yield r_{ep}.
   e. Moment at remaining point consistent with rep.

340

f. Change in maximum deflection.

g. Total maximum deflection.

Note:

An element fixed on three or four sides exhibits three or more yields (either in the horizontal or vertical direction). Therefore, repeat Step 6 as many times as necessary to obtain properties at the various yield points.

Step 7. Compute properties at final yield (ultimate unit resistance)

a. Ultimate unit resistance.

b. Change in resistance between ultimate unit resistance and resistance at prior yield.

c. Change in maximum deflection.

d. Total maximum deflection.

Step 8. Draw the actual resistance-deflection curve (fig. 3-39).

Step 9. Calculate equivalent maximum elastic deflection of the element.

Example: 3A-2 Resistance-Deflection Function

Required: The actual and equivalent resistance-deflection function (curve) in the elasto-plastic region for the two-way structural steel element.

Solution:

Step 1. Given:

a. $L = 240$ in. $H = 168$ in.

b. Fixed on three sides and free at the fourth.

Step 2. Same as step 3 of example 3A-1(A), part a.

Step 3. Static properties.

a. Modulus of elasticity, E_s for steel

$E_s = 29 \times 10^6$ psi

b. Considering a 1-inch strip (b = 1 inch)

Assume $I = 144$ in^4

Step 4. For points of interest, see figure 3A-6.

Step 5. Properties at first yield.

341
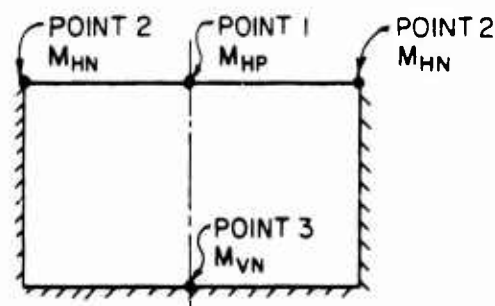
Figure 3A-6

From figure 3-27 for H/L = 0.7

$\beta_1 = 0.077$ $\qquad$ $\beta_2 = 0.160$ $\qquad$ $\beta_3 = 0.115$

$\gamma_1 = 0.012$ $\qquad$ $\upsilon = 1/6$

a. $M_{HP} = M_{HN} = M_{VP} = M_{VN} = 20,000$ in-lbs/in

$M_p = \beta r H^2$

$r = M/\beta H^2$

$r_1 = 20,000/[(0.077)(168)^2] = 9.20$ psi

$r_2 = 20,000/[(0.160)(168)^2] = 4.43$ psi

$r_3 = 20,000/[(0.115)(168)^2] = 6.16$ psi

First yield at point 2 (smallest r)

b. $r_e = 4.43$ psi

c. M_p (Point 1) = $(0.077)(4.43)(168)^2 = 9,627$ in-lbs/in

M_N (Point 3) = $(0.115)(4.43)(168)^2 = 14,379$ in-lbs/in

d. $D = EI/b(1-v^2)$

$\qquad = 29 \times 10^6 \times 144/1[1-(0.1667)^2] = 43.0 \times 10^8$ in-lbs

$X_e = \gamma_1 r_e H^4/D = (0.0120)(4.43)(168)^4/43(10^8) = 0.0098$ in

Step 6. Properties at second yield.

After first yield element assumes a simple-simple-fixed-free stiffness, therefore from figure 3-29 for $H/L = 0.7$.

$\beta_1 = 0.120$ $\qquad$ $\beta_3 = 0.220$

$\gamma_1 = 0.045$ $\qquad$ $\upsilon = 0.3$

a. $\quad M_P$ (Point 1) $= M_{HP} - M_p$ (at r_e)

$\qquad = 20,000 - 9627 = 10373$ in-lbs/in

$\quad M_N$ (Point 3) $= M_{VN} - M_p$ (at r_e)

$\qquad = 20,000 - 14,379 = 5621$ in-lbs/in

b. $\quad M_P$ (Point 1) $= 10373$ in-lbs/in $= \beta_1 \Delta r H^2$

$\qquad \Delta r = 10373/(0.120)(168)^2 = 3.06$ psi

$\quad M_n$ (Point 3) $= 5,621$ in-lbs/in $= \beta_3 \Delta r H^2$

$\qquad \Delta r = 5,621/[(0.220)(168)^2] = 0.90$ psi

Second yield at Point 3 (smaller Δr)

c. $\quad \Delta r = 0.90$ psi

d. $\quad r_{ep} = r_e + \Delta r = 4.43 + 0.90 = 5.33$ psi

e. $\quad M_P$ (Point 1) $= 0.120(0.90)(168)^2$

$\qquad = 3,048$ in-lbs/in

f. $\quad D = EI/b(1-v^2) = (29)(10^6)(144)/1[1-(0.3)^2]$

$\qquad = 45.9 \times 10^8$ in-lbs/in

$\Delta x = \gamma_1 \Delta r H^4/D = 0.030(0.90)(168)^4/45.9(10)^8$

$\qquad = 0.0047$ in

g. $\quad X_{ep} = X_e + \Delta X = 0.0098 + 0.0047 = 0.014$ in

Step 7. Properties at final yield (ultimate unit resistance). After second yield element assumes a simple-simple-simple-free stiffness, therefore from figure 3-30 for $H/L = 0.7$.

$\gamma_1 = 0.045$ $\qquad$ $\upsilon = 0.3$

a. $\quad r_u = 10.6$ psi (part a, example 3A-1(A))

b. $\quad \Delta r = r_u - r_{ep} = 10.6 - 5.33 = 5.27$ psi

343

c. $D = EI/b(1-v^2) = 29(10^6)(144)/1[1-(0.3)^2]$

$= 45.9 \times 10^8$ in-lbs

$\Delta x = \gamma_1 \; rH^4/D = (0.045)(5.27)(168)^4/45.9 \times 10^8$

$= 0.041$ in

d. $X_p = X_{ep} + \Delta X = 0.014 + 0.041 = 0.055$ in

Step 8. For actual resistance-deflection curve, see figure 3A-7.

Step 9. $X_E = X_e(r_{ep}/r_u) + X_{ep}[1-(r_e/r_u)] + X_p[1-(r_{ep}/r_u)]$

Equation 3-35

$= 0.0098(5.33/10.6) + 0.014 [1-(4.43/10.6)]$

$+ 0.055[1-(5.33/10.6)]$

$= 0.00493 + 0.0081 + 0.0273$

$= 0.04033$ in

The equivalent resistance-deflection curve is shown in figure 3A-7.

Problem 3A-3 Dynamic Design Factors For A One Way Element

Problem: Determine the plastic load, mass and load-mass factors for a one-way element.

Procedure:

Step 1. Establish design parameters.

Step 2. Determine deflected shape.

    a. geometry of element
    b. support conditions
    c. type of load and mass

Step 3. Determine maximum deflection

Step 4. Determine deflection function

    a. For distributed load and/or continuous mass determine the deflection at any point.

344

Figure 3A-7

345
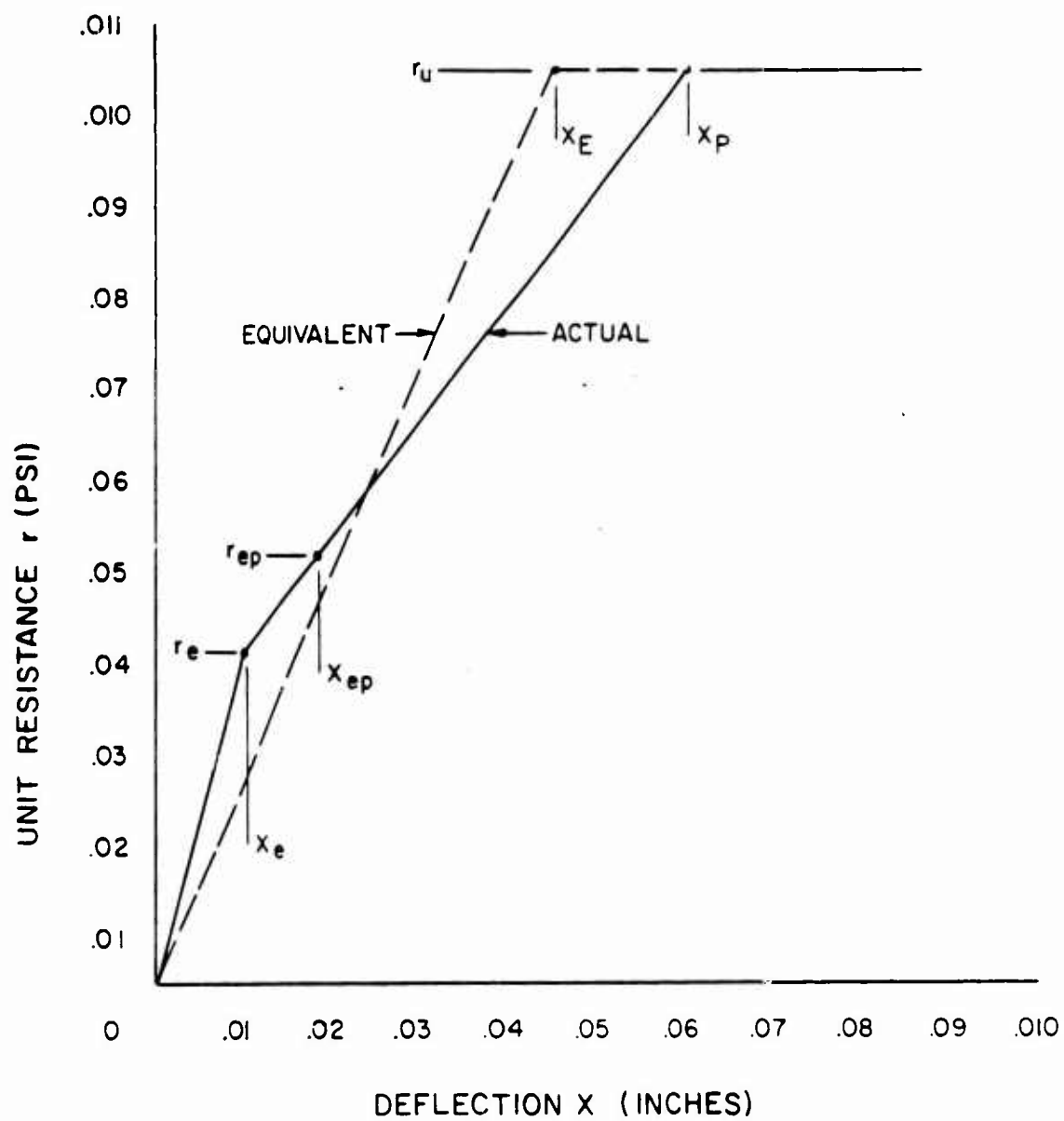
b. For concentrated loads and concentrated mass determine the deflection at the load.

Step 5.   Calculate the shape function

a. For distributed load and/or continuous mass calculate $\phi(x)$, equation 3-43.

b. For concentrated load and concentrated mass calculate ϕ_r, equation 3-46.

Step 6.   Calculate the load factor, K_L.

a. Use equations 3-41 and 3-42 for a distributed load.

b. Use equations 3-41 and 3-45 for a concentrated load

Step 7.   Calculate the mass factor, K_M.

a. Use equations 3-47 and 3-48 for a continuous mass

b. Use equations 3-44 and 3-49 for concentrated mass

Step 8.   Calculate the load-mass factor K_{LM}, from equation 3-53.

Example 3A-3(A)   Dynamic Design Factors For A One-Way Element

Required: The load, mass and load-mass factors for a structural steel beam in the elastic range, with a distributed load.

Solution:

Step 1:   Given structural steel beam shown in figure 3A-8
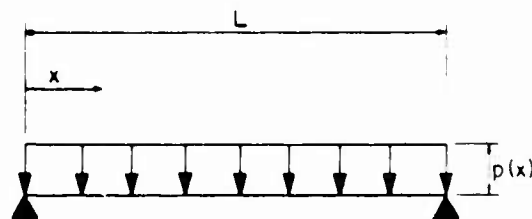
Figure 3A-8

a.   L = 120 in.
b.   Simply supported on both edges
c. $p(x) = 2,000 \ \text{lb/in}$
   $m(x) = 0.0055(\text{lb-s}^2/\text{in}^4)/\text{in}$

346
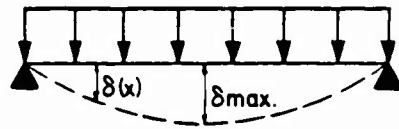
Figure 3A-9

Step 2: Assumed deflected shape for elastic range is shown in figure 3A-9

Step 3: The maximum deflection at the center is

$$\delta_{max} = \frac{5p(x)L^4}{384\ EI}$$

Step 4: Determine deflection function

$$\delta(x) = \frac{p(x)}{24EI}\ (L^3 - 2Lx^2 + x^3)$$

Step 5: Calculate the shape function using equation 3-43

$$\phi = \frac{\delta(x)}{\delta_{max}} = \frac{p(x)x}{24EI}\ (L^3 - 2Lx^2 + x^3)\ \frac{384EI}{5p(x)L^4}$$

$$= \frac{16}{5L^4}(L^3x - 2Lx^3 + x^4)$$

Step 6: a. Using equation 3-42, determine equivalent force

$$F_E = \int_0^L p(x)\phi(x)dx = \int_0^{120}(2{,}000\ \text{lb/in})\ \frac{16}{5L^4}(L^3x - 2Lx^3 + x^4)dx$$

$$= \frac{6{,}400}{L^4}\ \frac{L^3x^2}{2} - \frac{2Lx^4}{4} + \frac{x^5}{5}\ \Big|_0^{120} = 1{,}280L/\Big|_0^{120}$$

$$= 153{,}600\ \text{lb.}$$

b. From equation 3-41, find the load factor

$$K_L = \frac{F_E}{F} = \frac{153{,}600\ \text{lb.}}{(2{,}000\ \text{lb/in} \times 120\ \text{in.})}$$

$K_L = 0.64$ in the elastic range

Step 7:   a. Find the equivalent mass from equation 3-48

$$M_E = \int_0^L m(x)\phi^2(x)dx = .0055 \frac{256}{25 L^8} \int_0^{120}(L^3 x - 2Lx^3 + 4)^2 dx$$

$$= \frac{1.408}{25 L^8} \int_0^{120}(L^5 x^2 - 4L^4 x^4 + 2L^3 x^5 + 4L^2 x^6 - 4Lx^7 + x^8)dx$$

$$= \frac{1.408}{25} \left. \frac{L^6 x^3}{3} - \frac{4L^4 x^5}{5} + \frac{2L^3 x^6}{6} + \frac{4L^2 x^7}{7} - \frac{4Lx^8}{8} + \frac{x^9}{9} \right|_0^{120}$$

$$= .00277 L \left. \right|_0^{120}$$

$$= 0.3325 \text{ lb} - s^2/in^3$$

   b. From equation 3-47, calculate the mass factor

$$K_M = \frac{M_E}{M} = \frac{0.3325 \text{ lb} - s^2/in^3}{(0.0055 \text{ lb} - s^2/in^4 \times 120 \text{ in})}$$

$K_M = 0.50$ in the elastic range

Step 8:   Calculate the load-mass factor as defined by equation 3-51

$$K_{LM} = K_M/K_L$$

$$= 0.50/0.64$$

$K_{LM} = 0.78$ in the elastic range

Example 3A-3(B)   Dynamic Design Factors For A One-Way Element

Required: The load, mass and load-mass factors for a structural
          steel beam in the plastic range with a distributed load.

Solution:

   Step 1. Given the structural steel beam shown in figure 3A-8

      a. L = 120 in.

      b. Simply-supported on both ends

      c. $p(x) = 2,000$ lb/in

      d. $m(x) = 0.0055$ (lb - s^2/in^4)/in

   Step 2. Assume deflected shape for the plastic range is shown in
          figure 3A-10

348
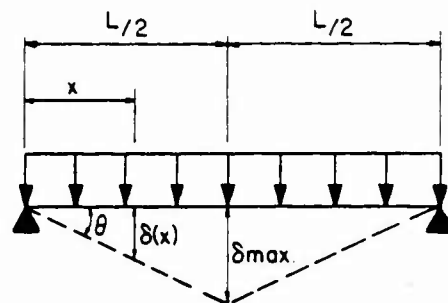
Figure 3A-10

Step 3. Determine maximum deflection

$$\delta_{max} = (L/2)\tan\Theta$$

Step 4. Determine the deflection at any point.

$$\delta(x) = x\tan\Theta \qquad\qquad x < L/2$$

Step 5. Calculate the shape function, equation 3-43

$$\phi(x) = \frac{\delta(x)}{\delta_{max}} = \frac{x\tan\Theta}{(L/2)\tan\Theta}$$

$$= 2x/L \quad x < L/2$$

Step 6:

    a. Find F_E using equation 3-42.

$$F_E = \int_0^L p(x)\phi(x)dx = 2\int_0^{60}(2,000\ lb/in)(2x/L)dx$$

$$= 4,000\ lb/in\ \ x^2/L\ \Big|_0^{60}$$

$$= 120,000\ lb$$

    b. From equation 3-41

$$K_L = \frac{F_E}{F} = \frac{120,000\ lb.}{(2,000\ lb/in)120\ in}$$

$$K_L = 0.5\ \text{in the plastic range}$$

Step 7:

    a. Use equation 3-48 to find the equivalent mass

$$M_E = \int_0^L m(x)\phi^2(x)dx = 2\int_0^{60}(1.0055)(4\ x^2/L2)dx$$

$$= 0.044\ \frac{x^3}{3L^2}\Big|_0^{60}$$

$$= 0.22\ lb - s^2/in^3$$

349

b. As defined by equation 3-47

$$K_M = \frac{M_E}{M} = \frac{0.22 \ lb - s^2/in^3}{(0.0055 \ lb - s^2/in^4)120 \ in}$$

$K_M = 0.33$ in the plastic range

Step 8. Calculate K_{LM} using equation 3-53

$$K_{LM} = K_M/K_L$$

$$= 0.33/0.5$$

$K_{LM} = 0.66$ in the plastic range

Example 3A-3(C) Dynamic Design Factors For A One-Way Element

Required: The load, mass and load-mass factors for a structural steel beam in the elastic range, with a concentrated load.

Solution:

Step 1: Given structural steel beam shown in figure 3A-11
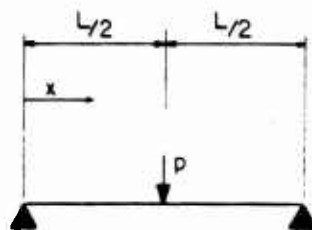
Figure 3A-11

a. L = 120 in.
b. Simply supported on both sides
c. F = 240 kips
    $m(x) = 0.0055(lb - s^2/in^4)/in.$

Step 2: Assume deflected shape for elastic range is shown in figure 3A-12

350
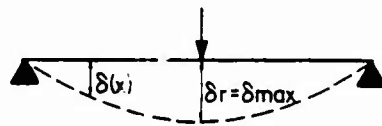
Figure 3A-12

Step 3: Determine maximum deflection

$$\delta_{max} = \frac{PL^3}{48EI}$$

Step 4: Determine deflection functions

a. for continuous mass,

$$\delta(x) = \frac{Px}{48EI} (3L^2 - 4x^2)$$

b. for concentrated load

$$\delta_r = \frac{PL^3}{48EI}$$

Step 5: Calculate shape functions

a. for continuous mass use equation 3-43

$$\phi(x) = \frac{\delta(x)}{\delta_{max}} = \frac{Px(3L^3 - 4x^2)}{48EI} \frac{48EI}{PL^3}$$

$$= (3L^2x - 4x^3)/L^3$$

b. for concentrated load, use equation 3-46

$$\phi_r = \frac{PL^3}{48EI} \frac{48EI}{PL^3}$$

$$= 1.0$$

Step 6:

a. Find equivalent force from equation 3-45

$$F_E = \sum_{r=1}^{i} F_r \phi_r = Px1 = 240 \text{ kips}$$

351

b. Using equation 3-41, calculate the load factor

$$K_L = \frac{F_E}{F} = \frac{240 \text{ kips}}{240 \text{ kips}}$$

$K_L = 1.0$ for the elastic range

Step 7: a. Equation 3-48 gives the equivalent mass.

$$M_E = \int_0^L m(x)\phi^2(x)dx = \int_0^{120} \frac{(0.0055)}{L^6} (9L^4x^2 - 24L^2x^4 + 16x^6)dx$$

$$= \frac{0.0055}{L^6} \left[3L^4x^3 - \frac{24L^2x^5}{5} + \frac{16x^7}{7} \right]_0^{120}$$

$$= 0.0027L/_0^{120}$$

$$= 0.321b - s^2/in^3$$

b. From equation 3-47, calculate the mass factor

$$K_M = \frac{M_E}{M} = \frac{0.321b - s^2/in^3}{(0.0055 \, 1b - s^2/in^4 \times 120in)}$$

$K_M = 0.49$ in the elastic range

Step 8: Calculate the load-mass factor, from equation 3-53

$$K_{LM} = K_M/K_L$$

$$= 0.49/1.0$$

$K_{LM} = 0.49$ for the elastic range

Example 3A-3(D)   Dynamic Design Factors For A One-Way Element

Required: Determine the load, mass and the load-mass factors for a structural steel beam, in the plastic range, with a concentrated load.

Solution:

Step 1. Given structural steel beams shown in figure 3A-11.

a. L = 120 in

b. Simply-supported at both edges

c. F = 240 kips

$$m(x) = 0.0055 \ (1b - s^2/in^4)/in$$

Step 2. Assumed deflected shape for the plastic range is shown in figure 3A-13
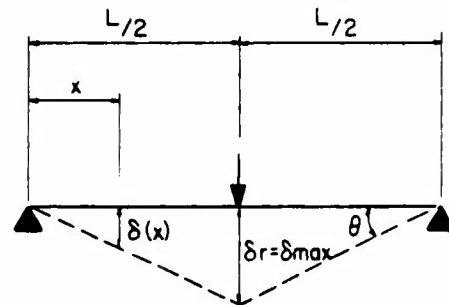
Figure 3A-13

Step 3: Determine maximum deflection

$$\delta_{max} = (L/2)\tan\Theta$$

Step 4: Determine deflection function.

a. for continuous mass

$$\delta(x) = x\tan\Theta \qquad\qquad x < L/2$$

b. for a concentrated load

$$\delta_r = (L/2)\tan\Theta$$

Step 5: Calculate shape factors using

a. equation 3-43 for continuous mass

$$\phi(x) = \frac{\delta(x)}{\delta_{max}} = \frac{x\tan\Theta}{(L/2)\tan\phi}$$

$$= 2x/L \qquad\qquad x < L/2$$

b. equation 3-46 for concentrated load

$$\phi_r = \frac{\delta_r}{\delta_{max}} = \frac{(L/2)\tan\Theta}{(L/2)\tan\Theta}$$

$$= 1.0$$

353

Step 6:   a. The equivalent force is found using equation 3-45

$$F_E = \sum_{r=1}^{i} F_r \phi_r = Px1$$

          = 240 kips

          b. Equation 3-41 gives the load factor

$$K_L = \frac{F_E}{F} = \frac{240 \text{ kips}}{240 \text{ kips}}$$

$K_L = 1.0$ for plastic range

Step 7:   a. The equivalent mass is found using equation 3-48

$$M_E = \int_0^L m(x)\phi^2(x)dx = 2\int_0^{60}(0.0055)(4x^2/L^2)dx$$

$$= 0.44 \left. \frac{x^3}{L^3} \right|_0^{60}$$

$$= 0.22 \text{ lb} - s^2/in^3$$

          b. Solve for K_M using equation 3-47

$$K_M = \frac{M_E}{M} = \frac{0.22 \text{ lb} - s^2/in^3}{(0.0055 \text{ lb} -s^2/in^4)120 \text{ in}}$$

$K_M = 0.33$ in the plastic range

Step 8:   From equation 3-53, calculate K_{LM}

$$K_{LM} = K_M/K_L$$

          = 0.33 in the plastic range

Problem 3A-4   Plastic Load-Mass Factor

Problem: Determine the platic load-mass factor K_{LM} for a two-way element
           using (1) general solution and (2) chart solution.

           Note: The determination of the plastic load-mass factor follows
           the calculations for the ultimate resistance, hence the structural
           configuration and the location of the plastic yield lines will be
           known.

Procedure: Part (a) - General Solution

           Step 1. See part a, problem 3A-1 for the structural configuration
                    and location of plastic yield lines. Denote sectors
                    formed by yield lines.

Step 2. Determine the load-mass factors properties I, c, and L'
for all sectors.
Step 3. Determine the factor I/cL' for all sectors.
Step 4. Calculate the total area of the element.
Step 5. With values obtained above, calculate the plastic load-mass factor for the element using equation 3-57.

Note: In the above problem, an element of uniform thickness was considered. For non-uniform elements, the load-mass factor is calculated using equation 3-53 where the mass of the individual sectors must be considered.

Procedure: Part (b) - Chart Solution

Step 1. See part b, problem 3A-1 for structural configuration and location of plastic yield lines in terms of x/L or y/H.

Step 2. For known value of X/L or y/H and support condition, determine the load-mass factor for the element from figure 3-44.

Note: Chart solution may be used only if the element conforms to the requirements listed in section 3-17.3

Example 3A-4   Plastic Load-Mass Factor

Required: Plastic load-mass factor for the element considered in example 3A-1(A) using (1) general solution and (2) chart solution.

Solution: Part (a) - General Solution

Step 1. Given structural configuration and location of yield lines shown
below (see part a, example 3A-1(A)) in figure 3A-14.

L = 240 in
H = 168 in
X = 120 in
y = 137.6 in
T_c = constant

Figure 3A - 14

355
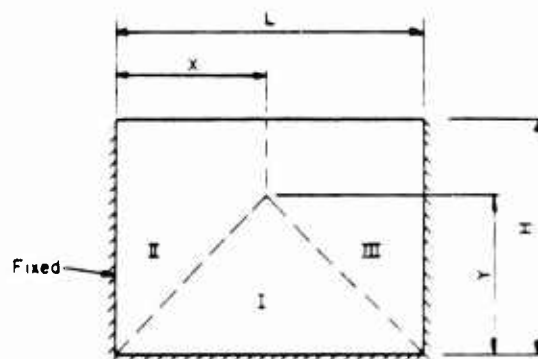
Step 2. Load-mass factor properties.

    a. Sector I.

$$L' = y = 137.6 \text{ in}$$

$$c = y/3 = 137.6/3$$

$$I = L(L')^3/12 = 240(137.6)^3/12$$

    b. Sector II
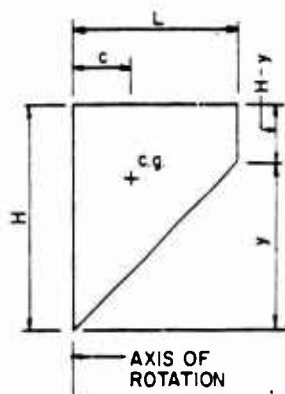
Figure 3A-15

Figure 3A - 16

$$L' = x = 120 \text{ in}$$

$$H - y = 168 - 137.6 = 30.4 \text{ in}$$

$$c = \frac{L'[H + 2(H-y)]}{3[H + (H-y)]} = \frac{120[168 + 2(30.4)]}{3(168 + 30.4)}$$

$$c = 120(0.384)$$

$$I = \frac{(H-y)(L')^3}{3} + \frac{y(L')^3}{12}$$

$$= \frac{30.4(120)^3}{3} + \frac{137.6(120)^3}{12} = 21.60(120)^3$$

Step 3. Calculate factor I/cL' for each sector:

Sector I. $\dfrac{I}{cL'} = \dfrac{\dfrac{240(137.6)^3}{12}}{(\dfrac{133.4}{3})(133.4)} = 8{,}256 \text{ in}^2$

Sector II. $\dfrac{I}{cL'} = \dfrac{21.60(120)^3}{(0.390 \times 120)(120)} = 6{,}646 \text{ in}^2$

Sector III. $\dfrac{I}{cL'} = 6{,}646 \text{ in}^2$

    Step 4. Area of panel

$$A = LH = 240(168) = 40{,}320 \text{ in}^2$$
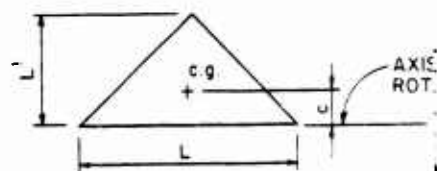
Step 5.   Load-mass factor

$$K_{LM} = \frac{I/cL'}{A} \qquad \text{(eq. 6-14)}$$

$$K_{LM} = \frac{8,256 + 2(6,646)}{40,320} = 0.534$$

Solution: Part (b) - Chart Solution

Step 1. Given: Panel fixed on 3 edges, 1 free and y/H = 0.803   (see part b, example 3A-1(A)).

Step 2. From figure 3-44, read load-mass factor

$$K_{LM} = 0.543$$

Problem 3A-5 Response of a Single-Degree-of Freedom System subject to Dynamic Load

Problem: Determine the maximum response and the corresponding time it occurs of a single-degree-of-freedom system subjected to dynamic load using (a) numerical methods and (b) design charts.

Procedure: Part (a) - Numeri. Methods

Step 1. Establish dimensional parameters of the system.

Step 2. Determine the natural period of vibration and integration time interval.

Step 3. Construct a table similar to table 3-14 of section 3-19.2. Note: For the first interval n=1, Equation 3-59 is used and subsequent intervals, the recurrence formula (eqn. 3-56) is used.

Procedure: Part (b) - Chart solution

Step 1. Same as step 1 of example 3A-5, part a.

Step 2. Determine the non-dimensional parameters.

Step 3. Determine the ratio of the maximum desplacement to the elastic displacement X_m/X_E and the ratio of the time at which this maximum displacement occurs to the duration of the blast load.

Example 3A-5 Maximum Response of Single-Degree-of-Freedom System Subjected to a Triangular Load.

Required: The maximum response and the time it occurs, of a single-degree-of-freedom system subjected to blast loads, using (a) numerical methods and (b) design charts.

357

Solution: Part (a) - Numerical Methods

Step 1. Given:
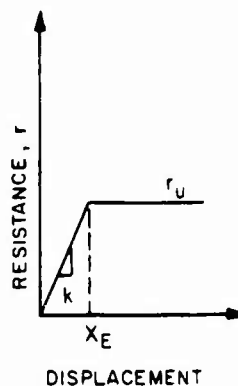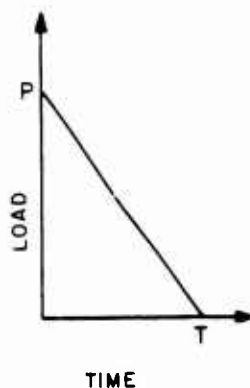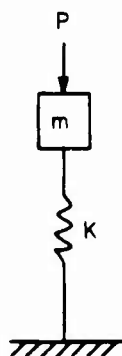
(a) Single-Degree-of-
Freedom System

(b) External Load

(c) Resistance
Function

Figure 3A-17   Single-Degree-of-Freedom System subjected to external loads.

$$m = 2.5 \text{ Kips-sec}^2/\text{ft}$$
$$K = 9,860 \text{ Kips/ft}$$
$$r_u = 750 \text{ Kips}$$
$$X_E = 0.076 \text{ ft}$$
$$T = 0.10 \text{ sec}$$
$$P = 1000 \text{ Kips}$$

Step 2. Natural period of vibration and integration time interval.

$$T_N = 2 \quad [m/K]^{1/2} = 2(\ ) [2.5/9,860]^{1/2} = 0.10 \text{ sec}$$

$$t = T_N/10 = 0.01 \text{ sec}$$

Step 3. Construct table as shown below.

358

1	2	3	4	5	6	7	8	9	10
n	t (sec)	P_n (Kips)	R_n (Kips)	P_n-R_n (Kips)	$A_n=(P_n-R_n)/m$ (ft/sec^2)	$a_n(\Delta t)^2$ (ft)	$2X_n$ (ft)	X_{n-1} (ft)	X_{n+1} (ft)
0	0	1000	0	1000	400	0.040	0.0	0.0	0.020
1	0.01	900	197.200	702.800	281.120	0.028112	0.0400	0.0	0.068112
2	0.02	800	671.584	128.426	51.366	0.05137	0.13622	0.020	0.121357
3	0.03	700	750	-50.0	-20.0	-0.00200	0.242714	0.06811	0.17261
4	0.04	600	750	-150.0	-60.0	-0.00600	0.34522	0.121357	0.21786
5	0.05	500	750	-250.0	-100.0	-0.0100	0.43573	0.17261	0.25312
6	0.06	40	750	-350.0	-140.0	-0.0140	0.050623	0.21786	0.27437
7	0.07	300	750	-450.0	-180.0	-0.0180	0.54874	0.25312	0.27762
8	0.08	200	750	-550.0	-220.0	-0.0220	0.55525	0.27437	0.25880
9	0.09								

Note: $P_n = f(t_n) = 1000\,[1-n(\Delta t/T)]$

$$R_n = \begin{cases} KX_n & \text{for } X_n < X_e \\ r_u = 750 & \text{for } X_n > X_e \end{cases}$$

$$X_{n+1} = 2X_n - X_{n-1} + a_n(\Delta t)^2$$

Note:

For n=0, X_{n+1} (Column 10) $= X_{0+1} = X_1 = (1/2)a_0(\Delta t)^2$

$$= (1/2)(0.040)$$

$$= 0.02 \text{ ft}$$

For n=1, $2X_n$ (Column 8) $= 2X_1 = 2[(1/2)a_0(\Delta t)^2]$

$$= 2(0.02) = 0.04 \text{ ft}$$

X_{n-1} (Column 9) $= X_0 = 0.0$

X_{n+1} (Column 10) $= X_2 \qquad = 2X_1 - X_0 + a_1(\Delta t)^2$

$$= 2(0.02) - 0 + 0.02811$$

$$= 0.06811 \text{ ft}$$

For n=2, $2X_n$ (Column 8) $= 2X_2 = 2(0.06811)$

$$= 0.13622 \text{ ft.}$$

$$X_{n-1} \text{ (Column 9)} \quad = X_1 = 0.02 \text{ ft.}$$

$$X_{n+1} \text{ (Column 10)} \quad = X_3 = 2X_2 - X_1 + a_2 (\Delta t)^2$$

$$= (2)(0.06811) - 0.02 + 0.005137$$

$$= 0.12357 \text{ ft.}$$

For n=3, 4,..., repeat the above procedure.

Solution: Part (b) - Design Charts

Step 1. Same as step 1 of example 3A-5, part a

Step 2. Non-dimensional parameters

    a. Natural period of vibration, T_n

$$T_n = 2\pi[m/K]^{12} = 2\pi[2.5/9,860]^{12} = 0.10 \text{ sec}$$

    b. Ratio of duration of blast load T to natural period T_N

$$T/T_N = 0.10/0.10 = 1.0$$

    c. Ratio of peak resistance r_u to peak load P

$$r_u/P = 750/1000 = 0.75$$

Step 3. Using the ratios calculated in step 2 and figures 3-54 and 3-55, determine the value of X_m/X_E and t_m/TN.

    For $T/T_N = 1$ and $r_u/P = 0.75$

    $X_m/X_E = 3.7$ from figure 3-54

    $t_m/T = 0.77$ from figure 3-55

Step 4. Determine X_m and t_m

    $X_m/X_E = 3.7$

    $X_m = (3.7)X_E = (3.7(r_u/K_E)$

        $= (3.7)(750/9,860) = 0.28144 \text{ ft.}$

    $t_m/T = 0.77$

    $t_m = (0.77)T = 0.77(0.10) = 0.077 \text{ sec}$

Problem 3A-6 Maximum Response of a Single-Degree-of-Freedom System to Bilinear Blast Loads

Problem: Determine X_m/X_E, t_m/T_N and t_E/T (when applicable) for a single-degree-of-freedom system subject to various bilinear blast loads.

Procedure: Part (a) - Solution in Region D

  Step 1. Establish normalized parameters

  Step 2. Enter table 3-15 with the given C parameters and determine which figures have to be used.

  Step 3. Enter each of the figures determined in step 2, with the given values of the other two parameters and determine the region where the intersection points are located.

  Step 4. Based on the region where the intersection points are located, enter the appropriate figure and find X_m/X_E, t_m/T_N and t_E/T.

Procedure: Part (b) - Solution in Region C - Graphical Interpolation.

  Step 1. Same as step 1 in part a.

  Step 2. Same as step 2 in part a.

  Step 3. Same as step 3 in part a.

  Step 4. Set up a table as shown in table 3A-1. Post each figure number and the corresponding values of C_1 and C_2, leaving a space between each line of information. Post in the spaces the appropriate valuesof C_1 and C_2 needed for interpolation. Enter each of the figures determined in Step 2 with the given parameters and find the values of X_m/X_E. Post these values in table 3A-1.

  Step 5. Use log-log graph paper to plot the points obtained in Step 4. Post these values in table 3A-1, using linear interpolation where necessary.

  Step 6. Plot on log-log graph paper the points which represent (X_m/X_E, C_2) for the given value of C. Use linear interpolation to find X_m/X_E for given value of C_2.

Procedure: Part (c) - Solution in Region C - Mathematical Interpolation

  Step 1. Same as step 1 in part a.

  Step 2. Same as step 2 in part a.

  Step 3. Same as step 3 in part a.

361

Step 4. Same as step 4 in part b.

Step 5. Solve for $\ln Y_a$ and $\ln Y_b$ using equations 3-83 and 3-84.

Step 6. Solve for $\ln Y$ using equation 3-85.

Step 7. Solve for Y using equation 3-86.

Example 3A-6 Maximum Response of a Single-Degree-of-Freedom System to Bilinear Blast Loads

Required: Determine X_m/X_E, t_m/T_N and t_E/T (when applicable) for a single-degree-of-freedom system subject to various bilinear blast loads.

Solution: Part (a) - Solution in Region D

Step 1. Given: $P/r_u = 1.0$

   $T/T_N = 3.0$

   $C_1 = 0.66$

   $C_2 = 50$

Step 2. Enter table 3-15 with $C_1 = 0.66$ and $C_2 = 50$. Note figures 3-119, 3-120, 3-147, and 3-148 apply.

Step 3. Enter each of the figures determined in step 2, with $P/r_u = 1.0$ and $T/T_N = 3.0$. Note that the intersection point is located to the right of the line of solid squares, defined as region D. In region D, the maximum dynamic response depends only on the shock load described by P/r_u and T/T_n; the gas load described by $C_1 P/r_u$ and $C_2 T/T_n$ does not influence the maximum dynamic response. Consequently, figures 3-64a and 3-64b for a single triangular load pulse apply. Enter figure 3-64a with $P/r_u = 1.0$ and $T/T_N = 3.0$ and find $X_m/X_E = 3.55$, $t_m/T_N = 0.98$, $t_E/T = 0.086$.

Solution: Part (b) - Solution in Region C - Graphical Interpolation

Step 1. Given: $P/r_u = 32$

   $T/T_N = 0.10$

   $C_1 = 0.06$

   $C_2 = 20$

Step 2. Enter table 3-15 with $C_1 = 0.06$ and $C_2 = 20$. Note figures 3-108, 3-109, 3-133 and 3-134 apply.

Step 3. Enter each of these figures with $P/r_u = 32$ and $T/T_n = 0.10$. Note that the intersection point is not located in regions A, B or D. Therefore the intersection points lie in region C and interpolation between charts is required to obtain a solution.

Step 4. Set up table as shown in table 3A-1 below. Post each chart number and the corresponding values of C_1 and C_2, leaving a space between each line of information. Post in the spaces the appropriate values of C_1 and C_2 needed for interpolation. Enter figure 3-108 with $P/r_u = 32$ and $T/T_N = 0.10$ and find $X_m/X_E = 112$. Post this value in the table. Enter figure 3-109 with $P/r_u = 32$ and $T/T_N = 0.10$ and find $X_m/X_E = 86$. Post this value in the table. Repeat this process for figures 3-133 and 3-134, and post values for X_m/X_E in the table.

Step 5. Use log-log graph paper to plot the points (112,0.068) and (86,0.046) which represent $(X_m/X_E, C_1)$ for $C_2 = 10$ as shown in figure 3-267. Use straight-line interpolation to find $X_m/X_E = 103$ for $C_1 = 0.060$. Post this value in the table. Repeat this process for $C_2 = 30$, and find $X_m/X_E = 251$ for $C_1 = 0.06$ as shown in figure 3-267.

Step 6. Plot on log-log graph paper the points (103,10) and (251,30) which represent $(X_m/X_E, C_2)$ for $C_1 = 0.060$. Use straight-line interpolation for find $X_m/X_E = 182$ for $C_2 = 50$ as shown in figure 3-267. Thus the solution is $X_m/X_E = 182$.

Table 3A-1

Figure No.	C_1	C_2	X_m/X_E		
3-108	0.068	10	112		
	0.060	10	--	103	
3-109	0.046	10	86		
	0.060	20	--		182
3-133	0.075	30	340		
	0.060	30	--	251	
3-134	0.056	30	230		

Solution: Part (c) – Solution in region C – Mathematical Interpolation

Step 1. Same as step 1 of part (b).

Step 2. Same as step 2 of part (b).

Step 3. Same as step 3 of part (b).

Step 4. Same as step 4 of part (b).

Step 5. Using equation 3-83 and 3-84, find $\ln Y_a$ and $\ln Y_b$.

$$\ln Y_a = \ln Y_1 + \frac{\ln(Y_2/Y_1)\ln(C_1/C_{11})}{\ln(C_{12}/C_{11})}$$

$$= \ln 112 + \frac{\ln(86/112)\ln(0.060/0.068)}{\ln(0.046/0.068)}$$

$$\ln Y_a = 4.6339$$

$$\ln Y_b = \ln Y_3 + \frac{\ln(Y_4/Y_3)\ln(C_1/C_{13})}{\ln(C_{14}/C_{13})}$$

$$= \ln 340 + \frac{\ln(230/340)\ln(0.06/o.075)}{\ln(0.056/0.075)}$$

$$\ln Y_a = 5.5304$$

Step 6. Find lnY from equation 3-85

$$\ln Y = \ln Y_a + \frac{\ln Y_b - \ln Y_a)\ln(C_2/C_{21})}{\ln(C_{23}/C_{21})}$$

$$= 4.6339 + \frac{(5.5304 - 4.639)\ln(20/10)}{\ln(30/10)}$$

$$\ln Y = 5.1995$$

Step 7. Solve for Y using equation 3-86

$$Y = e^{\ln Y}$$

$$= e^{5.1995}$$

$$Y = 181$$

APPENDIX 3B

LIST OF SYMBOLS

365

APPENDIX 3B - LIST OF SYMBOLS

a   (1)   acceleration $(in./ms^2)$

              (2)   depth of equivalent rectangular stress block (in.)

A area $(in.^2)$

A_a area of diagonal bars at the support within a width b $(in.^2)$

A_o area of openings (ft^2)

A_s area of tension reinforcement within a width b $(in.^2)$

A_s' area of compression reinforcement within a width b $(in.^2)$

A_{sH} area of flexural reinforcement within a width b in the horizontal

            direction on each face $(in.^2)$*

A_{sV} area of flexural reinforcement within a widtn b in the vertical

            direction on each face $(in.^2)$*

A_v total area of stirrups or lacing reinforcement in tension within a

            distance, s_s or s_1 and a width b_s or b_1 $(in.^2)$.

A_I, A_{II} area of sector I and II, respectively $(in._2)$

b   (1)   width of compression face of flexural member (in.)

             (2)   width of concrete strip in which the direct shear stresses at

                    the supports are resisted by diagonal bars (in.)

b_s width of concrete strip in which the diagonal tension stresses are

            resisted by stirrups of area A_v (in.)

b_1 width of concrete strip in which the diagonal tension stresses are

            resisted by lacing of area A_v (in.)

B   constant defined in pargraph

---

* See note at end of symbols.

c	(1) distance from the resultant applied load to the axis of rotaton (in.)
	(2) damping coefficient
c_I, c_{II}	distance from the resultant applied load to the axis of rotation for sectors I and II, respectively (in.)
c_s	dilatational velocity of concrete (ft/sec)
C	shear coefficient
C_{cr}	critical damping
C_d	shear coefficient for ultimate shear stress of one-way elements
C_f	post-failure fragment coefficient (lb^2-$ms^4/in.^8$)
C_{ra}	peak reflected pressure coefficient at angle of incidence a
C_s	shear coefficient for ultimate support shear for one-way elements
C_{sH}	shear coefficient for ultimate support shear in horizontal direction for two-way elements*
C_{sV}	shear coefficient for ultimate support shear in vertical direction for two-way elements*
C_D	drag coefficient
$C_D q$	drag pressure (psi)
$C_D q_o$	peak drag pressure (psi)
C_E	equivalent load factor
C_H	shear coefficient for ultimate shear stress in horizontal direction for two-way elements*
C_L	leakage pressure coefficient

---

* See note at end of symbols.

C_M maximum shear coefficient

C_u impulse coefficient at deflection X_u (psi-ms^2/in.^{2})

C_u' impulse coefficient at deflection X_m (psi-ms^2/in.^{2})

C_v shear coefficient for ultimate shear stress in vertical direction for two-way elements*

C_1 (1) impulse coefficient at deflection X_1 (psi-ms^2/in.^{2})

(2) parameter defined in figure

(3) ratio of gas load to shock load

C_1' impulse coefficient at deflection X_m (psi-ms^2/in.^{2})

C_2 ratio of gas load duration to shock load duration

d distance from extreme compression fiber to centroid of tension reinforcement (in.)

d' distance from extreme compression fiber to centroid of compression reinforcement (in.)

d_c distance between the centroids of the compression and tension reinforcement (in.)

d_e distance from support and equal to distance d or d_c (in.)

d_i inside diameter of cylindrical explosive container (in.)

d_l distance between center lines of adjacent lacing bends measured normal to flexural reinforcement (in.)

d_{co} diameter of steel core (in.)

d_1 diameter of cylindrical portion of primary fragment (in.)

---

* See note at end of symbols.

D	(1) unit flexural rigidity (lb-in.)
	(2) location of shock front for maximum stress (ft)
	(3) minimum magazine separation distance (ft)
D_o	nominal diameter of reinforcing bar (in.)
D_E	equivalent loaded width of structure for non-planar wave front (ft)
DIF	dynamic increase factor
DLF	dynamic load factor
e	base of natural logarithms and equal to 2.71828...
$(2E')^{1/2}$	Gurney Energy Constant (ft/sec)
E	modulus of elasticity
E_c	modulus of elasticity of concrete (psi)
E_s	modulus of elasticity of reinforcement (psi)
f	unit external force (psi)
f'_c	static ultimate compressive strength of concrete at 28 days (psi)
f'_{dc}	dynamic ultimate compresive strength of concrete (psi)
f_{ds}	dynamic design stress for reinforcement (psi)
f_{du}	dynamic ultimate stress of reinforcement (psi)
f_{dy}	dynamic yield stress of reinforcement (psi)
f_s	static design stress for reinforcement (a function of f_y, f_u and θ (psi)
f_u	static ultimate stress of reinforcement (psi)
f_y	static yield stress of reinforcement (psi)
F	(1) total external force (lbs)
	(2) coefficient for moment of inertia of cracked section

(3) function of C_2 & C_1 for bilinear triangular load

F_0 force in the reinforcing bars (lbs)

F_E equivalent external force (lbs)

g   variable defined in table 4-3

h   charge location parameter (ft)

H   (1) span height (in.)

        (2) distance between reflecting surface(s) and/or free edge(s) in

            vertical direction (ft)

H_c height of charge above ground (ft)

H_c scaled height of charge above ground $(ft/lb^{1/3})$

H_s height of structure (ft)

H_T scaled height of triple point $(ft/lb^{1/3})$

i   unit positive impulse (psi-ms)

i-   unit negative impulse (psi-ms)

$\bar{i}_a$ sum of scaled unit blast impulse capacity of receiver panel and

       scaled unit blast impulse attenuated through cocnrete and sand

       in a composite element $(psi-ms/lb^{1/3})$

i_b unit blast impulse (psi-ms)

$\bar{i}_b$ scaled unit blast impulse $(psi-ms/lb^{1/3})$

$\bar{i}_{bt}$ total scaled unit blast impulse capacity of composite element

       $(psi-ms/lb^{1/3})$

$\bar{i}_{ba}$ scaled unit blast impulse capacity of receiver panel of composite

       element $(psi-ms/lb^{1/3})$

$\bar{i}_{bd}$ scaled unit blast impulse capacity of donor panel of composite

       element $(psi-ms/lb^{1/3})$

371

i_e unit excess blast impulse (psi-ms)

i_r unit positive normal reflected impulse (psi-ms)

i_r-   unit negative normal reflected impulse (psi-ms)

i_s unit positive incident impulse (psi-ms)

i_s-   unit negative incident impulse (psi-ms)

I moment of inertia (in.^{4})

I_a average of gross and cracked moments of inertia of width b (in.^{4})

I_c moment of inertia of cracked concrete section of width b (in.^{4})

I_g moment of inertia of gross concrete section of width b (in.^{4})

I_m mass moment of inertia (lb-ms^2-in.)

j ratio of distance between centroids of compression and tension forces to the depth d

k constant defined in paragraph

K (1)   unit stiffness (psi-in for slabs) (lb/in/in for beams)

            (2)   constant defined in paragraph

K_e elastic unit stiffness (psi/in for slabs) (lb/in/in for beams)

K_{ep} elasto-plastic unit stiffness (psi-in for slabs) (psi for beams)

K_E equivalent elastic unit stiffness (psi-in for slabs) (psi for beams)

            equivalent spring constant

K_L load factor

K_{LM} load-mass factor

$(K_{LM})_u$ load-mass factor in the ultimate range

$(K_{LM})_{uD}$ load-mass factor in the post-ultimate range

K_M mass factor

K_R	resistance factor
K_1	factor defined in paragraph
KE	kinetic energy
l	charge location parameter (ft)
l_p	spacing of same type of lacing bar (in.)
L	(1) span length (in.) except in chapter 4 (ft)*
	(2) distance between reflecting surface(s) and/or free edge(s) in horizontal direction (ft)
L_1	length of lacing bar required in distance s_1 (in.)
L_o	embedment length of reinforcing bars (in.)
L_w	wave length of positive pressure phase (ft)
L_w-	wave length of negative pressure phase (ft)
L_{wb}, L_{wd}	wave length of positive pressure phase at points b and d, respectively (ft)
L_1	total length of sector of element normal to axis of rotation (in.)
m	unit mass (psi-ms^2/in.)
m_a	average of the effective elastic and plastic unit masses (psi-ms^2/in.)
m_e	effective unit mass (psi-ms^2/in.)
m_u	effective unit mass in the ultimate range (psi-ms^2/in.)
m_{up}	effective unit mass in the post-ultimate range (psi-ms^2/in.)
M	(1) unit bending moment (in-lbs/in.)
	(2) total mass (lb-ms^2/in.)

---

* See note at end of symbols.

M_e effective total mass (lb-ms^2/in.)

M_u ultimate unit resisting moment (in-lbs/in.)

M_c moment of concentrated loads about line of rotation of sector (in.-lbs)

M_A fragment distribution parameter

M_E equivalent total mass (lb-ms^2/in.)

M_{HN} ultimate unit negative moment capacity in horizontal direction (in.-lbs/in.)*

M_{HP} ultimate unit positive moment capacity in horizontal direction (in.-lbs/in.)*

M_N ultimate unit negative moment capacity at supports (in.-lbs/in.)

M_P ultimate unit positive moment capacity at midspan (in.-lbs/in.)

M_{VN} ultimate unit negative moment capacity in vertical direction (in.-lbs/in.)*

M_{VP} ultimate unit positive moment capacity in vertical direction (in.-lbs/in.)*

n (1) modular ratio

        (2) number of time intervals

N number of adjacent reflecting surfaces

N_f number of primary fragments larger than W_f

p reinforcement ratio equal to $\dfrac{A_s}{bd}$ or $\dfrac{A_s}{bd_c}$

---

*   See note at end of symbols.

374

p'	reinforcement ratio equal to $\dfrac{A_s'}{bd}$ or $\dfrac{A_s'}{\overline{bd}_c}$
p_b	reinforcement ratio producing balanced conditions at ultimate strength
p_m	mean pressure in a partially vented chamber (psi)
p_{mo}	peak mean pressure in a partially vented chamber (psi)
p_H	reinforcement ratio in horizontal direction on each face*
p_T	reinforcement ratio equal to $p_H + p_v$
p_v	reinforcement ratio in vertical direction on each face*
$p(x)$	distributed load per unit length
P	(1) pressure (psi)
	(2) concentrated load (lbs)
$P-$	negative pressure (psi)
P_i	interior pressure within structure (psi)
P_i	interior pressure increment (psi)
P_f	fictitious peak pressure (psi)
P_o	peak pressure (psi)
P_r	peak positive normal reflected pressure (psi)
P_r-	peak negative normal reflected pressure (psi)
P_{ra}	peak reflected pressure at angle of incidence a (psi)
P_s	positive incident pressure (psi)
P_{sb}, P_{se}	positive incident pressure at points b and e, respectively (psi)
P_{so}	peak positive incident pressure (psi)
$P_{so}-$	peak negative incident pressure

---

* See note at end of symbols.

P_{sob}, P_{sod}, peak positive incident pressure at points b, d, and e,

P_{soe} respectively (psi)

q dynamic pressure (psi)

q_b, q_e dynamic pressure at points b and e, respectively (psi)

q_o peak dynamic pressure (psi)

q_{ob}, q_{oe} peak dynamic presure at points b and e, respectively (psi)

r (1) unit resistance (psi)

          (2) radius of spherical TNT (density equals 95 lb/ft^3 charge

             (ft))

$r-$ unit rebound resistance (psi)

r change in unit resistance (psi)

r_e elastic unit resistance

r_{ep} elasto-plastic unit resistance (psi)

r_u ultimate unit resistance (psi, for slabs) (lb/in for beams)

r_{up} post-ultimate unit resistant (psi)

r_1 radius of hemispherical portion of primary fragment (in.)

R (1) total internal resistance (lbs)

          (2) slant distance (ft)

R_f distance traveled by primary fragment (ft)

R_1 radius of lacing bend (in.)

R_A normal distance (ft)

R_E equivalent total internal resistance (lbs)

R_G ground distance (ft)

R_u total ultimate resistance

R_I, R_{II} total internal resistance of sectors I and II, respectively (lbs)

376

s_s	spacing of stirrups in the direction parallel to the longitudinal reinforcement (in.)
s_l	spacing of lacing in the direction parallel to the longitudinal reinforcement (in.)
S	height of front wall or one-half its width, whichever is smaller (ft)
SE	strain energy
t	time (ms)
t	time increment (ms)
t_a	any time (ms)
t_b, t_e, t_f	time of arrival of blast wave at points b, ϵ, and f, respectively (ms)
t_c	(1) clearing time for reflected pressures (ms)
	(2) container thickness of explosive charges (in.)
t_d	rise time (ms)
t_E	time to reach maximum elastic deflection
t_m	time at which maximum deflection occurs (ms)
t_o	duration of positive phase of blast pressure (ms)
t_o-	duration of negative phase of blast pressure (ms)
t_{of}	fictitious positive phase pressure duration (ms)
$t_{of}-$	fictitious negative phase pressure duration (ms)
t_r	fictitious reflected pressure duration (ms)
t_u	time at which ultimate deflection occurs (ms)
t_y	time to reach yield (ms)
t_A	time of arrival of blast wave (ms)

t_1	time at which partial failure occurs (ms)
T	duration of equivalent triangular loading function (ms)
T_c	thickness of concrete section (in.)
T_c	scaled thickness of concrete section ($ft/lb^{1/3}$)
T_N	effective natural period of vibration (ms)
T_r	rise time (ms)
T_s	thickness of sand fill (in.)
T_s	scaled thickness of sand fill ($ft/lb^{1/3}$)
u	particle velocity (ft/ms)
u_u	ultimate flexural or anchorage bond stress (psi)
U	shock front velocity (ft/ms)
v	velocity (in./ms)
v_a	instantaneous velocity at any time (in./ms)
v_b	boundary velocity for primary fragments (ft/sec)
v_c	ultimate shear stress permitted on an unreinforced web (psi)
v_f	maximum post-failure fragment velocity (in./ms)
v_f (avg.)	average post-failure fragment velocity (in./ms)
v_i	velocity at incipient failure deflection (in./ms)
v_o	initial velocity of primary fragment (ft/sec)
v_r	residual velocity of primary fragment after perforation (ft/sec)
v_s	striking velocity of primary fragment (ft/sec)
v_u	ultimate shear stress (psi)
v_{uH}	ultimate shear stress at distance d_e from the horizontal support (psi)*

---

* See note at end of symbols.

v_{uV} ultimate shear stress at distance d_e from the vertical support (spi)*

V volume of partially vented chamber (ft^3)

V_d ultimate direct shear capacity of the concrete of width b (lbs)

V_{dH} shear at distance d_e from the vertical support on a unit width (lbs./in.)*

V_{dV} shear at distance d_e from the horizontal support on a unit width (lbs/in.)*

V_o volume of structure (ft^3)

V_s shear at the support on a unit width (lbs/in)*

V_{sH} shear at the vertical support on a unit width (lbs/in.)*

V_{sV} shear at the horizontal support on a unit width (lbs/in.)*

V_u total shear on a width b (lbs).

w weight density of concrete (lbs/ft^3)

w_s weight density of sand (lbs/ft^3)

W charge weight (lbs)

W_c total weight of explosive containers (lbs)

W_f weight of primary fragment (oz)

W_{co} total weight of steel core (lbs)

W_{c1}, W_{c2} total weight of plates 1 and 2, respectively (lbs)

W_s width of structure (ft)

WD   work done

x yield line location in horizontal direction (in.)*

---

*   See note at end of symbols.

X	deflection (in.)
X_a	any deflection (in.)
X_e	elastic deflection (in.)
X_{ep}	elasto-plastic deflection (in.)
X_f	maximum penetration into concrete of armor-piercing fragments (in.)
X_f'	maximum penetration into concrete of fragments other than armor-piercing (in.)
X_m	maximum transient deflection (in.)
X_p	plastic deflection (in.)
X_s	(1) maximum penetration into sand of armor-piercing fragments (in.)
	(2) static deflection
X_u	ultimate deflection (in.)
X_E	equivalent elastic deflection (in.)
X_1	partial failure deflection (in.)
y	yield line location in vertical direction (in.)*
Z	scaled slant distance $(ft/lb^{1/3})$
Z_A	scaled normal distance $(ft/lb^{1/3})$
Z_G	scaled ground distance $(ft/lb^{1/3})$
α	(1) angle formed by the plane of stirrups, lacing, or diagonal reinforcement and the plane of the longitudinal reinforcement (deg)

---

*   See note at end of symbols.

α	(2)	angle of incidence of the pressure front (deg)
β	(1)	coefficient for determining elastic and elasto-plastic resistances
	(2)	particular support rotation angle (deg)
γ		coefficient for determining elastic and elasto-plastic deflections
λ		increase in support rotation angle after partial failure (deg)
θ		support rotation angle (deg)
θ̈		angular acceleration (rad/ms^2)
θ$_{max.}$		maximum support rotation angle (deg)
θ$_H$		horizontal rotation angle (deg)*
θ$_V$		vertical rotation angle (deg)*
Σo		effective perimeter of reinforcing bars (in.)
ΣM		summation of moments (in.-lbs)
ΣM$_N$		sum of the ultimate unit resisting moments acting along the negative yield lines (in.-lbs)
ΣM$_P$		sum of the ultimate unit resisting moments acting along the positive yield lines (in.-lbs)
μ		ductility factor
ν		Poisson's ratio
Φ	(1)	capacity reduction factor
	(2)	bar diameter (in.)
φ$_r$		assumed shape function for concentrated loads

---

* See note at end of symbols.

381

$\varphi(x)$ assumed shape function for distributed loads

———— free edge

═══════ simple support

χχχχχχχχ fixed support

XXXXXXXXXX either fixed, restrained, or simple support

* Note. This symbol was developed for two-way elements which are used as walls. When roof slabs or other horizontal elements are under consideration, this symbol will also be applicable if the element is treated as being rotated into a vertical position.

APPENDIX 3C

BIBLIOGRAPHY

APPENDIX 3C - BIBLIOGRAPHY

1. Blast Resistant Design, NAVFAC Design Manual 2.8, Department of the Navy, Naval Facilities Engineering Command, Alexandria, VA 22332, April 1982.

2. Design of Structures to Resist Nuclear Weapons Effects, ASCE Manual of Engineering Practice, No. 42, American Society of Civil Engineers, New York, NY, 1961. (1983 Edition under preparation)

3. Designing Facilities to Resist Nuclear Weapons Effects, Structures, TM5-858-3, Headquarters, Department of the Army, Washington, DC.

4. Structures to Resist the Effects of Accidental Explosions, Technical Manual TM5-1300, Navy Publication NAVFAC P-397, Air Force Manual AFM 88-22, Department of the Army, the Navy, and the Air Force, Washington, DC, June 1969.

5. Crawford, R. E., et al, The Air Force Manual for Design and Analysis of Hardened Structures, AFWL-TR-74-102, Air Force Weapons Laboratory, Kirtland Air Force Base, New Mexico, 87117.

6. Healey, J., et at, Design of Steel Structures to Resist the Effects of HE Explosions, by Ammann & Whitney, Consulting Engineers, New York, NY, Technical Report 4837, Picatinny Arsenal, Dover, NJ, August 1975.

7. Hopkins, J., Charts for Predicting Response of a Simple Spring-Mass System to a Bilinear Blast Load, Technical Note N-1450, Naval Civil Engineering Laboratory, Port Hueneme, CA, April 1983.

8. Stea, W., et al, Nonlinear Analysis of Frame Structures Subjected to Blast Overpressures, by Ammann & Whitney, Consulting Engineers, New York, NY, Contractor report ARLCD-CR-77008, U.S. Army Armament Research and Development Command, Large Caliber Weapon Systems Laboratory, Dover, NJ, May 1977.

9. Stea, W. Weissman, S., and Dobbs, N., Overturning and Sliding Analysis of Reinforced Concrete Protective Structures, by Ammann & Whitney, consulting Engineers, New York, NY, Technical Report 4921, Picatinny Arsenal, Dover, NJ, February 1976.

10. Javornicky, J. and Van Amerongen, C., Tables for the Analysis of Plates, Slabs and Diaphragms Based on the Elastic Theory, Bauverlag GmbH., Wiesbaden/Germany (2nd Edition 1971).

11. Roark, R.J. and Young, W. C., Formulas for Stress and Strain, McGraw Hill, New York (5th Edition 1975).

12. Cohen, E. and Dobbs, N., Design Procedures and Details for Reinforced Concrete Structures Utilized in Explosive Storage and Manufacturing Facilities, Ammann & Whitney, Consulting Engineers, New York, NY, Annals of the New York Academy of Sciences, Conference on Prevention of and Protection against Accidental Explosion of Munitions, Fuels and Other Hazardous Mixtures, Volume 152, Art. 1, October 1968.

Commander
Armament Research and Development Center
US Army Armament, Munitions and Chemical Command
ATTN: DRSMC-TSS(D) (5)
         DRSMC-LCM(D)
         DRSMC-LCM--SP(D) (10)
         DRSMC-LCM-M(D)
         DRSMC-SF(D)
Dover, NJ   07801

Administrator
Defense Technical Information Center
ATTN: Accessions Division (12)
Cameron Station
Alexandria, VA 22314

Director
Ballistics Research and Development Center
US Army Armament, Munitions and Chemical Command
ATTN: DRSMC-BLA-S(A)
       DRSMC-BLT(A) (2)
Aberdeen Proving Ground, MD   21005

Commander
US Army Armament, Munitions and Chemical Command
ATTN: DRSMC-LEP-L(R)
       DRSMC-SF(R)
       DRSMC-IR(R)
       DRSMC-EN(R)
Rock Island, IL   61299

Commander/Director
Chemical Research and Development Center
US Army Armament, Munitions and Chemical Command
ATTN: DRSMC-CLJ-L(A)
       DRSMC-CLB-PA(A)   •
APG, Edgewood Area, MD   21010

Commander
US Army Materiel Development and Readiness Command
ATTN: DRCSF
5001 Eisenhower Avenue
Alexandria, VA 22333

Director
DARCOM Field Safety Activity
ATTN: DRXOS
Charleston, IN 47111

Chief
Benet Weapons Laboratory, LCWSL
Armament Research and Development Center
US Army Armament, Munitions and Chemical Command
ATTN: DRSMC-LCB-TL
Watervliet, NJ 12189

Director
US Army Materiel Systems Analysis Activity
ATTN: DRXSY-MP
Aberdeen Proving Ground, MD 21005

ARDC Resident Operations Office
ATTN: DRSMC-TSE-OA
National Space Technology Laboratories
NSTL, MS 39529

Chairman
Department of Defense Explosives Safety Board
ATTN: Dr. T. Zaker (2)
      P. Price
Hoffman Bldg 1, Rm 856C
2461 Eisenhower Avenue
Alexandria, VA 22331

HQUSACE
ATTN: DAEN-ECE-T (10)
      DAEN-RDM
Washington, D.C. 20314

Commander
US Army Engineering Division
ATTN: HNDED-CS (R. Lein) (10)
P.O. Box 1600
Huntsville, AL 35807

Commander/Director
US Army Construction Engineering Research Laboratory
P.O. Box 4005 (2)
Champaign, IL 61820

Commander/Director
US Army Cold Regions Research and Engineering Laboratory
P.O. Box 282 (2)
Hanover, NH 03755

Commander/Director
US Army Engineer Waterways Experiment Station
P.O. Box 631 (2)
Vicksburg, MS 39180

Commander
Naval Facilities Engineering Command
ATTN: Code 04T5 (20)
200 Stovall Street
Alexandria, VA 22332

Commanding Officer
Naval Civil Engineering Laboratory
ATTN: Code L51P1 (15)
Port Hueneme, CA 93043

388

Chief of Naval Operations
Department of the Navy
ATTN: NOP-411F
Washington, D.C. 20350

Commander
Naval Sea Systems Command
ATTN: SEA-06H1
Naval Sea Systems Command Headquarters
Washington, D.C. 20362

Commander
David W. Taylor Naval Ship Research
  and Development Center
Bethesda, MD 20084

Commander
Naval Surface Weapons Center
ATTN: G10 (J. Proctor)
      R12 (W. Filler)
      R15 (J. Connor)
      R15 (R. Lorenz)
      R15 (M. Swisdak)
White Oak Laboratory
Silver Spring, MD 20910

Facilities and Maintenance Branch
Department of Energy
Albuquerque Operations
Amarillo Area Office
ATTN: Mr. L. M. Paradee, Chief (5)
P.O. Box 30030
Amarillo, TX 79120

Department of Energy
Facilities and Construction Maintenance Division
Albuquerque Operations
ATTN: Mr. Manuel G. Martinez (5)
P.O. Box 5400
Albuquerque, NM 87115

AFESC/RDC
ATTN: W. C. Buchholtz (5)
Tyndall AFB, FL 30403

Ammann & Whitney Consulting Engrs.
ATTN: N. Dobbs, 17th Floor (5)
2 World Trade Center
New York, NY 10048

Southwest Research Institute
ATTN: Mark G. Whitney (5)
P.O. Drawer 28510
6220 Culebra Road
San Antonio, TX 78284

389

Wilfred Baker Engineering
218 E. Edgewood Place (5)
San Antonio, TX 78209

Illinois Institute of Technology Research
ATTN: H. S. Napadensky
10 West 35th Street
Chicago, IL 60616